



22nd International Symposium on Ballistics

Vancouver BC, Canada

14-18 November 2005

Agenda

Tuesday, 15 November 2005

Invited Presentation: by From Columbia To Discovery: Understanding the Impact Threat to the Space Shuttle, by James D. Walker, Southwest Research Institute

General Oral Session #1

- Plasma Ignition of a 30mm Cannon, Richard A. Beyer, Andrew L. Brant, Joseph J. Colburn, US Army Research Laboratories
- Numerical Computations of Subsonic and Supersonic Flow Choking Phenomena in Grid Finned Projectiles, Nicolas Parise, SNC Technologies, Inc; Alain Dupuis, Precision Weapons Section, Defense Research and Development Canada
- The Use of Electric Power in Active Armour Applications, Martin van de Voorde, R. Boeschoten, TNO Defence, Security and Safety
- Prevention of Sympathetic Detonation Between Reactive Armor Sandwiches, Andreas Holzwarth, Fraunhofer-Institut Fur Kurzzeitdynamik

Terminal Ballistics Oral Session #1

- Bullet Impact on Steel and Kevlar®/Steel Armor - Experimental Data and Hydrocode Modeling with Eulerian and Lagrangian Methods, Dale S. Preece, Vanessa S. Berg, and Loyd R. Payne, Sandia National Laboratories
- Progress on the NDE Characterization of Impact Damage in Armor Materials, Joseph M. Wells, JMW Associates
- The influence of sabot threads on the performance of KE penetrators, Nick Lynch and John Stubberfield, QinetiQ
- The Use of Electric Power in Active Armour Applications, Martin van de Voorde, R. Boeschoten, TNO Defence, Security and Safety
- Prevention of Sympathetic Detonation Between Reactive Armor Sandwiches, Andreas Holzwarth, Fraunhofer-Institut Fur Kurzzeitdynamik

Exterior Ballistics Oral Session #1

- Micro-Adaptive Flow Control Applied to a Spinning Projectile, Dr. Jubaraj Sahu, U.S. Army Research Laboratory
- Micro-Adaptive Flow Control and Nonlinear Aerodynamics (Combustion Gas Generators), Dr. Jubaraj Sahu and Ms. Karen Heavey, U.S. Army Research Laboratory
- Aerodynamic Characteristics of a Grid Finned Projectile from Free-Flight Tests at Supersonic Velocities, Alain Dupuis, DRDC - Valcartier; Claude Berner, French-German Research Institute
- Recent Computations and Validations of Projectile Unsteady Aerodynamics, Roxan Cayaz, Eric Carette, Giat Industries; Remy Thepot, Patrick Champigny, Office National D'Etudes et de Recherches Aerospatiales
- Research of Flight Characteristics of Rod-Type Projectile with Triangular Cross-section, Dr. Wenjun Yi, Prof. Xiaobing Zhang, and Prof. Jianping Qian, Ballistic Research Laboratory of China

Wednesday, 16 November 2005

Exterior Ballistics Oral Session #2

- Impact of Nose-Mounted Micro-Structures on the Aerodynamics of a Generic Missile, Dr. Daniel Corriveau, Defence R&D Canada (DRDC - Valcartier)
- Analyses of Gliding Control for an Extended-Range Projectile, Prof. Zhongyuan Wang, Prof. Houqian Xu, Dr. Jinguang Shi, Dr. Wenjun Yi, Prof. Shaosong Chen, Ballistic Research Laboratory of China
- Theoretical Design for a Guided Supersonic Projectile, Pierre Wey, Claude Berner, Eckhart Sommer, Volker Fleck, Henry Moulard, French-German Research Institute of Saint-Louis (ISL)

Interior Ballistics/Launch Dynamics Oral Session #1

- Ceramic Gun Barrel Technologies, Larry Burton, Jeff Swab, Rob Carter, Ryan Emerson, U.S. Army Research Laboratory, Weapons & Materials Research Directorate
- M865 TID Improvement Study, Kerry Henry, Army Research Development & Engineering Center; Jason W. Gaines, General Dynamics-OTS
- Two-Dimensional Modeling of Mortar Internal Ballistics, Clive R. Woodley, David Finbow, QinetiQ; Vladimir Titarev, Eleuterio Toro, Umeritek Limited
- The Mechanism Analysis of Interior Ballistics of Serial Chamber Gun, Dr. Sanjiu Ying, Charge Design Laboratory of China; Prof. Xiaobing Zhang, Prof.

Yaxiong Yuan, and Dr. Yan Wang, Ballistic Research Laboratory of China

Terminal Ballistics Oral Session #2

- Behind Armor Debris Computations with Finite Elements and Meshless Particles, Gordon R. Johnson and Robert A. Stryk, Network Computing Services, Inc.
- Experimental and Numerical Study of the Penetration of Tungsten Carbide Into Steel Targets During High Rates of Strain, Eva K. Friis, Nammo Raufoss AS; Oyvind Froyland and John F. Moxnes, FFI (Norwegian Defence Research Establishment)
- Mine Neutralisation with Small Calibre Projectile Impact, Mark Dijkstra, J.H. Meulman, TNO Defence Safety and Security

Vulnerability, Lethality and Wound Ballistics Oral Session

- The Application of Critical Perforation Analysis (CPA) to Military Personal Armour Research and Evaluation, Catherine H. Crawford and Philip Gotts, Defence Clothing Research and Project Support
- Fragment Patterns Behind Concrete Structures Caused by KE Projectiles, S. Lampert, Fene Jeanquartier, D. Hoffmann, and B. Lehmann, Armasuisse
- Mine Neutralisation with Small Calibre Projectile Impact, Mark Dijkstra, J.H. Meulman, TNO Defence Safety and Security

Thursday, 17 November 2005

Warhead Mechanisms Oral Session #1:

- Soft-Recovery of Explosively Formed Penetrators, David Lambert and Matthew Pope, Air Force Research Laboratory, Munitions Directorate; Stanley E. Jones and Jonathan Muse, Aerospace Engineering and Mechanics, University of Alabama
- The Gurney Velocity: A “Constant” Affected by Previously Unrecognized Factors, Joseph E. Backofen, BRIGS Co.
- The Influence of Post Detonation Burning Process on Blast Wave Parameters in Air, Meir Mayselless and I. Belsky, IDF, Armor Branch; E. Muzychuk, IMI, Central Laboratory

Interior Ballistics/Launch Dynamics Oral Session #2

- 3-D Finite-Element Gun Launch Simulation of a Surrogate Excalibur 155-mm Guided Artillery Projectile - Modeling Capabilities and its Implications, M.R. Chowdhury and A. Frydman, US Army Research Laboratory; J. Cordes, L. Reinhardt and D. Carlucci, US Army ARDEC, Analysis and Evaluation Division
- Caseless Ammunition and Advances in the Characterization of High Ignition Temperature Propellant (HITP), Paul Shipley, AAI Corporation; Erin K. Hardmeyer, US Army ARDEC; and Ben Ashcroft, Alliant Technical Systems
- Ballistic Launch to Space, Ed Schmidt and Mark Bundy, Army Research Laboratory
- A Novel Launcher for Cavitating Weapons, Chris Weiland and Pavlos Vlachos, Mechanical Engineering Department, Virginia Polytechnic Institute and State University; and Jon Yagla, Engagement Systems Department, Naval Surface Warfare Center

Warhead Mechanisms Oral Session #2

- The Role of Rayleigh Taylor Instability in Shaped Charge Jets Formation and Stability, Dr. Simcha Miller, Mr. Gershon Kliminz, Rafael Ballistic Center,
- Simulation of Cylinder Expansion Tests Using an Eulerian Multiple-Material Approach, Laura Donahue, R.C. Ripley, Martec, Ltd
- Application of Powder Tantalum Material for Explosively Formed Penetrator (EFP) Warhead, Richard Fong, Mike Hesp, William Ng, and Steven Tang, US Army ARDEC
- Oilwell Perforators: Theoretical Considerations, Brenden Grove, Schlumberger Reservoir Completions Center
- The Study on Lethality Simulation Method for Fragmentation Warhead, Yang Yunbin, Qu Ming, and Qian Lixin, Institute of Structural Mechanics, China Academy of Engineering Physics

Friday, 18 November 2005

Terminal Ballistics Oral Session #3:

- Performance Evaluation of Multi-Threat Body Armour Systems, B. Anctil and M. Keown, Biokinetics and Associates Ltd.; G. Pageau, M. Bolduc, and D. Bourget, Defence R&D Canada - Valcartier
- The Residual Damage in CFRP Composite After Ballistic Impacts (Experiments & Simulations), Koen Herlaar, TNO Defence, Security and Safety
- The Effect of Boundary Conditions on the Ballistic Performance of Textile Fabrics, Colin R. Cork, University of Manchester, School of Materials

General Oral Session #2

- Wind Tunnel Verification of the Performance of a Smart Material Canard Actuator, Paul Weinacht, William F. Drysdale, Travis Bogetti, and Rod Don, US Army Research Laboratory; James T. Arters, Jack R. Vinson, Aaron R. Hickman, University of Delaware; Lamar Auman, US Army Aviation and Missile RD&E Center; Oded Rabinovitch, Technion Israel Institute of Technology
- The Fragmentation of Metal Cylinders Using Thermobaric Explosives, William Andrews, Royal Military College of Canada; Michael Dunning, Defence R&D Canada – Suffield; and Kevin Jaansalu, Montana Tech (University of Montana)
- A Novel Test Methodology to Assess the Performance of Ballistic Helmets, B. Anctil and M. Keown, Biokinetics and Associates Ltd.; G. Pageau and D. Bourget, Defence R&D Canada - Valcartier
- Ballistic Analysis of Bulgarian Electroslag Remelted Dual Hard Steel Armor Plate, William Gooch, Matthew Burkins, and David Mackenzie, US Army Research Laboratory Weapons and Materials Research Directorate; Stefan Vodenicharov, Institute of Metal Science, Bulgarian Academy of Sciences



22ND INTERNATIONAL SYMPOSIUM ON BALLISTICS

November 14-18, 2005



Vancouver
BC, Canada
Event #6210



International Symposium on Ballistics 2005

International Symposium on Ballistics 2005 is jointly organized and supported by the National Defense Industrial Association, USA in conjunction with the International Ballistics Committee

Symposium Co-Chairman: William Flis
Symposium Co-Chairman: Brian Scott

PREVIOUS INTERNATIONAL SYMPOSIA ON BALLISTICS

1st	Orlando, Florida, USA	1974
2nd	Daytona, Florida, USA	1976
3rd	Karlsruhe, Germany	1977
4th	Monterey, California, USA	1978
5th	Toulouse, France	1980
6th	Orlando, Florida, USA	1981
7th	The Hague, The Netherlands	1983
8th	Orlando, Florida, USA	1984
9th	Shrivenham, UK	1986
10th	San Diego, California, USA	1987
11th	Brussels, Belgium	1989
12th	San Antonio, Texas, USA	1990
13th	Stockholm, Sweden	1992
14th	Quebec City, Canada	1993
15th	Jerusalem, Israel	1995
16th	San Francisco, California, USA	1996
17th	Midrand, South Africa	1998
18th	San Antonio, Texas, USA	1999
19th	Interlaken, Switzerland	2001
20th	Orlando, Florida, USA	2002
21st	Adelaide, South Australia	2004
22nd	Vancouver, BC Canada	2005

SYMPOSIUM SCOPE AND OBJECTIVES

The objective of the 22nd International Symposium on Ballistics is to focus on potential technical advances and break-throughs in the 21st century in the general areas of:

- Interior Ballistics
- Launch Dynamics
- Exterior Ballistics
- Projectile and Warhead Design
- Terminal Ballistics
- Vulnerability
- Modeling and Simulation
- Wound Ballistics

Over 200 papers will be presented by authors from 26 countries.

SYMPOSIUM PROGRAM

Monday, November 14, 2005

2:00 pm - 5:00 pm Registration
 5:00 pm - 6:30 pm Reception in Exhibit Area

Tuesday, November 15, 2005

7:00 am Continental Breakfast and Registration
 7:00 am - 6:00 pm Exhibits Open
 8:00 am Opening Remarks
C. Samuel Campagna, National Defense Industrial Association
 8:10 am Welcome and Opening Remarks
William Flis, DE Technologies, Inc. & *Brian Scott*, US Army Research Laboratory
 8:20 am **Keynote Address**
Dr. Robert Walker, Director-General, Research and Development Programs
 (DGRDP), Defense Research and Development Canada
 9:05 am **Invited Presentation**
 From Columbia to Discovery: Understanding the Impact Threat to the Space Shuttle
James D. Walker, Southwest Research Institute
 9:50 am Morning Break

General Oral Session #1 **Chairpersons: *B. Janzon* and *J. Carleone***

10:20 am Plasma Ignition of a 30mm Cannon
Richard A. Beyer, Andrew L. Brant, Joseph J. Colburn, US Army Research Laboratories
 10:40 am Numerical Computations of Subsonic and Supersonic Flow Choking Phenomena in Grid Finned Projectiles
Nicolas Parisé, SNC Technologies, Inc.; *Alain Dupuis*, Precision Weapons Section, Defense Research and Development Canada
 11:00 am Multiple Explosively Formed Penetrator (MEFP) Warhead Technologies for Mine and Improvised Explosive Device (IED) Neutralization
Richard Fong, William Ng, Steve Tang, LaMar Thompson, U.S. Army Armament Research, Development and Engineering Center
 11:20 am The Use of Electric Power in Active Armour Applications
Martin van de Voorde, R. Boeschoten, TNO Defence, Security and Safety
 11:40 am Prevention of Sympathetic Detonation between Reactive Armor Sandwiches
Andreas Holzwarth, Fraunhofer-Institut für Kurzzeiddynamik
 12:00 pm Lunch

22nd International Symposium on Ballistics

1:30 pm - 3:10 pm	Exterior Ballistics Poster Session Chairpersons: Z. Wang and P.A. Karsten
	Terminal Ballistics Oral Session #1 Chairpersons: E. Lindén and C. Anderson
1:30 pm	Bullet Impact on Steel and Kevlar®/Steel Armor – Experimental Data and Hydrocode Modeling with Eulerian and Lagrangian Methods* Dale S. Preece, Vanessa S. Berg, Mathew A. Risenmay , Sandia National Laboratories
1:50 pm	Progress on the NDE Characterization of Impact Damage in Armor Materials Joseph M. Wells , JMW Associates
2:10 pm	Design, Analysis, and Testing of an Unconfined Ceramic Target to Induce Dwell Timothy J. Holmquist , Network Computing Services, Inc.; C. Anderson, Jr. , Southwest Research Institute; Thilo Behner , Ernst-Mach-Institut
2:30 pm	The Influence of Sabot Threads on the Performance of KE Penetrators against multiple plate targets Nick J. Lynch, J. Stubberfield , QinetiQ
2:50 pm	Visualization of Wave Propagation and Impact Damage in a Polycrystalline Transparent Ceramic - AlON Elmar Strassburger , Fraunhofer Institut für Kurzzeitdynamik; Parimal Patel, James W. McCauley , US Army Research Laboratory; Douglas W. Templeton , US Army TARDEC
3:10 pm	Afternoon Break
3:40 pm - 5:20 pm	Terminal Ballistics Poster Session #1 Chairpersons: A. Diederer
	Exterior Ballistics Oral Session Chairpersons: W. Reinecke and A. Dupuis
3:40 pm	Advanced Time-Accurate CFD/RBD Simulations of Projectiles in Free Flight Jubaraj Sahu , US Army Research Laboratory
4:00 pm	Aerodynamic Characteristics of a Grid Finned Projectile from Free-Flight Tests at Supersonic Velocities Alain Dupuis , DRDC - Valcartier; Claude Berner , French-German Research Institute
4:20 pm	Recent Computations and Validations of Projectile Unsteady Aerodynamics Roxan Cayaz, Eric Carette , Giat Industries; Rémy Thépot, Patrick Champigny , Office National d'Études et de Recherches Aérospatiales
4:40 pm	The Derivation of Spin Stabilised Projectile Yaw Rates and Ballistic Model Coefficients Using Conventional CW Doppler Radar Systems John Tate , FLEET
5:00 pm	Research of Flight Characteristics of Rod-Type Projectile with Triangular Cross-Section Wenjun Yi, Xiaobing Zhang, Jianping Qian , Ballistic Research Laboratory of China, Nanjing University of Science & Technology
5:20 pm	Adjourn for the Day

22nd International Symposium on Ballistics

Wednesday, November 16, 2005

7:00 am	Continental Breakfast and Registration
7:00 am - 5:00 pm	Exhibits Open
8:00 am	Administrative Remarks
8:10 am - 9:50 am	Terminal Ballistics Poster Session #2 Chairpersons: J. Riegel and E. Hirsch
	Exterior Ballistics Oral Session #2 Chairpersons: P. Nel and E. Schmidt
8:10 am	Impact of Nose-Mounted Micro-Structures on the Aerodynamics of a Generic Missile <i>Daniel Corriveau</i> , Defence R&D Canada (DRDC - Valcartier)
8:30 am	Ballistic Simulations and Wind Tunnel Testing of 120 mm Mortar Bomb Tail Fin Geometries – In Search for Extra Range <i>Jukka Tiainen, Ari Makkonen</i> , Patria Weapon Systems Oy; <i>Mikko Korhonen, Timo Sillaranta</i> , TKK/Laboratory of Aerodynamics
8:50 am	Bringing Solid Fuel Ramjet Projectiles Closer to Application – An Overview of the TNO/RWMS Technology Demonstration Programme <i>Ronald G. Veraar</i> , TNO Defence, Security and Safety Research Group Rocket Technology; <i>Guido Giusti</i> , Rheinmetall Waffe Munition Schweiz AG
9:10 am	Analysis of Gliding Control for an Extended-Range Projectile <i>Zhongyuan Wang, Houqian Xu, Jinguang Shi, Wenjun Yi, Shaosong Chen</i> , Ballistic Research Laboratory of China, Nanjing University of Science & Technology
9:30 am	Theoretical Design for a Guided Supersonic Projectile <i>Pierre Wey, Claude Berner, Eckhart Sommer, Volker Fleck, Henry Moulard</i> , French-German Research Institute of Saint-Louis (ISL)
9:50 am	Morning Break
10:20 am - 12:00 pm	Warhead Mechanisms Poster Session Chairpersons: R. Fong and F. Mostert
	Interior Ballistics/Launch Dynamics Oral Session #1 Chairpersons: C. Candland and C. Woodley
10:20 am	Ceramic Gun Barrel Technology <i>Lawrence W. Burton, Jeffrey J. Swab, Ryan Emerson, Robert Carter</i> , US Army Research Laboratory, Weapons & Materials Research Directorate
10:40 am	M865E3 Cold Target Impact Dispersion Study <i>Kerry Henry</i> , Army Research Development & Engineering Center; <i>Jason W. Gaines</i> , General Dynamics-OTS
11:00 am	An Alternative Technique to Evaluate and Characterize Pressure Waves in Large Calibre Guns <i>Victor Schabot</i> , Denel Land Systems Western Cape
11:20 am	Two-Dimensional Modelling of Mortar Internal Ballistics <i>Clive R. Woodley, David Finbow</i> , QinetiQ; <i>Vladimir Titarev, Eleuterio Toro</i> , Numeritek Limited

22nd International Symposium on Ballistics

11:40 am	The Mechanism Analysis of Interior Ballistics of Serial Chamber Gun Sanjiu Ying , Charge Design Laboratory of China, Nanjing University of Science & Technology; Xiaobing Zhang, Qaxiong Yuan, Yan Wang , Ballistic Research Laboratory of China, Nanjing University of Science & Technology
12:00 pm	Lunch
Terminal Ballistics Oral Session #2 Chairpersons: M. Mayseless and T. Holmquist	
1:30 pm	Behind Armor Debris Computations with Finite Elements and Meshless Particles Gordon R. Johnson, Robert A. Stryk , Network Computing Services, Inc.
1:50 pm	Expirmental and Numerical Study of the Penetration of Tungsten Carbide into Steel Targets During High Rates of Strain Eva K. Friis , Nammo Raufoss AS, Oyvind Froyland, John F. Moxnes , FFI (Norwegian Defence Researhd Establishment)
2:10 pm	Fragmentation Behavior of Tungsten Alloy Cubes on Normal Aluminum Plate Targets Karl Weber , Fraunhofer-Institut für Kurzzeitdynamik, Ernst-Mach Institut
2:30 pm	The Failure Kinetics of High Density DEDF Glass Against Rod Impact at Velocities From 0.4 to 2.5 km/s Thilo Behner, V. Hohler, M. Moll , Fraunhofer Institut für Kurzzeitdynamik (Ernst-Mach Institut); Ch. E. Anderson Jr. , Southwest Research Institute; D. L. Orphal , International Research Associates, Inc.; D. W. Templeton , US Army RDECOM-TACOM
2:50 pm	Mine Neutralisation with Small Calibre Projectile Impact Mark Dijkstra, J.H. Meulman , TNO Defence, Safety and Security
3:10 pm	Afternoon Break
Vulnerability, Lethality and Wound Ballistics Oral Session Chairpersons: R. Vaziri, A. Persson	
3:40 pm	The Application of Critical Perforation Analysis (CPA) to Military Personal Armour Research and Evaluation Catherine H. Crawford, Philip Gotts , Defence Clothing Research and Project Support
4:00 pm	An Efficient Mechanistic Approach to Modelling the Ballistic Response of Multi-Layer Fabrics Ali Shahkarami, Reza Vaziri, Anounsh Poursartip , Composites Group, Departments of Civil Engineering and Materials Engineering The University of British Columbia; Navin Tajani , DuPont Advanced Fibers Systems
4:20 pm	Pencilling – A Novel Behind Armour Blunt Trauma Injury Eluned A. Lewis , Defence Clothing Research and Project Support; Ian Horsfall, Celia Watson , Engineering Systems Department, Royal Military College of Science, Cranfield University
4:40 pm	Scaling the Dynamic Response of Armored Vehicle's Floor Subjected to a Large Buried Charge Avidov Neuberger , MOD, Tank Program Management; S. Peles , IMI, Central Laboratory Division; D. Rittel , Technion, Israel Institute of Technology, Faculty of Mechanical Engineering

5:00 pm Fragment Patterns Behind Concrete Structures Caused by KE Projectiles
René Jeanquartier, D. Hoffmann, S. Lampert, B. Lehmann, Armasuisse

5:20 pm Adjourn for the Day

Thursday, November 17, 2005

7:00 am Continental Breakfast and Registration

8:00 am - 11:00 am Exhibits Open

8:00 am Adminstrative Remarks

8:10 am - 9:50 am **Interior Ballistics/Launch Dynamics Poster Session**

Chairpersons: C. Woodley and C. Candlant

Warhead Mechanisms Oral Session #1

Chairpersons: M. Murphy and P.Y. Chanteret

8:10 am Soft-Recovery of Explosively Formed Penetrators

David E. Lambert, Matthew Pope, Air Force Research Laboratory, Munitions Directorate; **Stanley Jones, Jonathan Muse**, University of Alabama, Aerospace Engineering and Mechanics

8:30 am The Gurney Velocity: A "Constant" Affected by Previously Unrecognized Factors
Joseph E. Backofen, BRIGS Co.

8:50 am Influence of Post Detonation Burning Process on Blast Wave Parameters in Air
Meir Mayseless, E. Muzychuk, IDF, Mil.; **M. Mayseless, I. Belsky, IMI**, Central Laboratory

9:10 am Steerable Fragment Masses
Manfred Held, TDW/EADS

9:30 am Penetration Performances of Tungsten-Copper Shaped Charge Liner
Seong Lee, Eun Pyo Kim, Youngmoo Kim, Sung Ho Lee, Moon-Hee Hong, Joon-Woong Noh, Agency for Defense Development

9:50 am Morning Break

10:20 am - 12:00 pm **Vulnerability/Lethality/Wound Ballistics Poster Session**

Chairpersons: W. Gooch

Interior Ballistics/Launch Dynamics Oral Session #2

Chairpersons: B. Burns and R. Cayzac

10:20 am 3-D Finite-Element Gun Launch Simulation of a Surrogate Excalibur 155-mm Guided Artillery Projectile - Modeling Capabilities and its Implications

M.R. Chowdhury, A. Frydman, US Army Research Laboratory; **J. Cordes, L. Reinhardt, D. Carlucci**, US Army ARDEC, Analysis and Evaluation Division

10:40 am Method of Calculating Initial Firing Data of Artillery Laser Terminal-Guidance Weapon System

Feipeng Zeng, Liren Liu, Faculty of Artillery Command, Nanjing Artillery Academy

22nd International Symposium on Ballistics

11:00 am	Caseless Ammunition & Advances in the Characterization of High Ignition Temperature Propellant Patricia M. O'Reilly, Erin Hardmeyer, Chad Sensemig , US Army ARDEC; Ben Ashcroft , Alliant Techsystems; Dave Cleveland , The Johns Hopkins University, 0Applied Physics Laboratory; Bo Engel, Paul Shipley , AAI Corporation
11:20 am	Ballistic Launch to Space Edward Schmidt, M. Bundy , US Army Research Laboratory
11:40 am	A Novel Launcher for Cavitating Weapons Chris J. Weiland , Pavlos P Vlachos, Dept of Mechanical Engineering Virginia Tech; Jon J Yagla, Mechanical Engineer Engagement Systems Department Naval Surface Warfare Center
12:00 pm	Lunch
	Warhead Mechanisms Oral Session #2 Chairpersons: R. Brown and M. Held
1:30 pm	The Role of Rayleigh Taylor Instability in Shaped Charge Jets Formation and Stability Simcha Miller, Gershon Kliminz , Rafael Ballistic Center
1:50 pm	Simulation of Cylinder Expansion Tests Using an Eulerian Multiple-Material Approach Laura K. Donahue, R.C. Ripley , Martec, Ltd.
2:10 pm	Application of Powder Tantalum Material for Explosively Formed Penetrator Warhead Richard Fong, William Ng, Steven Tang, Michael Hespos , US Army Armament Research, Development and Engineering Center
2:30 pm	Oilwell Perforators: Theoretical Considerations Brenden M. Grove , Schlumberger Reservoir Completions Center
2:50 pm	Planar Cutting Jets from Shaped Charges Geoffery EB Tan, T.K. Lam, Y.K. Tham , DSO National Laboratories
3:10 pm	The Study on Lethality Simulation Method for Fragment Warhead Yang Yunbin, Qu Ming, Qian Lixin , Institute of Structural Mechanics, China Academy of Engineering Physics
3:30 pm	Adjourn for the Day
4:00 pm - 5:30 pm	Reception
<u>Friday, November 18, 2005</u>	
7:00 am	Continental Breakfast and Registration
8:00 am	Administrative Remarks
	Terminal Ballistics Oral Session #3 Chairpersons: I. Cullis and D. Nandlall
8:10 am	Performance Evaluation of Multi threat Body Armour Systems B. Ancil, M. Keown , Biokinetics and Associates Ltd.; G. Pageau, M. Bolduc D. Bourget , Defence R&D Canada – Valcartier

22nd International Symposium on Ballistics

8:30 am	Finite Element Simulations and Experiments to Determine the Residual Damage of a CFRP Composite Material After Ballistic Impacts <i>Koen Herlaar, M. Van der Jagt-Deutekom</i> , TNO Defence, Security and Safety
8:50 am	The Effect of Boundary Conditions on the Ballistic Performance of Textile Fabrics <i>Colin R. Cork</i> , University of Manchester, School of Materials
9:10 am	Terminal Ballistic Effects of Low Density Materials Used as Confinement Plates for Explosive Reactive Armours <i>Hanspeter Kaufmann</i> , RUAG Land Systems; <i>André Koch</i> , Armasuisse
9:30 am	Quantification of the Effect of Using the Johnson-Cook Damage Model in Numerical Simulations of Penetration and Perforation <i>Charles E. Anderson Jr., T. R. Sharron</i> , Southwest Research Institute; <i>Timothy J. Holmquist</i> , Network Computing Services, Inc.
9:50 am	Morning Break
General Oral Session #2 Chairpersons: V. Sanchez-Galvez and P. Cuniff	
10:20 am	Comparisons of Internal Ballistics Simulations of the AGARD Gun <i>Clive R. Woodley</i> , QinetiQ; <i>Alain Carriere, Patrice Franco, Dieter Hensel, Julien Nussbaum</i> , Institut Franco-Allemand de Recherches de Saint-Louis (ISL); <i>Tatjana Gröge</i> , Ernst-Mach-Institut (EMI); <i>Stefan Kelzenberg</i> , Fraunhofer-Institut für Chemische Technologie (ICT), <i>Baptiste Longuet</i> , DGA/DCE/ETBSr3
10:40 am	Wind Tunnel Verification of the Performance of a Smart Material Canard Actuator <i>Paul Weinacht, William F. Drysdale, Travis Bogetti, Rod Don</i> , US Army Research Laboratory; <i>James T. Arters, Jack R. Vinson, Aaron R. Hickman</i> , University of Delaware; <i>Lamar Auman</i> , US Army Aviation and Missile RD&E Center; <i>Oded Rabinovitch</i> , Technion Israel Institute of Technology
11:00 am	Fragmentation of Metal Cylinders Using Thermobaric Explosives <i>M.R. Dunning</i> , Defence Research and Development - Suffield, <i>W.S. Andrews</i> , Department of Chemistry and Chemical Engineering, Royal Military College of Canada; <i>K.M. Jaansalu</i> , Department of Metallurgical and Materials Engineering, The University of Montana
11:20 am	A Novel Test Methodology to Assess the Performance Ballistic Helmets <i>B. Anctil, M. Keown</i> , Biokinetics and Associates Ltd.; <i>D. Bourget, G. Pageau</i> , Defence R&D
11:40 am	Ballistic Analysis of Bulgarian Electroslag Remelted Dual Hard Steel Armor Plate <i>William Gooch, Matthew Burkins and David Mackenzie</i> , US Army Research Laboratory, Weapons and Materials Research Directorate; Stefan Vodenicharov, Institute of Metal Science, Bulgarian Academy of Sciences
12:00 pm	Presentation of Awards The Rosalind and Pei Chi Chou Award for Young Authors The Neil Griffiths Memorial Award The Louis and Edith Zernow Award
12:15 pm	Invitation to the 23rd International Symposium on Ballistics, Tarragona, Spain, 2007
12:25 pm	Closing <i>William Flis</i> , DE Technologies, Inc. & <i>Brian Scott</i> , US Army Research Laboratory

POSTER SESSIONS START HERE

Exterior Ballistics Poster Session
1:30 pm - 3:10 pm Tuesday, November 15

1913 Fractional Calculus for Design of Aerodynamic Missile's Autopilot and Digital Realization

Bangchu Zhang, Chenming Li, Zipeng Han, Zou Yun, Fuming Xu, Ballistic Research Laboratory of China, Nanjing University of Science & Technology

1915 The Simulation of Rocket Trajectory in Simulink

Xin Changfan, Nanjing University of Science & Technology

1924 Establishing a Pitch Damping Test Capability at CSIR Defencetek

Fabrizio Dionisio, CSIR, Defencetek

1944 The Investigation About Using Different Guidance Laws on Improving Impact Point Deviation of a Rocket

Handong Zhao, Fang Wang, Qingshang Liu, Key Laboratory of Instrumentation and Dynamic Measurement, North University of China

1951 Numerical Integration Method Based on 4th Lagrange Polynomial of Strap-Down INS System

Guoguang Chen, Xiaoli Tian, Changfan Xin, Yaqi Bao, North University of China

1952 Research on Real Time Trajectory Measure Device of Range

Changfan Xin, Guoguang Chen, Xiaoli Tian, North University of China

1953 Research on Attitude Control Strategy of Glide Range Extend Rocket

Xiaoli Tian, Guoguang Chen, Changfan Xin, North University of China

1954 Optimal Algorithm of Glide Range Extend Rocket's Trajectory

Guoguang Chen, Xiaoli Tian, Changfan Xin, North University of China

1978 Practical Propulsion by Directed Energetic Processes

Joseph P. Backofen, BRIGS Co.

2014 Investigating the Method of Obtaining Ammunition Roll Attitude by Detecting the Geomagnetic Vector

Hongsong Cao, Guoguang Chen, Department of Mechatronics Engineering, North University of China

2065 External Ballistic Trajectory Computations for Direct/Indirect Fire Weapon Systems

David J. Norton, General Dynamics Canada

2087 The Influence of Laser Rangefinder Parameters on the Hit Probability in Direct Tank Fire

Vladimir Cech, OPROX, Inc., **Jiri Jevicky**, Department of Mathematics, University of Defense

2123 Flight Dynamics Modeling and Experiment for Composite Concepts. Application to Ribbon Aerodynamic Stabilization

Christopher Grignon, S. Heddadj, Giat Industries

2128 Onboard Measurements with Magnetic Sensors: Determination of the Attitude and the trajectory Position

V. Fleck, E. Sommer, S. Changey, French-German Research Institute (ISL); **D. Beauvois**, Ecole Superirure d'Electrecite (Supelec)

2133 Aerodynamic Characteristics of a Long Range Spinning Artillery Shell Obtained from 3D Magnetic Sensors

V. Fleck, E. Sommer, C. Berner, French-German Research Institute (ISL); **A. Dupuis**, DRDC

2143 Experimental Testing and Numerical Simulation of Separation Disturbances for Two-Stage Kinetic Energy Missiles

Nicolas Parisé, SNC Technologies, Inc.; **Richard Lestage, Francoise Lesage**, Precision Weapons Section, Defense Research and Development Canada Valcartier

2147 Numerical Study on the Base Drag Characteristics of a Base Bleed Projectile with a Central Propulsive Jet

Chang-Kee Kim, Agency for Defense Development; **J.Y. Choi**, Pusan National University, Department Aerospace Engineering

2169 Solid Fuel Ramjet (SFRJ) Propulsion for Artillery Projectile Applications – Dynamic Testing Progress
Anton Stockenström, Dynax

3010 Pitch and Bending During In-Flight Extension
W. G. Reinecke, Institute for Advanced Technology; **M. G. Miller**, Physical Sciences, Inc.

4004 Improvements in Aerodynamic Design for KE Less-Lethal Projectiles
Jamie H. Cuadros, Arts & Engineering

Terminal Ballistics Poster Session #1
3:40 pm - 5:20 pm Tuesday, November 15

1001 Numerical Simulations of Silicon Carbide Tiles Impacted by Tungsten Carbide Spheres
Constantine G. Fountzoulas, **Jerry C. LaSalvia**, **Bryan A. Cheeseman**, Weapons and Materials Research Directorate; **Michael J. Normandia**, Ceradyne, Inc.

1007 Shock Mitigation for Blast Protection Using Hertzian Tapered Chains
Robert Doney, US Army Research Laboratory; **Surajit Sen**, Department of Physics, State University of New York at Buffalo

1011 A Predictive Model for the Dwell/Penetration Transition Phenomenon
Jerry C. LaSalvia, US Army Research Laboratory

1012 Effect of Ceramic Thickness on the Dwell/Penetration Transition Phenomenon
Jerry C. LaSalvia, US Army Research Laboratory

1014 The Development of Hybridized Thermoplastic-Based Structural Materials with Applications to Ballistic Helmets
Shawn Walsh, **Brian R. Scott**, **David M. Spagnuolo**, AMSRD-ARL-WM-MB

1015 Time Resolved Observation of the Deformation and Surface Strain of a Textile Fabric Subject to Ballistic Impact
Brian Scott, **Peter Dehmer**, US Army Research Laboratory; **Timothy Schmidt**, Trilion Quality Systems

1016 Analytic Design Trends of Fabric Armor
Brian Scott, **Chian-Fong Yen**, US Army Research Laboratory

1018 High-Speed Photographic Study of Wave and Fracture Propagation in Fused Silica
Elmar Strassburger, Fraunhofer-Institut für Kurzzeitdynamik, Ernst-Mach-Institut (EMI); **Parimal Patel**, **James W. McCauley**, US Army Research Laboratory; **Douglas W. Templeton**, US Army TARDEC

1022 Low Velocity Ballistic Properties of Shear Thickening Fluid (STF)–Fabric Composites
M. J. Decker, **R. G. Egres**, **N. J. Wagner**, University of Delaware, Dept. of Chemical Engineering and Center for Composite Materials; E. D. Wetzel, U.S. Army Research Laboratory

1023 An Approximate Solution of the Long-Rod Penetration Equations
William Walters, **Cyril Williams**, ARL, Terminal Effects Division

1901 Tubular Projectile Interaction with Stationary and Moving Oblique Plates
Olof Andersson, Swedish Defence Research Agency (FOI), Weapons and Protection Division

1911 A Study on the Moving Features of Double-Layer Explosive Reactive Armor with Definite Angle by Numerical Simulation and Experiments
Zhengxiang Huang, **Xianfeng Zhang**, **Gang Li**, School of Mechanical Engineering, Nanjing University of Science & Technology

1927 Mechanics of Structural Design of EPW Warhead
X.W. Chen, Institute of Structural Mechanics, China Academy of Engineering Physics

1928 Armour Qualification Utilizing Maximum Likelihood Ballistic Limit Calculation
Moshe Ravid, **Shlomo Galperin**; Rimat Advanced Technologies, Ltd.

1934 Perforation of Concrete Targets by an Eroding Tungsten-Alloy Rod
Stephan Lampert, Rene Jeanquartier, Armasuisse

1955 Ballistic Properties of Single-Melt Titanium-6Aluminum-4Vanadium Alloy Plate
Brij J. Roopchand, US Army Tank-Automotive and Armament Command, Armament Research, Development, & Engineering Center

1987 Preliminary Investigations of Potential Light Weight Metallic Armour Applications
Martin van de Voorde, A.M. Dierderen, K. Herlaar, TNO Defence, Safety and Security

2001 Oblique Warhead Penetration and Perforation of Multi-Layered Metallic Targets
Yongxiang Dong, Feng Shunshan, Wang Fang, State Key Laboratory of Explosion Science & Technology, Beijing Institute of Technology

2019 Influence of Projectile Material on Yawed Long Rod Projectiles Penetrating Oblique Plates
Ewa Lidén, Swedish Defence Research Agency (FOI), Weapons and Protection Division

2035 Advanced Aliphatic Polyurthane Resins for High Durability and Superior Ballistic Performance Laminated Glass
Francisco Folgar, INTER Materials, LLC

2037 Impact and Penetration of B4C Ceramic, Aluminum, and Beryllium by Depleted Uranium Rods at 2.0 KM/S
Scott A. Mullin, James D. Walker, Carl E. Weiss, Southwest Research Institute; **Paul O. Leslie**, Los Alamos National Laboratories

2122 A Comparison of Some Analytical and Empirical Models for Kinetic Energy Penetration of Semi-Infinite and Finite Thickness Steel Targets
Nick J. Lynch, J T Mills, QinetiQ

2181 Computed Tomography of High-Speed Events
Karsten Michael, Philip Helberg, Fraunhofer Institute for High Speed Dynamics, Ernst-Mach-Institut

2186 Characterization of Behind-Armor Debris Particles from Tungsten Penetrators
Brad A. Pedersen, S. Bless, Institute for Advanced Technology

Terminal Ballistics Poster Session #2
8:10 am - 9:50 am Wednesday, November 16

2050 On the Critical Thickness of Ceramic to Shatter WC-Co Bullet Cores
Paul J. Hazell, Engineering Systems Department, Cranfield University, Royal Military College of Science; **C. J. Roberson**, Advanced Defence Materials Limited

2060 The Effect of Spaced Armour on the Penetration of Shaped Charge Warheads
James D. Shattock, Cranfield University

2072 Modeling Impact and Penetration Using a Deterministic and Probabilistic Design Tool
David S. Riha, Jason B. Pleming, Ben H. Tucker, Scott A. Mullin, James D. Walker, Carl E. Weiss, Southwest Research Institute; **Edward A. Rodriguez, Paul O. Leslie**, Los Alamos National Laboratories

2106 On the Ballistic Efficiency of the Three Layered Metallic Targets
Stanislav Rolc, Military Technical Institute of Protection; **Jaroslav Buchar**, Mendel University; **Giovanni Cozzani**, OTO MELARA S.p.A **Vojtech Hruba**, University of Defence

2107 Effect of the Temperature on the Ballistic Efficiency of Plates Made From Cast Iron
Stanislav Rolc, Military Technical Institute of Protection; **Jaroslav Buchar**, Mendel University

2113 Displacement Device to Measure the Acceleration of the Bulge of RHA Plates Under Anti-Tank Mine Blast
Manfred Held, TDW/EADS; **Peter Heeger**, WTD; **Josef Kiermeir**, CONDAT

2116 Defeating Mechanisms of Explosive Reactive Armour Sandwiches

Manfred Held, TDW/LFK/EADS

2121 Comparisons of Unitary and Jacketed Rod Penetration into Semi-Infinite and Oblique Plate Targets at System Equivalent Velocities

John Stubberfield, N J Lynch, QinetiQ; **I Wallis**, QinetiQ Farnborough

2126 Finite Element Simulations and Experiments of Ballistic Impacts on High Performance PE Composite Material

Koen Herlaar, M. Van der Jagt-Deutekom, TNO Defense, Security and Safety

2129 The Use of Foam Structures in Armoured Vehicle Protection Against Landmines

David A. Cendón, Vincente Sanchez-Galvez, Francisci Galvez, Alejandro Enfedaque, Departamento de Ciencia de Materiales, E.T.S.I. Caminos, Canales y Puertos, Universidad Politecnica de Madrid, Spain

2136 The Numerical Simulation of the Impact of an Aluminum Cylinder into a Steel Cone

Izak M. Snijman, Defencetek Landwards Programme, CSIR

2139 Characterization of Al 6061-T6 using Split Hopkinson Bar Tests and Numerical Simulations

Amal Bouamoul, Manon Bolduc, DRDC - Valcartier

2145 Finite Element Modeling of Light Armoured Vehicles (LAV) Welds Heat Affected Zones Subjected to an Anti-Vehicular (AV) Blast Landmine Loading: A Summary of the Numerical Model and Experiment

Patrice Gaudreault, Defence Research & Development Canada; **Amal Bouamoul, Robert Durocher, Benoit St-Jean**, DRDC Valcartier

2151 Designer Projectiles by Density Variation: Towards the Nano-Projectile

John P. Curtis, QinetiQ

2160 Numerical Simulation for the Front Section Effect of Missile Warhead on the Target Perforation

Ho Soo Kim, Ki-Sun Yeom, Seong Shik Kim, Agency for Defense Development (ADD); Larry Sotsky, US Army ARDEC

2180 The Penetration Process of Projectiles into Long Bars in the Axial Direction

Dan Yaziv, G. Gans, Y. Reifen, RAFAEL

2199 The Electromagnetic Launch Trends Utilization for Shaped Charge Jets Penetration Depth Decrease

S.V. Demidkov, Effective Soft Ltd.

3003 Simulation of the Perforation of Low Mass Long L/D Rods Against Finite RHA Plates

P. Church, I. Cullis, A Bowden, D Gibson, QinetiQ, Ltd.

3011 Deflection and Fracture of Tungsten Rods by Yawed Impact

S. Bless, R. Russell, Institute for Advanced Technology; **K. Tarcza**, US Army ARDEC; **E. Taleff**, Department of Mechanical Engineering, The University of Texas at Austin; **M. Huerta**, The University of Texas at El Paso

3012 Anomalies in the Strength of Alumina under Dynamic Compression

T. Beno, S. Bless, S. Nichols, Institute for Advanced Technology

3014 On the 3D Visualization of Ballistic Damage in Ti-6AL-4V Applique Armour with X-Ray Computed Tomography

J.M. Wells, JMW Associates; **W.H. Green, N.L. Rupert**, US Army Research Laboratory, Weapons & Materials Research Division; **John M. Winter, Jr.**, ORISE Contractor at WMRD; **S.J. Cimpoeru**, DSTO Melbourne

4012 Analytical Models for Foam, Ice and Ablator Impacts into Space Shuttle Thermal Tiles

James D. Walker, Sidney Chocron, Walt Gray, Southwest Research Institute

4013 CTH Simulations of Foam and Ice Impacts into the Space Shuttle Thermal Protection System Tiles

Sidney Chocron, Walt Gray, James D. Walker, Southwest Research Institute

4016 Damage Created in Composite Sheet by Explosives – Effects of Fibre Type, Explosive Mass and Attenuating Material

M. R. Edwards, R. Unwin, Centre for Materials Science and Engineering, Cranfield University

Warhead Mechanisms Poster Session
10:20 am - 12:00 pm, November 16

1914 Experimental Investigation of Equivalent Blast Characteristics for Aluminiferous Explosive in Shallow Underwater
Wenbin Gu, Jianqing Liu, Qingli Su, Weiping Zhou, Ballistic Research Laboratory of China, Nanjing University of Science & Technology

1935 Break-up of Copper Shaped – Charge Jets: A Combined Experimental/Numerical/Analytical Approach
Jacques Petit, Centre d'Etudes de Gramat; **V. JeanClaude, C. Fressengeas**, Laboratoire de Physique et Mecanique des Materiaux, Universite de Metz/CNRS

1949 A Theoretical Analysis for Initial Fragment Velocity and Peak Overpressure of a Blast Fragmentation Device
Jin Jianming, Institute of Structural Mechanics, China Academy of Engineering Physics

1963 Scaling the Dynamic Response of Armored Vehicle's Floor Subjected to a Large Buried Charges
Avidov Neuberger, IMOD, MANTAK, Tank Program Management; **S. Peles**, IMI Central Laboratory Division; **D. Rittel**, Technion, Israel Institute of Technology, Faculty of Mechanical Engineering

1984 High-Speed Flash X-Ray Computed Tomo-Cinematography
Philip Helberg, Karsten Michael, Fraunhofer Institute for High-Speed Dynamics, Ernst-Mach-Institut

2002 The Influence of Parameters Other Than Liner Velocity on Shaped Charge Jet Coherence
Frederik Mostert, CSIR Defencetek; **C. J. Terblanche**, Denel Land Systems - Western Cape; **M. F. Maritz**, Department of Applied Mathematics, University of Stellenbosch

2053 Comparison of Vulnerability and Performances of Insensitive Munitions (IM) and Non IM Directed Energy Warheads
Frederic Peugeot, MSIAC, NATO HQ

2059 Trumpet Shaped Liners' Influence on Slug Properties
Eitan Hirsch, Consultor; **Meir Mayseless**, IMI Central Laboratory

2077 A Study on the Structure of Small Caliber EFP
Chen Zhigang, Zhao Taiyong, Hou Xiucheng, Dong Surong, The Research Institute of Explosive Demolition & Defence Technology, North University of China; **You Zheng**, Department of Precision Instruments and Mechanics, Tsinghua University

2078 A Framework for the Analyses and Visualization of X-Ray Computed Tomography Image Data using a Compute Cluster
Jeffrey R. Wheeler, US Army Research Laboratory; **William H. Green**, US Army Research Laboratory, Weapons & Materials Research Division; **Michael Schuresko**, Baskin School of Engineering, University of California; **Michael Patrick Lowery**, Computational Mathematics Department, University of California

2137 An Artillery Shell for Anti-Bunker Applications (155 ABS)
Rémi Boulanger, Giat Industries; **Anders Vangen Jordet, Dagfinn Hoff**, NAMMO Raufoss

2141 Development of a TMRP-6 Surrogate Mine
Yves Baillargeon, A. Sirois and G. McIntosh; DRDC Valcartier

2148 Use of Foamed TNT Mixtures as a Dispersion Charge of Submunitions
Jun Sik Hwang, S.-K. Kwon, C.-K. Kim, S.-W. Kwon, S.-S. Kim, S.-H. Moon, Explosive Trains and Gun Propellant Team, Agency for Defense Development

2152 Wall Breaching Tandem Warhead
Andreas Helte, Torgny Carlsson, Håkan Hansson, Svante Karlsson, Jonas Lundgren, Lars Westerling, Håkan Örnhed, Swedish Defence Research Agency, FOI, Weapons and Protection Division

2156 An Analytical Penetration Model for Jets with Varying Mass Density Profiles
Milton F. Maritz, Stellenbosch University; **Klaus D. Werneyer**, TTP Products; **Frederik J. Mostert**, Defencetek

2168 Peripheral Initiation Technology Development

Arthur S. Daniels, Ernest L. Baker, William J. Poulos, Vladimir M. Gold, B. Fuchs, US Army ARDEC

2175 Shaped-Charge Jet Stability Calculations: The Role of Initial and Boundary Conditions

James S. Stolken, S. Christian Simonson, Mukul Kumar, Lawrence Livermore National Laboratory

3007 Enhanced Focused Fragmentation Warhead Study

Richard Fong, William Ng, Peter Rottinger, Steve Tang, US Army Armaments Research, Development and Engineering Center

4015 Microstructure and Properties of the Explosively Formed Petals in Aluminium Alloys

M. R. Edwards, J. M. Cassar, Centre for Materials Science and Engineering, Cranfield University

Interior Ballistics/Launch Dynamics Poster Session

8:10 am - 9:50 am November 17

1017 In-Bore Mechanics Analysis of the M855 Projectile

Joseph T. South, James F. Newill, US Army Research Laboratory

1020 Dynamic Strain Measured in a 105-mm Composite Gun Barrel - A Fiction or Reality

Jerome T. Tzeng, US Army Research Laboratory

1916 A Vector Way for Calculating Propellant's Combustion Performance

Wei Zhifang, Department of Mechanical and Electronic Engineering, North University of China

1931 Interior Ballistics Code Applied to ETC Concept: Computations and Validations

Gilles Légeret, Dominique Boisson, Giat Industries

2004 The FHIBS Internal Ballistics Code

Clive R. Woodley, Steve Billett, QinetiQ; **Caroline Lowe**, Department of Applied Mathematics and Theoretical Physics, Centre for Mathematical Studies, University of Cambridge; **William Speares**, The Cylinders; **Eleuterio Toro** Laboratory of Applied Mathematics, Faculty of Engineering, University of Trento

2005 Modelling the Ignition of 40mm Gun Charges

Clive R. Woodley, QinetiQ

2020 Thermo-Mechanical Erosion Study of the 120mm Chromium Coated Gun Barrel: Computation and Validation of the Heat Exchange Boundary Condition

Dominique Boisson, Gilles Légeret, Roxan Cayzac, Giat Industries

2031 MOBIDIC-NG: A 1D/2D CFD Code Suitable for Interior Ballistics and Vulnerability Modelling

Baptiste Longuet, Pascal Millet, Eric Taiana, ETBS; **Patrick Della, Pieta Christiane Reynaud**, SNPE Matériaux Energétiques CRB; **Patrice Franco, Alain Carrère**, Institut Franco-Allemand de Recherches de Saint-Louis (ISL); **Gilles Légeret, Dominique Boisson**, Giat Industries; **Alexandre Papy**, ERM ABAL 30

2070 Barrell Life Results of the 5.56 mm XC77A1 Cartridge

Etienne Munger, SNC Technologies, Inc.

2117 Further Investigation of the Effect Known as Electrothermal Pyrolysis

Steve R. Fuller, M.J. Taylor, QinetiQ

2150 Determination of Force and Temperature Impact on Missile's Fuel Charge in Process of Ignition

Dmitriy Orlov, GDT Software Group

2161 Unsteady Intermediate Ballistics: 2D and 3D CFD Modelling, Application to Sabot Separation

Roxan Cayzac, Eric Carette, Giat Industries, Division Munitions; **Thierry Alziary de Roquefort**, Université de Poitiers, Laboratoire d'Études Aérodynamiques; **Philippe Bidorini, Emmanuel Bret, Pascal Delusier, Serge Secco**, DGA/ETBS, Direction de l'Expertise Technique

2166 Large Caliber Firing with Electro Thermal-Chemical Ignition (ETI)
Jonathan D. Shin, John J. O'Reilly, David T. Keyser, US Army Research, Development and Engineering Center - TACOM; **Jahn Dyvik**, United Defense L.P.

3006 Rail Gun Test Projectile for Improved Developmental Testing of Precision Munition Electronics
T. Myers, D. Carlucci, J.A. Cordes, US Army ARDEC, Analysis and Evaluation Division, Fuze and Precision Munitions Technology Directorate

4010 Improved Mortar Barrel Thermal Model
M. Pocock, C. Guyott, Frazer-Nash Consultancy Ltd; **P. Locking**, BAE Systems, Land Systems

Vulnerability/Lethality/Wound Ballistics Poster Session
10:20 am - 12:00 pm November 17

1855 On Incorporating XCT into Predictive Ballistic Impact Damage Modeling
Joseph M. Wells, JMW Associates

1878 New Soft-Target Failure Criteria for System-Analytical Considerations
Markus J. Estermann, RUAG Defence, Warhead Division; **Beat P. Kneubuhl**, Aramasuisse

1941 Protecting Vehicles from Landmine Blasts
Sheri L. Hlady, Denis Bergeron, Defence R&D Canada – Suffield; **Rene Gonzalez**, US Army, PM Light Tactical Vehicles

1957 Office of Naval Research Limb Protection Program
Graham K. Hubler, NRL

1980 Survivability and Lethality Assessment Software Based on Virtual Mode Technology
Lu Yonggang, Qian Lixin, Yang Yubin, Liu Tong, Institute of Structural Mechanics, CAEP

1981 “TBM-Xpert” - A New Endgame Code: Features and Validation
Werner Arnold, EADS-TDW Gesellschaft für verteidigungstechnische; **E. Rottenkolber**, NUMERICS GmbH

1989 The Use of Ballistic Knowledge in Ammunition Safety Cases
Martin van de Voorde, TNO Defence, Safety and Security

2011 A Note on the Roecker-Ricchiazzi Model of Penetrator Trajectory Instability
William J. Flis, DE Technologies, Inc.

2022 Numerical Calculation and Simulation of Missile Jet-Airplane Interaction
Feipeng Zeng, Faculty of Artillery Command, Nanjing Artillery Academy

2111 Need for Enhanced Protection Against Blast Threats for Soldiers Exposed to Roadside Improvised Explosive Devices (IEDs)
François-Xavier Jetté, Jean-Philippe Dionne, Aris Makris, Med-Eng Systems, Inc.; **Karl Masters**, PEO Soldier; **Christine Perritt**, PM Soldier Equipment

2119 WitnessMan: The Software Tool to Design, Analyse and Assess a Witness Pack with Respect to Military and Medical Effects on an (Un)protected (Dis)mounted Soldier.
Theo L.A. Verhagen, R. Kemper, H. Huisjes, S.G. Knijnenburg, A. Pronk, M.H. van Klink, TNO Defence, Security and Safety

2154 Injury Risks Resulting from Deminer Position
François-Xavier Jetté, Jean-Philippe Dionne, Ismail El Maach, Aris Makris, Matt Ceh, Med-Eng Systems, Inc.; **Denis Bergeron**, Defence R&D Canada Suffield

2163 RPG Mitigation for Military Vehicles
Karl Pfister, Dipl. Ing (FH) Armatec Survivability Corporation

2164 Protection Against Closely-Spaced Impacts by Small Arms Bullets

Michael J. Iremonger, Cranfield University, Royal Military College of Science; **Abdullah Alsalmi**

3013 Vulnerability Evaluations of 30mm Airburst Ammunition

Quoc Bao Diep, Eimund Smedstad, Nammo Raufoss AS; **Nick Rogers**, System Design Evaluation (SDE)

3018 Challenges and a Solution in Determining Land Mine or IED Neutralization Effectiveness

Robert Colbert, Mark Majerus, William Clark, DE Technologies, Inc.

4011 Numerical and Experimental Analysis of the Detonation of Sand-Buried Mines

N. Heider, A. Klomfass, Fraunhofer-Institut für Kurzzeitdynamik, Ernst-Mach-Institut

The symposium registration fees are:

	Regular	Late/Onsite after 10/28/05
	\$950 (US)	\$1045 (US)
IBC Committee Appreciation Dinner	\$75 (US)	
Guest at Both Receptions	\$75 (US)	
Guest at One Reception	\$50 (US)	

The symposium registration fee includes attendance at all sessions, bound symposium proceedings with CD, continental breakfasts, coffee breaks, lunches, receptions, and administrative costs. The registration fee will also include a compact disc (CD) which contains a cumulative database of titles, authors and abstracts of all of the 22 Ballistics Symposia.

To register online for this conference visit: <http://register.ndia.org/interview/register.ndia?~Brochure~6210>. You can also visit the NDIA website at www.ndia.org and select "Schedule of Events". Then select 2005 November and scroll down to the 22nd International Symposium on Ballistics. Once there, select the blue "Register" link in the lower left hand corner of your screen. Review your information and then select "submit" one time only and then select "confirm". On-line registration will close at 5:00 pm EST on October 28, 2005. You must register on-site after this date.

-or-

You may fax the completed registration form contained in this brochure to (703) 522-1885.

-or-

You may mail the completed registration form contained in this brochure to: Event # 6210, National Defense Industrial Association, 2111 Wilson Boulevard, Suite 400, Arlington, VA 22201-3061.

Payment must be made at the time of registration. Registrations will not be taken over the phone.

Cancellations and Refund Policy

Registrants who cannot attend the 22nd International Symposium on Ballistics must provide written notification via email to bbommelje@ndia.org or fax to (703) 522-1885 on or before September 16, 2005 to avoid a cancellation fee.

Cancellations received between September 16, 2005 and October 28, 2005 will receive a refund minus a \$75 cancellation fee. No refunds will be given to cancellations received after October 28, 2005 however, **SUBSTITUTIONS ARE WELCOME IN LIEU OF CANCELLATIONS**.

You must have a government picture identification (drivers license, passport, military ID, etc.) to receive a symposium badge. Badges must be worn at all times during the symposium.

Special Needs

NDIA supports the Americans with Disabilities Act of 1990. Attendees with special needs should call (703) 522-1820 prior to October 3, 2005.

Hotel Accommodations

A limited block of rooms have been reserved at the Fairmont Waterfront Hotel. The industry room rate is \$219 Canadian (approximately \$180 US). The government symposium room rate is approximately \$114 Canadian (\$94 US). Please call (604) 691-1991 to make reservations.

In order to ensure the discounted NDIA rate, please make reservations early and ask for the NDIA room block. Rooms will not be held after Tuesday, October 11, 2005 and may sell out before then. Rates are also subject to increase after this date.

**The government room rate applies only to active duty military and civilian government employees. It is not available to government contractors, retired military or retired civilian government employees. ID cards and/or travel orders will be required at check-in to verify rate eligibility.*

GENERAL INFORMATION

Symposium Attire

Appropriate dress for this symposium is business for civilians (coat and tie) and class A uniform for military.

Inquiries

For more information regarding the symposium contact Britt Bommelje, Meeting Planner at (703) 247-2587 or bbommelje@ndia.org.

Promotional Partnerships

Increase your company or organization exposure at this premier event by becoming a Promotional Partner. A Promotional Partnership (\$5,000) will add your company name to the back cover of the on-site brochure as well as main platform recognition throughout the conference, signage at all events including the opening reception and a 350-word organization description in the conference agenda. For more information, please contact Sam Campagna at 703-247-2544 or scampagna@ndia.org.

www.defensejobs.com

The Defense Industry's leading employment website; find a job, post a job listing, post a resume, and search resumes. For more information please contact info@defensejobs.com or (703) 247-9461. Please visit www.defensejobs.com

IBC Committee Appreciation Dinner

The IBC Committee Appreciation Dinner will be held on Friday, November 18, 2005 in Vancouver. This dinner is open to IBC Committee members and their guests only. If you and your guest would like to attend, please make a note of it on the registration form. There is a \$75 charge per person to attend.

"The Department of Defense finds this event meets the minimum regulatory standards for attendance by DoD employees. This finding does not constitute a blanket approval or endorsement for attendance. Individual DoD component commands or organizations are responsible for approving attendance of its DoD employees based on mission requirements and DoD regulations."

Organization Information

Organization Name (as it should appear on booth sign -- limited to 40 characters and spaces)

Point of Contact (for fees and exhibitor service kit) Title

Street Address	City	State	Zip Code
----------------	------	-------	----------

Telephone	Fax	E-mail
-----------	-----	--------

Reserve your booth and register your exhibit staff at <http://exhibits.ndia.org>

Exhibit Space Information:

Corporate Members and bona-fide government organizations:

Please reserve _____ 10' x 10' booth(s) at \$2,650 each

Non-Corporate Members:

Please reserve _____ 10' x 10' booth(s) at \$3,250 each

Remember:

Add an additional \$250 for corner booth space

Add an additional \$500 for island space

PAYMENT POLICY:

Total booth cost is due with this application to guarantee space. Booths will be assigned on a first-paid, first-served basis. Purchase orders are not acceptable as payment unless paid in advance of show dates. This contract is your invoice. All payments are due by September 30, 2005.

CANCELLATION POLICY:

Fees will be refunded, less a service charge of 50% of total booth fee, if written notice of cancellation is received by September 30, 2005. No refunds will be given for cancellations received after September 30, 2005.

Booth Choices: (List booth number(s) in order of preference)

1st _____ 2nd _____ 3rd _____

Payment Computation:

\$ _____ Booth Fee x _____ sq. ft + \$ _____ Corner Fee = \$ _____ Total

Check (payable to NDIA, Event #6210-3140)

VISA

Diners Club

MasterCard

American Express

Credit Card Number

Expiration Date

Authorized Signature

The undersigned agrees to abide by the rules and regulations set forth by NDIA on show web site and the Exhibitor Service Kit.

AUTHORIZED SIGNATURE

DATE

Contact: Tina Lynn Mercardo - NDIA, 2111 Wilson Blvd., Suite 400, Arlington, VA 22201

TEL: (703)247-2582 ~ FAX: (703)522-1885 ~ E-MAIL:tmercardo@ndia.org

22nd International Symposium on Ballistics

Vancouver Convention Center

Vancouver, BC, CANADA

November 14-18, 2005

The objective of the 22nd International Symposium on Ballistics is to focus on potential technical advances and breakthroughs in the 21st century in the general area of: interior ballistics, launch dynamics, exterior ballistics, projectile and warhead design, vulnerability, wound ballistics, and armored and personal protection. The symposium is an opportunity for ballistic scientists, engineers and others to report, share and discuss current research and advances in ballistics and visions of the future.

NDIA invites you to take advantage of this tremendous opportunity to demonstrate your organization's products and services to this specialized community by exhibiting at this year's event.

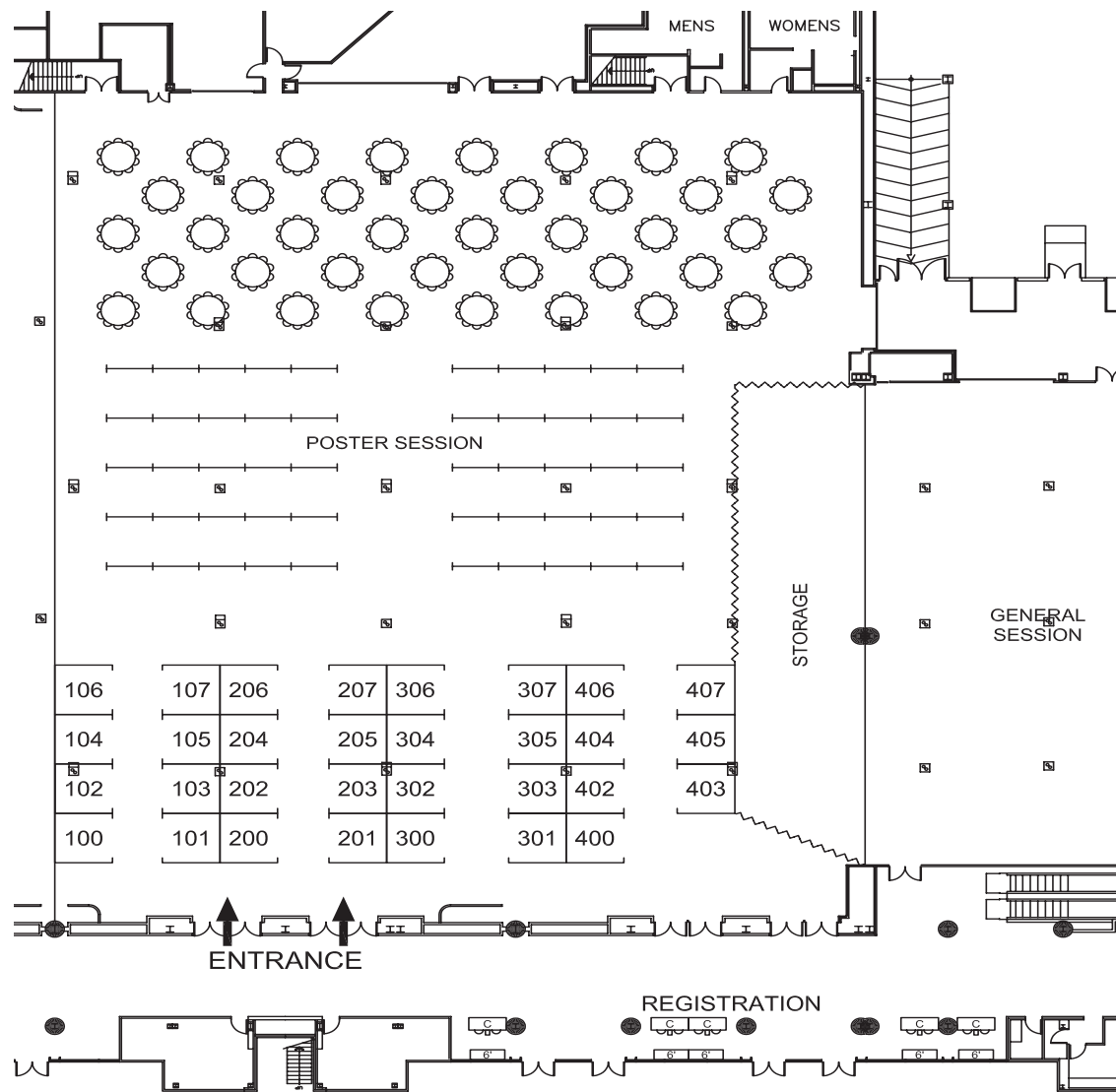


Exhibit Rate:

- \$2,650 per 10' x 10' booth space for NDIA corporate members/Government organizations
- \$3,250 for non-members and Industry
- Add \$250 for corner booths
- Add \$500 for island booths

Tentative Exhibit Schedule*:

- Monday, November 14: 4:00pm - 7:30pm
- Tuesday, November 15: 7:00am - 6:00pm
- Wednesday, November 16: 7:00am - 5:00 pm
- Thursday, November 17: 8:00am - 11:00am
- Friday, November 18: 8:00am - 11:00am

**Show days only. Does not include move-in and move-out. For complete exhibit schedule go to <http://exhibits.ndia.org>.*

Reserve your booth on-line and in real time. Go to <http://exhibits.ndia.org>

Questions? Contact Tina Lynn Mercardo at TMercardo@ndia.org or 703-247-2582

**22nd International Symposium on Ballistics
Vancouver Convention Center
November 14-18, 2005 • Event #6210**

National Defense Industrial Association
2111 Wilson Boulevard, Suite 400
Arlington, VA 22201-3061
(703) 522-1820 • (703) 522-1885 fax
www.ndia.org



3 Ways to sign up:

1. Online with a credit card at www.ndia.org
2. By fax with a credit card — Fax: 703-522-1885
3. By mail with a check or credit card

Address change needed

By completing the following, you help us understand who is attending our meetings.

NDIA Master ID/Membership # _____ Social Security # _____
(if known—hint: on mailing label above your name) (last 4 digits – optional)

Prefix _____
(e.g. RADM, COL, Mr., Ms., Dr., etc.)

Name First _____ MI _____ Last _____

Military Affiliation _____ Nickname _____
(e.g. USMC, USA (Ret.) etc.) (for Meeting Badges)

Title _____

Organization _____

Street Address _____

Address (Suite, PO Box, Mail Stop, Building, etc.) _____

City _____ State _____ Zip _____ Country _____

Phone _____ ext. _____ Fax _____

E-Mail _____

Signature* _____ Date _____

Preferred way to receive information

Conference information address above Alternate (print address below) E-mail

Subscriptions address above Alternate (print address below)

Alternate Street Address _____

Alternate Address (Suite, PO Box, Mail Stop, Building, etc.) _____

City _____ State _____ Zip _____ Country _____

* By your signature above you consent to receive communications sent by or on behalf of NDIA, its Chapters, Divisions and affiliates (NTSA, AFEI, PSA, NCWG, WID) via regular mail, e-mail, telephone, or fax. NDIA, its Chapters, Divisions and affiliates do not sell data to vendors or other companies.

Primary Occupational

Classification. Check ONE.

- A. Defense Business/Industry
- B. R&D/Laboratories
- C. Army
- D. Navy
- E. Air Force
- F. Marine Corps
- G. Coast Guard
- H. DOD/MOD Civilian
- I. Gov't Civilian (Non-DOD/MOD)
- J. Trade/Professional Assn.
- K. Educator/Academia
- L. Professional Services
- M. Non-Defense Business
- N. Other _____

Current Job/Title/Position.

Check ONE.

- A. Senior Executive
- B. Executive
- C. Manager
- D. Engineer/Scientist
- E. Professor/Instructor/Librarian
- F. Ambassador/Attaché
- G. Legislator/Legislative Aide
- H. General/Admiral
- I. Colonel/Navy Captain
- J. Lieutenant Colonel/Commander/Major/Lieutenant Commander
- K. Captain/Lieutenant/Ensign
- L. Enlisted Military
- O. Other _____

Year of birth _____
(Optional)

Registration Fees

	Regular	Late after 10/28/05
All Attendees	\$950	\$1045
IBC Committee Appreciation Dinner	\$75	
Number of people attending the dinner	_____	
Guest at Both Receptions	\$75	_____
Guest at One Reception	\$50	_____

No refunds for cancellations received after 10/28/05. **Substitutions are welcome in lieu of cancellation.**

Payment Options

Check (payable to NDIA)

Cash

Government PO/Training Form # _____

VISA

MasterCard

American Express

Diners Club

If paying by credit card, you may return by fax to (703) 522-1885.

Credit Card Number

--	--	--	--	--	--	--	--	--	--	--	--	--	--	--	--	--	--	--	--

Exp. date

 /

Signature _____

Date _____

Questions? Contact Meeting Planner, Britt Bommelje (703) 247-2587 email: bbommelje@ndia.org
Mail to: NDIA, Event #6210 2111 Wilson Boulevard, Suite 400 Arlington, VA 22201
Fax to: (703) 522-1885



2111 Wilson Blvd.
Suite 400
Arlington, VA 22201

Performance Evaluation of Multi-Threat Body Armour Systems

Presented by:
B. Anctil

Co-authors:
M. Keown
Biokinetics and Associates Ltd.

G. Pageau, M. Bolduc, D. Bourget
Defence R&D Canada



22nd International Symposium on Ballistics
Vancouver, Canada, November 14-18, 2005



The Problem

- Is it possible to find light-weight and flexible body armours capable of defeating multiple threats?



Why should we care?

- Common threats to military and law enforcement personnel:
 - Small arm projectiles*
 - Fragmentation from explosive devices (e.g. IEDs)*
 - Knife, spike, flechette*
- Can they be protected against all these threats with a single body armour system?

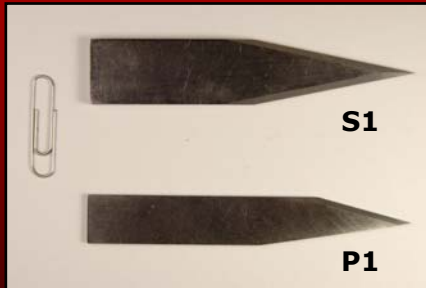


Our Strategy

- ▶ Established multiple performance requirements
- ▶ Select appropriate test methods
- ▶ Contact mfgs to propose solutions and provide test samples
- ▶ Evaluate armour materials

Performance Requirements & Test Methods

Threat	Stab S1, P1
Test Standard	NIJ 0115.00
Performance Requirement (necessary)	Level 1 24J / 36J
Performance Requirement (desired)	Level 2 33J / 50J



Performance Requirements & Test Methods

Threat	Stab S1, P1	Spike
Test Standard	NIJ 0115.00	NIJ 0115.00
Performance Requirement (necessary)	Level 1 24J / 36J	Level 1 24J / 36J
Performance Requirement (desired)	Level 2 33J / 50J	Level 2 33J / 50J



Performance Requirements & Test Methods

Threat	Stab S1, P1	Spike	Flechette Artillery
Test Standard	NIJ 0115.00	NIJ 0115.00	STANAG 2920
Performance Requirement (necessary)	Level 1 24J / 36J	Level 1 24J / 36J	$V_{50} \geq$ 250 m/s or equivalent
Performance Requirement (desired)	Level 2 33J / 50J	Level 2 33J / 50J	$V_{50} \geq$ 400 m/s or equivalent



- ▶ **Ballistic method**
 - *flight stability problem*
- ▶ **Drop mass method equivalent?**
 - *based on NIJ 0115.00*

Performance Requirements & Test Methods

Threat	Stab S1, P1	Spike	Flechette Artillery	17gr FSP
Test Standard	NIJ 0115.00	NIJ 0115.00	STANAG 2920	STANAG 2920
Performance Requirement (necessary)	Level 1 24J / 36J	Level 1 24J / 36J	$V_{50} \geq$ 250 m/s or equivalent	$V_{50} \geq$ 600 m/s
Performance Requirement (desired)	Level 2 33J / 50J	Level 2 33J / 50J	$V_{50} \geq$ 400 m/s or equivalent	$V_{50} \geq$ 750 m/s



Performance Requirements & Test Methods

Threat	Stab S1, P1	Spike	Flechette Artillery	17gr FSP	1gr Sphere
Test Standard	NIJ 0115.00	NIJ 0115.00	STANAG 2920	STANAG 2920	STANAG 2920
Performance Requirement (necessary)	Level 1 24J / 36J	Level 1 24J / 36J	$V_{50} \geq$ 250 m/s or equivalent	$V_{50} \geq$ 600 m/s	$V_{50} \geq$ 850 m/s
Performance Requirement (desired)	Level 2 33J / 50J	Level 2 33J / 50J	$V_{50} \geq$ 400 m/s or equivalent	$V_{50} \geq$ 750 m/s	$V_{50} \geq$ 1000 m/s



Performance Requirements & Test Methods

Threat	Stab S1, P1	Spike	Flechette Artillery	17gr FSP	1gr Sphere	9x19 mm FMJ
Test Standard	NIJ 0115.00	NIJ 0115.00	STANAG 2920	STANAG 2920	STANAG 2920	NIJ 0101.04
Performance Requirement (necessary)	Level 1 24J / 36J	Level 1 24J / 36J	$V_{50} \geq$ 250 m/s or equivalent	$V_{50} \geq$ 600 m/s	$V_{50} \geq$ 850 m/s	$V_{proof} \geq$ 367±9 m/s (Level 2)
Performance Requirement (desired)	Level 2 33J / 50J	Level 2 33J / 50J	$V_{50} \geq$ 400 m/s or equivalent	$V_{50} \geq$ 750 m/s	$V_{50} \geq$ 1000 m/s	$V_{proof} \geq$ 436±9 m/s (Level 3A)



Performance Requirements & Test Methods

Threat	Stab S1, P1	Spike	Flechette Artillery	17gr FSP	1gr Sphere	9x19 mm FMJ	9x19 mm Bofors HP
Test Standard	NIJ 0115.00	NIJ 0115.00	STANAG 2920	STANAG 2920	STANAG 2920	NIJ 0101.04	NIJ 0101.04
Performance Requirement (necessary)	Level 1 24J / 36J	Level 1 24J / 36J	$V_{50} \geq$ 250 m/s or equivalent	$V_{50} \geq$ 600 m/s	$V_{50} \geq$ 850 m/s	$V_{proof} \geq$ 367±9 m/s (Level 2)	$V_{50} \geq$ 367 m/s
Performance Requirement (desired)	Level 2 33J / 50J	Level 2 33J / 50J	$V_{50} \geq$ 400 m/s or equivalent	$V_{50} \geq$ 750 m/s	$V_{50} \geq$ 1000 m/s	$V_{proof} \geq$ 436±9 m/s (Level 3A)	$V_{50} \geq$ 420 m/s



Test Samples

Armour Sample	Description	Protection	Areal Density (kg/m ²)
1	Steel sheets and woven fabric, 15 layers total	PSDB Level KR1	6.0
2	Coated woven aramid, 30 layers	NIJ Stab Level 2	10.2
3	Coated woven aramid, 30 layers	NIJ Stab Level 2	9.9
4	Coated woven polyethylene, 27 layers	NIJ Stab Level 2	9.9
5	2 types of woven aramid, 32 layers total	Custom	9.9
6	2 types of woven aramid, 31 layers total	Custom	8.4
7*	Multi-layers of dense woven aramid, 18 layers	NIJ Spike Level 2	2.2
8	Woven aramid and laminated polyethylene, 26 layers total	NIJ Ballistic Class II NIJ Stab Level 2	6.3
9	Woven PBO and aramid, laminated polyethylene, 50 layers total	NIJ Ballistic Class IIIA NIJ Spike Level 2	6.6
10**	Woven PBO, 20 layers	Custom	2.7
11**	Coated woven aramid, woven aramid, laminated polyethylene, 41 layers total	Custom	11.9
12**	Coated woven aramid, woven PBO, laminated polyethylene, 51 layers total	Custom	12.3
13**	Woven PBO, unidirectional aramid, 38 layers total	Custom	6.3

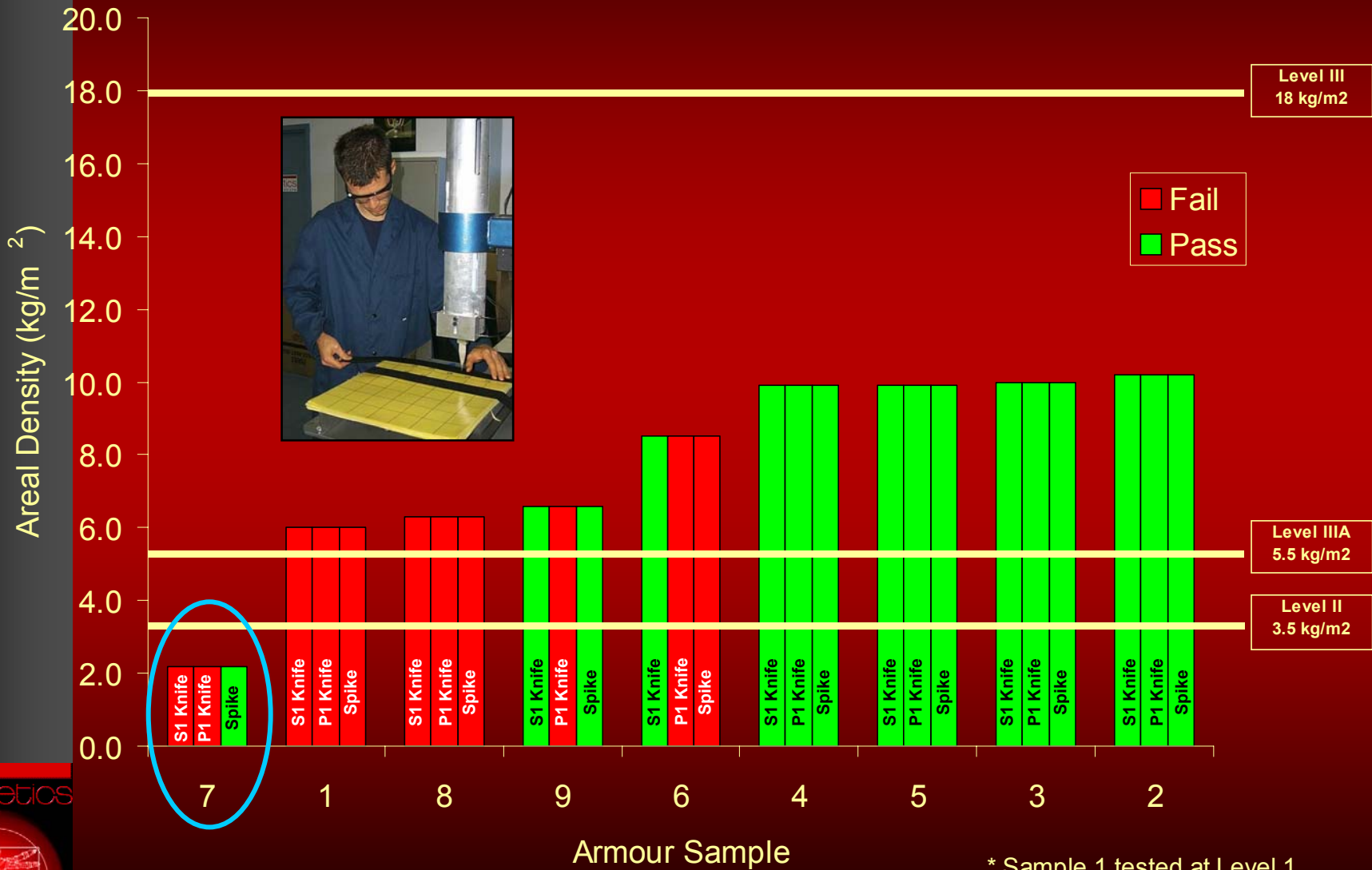
Test Samples

Armour Sample	Description	Protection	Areal Density (kg/m ²)
1	Steel sheets and woven fabric, 15 layers total	PSDB Level KR1	6.0
2	Coated woven aramid, 30 layers	NIJ Stab Level 2	10.2
3	Coated woven aramid, 30 layers	NIJ Stab Level 2	9.9
4	Coated woven polyethylene, 27 layers	NIJ Stab Level 2	9.9
5	2 types of woven aramid, 32 layers total	Custom	9.9
6	2 types of woven aramid, 31 layers total	Custom	8.4
7*	Multi-layers of dense woven aramid, 18 layers	NIJ Spike Level 2	2.2
8	Woven aramid and laminated polyethylene, 26 layers total	NIJ Ballistic Class II NIJ Stab Level 2	6.3
9	Woven PBO and aramid, laminated polyethylene, 50 layers total	NIJ Ballistic Class IIIA NIJ Spike Level 2	6.6
10**	Woven PBO, 20 layers	Custom	2.7
11**	Coated woven aramid, woven aramid, laminated polyethylene, 41 layers total	Custom	11.9
12**	Coated woven aramid, woven PBO, laminated polyethylene, 51 layers total	Custom	12.3
13**	Woven PBO, unidirectional aramid, 38 layers total	Custom	6.3

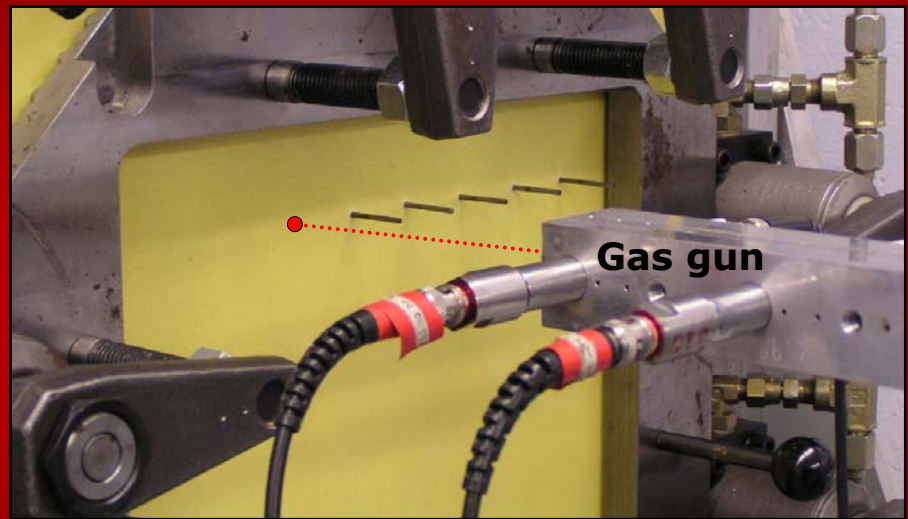
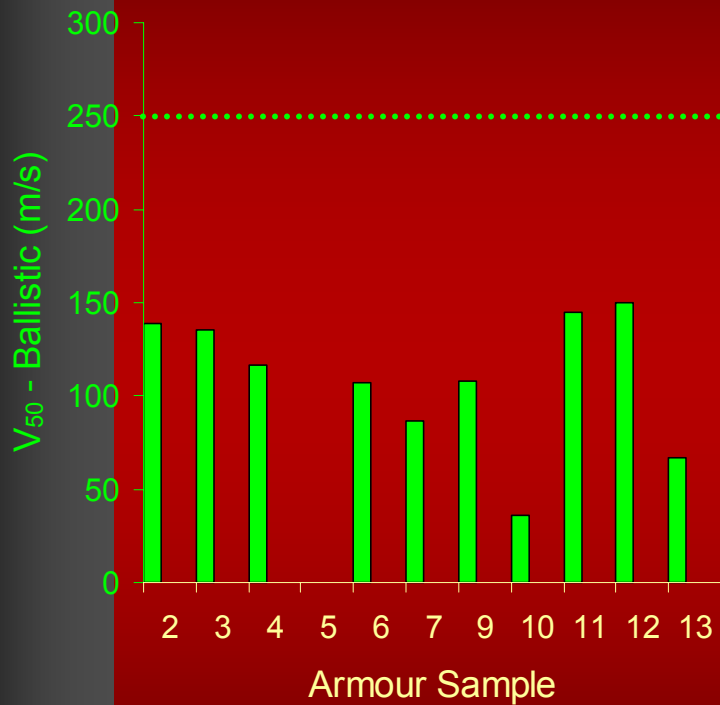
Test Samples

Armour Sample	Description	Protection	Areal Density (kg/m ²)
1	Steel sheets and woven fabric, 15 layers total	PSDB Level KR1	6.0
2	Coated woven aramid, 30 layers	NIJ Stab Level 2	10.2
3	Coated woven aramid, 30 layers	NIJ Stab Level 2	9.9
4	Coated woven polyethylene, 27 layers	NIJ Stab Level 2	9.9
5	2 types of woven aramid, 32 layers total	Custom	9.9
6	2 types of woven aramid, 31 layers total	Custom	8.4
7*	Multi-layers of dense woven aramid, 18 layers	NIJ Spike Level 2	2.2
8	Woven aramid and laminated polyethylene, 26 layers total	NIJ Ballistic Class II NIJ Stab Level 2	6.3
9	Woven PBO and aramid, laminated polyethylene, 50 layers total	NIJ Ballistic Class IIIA NIJ Spike Level 2	6.6
10**	Woven PBO, 20 layers	Custom	2.7
11**	Coated woven aramid, woven aramid, laminated polyethylene, 41 layers total	Custom	11.9
12**	Coated woven aramid, woven PBO, laminated polyethylene, 51 layers total	Custom	12.3
13**	Woven PBO, unidirectional aramid, 38 layers total	Custom	6.3

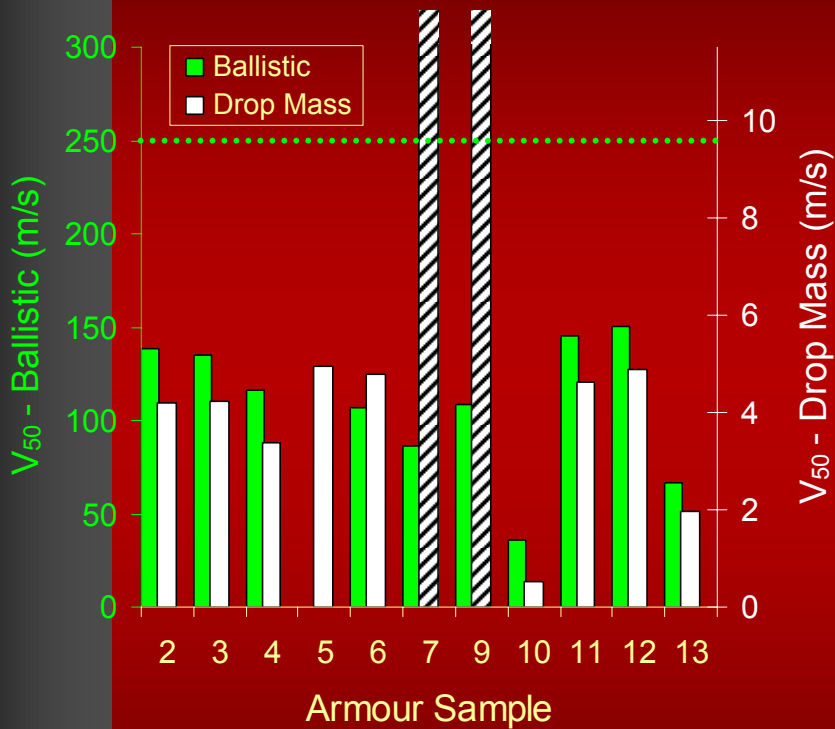
Stab Resistance (Level 2)



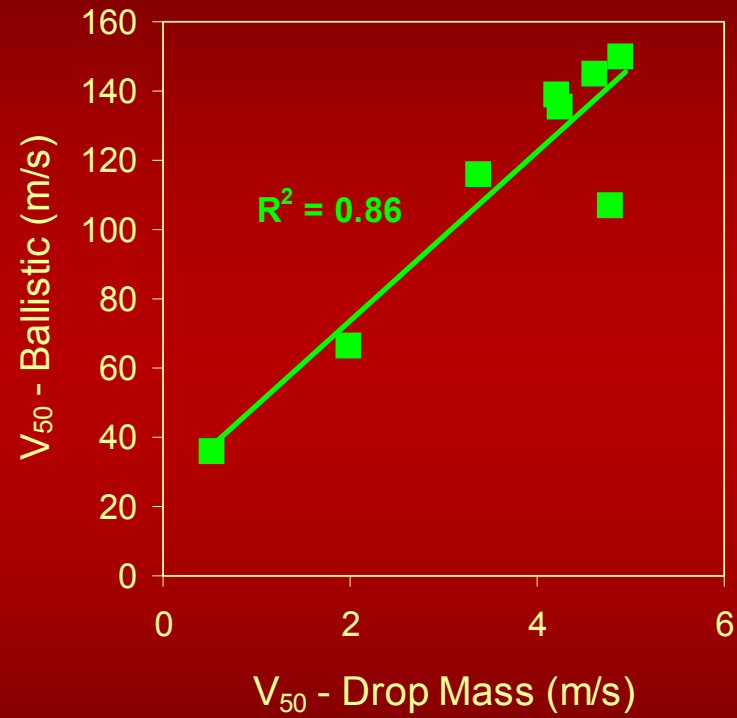
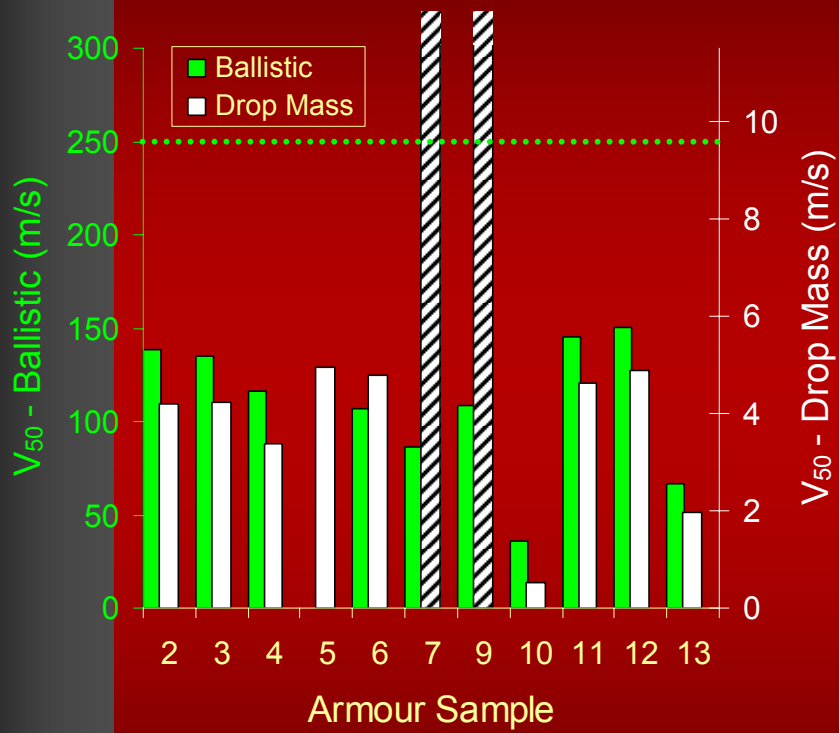
Flechette Resistance



Flechette Resistance

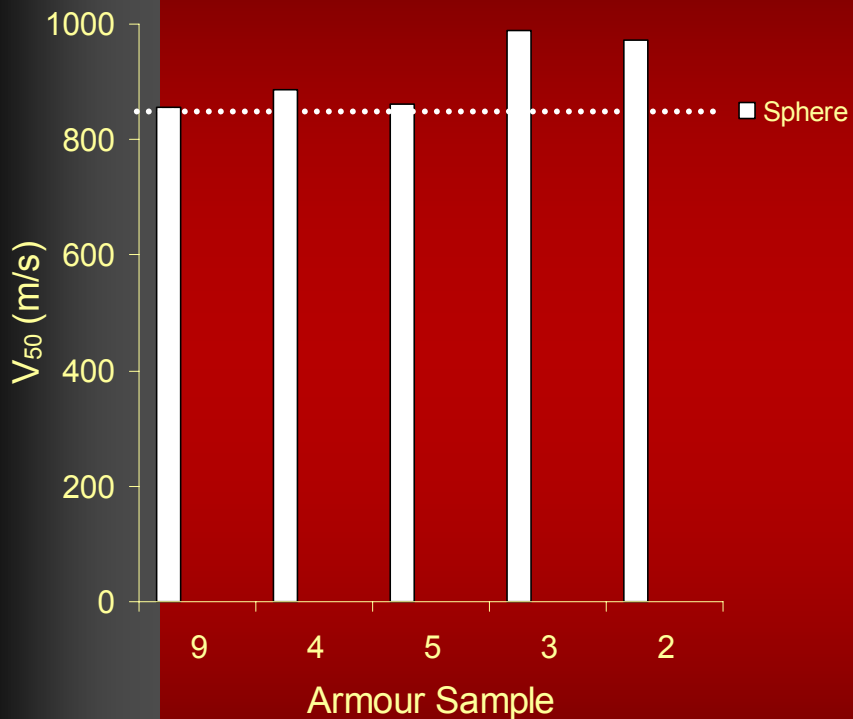


Flechette Resistance



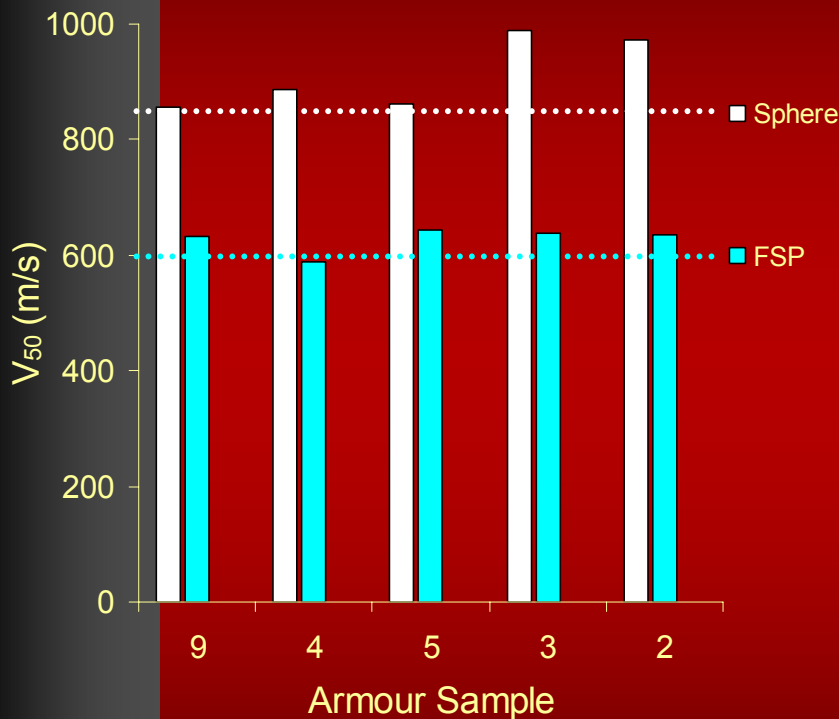
Fragmentation / Bullet Resistance

Ballistic Limit



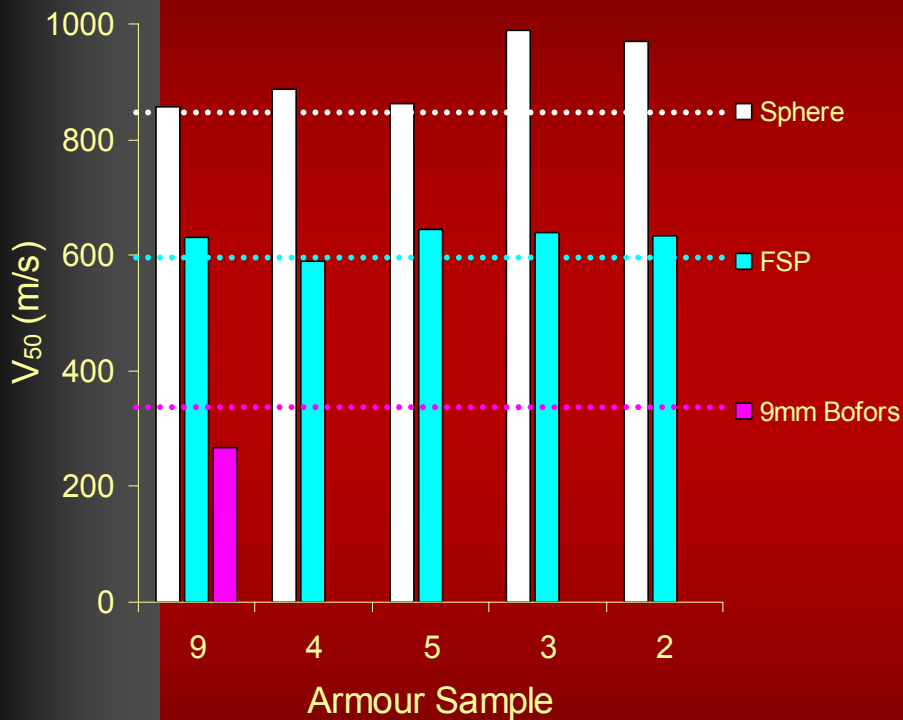
Fragmentation / Bullet Resistance

Ballistic Limit



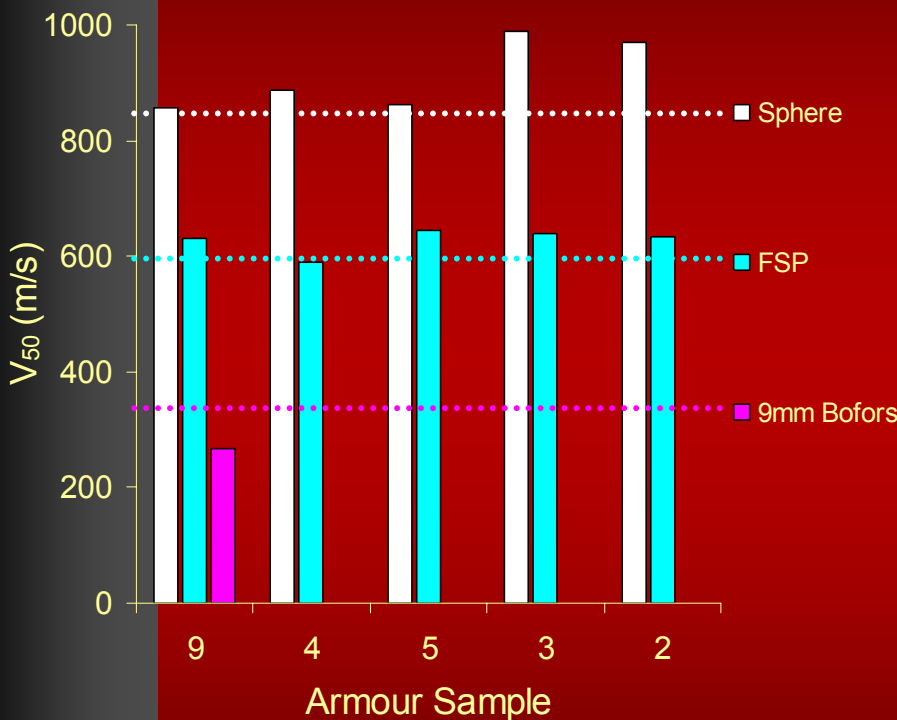
Fragmentation / Bullet Resistance

Ballistic Limit

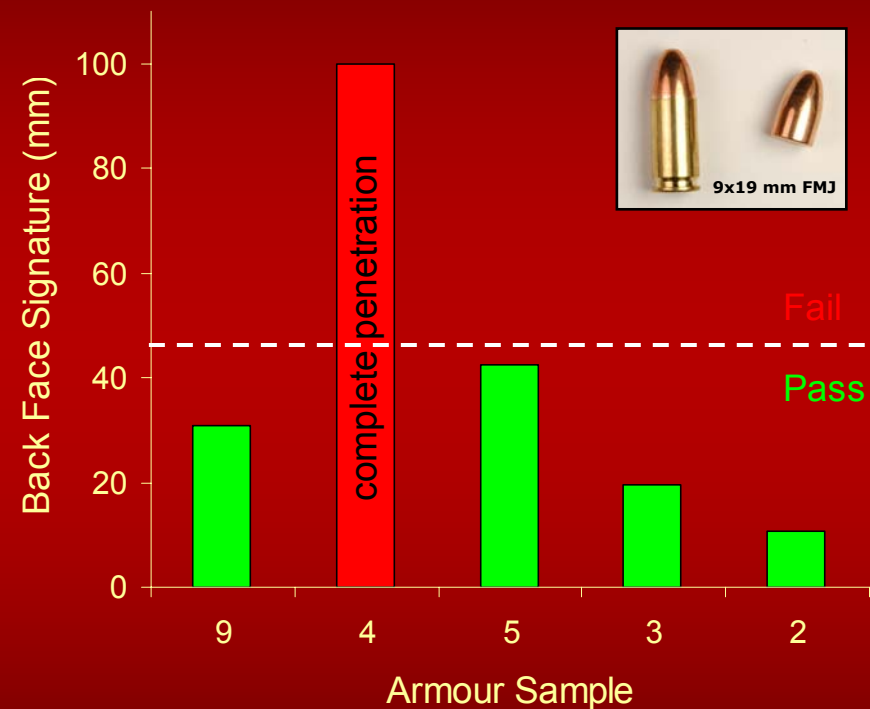


Fragmentation / Bullet Resistance

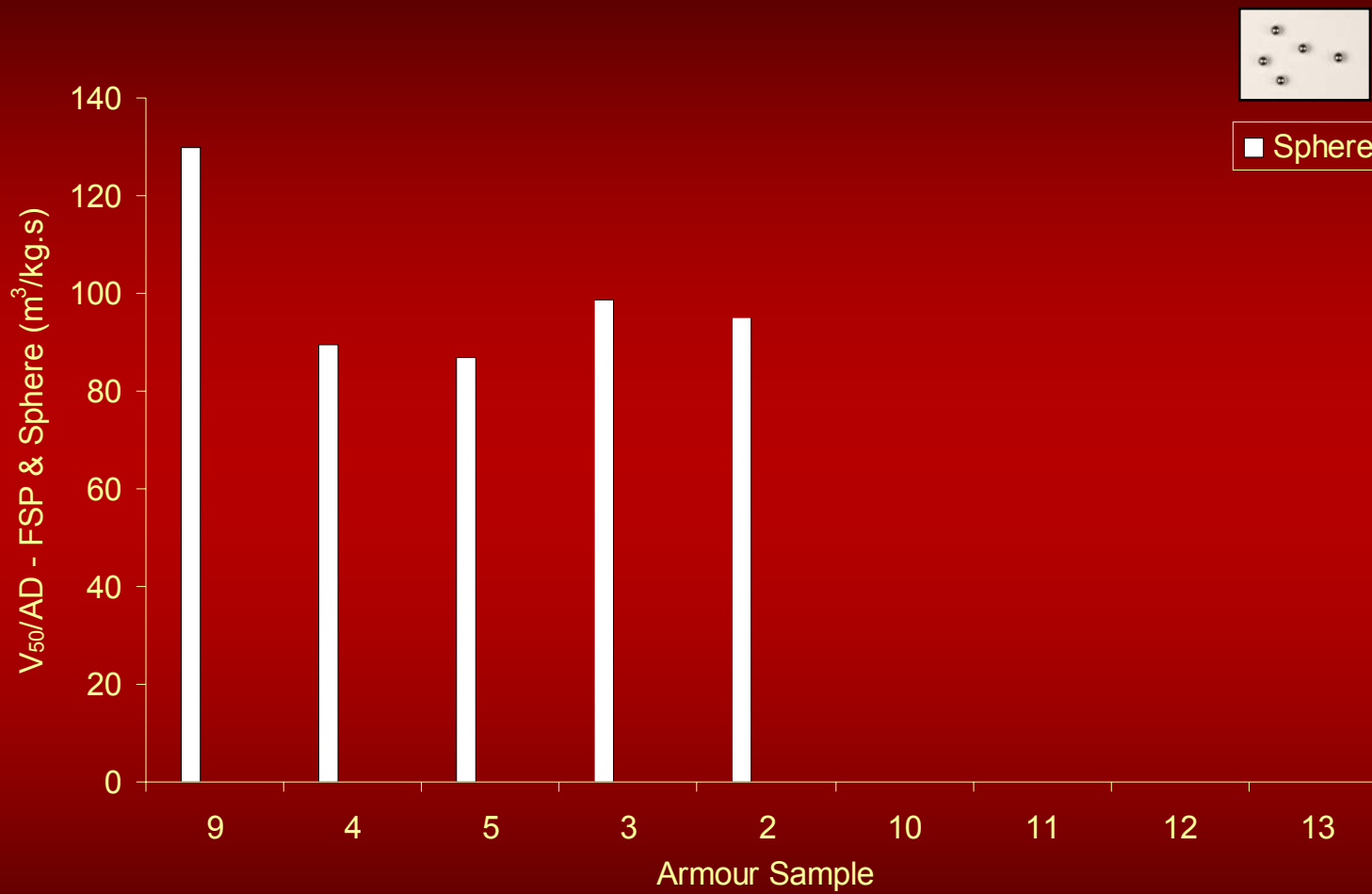
Ballistic Limit



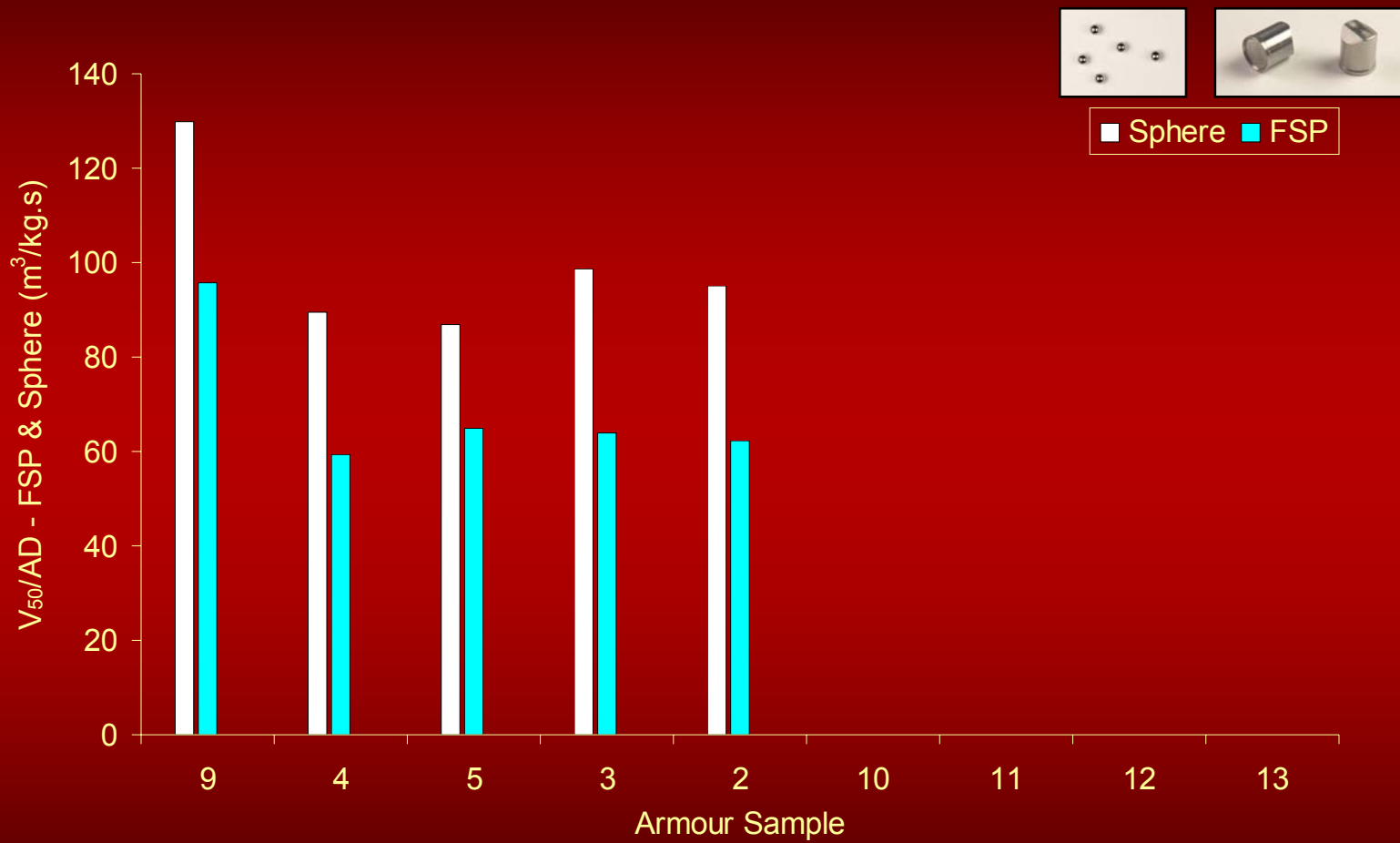
Back Face Signature



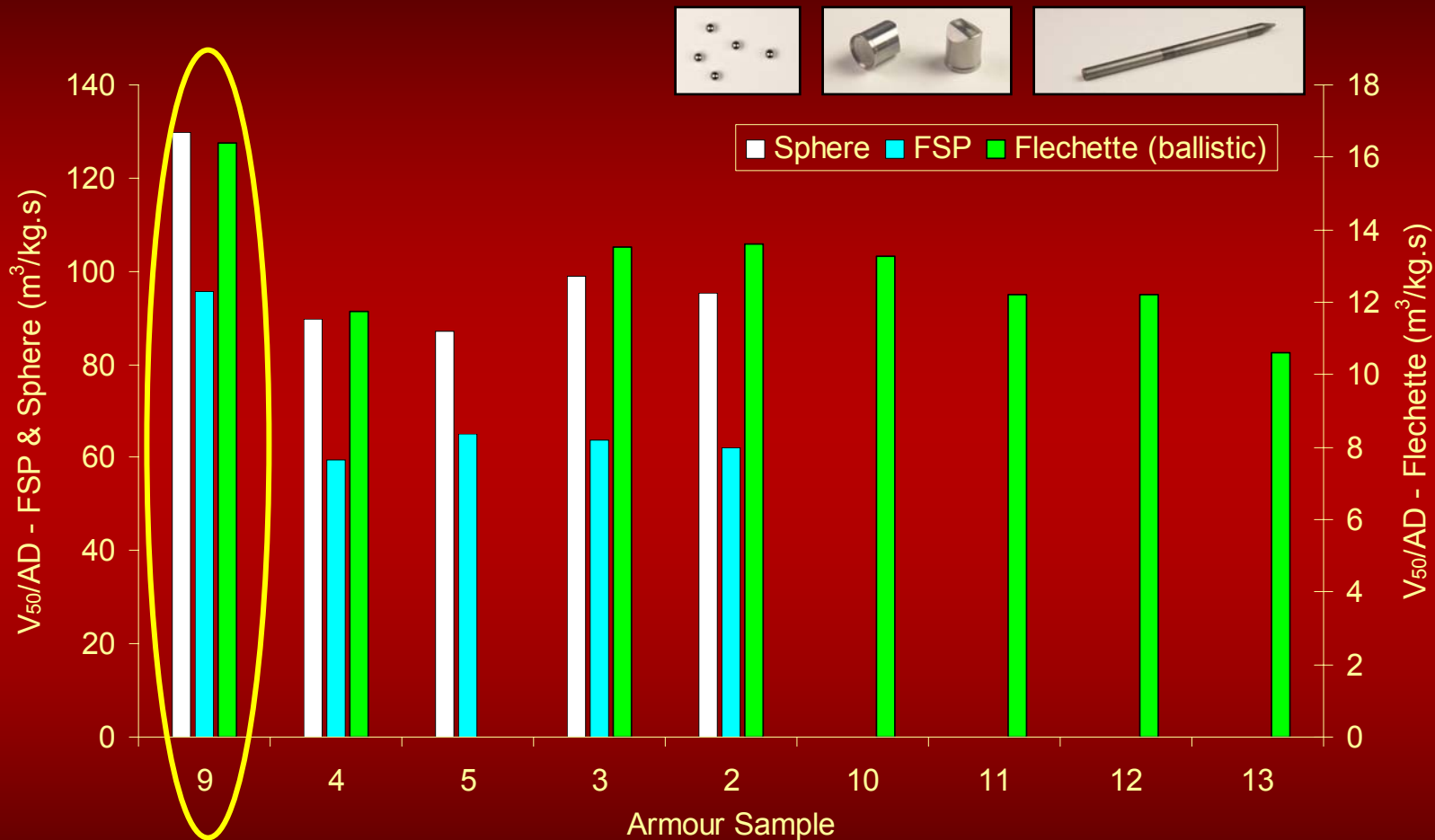
Performance Comparison – Ballistic Limit



Performance Comparison – Ballistic Limit

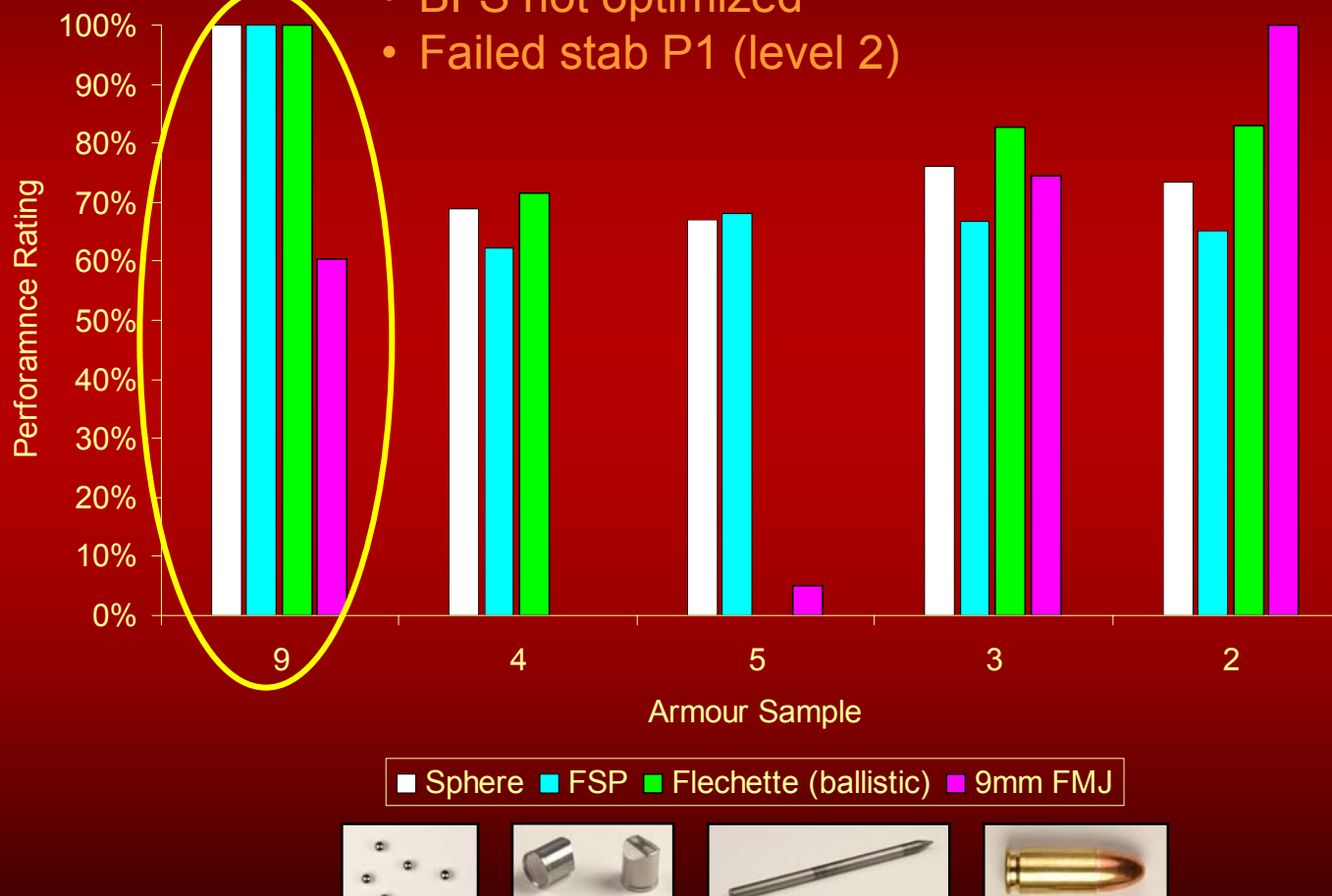


Performance Comparison – Ballistic Limit



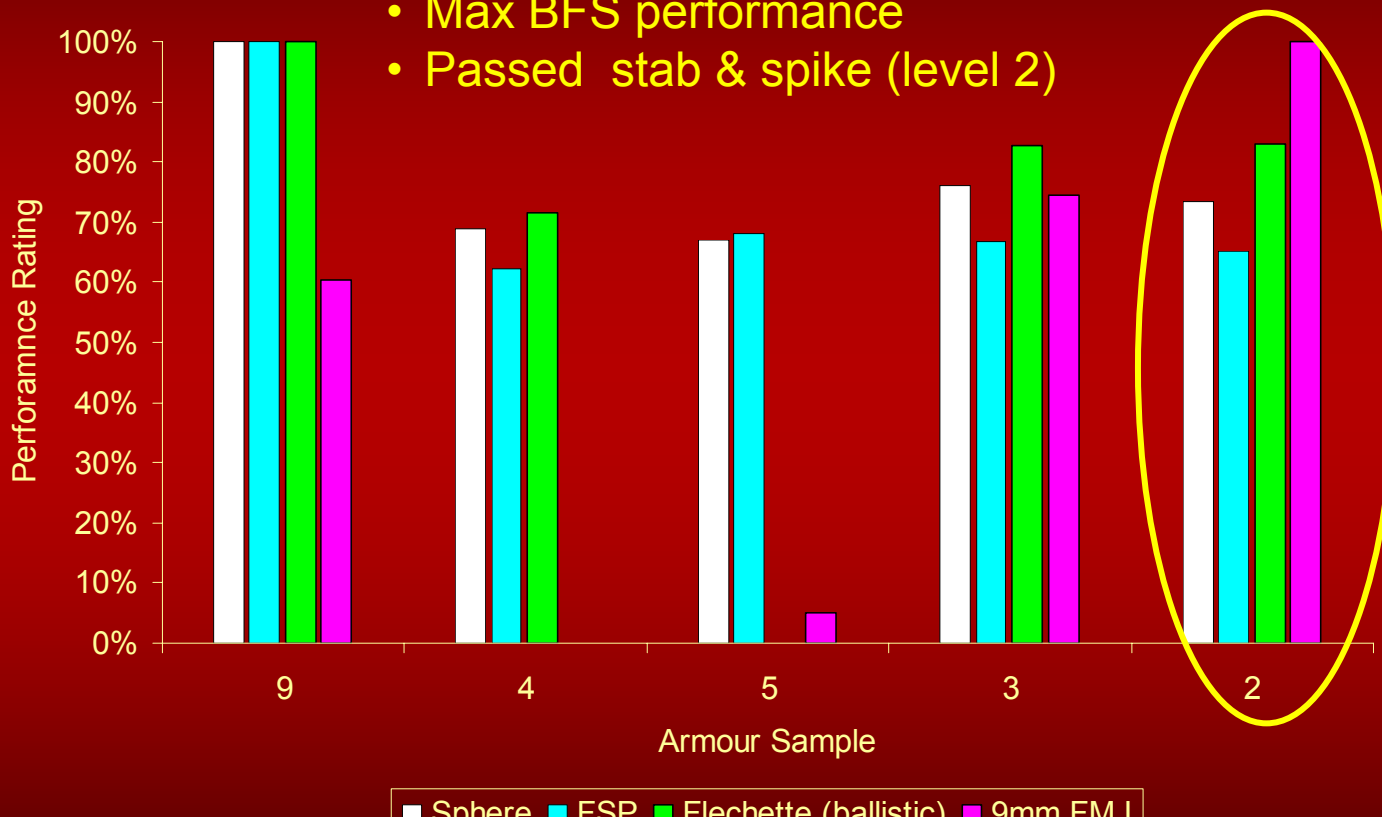
Performance Rating - Ballistic

- Max performance ballistic penetration
- BFS not optimized
- Failed stab P1 (level 2)



Performance Rating - Ballistic

- Good performance ballistic penetration
- Max BFS performance
- Passed stab & spike (level 2)



Conclusions

- Current technologies can provide minimum protection against stab, flechette, and ballistic threats.
- a.d. $\geq 9.9 \text{ kg/m}^2$ for 3 stab threats (level 2)
- Preliminary assessment of flechette resistance possible with drop mass method
- Performance optimization possible through # of layers, sequence, material combination
- Desired requirements can not be achieved for a.d. $< 10 \text{ kg/m}^2$ (9mm HP Bofors and flechette)

Way ahead

- ▶ Test all samples for stab Level 1
- ▶ Refine drop mass method: reduce weight to increase velocity, modify flechette simulator
- ▶ Complete ballistic test evaluation for samples No. 11 and 12
- ▶ Evaluate semi-rigid solutions (metallic or ceramic tiles) for high performance bullets
- ▶ Optimize performance with minimum aerial density
- ▶ Consider zones with different protection levels

Acknowledgment

- ▶ This work was supported by
 - *Defence R&D – Valcartier*
 - *Directorate of Land Requirements of DND Canada*
- ▶ Co-authors
 - *M. Keown (Biokinetics and Associates Ltd.)*
 - *G. Pageau, M. Bolduc, and D. Bourget (Defence R&D Canada)*

Engineered Solutions for Impact Protection



22nd International Symposium on Ballistics

Contact Information

- ▶ Name: Benoit Anctil
- ▶ Phone No.: (613) 736-0384 ext.223
- ▶ Company: Biokinetics and Associates Ltd.
- ▶ E-mail: anctil@biokinetics.com

A Novel Test Methodology to Assess the Performance of Ballistic Helmets

Presented by:

B. Anctil

Co-authors:

M. Keown

Biokinetics and Associates Ltd.

D. Bourget and G. Pageau

Defence R&D Canada

22nd International Symposium on Ballistics
Vancouver, Canada, November 14-18, 2005

The Problem

- ▶ New lightweight composite helmets have increased protection against penetration
- ▶ Result in large back-face deformation
- ▶ Increased risk of serious skull/brain injuries
- ▶ No widely accepted evaluation procedure



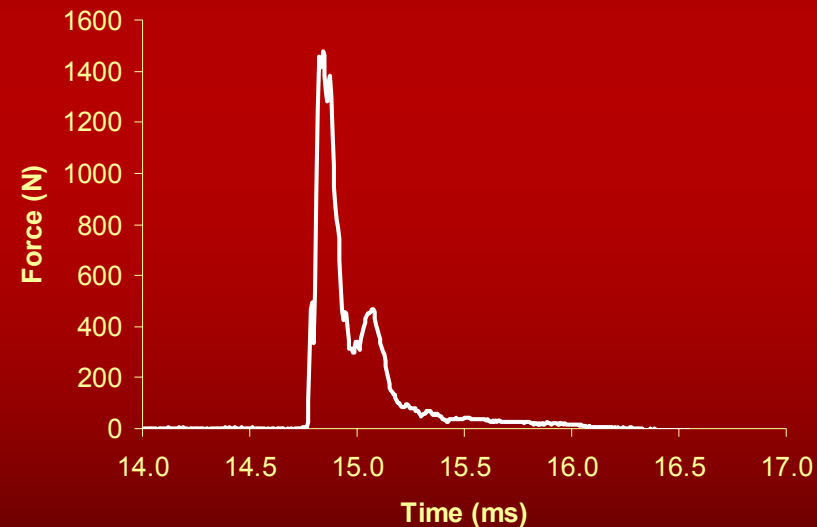
Our Strategy

- ▶ Implement an impact force measurement headform
- ▶ Based on injury model developed by Bass et al. (2003) using localized skull pressure data
- ▶ Develop test procedure
- ▶ Conduct experimental trials with current combat helmet models
- ▶ Define injury function



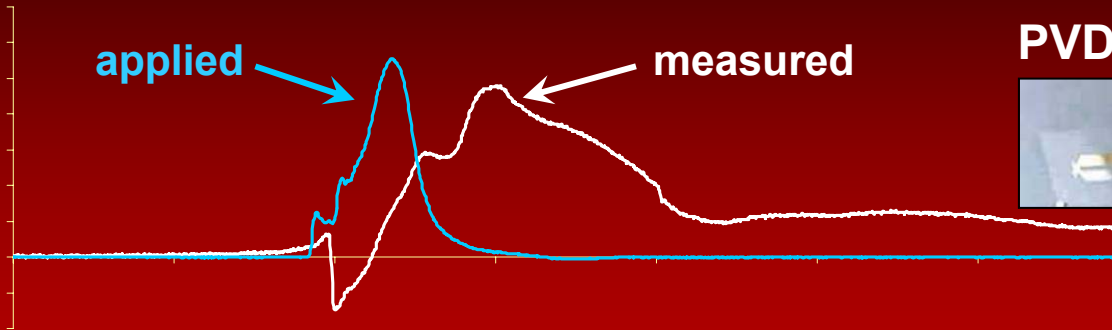
Measurement System Requirements

- ▶ **Dynamic Loads**
 - *Force < 5,000 N*
 - *Duration < 2 ms*
- ▶ **PVDF gauge**
- ▶ **Load cell**
- ▶ **Evaluation under ballistic loading conditions**

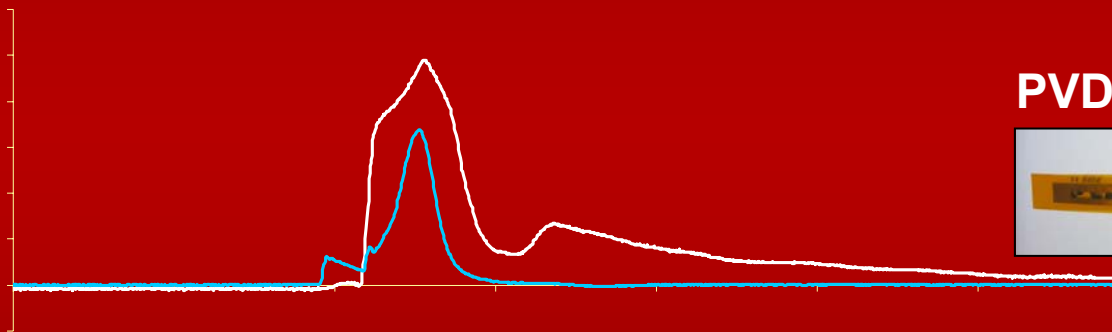


Instrumentation Selection

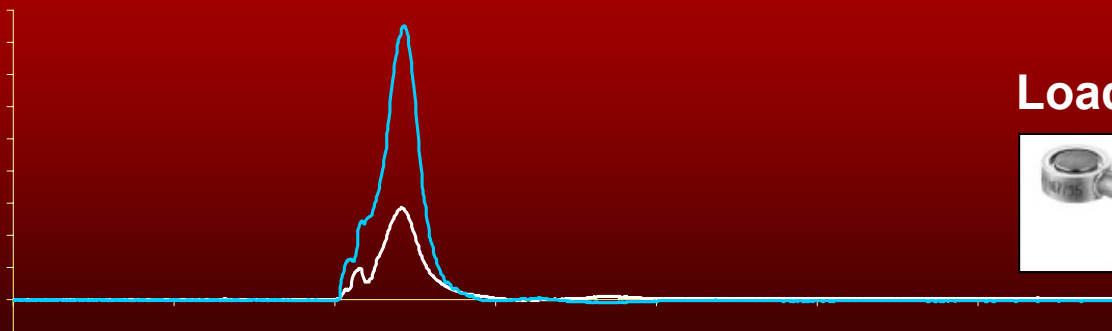
applied → measured ←



PVDF Gauge (Ktech)



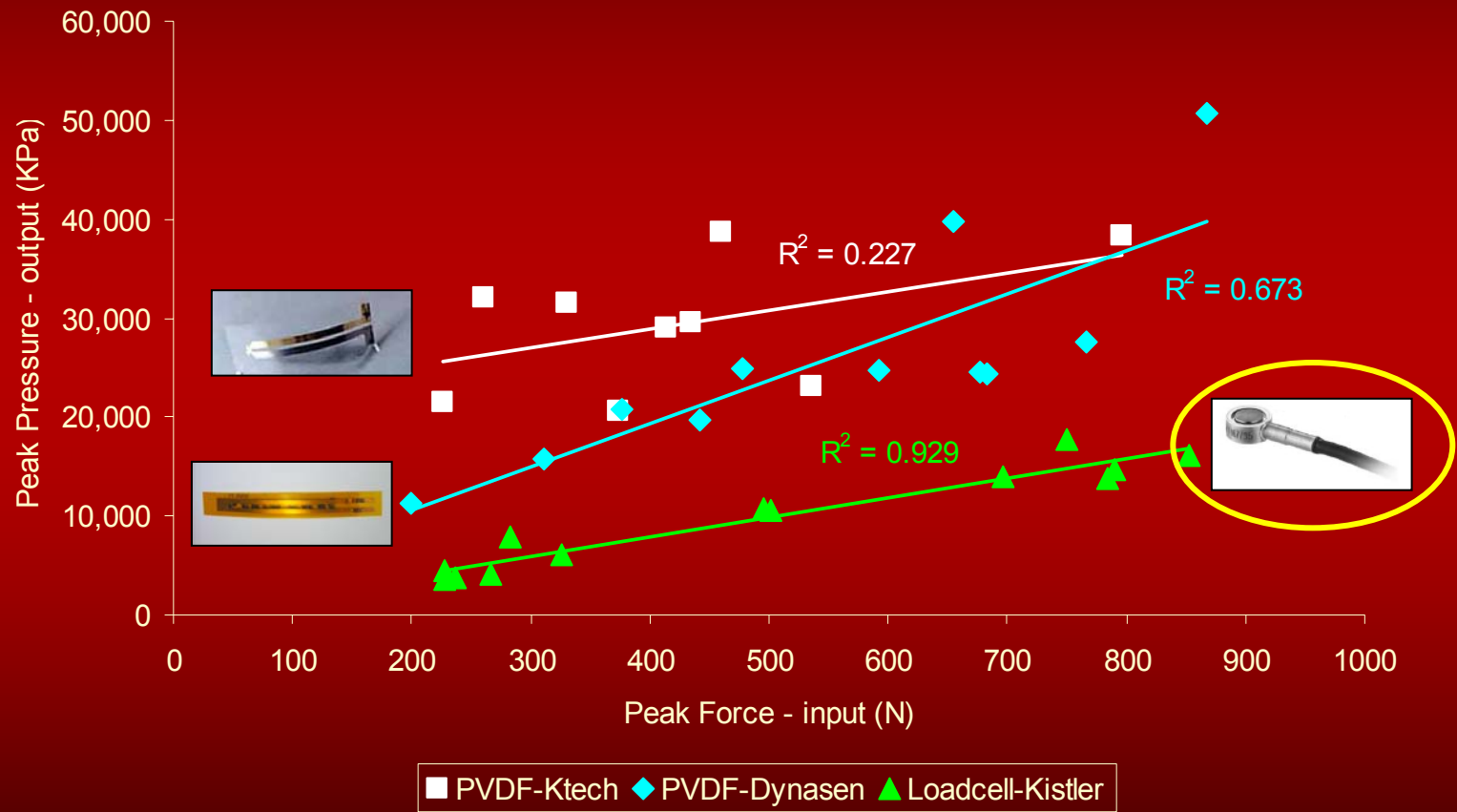
PVDF Gauge (Dynasen)



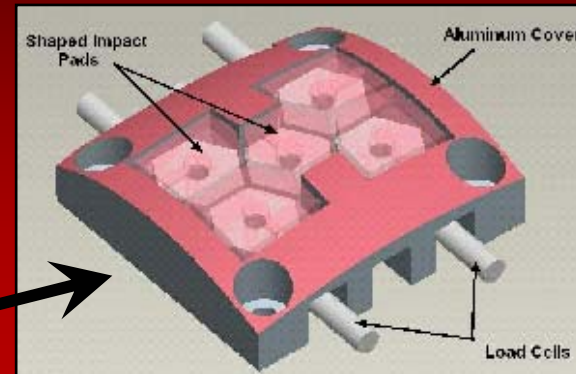
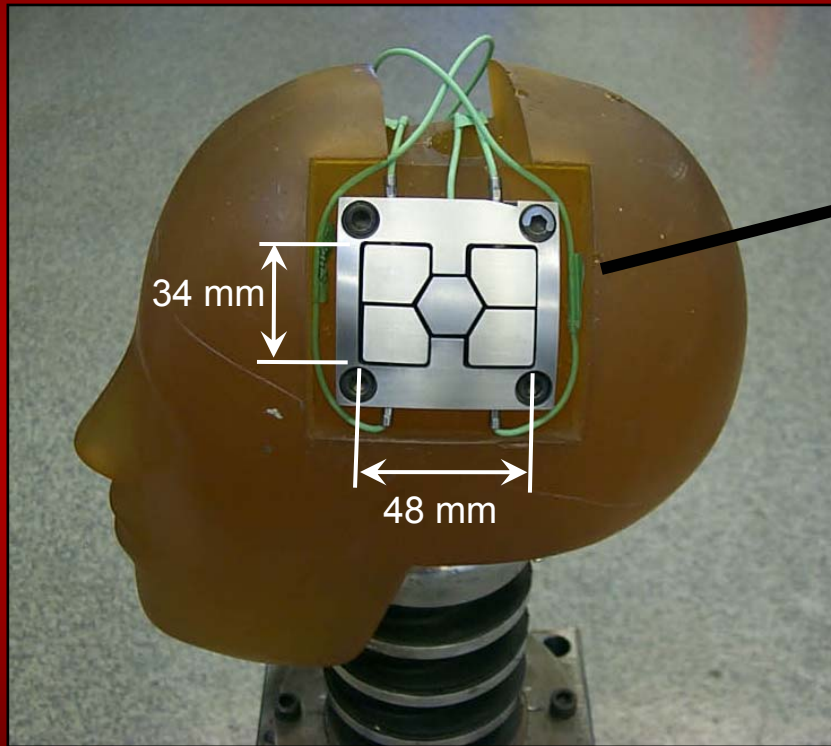
Load cell (Kistler)



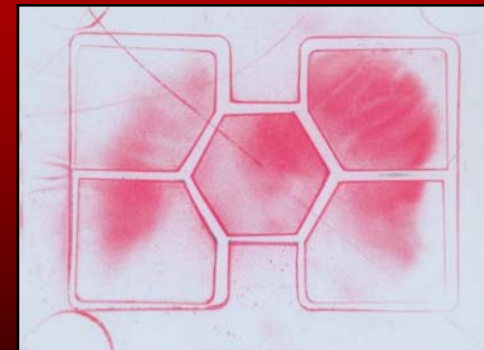
Force applied vs. measured



Impact Force Measurement Headform



Pressure sensitive film to measure loading area



Helmet Performance Evaluation

- 3 Combat Helmet Models
- Similar Ballistic Limit (V_{50})
- 9mm FMJ
- $350 \text{ m/s} < v < 450 \text{ m/s}$



Helmet A



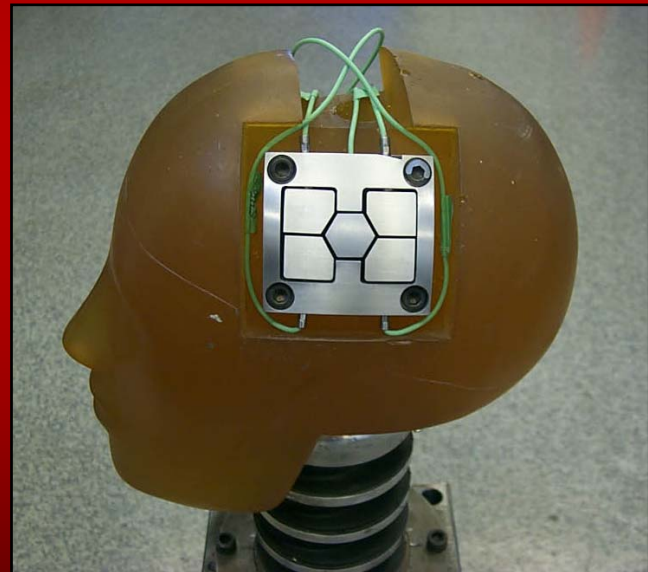
Helmet B



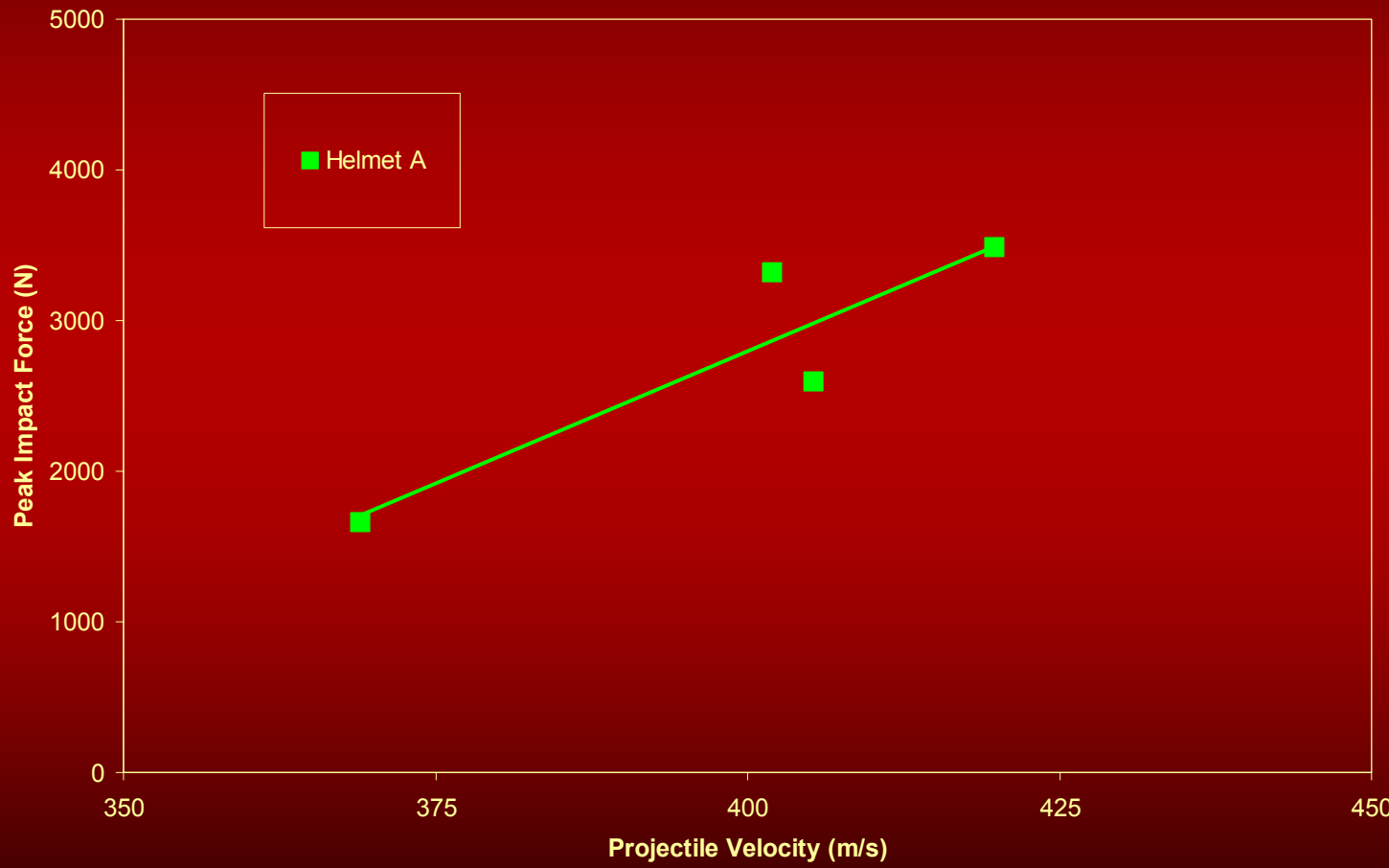
Helmet C

Headform Response

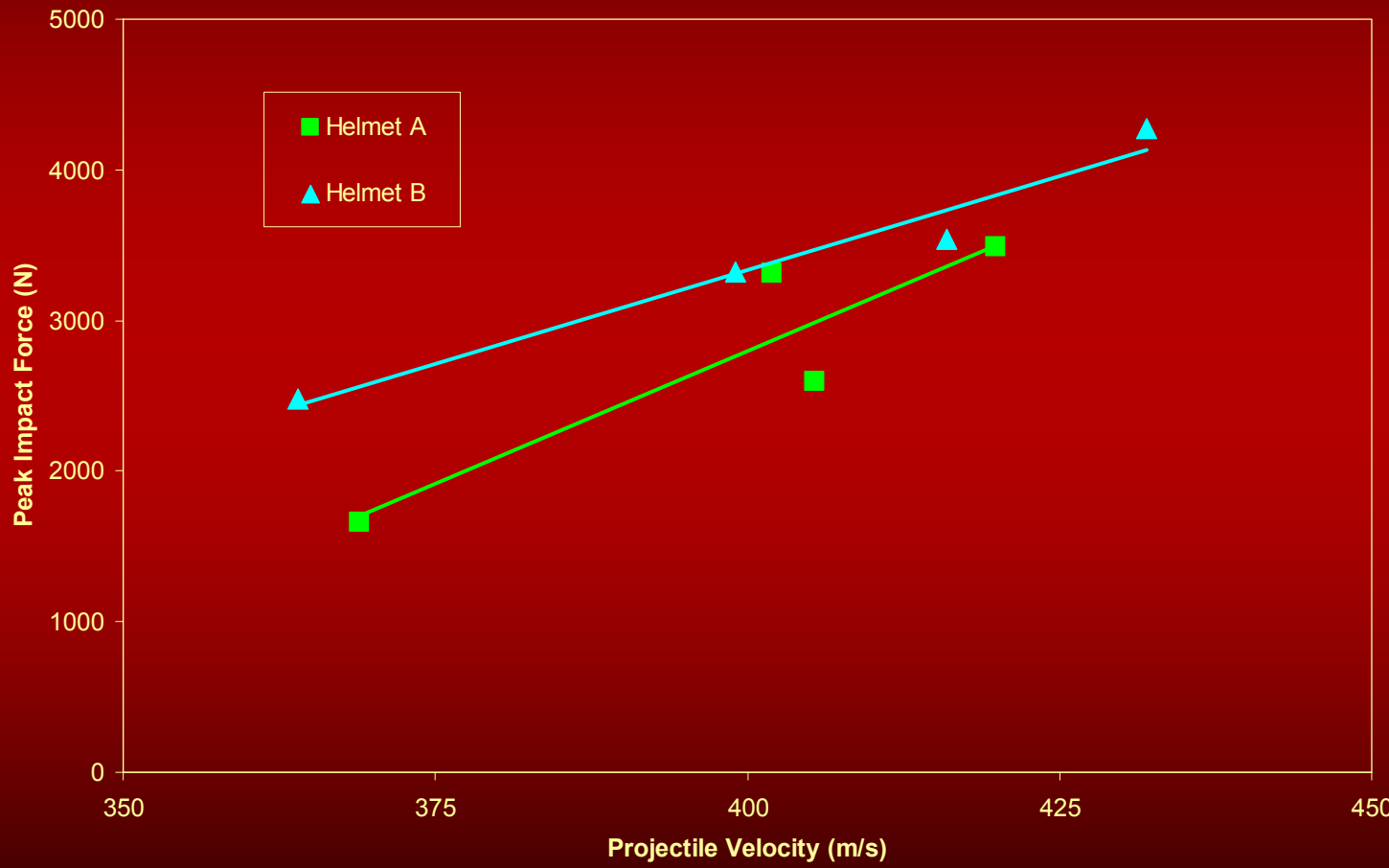
- ▶ Peak Force of Individual Load Cells
- ▶ Peak Force of Sum of Load Cells
- ▶ Impulse



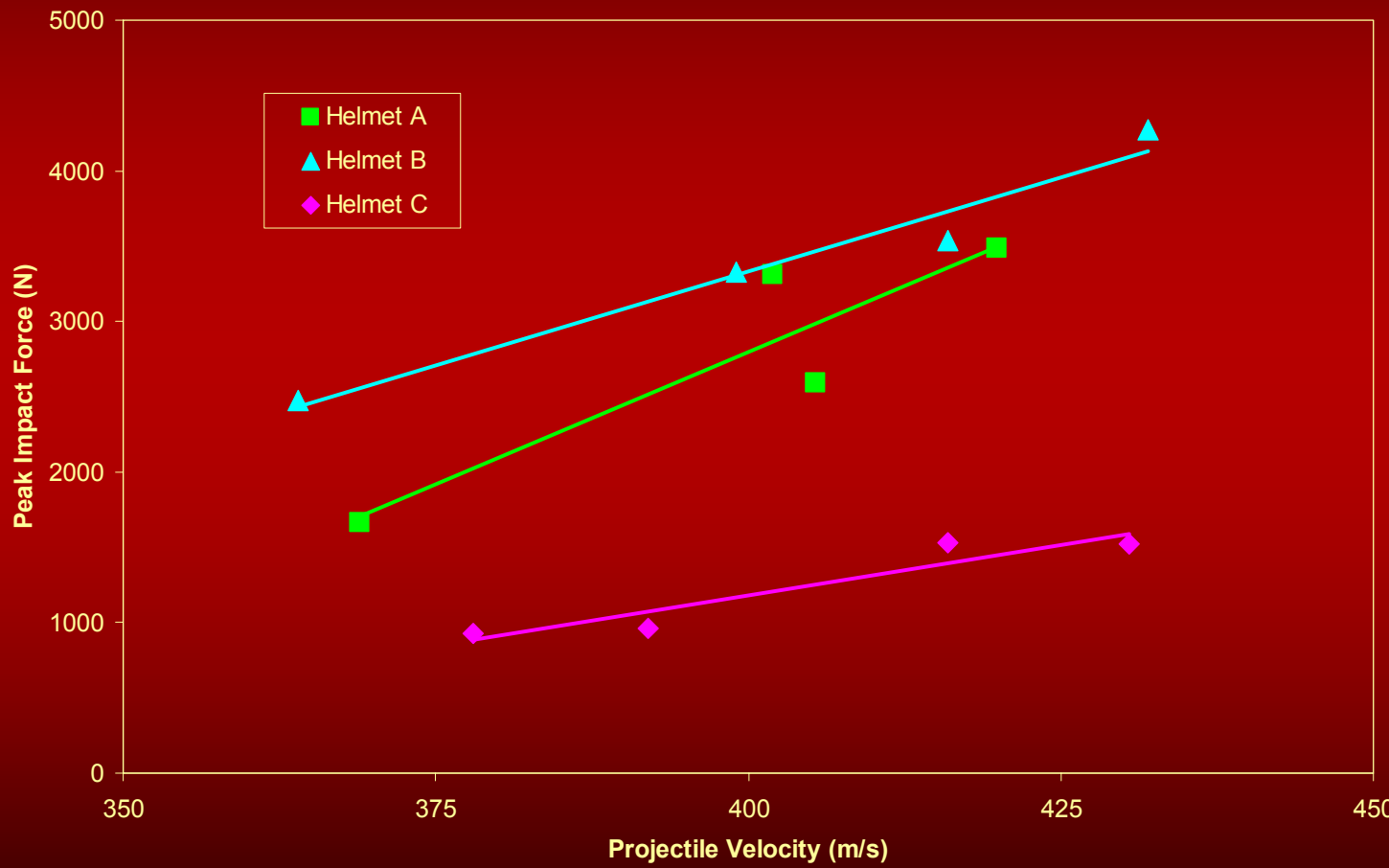
Individual Peak Forces



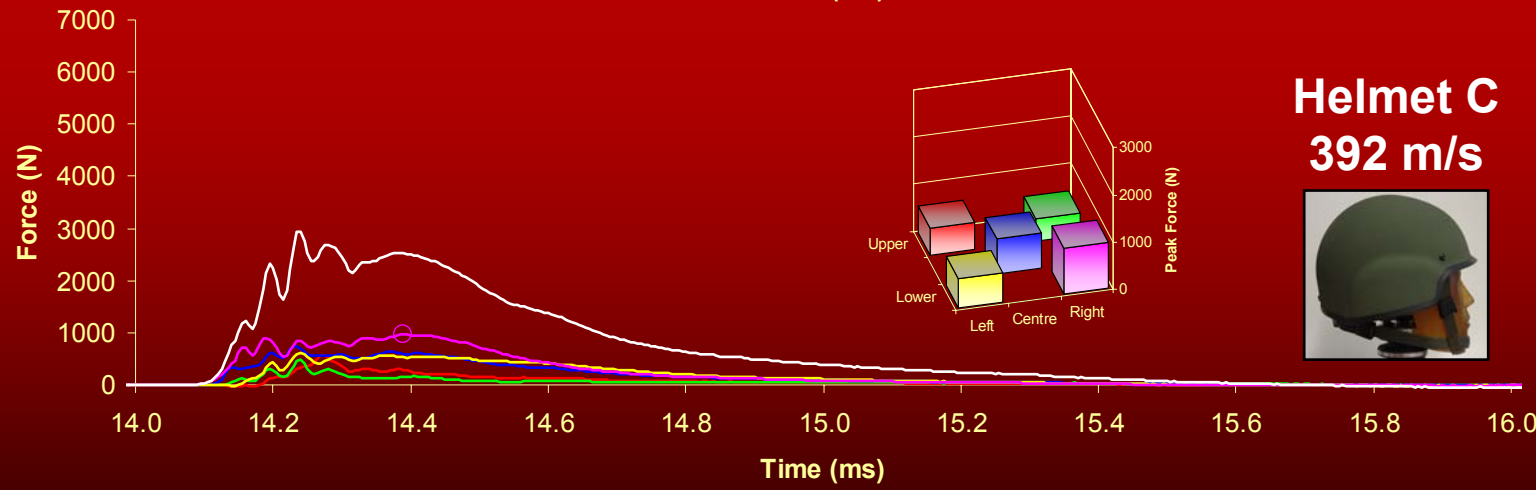
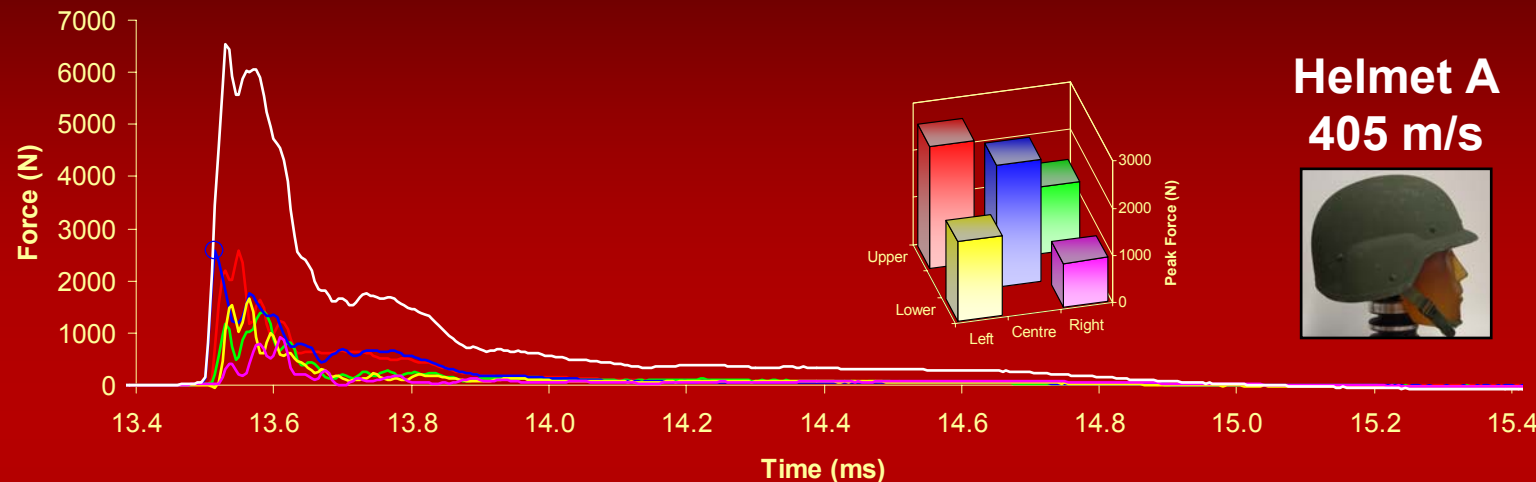
Individual Peak Forces



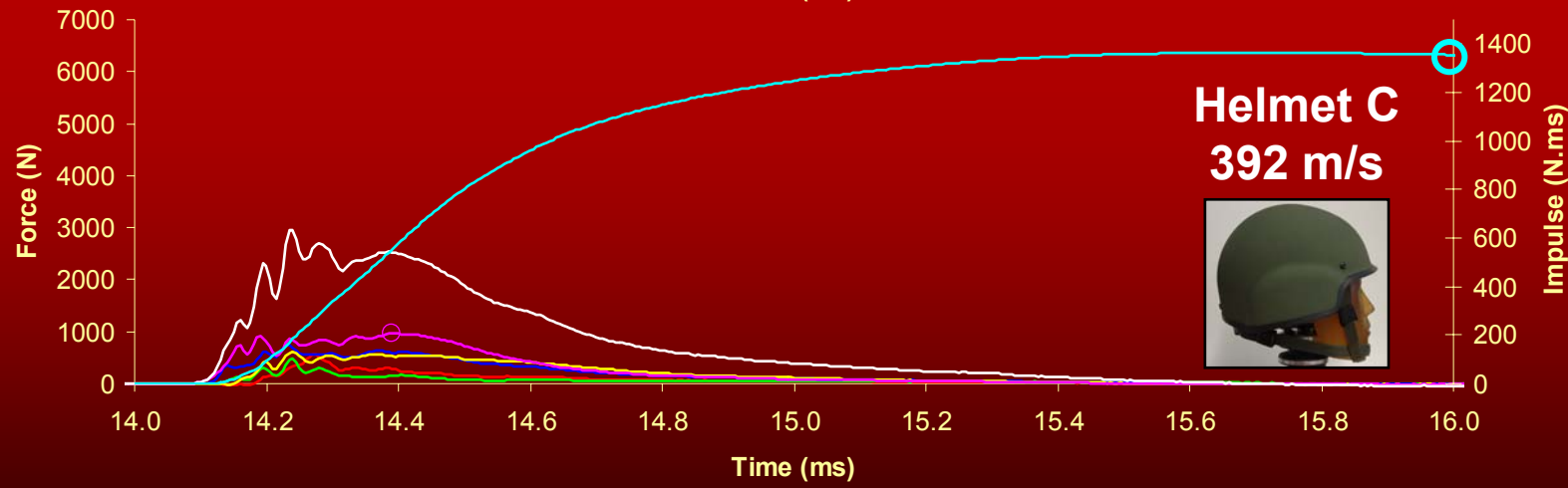
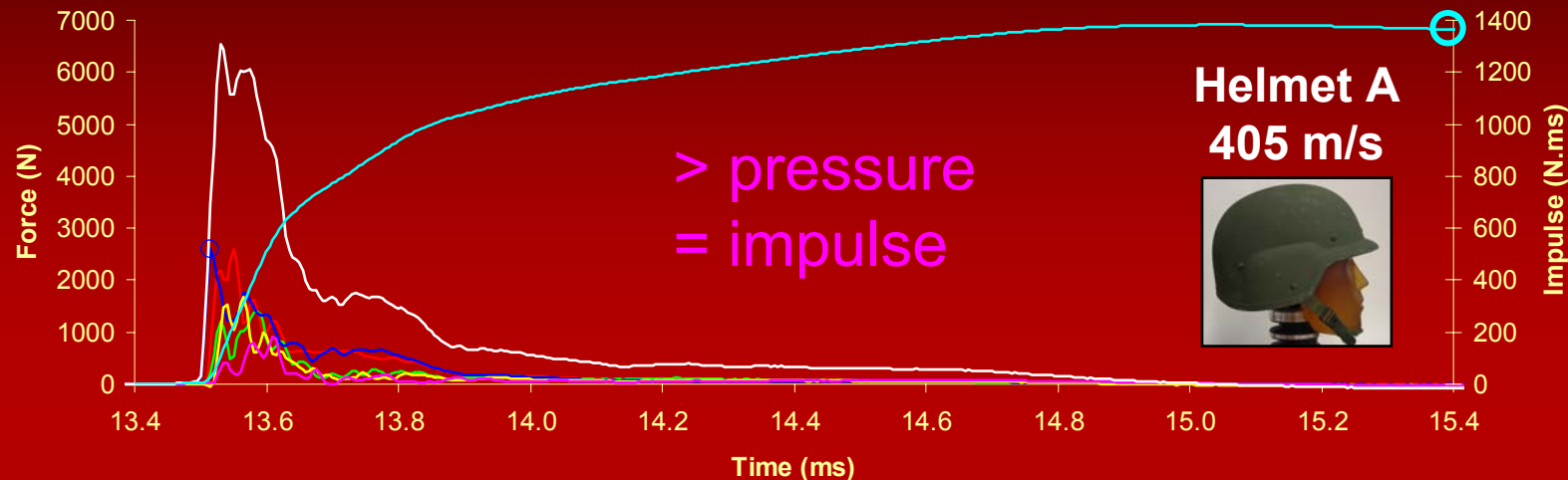
Individual Peak Forces



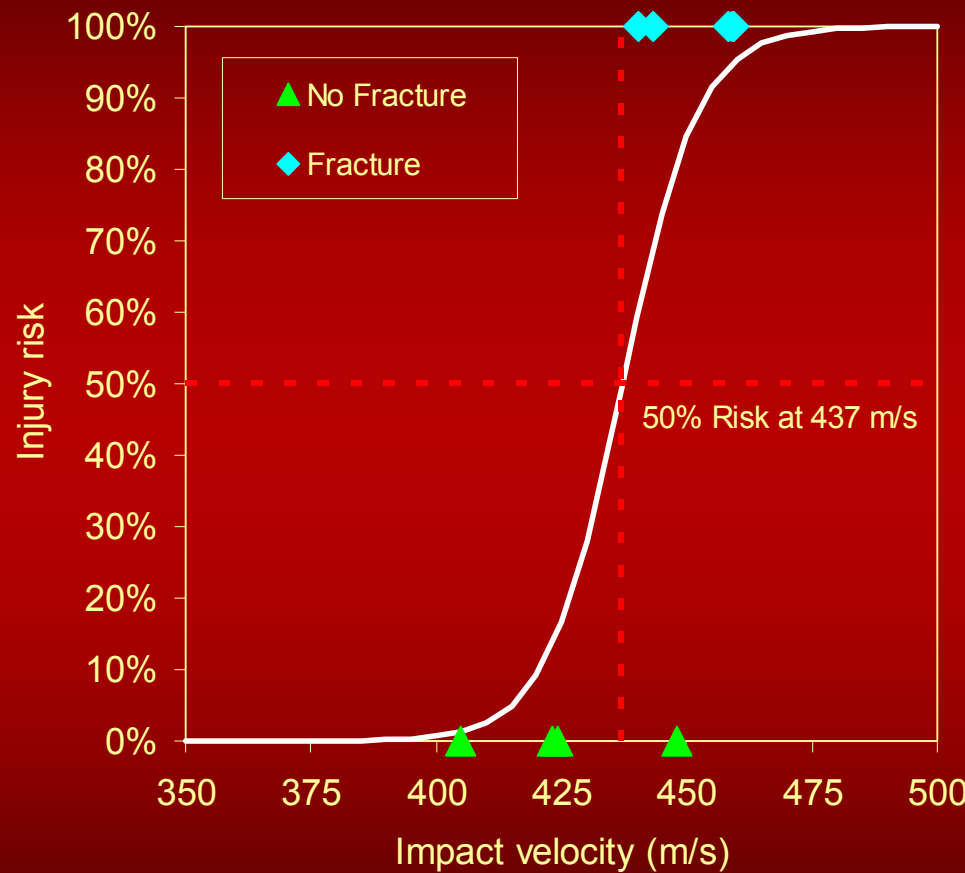
Impact Force Measurements



Impulse

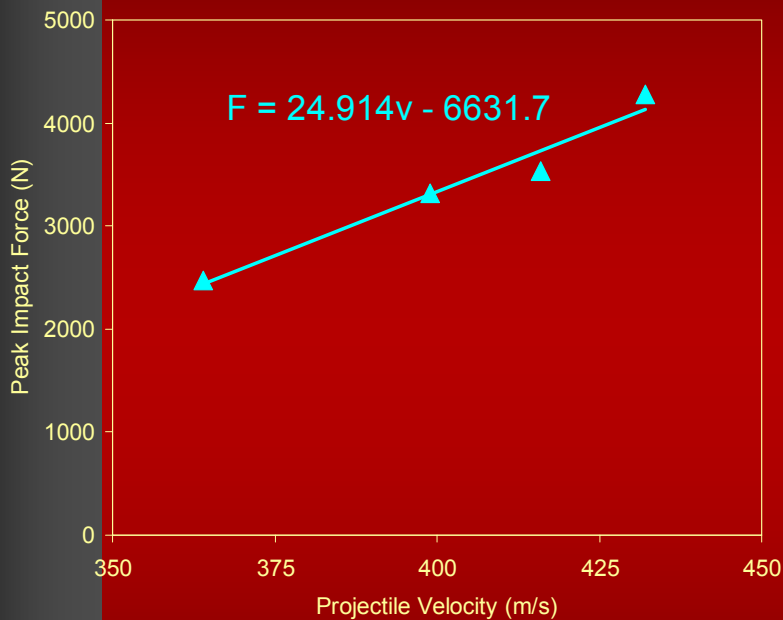


Skull Fracture Injury Function

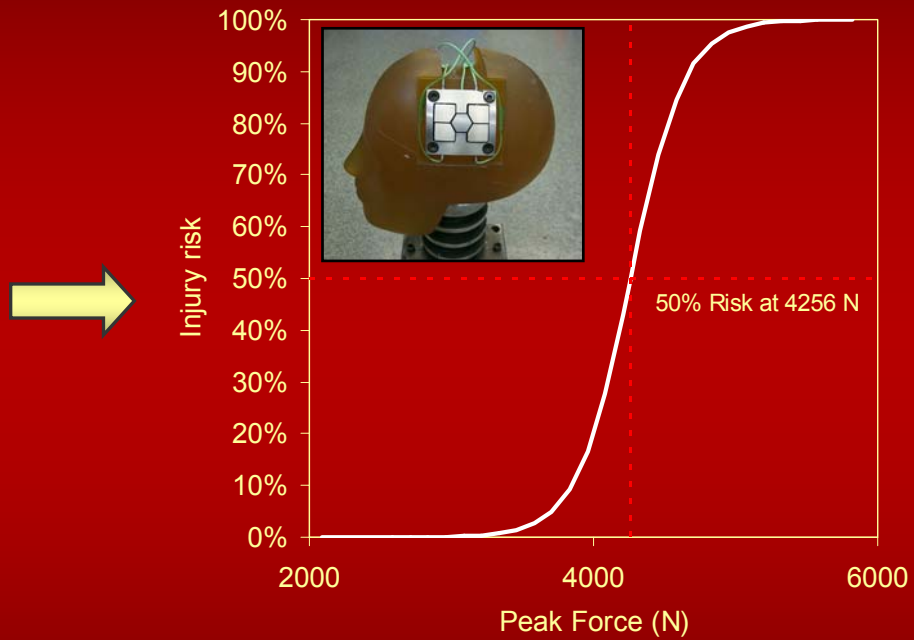


Helmet B / PMHS
(Bass et al. 2003)

Transfer Function

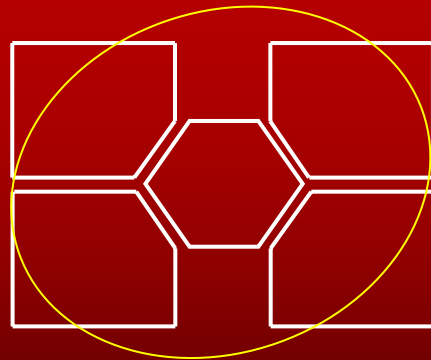
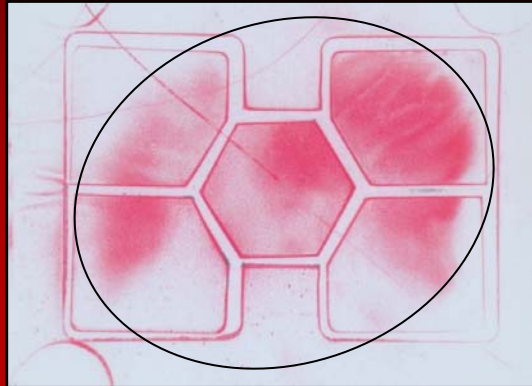


Force vs. velocity



valid only for concentrated load

Load Distribution



$$P_e = \frac{\sum_{i=1}^5 F_i(t)}{A_e}$$

Average Peak Pressure

Conclusions

- ▶ Miniature load cell suitable to measure helmet backface loading
- ▶ Instrumented headform was able to quantify the performance of ballistic helmets
- ▶ Can be used to predict the risk of skull fracture

Limitations

- ▶ Injury function valid only for concentrated load
- ▶ Contact area > sensing area
- ▶ Peak force must be within sensing area
- ▶ Does not address distributed forces (rigid helmets)

Way ahead

- ▶ Additional impact locations (e.g. front, rear)
- ▶ Consider other measurements (head acceleration)
- ▶ Review data analysis procedure (peak, sum, impulse)
- ▶ Calibration procedure
- ▶ Laboratory re-enactments of injurious cases

Acknowledgment

- ▶ This work was supported by
 - *Defence R&D – Valcartier*
 - *Directorate of Land Requirements of DND Canada*
 - *International Counter Terrorism Research and Development Program Agreement between US and Canada*
 - *OLES and NIJ*
- ▶ Co-authors
 - *M. Keown (Biokinetics and Associates Ltd.)*
 - *D. Bourget and G. Pageau (Defence R&D Canada)*

Engineered Solutions for Impact Protection



22nd International Symposium on Ballistics

Contact Information

- ▶ Name: Benoit Anctil
- ▶ Phone No.: (613) 736-0384 ext.223
- ▶ Company: Biokinetics and Associates Ltd.
- ▶ E-mail: anctil@biokinetics.com



Contact Information

- Captain Michael Dunning
Military Engineering Section
Defence R&D Canada – Suffield
Mike.Dunning@drdc-rddc.gc.ca
(403) 544-4269
- Dr Bill Andrews
Dept of Chemistry and Chemical Engineering
Royal Military College of Canada
Andrews-w@rmc.ca
(613) 541-6000 ext. 6052
- Dr Kevin Jaansalu
Dept of Metallurgical & Materials Engineering
Montana Tech (University of Montana)
kjaansalu@mtech.edu
(406) 496-4305





THE FRAGMENTATION OF METAL CYLINDERS USING THERMOBARIC EXPLOSIVES

Michael Dunning, Defence R&D Canada – Suffield

William Andrews, Royal Military College of Canada

Kevin Jaansalu, Montana Tech (University of Montana)

18 Nov 05



Defence Research and
Development Canada

Recherche et développement
pour la défense Canada

Canada



Outline

- Research goal
- Basic principles of TBX
- Experimental set-up
- Secondary combustion
- Fragment mass results
- Fragment velocity results
- Conclusions
- Future work

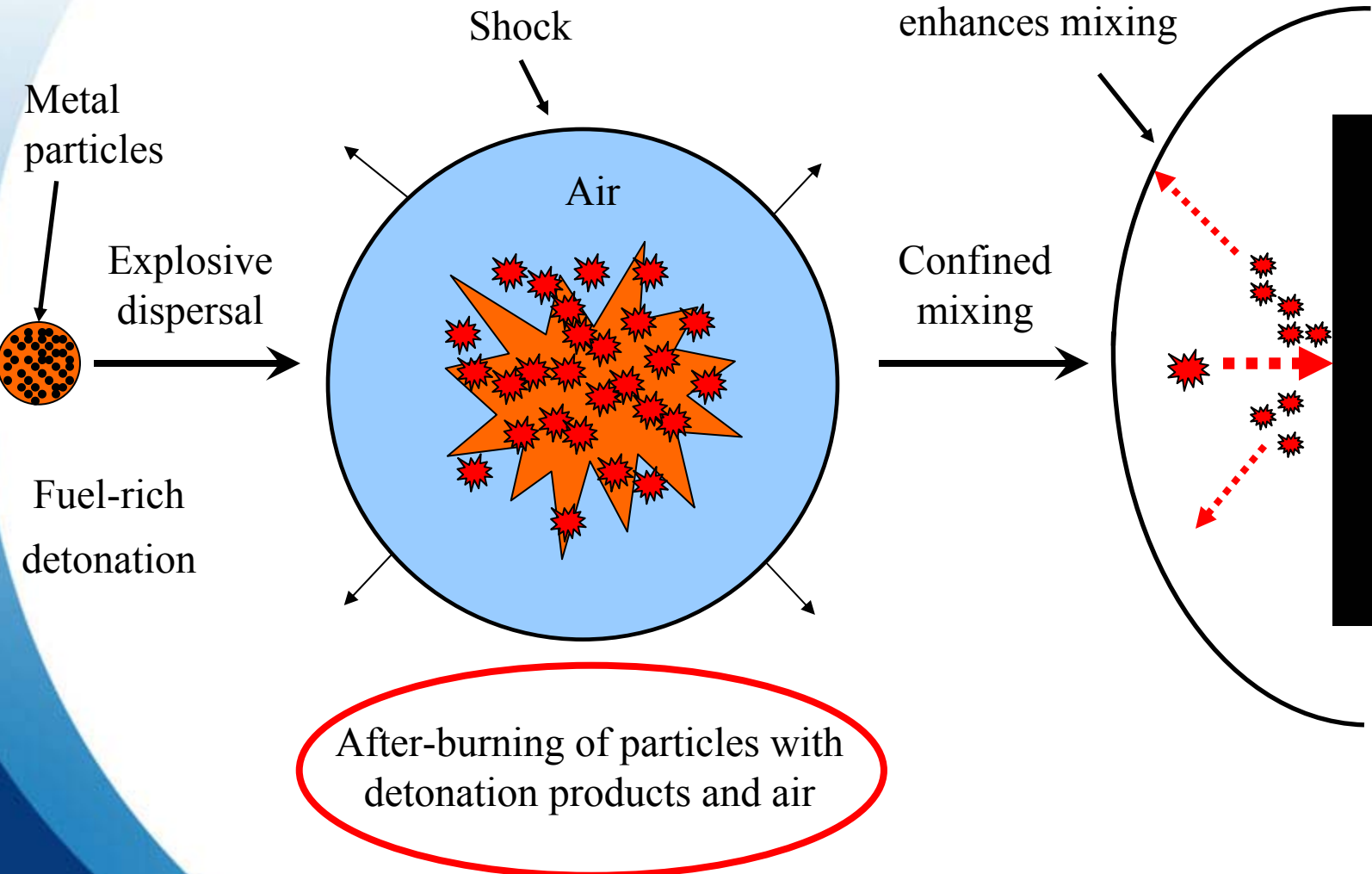


Research Goal

To assess the ability of TBXs to generate fragments.

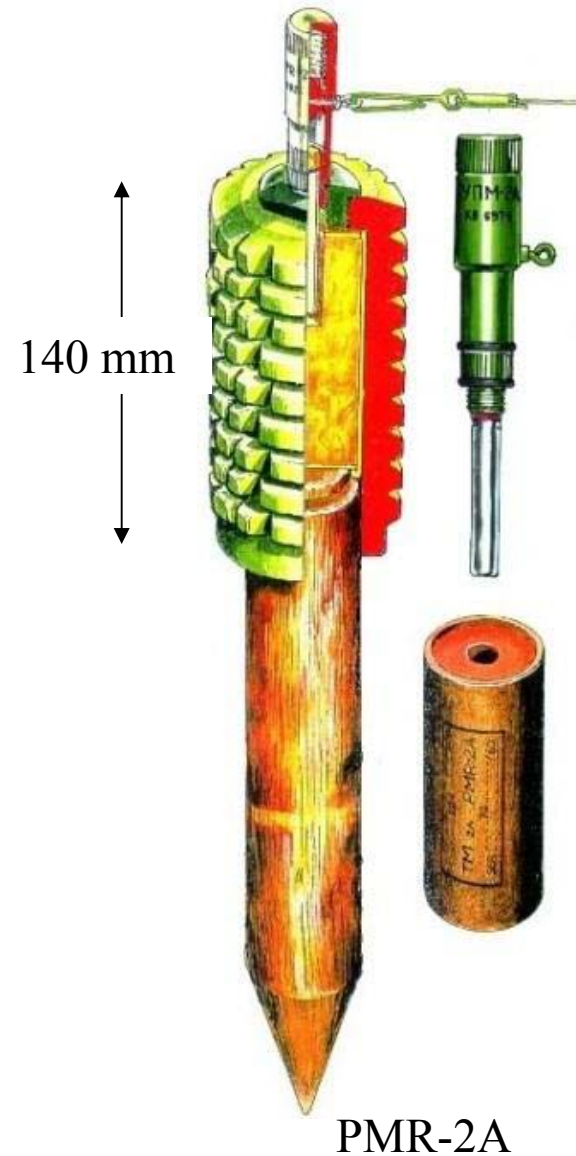
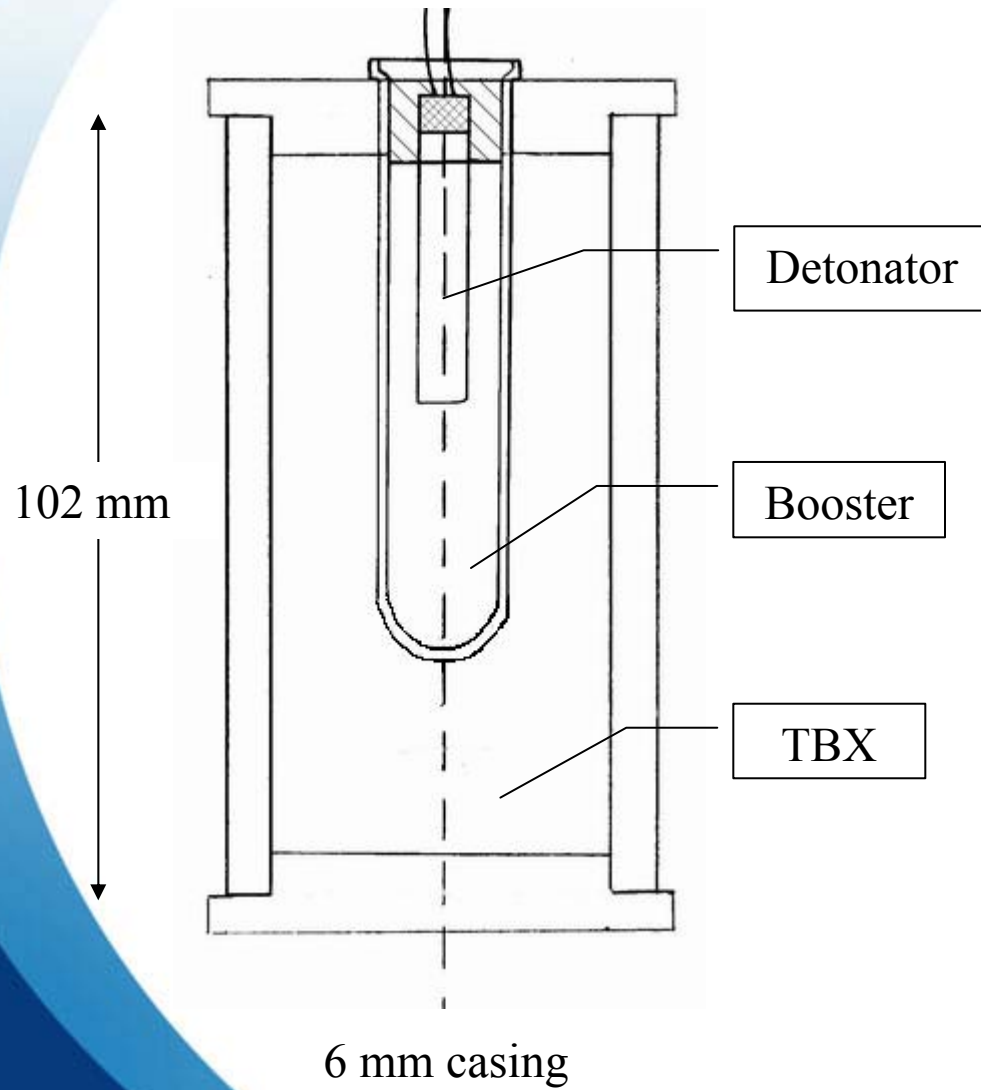


Basic TBX Concept



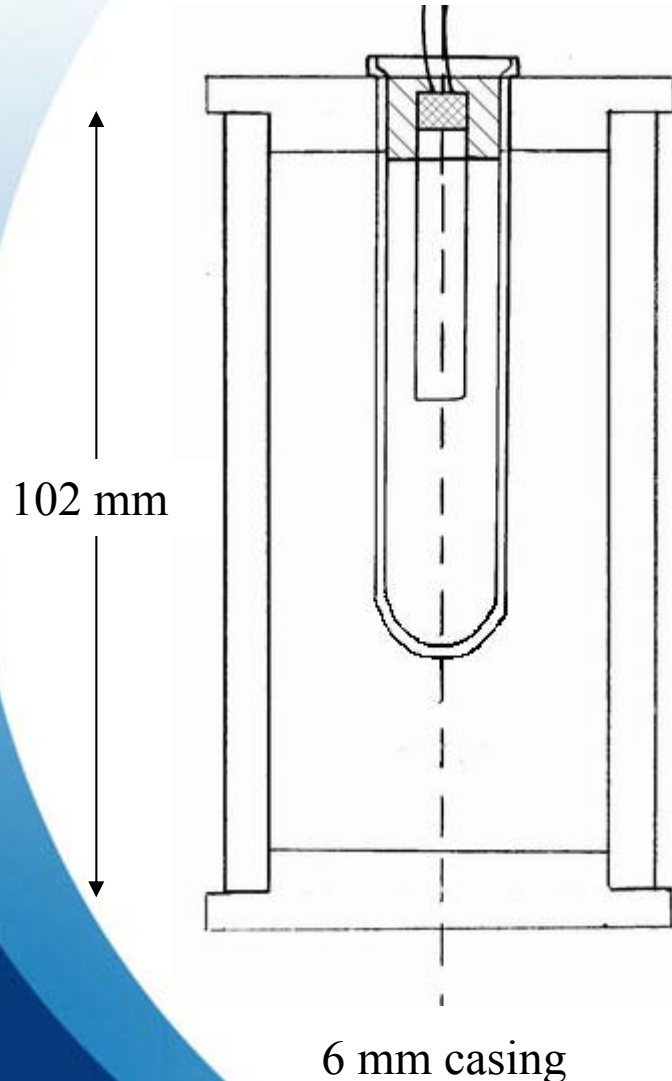


Experimental Charge





Trial Variables



- Explosives
 - TBX 1, 2, 3
 - C4 (baseline)
- Wall thickness
 - 3.8 mm, 6 mm, 8 mm, and 9.5 mm
- Casing material
 - 1026 steel
 - Ductile cast iron (DCI)
 - Grey cast iron (GCI)



TBX formulations

TBX 1

Monopropellant and magnesium particles

TBX 2

Nitromethane and aluminium (60/40 %wt)

TBX 3

Monopropellant, aluminium and RDX





Mine Effects Site





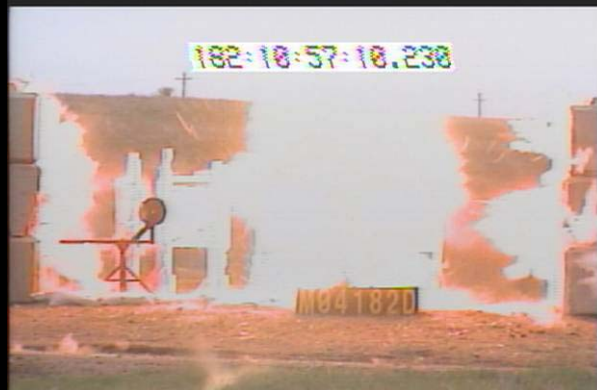
Witness Packs





Secondary Combustion

First fragment impacts





Witness Pack Analysis

Software converts hole size and depth of penetration to mass and velocity

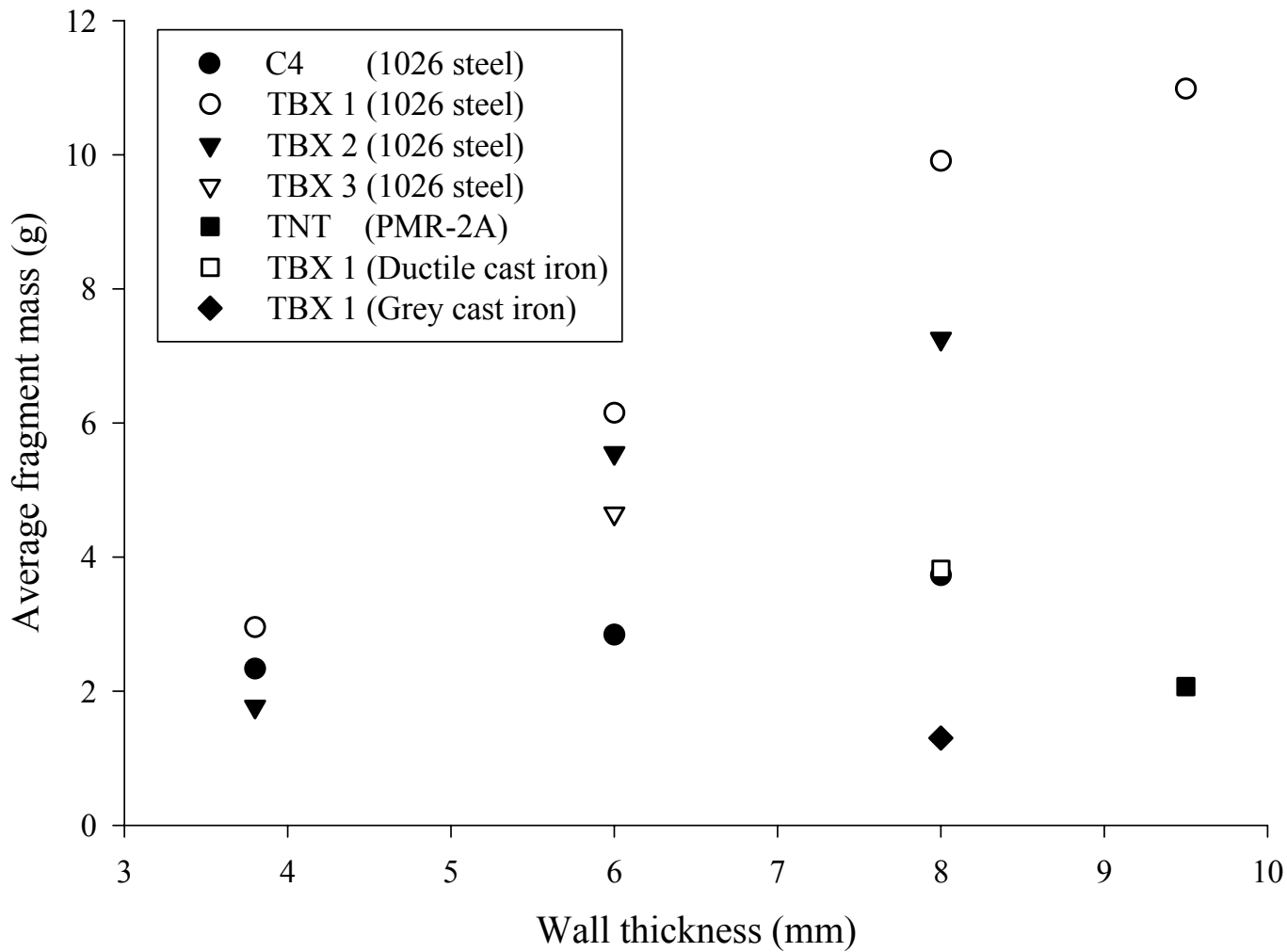
- Mass distribution results were compared to literature values
- The average velocities were compared to other methods.



C4-filled, 6 mm, 1026 steel casing

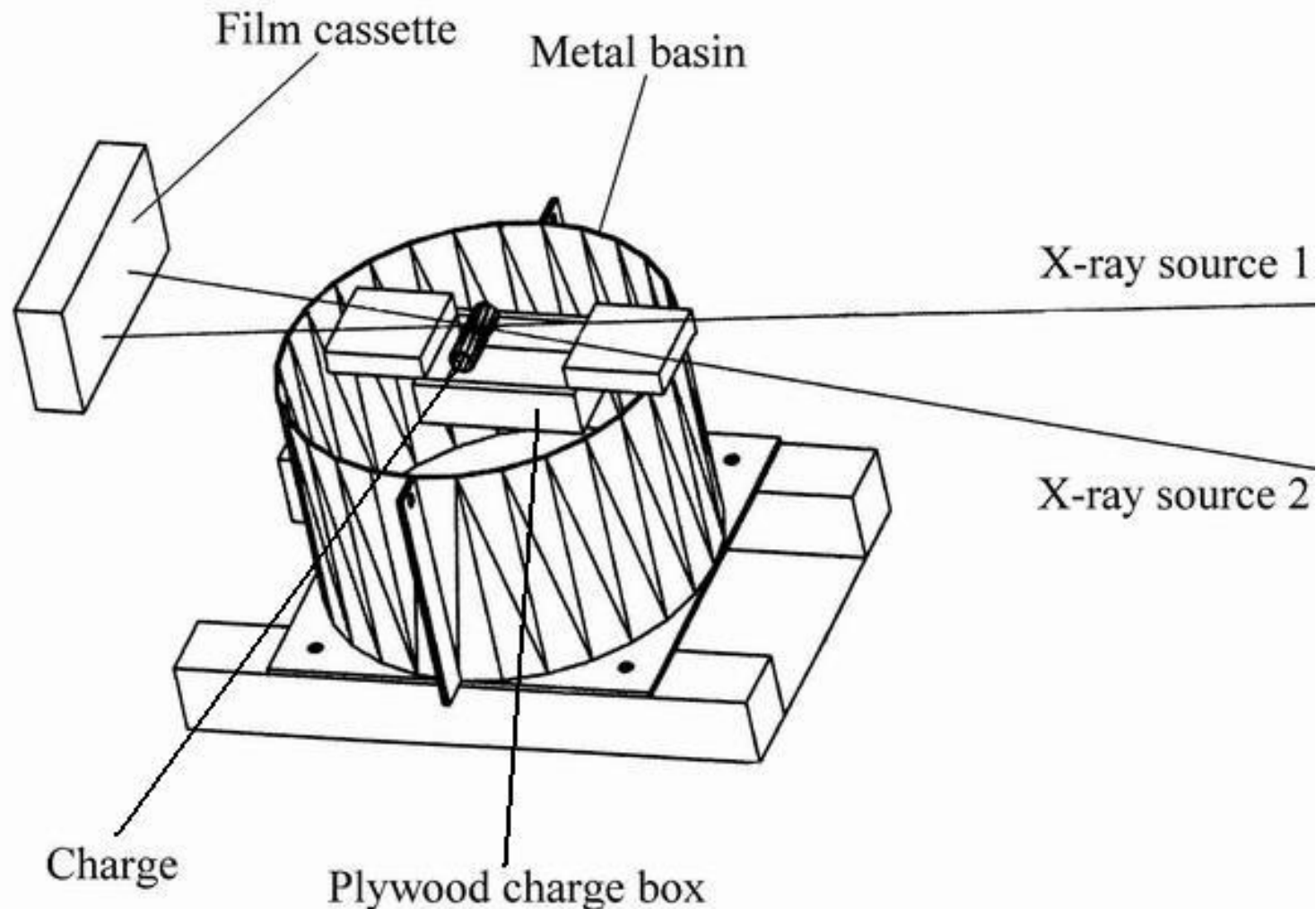


Average Fragment Mass





Flash X-ray Site (1/2)

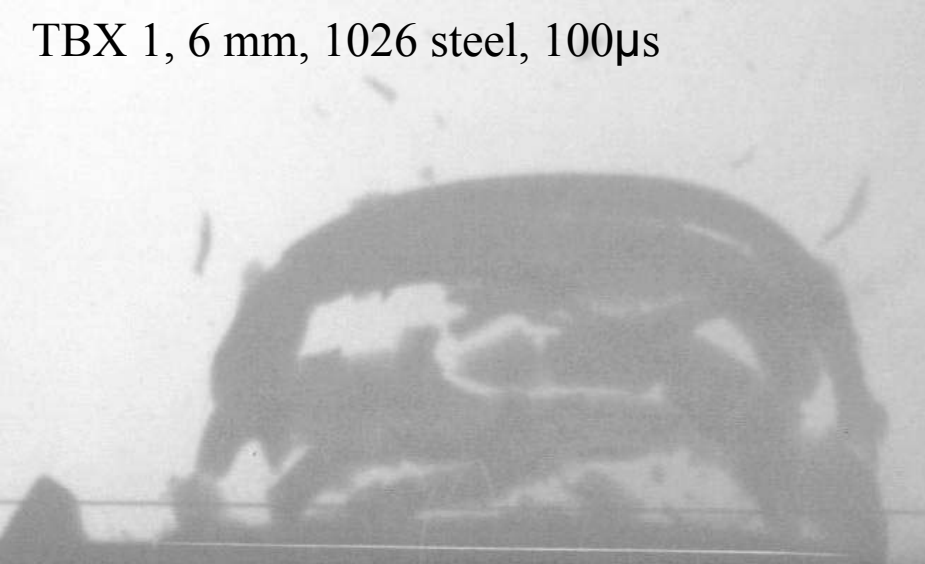




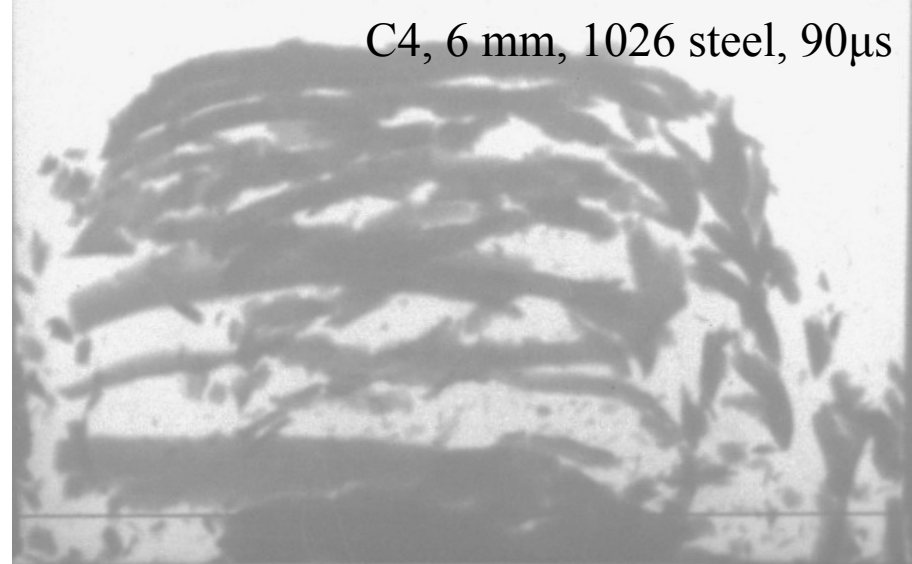
Flash X-ray Site (2/2)



TBX 1, 6 mm, 1026 steel, 100 μ s



C4, 6 mm, 1026 steel, 90 μ s

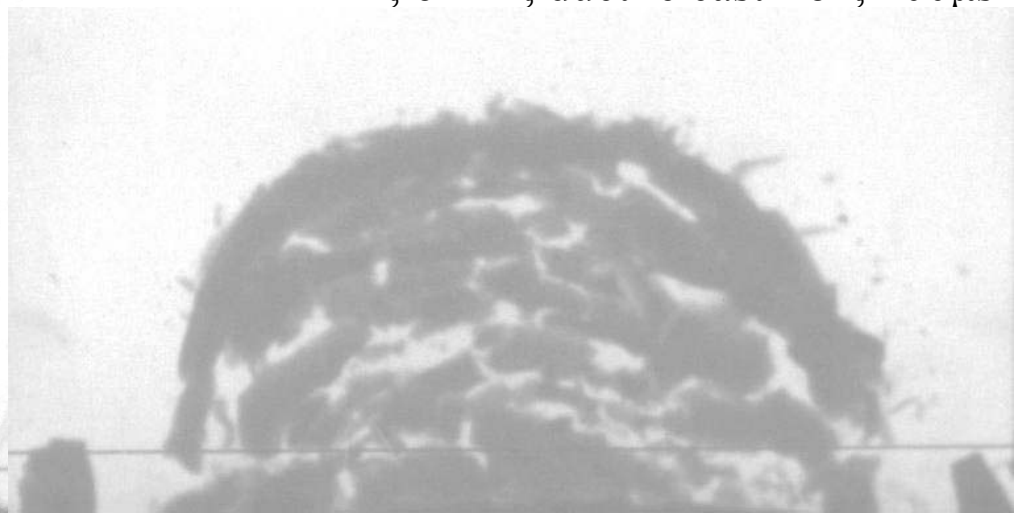


X-ray Images

TBX 1, 3.8 mm, 1026 steel, 100 μ s



TBX 1, 6 mm, ductile cast iron, 100 μ s





Predicting Fragment Velocity

Gurney equation

- Simple and long-standing
- Geometry-specific

$$v = \sqrt{2E} \left(\frac{M}{C} + \frac{1}{2} \right)^{-\frac{1}{2}}$$

M = mass of casing

C = mass of explosive

$\sqrt{2E}$ = Gurney constant

SplitX

- Gurney-based computer code that considers:
 - End confinement
 - Shock wave interaction and propagation
 - User-controlled geometry



Fragment Velocity (m/s)

Explosive	Wall thickness	Casing	Gurney ^a (+/- 12%)	SplitX ^a	Witness packs ^b	X-ray images ^a (+/- 50)
C4	6 mm	1026	1460	1360	610	1400
C4	8 mm	1026	1260	1150	590	---
TBX 1	3.8 mm	1026	1010	990	450	1000
TBX 1	6 mm	1026	700	770	430	800
TBX 1	6 mm	DCI	740	820	---	800
TBX 1	6 mm	GCI	640	810	---	750
TBX 2	6 mm	1026	990	930	460	---
TBX 3	6 mm	1026	1030	970	490	1000

a – Maximum fragment velocity

b – Average fragment velocity



Conclusions



- TBXs are capable of fragmenting metal casings:
 - Fragment mass distributions were consistent with literature values; and
 - Fragment velocities were well predicted using means that assume an instantaneous release of detonation energy.



Future Work



- Determine how the casing thickness and material disrupt the TBX shock wave.
 - Sacrificing the “thermobaric effect” to have fragments
- Determine how the fragmentation trends of the base explosives are altered by the additives.
 - Run trials with pure NM, and with silicon as an additive
- Determine why the casing material appears to have little effect on fragment velocity.
 - High strain rate failure and gas dynamics problem



Acknowledgements

- DRDC Valcartier
 - Weapons Effects Section
 - Y. Baillargeon for witness pack support
- DRDC Suffield (funding)
 - Neutralization and Protection Group
 - R. Fall for Mine Effects Site assistance
 - Threat Assessment Group
 - T. Storrie for Flash X-ray Site assistance
 - P. Lambert for mixing the explosives
 - Dr. J. Anderson for scientific support

DEFENCE



DÉFENSE

QUESTIONS ?

End of Presentation



Follow-on Slides



Fragment Energy (J)

Explosive	Casing thickness	Material	Average mass (g)	Max velocity (m/s)	Energy (J)	Number of fragments
C4	3.8 mm	1026	2.3	1750	3500	180
C4	6 mm	1026	2.8	1400	2700	240
C4	8 mm	1026	3.7	1200	2700	260
TBX 1	3.8 mm	1026	3.0	1000	1500	140
TBX 1	6 mm	1026	6.7	800	2100	100
TBX 1	8 mm	1026	9.9	650	2100	100
TBX 1	9.5 mm	1026	11.0	550	1700	110
TBX 1	8 mm	DCI	3.8	800	1200	220
TBX 1	8 mm	GCI	1.3	750	370	670
TBX 2	3.8 mm	1026	1.8	1200	1300	230
TBX 2	6 mm	1026	5.6	970	2600	120
TBX 2	8 mm	1026	7.3	850	2600	130
TBX 3	6 mm	1026	4.7	1000	2400	150
TNT (PMR 2A)	9.5 mm	GCI	2.1	570	340	740



Fragment Mass Distribution Mott Approach

$$N(m) = \frac{M_o}{2M_K^2} e^{-\left(\frac{\sqrt{m}}{M_K}\right)}$$

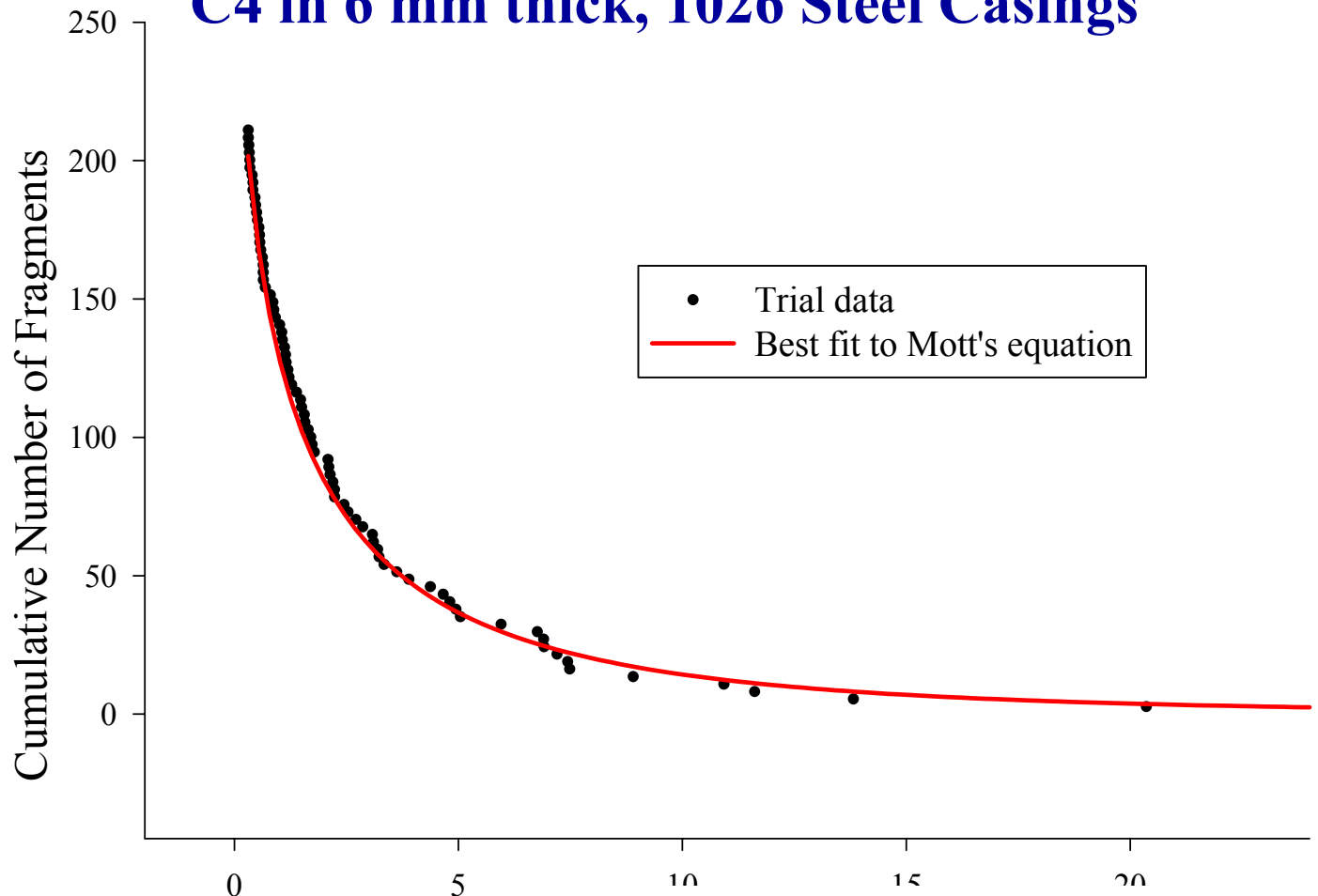
$N(m)$ = number of fragments
heavier than mass m
 M_o = casing mass

$$M_K = B t^{\frac{5}{6}} d^{\frac{1}{3}} \left(1 + \frac{t}{d} \right)$$

t = casing thickness
 d = casing interior diameter
 B = Mott coefficient



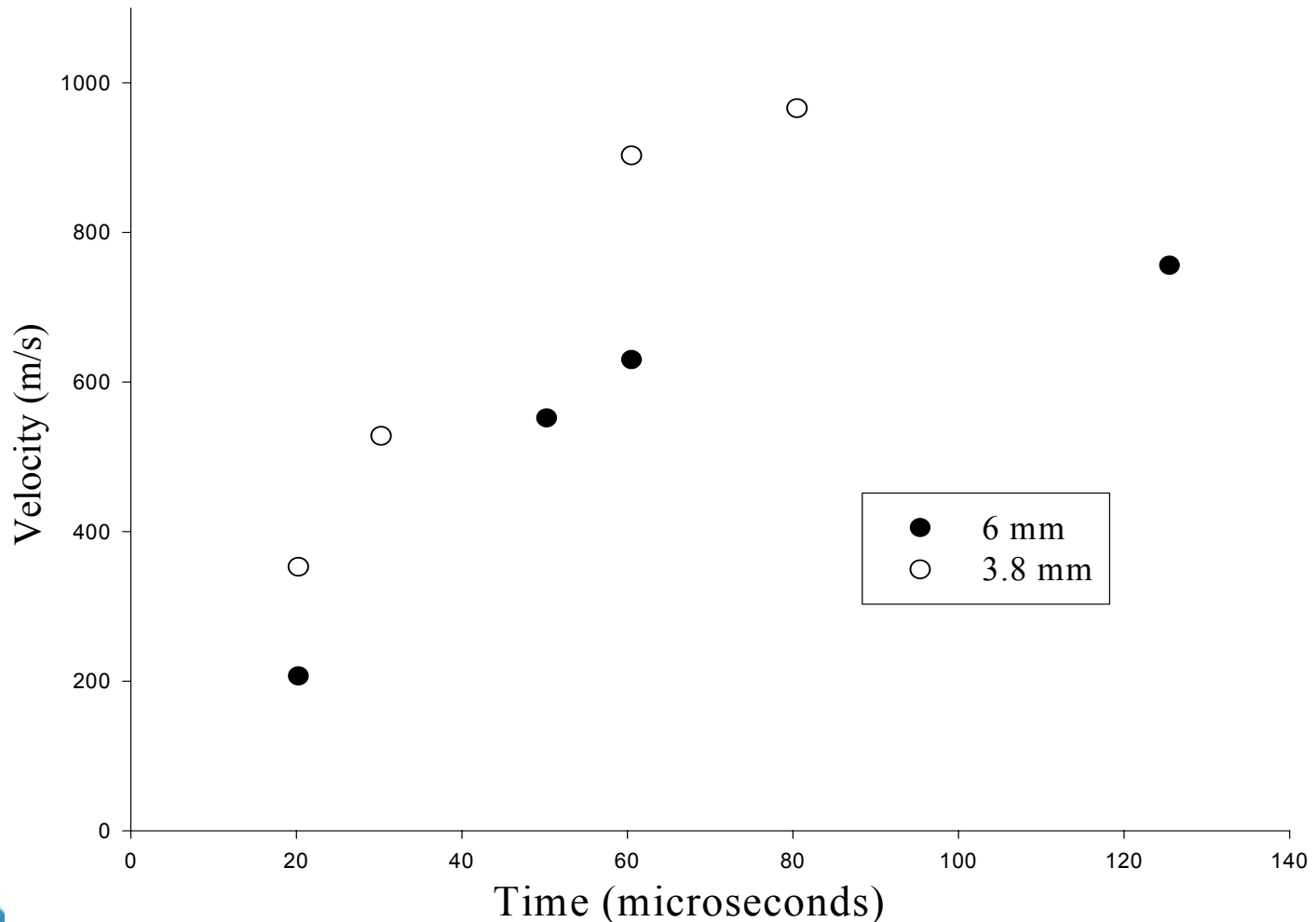
Fragment Mass Distribution C4 in 6 mm thick, 1026 Steel Casings





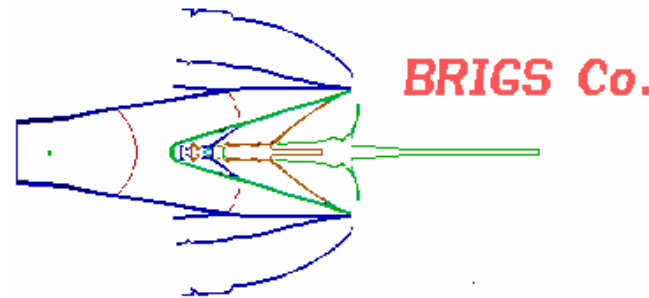
Fragment Velocity vs. Time

TBX 1 in 1026 steel casings



Oral Presentation Cover for Abstract 1943

Joseph E. Backofen



2668 Petersborough St.
Herndon, VA 20171

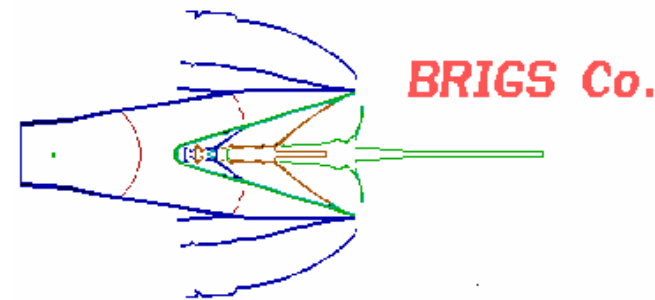
4192 Hales Ford Rd.
Moneta, VA 24121

703-476-6448

jebackofen@earthlink.net

The Gurney Velocity: A “Constant” Affected by Previously Unrecognized Factors

Joseph E. Backofen



2668 Petersborough St.
Herndon, VA 20171

4192 Hales Ford Rd.
Moneta, VA 24121

The Gurney Velocity – Key to the Equations

$$V_f = (2Eg)^{1/2} [(M/C) + 1/2]^{-1/2} \text{ Cylinder}$$

$$= V_g (\rho_{cyl} / \rho_{ex})^{-1/2} [(t_{cyl} / R_{ex})^2 + 2 (t_{cyl} / R_{ex}) + 0.5 (\rho_{ex} / \rho_{cyl})]^{-1/2}$$

$$V_f = (2Eg)^{1/2} [(M/C) + 1/3]^{-1/2} \text{ Symmetric Sandwich}$$

$$V_f = (2Eg)^{1/2} [(M/C) + 3/5]^{-1/2} \text{ Spherical Shell}$$

Values for the Gurney Velocity $(2Eg)^{1/2}$ derived from experiments using different cylinder materials

	Steel (m/s)	Copper (m/s)
Comp. A-3 (RDX)	2416	2630
Cyclotol (75/25 cast)	2320	2790
Comp. B	2310	2700
TNT (cast)	2040	2370
Tetryl	2209	2500

Gurney Velocity / Detonation Rate relationships:

$$V_g / D \approx 0.337 \quad (\text{P.W. Cooper})$$

$$V_g / D \approx (0.605 / [\Gamma - 1]) \quad (\text{J. Roth per J.E. Kennedy})$$

where Γ = the adiabatic exponent for the gaseous products

$$V_g / D \approx (0.60 \phi^{-1/2} + 0.648 \rho_o^{1/2}) / (1.01 + 1.313 \rho_o)$$

where $\phi = N M^{1/2} Q^{1/2}$; N = moles of gaseous detonation products

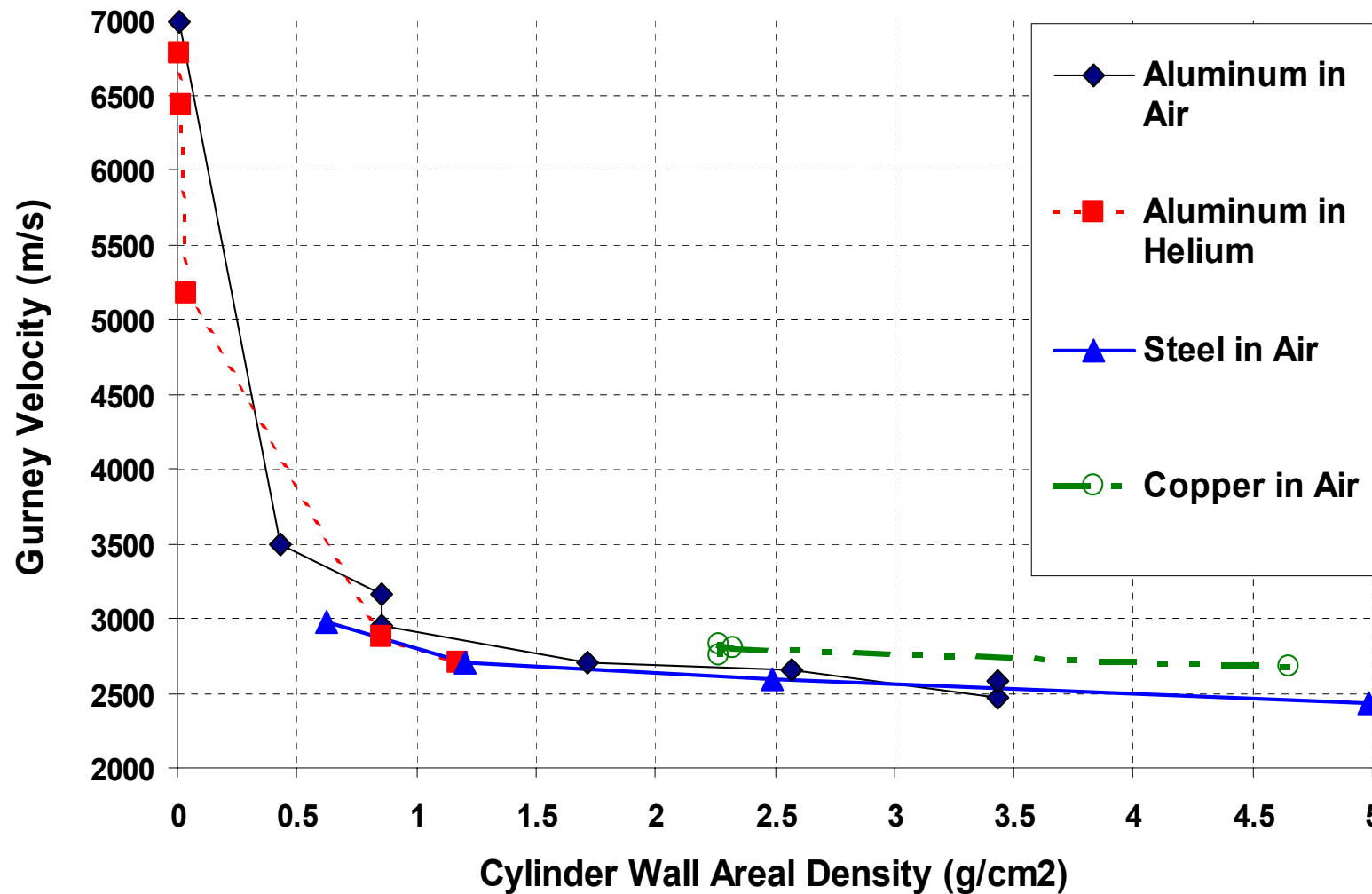
M = average weight of gases, and Q = chemical energy of detonation

(Hardesty & Kennedy / Kamlet & Hurwitz)

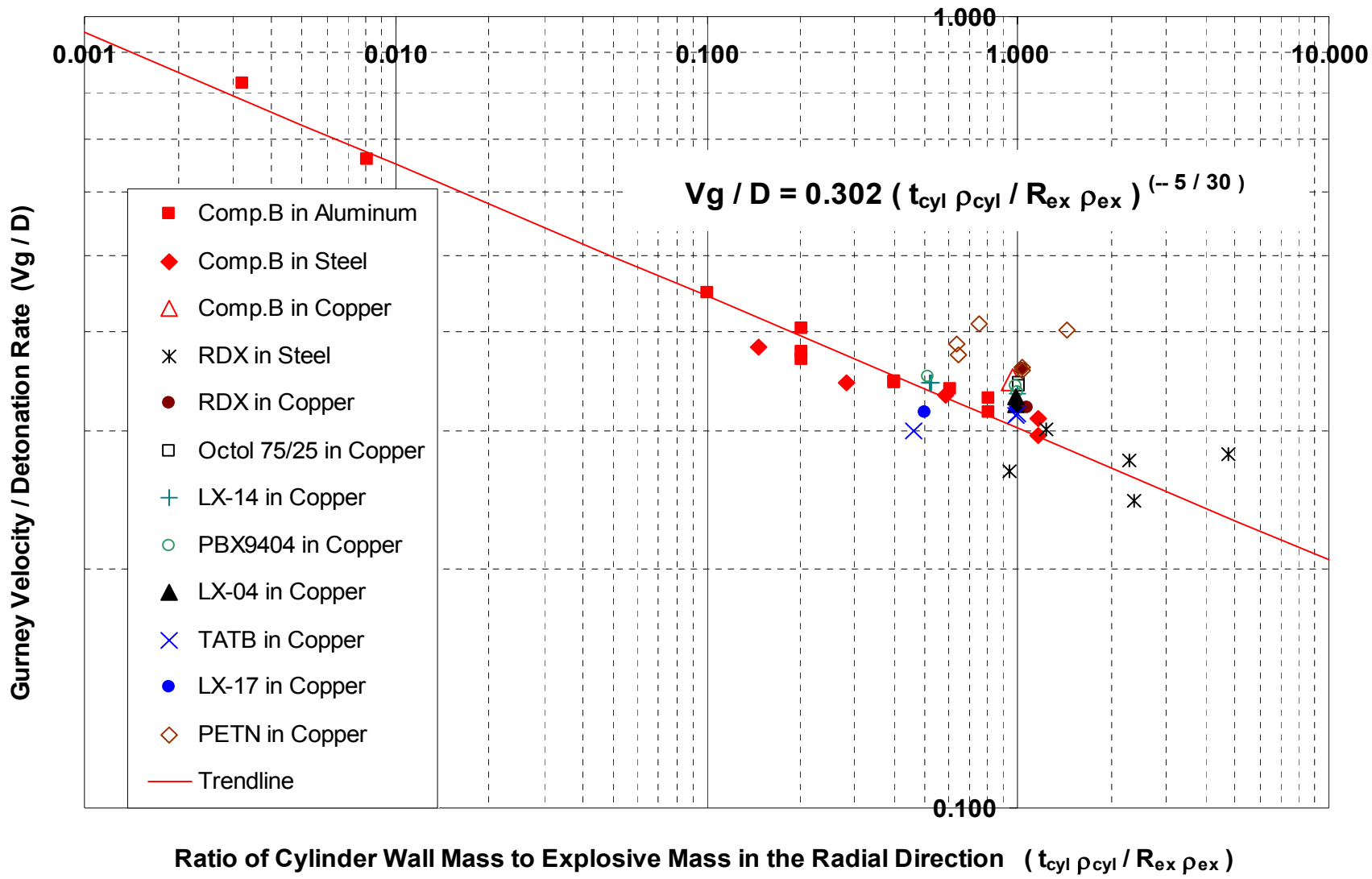
Copper Cylinders

<u>V_g / D</u>	<u>Exp. (Licht)</u>	<u>Cooper</u>	<u>Roth</u>	<u>HK/ KH</u>
TNT	0.346	0.346	0.350	0.351
Comp B	0.345	0.343	0.355	0.385
Octol	0.335	0.330	0.331	0.328
LX-14	-----	0.326	0.348	-----
PETN	0.359	0.355	0.369	0.331

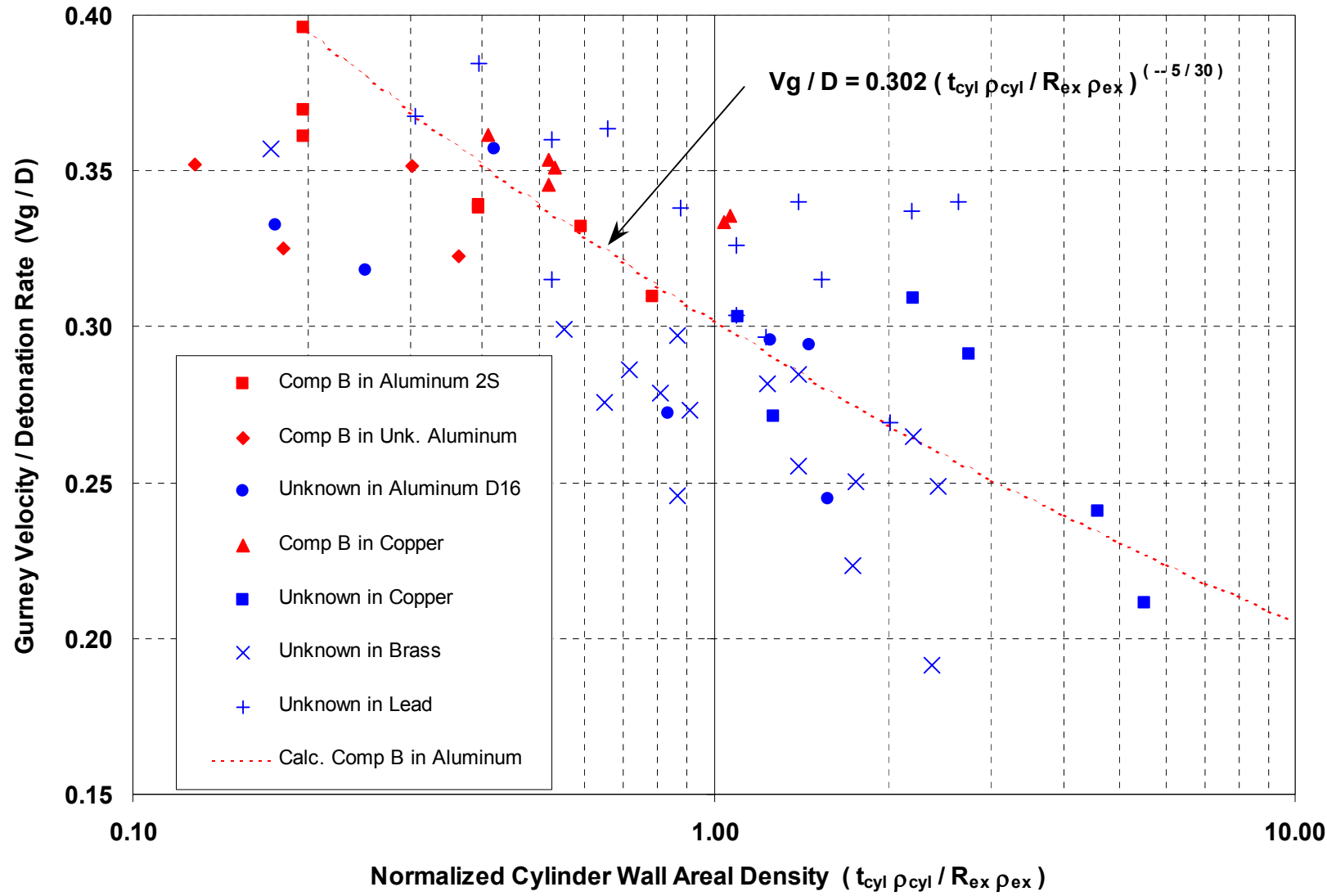
Comparison of Gurney Velocities on the Basis of Cylinder Wall Areal Density from 2-inch Diameter Cylinder Tests Using Comp. B Explosive



Ratio of the Gurney Velocity to an Explosive's Detonation Rate versus a Radial-Projection Areal Density Ratio



Normalized Gurney Velocity Data from Measurements of Cylinder Wall Velocity at Fracture Time



BRIGS Two-Step Detonation-Driven Propulsion Model

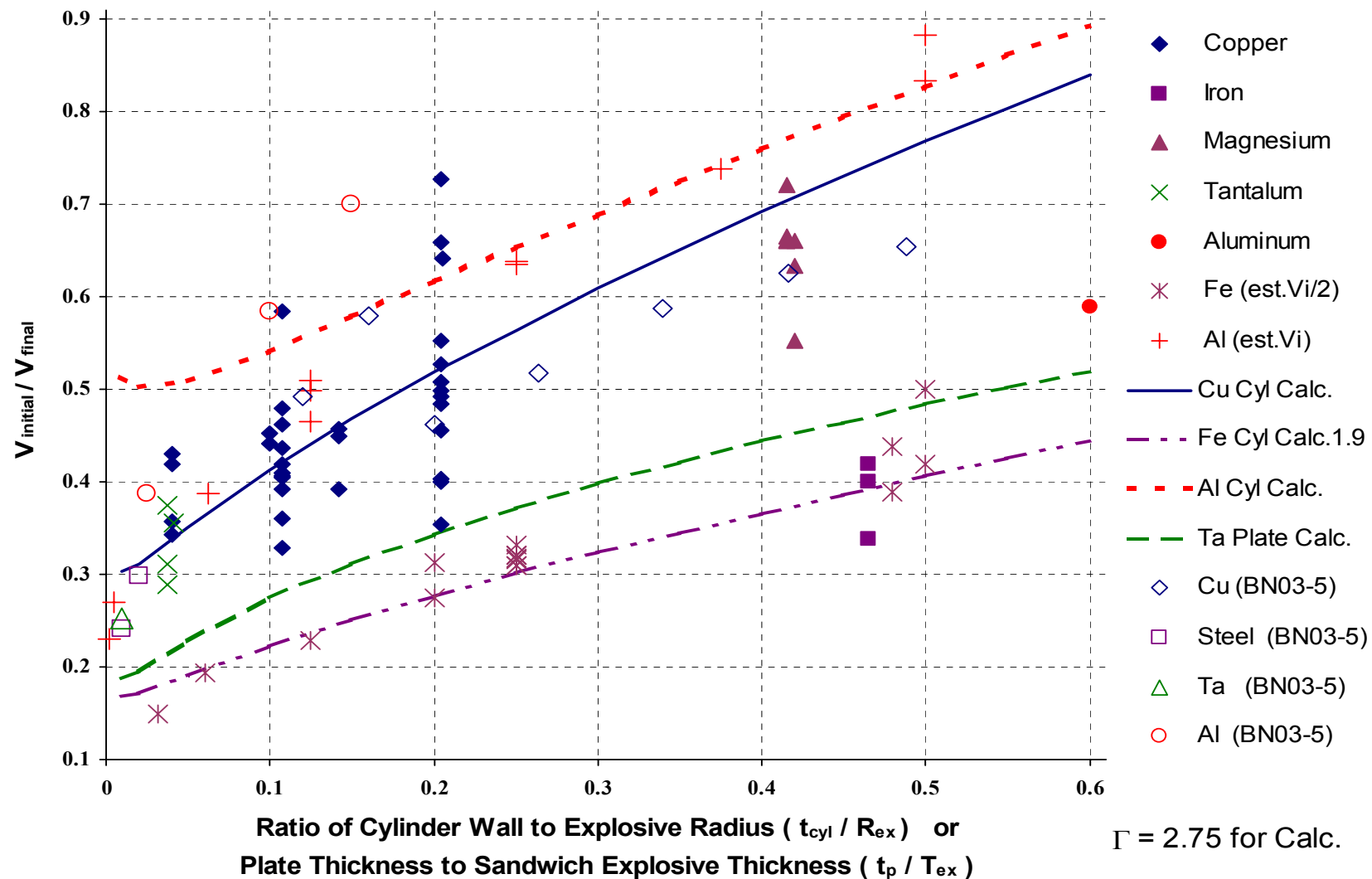
Initial motion:

- imparted by a brisant shock-dominated process that depends upon intimate contact of explosive with propelled material
- envisioned as caused by higher-pressure region of detonation front (envision the von Neumann spike or reaction zone region as a finite thickness of solid material squeezed at high pressure)

Gas-push (*gas-dynamic*) propulsion:

- envisioned similar to that assumed by Gurney modeling (gaseous product expansion from a homogeneous “all burnt” condition while pushing confining boundaries to a final “steady-state” velocity as the pressure drops)

$V_{\text{initial}} / V_{\text{final}}$ Data Plotted for Cylinders and Plates of Various Inert Materials and Explosives



New *formulas* improving insight into detonation-driven propulsion

Initial velocity imparted to cylinder wall

$$V_i / D = 0.2085 (\rho_{cyl} / \rho_{ex})^{-1/2} (t_{cyl} / R_{ex})^{-3/40}$$

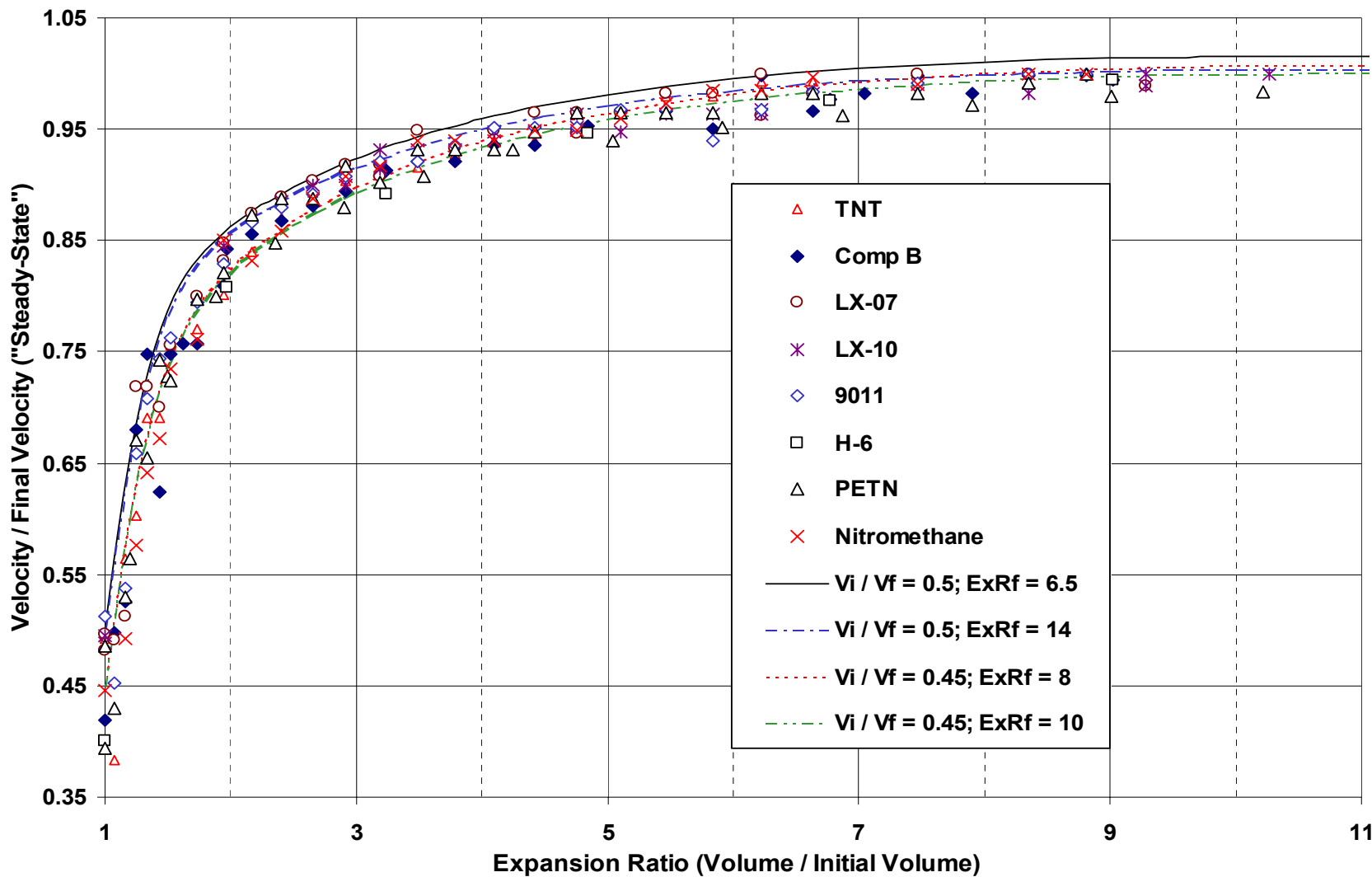
Equation for cylinders describing *ratio* of velocity imparted by *initial* coupling *to final* velocity

$$V_i / V_f = 0.3446 [\Gamma - 1] (t_{cyl} \rho_{cyl} / R_{ex} \rho_{ex})^{(5/30)} (t_{cyl} / R_{ex})^{-3/40} \\ [(t_{cyl} / R_{ex})^2 + 2 (t_{cyl} / R_{ex}) + 0.5 (\rho_{ex} / \rho_{cyl})]^{1/2}$$

V_i = initial free-surface velocity
 V_f = final “steady-state” velocity

Transition Pressure (Gpa)	
Aluminum	20.5
Carbon (pressed graphite)	23
Iron (0.2 wt% Carbon)	14.7
Iron (0.5 wt% Carbon)	13
Titanium	9.4

Normalized Velocity Data for Eight Explosives Driving Copper Cylinders



Equation for *instantaneous* velocity (Ver) as a function of the gaseous detonation products expansion ratio (ExR)

$$Ver / Vf = V1 / Vf + V2 / Vf$$

$$V1 / Vf = (Vi / Vf) [(e^{-ExR} - e^{-ExR^3}) + (\{ ExR / ExRf \}^{-1/2} / [1 / ExRf]^{-1/2})]$$

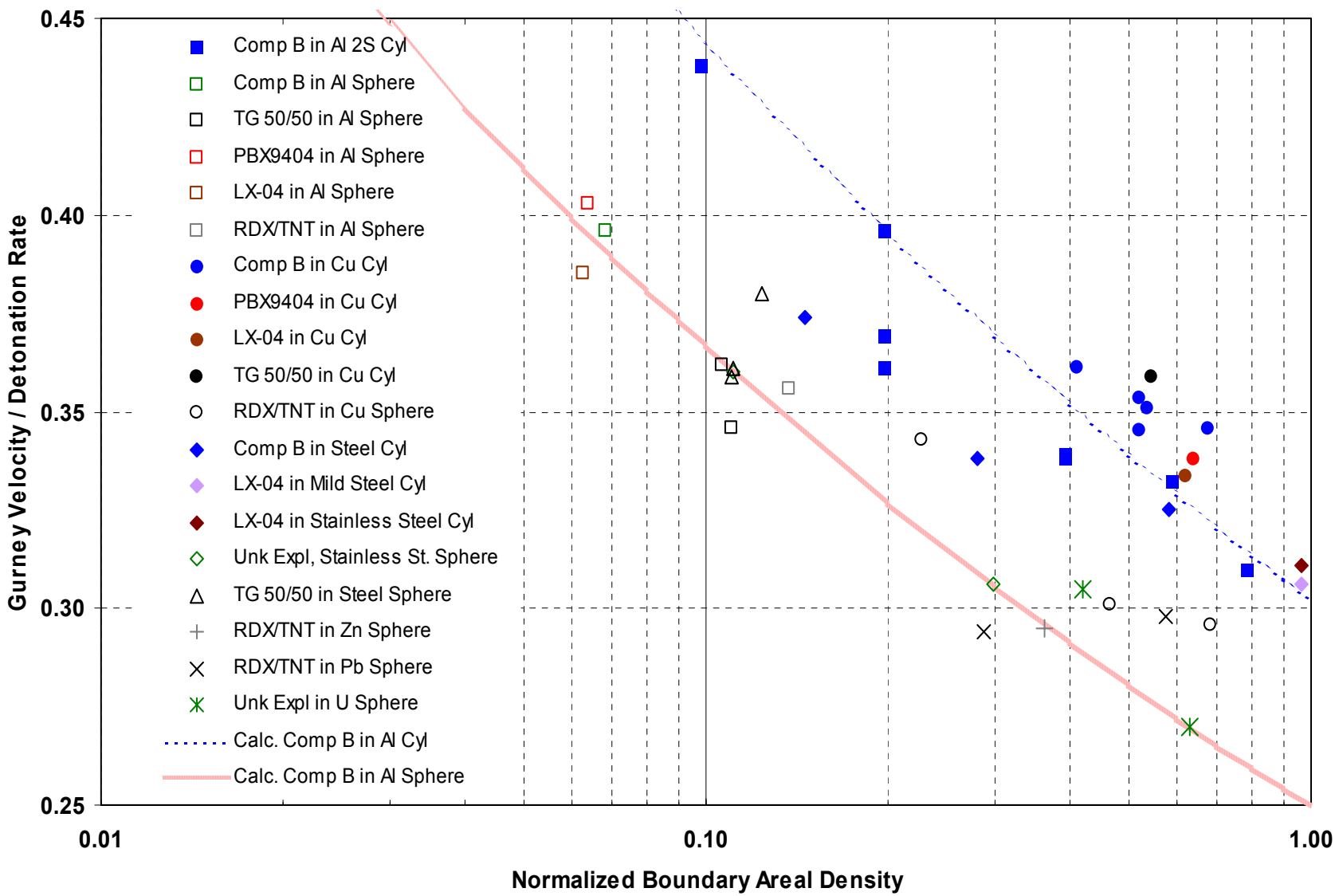
$$V2 / Vf = [1 - \{ (Vi / Vf) / (1 / ExRf) \}^{-1/2}] (ExR / ExRf)^{-1/3} [\log (ExR) / \log (ExRf)]$$

Vi = initial free-surface velocity

Vf = final “steady-state” velocity at final expansion ratio (ExRf)

(Equation was fitted “by eye” using MathCad™ software.)

Normalized Gurney Velocity Data for Some Explosives in Cylinders and Spheres of Different Materials



The important message is

material properties and geometry
affect Gurney Velocity measurement

The trend of these effects was demonstrated in:

- Cylinder tests (copper, aluminum, and steel)
- Fragmentation tests (copper, aluminum, etc.)

New data and analysis are needed:

- Published data were not specifically taken to reveal the effects
- Most copper cylinder test data taken at $(t_{cyl} \rho_{cyl} / R_{ex} \rho_{ex}) \approx 1.0$
- Gurney (Lagrange) assumptions may not be valid

New opportunities:

- Gurney values would reflect materials & geometry
- To define effect of cylinder wall phase transitions

Another important message is

**that *gas-dynamic* propulsion by
many explosives is similar**

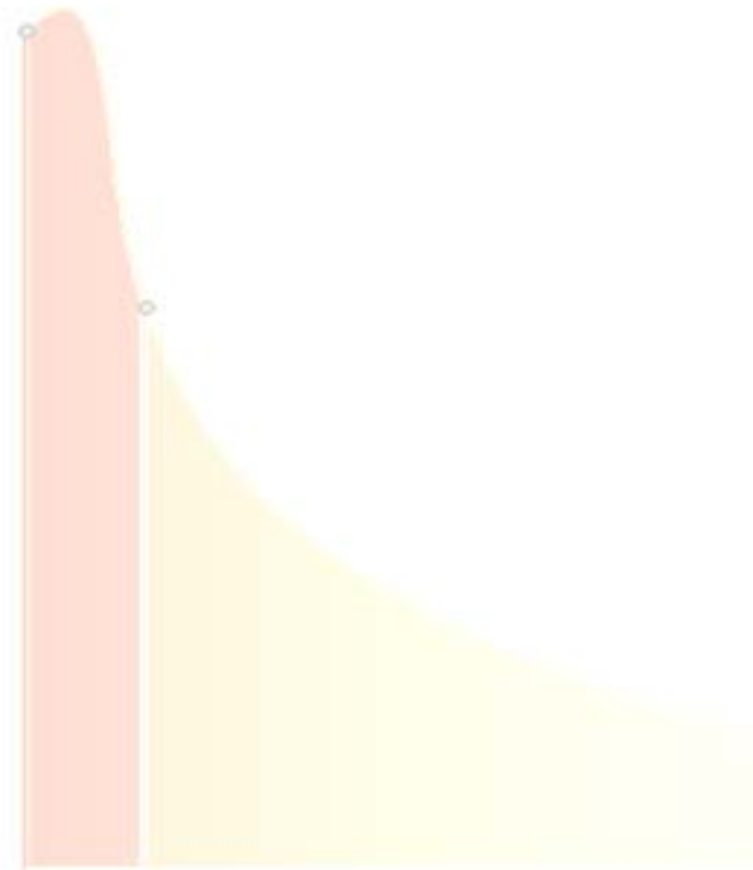
Differences between explosives arise from:

- V_i (solid-state detonation coupling effects)
- Total convertible energy (i.e. V_g from V_f at ExR_f)
- Time needed to convert total energy to kinetic energy of boundary materials & detonation products

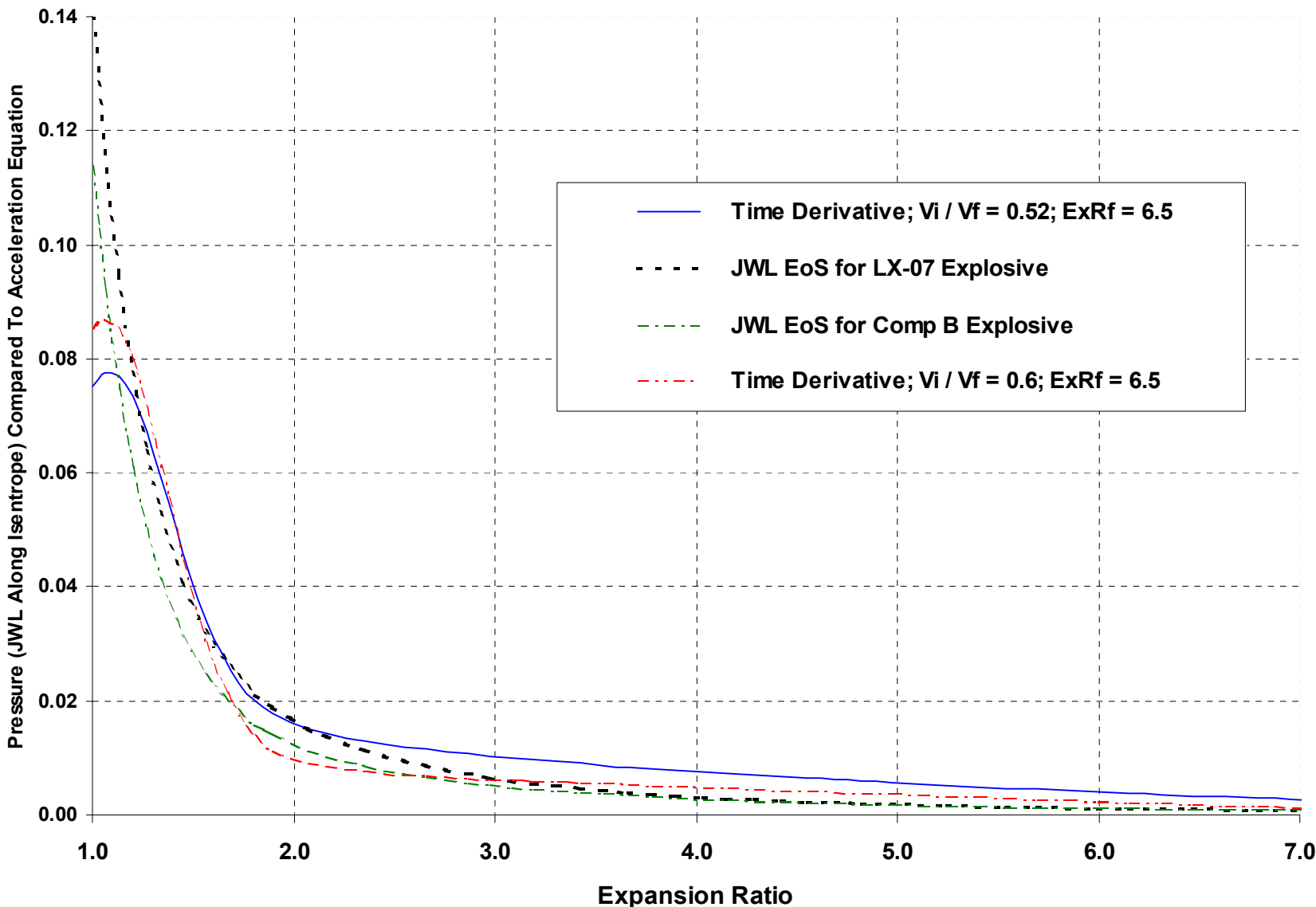
New, more accurate data are needed:

- V_i [grazing wave] using interferometry and various materials subject to phase transitions
- V_f data at larger ExR_f [beyond 6.5 to 10 - 14]
- Not sure that Gurney (Lagrange) assumptions valid [need more data from V_i to $ExR = 2$ & beyond]

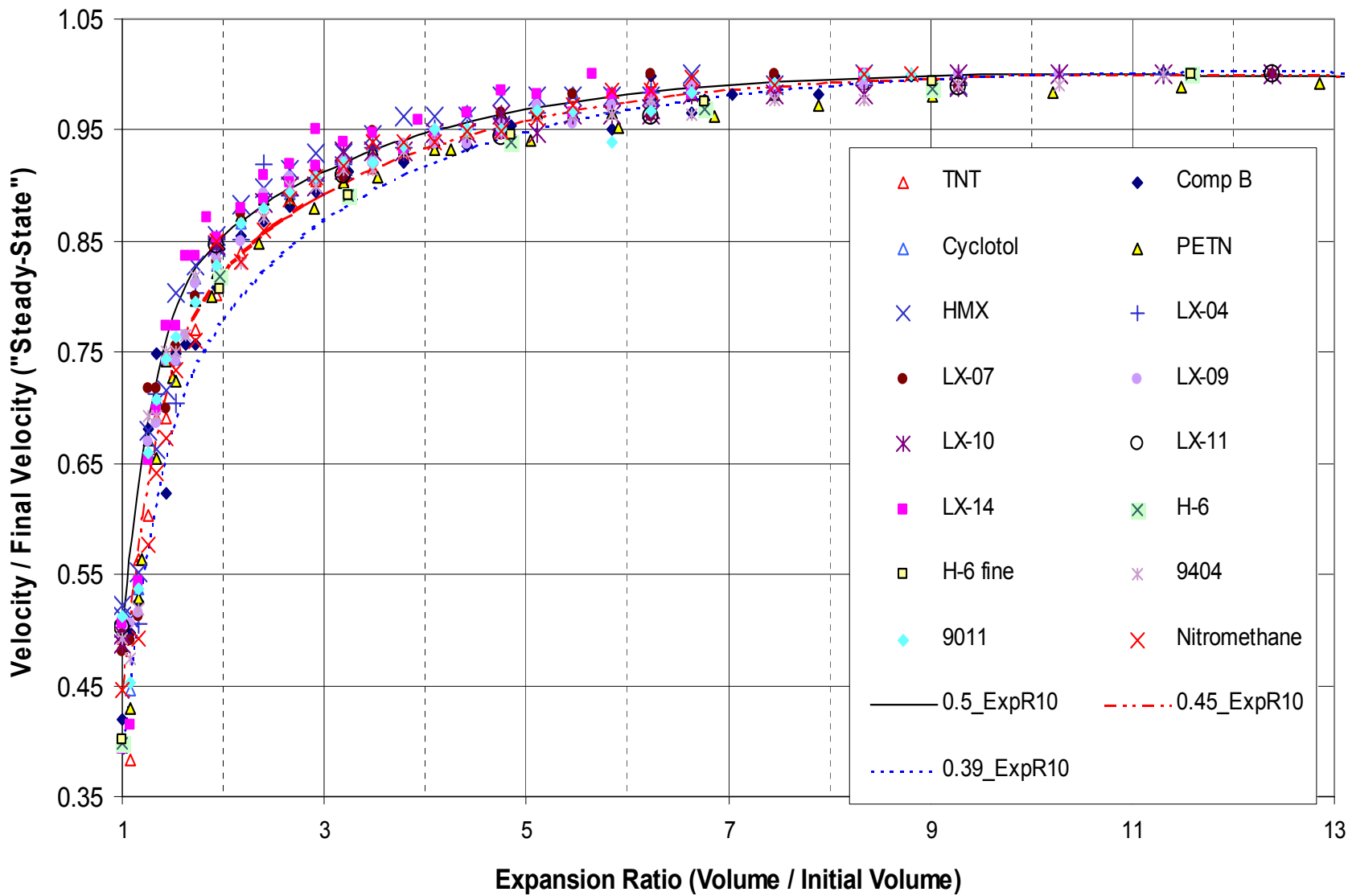
Additional Backup Information
Follows



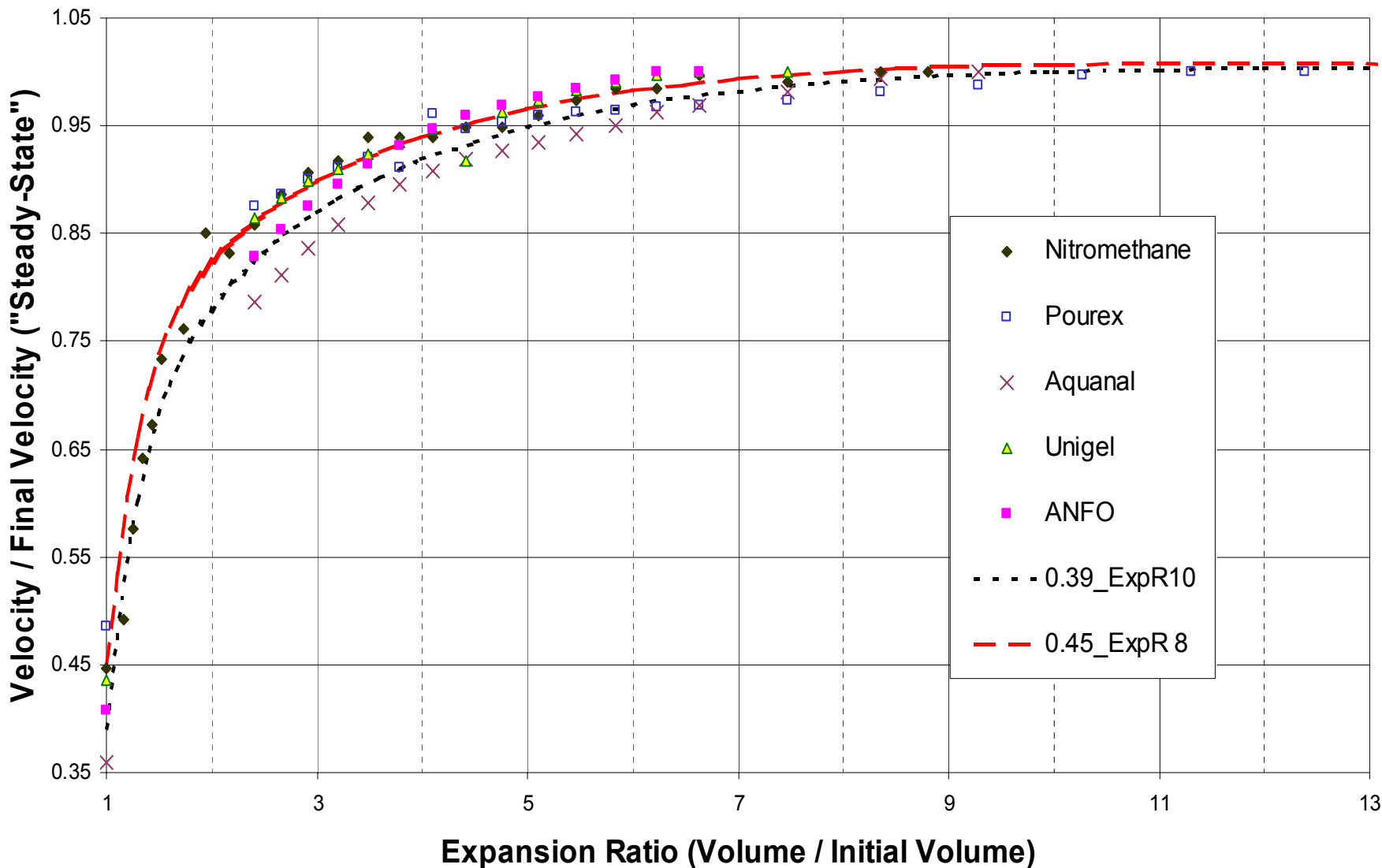
Comparison of JWL Calculated Pressures to the *Time Derivative* of the *Instantaneous Velocity* Equation for an Expanding Cylinder



Non-Dimensional Velocity as a Function of Explosive Volume Expansion for Sixteen "Ideal" Explosives



Non-Dimensional Velocity as a Function of Explosive Volume Expansion for Five Commercial Explosives



Currently available trend-line

$$Vg / D \cong (0.605 / [\Gamma-1]) (t_{cyl} \rho_{cyl} / R_{ex} \rho_{ex})^{-5/30}$$

(J. Roth per J.E. Kennedy) -- expanded

For use with

$$Vf = Vg (\rho_{cyl}/\rho_{ex})^{-1/2} [(t_{cyl}/R_{ex})^2 + 2 (t_{cyl}/R_{ex}) + 0.5 (\rho_{ex}/\rho_{cyl})]^{-1/2}$$

Future work

$$Vg / D \cong (0.60 \phi^{-1/2} + 0.648 \rho_o^{1/2}) / (1.01 + 1.313 \rho_o)$$

(Hardesty & Kennedy / Kamlet & Hurwitz)

$$Vg-p / D \cong (0.541 / [\Gamma-1]) (t_{cyl} \rho_{cyl} / R_{ex} \rho_{ex})^{-5/30}$$

(Gas - push contribution model)



3-D Finite-Element Gun Launch Simulation of a Surrogate Excalibur 155-mm Guided Artillery Projectile - Modeling Capabilities and its Implications

22nd International Symposium on **BALLISTICS**

Interior Ballistics/Launch Dynamics Oral Session #2

17 November 2005

Authors: M.R. Chowdhury² and A. Frydman²,
J. Cordes³, L. Reinhardt³ and D. Carlucci³

² U.S. Army Research Laboratory, AMSRD-ARL-WM-MB (ALC), Weapons & Materials Research Directorate, Adelphi, MD 20783-1145; POC Phone: (301) 394-6308; email: mchowdhury@arl.army.mil;

³ U.S. Army ARDEC, Analysis and Evaluation Division, AMSRD-AAR-AEP-E, Picatinny, N.J. 07806-5000



Overview



- ❖ Objectives
- ❖ XM-982 - Excalibur Projectile
- ❖ Challenges
- ❖ SRV FEM Models
- ❖ Results & Impacts to Excalibur Program
 - ❖ Validation & Verification.
 - ❖ Utility of 3D FE Models.
- ❖ Conclusions & Recommendations.



Objectives



155-mm, extended-range, guided munition

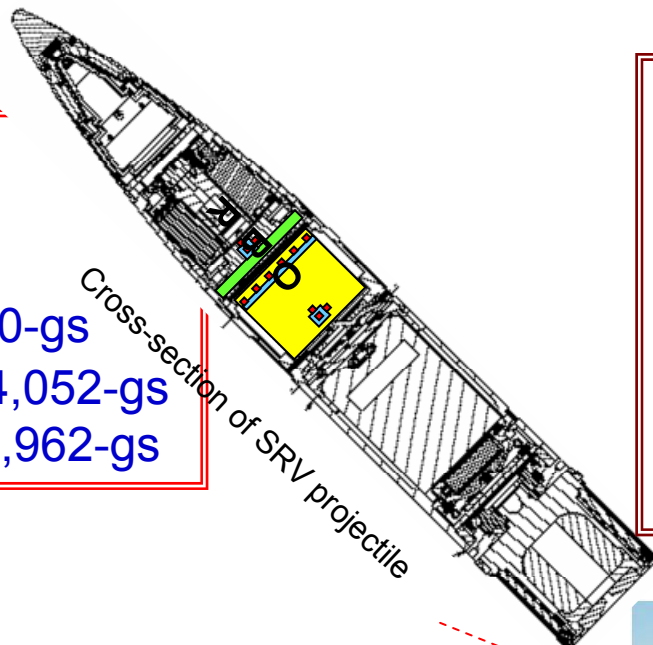
- To develop and validate a 3D FE model capable of simulating launch environment of the Excalibur projectile.
- To predict component loads and support the design of artillery launched guided projectile components.
- To support failure investigation of critical projectile units in an evolving design environment.



XM-982, Excalibur Artillery Launched Guided Projectile

Demanding g Requirements

- In Bore: Axial- 15,800-gs
- Muzzle Exit: Axial - 4,052-gs and balloting 3,962-gs



ISSUES

- Increasing use of sensitive electronics in a guided projectile.
- Survivability of MEMS is a major concern.

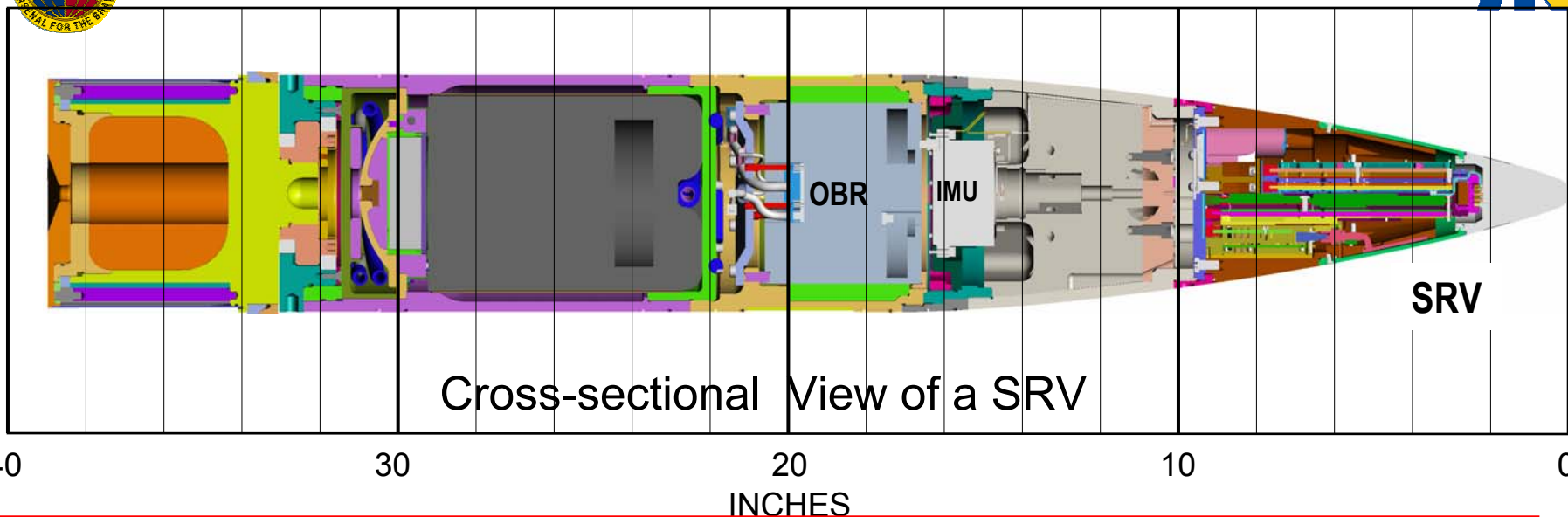
Design Development Methods

- Limited field tests
- Virtual simulation of launched environment using a detailed 3D FEM.





Challenges

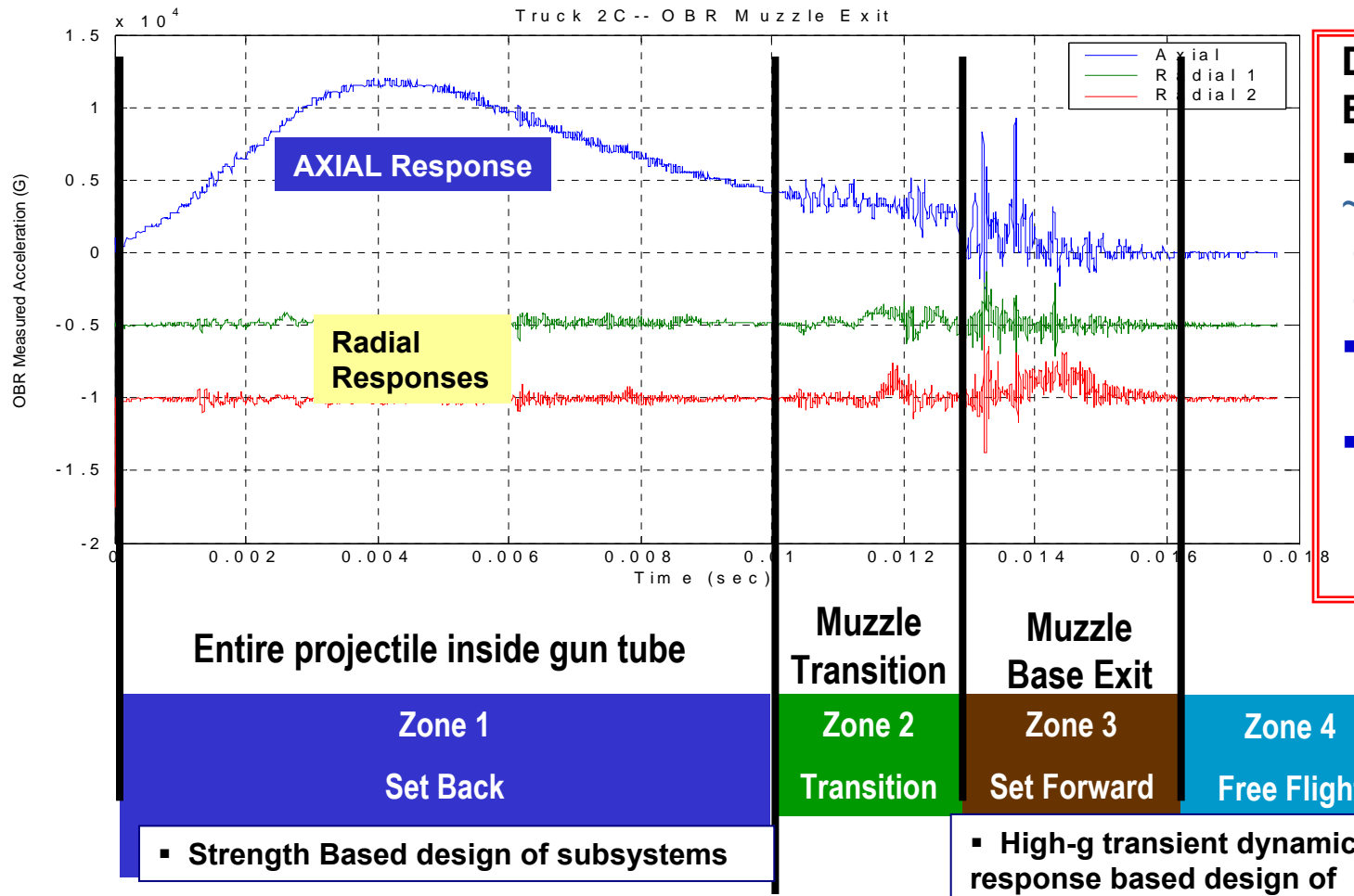


- Obtain physics-based representation of a highly complex structural configurations & interactions
- Provide real-time design driving guidance to evolving development of projectile's structure
- Achieve "fast-turn-around" version of a representative 3D transient model inherently "lengthy"
- Obtain accurate & representative validation test data- difficult to keep up with the test program
- Address "test-based" malfunctions or failures



Artillery Launched Guided Projectile –

Typical Launch Response Environment



✓ Uncertain Design Environments

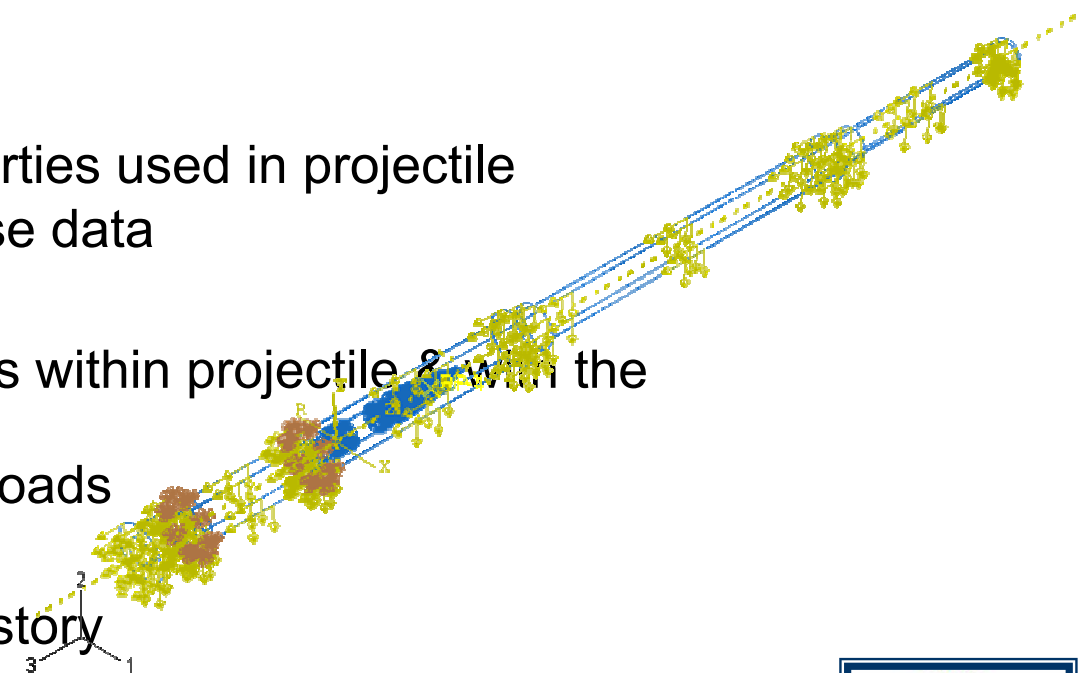


3D FEM of SRV Projectile –

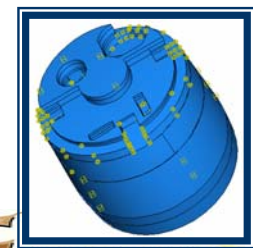
Modeling Barriers & Issues



- Geometry
 - Degree of defeathering
 - Degree of compatibility of CAD and CAE platforms
 - Art and Science
- Material Models
 - Inexact material properties used in projectile
 - Correlate with response data
- Internal constraints
 - Ties vs contact of parts within projectile & within the gun
 - Joints and transfer of loads
- Loads
 - Base pressure time history
 - Gun & geometry
- Boundary Conditions
 - Trunions' effect



Original



Defeatured



3D FEM of SRV Projectile –

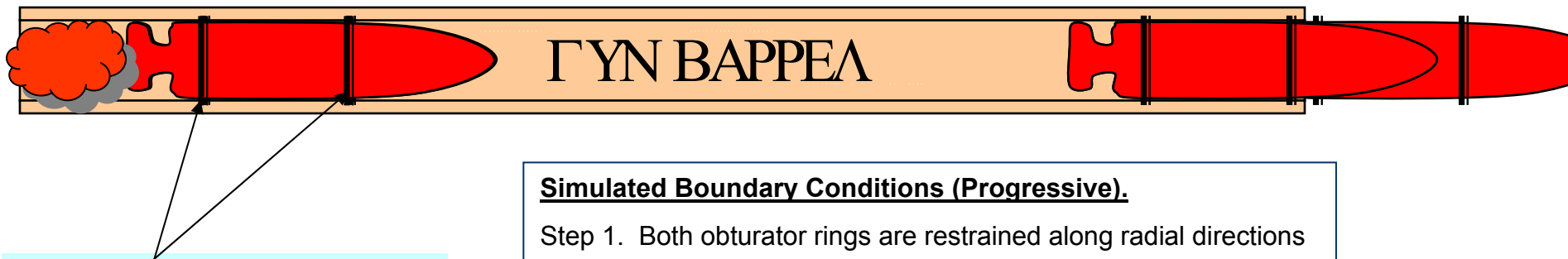
Modeling Cases & Conditions

- ❖ Over 50 modeling cases were run including:
 - Projectile systems & variations
 - Subsystem/components – [IMU](#), [GNU](#) etc.
 - Gun barrel interactions
 - Spinning and balloting effects
 - Verification/validation/model consistency check
 - Sensitivity analyses
 - Joint compliance/joint loads
 - Gravity gun droop
- ❖ A selected subset of cases is discussed next.



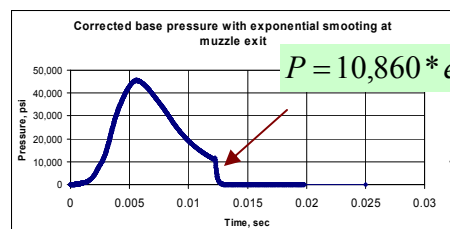
3D FEM of SRV Projectile –

NO Gun Barrel in Model (old SRV)



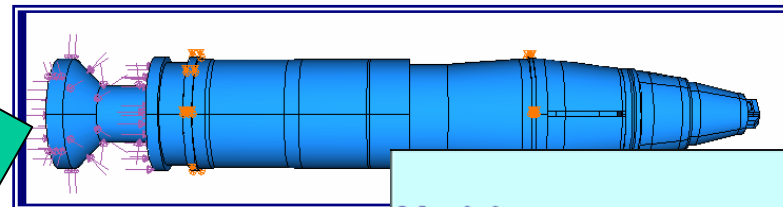
Simulated Boundary Conditions (Progressive).

- Step 1. Both obturator rings are restrained along radial directions
- Step 2. Only back ring is restrained along radial dir.
- Step 3. Free- BCs



High-g impulsive thrust (Typical)

“Projectile-only” FEM is capable of predicting Design loads for most subsystem design.



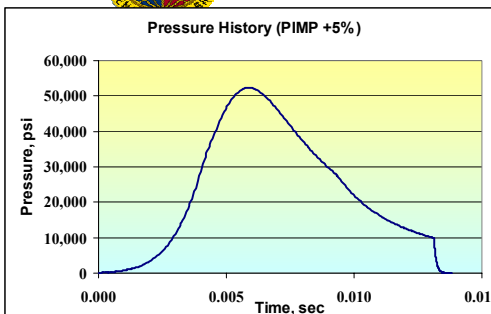
Model	Bp1-Step3-Tie-P76-V5
# DOFs	556,680
# Elements	123,399
Total weight in lbs	104.58
C.G. from the bottom of Boom	
Base in in.	16.87
CPU Time in sec, 8 CPUs	748.041



3D FEM of SRV Projectile –

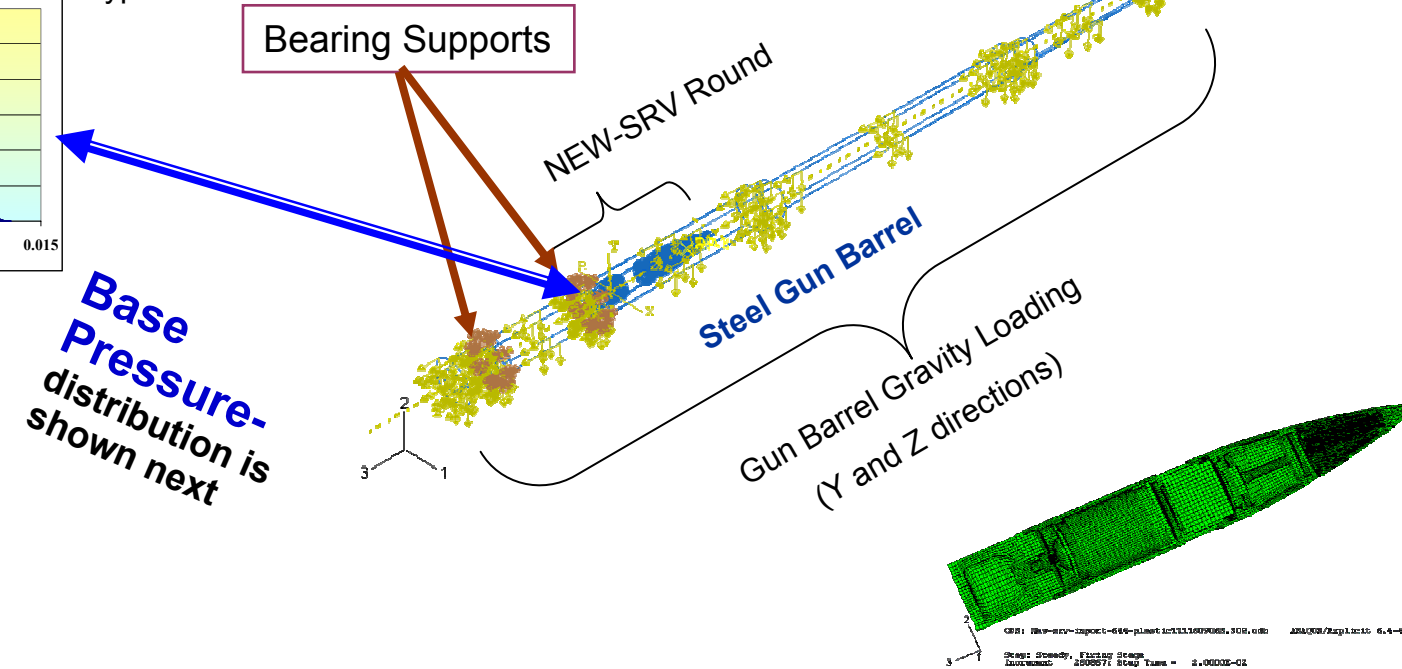


Gun Barrel/Projectile Interaction Model



Typical

Base Pressure-
distribution is
shown next

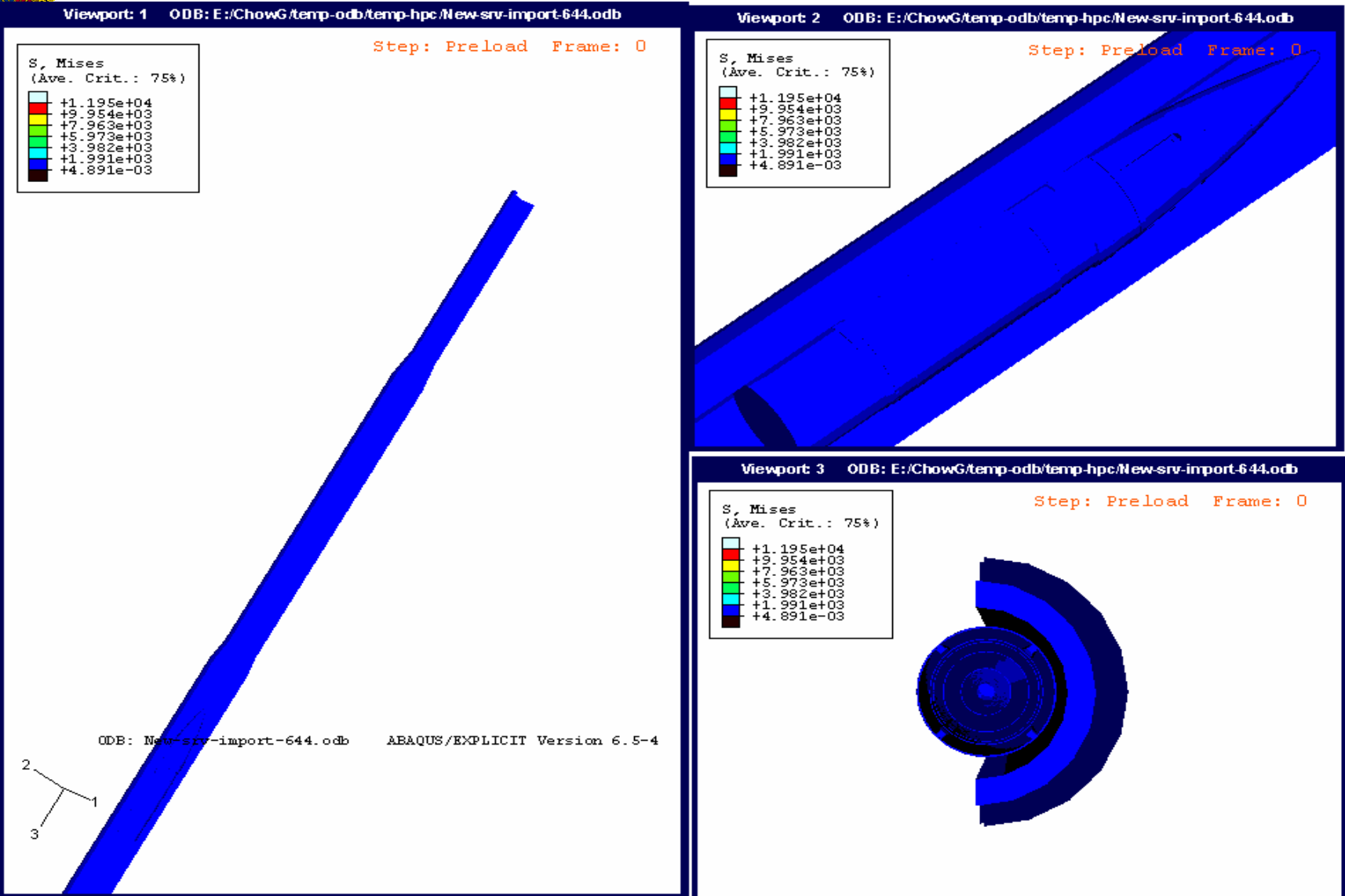


Model	New-SRVspin import-644.dat
# DOFs	1,124,979
# Elements	374,992
Total weight in lbs (Projectile)	105.78
C.G. from the bottom of Base in in.	13.78

CPU time r.t. No barrel ~ 3-4 X



Sample Analysis Results 3D SRV FEM- Components shock environment





3-D FEM of SRV Projectile –

FEM With and Without Gun Barrel – advantages & disadvantages



- **Gun Launch Simulation FEM with Barrel**
 - Increases the computational cost; dof's are almost twice the no-gun simulation case
 - Gun barrel interaction phenomena is critical to electronics' survivability analysis
 - High-g transient load for design of embedded electronics components can be predicted using this FEM.
- **Gun Launch Simulation FEM without Barrel**
 - Design loads for stress adequacy of subsystems can be effectively predicted.

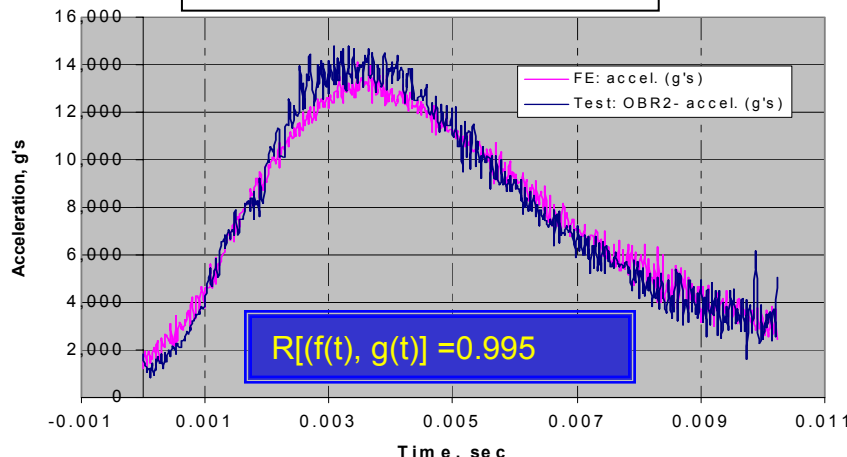


FEM Validation - during launch process in 155-mm Gun

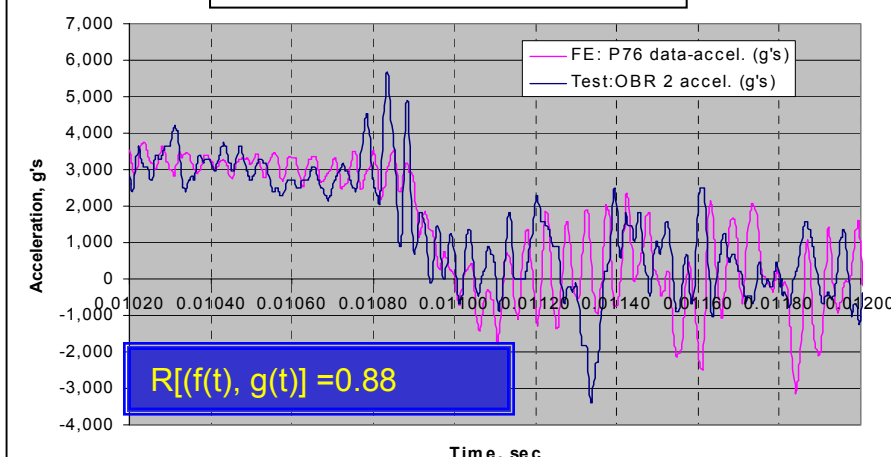
Comparison of **Simulation vs. Test** response at OBR Location



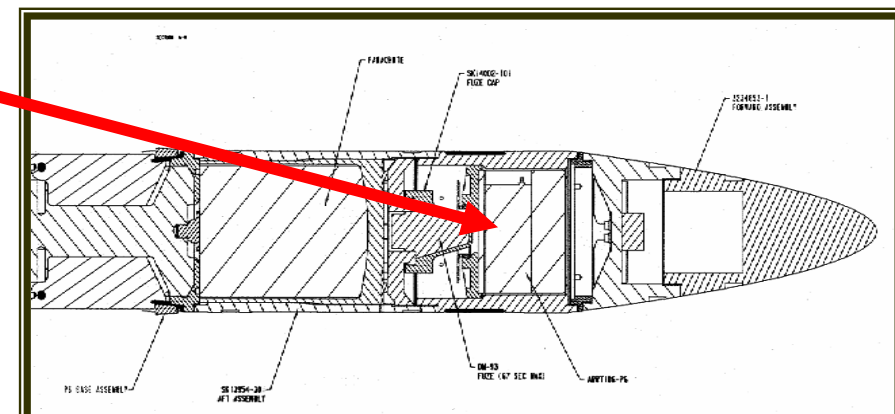
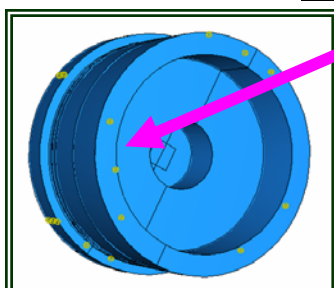
Setback Axial Response



Muzzle Exit Axial Response



OBR accelerometer

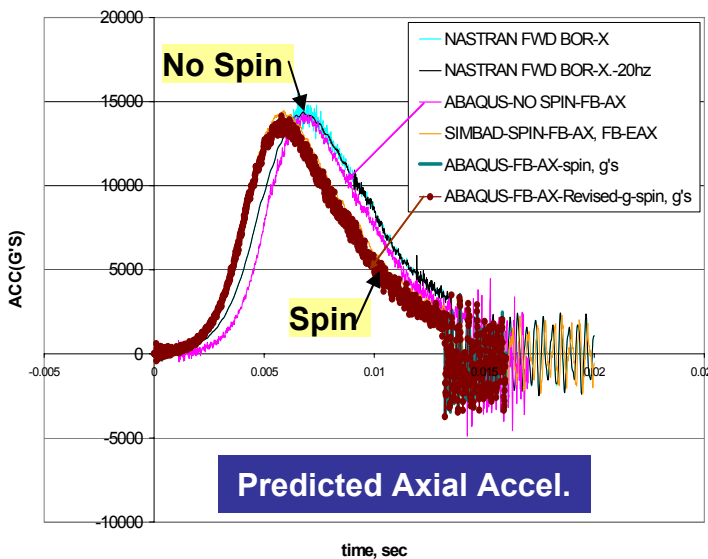
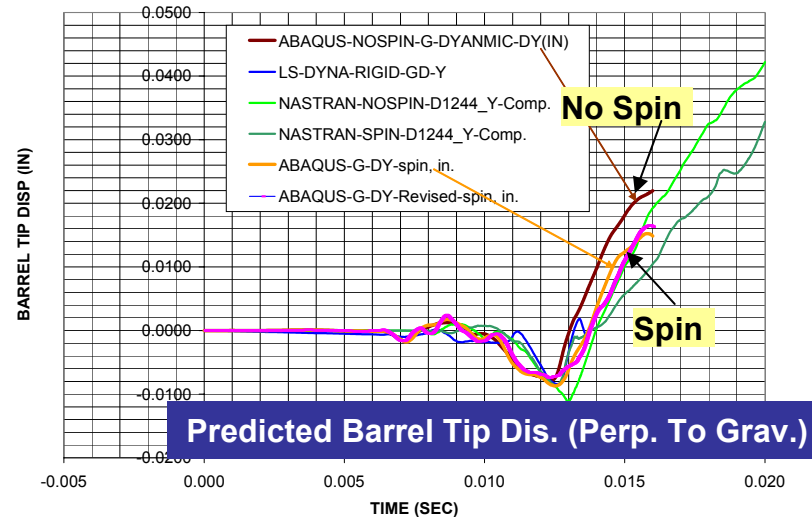
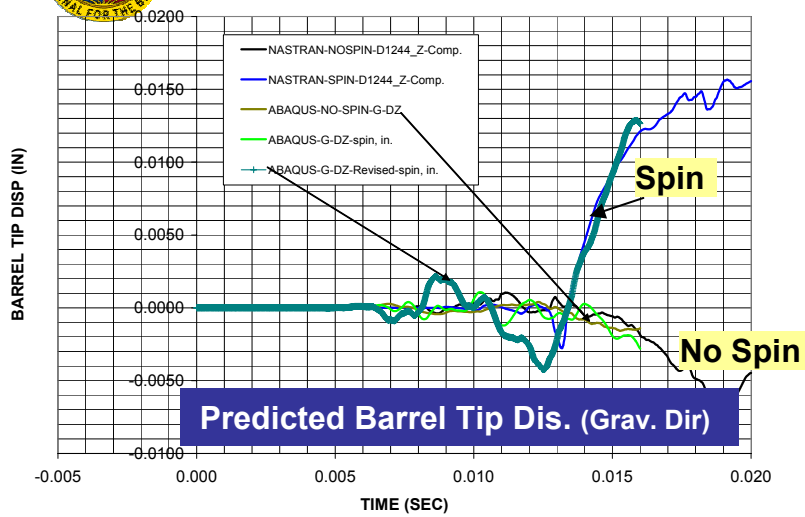


- Predicted and test responses are reasonably well correlated for the event
- BP1 Configuration with NO gun FEM

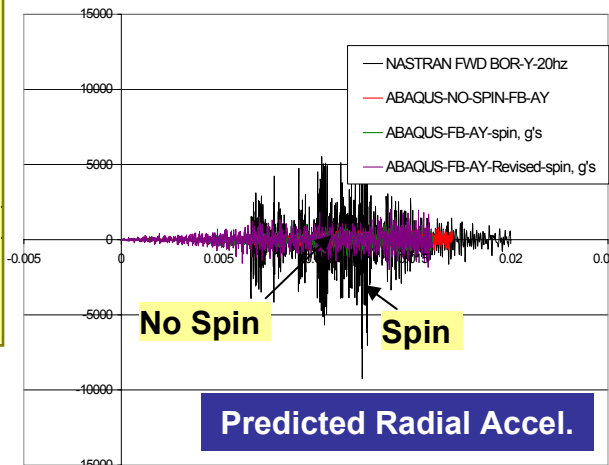


Multiple FEM Verification – barrel projectile model

Comparison of Simulated Spin vs. No Spin Responses using Different FE Codes



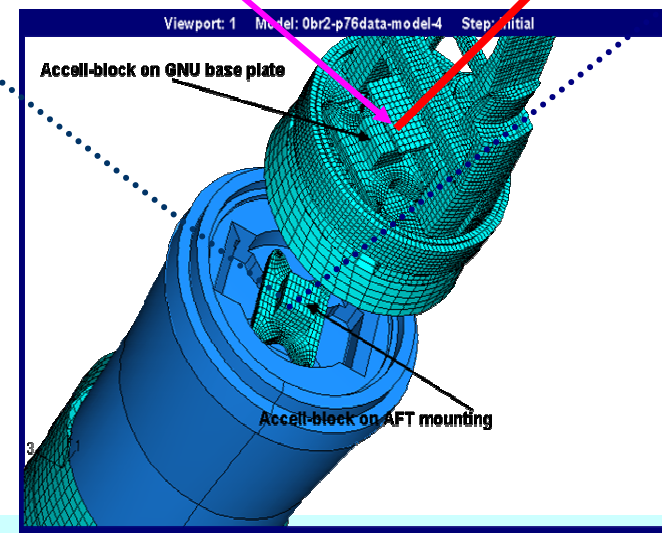
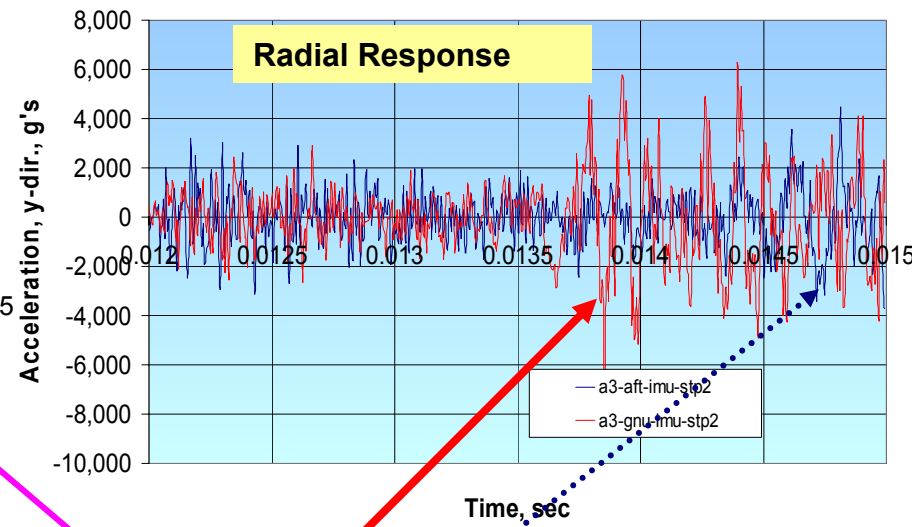
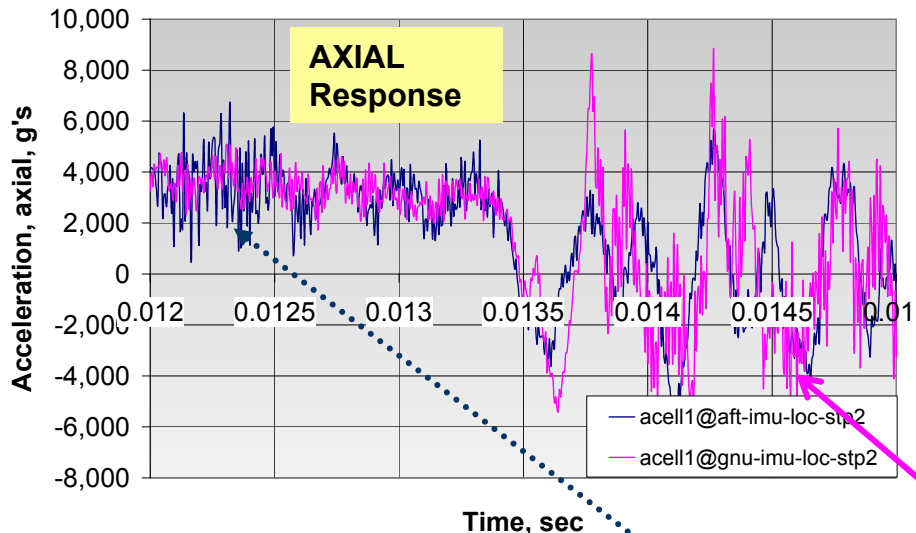
Qualitative agreement among predicted results using various FE codes **verifies** the effectiveness of the FEM.





Utility of 3D Transient SRV FEM -

Locating suitable mounting locations of sensitive electronics components



□ Comparison of simulated responses:

G's at Forward location ~ 8,500

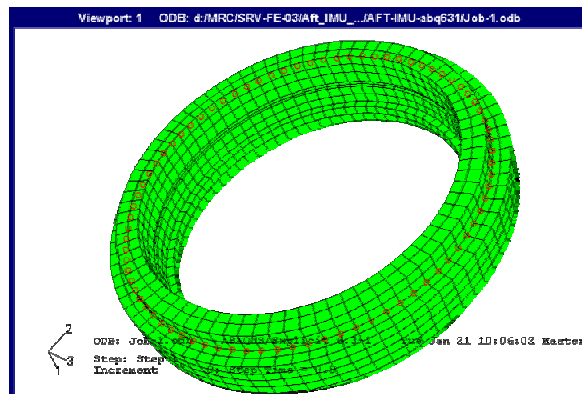
G's at AFT location ~ 3,000

Demonstrates the effectiveness of FEM in evaluating design concepts.



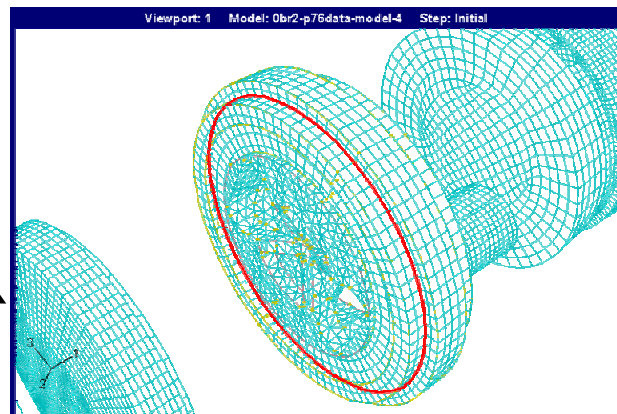
Utility of 3D Transient SRV FEM -

Sub Modeling Analysis –Micro-Level failure Investigation of IMU

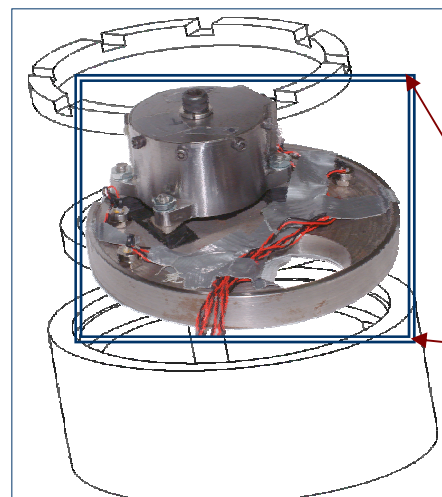


Top Driven Nodes from Global Model

ABAQUS Global Response From 3D FEM



Bottom Driven Nodes from Global Model



Time Saving Estimate $\geq 10X$

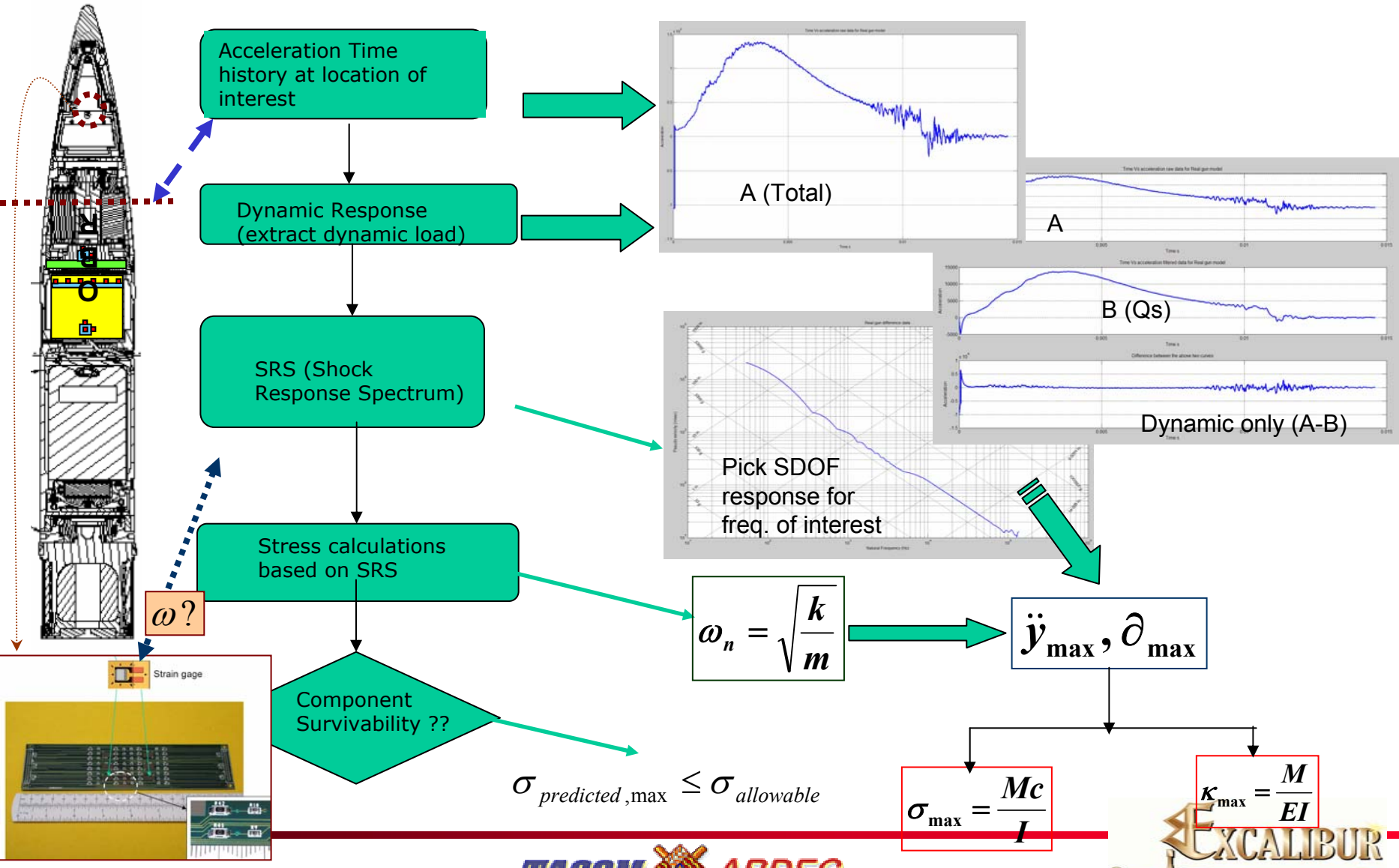
❖ Local detail FEM of IMU
❖ Global FEM provides input loads for this Local FEM

- Predicted global Accel. for driven nodes are used for sub modeling evaluation of the IMU device.
- Local detail FEM of the IMU is used thereby saving computational time.



Utility of 3D Transient SRV FEM –

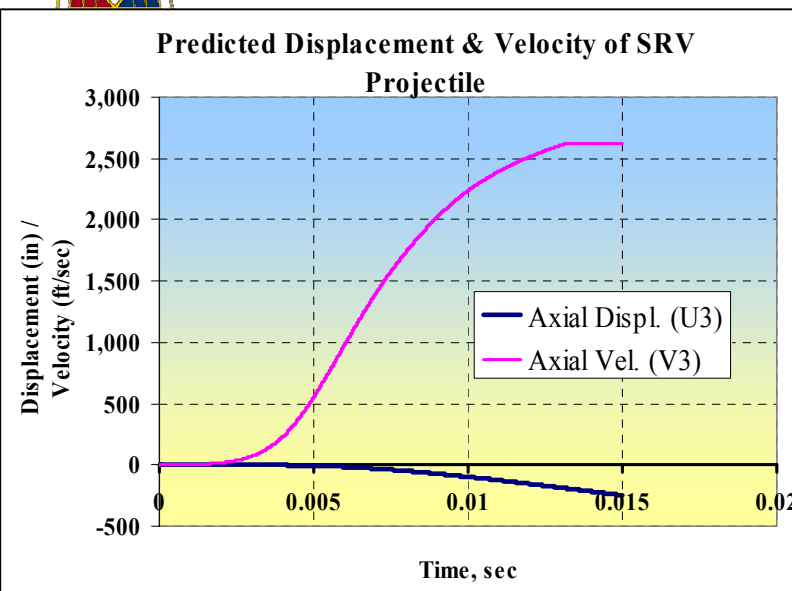
Failure Investigation of MEMS



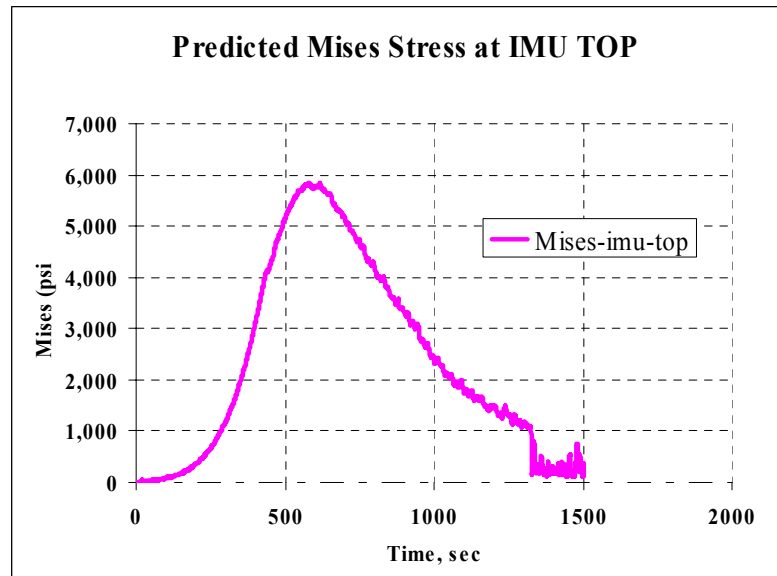
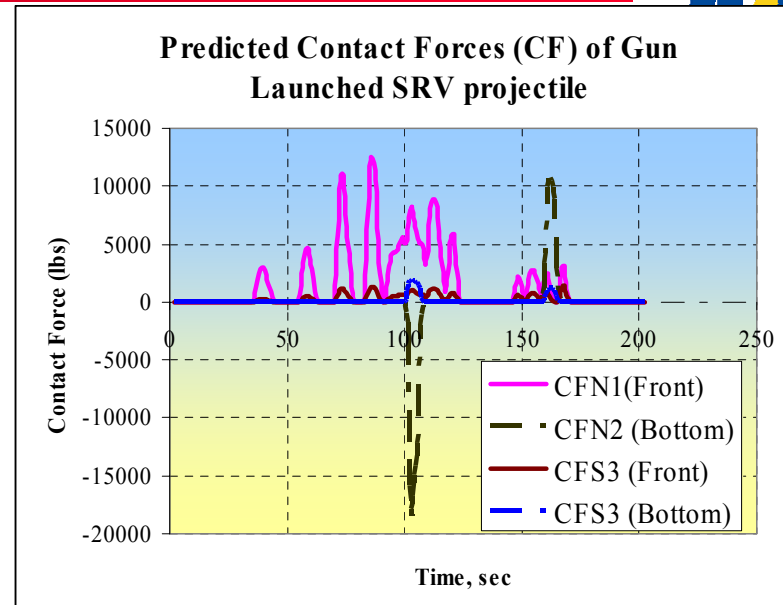


Predictive Capability of SRV FEM-

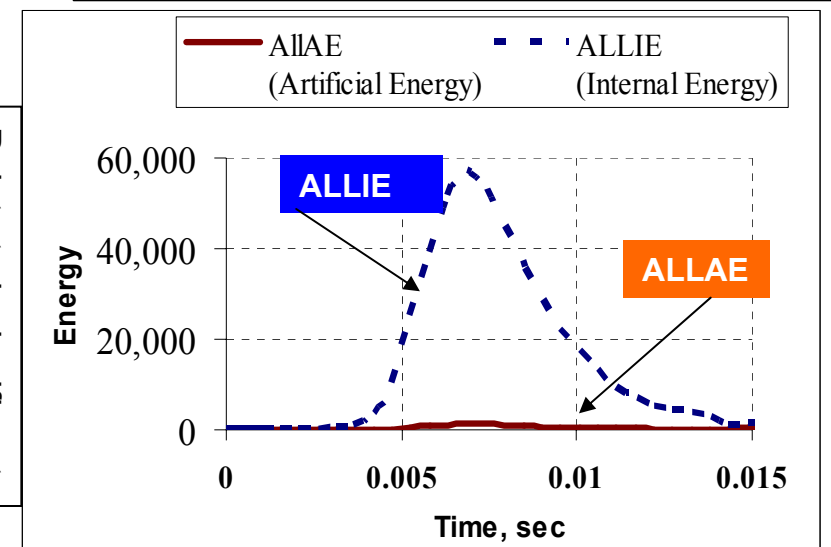
General behavior is explained



Traveled distance and the muzzle velocity compared closely with field values



Points to insignificant hourglass problem.



ALLAE vs. ALLIE



Conclusions & Recommendations

- ❖ Virtual simulation of a system behavior using a validated and verified FEM provides a flexible and powerful design evaluation tool for the future sophisticated systems.
- ❖ Gradual development of FEM starting with a simple model and then progressively adding features to improve the model capability is important in the development of a complex system such as the SRV projectile discussed here.
- ❖ Validation of FEM with measured results is desired, however, verification with alternative predictive tools may be used as an alternative.

School of Materials

**The Effect of Boundary Conditions on the
Ballistic Performance of Textile Fabrics**

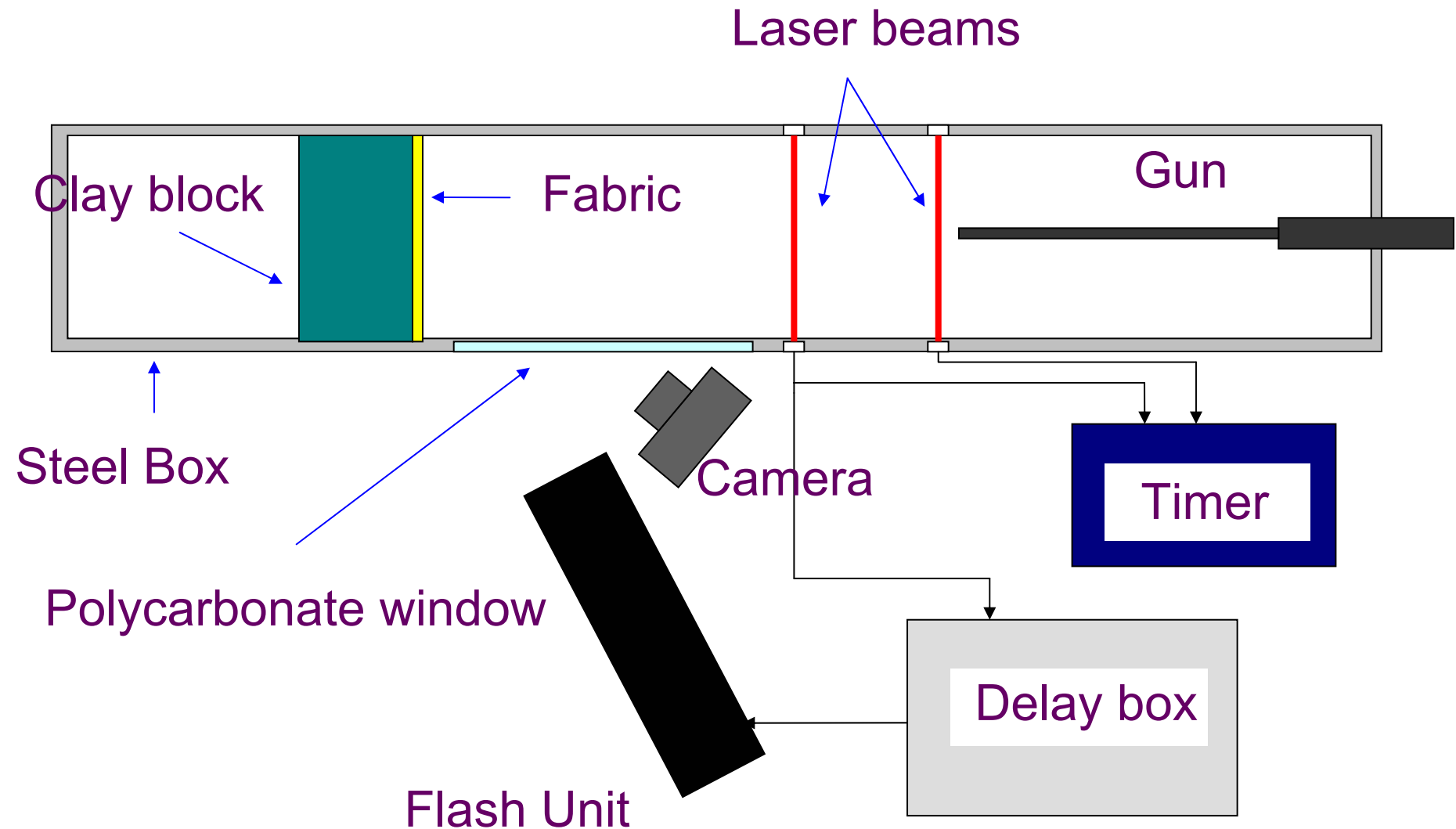
Colin Cork

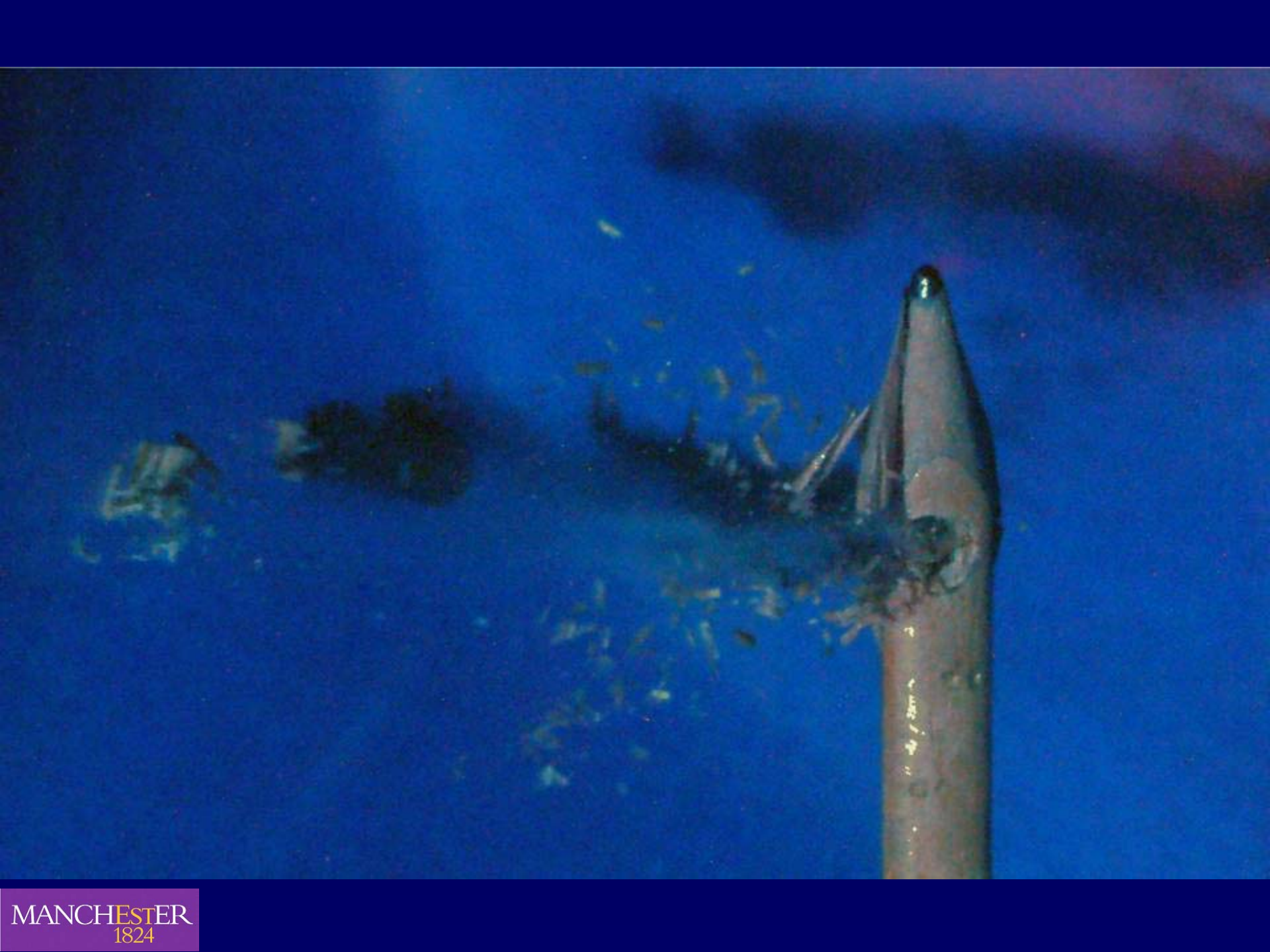
colin.cork@manchester.ac.uk



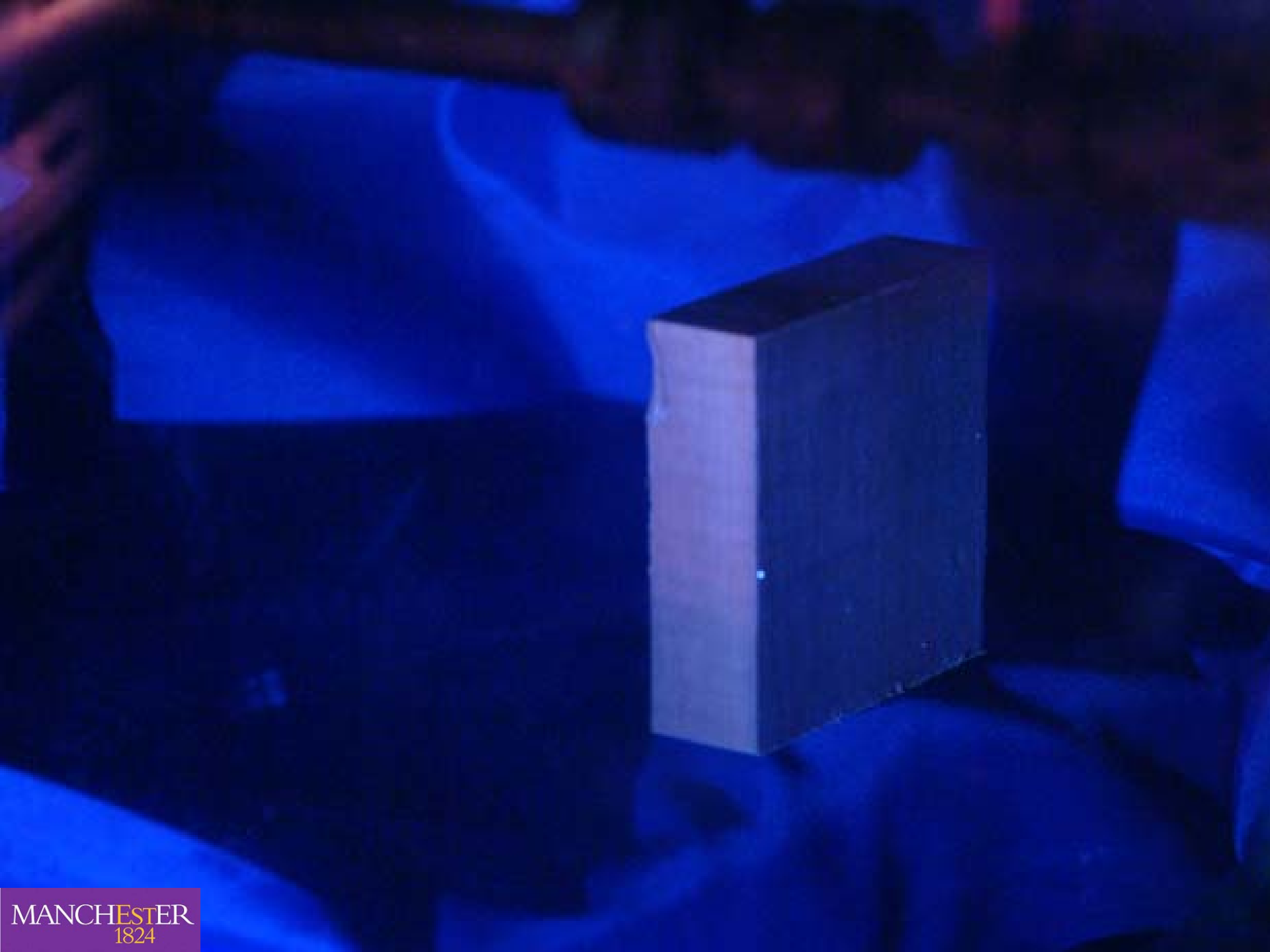








MANCHESTER
1824



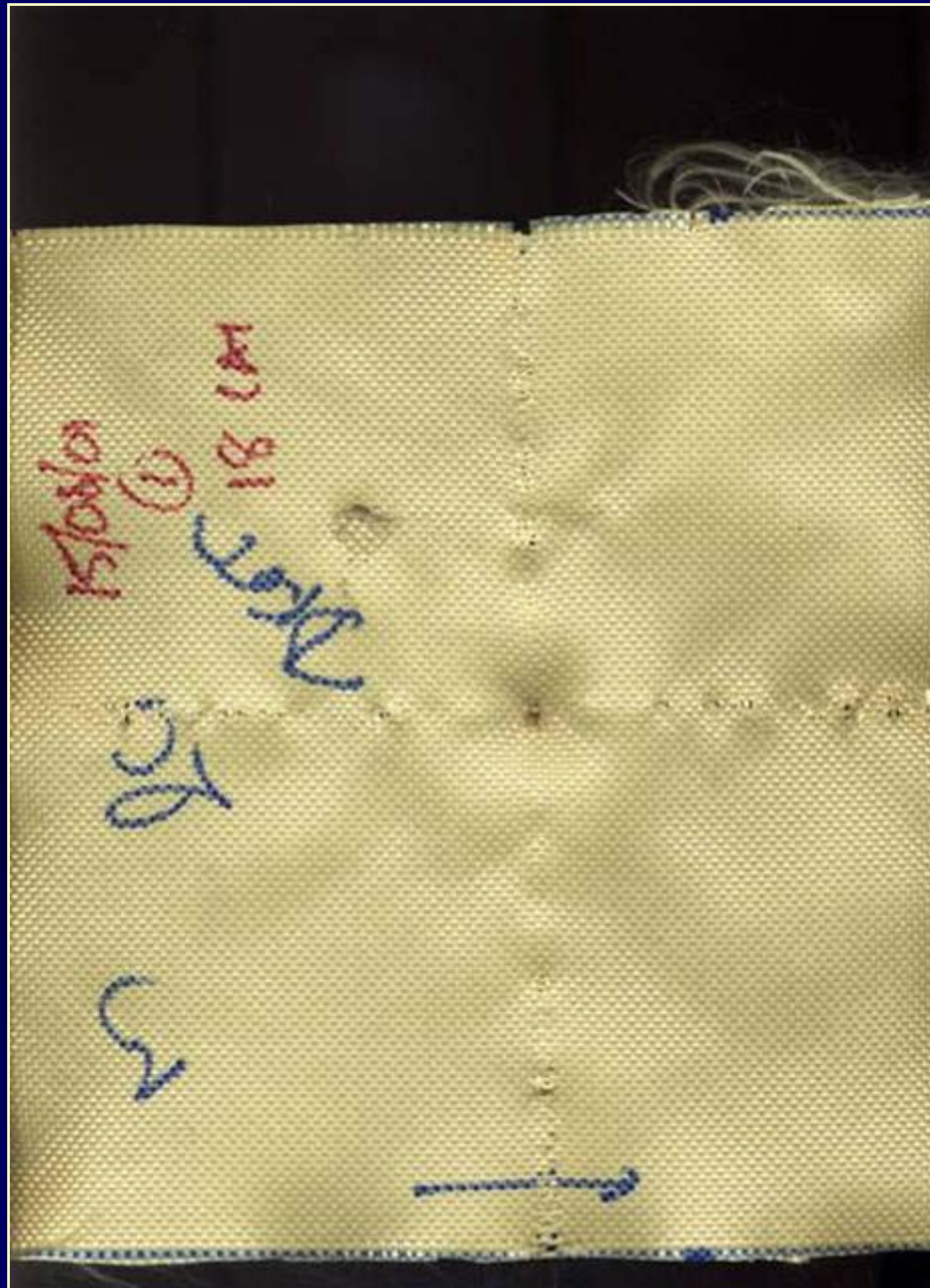
MANCHESTER
1824



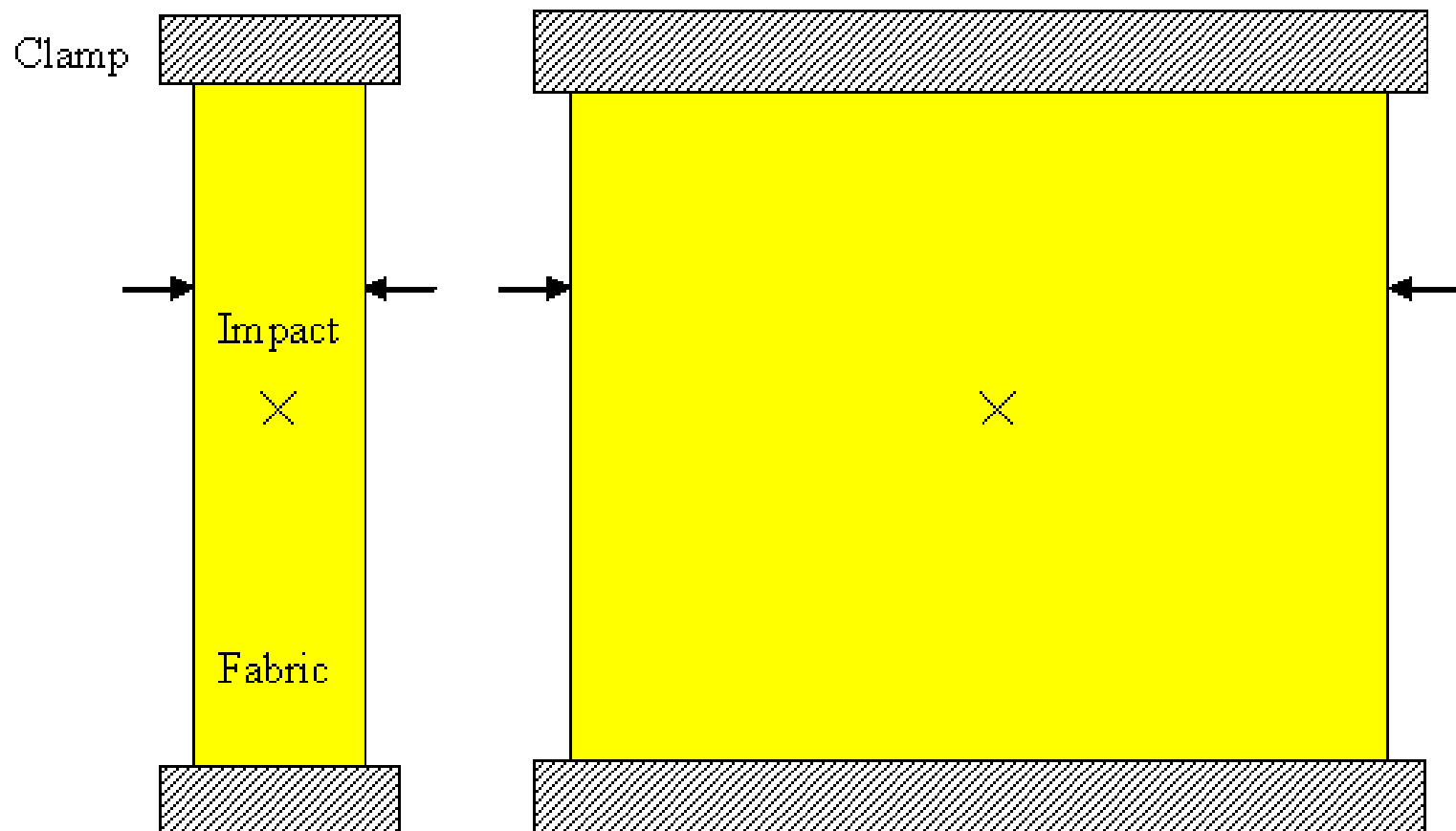
MANCHESTER
1824

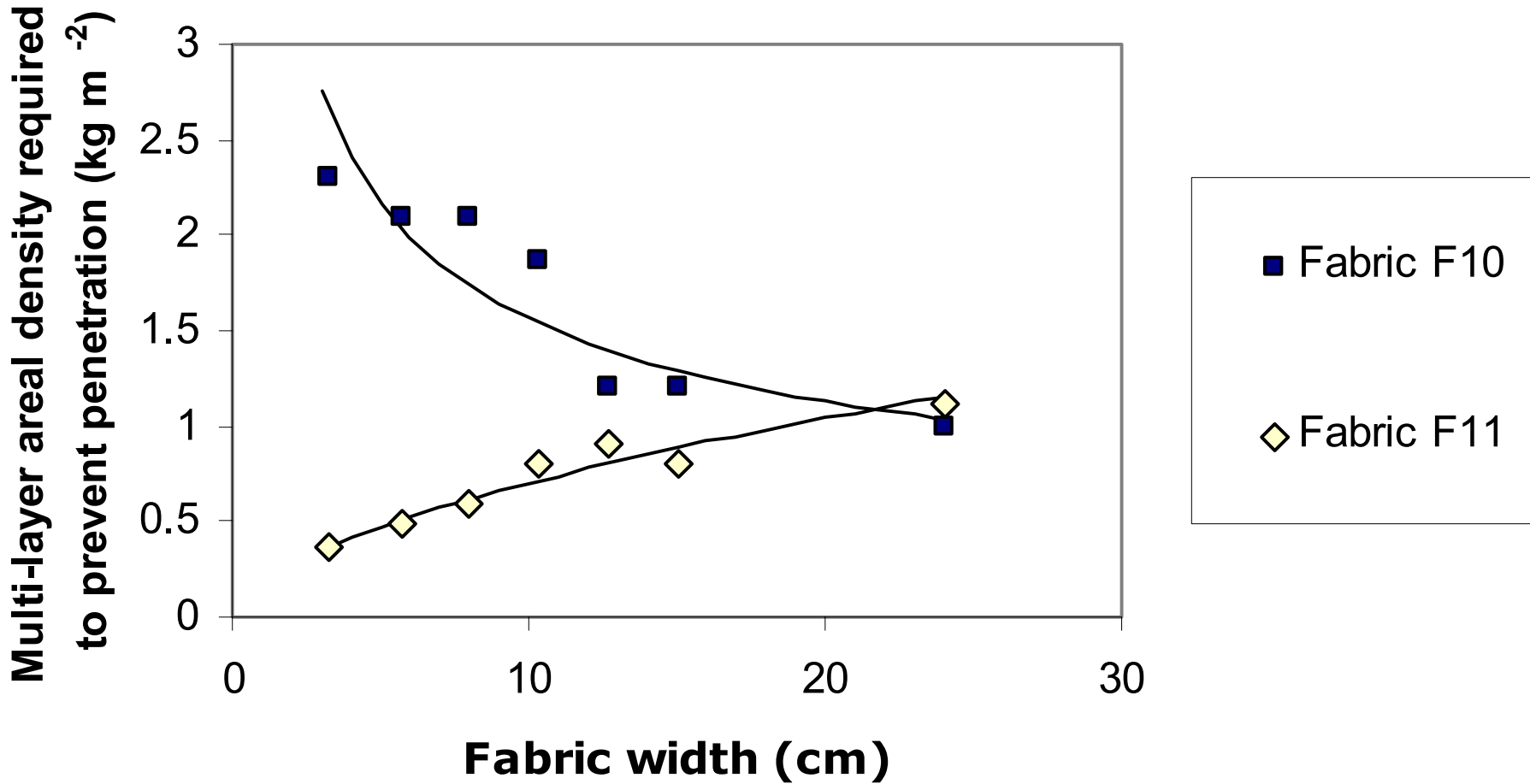


MANCHESTER
1824



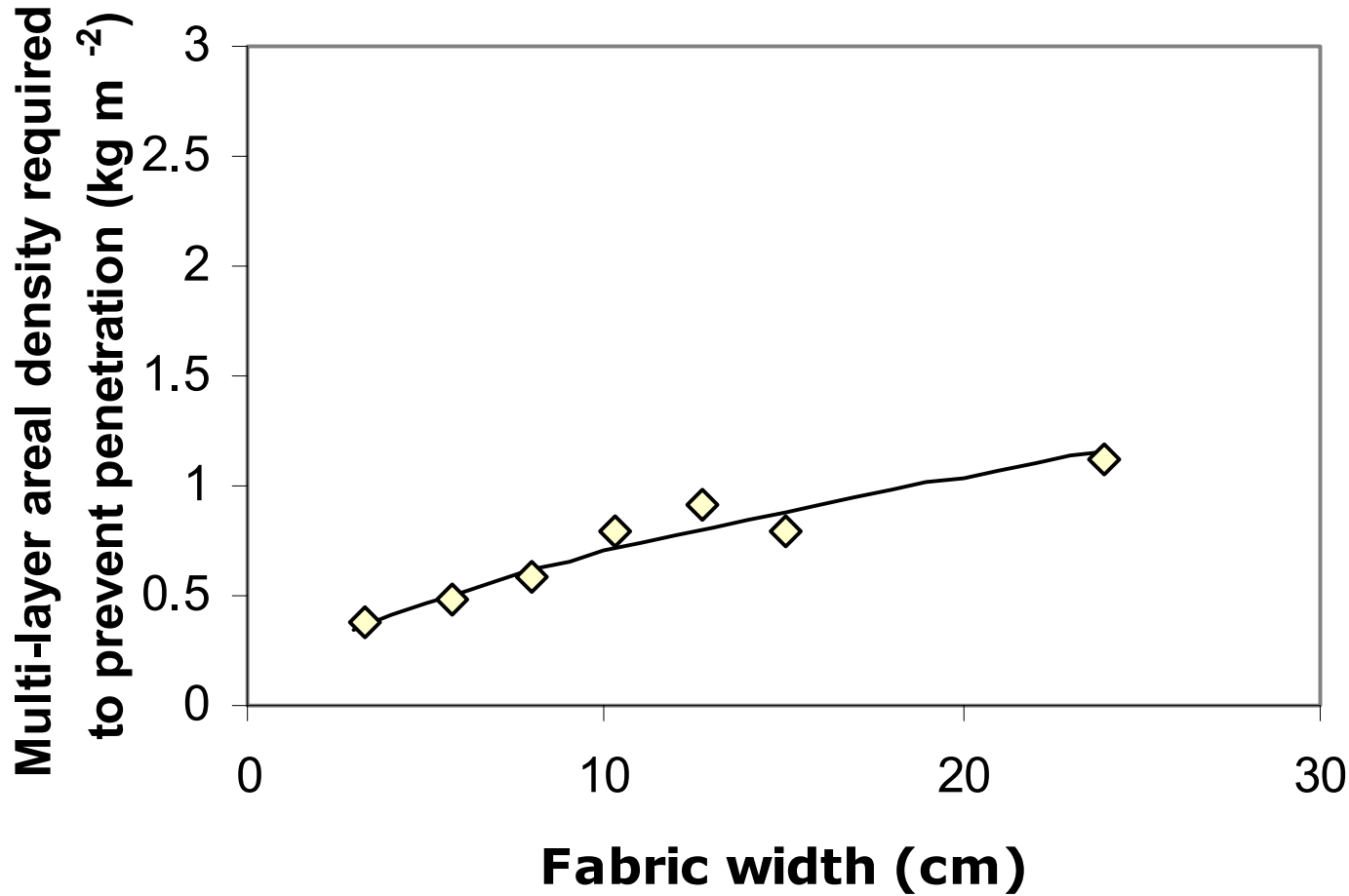






Weight of fabric required to prevent penetration vs. width of fabric strip.

	Fibre	Thread Density		Linear density of yarn		Structure	
		Picks/ cm	Ends/ cm	Weft (tex)	Warp (tex)		
F10	Kevlar	129	6.7	6.63	167	167	Plain weave
F11	Kevlar	49	22.4	22.4	23	23	Plain weave



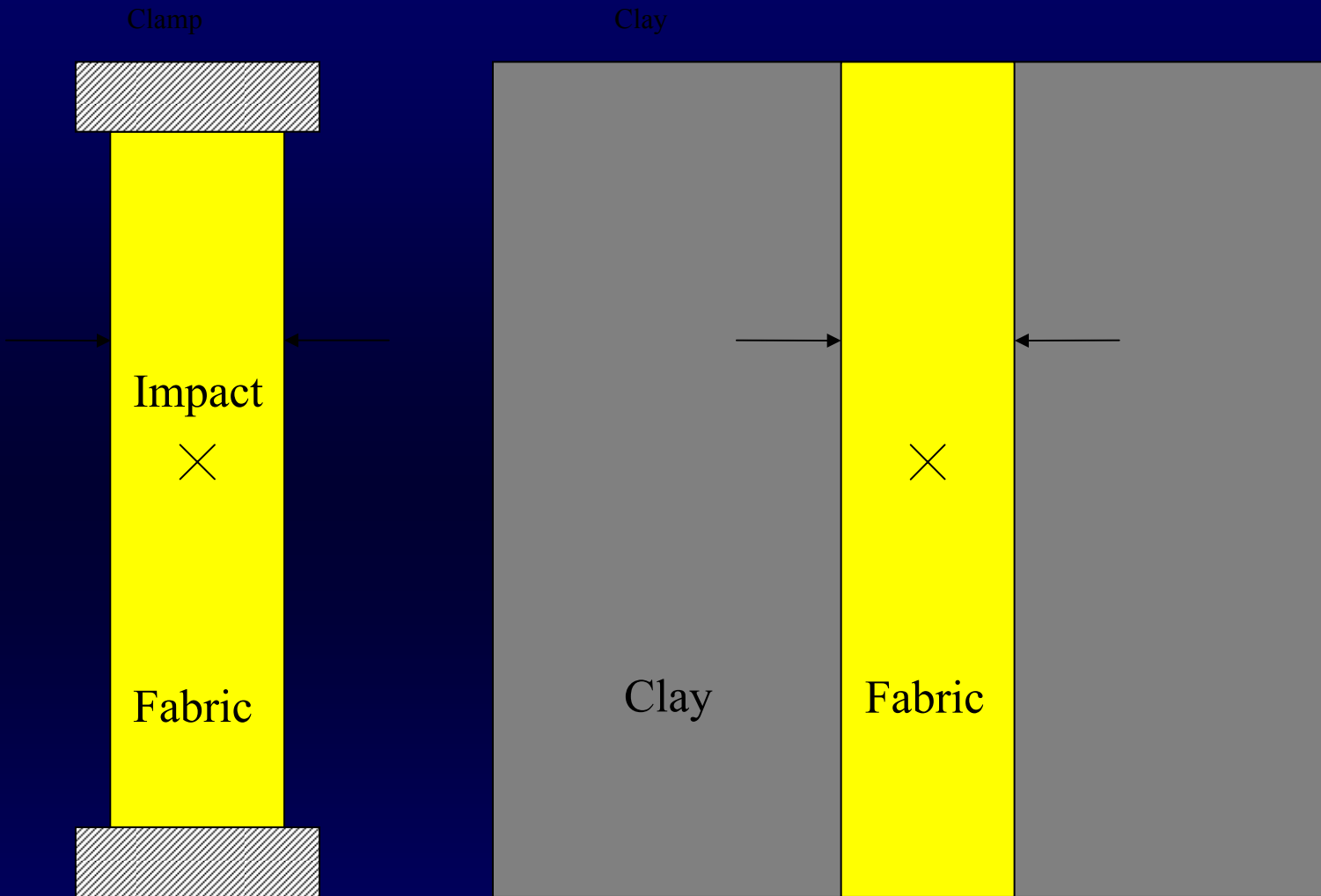
◇ Fabric F11

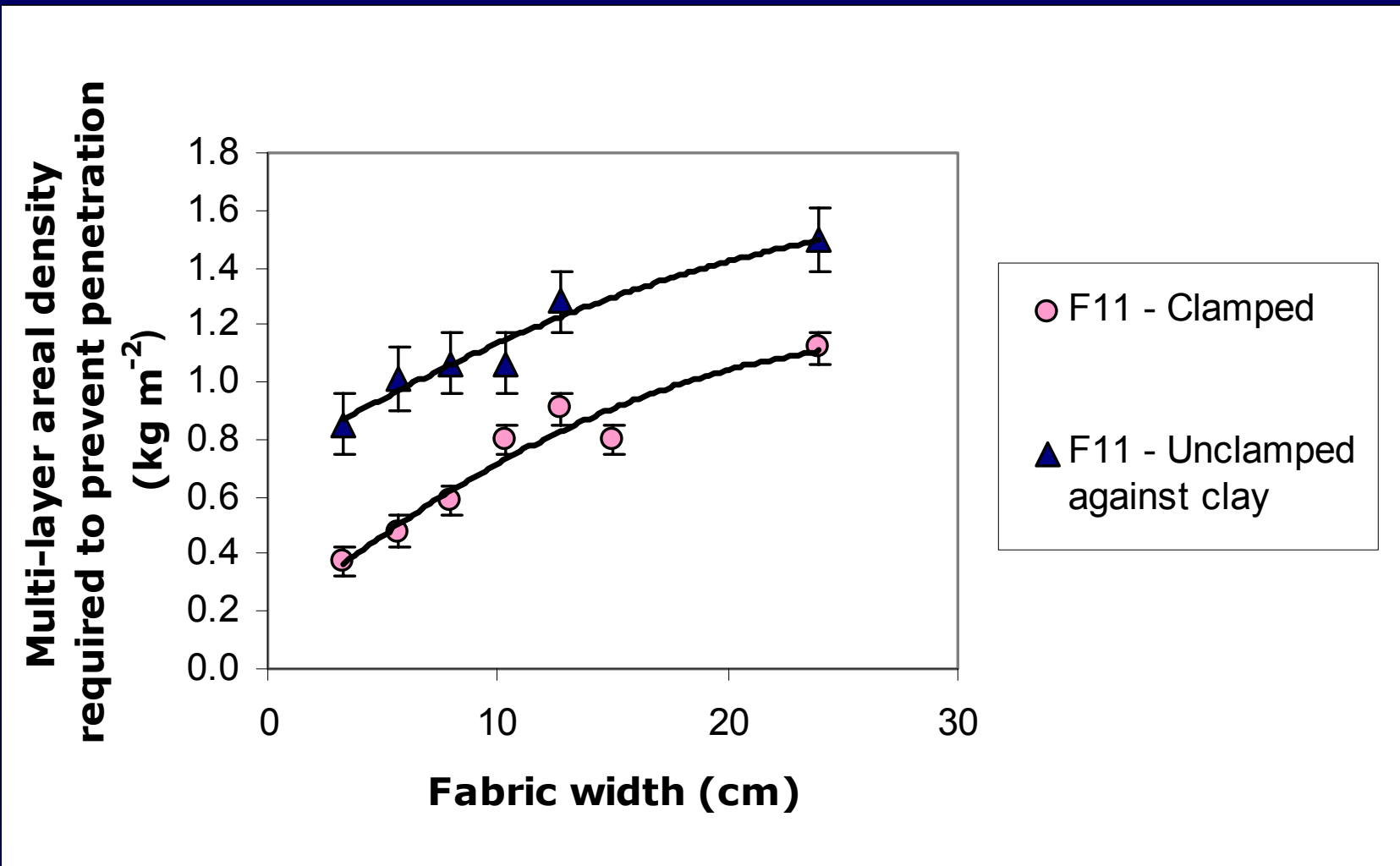
Weight of fabric required to prevent penetration vs. width of fabric strip

Width of strip (cm)	Weight of fabric required to prevent penetration (kg/sq m)
24	1.12
3.3	0.37

Weight saving (%)	67
-------------------	----

Example of the effect of reducing fabric width for direct impact onto a clamped narrow fabric.





Weight of fabric required to prevent penetration vs. width of fabric strip

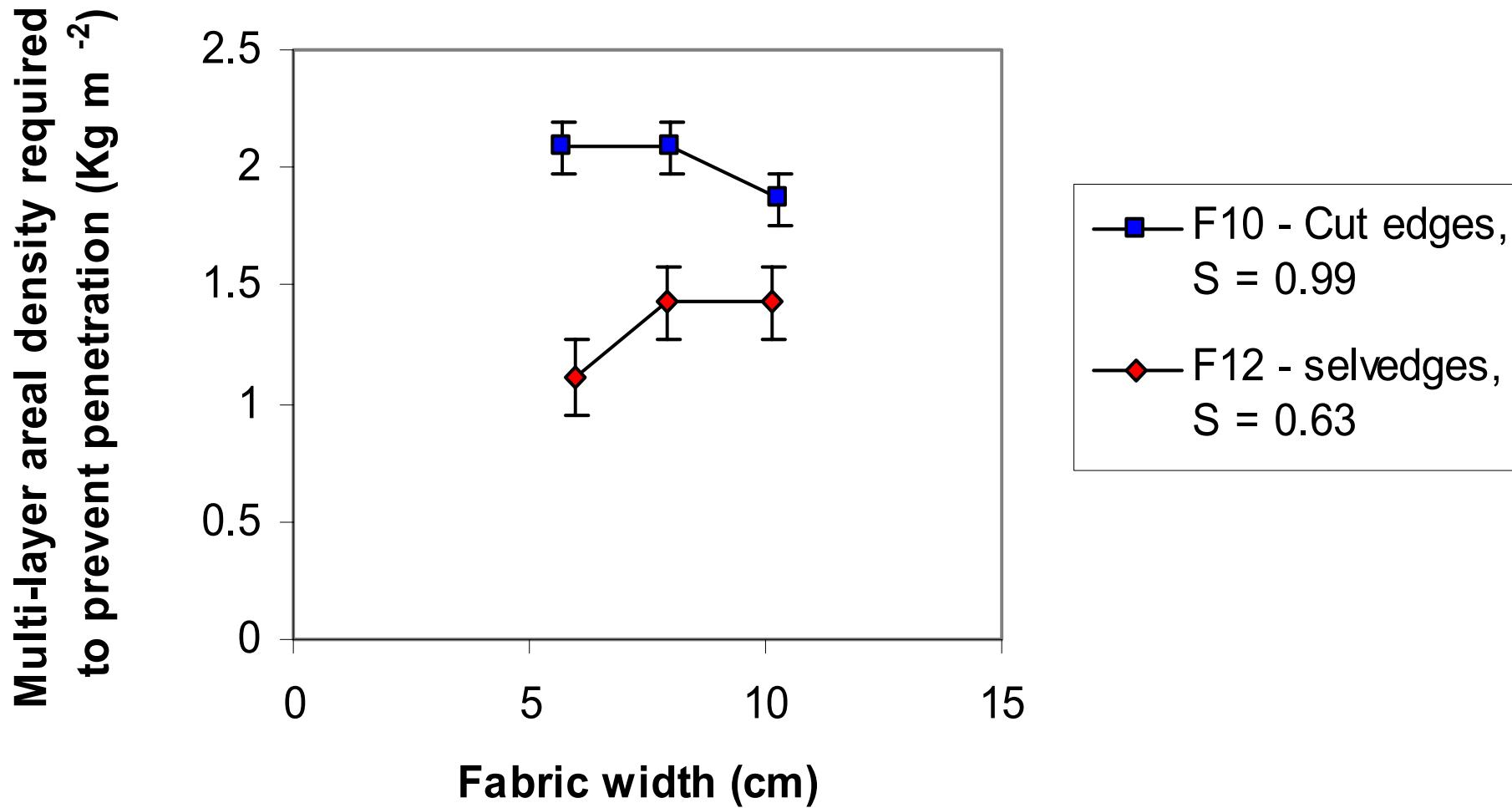


a) cut edges

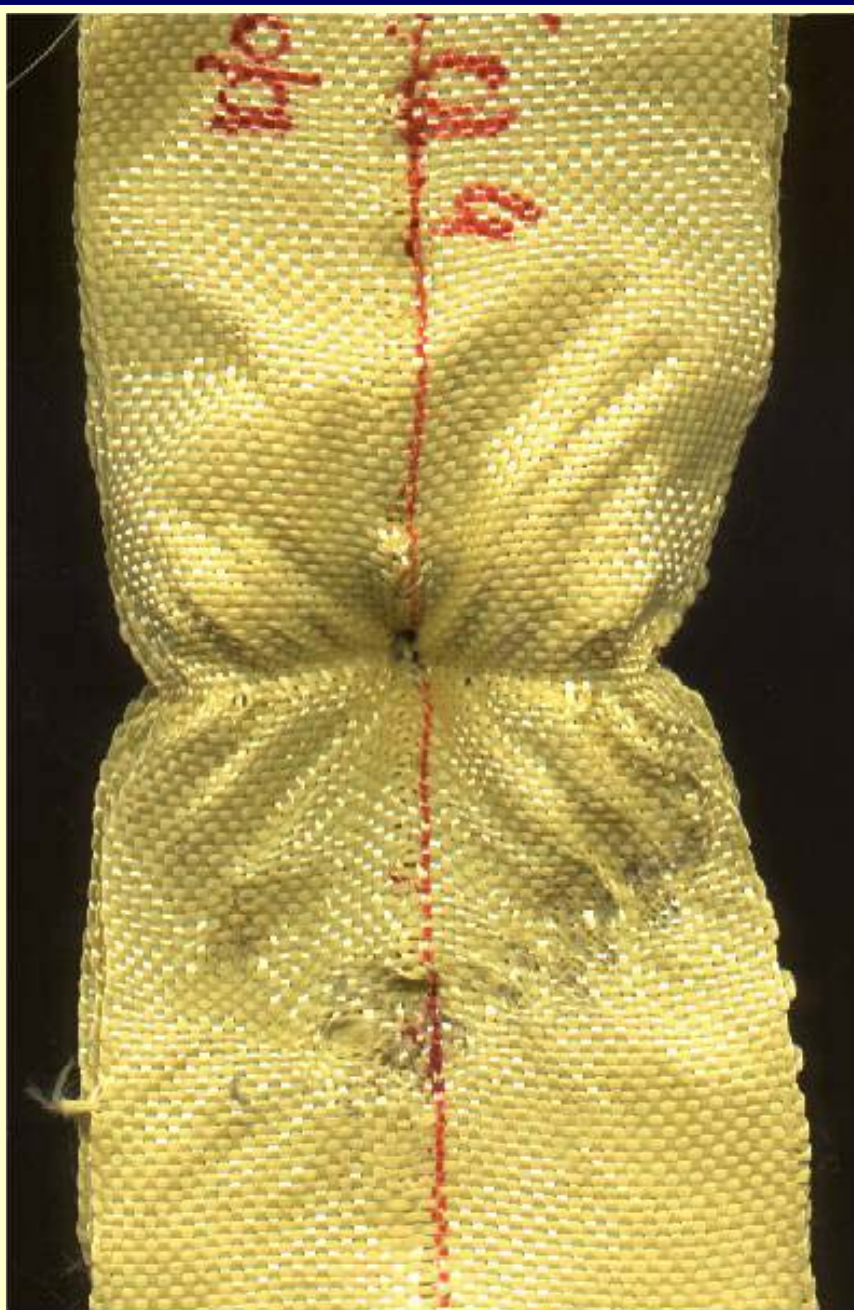


b) conventional selvedges

Schematic of cross-section through narrow fabrics



Weight of fabric required to prevent penetration vs. width of fabric strip



Mechanics of impact. Initially narrow fabric deformations are similar to those found for a regular fabric panel.

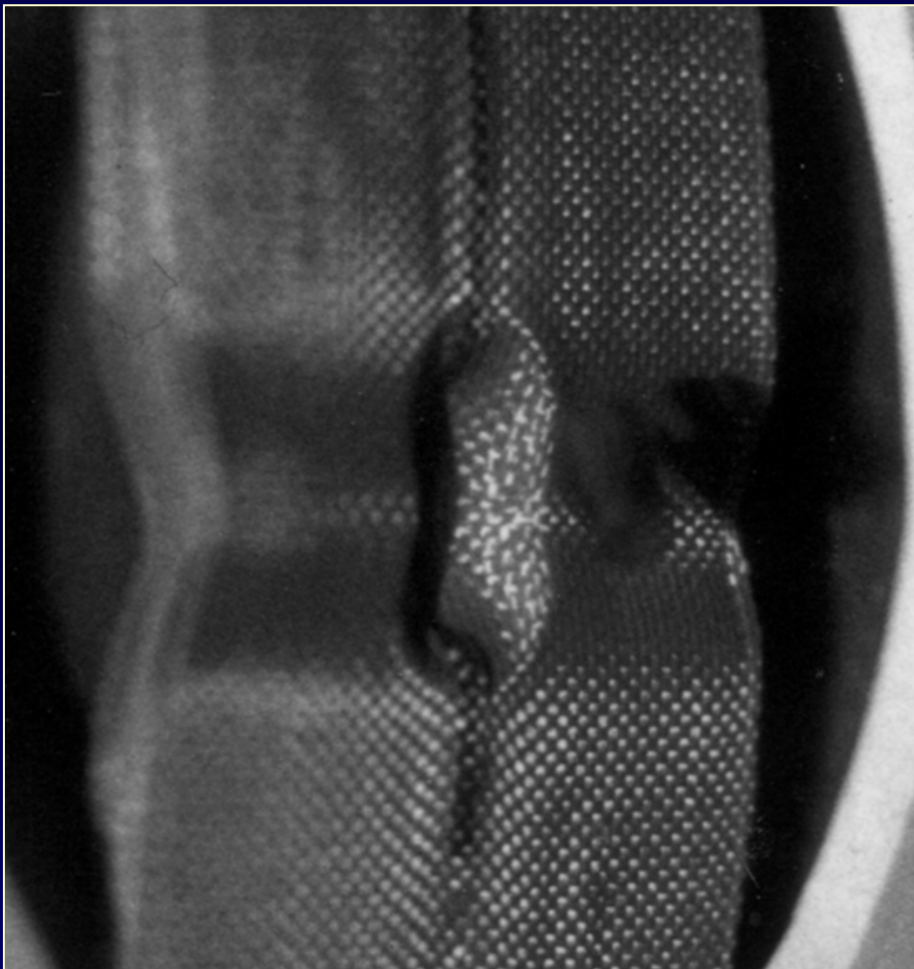


Regular fabric panel



Narrow fabric

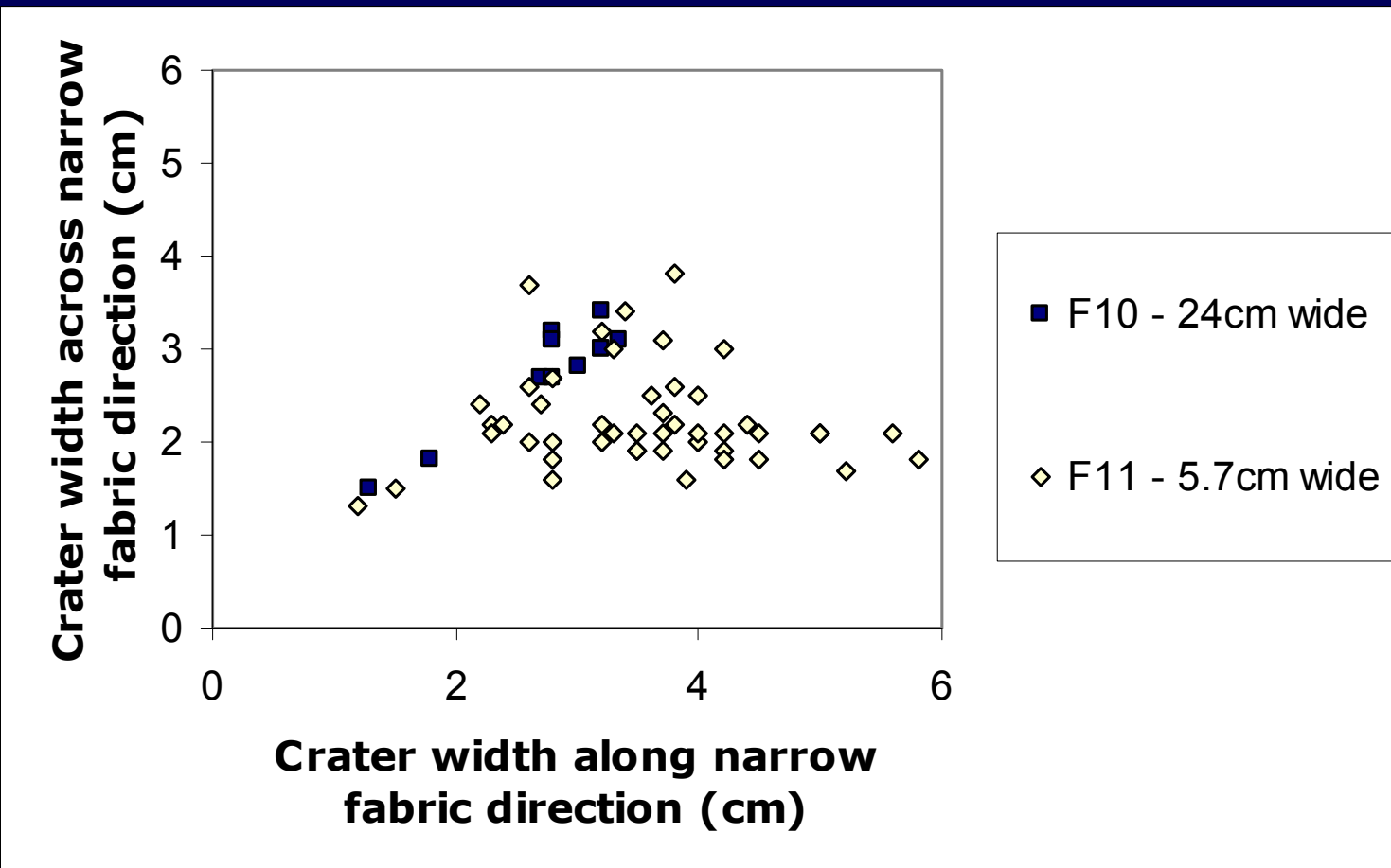
Later, in the case of narrow fabrics, deformation extends further in a direction parallel to the long sides. Typically, a peanut shaped deformation is observed.



This is reflected in the residual deformations.



Analysis of dimensions of crater left in clay

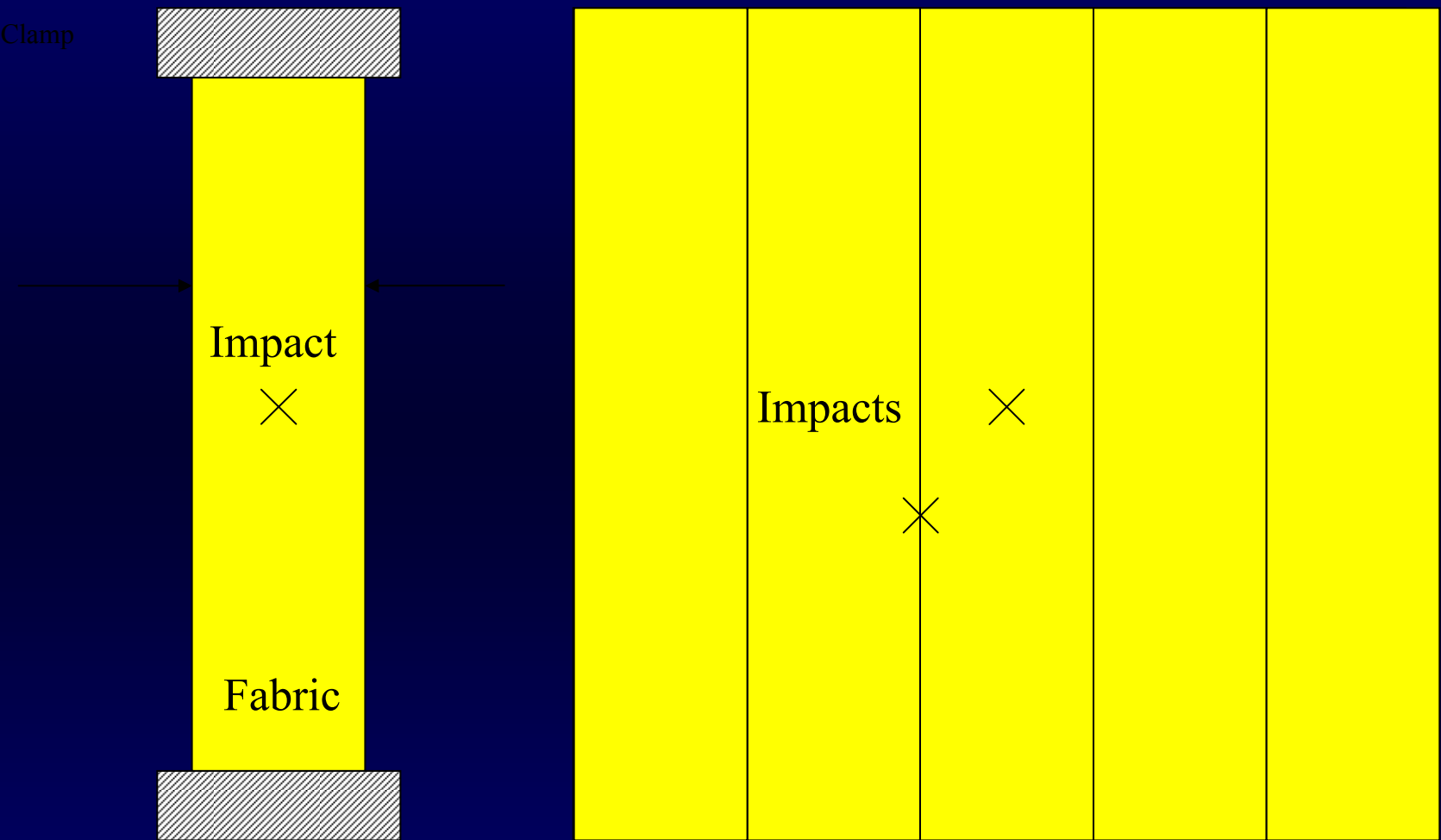


Comparison of crater widths in the two fabric directions

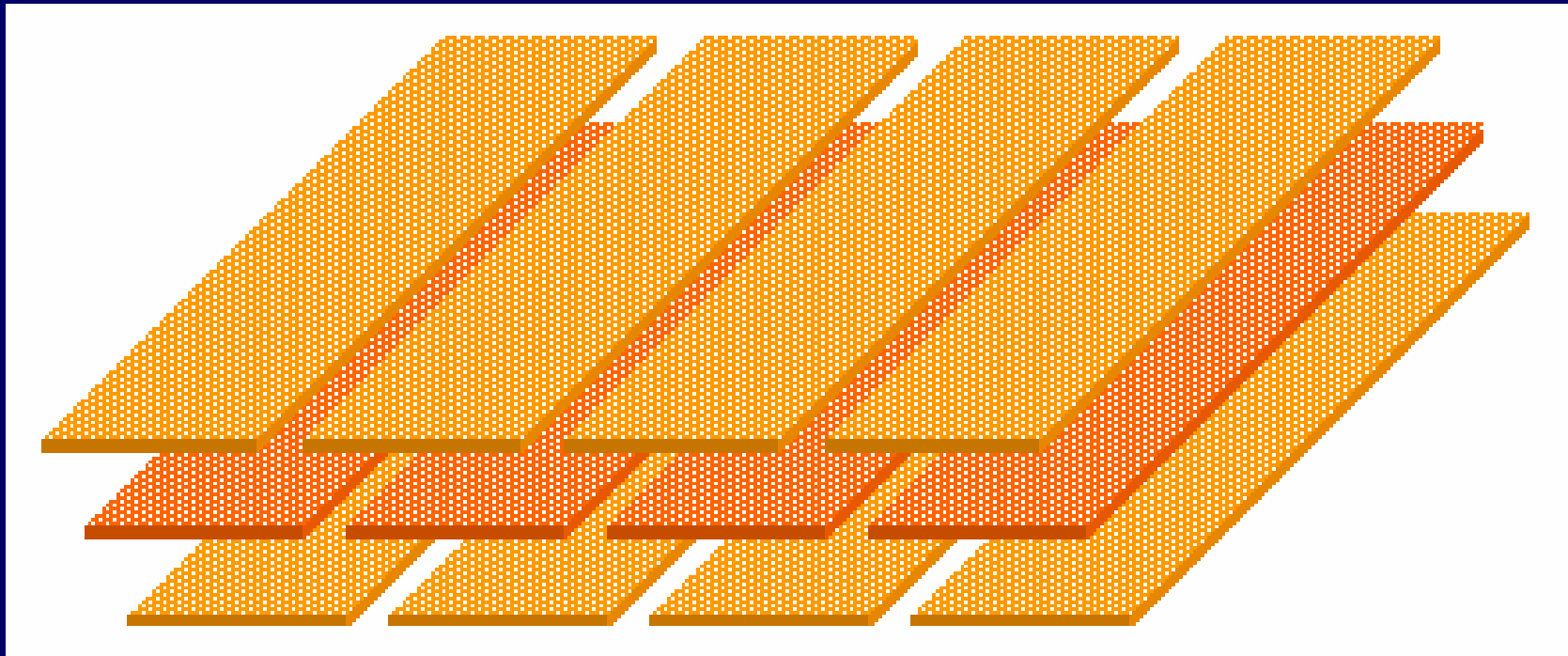
There are two problems in making practicable armour from narrow fabrics:

Impact

1. The weakness of the joins between fabric strips.
2. The weight and stiffness of any structure for holding the fabric on two sides.



Joins



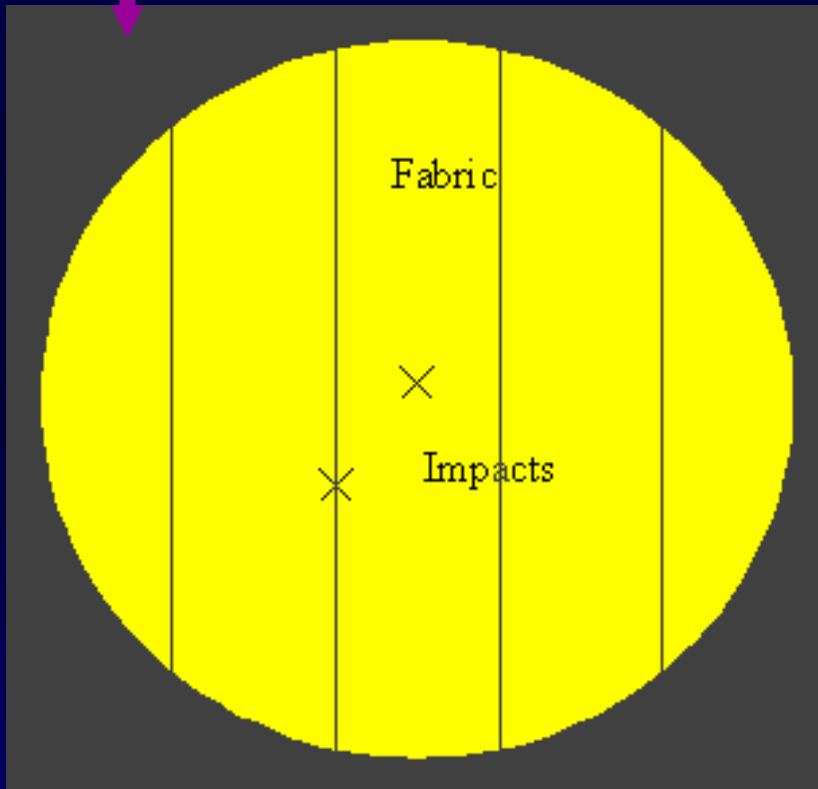
Narrow fabrics can be offset in different layers but the joins still contribute to an overall weakening of the fabric panel

Holding the fabric

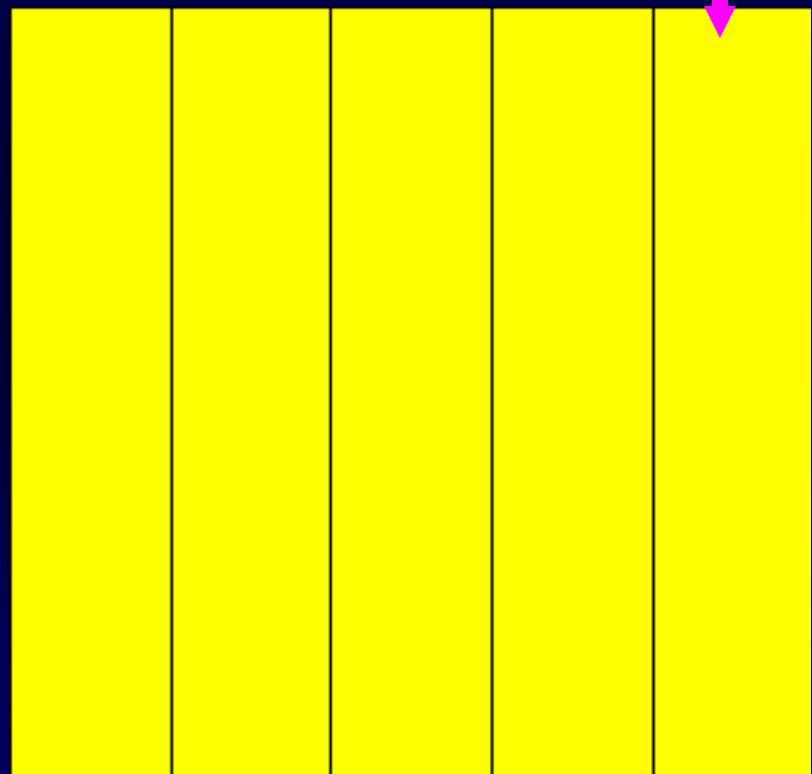
Various structures for holding the fabrics were investigated but were eliminated, either because of weight, because the grip was insufficient, or because they were destroyed by impact.

The solution was to use expanded polystyrene board.
The fabric strips were simply glued along the short sides

Polystyrene board (Weight = 28g)

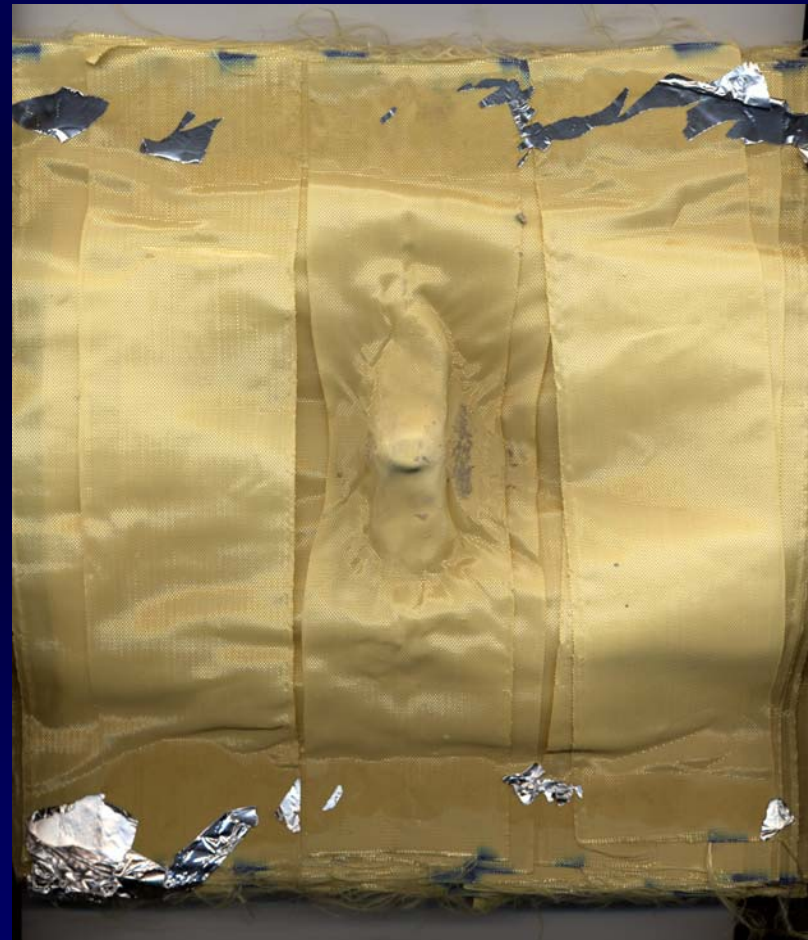
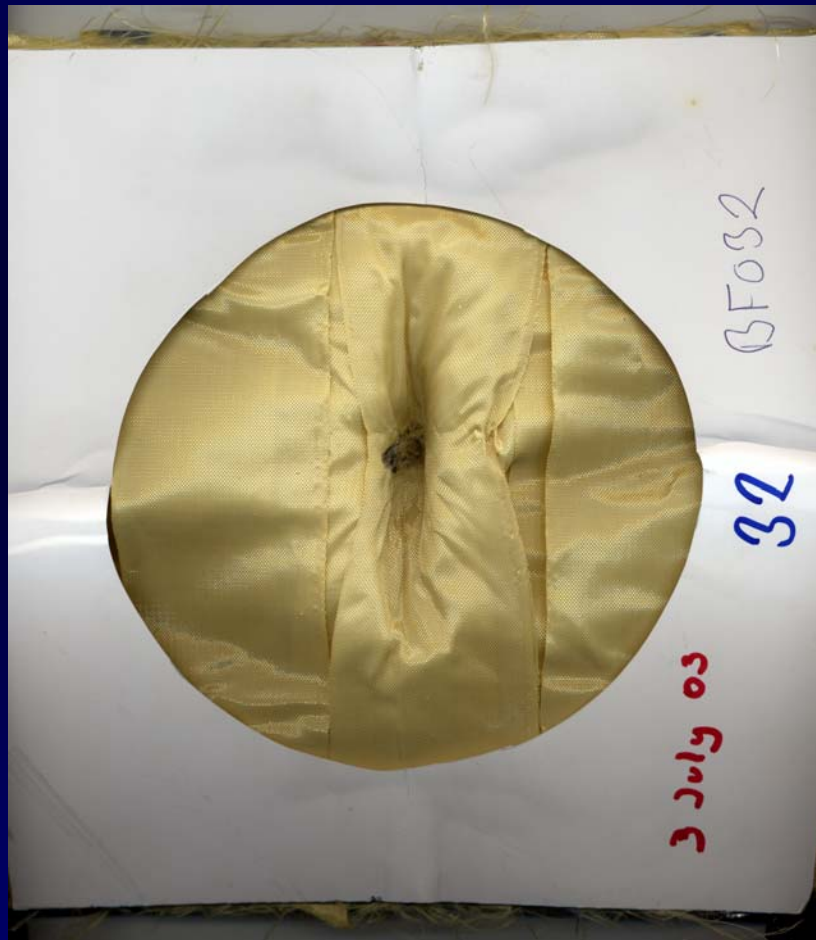


Glued edge



Face and back of the armour panel.

Impacted samples



Crater Depth in clay backing

Not only must armour arrest a projectile, but it must do it without excessive deformations. For example, it is of no use stopping a projectile if it takes a metre to do so.

Crater Depth in clay backing

	Crater Depth (cm)	Standard deviation (cm)
Benchmark (Fabric F10)	1.6	0.6
Narrow fabric assembly (Fabric F11)	1.4	0.2

Crater depth for narrow and benchmark fabric of equal areal densities.

Performance of narrow fabric assemblies

Multi-layer areal density required to prevent penetration

Impact velocity	Benchmark - Fabric F10	Narrow fabric assembly - Fabric F11	Weight reduction
(m s⁻¹)	(kg m⁻²)	(kg m⁻²)	(%)
400	1.6	1.1	31
520	3.4	3.2	6

Weight saving - Narrow fabric panel compared to control fabric. Results based on weight of **whole assembly**.

Performance of narrow fabric assemblies

Multi-layer areal density required to prevent penetration

Impact velocity	Benchmark Fabric F10	Narrow fabric assembly - Fabric F11	Weight reduction
(m s⁻¹)	(kg m⁻²)	(kg m⁻²)	(%)
400	1.6	0.6	63
520	3.4	2.6	24

Weight saving - Narrow fabric panel compared to control fabric. Results based on weight of **fabric alone**.

What we do not know about narrow fabrics

The minimum forces required to grip the fabrics (Can the weight of a soldier's equipment be utilised to hold the narrow fabrics under tension?)

The weave/width combination required to maximise ballistic performance.

The selvedge construction required to maximise ballistic performance.

What we **do not know** about narrow fabrics (Continued)

The fibre properties required to maximise the ballistic performance (Should they be different in warp and weft).

The frictional properties of yarns required to maximise the ballistic performance.

The relationship between ballistic performance and fabric length.

The relationship between ballistic performance and impact velocity.

What we **know** about narrow fabrics

The deformations of narrow fabrics undergoing ballistic impact differ to those for regular fabrics.

With the appropriate choice of narrow fabric construction, width, selvedge and method of gripping significant improvements in ballistic performance can be achieved.

Incorporating narrow fabrics into ballistic panels results in improvements in performance-to-weight ratios despite the weaknesses introduced by fabric joins.

Where some existing structure is present, such as an aircraft fuselage, still greater performance-to-weight ratios can be achieved.

School of Materials

THE END

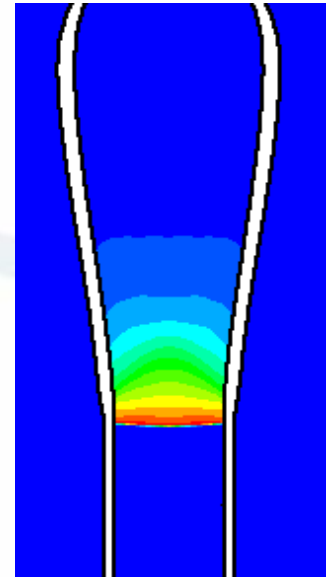
Simulation of Cylinder Expansion Tests Using an Eulerian Multiple-Material Approach

**L. Donahue, R.C. Ripley
Combustion Dynamics Group
Martec Limited
17 November 2005**



Outline

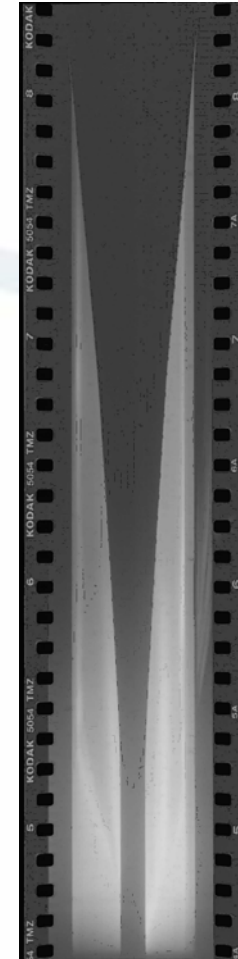
- Introduction
- Numerical Models
- Preliminary Calculations
- Cylinder Expansion Test Simulations
- Discussion
- Future Work



Introduction

- Cylinder Expansion (CYLEX) tests conducted to determine explosive performance
 - New conventional explosives
 - Non-standard mixes
- Explosive cased in a copper cylinder is detonated
- Resultant expanding wall velocities recorded
- Explosive energy can be determined
- Allows for determination of parameters for detonation product gas equation of state

Cylinder Expansion Test



Images Courtesy of DRDC Suffield

Objectives

- Simulation of cylinder expansion tests for three increasingly energetic explosives:
 - Nitromethane
 - TNT
 - Composition B3 (60 wt% RDX, 40 wt% TNT)
- Validation of Chinook CFD code
 - Multiple-material model
 - Reaction model

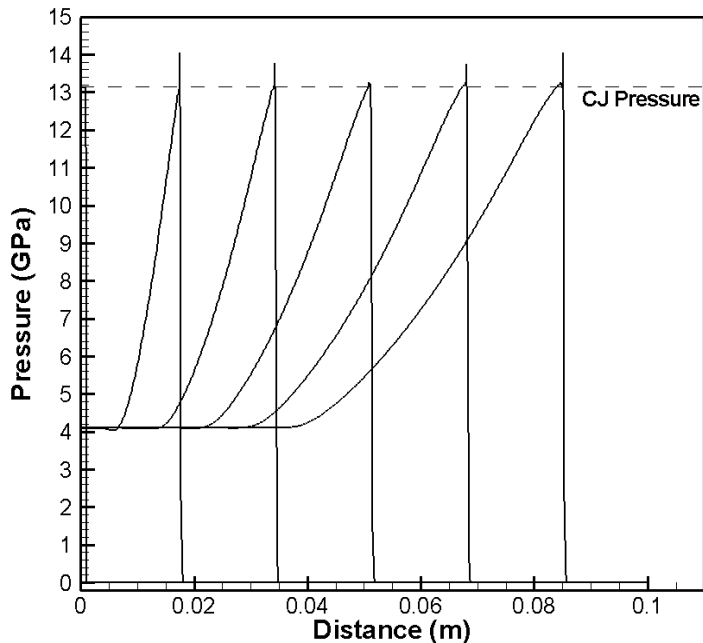
Background

- Multiple-material model previously applied to (non-reactive) underwater explosion and landmine simulations
- One of earliest calculations after implementation of advanced energetic material modelling capability in Chinook
- Calculations performed using Eulerian formulation

Model Theory

- Continuum approach – mixed cells with uniform pressure and velocity
- Allows for several equations of state to be used in a calculation
 - Mie-Gruneisen (HOM) for condensed explosive and tube wall
 - JWL for explosive products
 - Ideal gas for air
- One-step Arrhenius reaction model converts reactants into products
 - User-specified heat of reaction

Preliminary Calculations

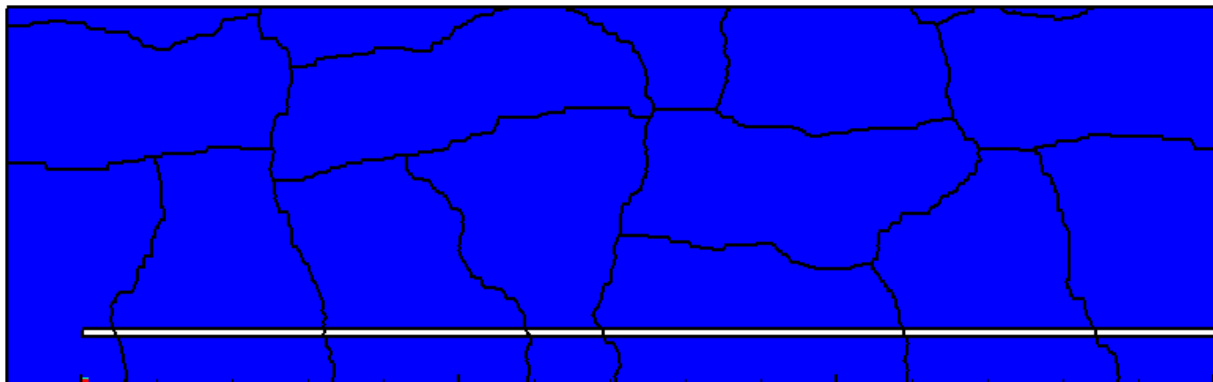


- 0.1 m long 1D domain
- Small initiation region at CJ state
- 0.2 mm cell size
- CJ pressure and detonation velocity extracted for each explosive

Explosive	Detonation Velocity (m/s)	CJ Pressure (GPa)
Nitromethane	6800 (2.8%)	13.27 (0.84%)
TNT	7280 (1.3%)	19.97 (-1.8%)
Comp B3	8400 (3.1%)	27.03 (-0.66%)

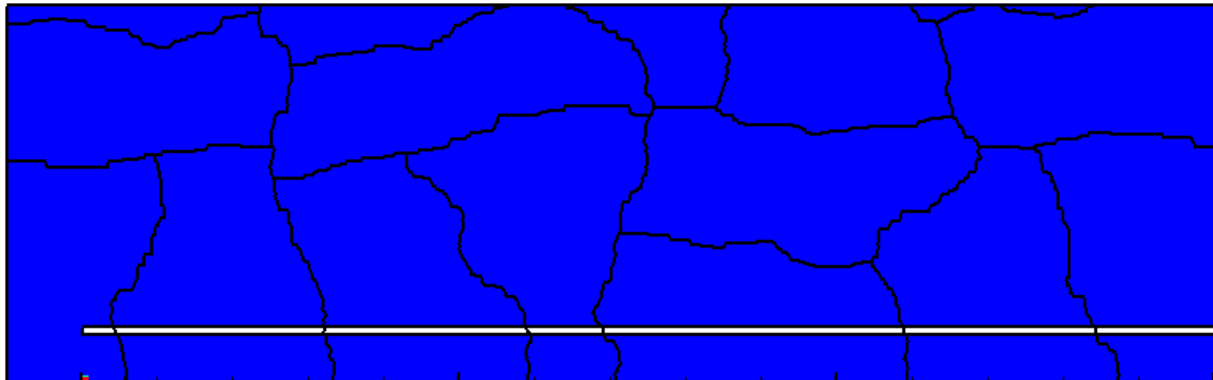
Cylinder Expansion Simulations

- 2D axi-symmetric analysis of cylinder tests
- 30 cm long by 2.54 cm diameter copper tube
- 0.2 mm cell size (structured quads)
- Expanding grids eliminate boundary reflections
- Approximately 1.1 million total cells
 - Utilize parallel computing



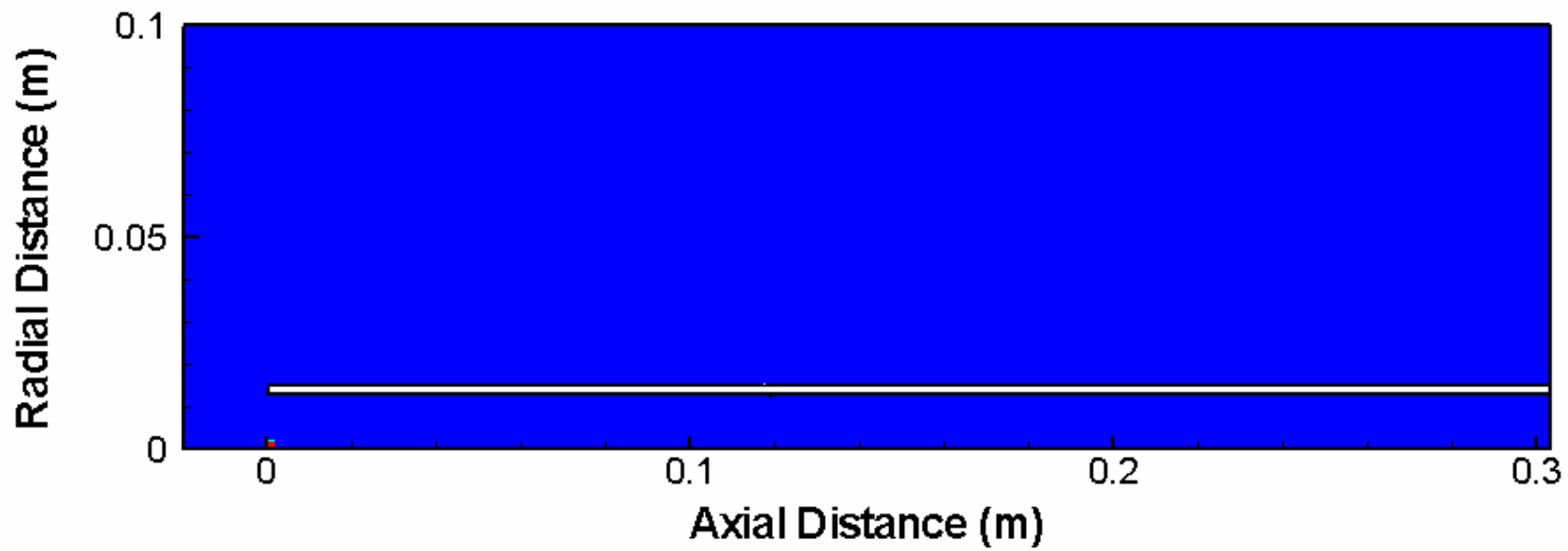
Cylinder Expansion Simulations

- Monitoring array placed 20 cm down tube
- Wall velocities extracted at 6 and 19 mm
- Wall position taken at 0.5 mass fraction copper



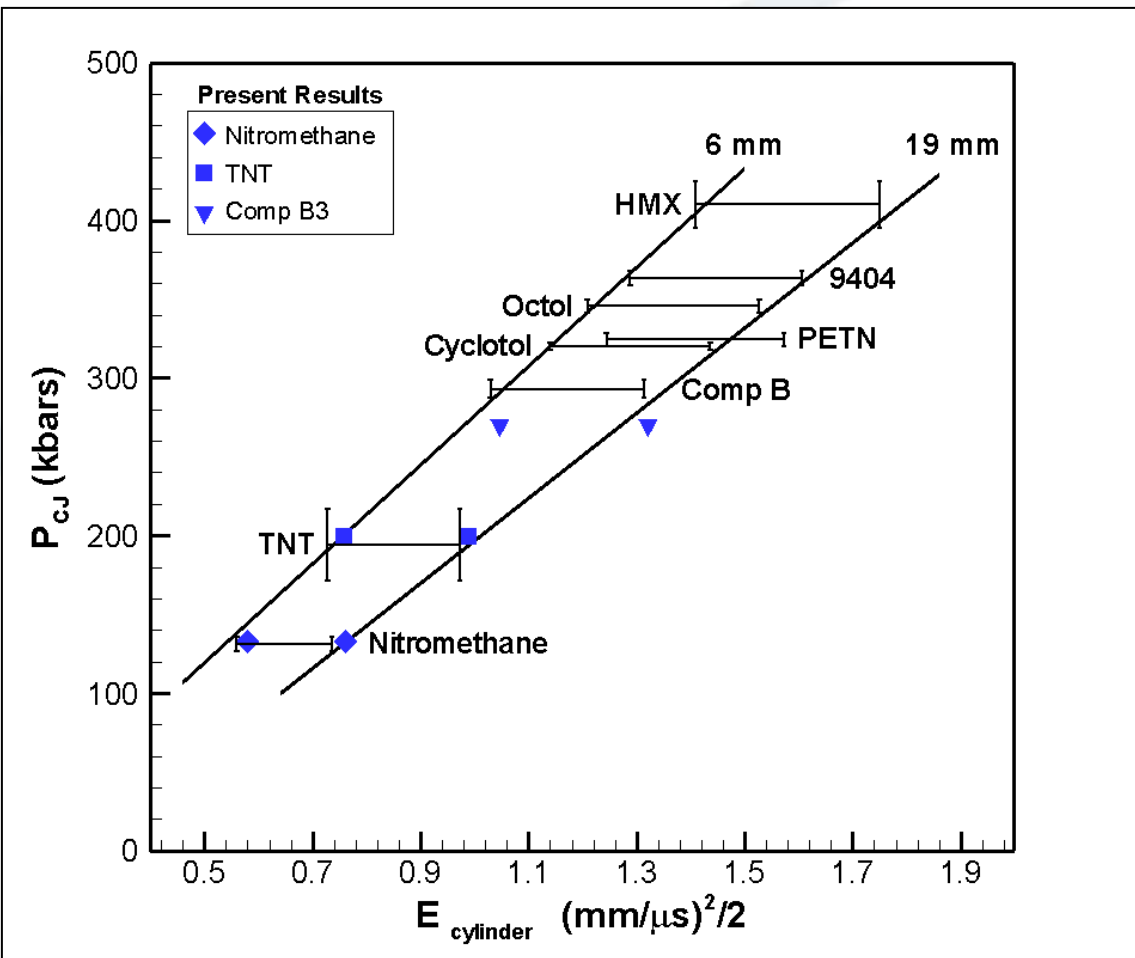
Wall Displacement

$t = 0.00000 \text{ ms}$



Pressure Contours

Comparison of Results



Discussion / Future Work

- Reasonable agreement with experimental results
 - CJ pressure / detonation velocity
 - Wall velocities
- Higher mesh resolution ?
- Eulerian approach results in some numerical diffusion
 - Adaptive mesh refinement
 - Material interface tracker
 - Lagrangian or moving mesh
- Next Step: Revisit this study and investigate explosives with higher reaction rates

Laura Donahue
Tel. 902.425.5101
Idonahue@martec.com

400-1888 Brunswick Street
Halifax, Nova Scotia
Canada B3J 3J8

www.martec.com



22nd International Symposium on Ballistics
November 14-18, 2005, Vancouver, Canada



Application of Powder Tantalum Material for Explosively Formed Penetrator (EFP) Warhead

U.S. Army ARDEC

Richard Fong, Mike Hespos, William Ng, *Steven Tang



Acknowledgment

Textron Systems Inc.

Aerojet Corporation

Outline

- Background
- Consolidation processes
 - Hot Isostatic Press
 - Extrusion
 - Resistance Sintered
- Near Net Process
- Material Evaluation
- Summary



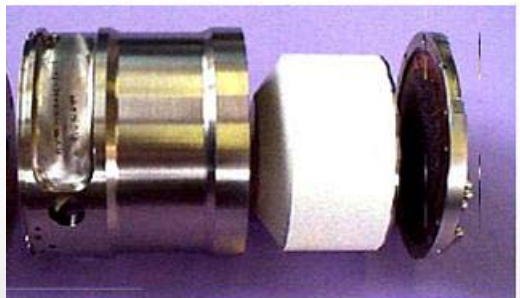
Explosively Formed Penetrator (EFP) Warheads



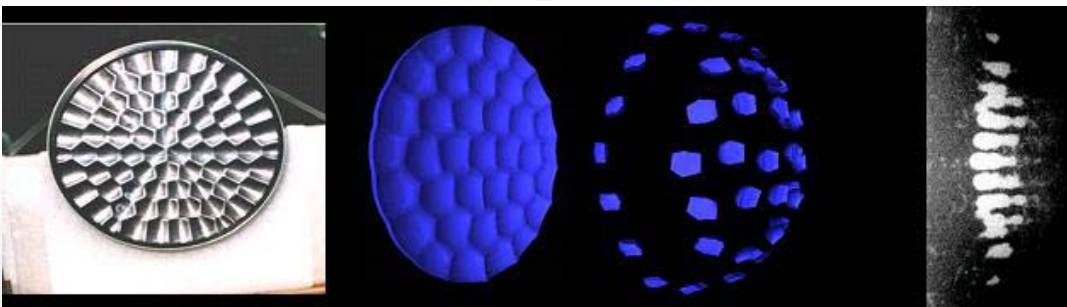
Single EFP



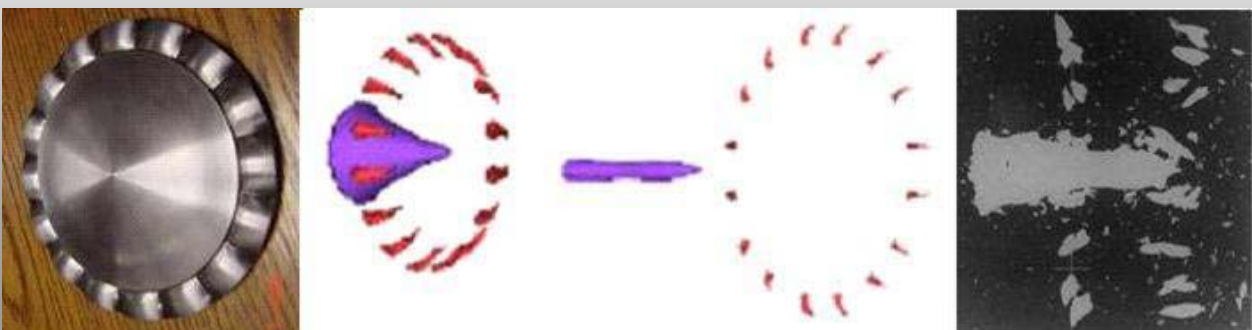
Warhead hardware



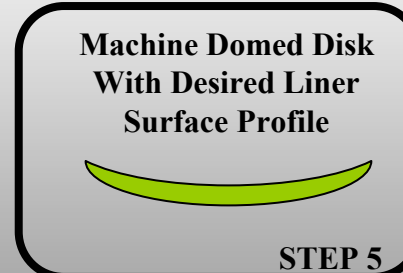
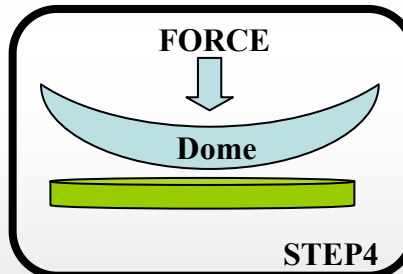
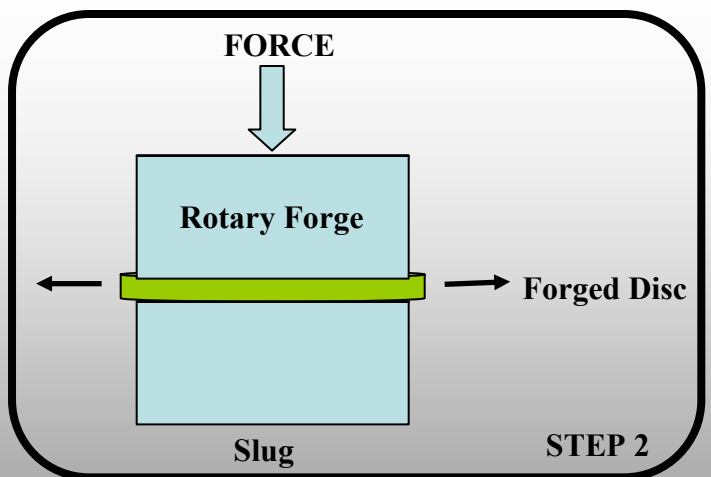
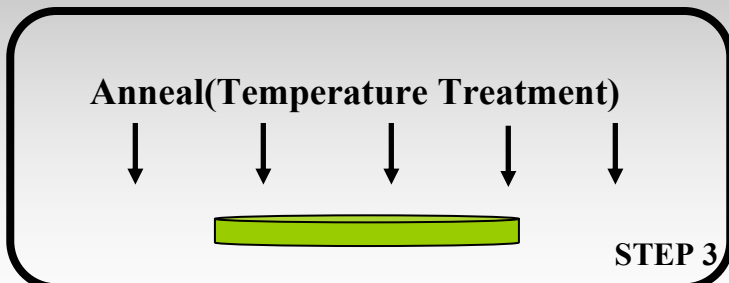
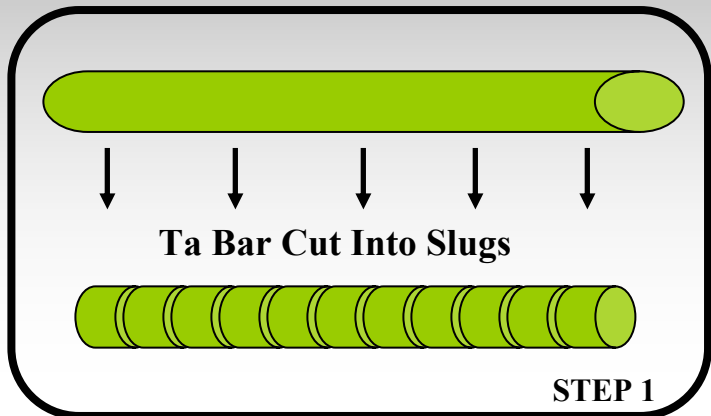
Multiple EFPs



Combined Effects EFP

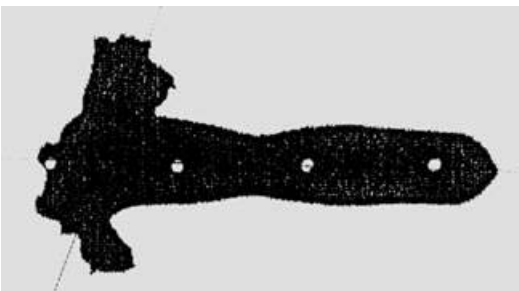


Conventional EFP Fabrication Process



EFP Formation Variation

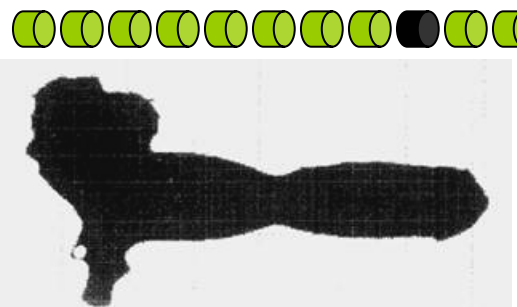
2nd Cut From Ta Bar



7th Cut From Ta Bar



9th Cut From Ta Bar





EFP Warhead Powder Tantalum Program



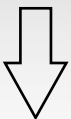
- Objectives: To develop
 - Powder process specification
 - Near net shape liner fabrication process
- Advantages of powder Tantalum approach
 - Availability
 - Consistency
 - Lower costs

Powder Consolidation Processes

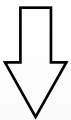
- Hot Isostatic Press
- Extrusion
- Resistance Sintered

HIP consolidation process

RAW POWDER



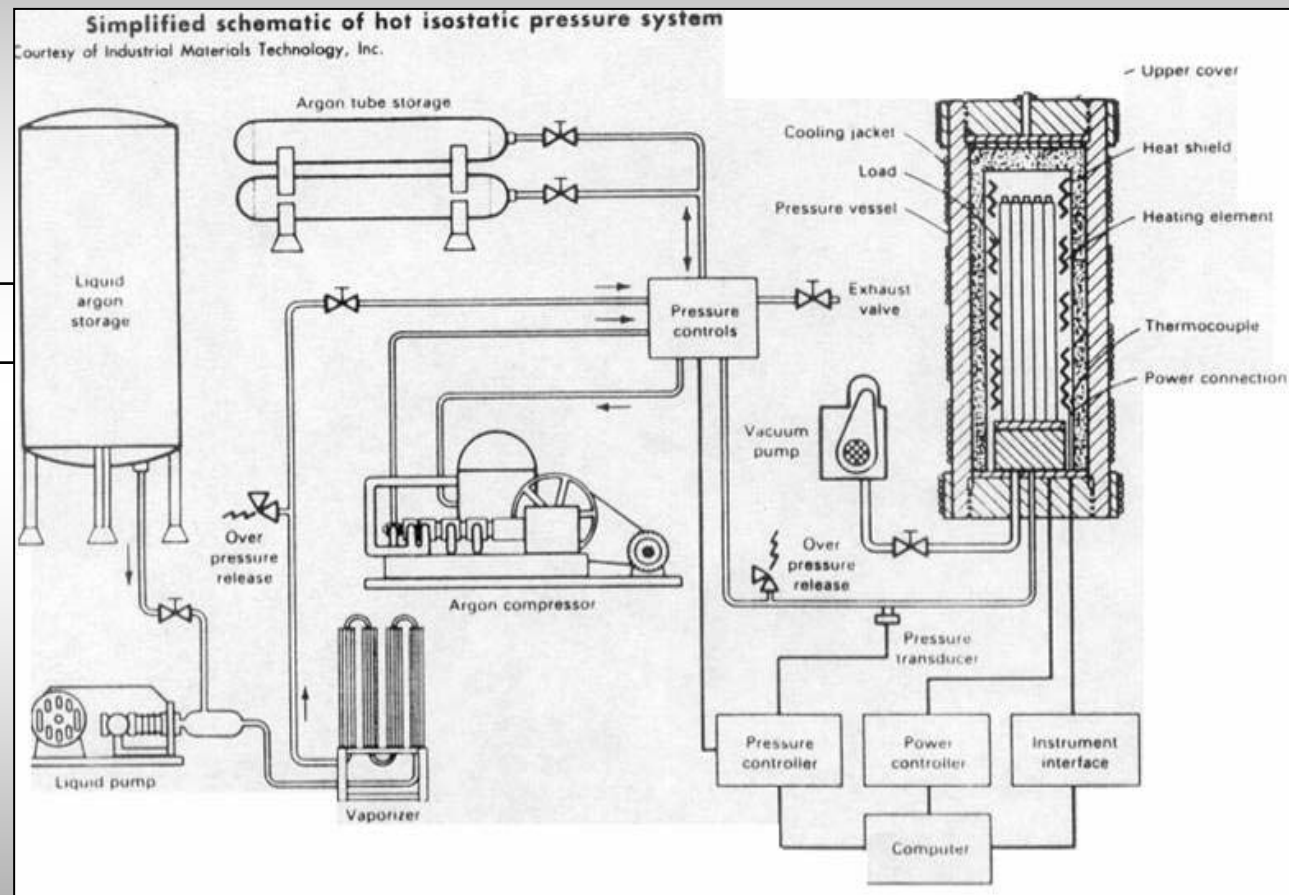
COLD ISOSTATIC PRESS



HOT ISOSTATIC PRESS



FINISHED BAR STOCK



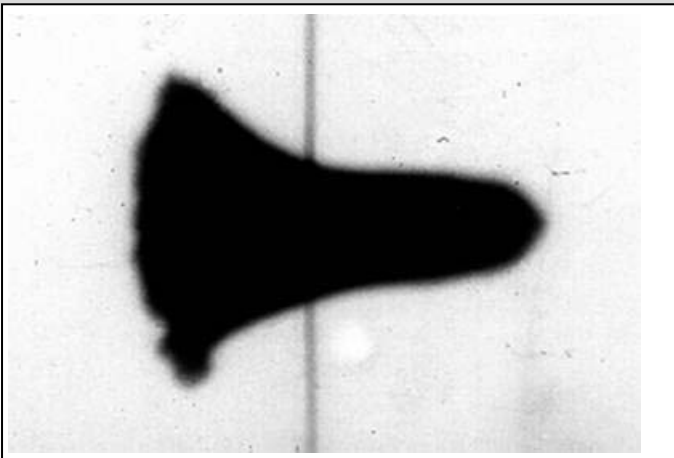


HIP Test Results

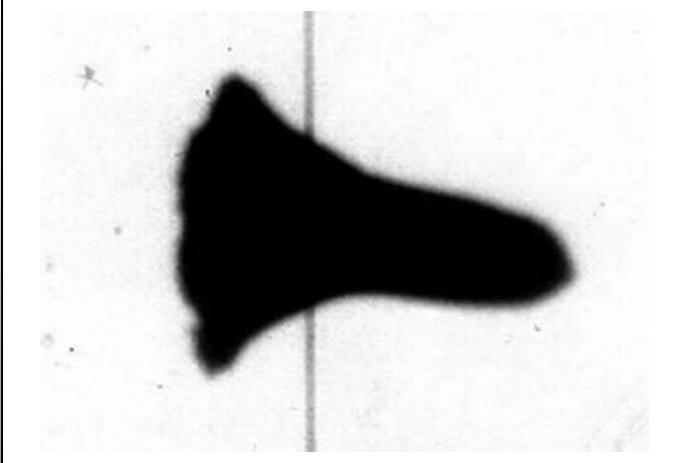


Orthogonal X-Ray Results

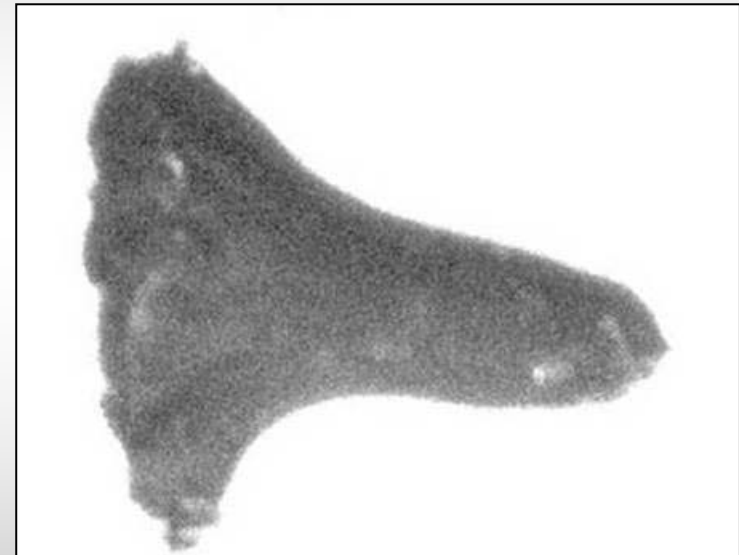
Horizontal



Vertical

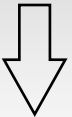


Cordin Photo Results

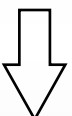


Extrusion consolidation process

RAW POWDER



COLD ISOSTATIC PRESS



EXTRUSION



FINISHED BAR STOCK



Extrusion Test Results

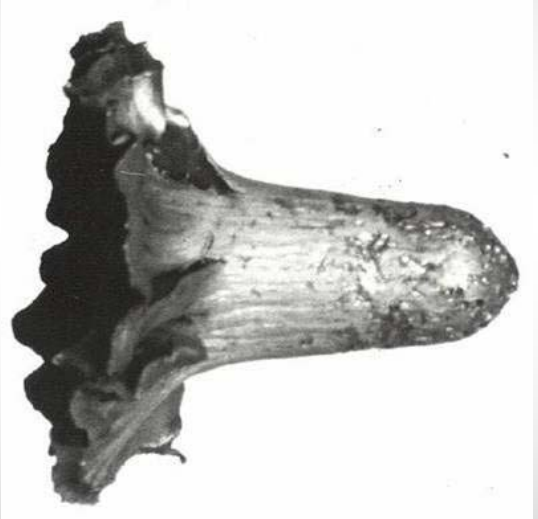
Orthogonal X-Ray Results

Horizontal

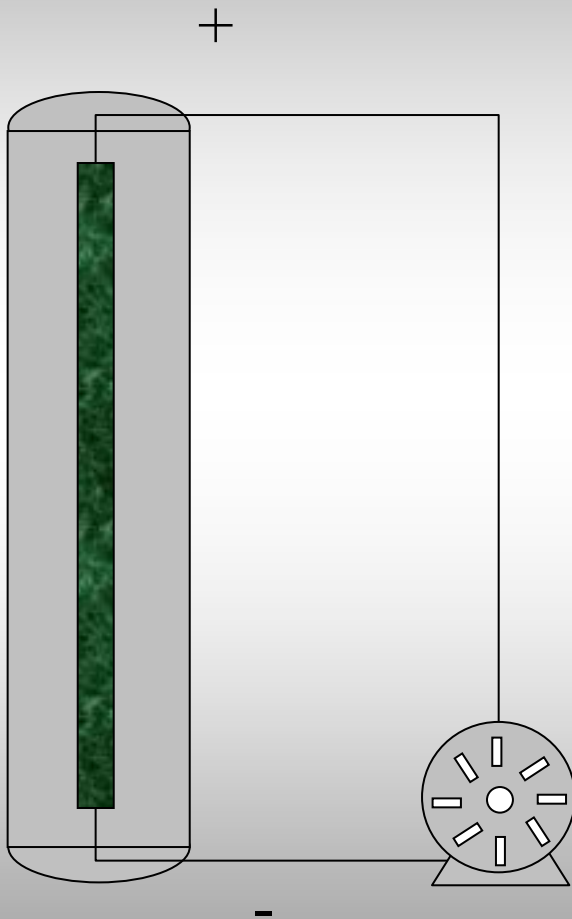
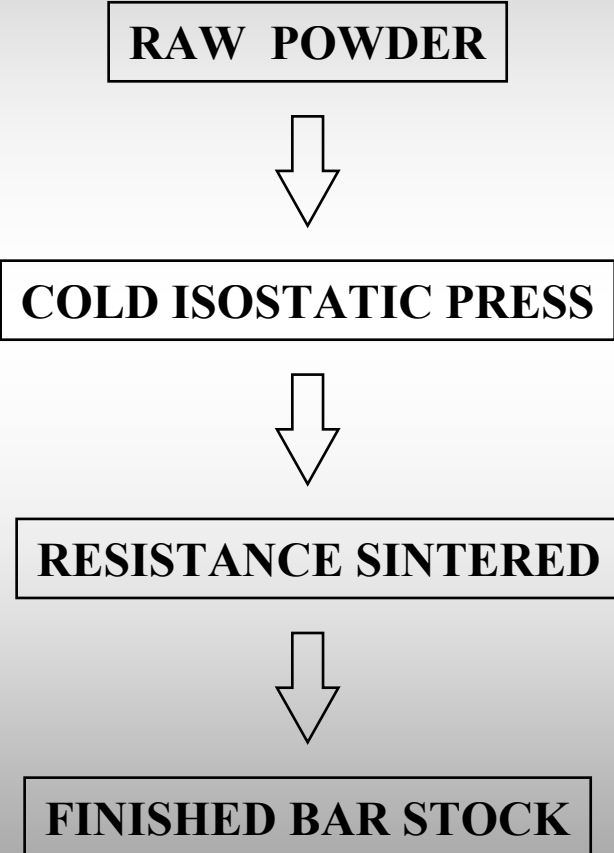


Vertical

Cordin Photo Results



Resistance Sintered consolidation process





Resistance Sintered Results



Horizontal



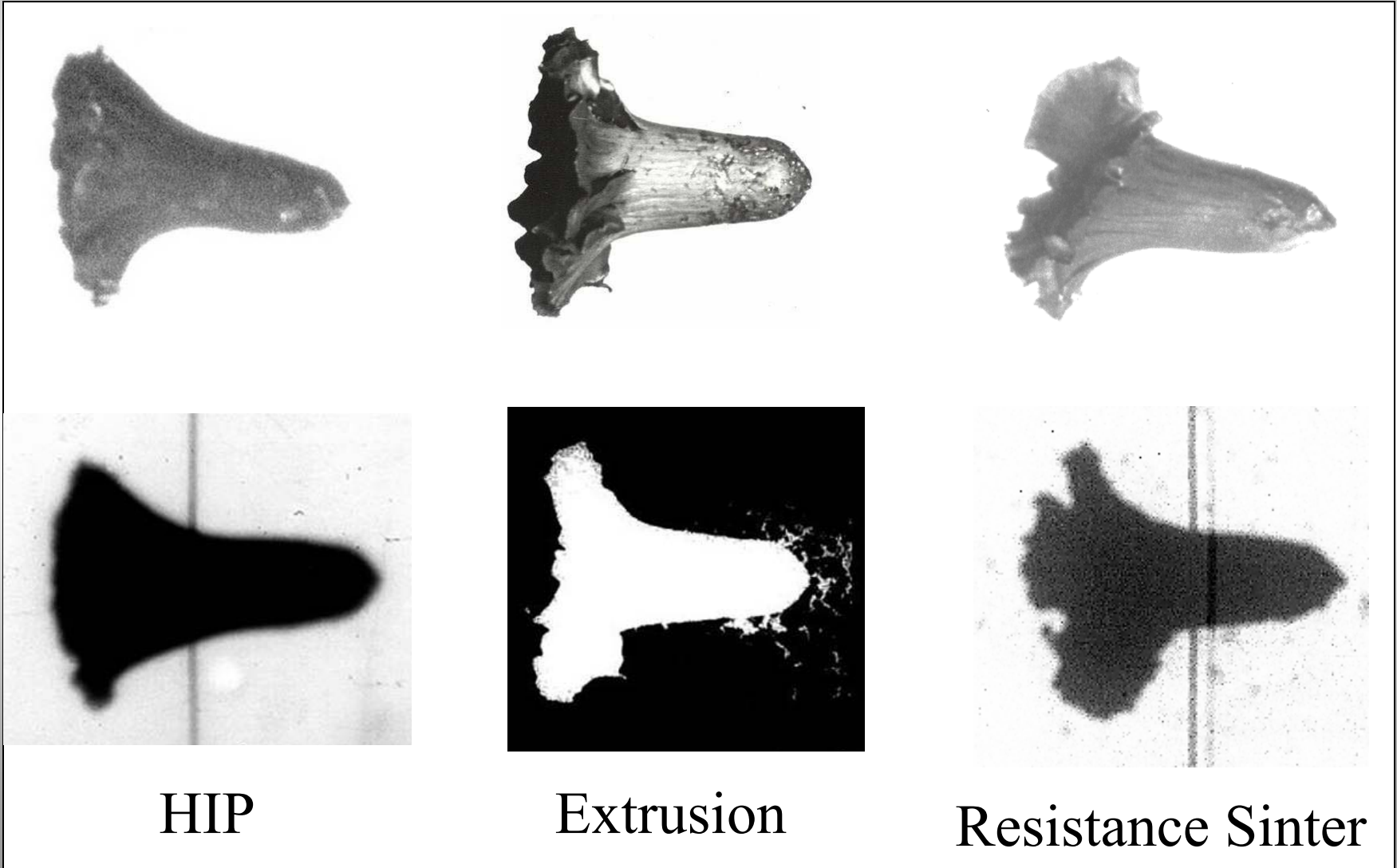
Vertical

Cordin Photo Results



Orthogonal X-Ray Results

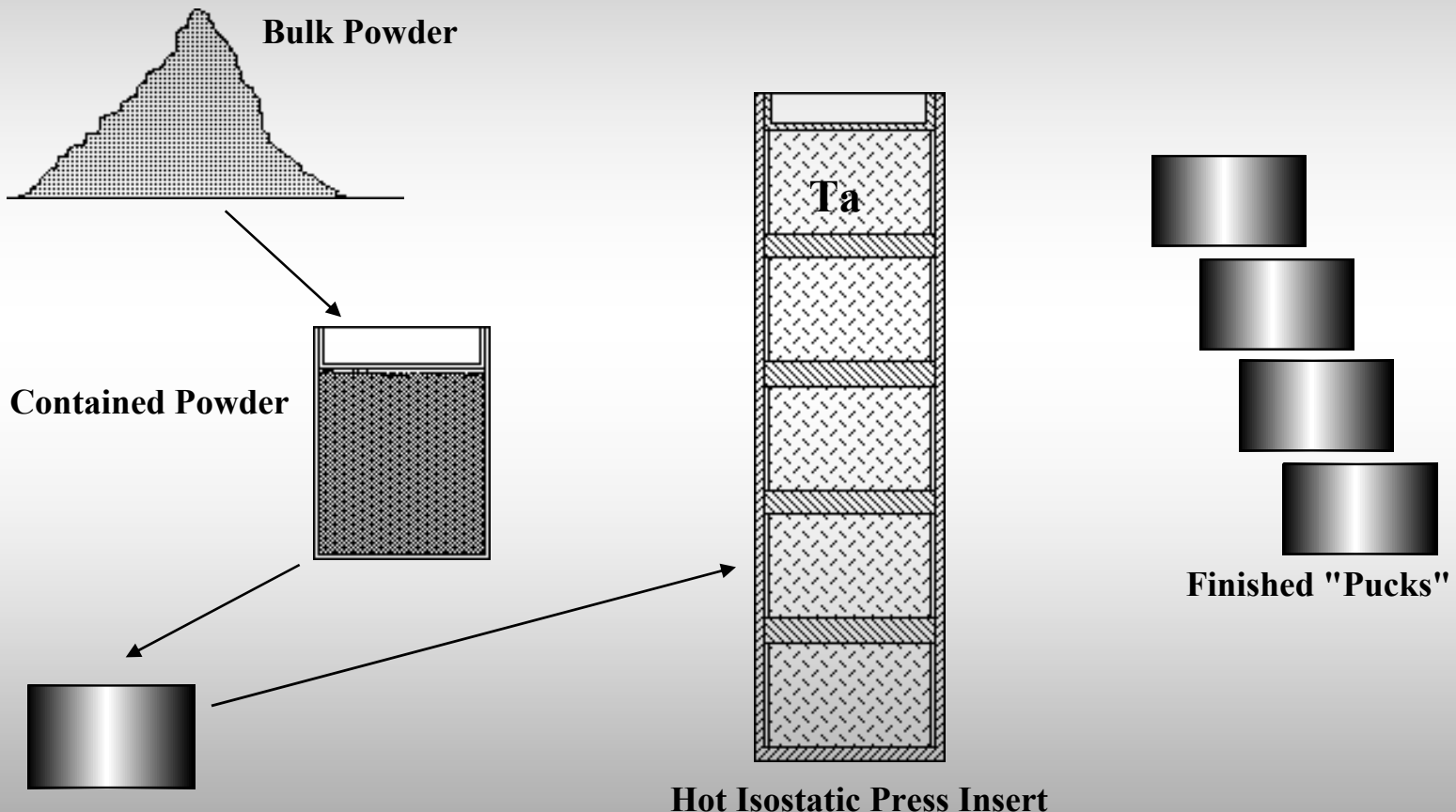
Comparison of Consolidation Processes





Near Net Process

Near-Net Process – Powder To “*Pucks*”



HIP To Puck Process

Consolidated Pucks



Pucks in Container



Pucks (Post-HIP) Containers removed



HIP



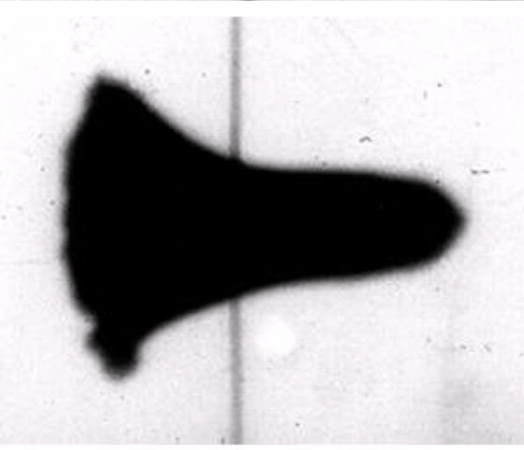
Test Data (HIP)

HIP to PUCK

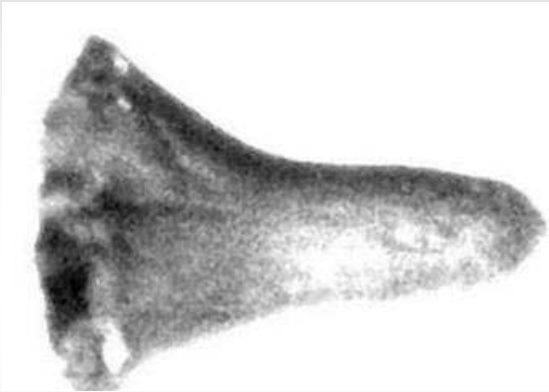
X-Ray Results



HIP to Bar



Cordin Photo Results





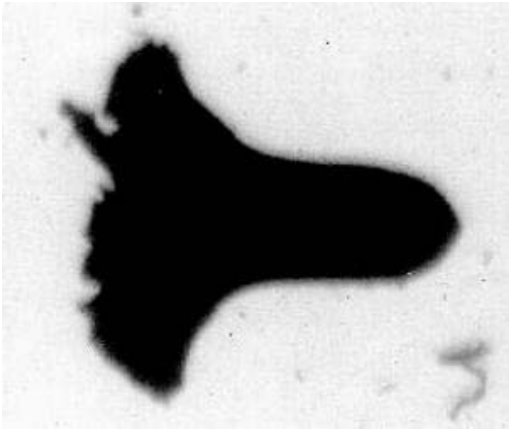
EFP Design and Material Evaluation



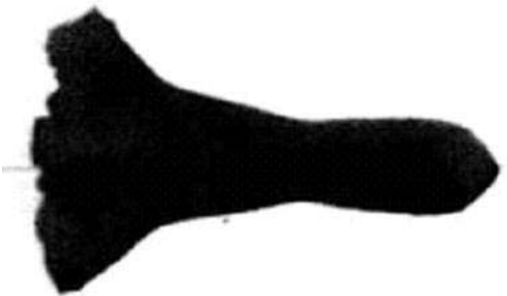
EFP Design Progression



Design #1



Design #2



Design #3



Material Evaluation



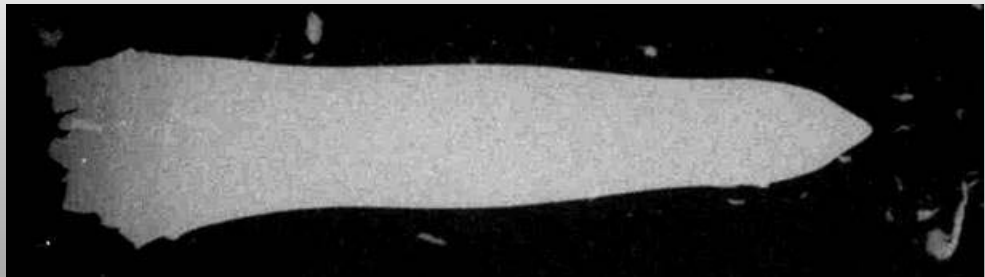
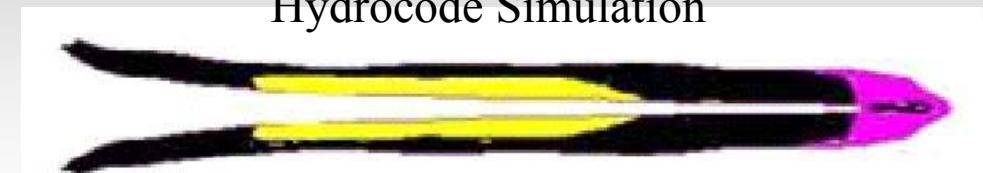
To assess Powdered Ta ductility for advance EFP designs

Advance EPF Design

EFP with pure Ta

EFP with TaW alloy

Hydrocode Simulation





Material Evaluation – Con't

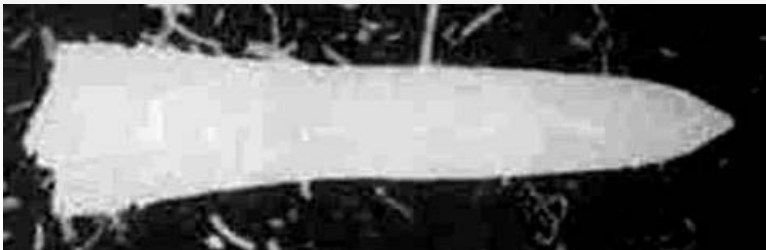


Powder Ta liner shot #1



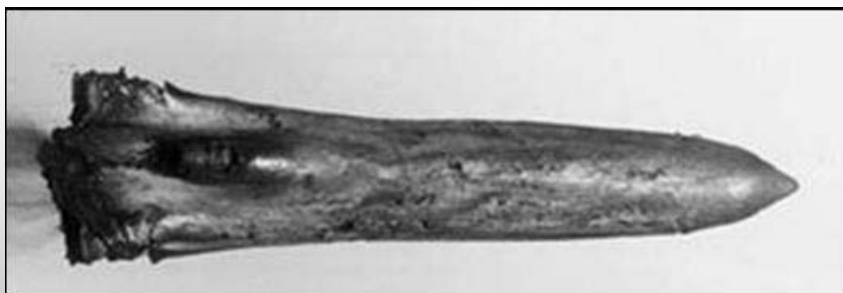
X-Ray

Powder Ta liner shot #2



X-Ray

Powder Ta liner shot #2



Cordin Photo

Pure Ta Bar



X-Ray



Summary

- Demonstrated lower cost repeatable EFP Liner fabrication process using Powder Tantalum.
- Eliminated lot-to-lot variations in material property
- Generated a powder tantalum material process and liner fabrication specification



WEAPONS AND MATERIALS RESEARCH DIRECTORATE

ARMOR MECHANICS BRANCH

BALLISTIC ANALYSIS OF BULGARIAN DUAL HARD STEEL PLATE

**MR. WILLIAM GOOCH, MR. MATTHEW BURKINS AND MR. DAVID MACKENZIE
U.S. ARMY RESEARCH LABORATORY
ABERDEEN PROVING GROUND, MD 21005-5066**

**PROFESSOR STEFAN VODENICHAROV
INSTITUTE OF METAL SCIENCE
BULGARIAN ACADEMY OF SCIENCES
SOFIA, BULGARIA**

**22nd INTERNATIONAL SYMPOSIUM ON BALLISTICS
VANCOUVER, BC, CANADA
MONTEREY, CA**

14-18 NOVEMBER 2005

**THIS PRESENTATION IS UNCLASSIFIED/DISTRIBUTION A
APPROVED FOR PUBLIC RELEASE**



METAL SOLUTIONS FOR TACTICAL VEHICLES



WEAPONS AND MATERIALS RESEARCH DIRECTORATE

ARMOR MECHANICS BRANCH

- MANY CURRENT ARMORED KITS FOR TACTICAL VEHICLES UTILIZE ROLLED HOMOGENEOUS ARMOR OR HIGH HARD STEEL SOLUTIONS
- SELECTION HAS BEEN DRIVEN BY EXPEDIENCY REQUIREMENTS, MATERIAL AVAILABILITY AND COST CONSIDERATIONS
- METAL SOLUTIONS ALSO PROVIDE VERY GOOD MULTIHIT FRAGMENT PROTECTION AGAINST IMPROVISED EXPLOSIVE DEVICES DUE TO THE TOUGHNESS OF THE PLATES
- ARL IS RE-EXAMINING METAL SOLUTIONS THAT COULD PROVIDE REDUCED WEIGHT AND/OR IMPROVED PROTECTION



POSSIBLE METAL TECHNOLOGIES



WEAPONS AND MATERIALS RESEARCH DIRECTORATE

ARMOR MECHANICS BRANCH

- **IMPROVED STEELS**
 - ULTRA HIGH HARD STEELS
 - **DUAL HARD STEELS**
- **HIGH STRENGTH ALUMINUM ALLOYS**
- **ALTERNATE TITANIUM ALLOYS TO Ti-6AL-4V**
 - BETA ALLOYS
 - DUAL HARD TITANIUM
- **METAL LAMINATES**
 - MILD STEEL/RHA OR HIGH HARD
 - STEEL/ALUMINUM LAMINATES
 - TITANIUM/ALUMINUM LAMINATES
- **METAL/POLYMER COMPOSITES**
 - METAL/POLYMERIC LAMINATES
 - METAL/FIBERCOMPOSITES



DUAL HARD STEEL DEVELOPMENT



WEAPONS AND MATERIALS RESEARCH DIRECTORATE

ARMOR MECHANICS BRANCH

- **DUAL HARD STEEL WAS DEVELOPED IN 1965 AT THE WATERTOWN ARSENAL, NOW ARL, FOR HELICOPTER ARMOR APPLICATIONS**
- **MIL-S-46099A, STEEL ARMOR PLATE, ROLL-BONDED, DUAL HARDNESS WAS ESTABLISHED IN NOVEMBER 1966**
- **PRODUCTION FEASIBILITY STUDIES FOR ROLL BONDED PLATE WERE CONDUCTED BY US STEEL IN 1968 AND THEN AT OTHER COMPANIES**
- **ALLEGHENY LUDLUM IS THE ONLY CURRENT PRODUCER OF K12® DUAL HARD ARMOR STEELS USING A PROPRIETARY PROCESS**



ALLEHGENY LUDLUM K12®

DUAL HARD STEEL



WEAPONS AND MATERIALS RESEARCH DIRECTORATE

ARMOR MECHANICS BRANCH

- **K12® DUAL HARD STEEL RESULTS FROM ROLL BONDING TWO NI-CR-MO PLATES THAT PRODUCE A HIGH HARDNESS FRONT SIDE AND A SOFTER BACK SIDE**
- **THE FRONT PLATE HAS A HARDNESS OF 601-712 BRINELL WITH THE REAR PLATE 461-534**
- **K12® IS NORMALLY FURNISHED IN THE ANNEALED STATE FOR SHAPING AND CUTTING AND IS THEN FINAL HEAT-TREATED**
- **MIL-S-46099C HAS A BALLISTIC ACCEPTANCE CRITERIA WITH PLATES FROM 0.170"-0.330" TESTED WITH THE 0.30-CAL APM2 AND PLATES FROM 0.290"- 0.585" WITH THE 0.50-CAL APM2**



RESEARCH GOAL



WEAPONS AND MATERIALS RESEARCH DIRECTORATE

ARMOR MECHANICS BRANCH

- **DUAL HARD STEEL ISSUES:**
 - DEBONDING OF ROLLED PLATES
 - PLATE SIZE LIMITATIONS
 - REAR PLATE DEFORMATION
 - ALTERNATE FABRICATION TECHNOLOGIES
- EXAMINE MIL-46099C FOR POSSIBLE ADDITION OF A NEW HARDNESS SPECIFICATION
- PAPER PROVIDES THE INITIAL RESULTS OF ARL'S EXAMINATION OF DUAL HARD STEEL PRODUCED BY THE ELECTROSLAG REMELTING PROCESS AS DEVELOPED BY THE INSTITUTE OF METAL SCIENCE (ISM) OF THE BULGARIAN ACADEMY OF SCIENCES
- BASELINE RHA AND HIGH HARD WERE ALSO RETESTED AS HISTORIC DATA IS INCOMPLETE



BULGARIAN INSTITUTE OF METAL SCIENCE DUAL HARD STEEL



WEAPONS AND MATERIALS RESEARCH DIRECTORATE

ARMOR MECHANICS BRANCH

- ELECTROSLAG REMELTING (ESR) PROCESS WAS HIGHLY DEVELOPED IN THE 1980'S, BUT WAS NOT WORKED ON AT THE ISM AFTER 1991 FOR LACK OF FUNDS
- ARL EXAMINED ISM DUAL HARD PLATES IN 2004 AND CONTRACTED WITH ISM TO RESTART THEIR ESR FURNACE AND PRODUCE A MODIFIED VERSION OF US DUAL HARD STEEL
- ARL SPECIFIED A FRONT PLATE WITH A HARDNESS OF 500-560 BRINELL WITH THE REAR PLATE 340-370 BRINELL
- PAPER EXAMINES THE BALLISTIC PROPERTIES OF DUAL HARD PLATE COMPARED AGAINST RHA AND HIGH HARD STEEL



ISM ESR016 ELECTROSLAG REMELTING FURNACE



WEAPONS AND MATERIALS RESEARCH DIRECTORATE

ARMOR MECHANICS BRANCH



**DR. STEFAN VODENICHAROV
INSTITUTE OF METAL SCIENCE
BULGARIAN ACADEMY
OF SCIENCES
SOFIA, BULGARIA**

**INGOTS WERE ESR CAST
FORGED AND ROLLED
HEAT-TREATED AND CUT
300mm X 300mm PLATES**

**PLATES WERE FABRICATED IN
THICKNESSES OF 5mm TO 80mm**

**ONLY 5-10mm PLATE DATA
PROVIDED IN THIS PAPER**

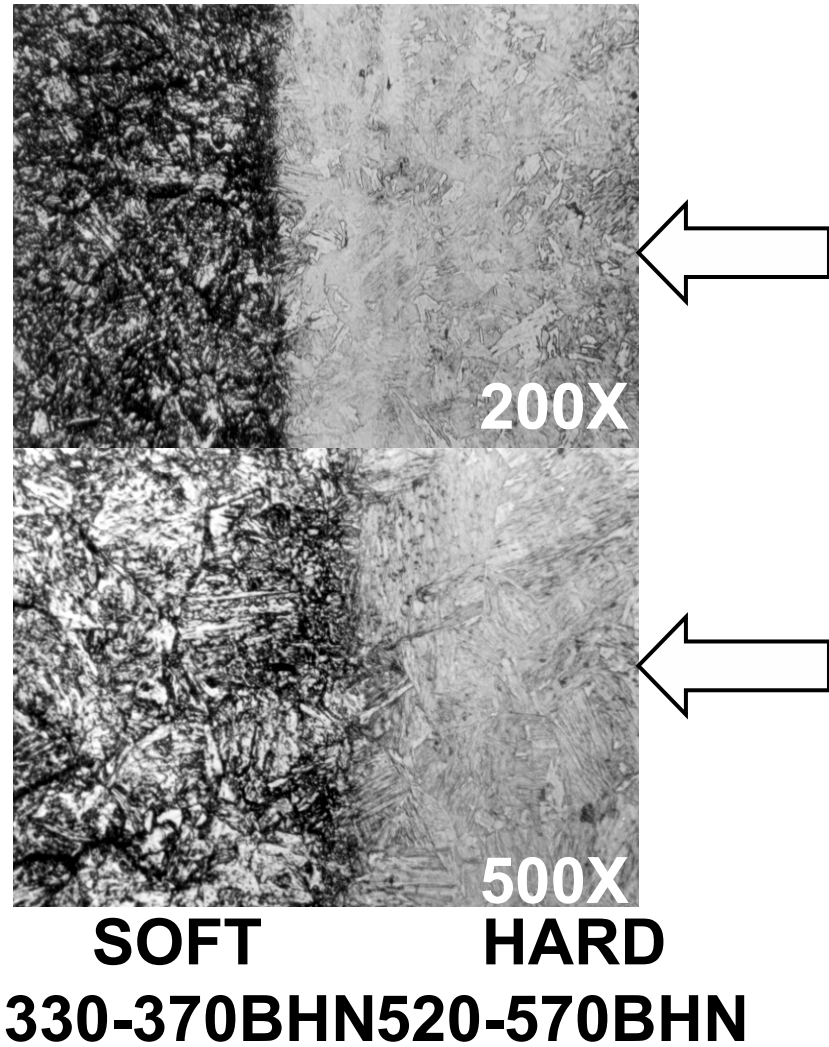
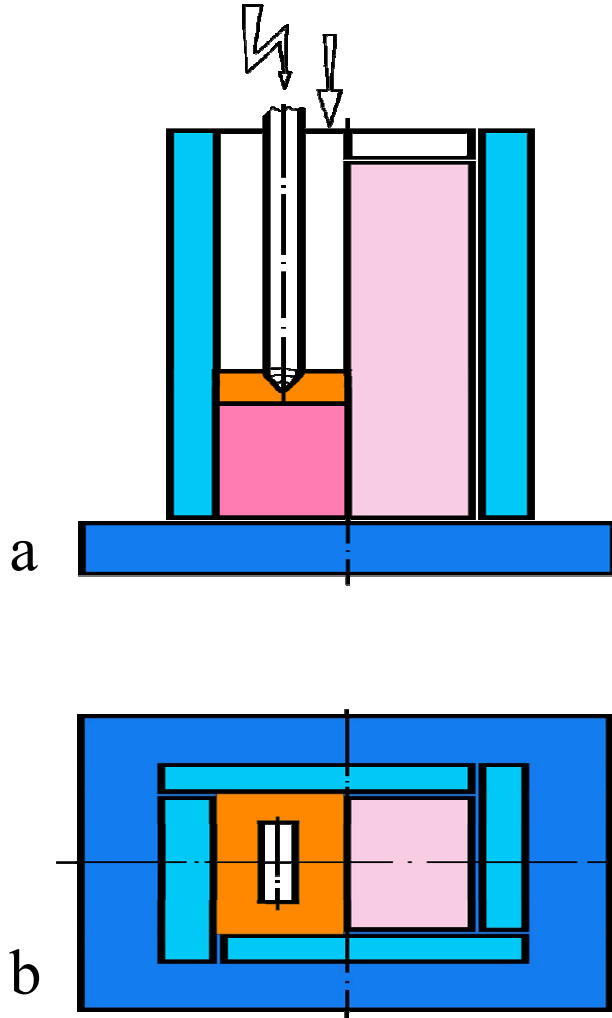


ISM ESR016 ELECTROSLAG REMELTING FURNACE



WEAPONS AND MATERIALS RESEARCH DIRECTORATE

ARMOR MECHANICS BRANCH



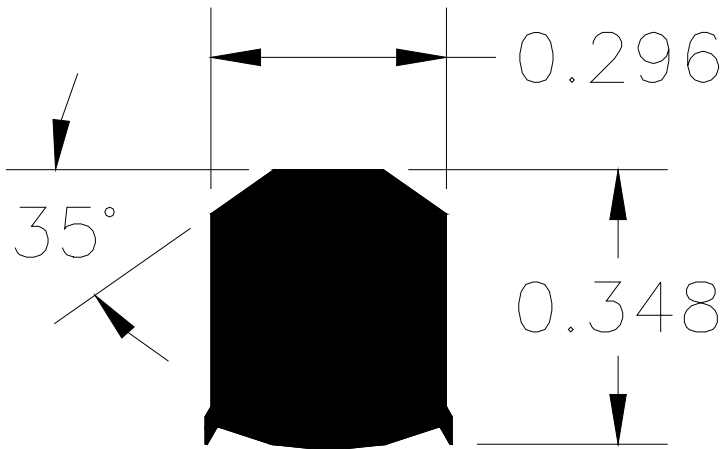


TEST PROJECTILES



WEAPONS AND MATERIALS RESEARCH DIRECTORATE

ARMOR MECHANICS BRANCH



**0.30-CALIBER 44-GRAIN
FRAGMENT SIMULATING
PROJECTILE**

**7.62mmx63 (0.30 CALIBER)
APM2 ARMOR PIERCING
PROJECTILE**



DUAL HARD TEST DATA



WEAPONS AND MATERIALS RESEARCH DIRECTORATE

ARMOR MECHANICS BRANCH

0.30-cal FSP V ₅₀ VELOCITY AT THICKNESS (0° OBLIQUITY) (m/s)						
Nominal Thickness	5mm	6mm	7mm	8mm	9mm	10mm
Actual Thickness	5.39	6.45	7.54	8.23	9.96	10.95
Front/Rear Hardness	523/365	572/375	561/373	537/363	544/340	557/337
Bulgarian Dual Hard	708	763	911	1063	1145	>1402

.30-cal APM2 V ₅₀ VELOCITY AT THICKNESS (0° OBLIQUITY) (m/s)						
Nominal Thickness	5mm	6mm	7mm	8mm	9mm	10mm
Actual Thickness	5.41	6.45	7.90	8.74	9.37	10.36
Front/Rear Hardness	523/365	572/375	568/366	547/361	531/340	539/345
Bulgarian Dual Hard	512	NA	693	691	703	705

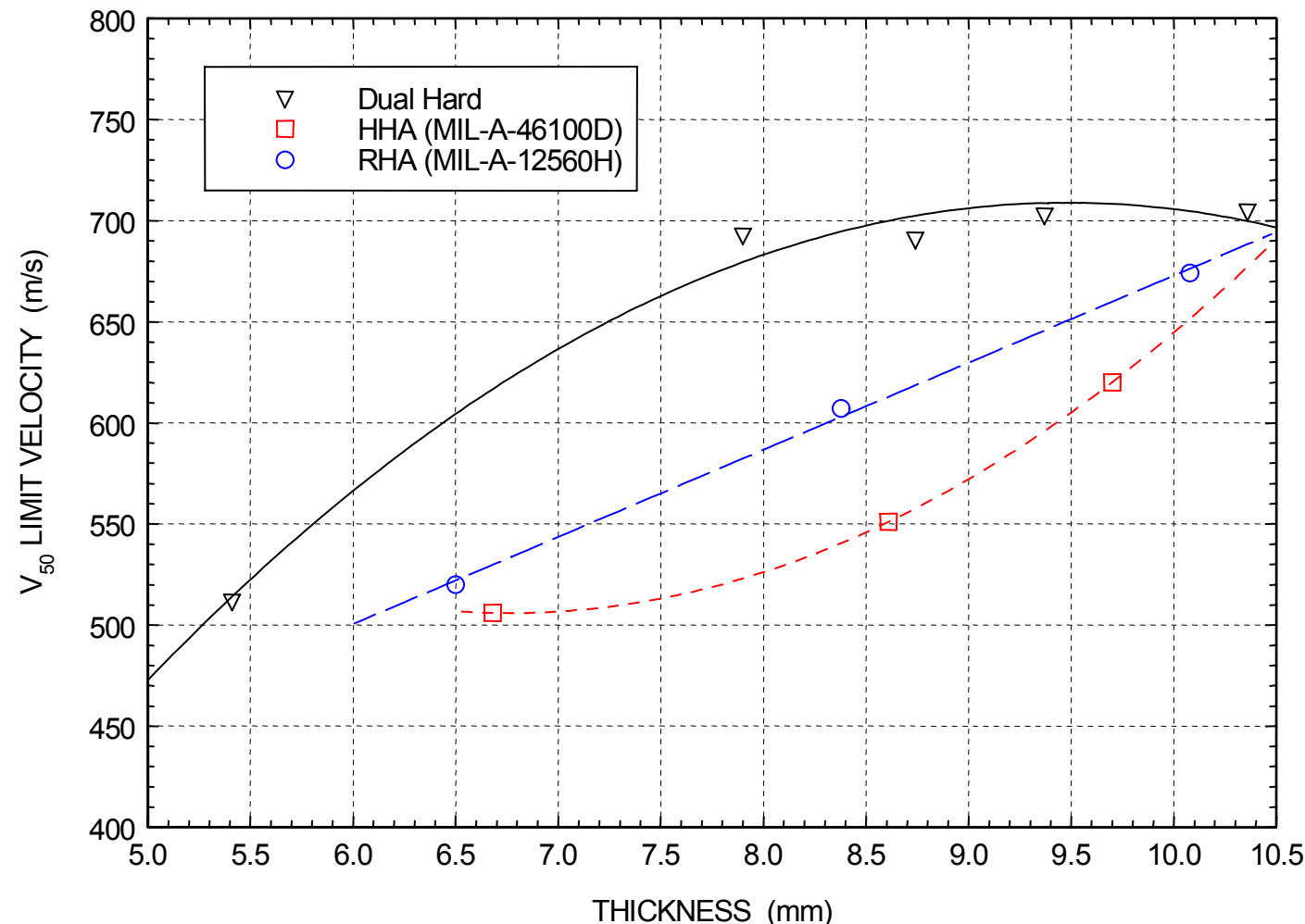


0.30 CALIBER APM2 @ 0°



WEAPONS AND MATERIALS RESEARCH DIRECTORATE

ARMOR MECHANICS BRANCH



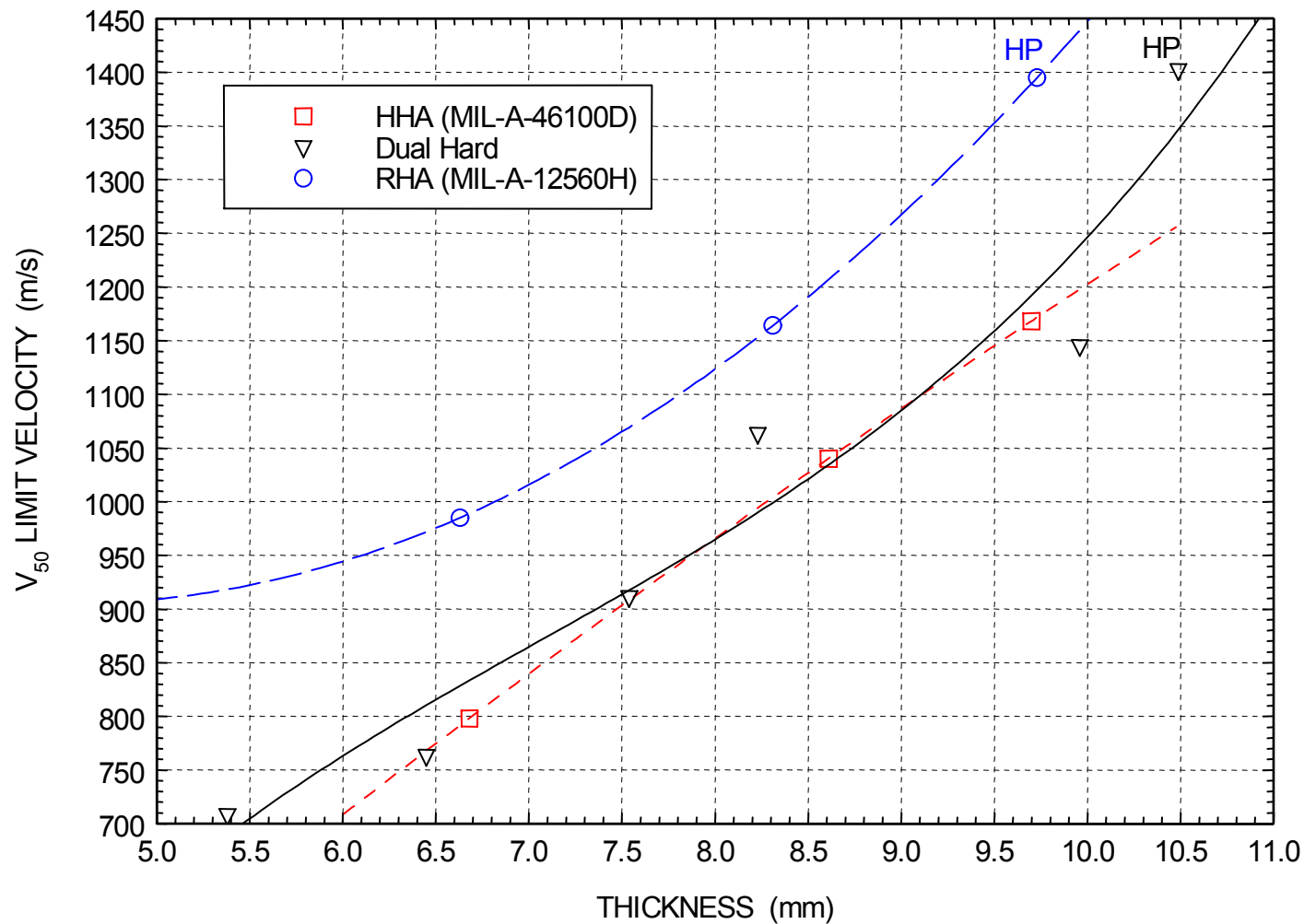


0.30 CALIBER FSP @ 0°



WEAPONS AND MATERIALS RESEARCH DIRECTORATE

ARMOR MECHANICS BRANCH



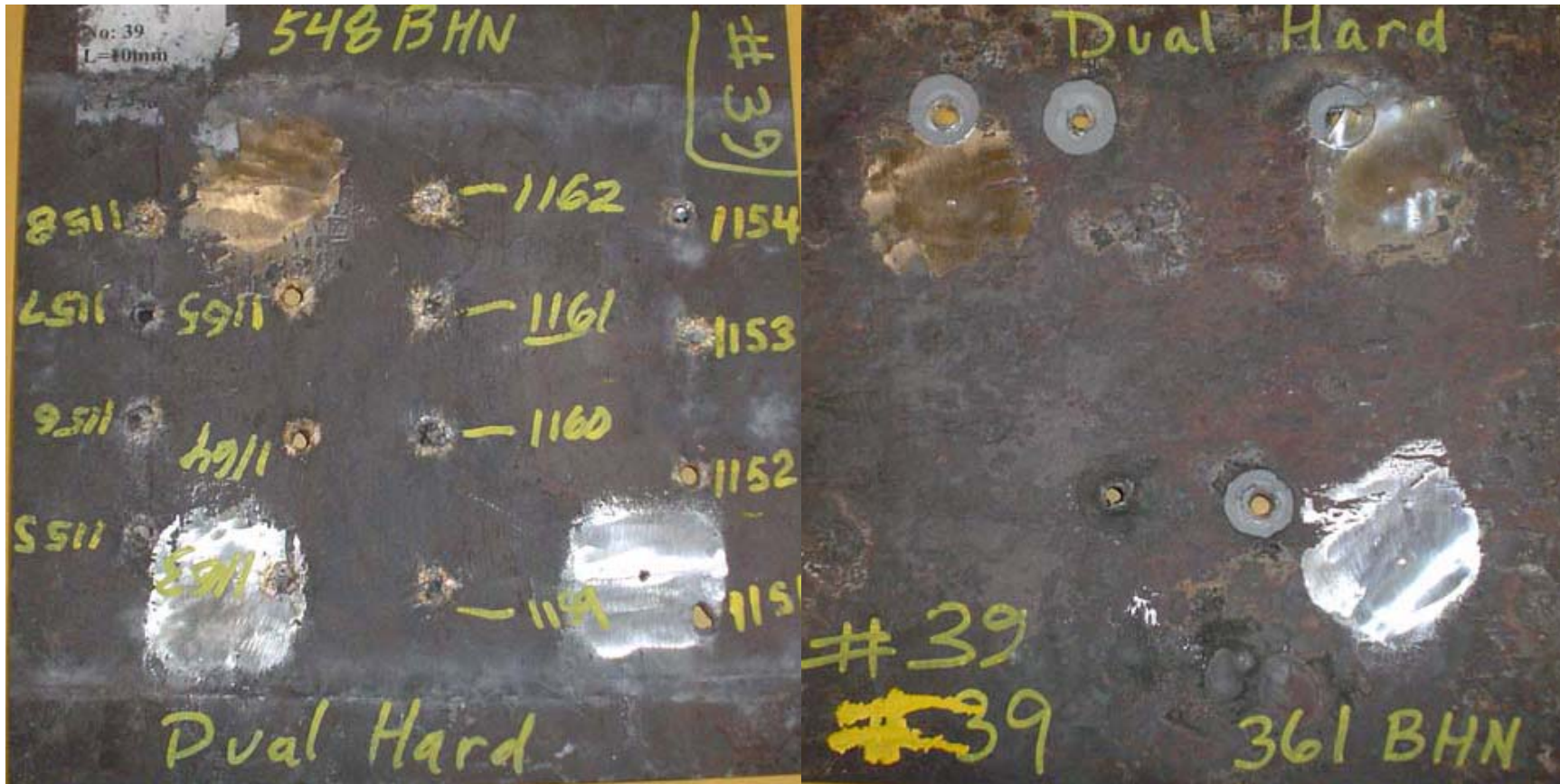


10mm TEST PLATE 0.30-CALIBER APM2



WEAPONS AND MATERIALS RESEARCH DIRECTORATE

ARMOR MECHANICS BRANCH



FRONT

REAR



10mm TEST PLATE 0.30-CALIBER FSP



WEAPONS AND MATERIALS RESEARCH DIRECTORATE

ARMOR MECHANICS BRANCH



FRONT



REAR

Oilwell Perforators: Theoretical Considerations

Brenden Grove

22nd International Symposium on Ballistics

November 17, 2005

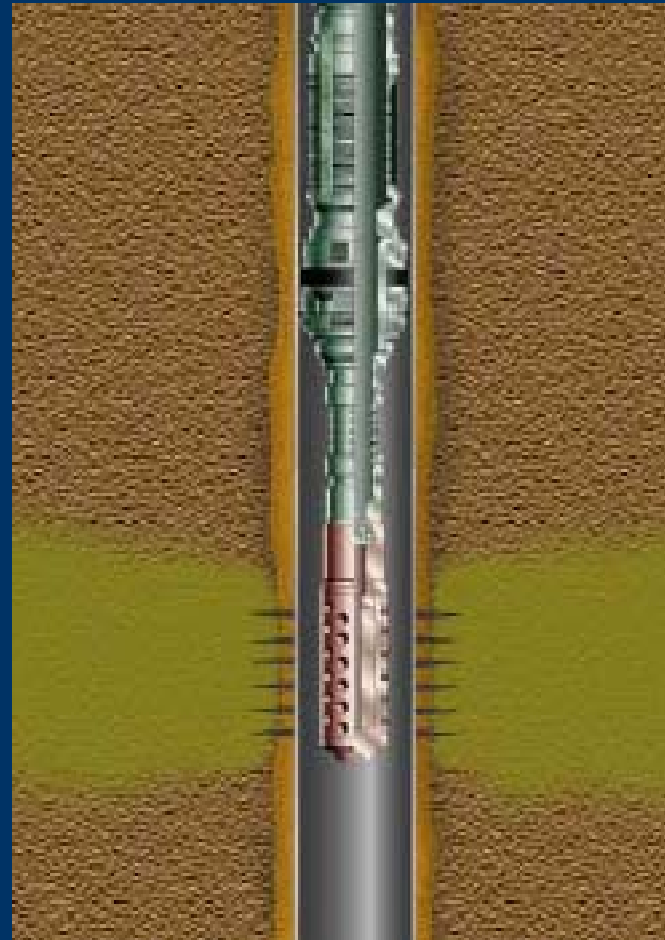
Schlumberger

Overview

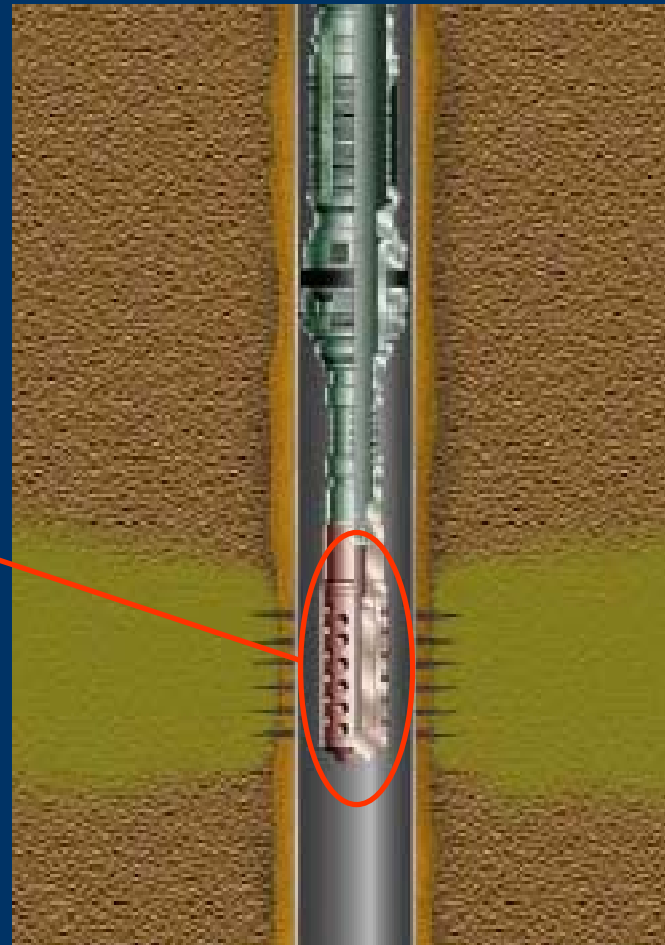
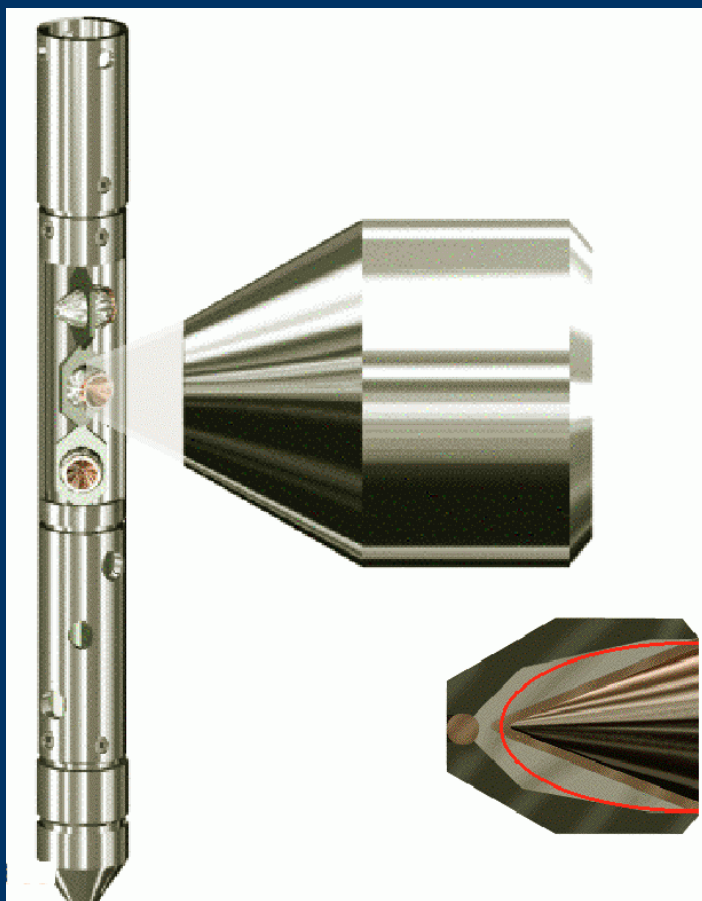
- Introduction / Background
- Compressible Jet Model
- Implications:
 - Hydrodynamic penetration depth
 - Impact pressure
 - Target strength
- Conclusions

Introduction / Background

- Oilwell perforators
→ 20-60mm
shaped charges
- Perforate casing,
cement, formation
rock
- Perf tunnels must
be clean to allow
subsequent fluid
flow



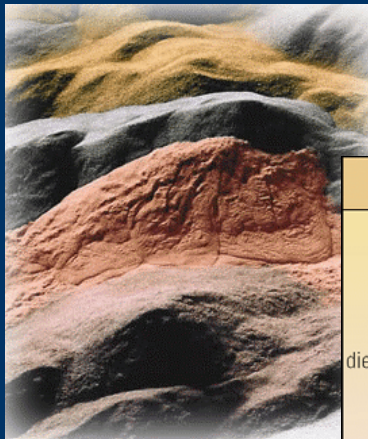
Introduction / Background



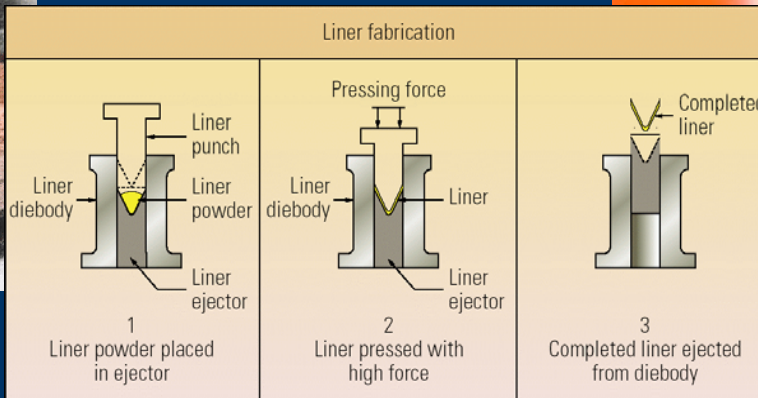
Introduction / Background

Liner:

- formed by powdered metallurgy (P/M)
- unsintered (green)

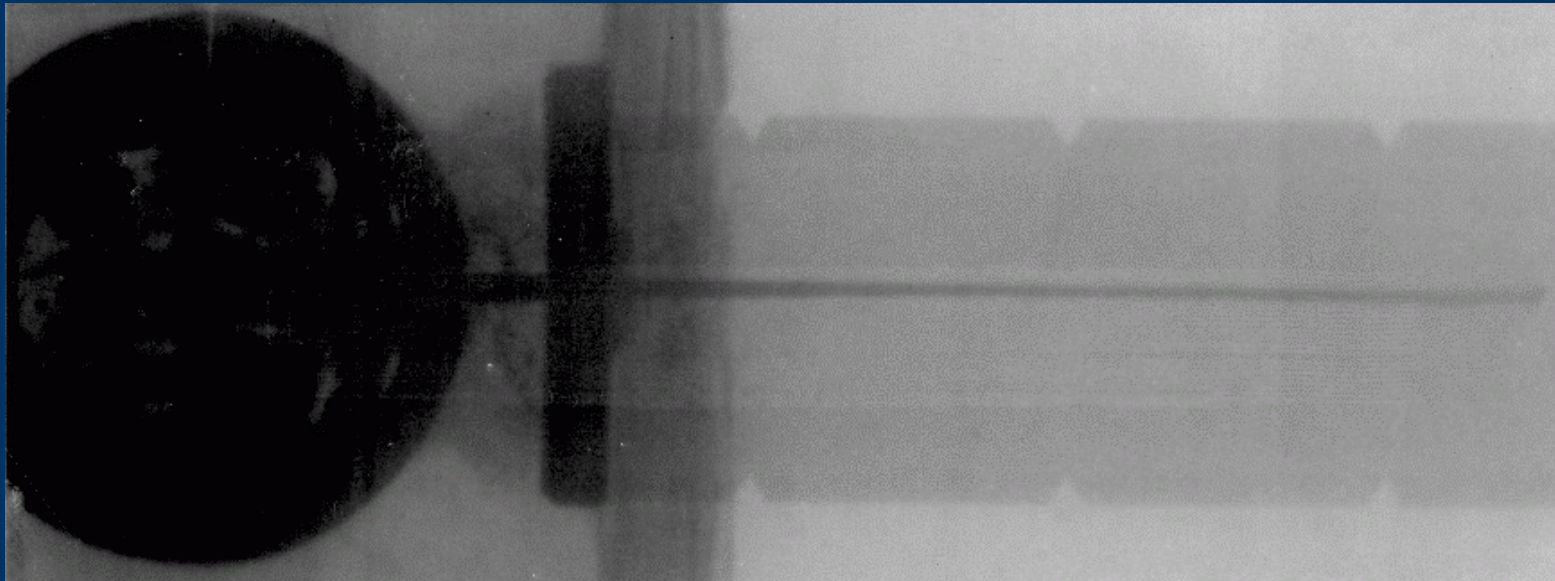


Metal powder photograph:
<http://www.mpif.org/IntroPM/makepowder.asp?linkid=5>



Introduction / Background

- Jet=millions of discrete powder particles
- How to model jet penetration?
 - *Traditional models underpredict penetration*

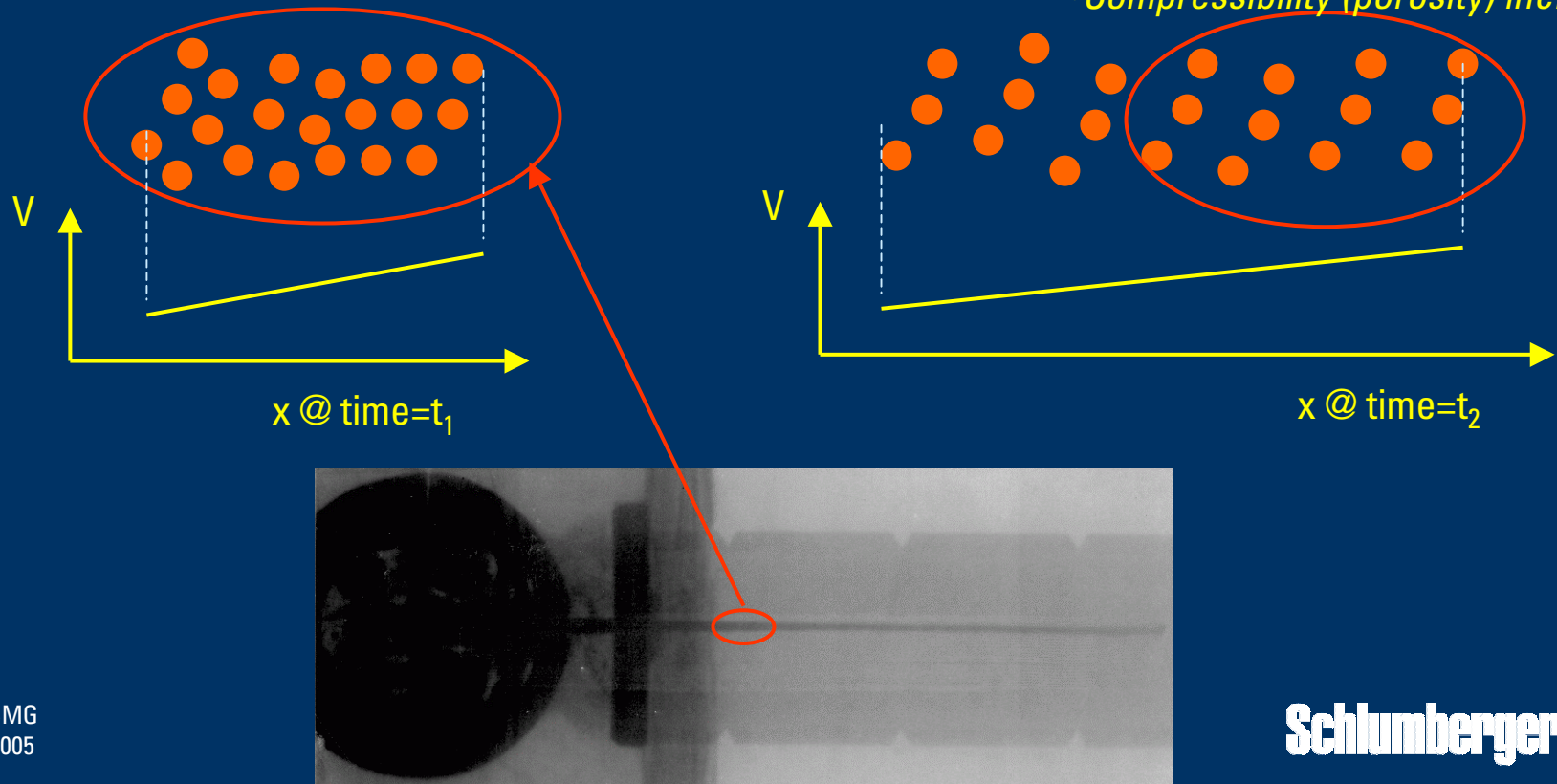


Introduction / Background

- Jet=millions of discrete powder particles
- How to model jet penetration?
 - *Density decrease*
 - *Compressibility*

- *Density decreases*

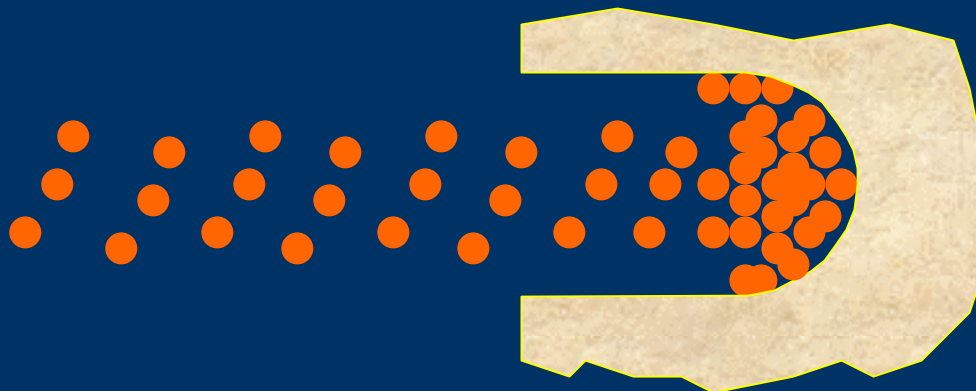
- Compressibility (porosity) increases



Compressible Jet

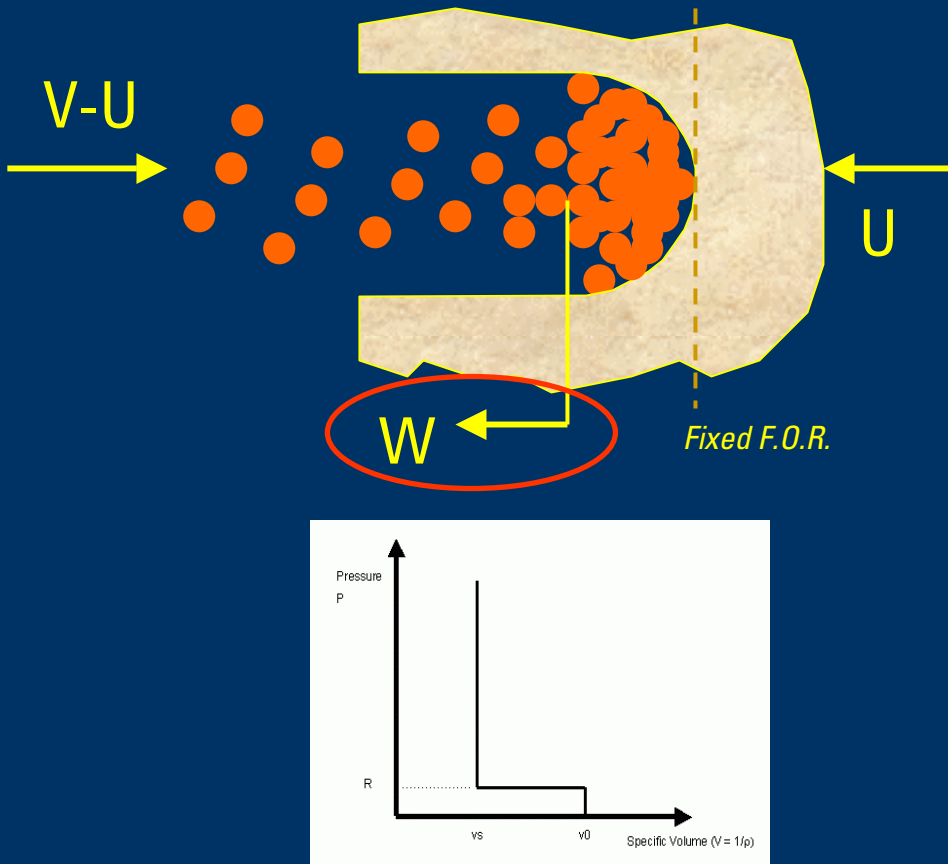
Penetration Theory

- Multiple discrete impacts; particles “pile up”?
- Macroscopically – jet compresses
- *Incompressible Bernoulli not applicable*



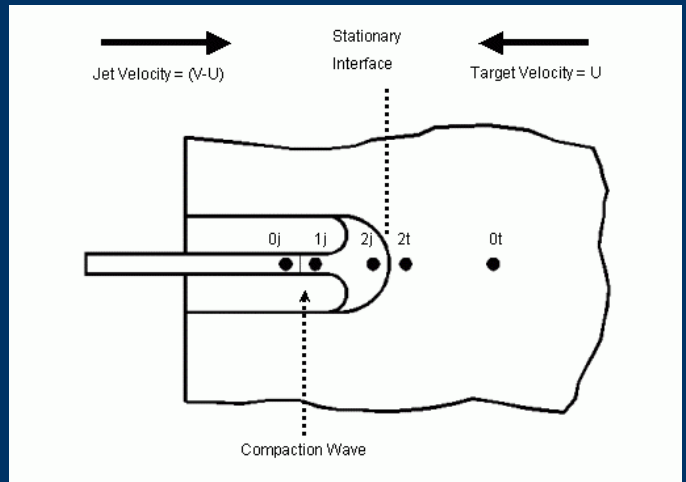
Compressible Jet

Penetration Theory



Jet Material Compaction Curve

- Flis & Crilly (18th ISB): compressible target
- Reverse their analysis here

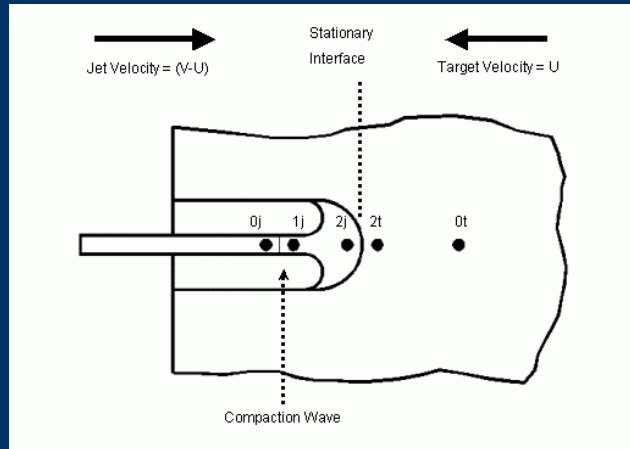


ρ_0 = initial (distended) jet density
 ρ_s = solid (pore-free) jet density
 $\phi = 1 - \rho_0 / \rho_s$ = jet porosity
 R = jet compaction initial resistance

Compressible Jet

Penetration Theory

- Distended jet at ρ_0 traveling at $(V-U)$
- Compacted to ρ_s , decelerated to w_{1j}



mass

$$\rho_{0j} w_{0j} = \rho_{1j} w_{1j} \quad w_{0j} = V - U$$

momentum

$$P_{0j} + \rho_0 (w_{0j})^2 = P_{1j} + \rho_1 (w_{1j})^2$$

full compaction

$$\rho_{1j} = \rho_{2j} = \rho_c$$

- Apply incompressible Bernoulli to compacted jet impact

Compressible Jet

Penetration Theory

Jet pressure

$$P_{2j} = R + \frac{1}{2} \rho_0 (V - U)^2 (1 + \phi)$$

Target pressure

$$P_{2t} = Y_t + \frac{1}{2} \rho_{0t} U^2$$

PD (hydrodynamic)

$$\frac{PD}{L} = \sqrt{\frac{\rho_0}{\rho_t} (1 + \phi)}$$

PD (target strength
important)

$$\frac{PD}{L} = \sqrt{\frac{\rho_0}{\rho_t} (1 + \phi)} - \frac{2\sigma}{\rho_t (V - U)^2}$$

Compressibility
Effect

Compressible vs. Incompressible Jet

Penetration Theory

Incompressible → Compressible

Jet Pressure

$$P_{2j} = Y_j + \frac{\lambda}{2} \rho_0 (V-U)^2 \longrightarrow P_{2j} = R + \frac{1}{2} \rho_0 (V-U)^2 (1+\phi)$$

Hydrodynamic
Penetration Depth

$$\frac{PD}{L} = \sqrt{\frac{\lambda \rho_j}{\rho_t}} \longrightarrow \frac{PD}{L} = \sqrt{\frac{\rho_0}{\rho_t} (1+\phi)}$$

$$\lambda \longrightarrow (1+\phi)$$

Compressible vs. Incompressible Jet

Penetration Theory

- $(1+\phi) \rightarrow \lambda$
- Porous jet model reduces to incompressible model at limits
- At upper limit ($\phi=1$; $\lambda=2$), $\rho \rightarrow$ zero
- For a given length and macroscopic density, porosity increases the following:
 - *Penetration depth*
 - *Impact pressure*

Jet Density, Length, Porosity

Summary

Consider 3 cases: *(Fixed mass, velocity, diameter)*

$$\rho L = \text{constant}$$

Case A: ρ_s , incompressible;
length = L_s



$\rightarrow V$

Case B: ρ_0 , compressible to ρ_s ;
length = L_0



$\rightarrow V$

Case C: ρ_0 , incompressible;
length = L_0



$\rightarrow V$

Jet Density, Length, Porosity Summary

Hydrodynamic Penetration Depth

Case A:

$$PD_A = L_s \sqrt{\frac{\rho_s}{\rho_t}}$$

Case B:

$$\begin{aligned} PD_B &= L_0 \sqrt{\frac{\rho_0}{\rho_t} (1 + \phi)} \\ &= PD_A \sqrt{\frac{1 + \phi}{1 - \phi}} \quad (\text{alternative form}) \\ &= PD_C \sqrt{1 + \phi} \quad (\text{alternative form}) \end{aligned}$$

Case C:

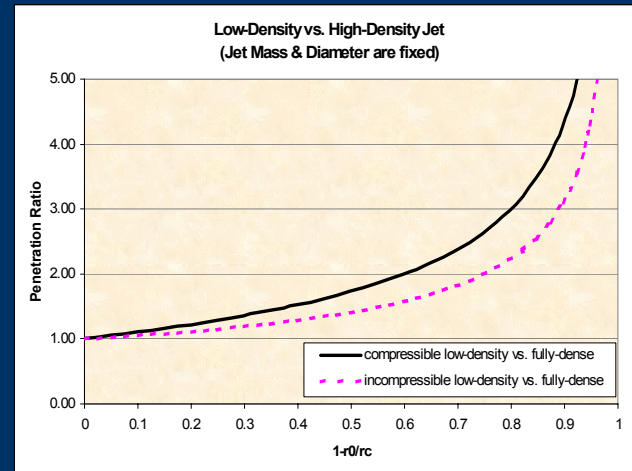
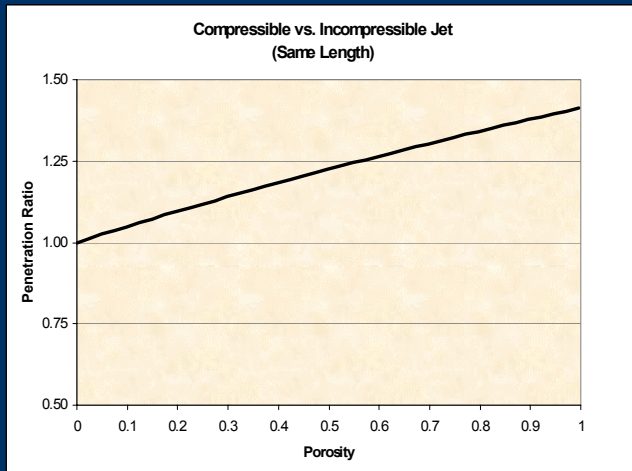
$$PD_C = L_0 \sqrt{\frac{\rho_0}{\rho_t}}$$

Jet Density, Length, Porosity Summary

Hydrodynamic Penetration Depth

$$PD_B > PD_C > PD_A$$

$$PD_B : PD_C : PD_A = \sqrt{\frac{1+\phi}{1-\phi}} : \sqrt{\frac{1}{1-\phi}} : 1$$



Jet Density, Length, Porosity Summary

Dynamic Jet Pressure

Case A:

$$P_A = \frac{1}{2} \rho_s (V - U)^2$$

Case B:

$$\begin{aligned} P_B &= \frac{1}{2} \rho_s (V - U)^2 (1 - \phi^2) \\ &= \frac{1}{2} \rho_0 (V - U)^2 (1 + \phi) \quad (\text{alternative form}) \end{aligned}$$

Case C:

$$P_C = \frac{1}{2} \rho_0 (V - U)^2$$

Jet Density, Length, Porosity Summary

Dynamic Jet Pressure

$$U = \frac{V}{1+\gamma}$$



$$\gamma_A = \sqrt{\frac{\rho_t}{\rho_s}}$$

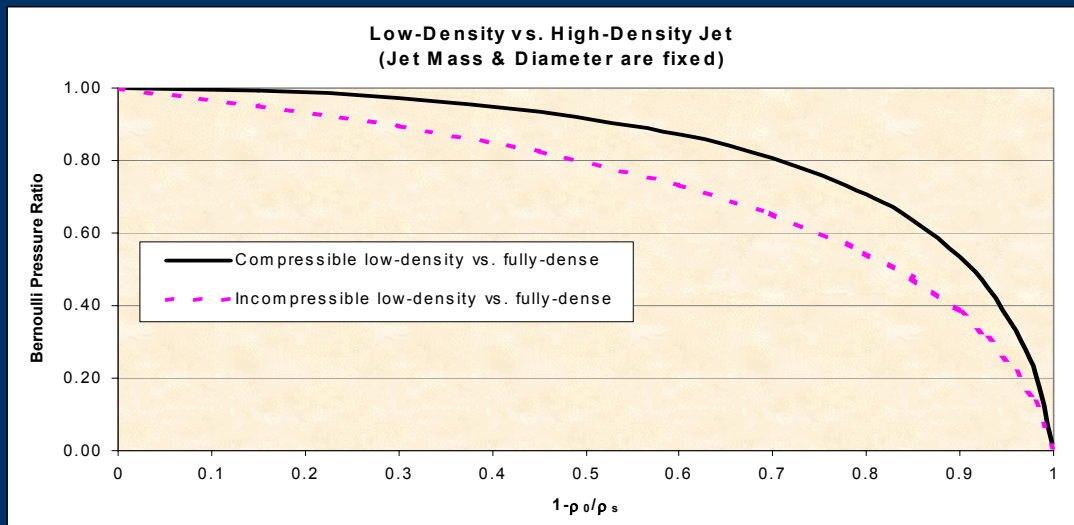
$$\gamma_B = \sqrt{\frac{\rho_t}{\rho_s(1-\phi^2)}} = \frac{\gamma_A}{\sqrt{1-\phi^2}}$$

$$\gamma_C = \sqrt{\frac{\rho_t}{\rho_0}} = \frac{\gamma_A}{\sqrt{1-\phi}}$$



$$P_A > P_B > P_C$$

$$P_A : P_B : P_C = 1 : \left[\frac{1 - \left(\frac{1}{1 + \frac{\gamma_A}{\sqrt{1-\phi^2}}} \right)^2}{1 - \left(\frac{1}{1 + \gamma_A} \right)} (1-\phi^2) \right] : \left[\frac{1 - \left(\frac{1}{1 + \frac{\gamma_A}{\sqrt{1-\phi}}} \right)^2}{1 - \left(\frac{1}{1 + \gamma_A} \right)} (1-\phi) \right]$$



Jet Density, Length, Porosity

Summary

Consider 3 cases: *(Fixed mass, velocity, diameter)*

$$\rho L = \text{constant}$$

Case A: ρ_s , incompressible;
length = L_s



Case B: ρ_0 , compressible to ρ_s ;
length = L_0

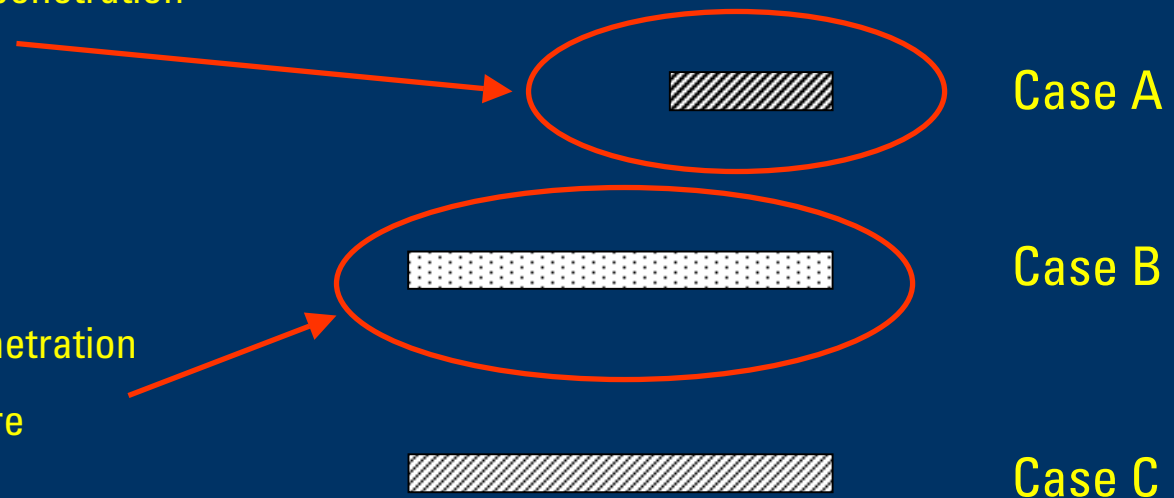


Case C: ρ_0 , incompressible;
length = L_0



Jet Density, Length, Porosity Summary

- Greatest impact pressure
- Shallowest hydrodynamic penetration



Impact Pressure & Target Strength

What about target strength?

Consider some critical point of interest (U_{crit} , P_{crit})

*Characteristic
target property*

$$U_{crit} = \sqrt{\frac{2(P_{crit} - Y_t)}{\rho_t}}$$

P_{crit} isobars in (ρ_j, V) coordinates

Incompressible; $1 \leq \lambda \leq 2$

$$\rho_j = \frac{\rho_t U_{crit}^2 + 2\sigma}{\lambda(V - U_{crit})^2}$$

Compressible

$$\rho_j = \rho_s(1 - \phi); \quad \phi = \sqrt{1 - \frac{\rho_t U_{crit}^2 + 2\sigma}{\rho_s(V - U_{crit})^2}}$$

*There is
no unique
 V_{min}*

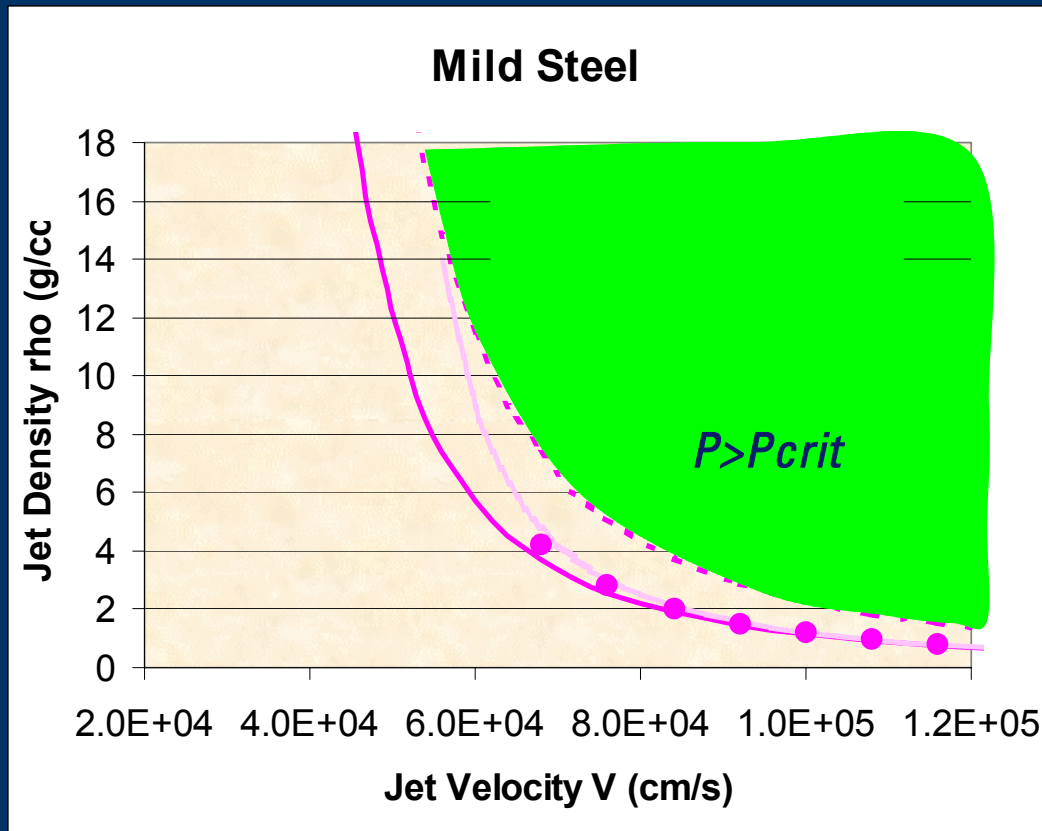
Impact Pressure & Target Strength

What do these isobars look like?

Target Material	ρ_t (g/cc)	Y_t (kbar)	P_{crit}	ρ_s (g/cc)	$R=Y_j$ (kbar)
Mild steel	7.86	3 (UTS)	$2Y_t$	16	0
Aluminium	2.7	3 (UTS)	"	"	"
Concrete	2.25	0.3 (UCS)	"	"	"
Sandstone	2.25	0.6 (UCS)	"	"	"

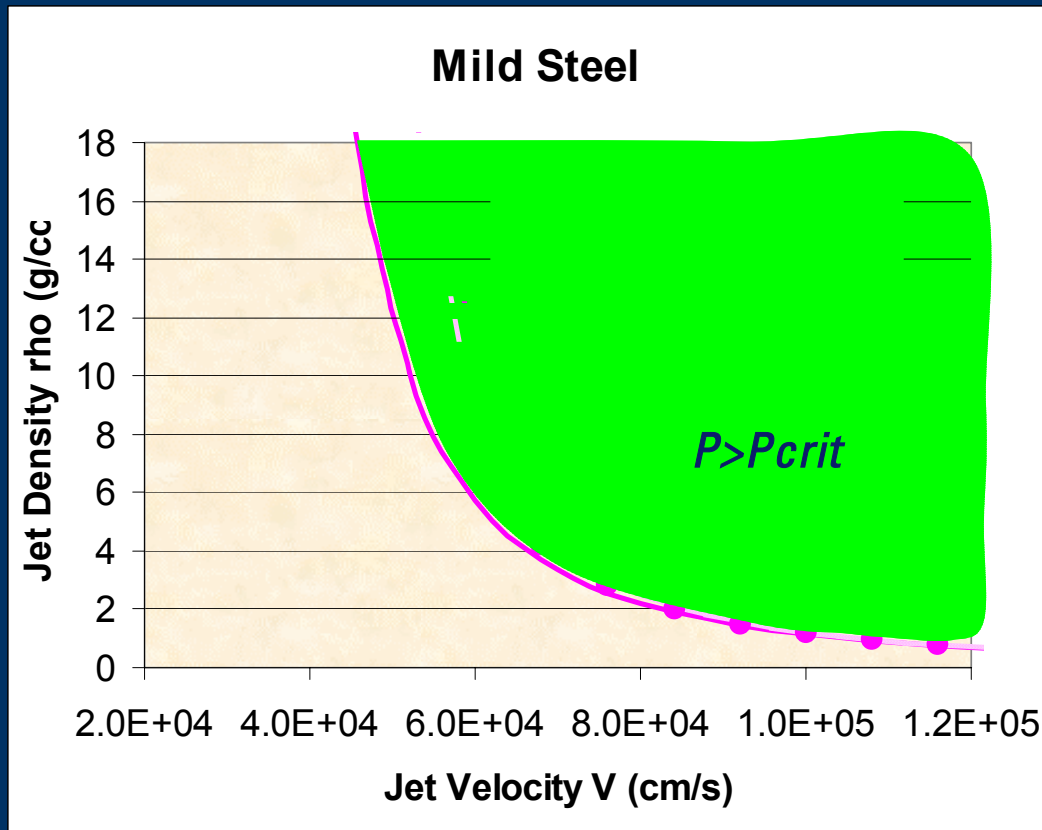
Impact Pressure & Target Strength

Isobars in (ρ_j, V) space



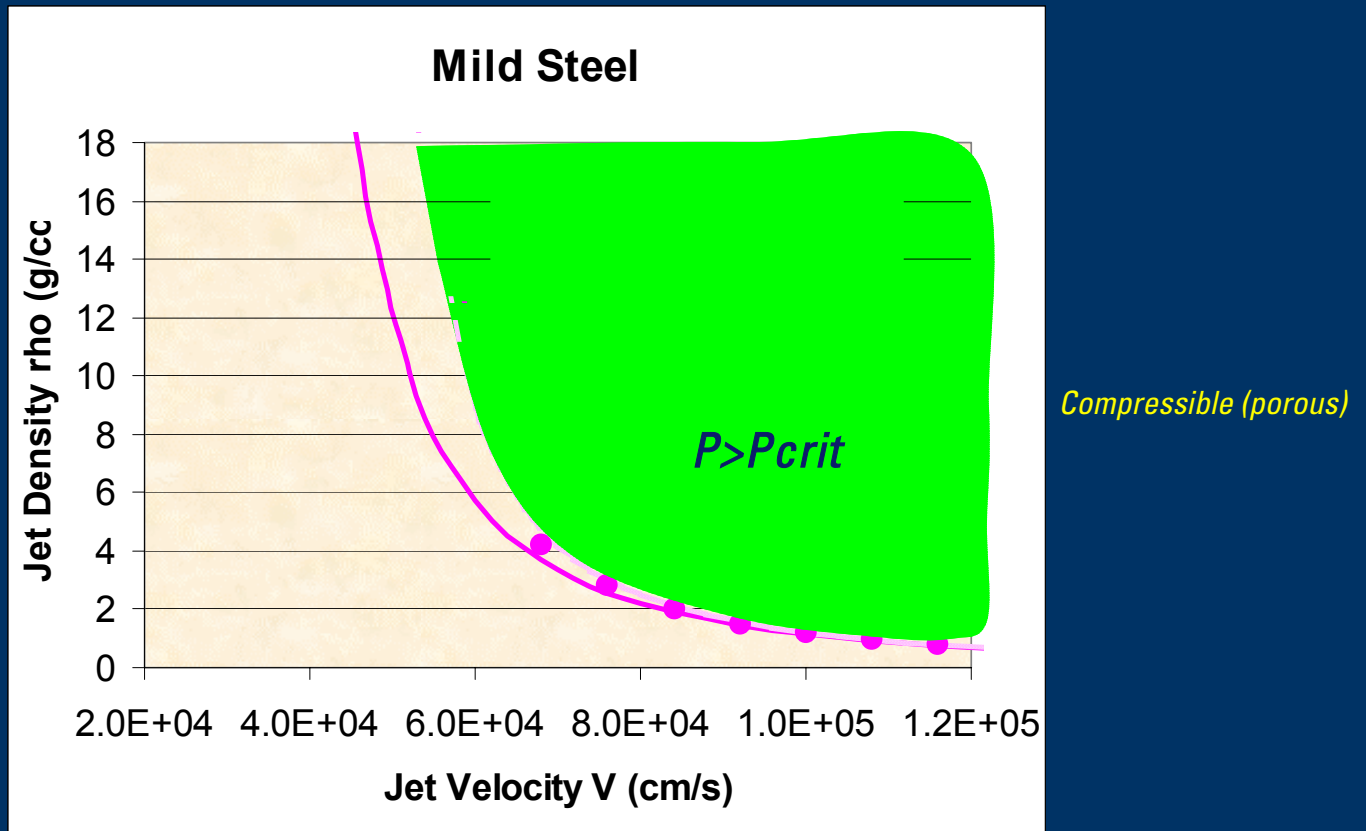
Impact Pressure & Target Strength

Isobars in (ρ_j, V) space



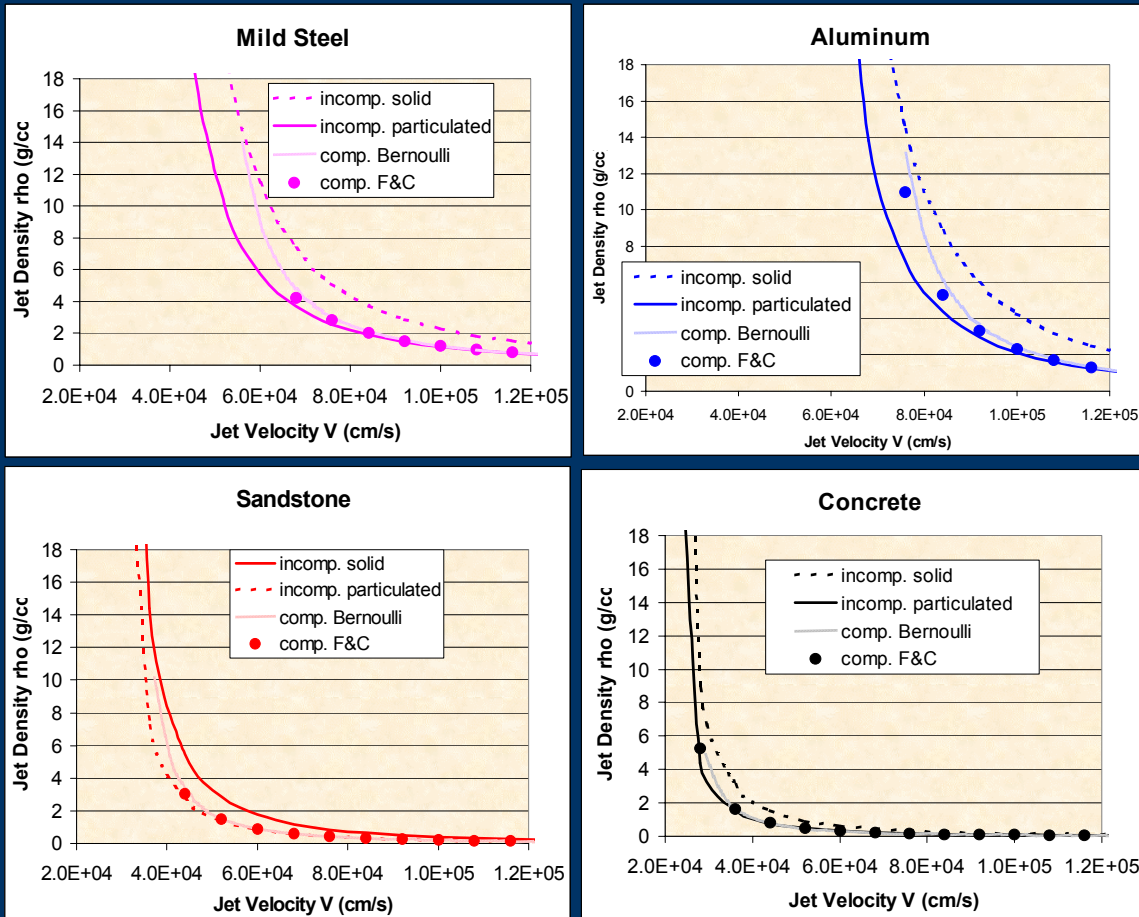
Impact Pressure & Target Strength

Isobars in (ρ_j, V) space



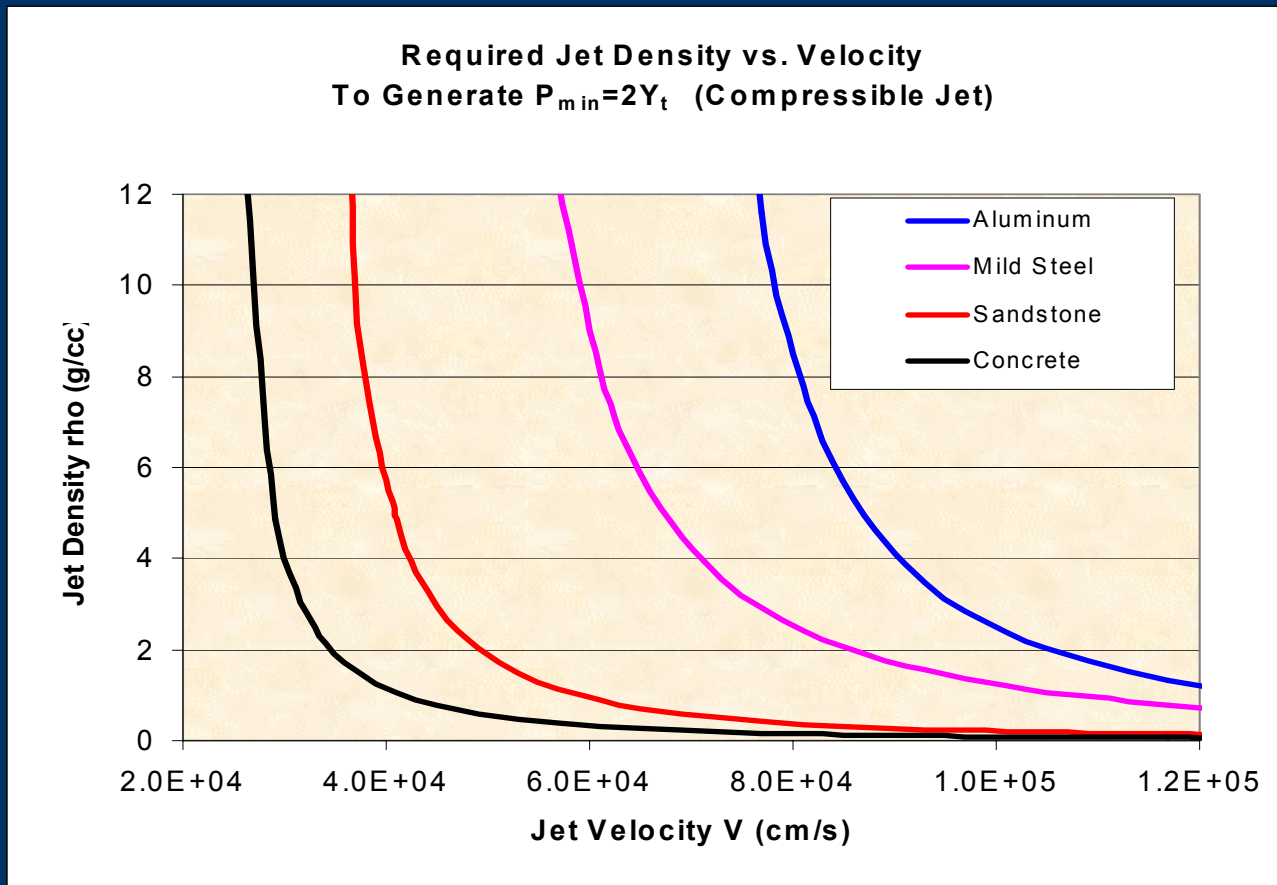
Impact Pressure & Target Strength

Isobars in (ρ_j, V) space



Impact Pressure & Target Strength

Isobars in (ρ_j, V) space



Conclusions (1)

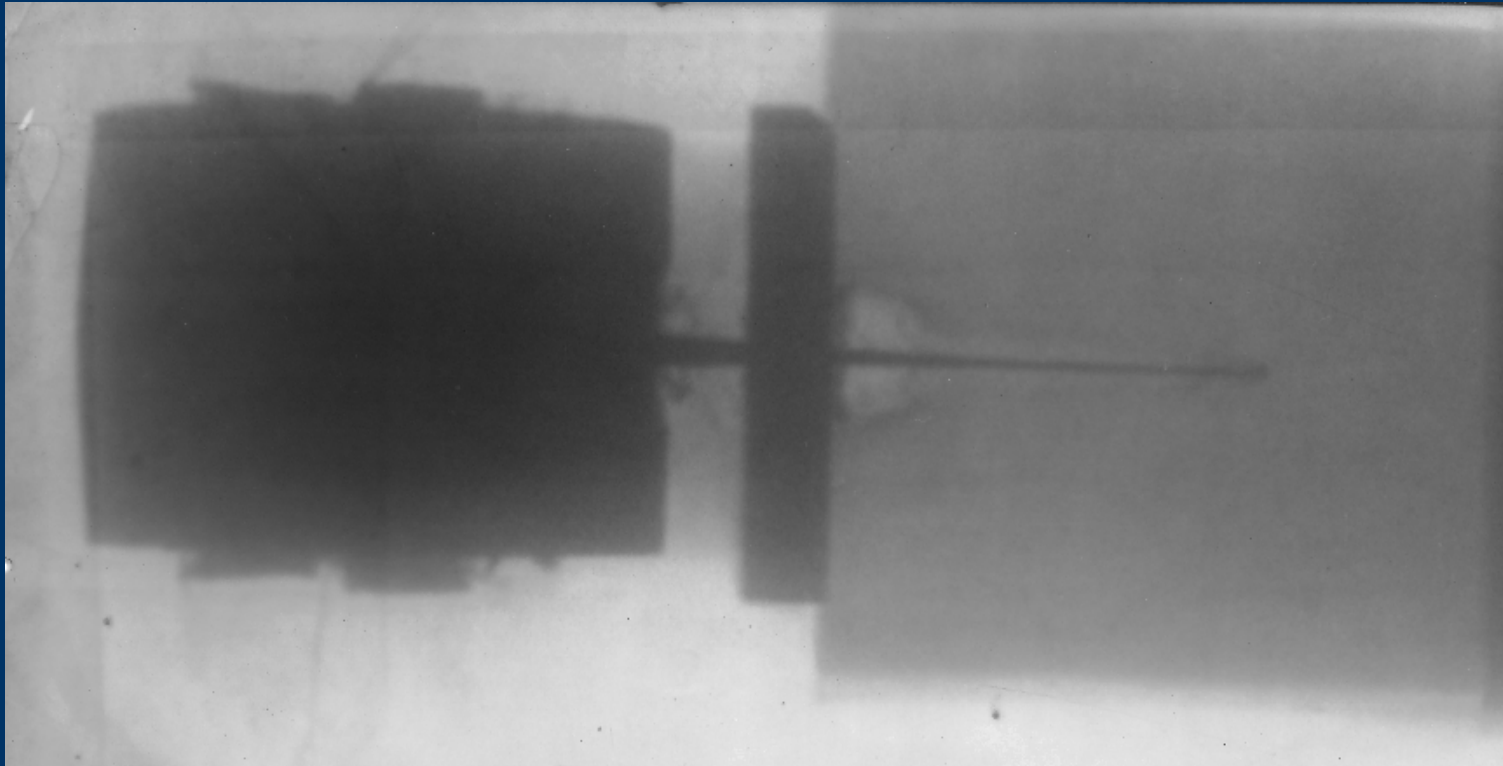
- Developed treatment of compressible jet
 - Reduces to well-known expressions for solid & fully-particulated jets
 - For a given mass, velocity, diameter:
 - Porous (compressible) penetrator penetrates deeper than incompressible penetrator of same L, ρ
 - ...also, deeper than shorter penetrator of higher ρ
 - ...produced impact pressure which is intermediate

Conclusions (2)

- Looked at steady-state impact pressure
 - Presented isobars in (ρ_j, V) coordinates
 - Compressible jet model interpolates between solid & fully-particulated incompressible jet model
 - Highly-distended, low-velocity jets may effectively penetrate moderate-strength geologic targets
- *This approach, so far, neglects transients*

Thank You

Questions??



Oilwell Perforators: Theoretical Considerations

Brenden Grove

22nd International Symposium on Ballistics

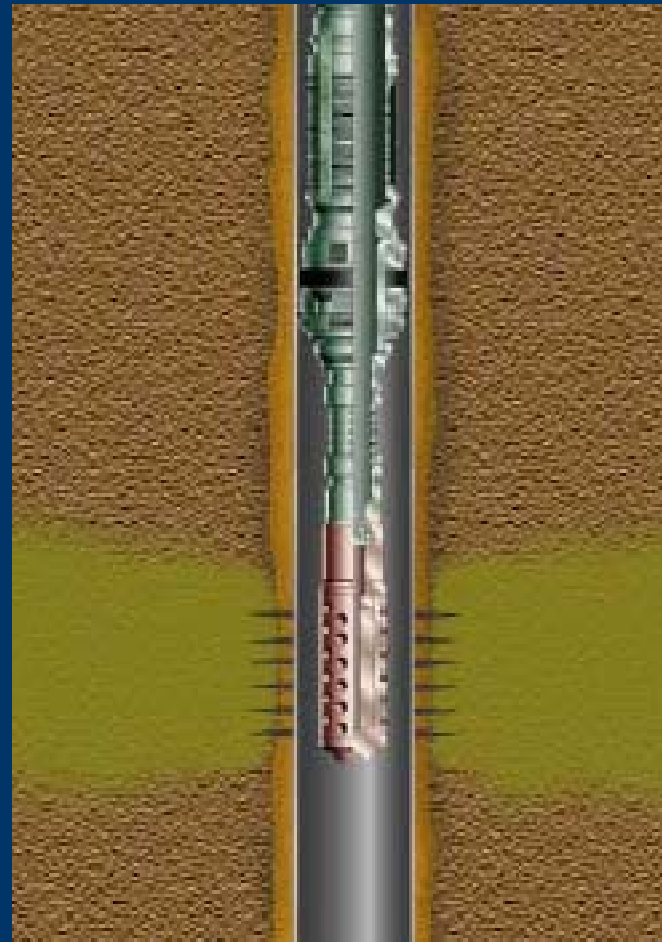
November 17, 2005

Overview

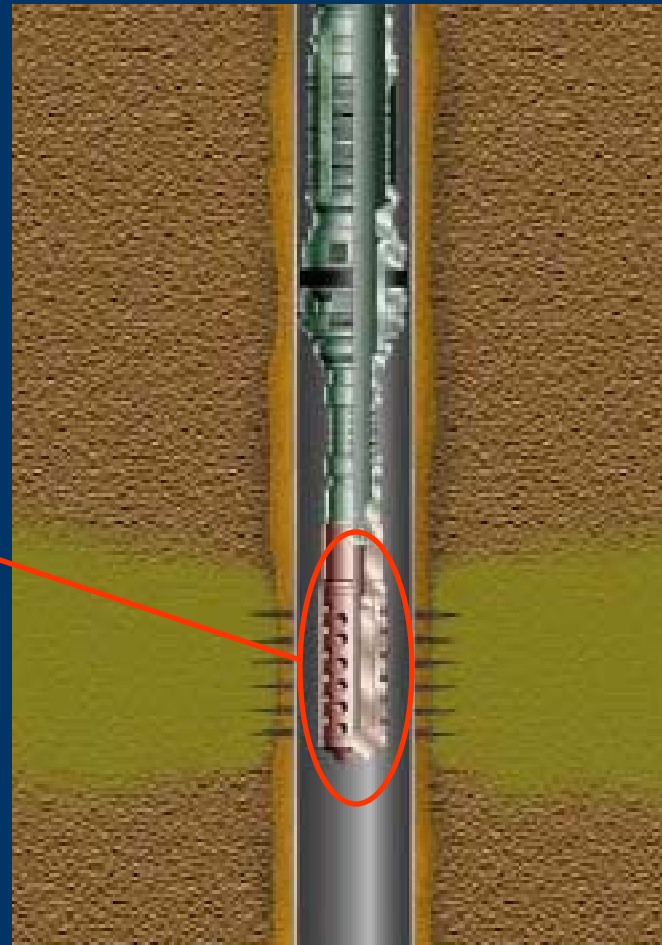
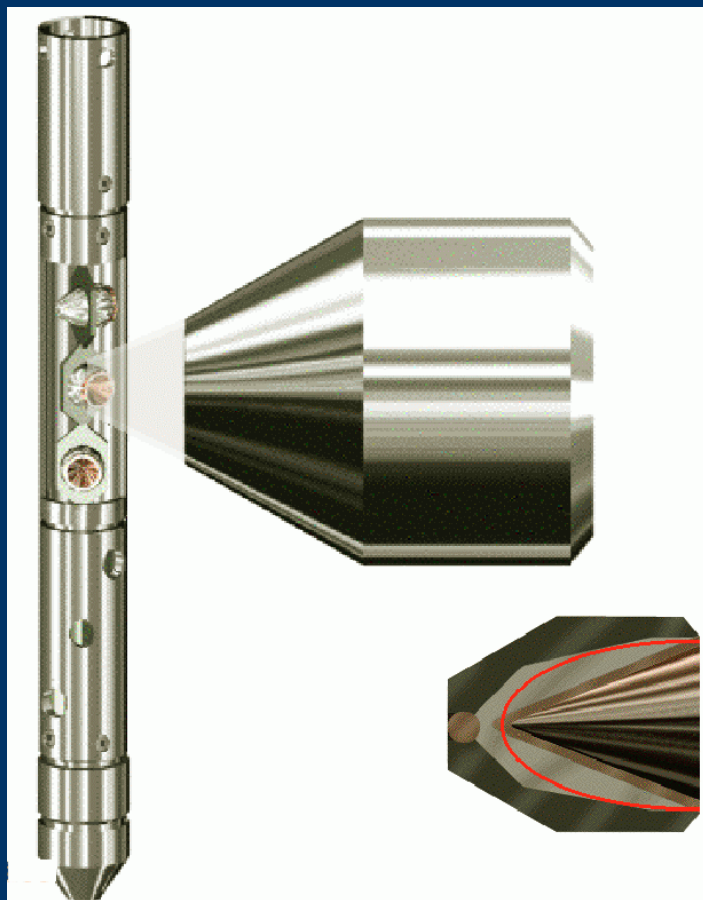
- Introduction / Background
- Compressible Jet Model
- Implications:
 - Hydrodynamic penetration depth
 - Impact pressure
 - Target strength
- Conclusions

Introduction / Background

- Oilwell perforators → 20-60mm shaped charges
- Perforate casing, cement, formation rock
- Perf tunnels must be clean to allow subsequent fluid flow



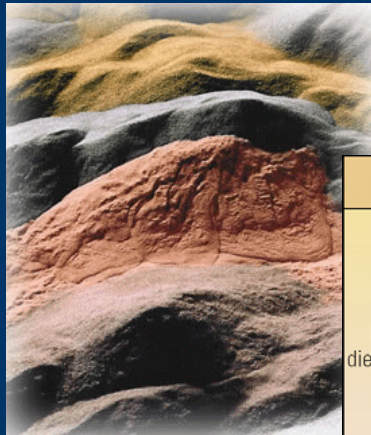
Introduction / Background



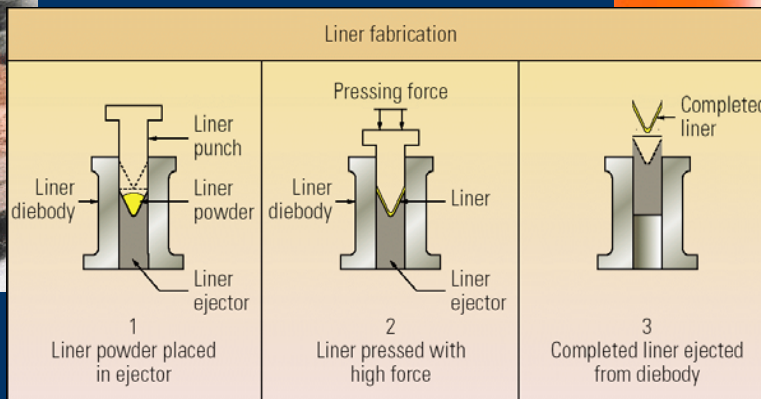
Introduction / Background

Liner:

- formed by powdered metallurgy (P/M)
- unsintered (green)



Metal powder photograph:
<http://www.mpif.org/IntroPM/makepowder.asp?linkid=5>



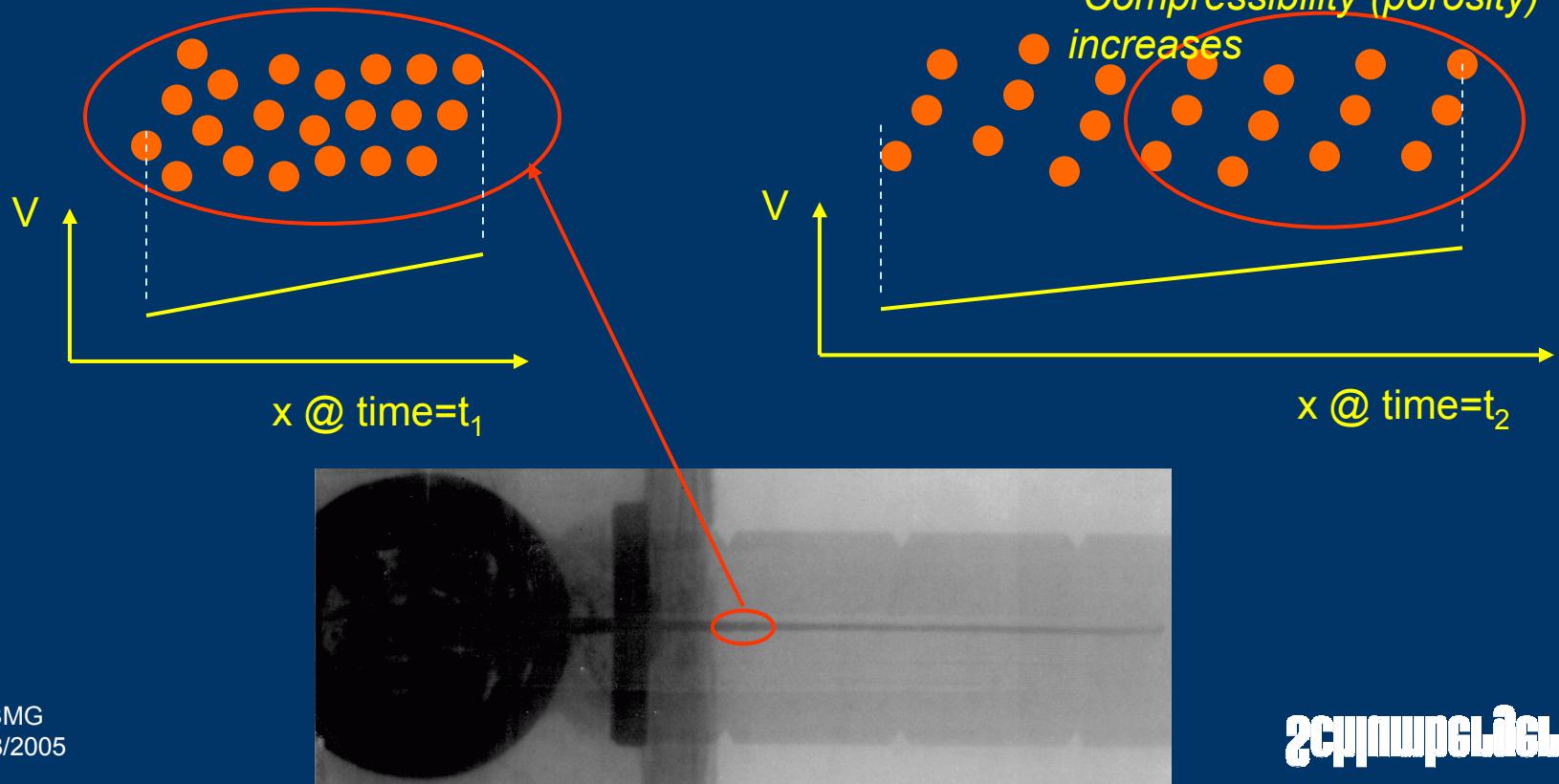
Introduction / Background

- Jet=millions of discrete powder particles
- How to model jet penetration?
 - *Traditional models underpredict penetration*



Introduction / Background

- Jet=millions of discrete powder particles
- How to model jet penetration?



Incompressible Jet

Penetration Theory

Incompressible Bernoulli

Jet pressure

$$P_{2j} = Y_j + \frac{\lambda}{2} \rho_0 (V - U)^2$$

Target pressure

$$P_{2t} = Y_t + \frac{1}{2} \rho_{0t} U^2$$

PD (hydrodynamic)

$$\frac{PD}{L} = \sqrt{\frac{\lambda \rho_j}{\rho_t}}$$

PD (target strength
important)

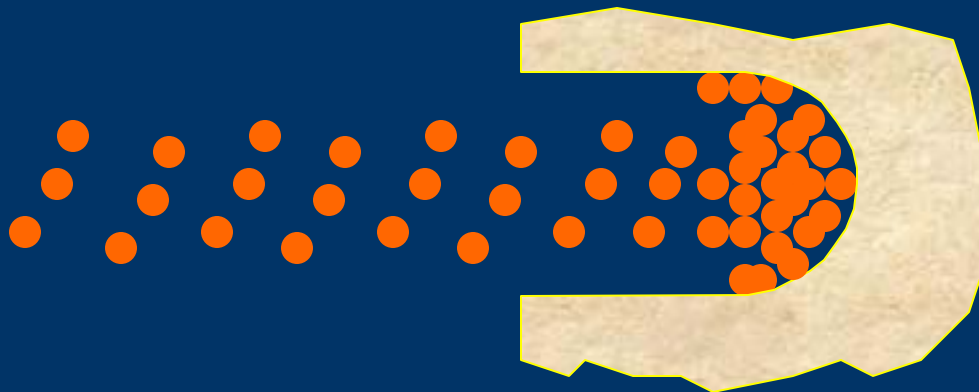
$$\frac{PD}{L} = \sqrt{\frac{\lambda \rho_j}{\rho_t} - \frac{2\sigma}{\rho_t (V - U)^2}}$$

$$\sigma = Y_t - Y_j$$

Compressible Jet

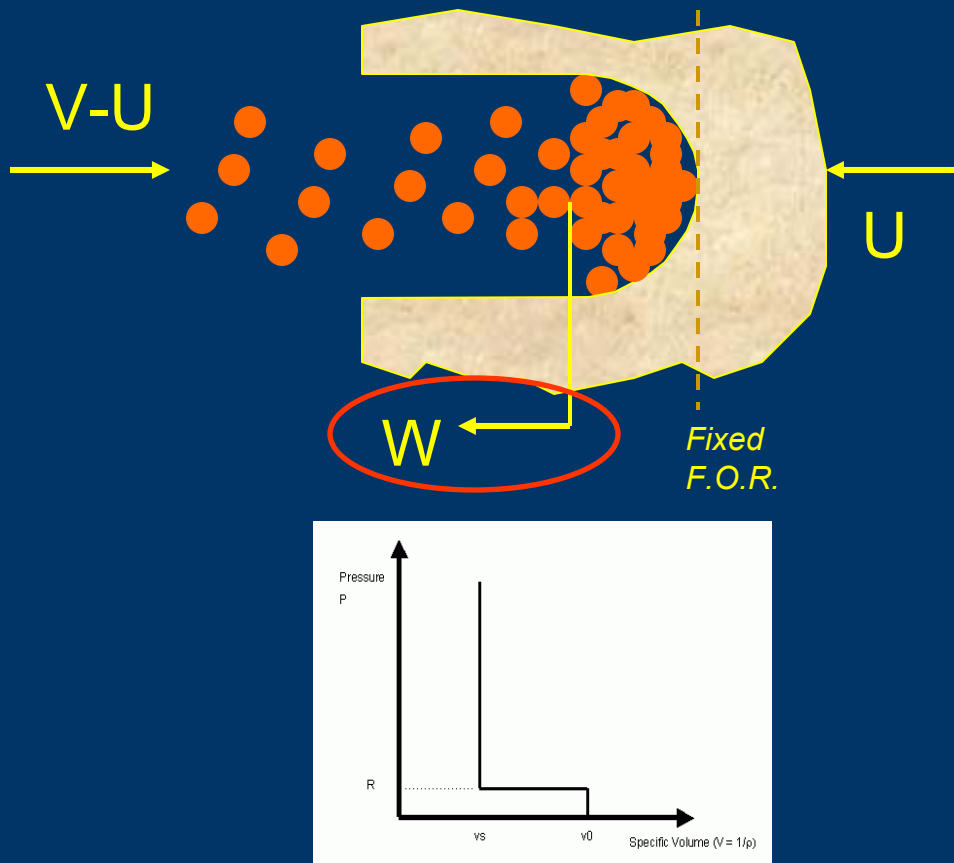
Penetration Theory

- Multiple discrete impacts; particles “pile up”?
- Macroscopically – jet compresses
- *Incompressible Bernoulli not applicable*

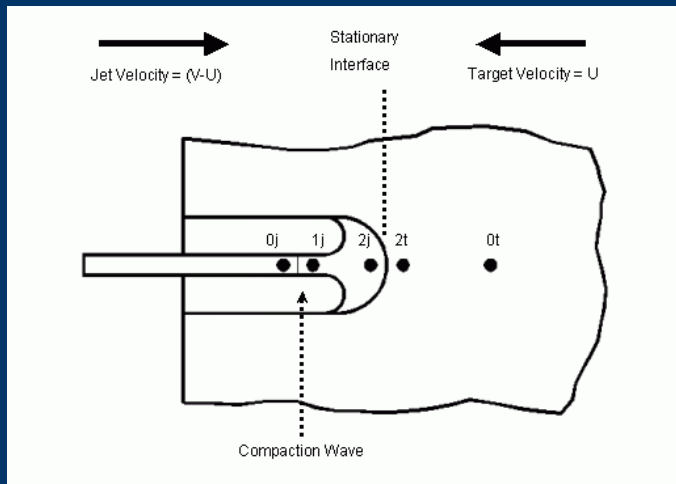


Compressible Jet

Penetration Theory



- Flis & Crilly (18th ISB): compressible target
- Reverse their analysis here



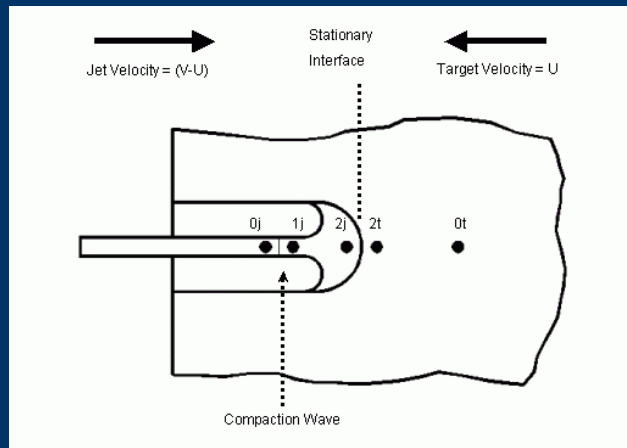
ρ_0 = initial (distended) jet density
 ρ_s = solid (pore-free) jet density
 $\phi = 1 - \rho_0 / \rho_s$ = jet porosity
 R = jet compaction initial resistance

Jet Material Compaction Curve

Compressible Jet

Penetration Theory

- Distended jet at ρ_o traveling at $(V-U)$
- Compacted to ρ_s , decelerated to w_{1j}



mass

$$\rho_{0j} w_{0j} = \rho_{1j} w_{1j}$$

$$w_{0j} = V - U$$

momentum

$$P_{0j} + \rho_0 (w_{0j})^2 = P_{1j} + \rho_1 (w_{1j})^2$$

full compaction

$$\rho_{1j} = \rho_{2j} = \rho_c$$

- Apply incompressible Bernoulli to compacted jet impact

Compressible Jet

Penetration Theory

Jet pressure

$$P_{2j} = R + \frac{1}{2} \rho_0 (V - U)^2 (1 + \phi)$$

Target pressure

$$P_{2t} = Y_t + \frac{1}{2} \rho_{0t} U^2$$

PD (hydrodynamic)

$$\frac{PD}{L} = \sqrt{\frac{\rho_0}{\rho_t} (1 + \phi)}$$

PD (target strength
important)

$$\frac{PD}{L} = \sqrt{\frac{\rho_0}{\rho_t} (1 + \phi)} - \frac{2\sigma}{\rho_t (V - U)^2}$$

Compressibilit
y
Effect

Compressible vs. Incompressible Jet

Penetration Theory

Incompressible \longrightarrow Compressible

Jet Pressure

Hydrodynamic Penetration Depth

$$P_{2j} = Y_j + \frac{\lambda}{2} \rho_0 (V - U)^2 \longrightarrow P_{2j} = R + \frac{1}{2} \rho_0 (V - U)^2 (1 + \phi)$$
$$\frac{PD}{L} = \sqrt{\frac{\lambda \rho_j}{\rho_t}} \longrightarrow \frac{PD}{L} = \sqrt{\frac{\rho_0}{\rho_t} (1 + \phi)}$$

$$\lambda \dashrightarrow (1 + \phi)$$

Compressible vs. Incompressible Jet

Penetration Theory

- $(1+\phi) \rightarrow \lambda$
- Porous jet model reduces to incompressible model at limits
- At upper limit ($\phi=1$; $\lambda=2$), $\rho \rightarrow$ zero
- For a given length and macroscopic density, porosity increases the following:
 - *Penetration depth*
 - *Impact pressure*

Jet Density, Length, Porosity

Summary

Consider 3 cases: (*Fixed mass, velocity, diameter*)

$$\rho L = \text{constant}$$

Case A: ρ_s , incompressible;
length = L_s



Case B: ρ_o , compressible to
 ρ_s ; length = L_o



Case C: ρ_o , incompressible;
length = L_o



Jet Density, Length, Porosity

Summary

Hydrodynamic Penetration Depth

Case A:

$$PD_A = L_s \sqrt{\frac{\rho_s}{\rho_t}}$$

Case B:

$$\begin{aligned} PD_B &= L_0 \sqrt{\frac{\rho_0}{\rho_t} (1 + \phi)} \\ &= PD_A \sqrt{\frac{1 + \phi}{1 - \phi}} \quad (\text{alternative form}) \\ &= PD_C \sqrt{1 + \phi} \quad (\text{alternative form}) \end{aligned}$$

Case C:

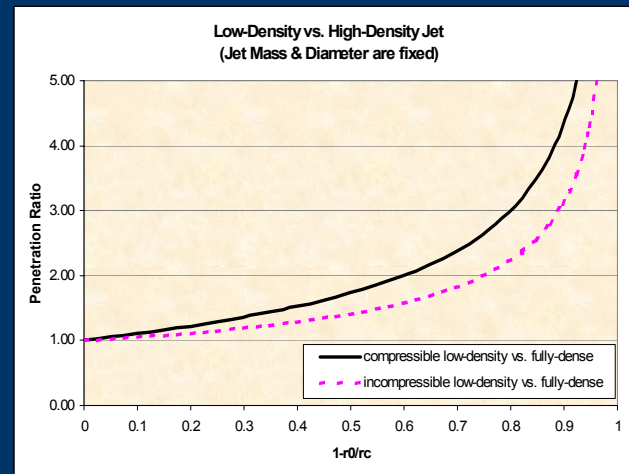
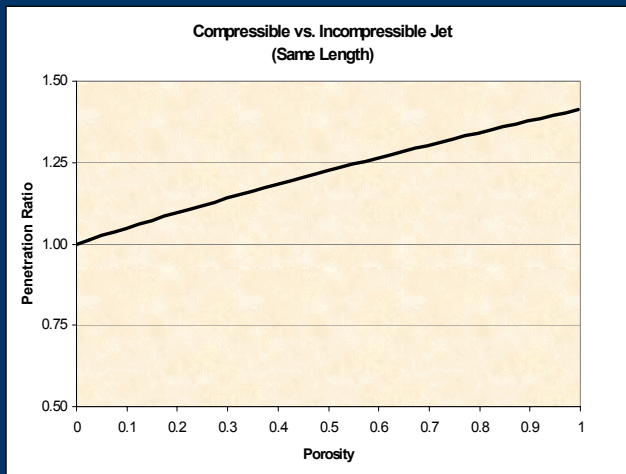
$$PD_C = L_0 \sqrt{\frac{\rho_0}{\rho_t}}$$

Jet Density, Length, Porosity Summary

Hydrodynamic Penetration Depth

$$PD_B > PD_C > PD_A$$

$$PD_B : PD_C : PD_A = \sqrt{\frac{1+\phi}{1-\phi}} : \sqrt{\frac{1}{1-\phi}} : 1$$



Jet Density, Length, Porosity

Summary

Dynamic Jet Pressure

Case A:

$$P_A = \frac{1}{2} \rho_s (V - U)^2$$

Case B:

$$\begin{aligned} P_B &= \frac{1}{2} \rho_s (V - U)^2 (1 - \phi^2) \\ &= \frac{1}{2} \rho_0 (V - U)^2 (1 + \phi) \quad (\text{alternative form}) \end{aligned}$$

Case C:

$$P_C = \frac{1}{2} \rho_0 (V - U)^2$$

Jet Density, Length, Porosity Summary

Dynamic Jet Pressure

$$P_A > P_B > P_C$$

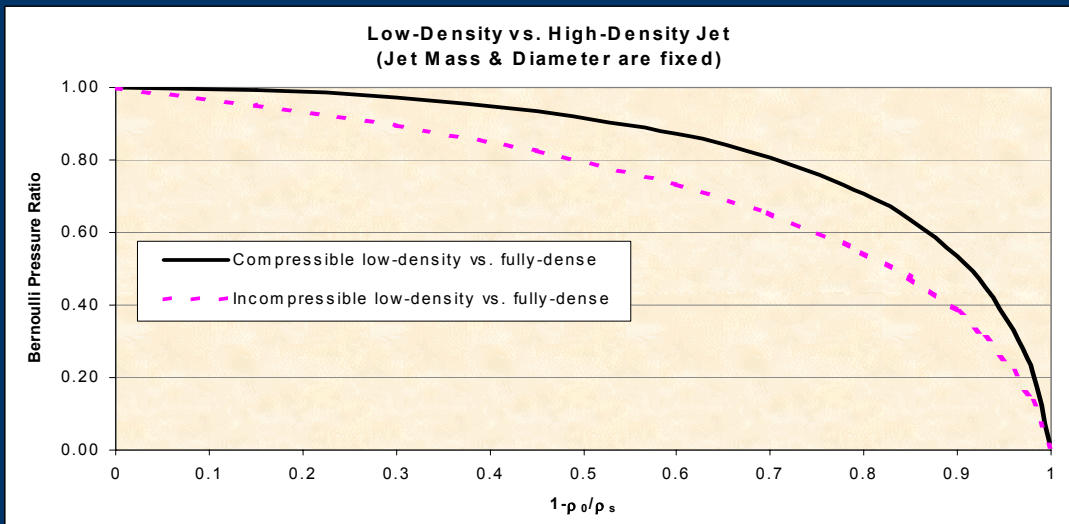
$$U = \frac{V}{1+\gamma}$$

$$\gamma_A = \sqrt{\frac{\rho_t}{\rho_s}}$$

$$\gamma_B = \sqrt{\frac{\rho_t}{\rho_s(1-\phi^2)}} = \frac{\gamma_A}{\sqrt{1-\phi^2}}$$

$$\gamma_C = \sqrt{\frac{\rho_t}{\rho_0}} = \frac{\gamma_A}{\sqrt{1-\phi}}$$

$$P_A : P_B : P_C = 1 : \left[1 - \left(\frac{1}{1 + \frac{\gamma_A}{\sqrt{1-\phi^2}}} \right)^2 (1-\phi^2) \right] : \left[1 - \left(\frac{1}{1 + \frac{\gamma_A}{\sqrt{1-\phi}}} \right)^2 (1-\phi) \right]$$



Jet Density, Length, Porosity

Summary

Consider 3 cases: (*Fixed mass, velocity, diameter*)

$$\rho L = \text{constant}$$

Case A: ρ_s , incompressible;
length = L_s



Case B: ρ_o , compressible to
 ρ_s ; length = L_o

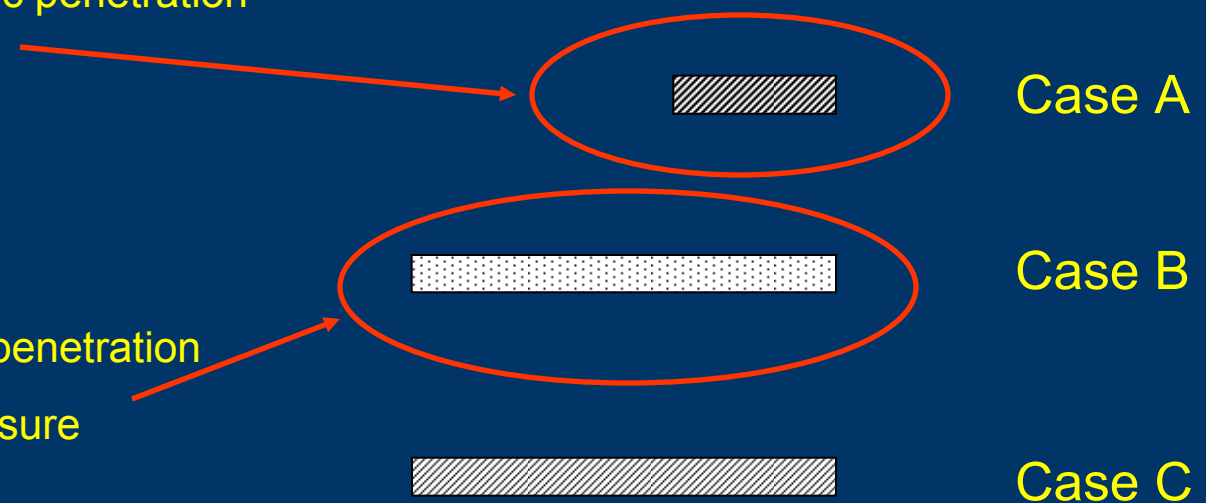


Case C: ρ_o , incompressible;
length = L_o



Jet Density, Length, Porosity Summary

- Greatest impact pressure
- Shallowest hydrodynamic penetration



Impact Pressure & Target Strength

What about target strength?

Consider some critical point of interest (U_{crit} , P_{crit})

*Characteristic
target property*

$$U_{crit} = \sqrt{\frac{2(P_{crit} - Y_t)}{\rho_t}}$$

P_{crit} isobars in (ρ_j, V) coordinates

Incompressible; $1 \leq \lambda \leq 2$

$$\rho_j = \frac{\rho_t U_{crit}^2 + 2\sigma}{\lambda(V - U_{crit})^2}$$

Compressible

$$\rho_j = \rho_s(1 - \phi); \quad \phi = \sqrt{1 - \frac{\rho_t U_{crit}^2 + 2\sigma}{\rho_s(V - U_{crit})^2}}$$

***There is
no
unique
 V_{min}
isobar***

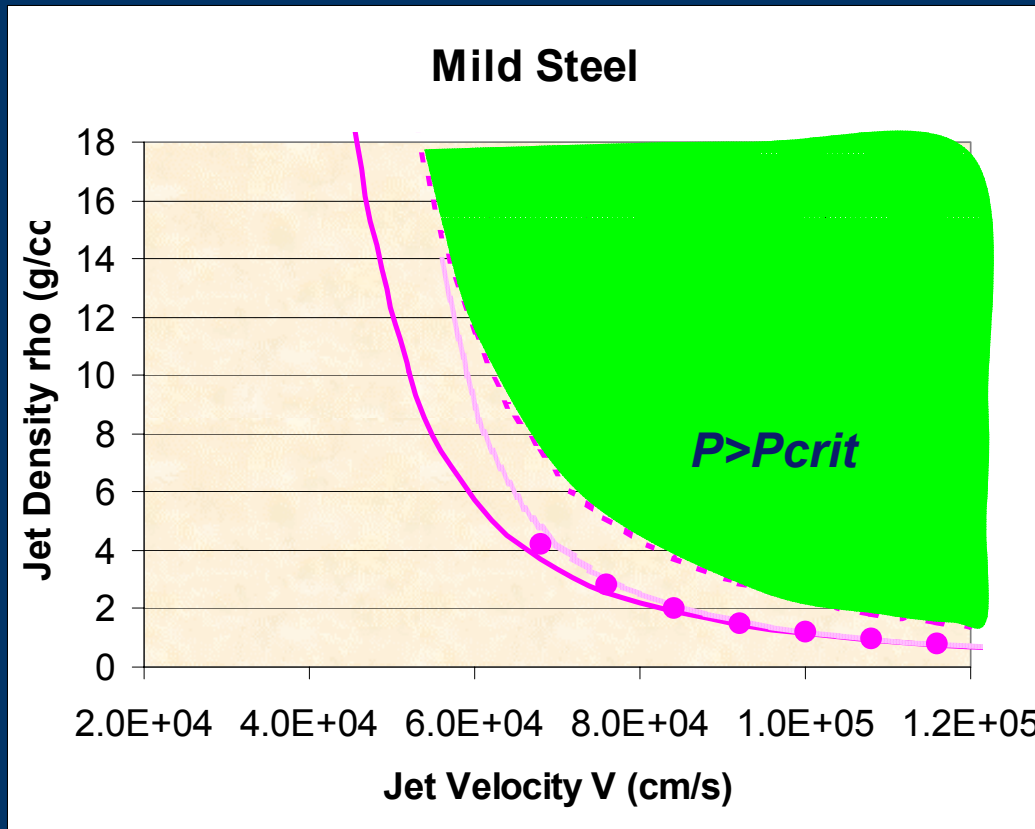
Impact Pressure & Target Strength

What do these isobars look like?

Target Material	ρ_t (g/cc)	Y_t (kbar)	P_{crit}	ρ_s (g/cc)	$R=Y_j$ (kbar)
Mild steel	7.86	3 (UTS)	$2Y_t$	16	0
Aluminium	2.7	3 (UTS)	"	"	"
Concrete	2.25	0.3 (UCS)	"	"	"
Sandstone	2.25	0.6 (UCS)	"	"	"

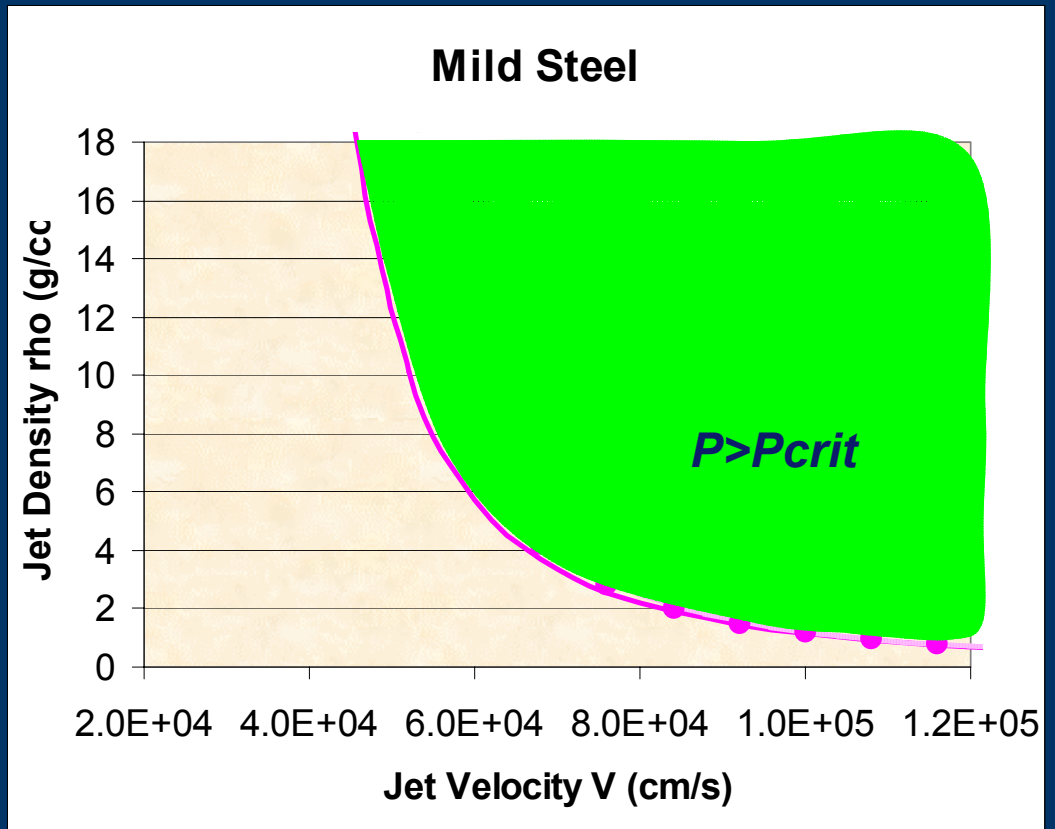
Impact Pressure & Target Strength

Isobars in (ρ_j, V) space



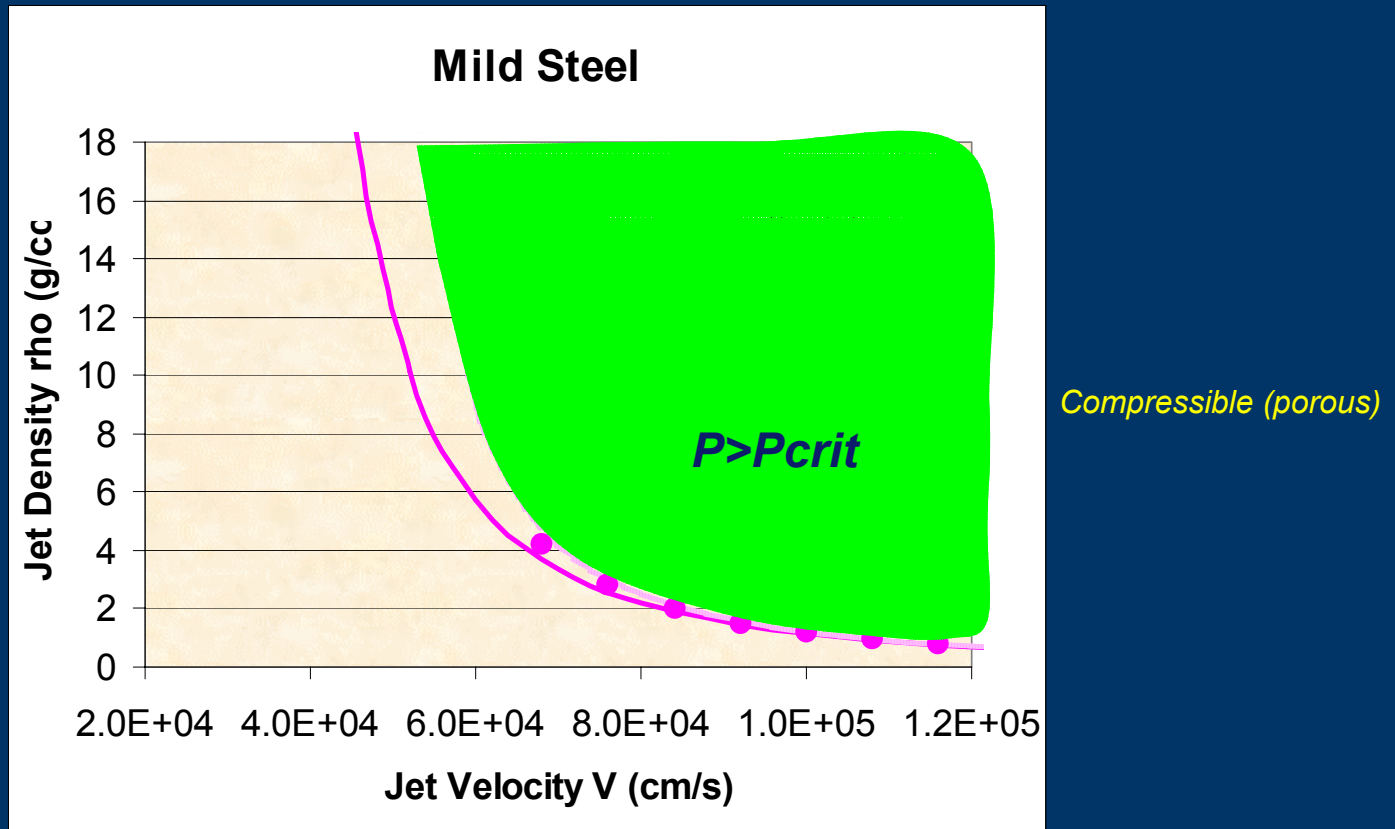
Impact Pressure & Target Strength

Isobars in (ρ_j, V) space



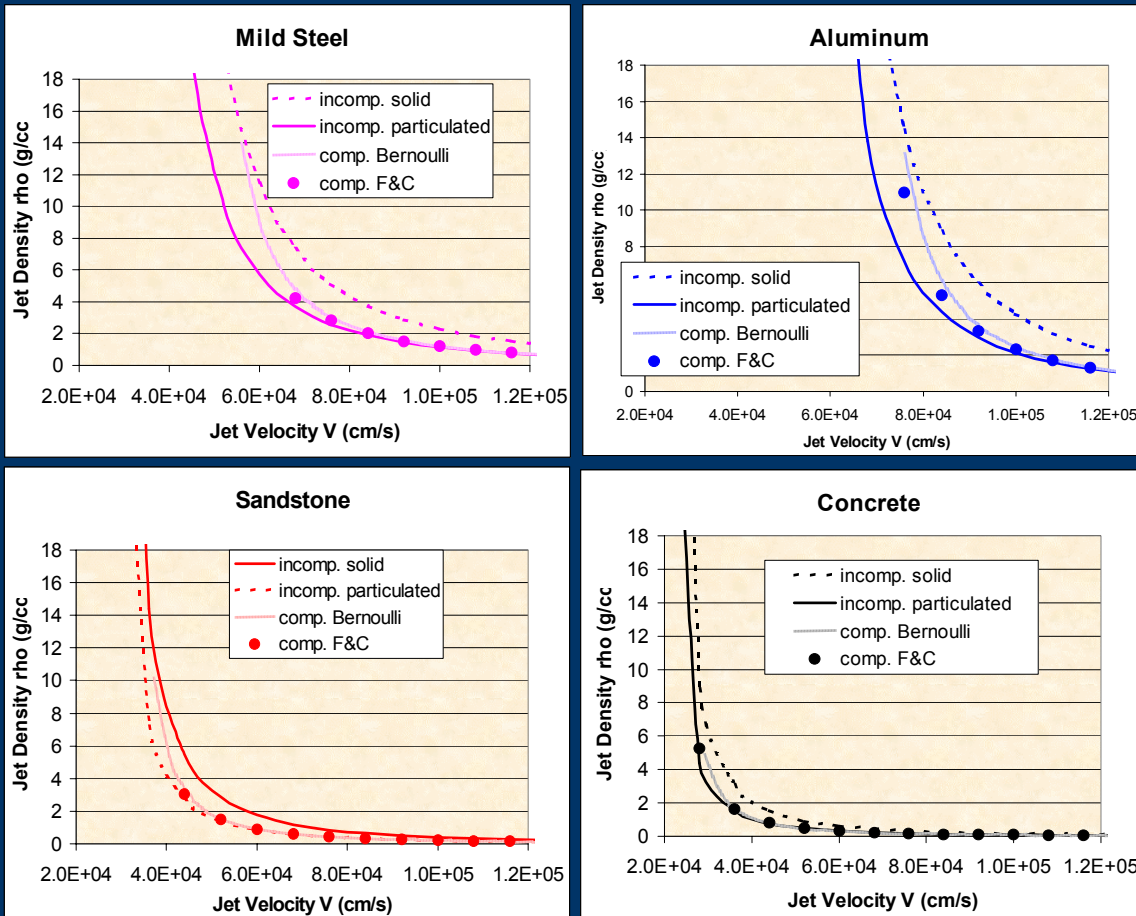
Impact Pressure & Target Strength

Isobars in (ρ_j, V) space



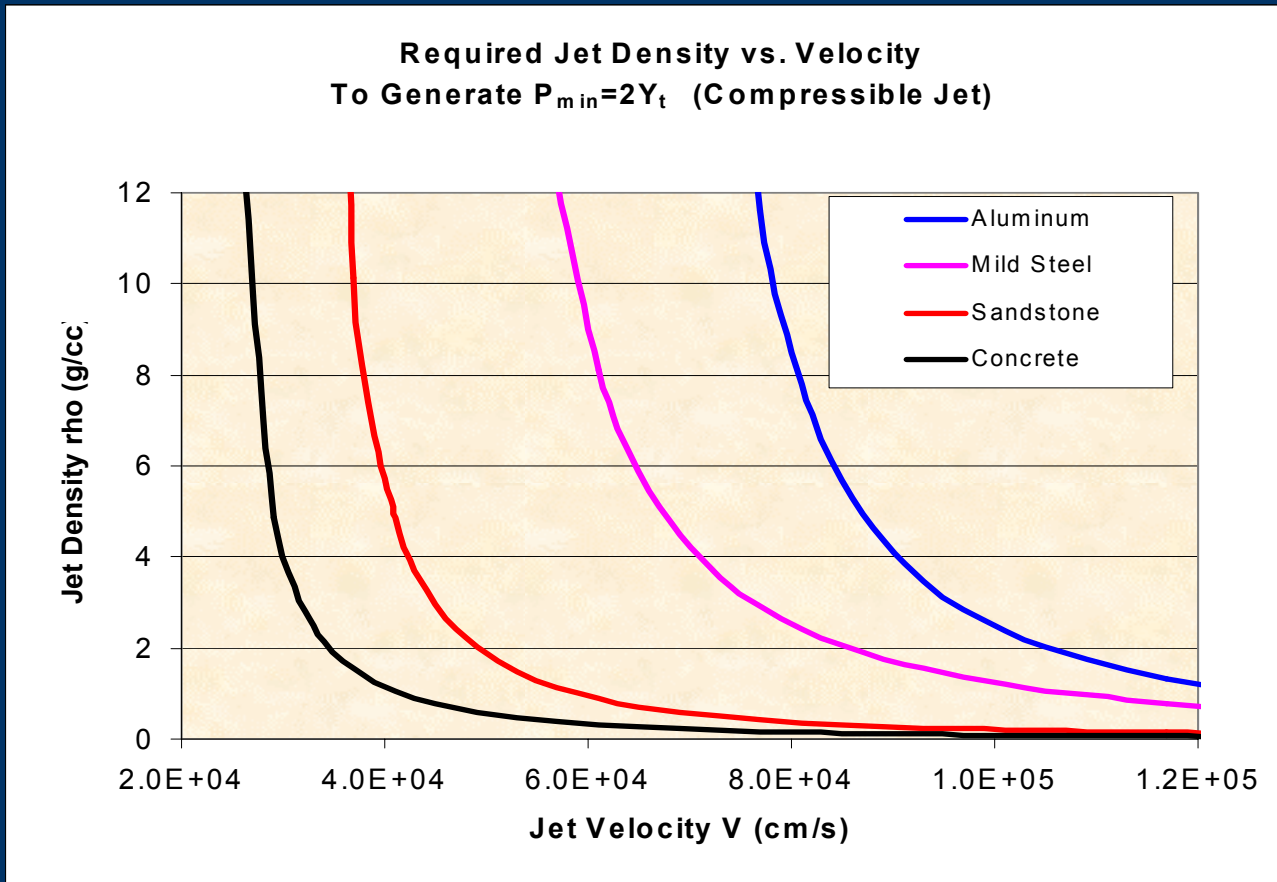
Impact Pressure & Target Strength

Isobars in (ρ_j, V) space



Impact Pressure & Target Strength

Isobars in (ρ_j, V) space



Conclusions (1)

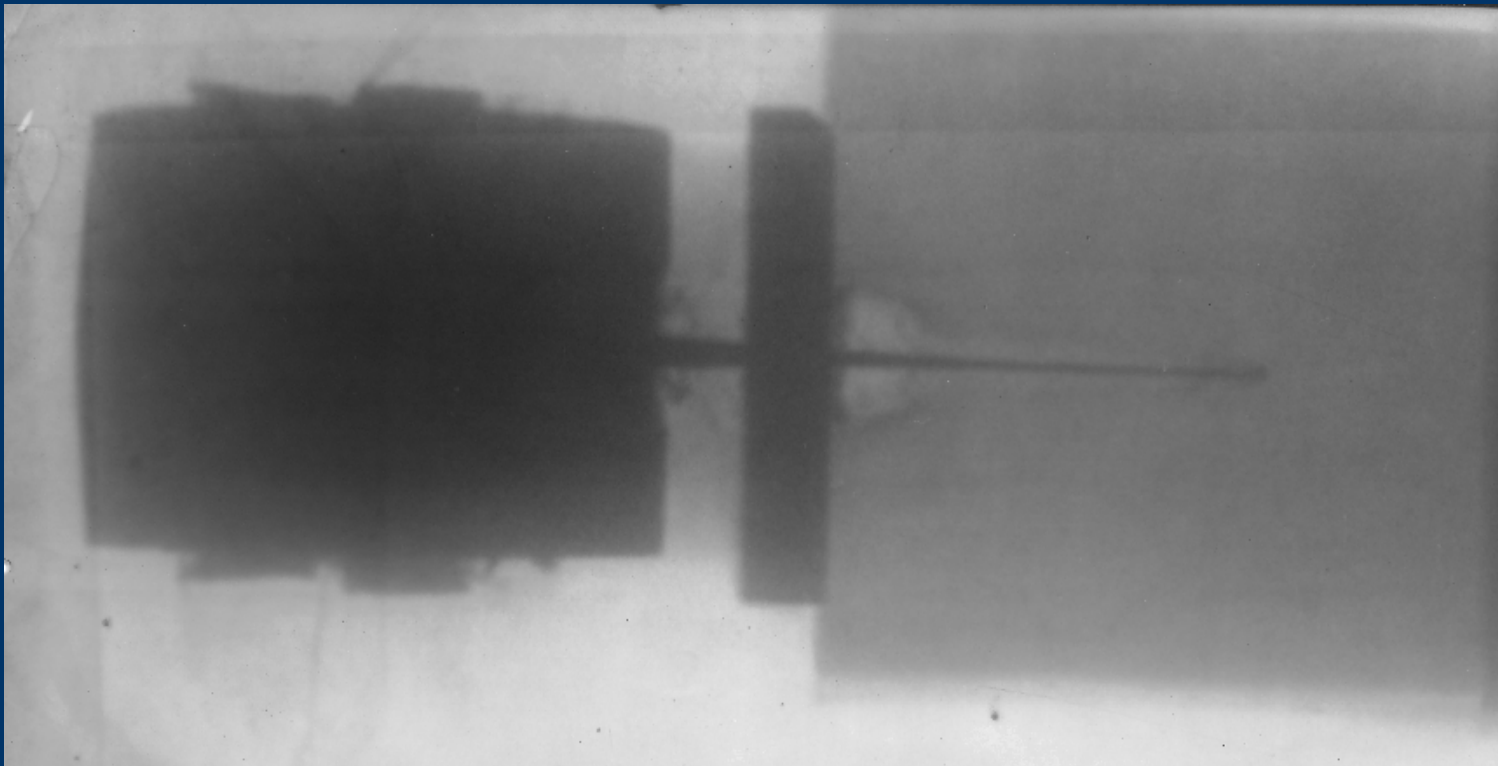
- Developed treatment of compressible jet
 - Reduces to well-known expressions for solid & fully-particulated jets
 - For a given mass, velocity, diameter:
 - Porous (compressible) penetrator penetrates deeper than incompressible penetrator of same L , ρ
 - ...also, deeper than shorter penetrator of higher ρ
 - ...produced impact pressure which is intermediate

Conclusions (2)

- Looked at steady-state impact pressure
 - Presented isobars in (ρ_j, V) coordinates
 - Compressible jet model interpolates between solid & fully-particulated incompressible jet model
 - Highly-distended, low-velocity jets may effectively penetrate moderate-strength geologic targets
- *This approach, so far, neglects transients*

Thank You

Questions??



The residual damage in CFRP composite after ballistic impacts (experiments & simulations)

Survivability of aircraft

TNO | Knowledge for business



Contents

- Introduction
- Ballistic test data
 - Residual velocity
 - Internal damage
- Material model of CFRP, AS4/3501
- Simulation results:
 - Residual velocity
 - Internal damage
- Conclusions and future work

Introduction

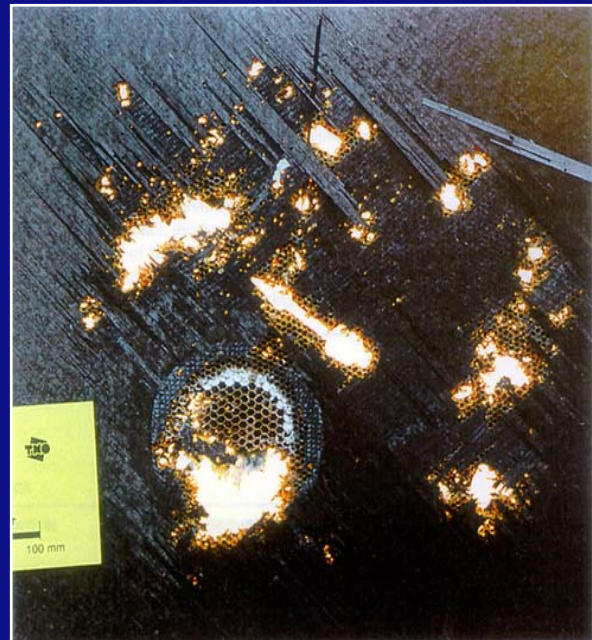


Survivability of aircraft:

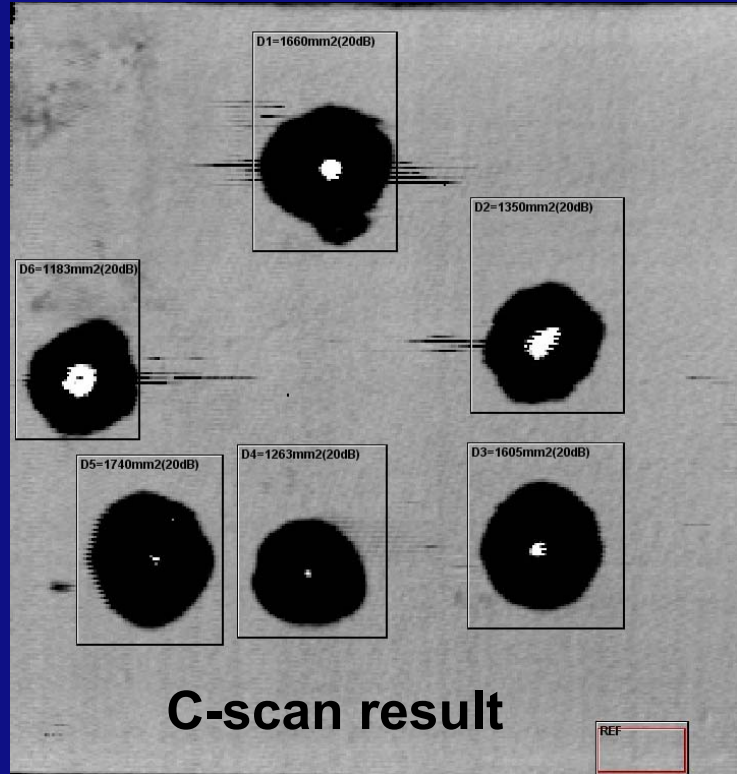
- Combined threats : both blast and projectile impacts
- Lighter platforms: more composite material

Combined threats + new materials

- ⇒ New failure models
- ⇒ New survivability tools

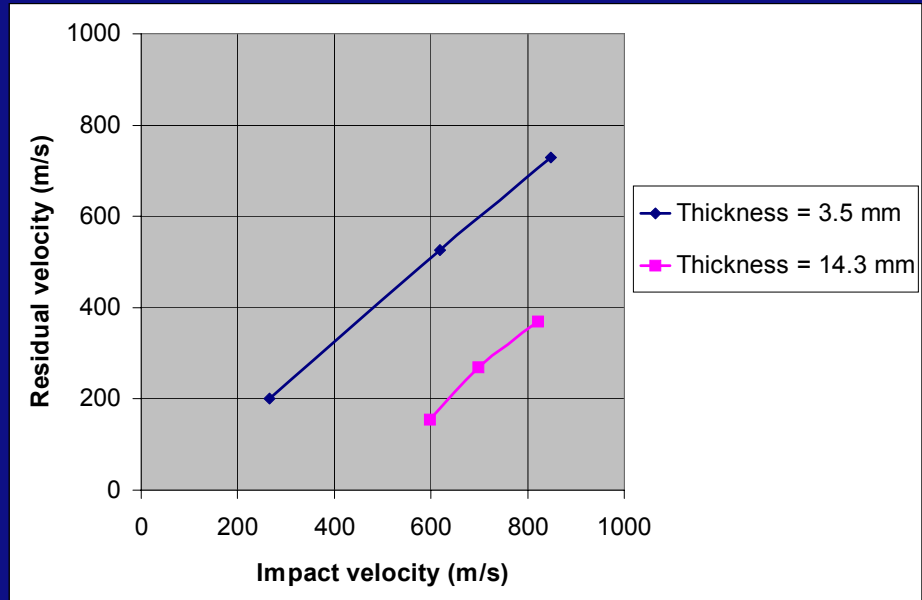


Ballistic tests

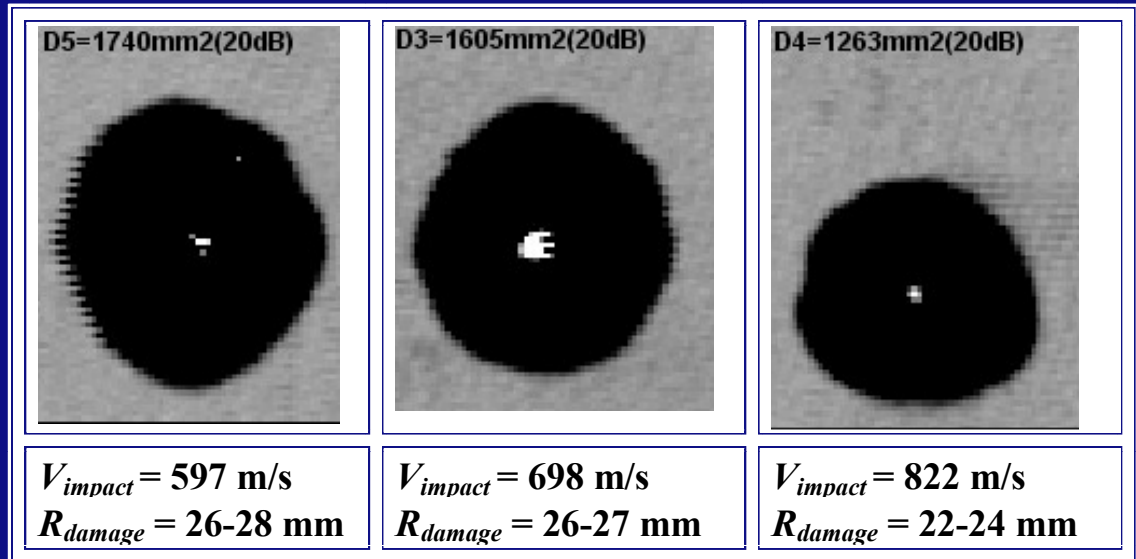


Ballistic tests

- Residual velocity:
Threat : 1.1 gram FSP
(Fragment Simulating Projectile)



- Internal damage
14.3 mm (C-Scan):



Contents

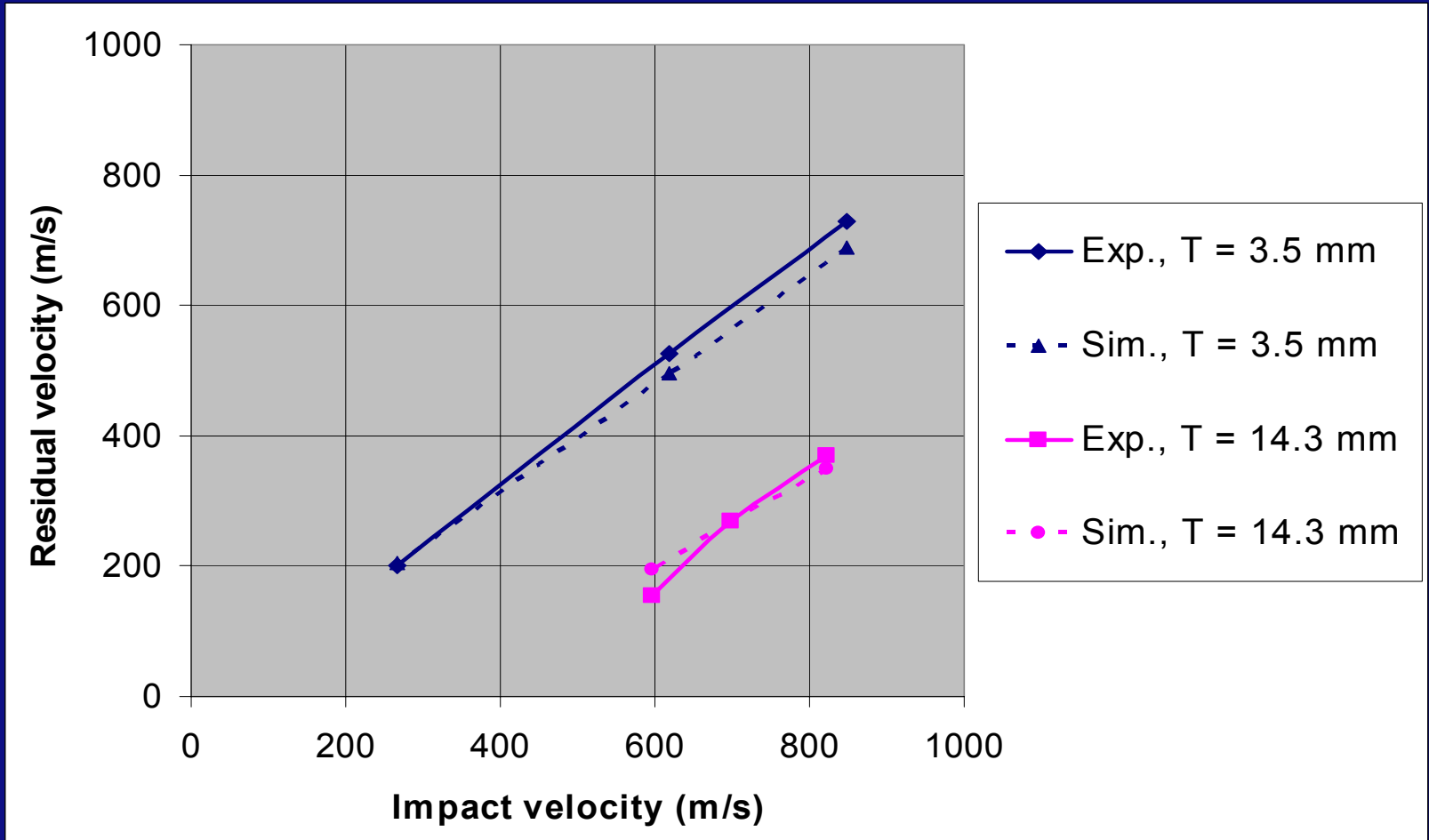
- Introduction
- Ballistic test data
 - Residual velocity
 - Internal damage
- **Material model**
- **Simulation results:**
 - **Residual velocity**
 - **Internal damage**
- Conclusions and future work

Material model of CFRP, AS4/3501

- Advanced Damage Material Model (ADAMMO) within AUTODYN® :
 - An orthotropic elastic model :
Parameters from quasi-static material tests (tension and V-notch)
 - A linear EOS (assumed linear; inverse flyer plate necessary)
- An orthotropic damage model with
 - Orthotropic failure criteria (tension and V-notch)
 - An orthotropic softening algorithm (data from literature)
 - Orthotropic post failure response; tensile stresses are still allowed in non-failed material directions

Simulation results

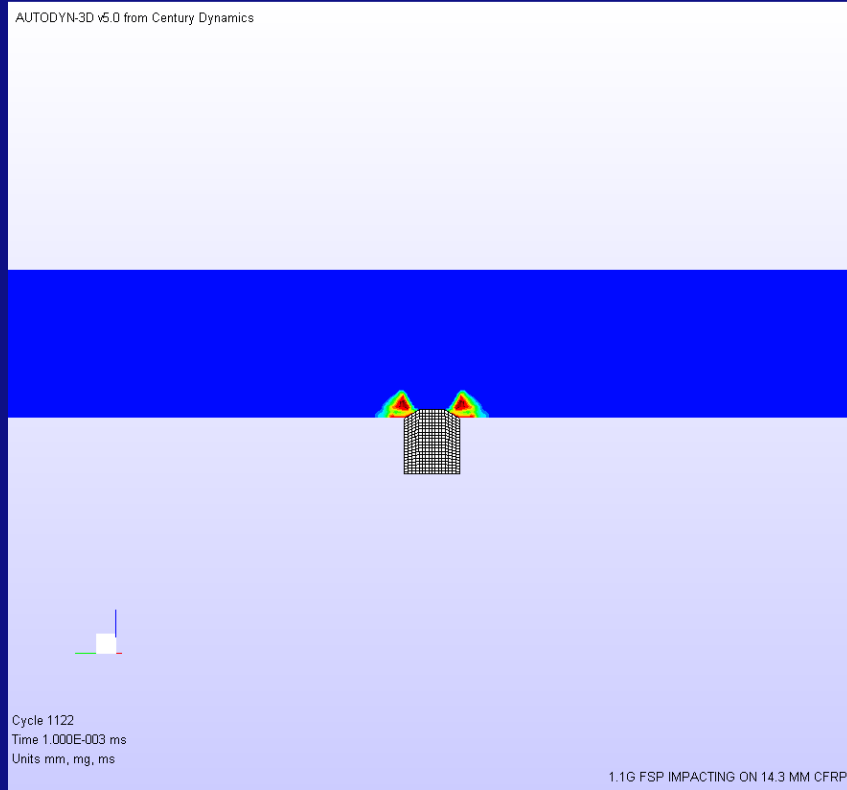
- Residual velocity (threat 1.1 gram fsp):



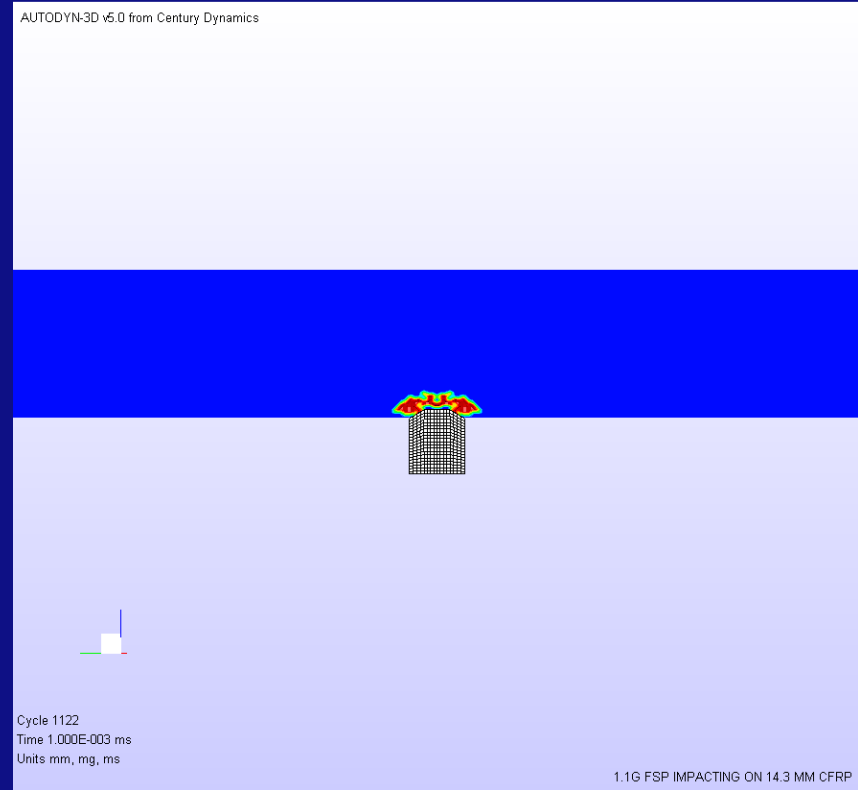
Simulation results

$V_{Impact} = 597 \text{ m/s}$, thickness = 14.3 mm

Delamination



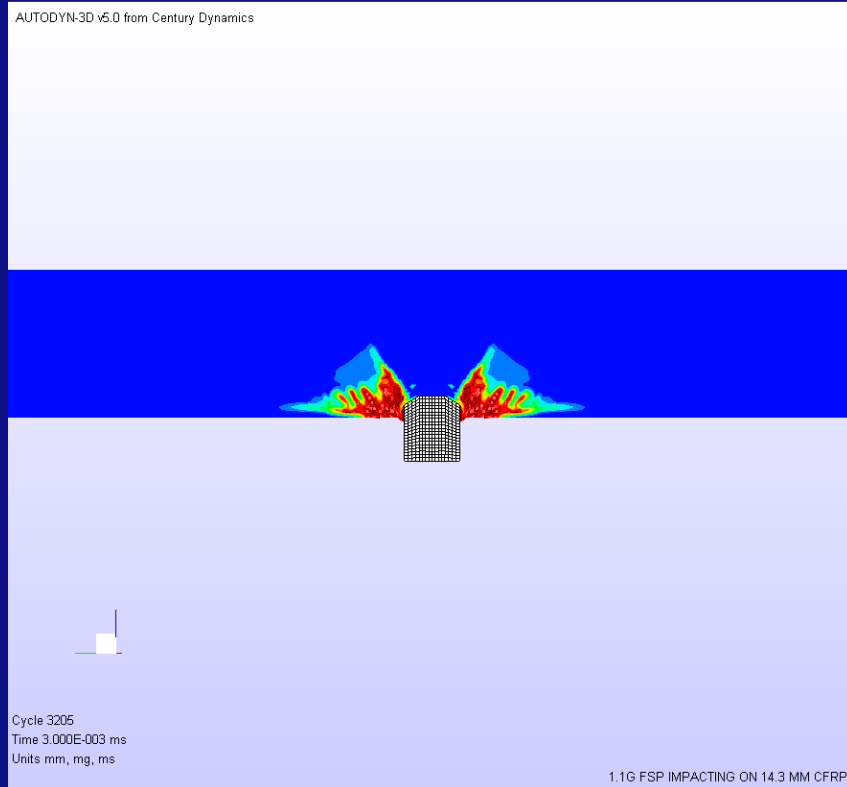
Fiber failure



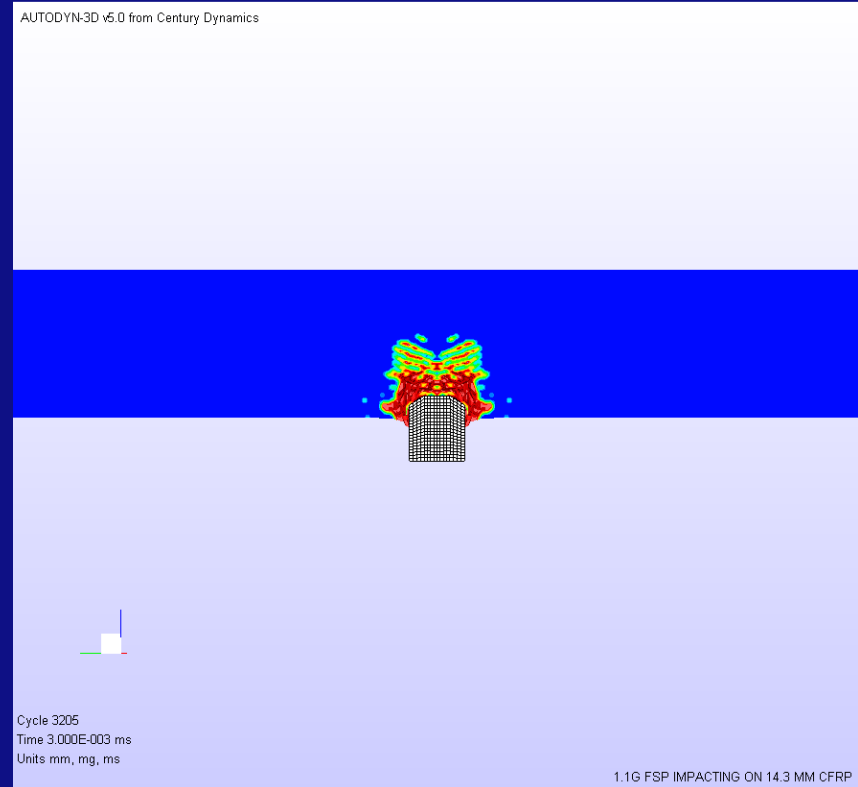
Simulation results

$V_{Impact} = 597 \text{ m/s}$, thickness = 14.3 mm

Delamination



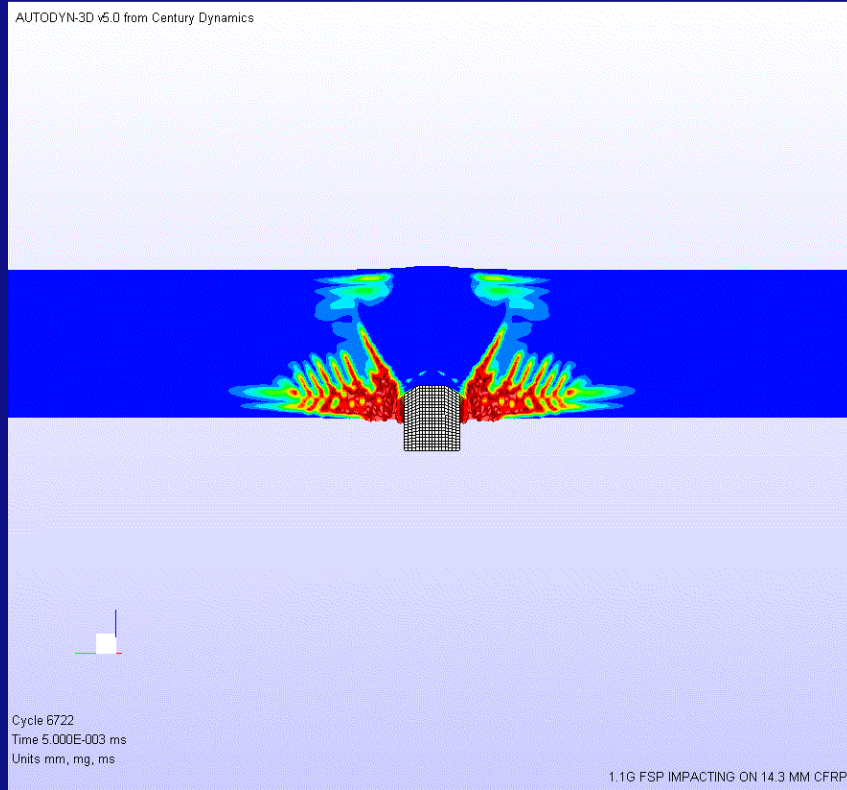
Fiber failure



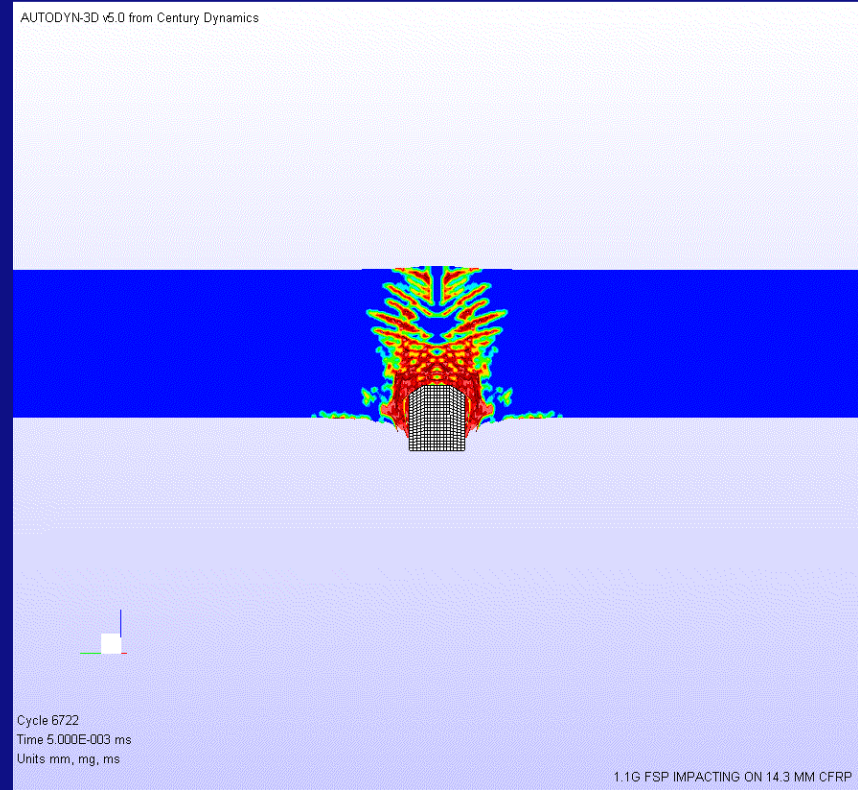
Simulation results

$V_{Impact} = 597 \text{ m/s}$, thickness = 14.3 mm

Delamination



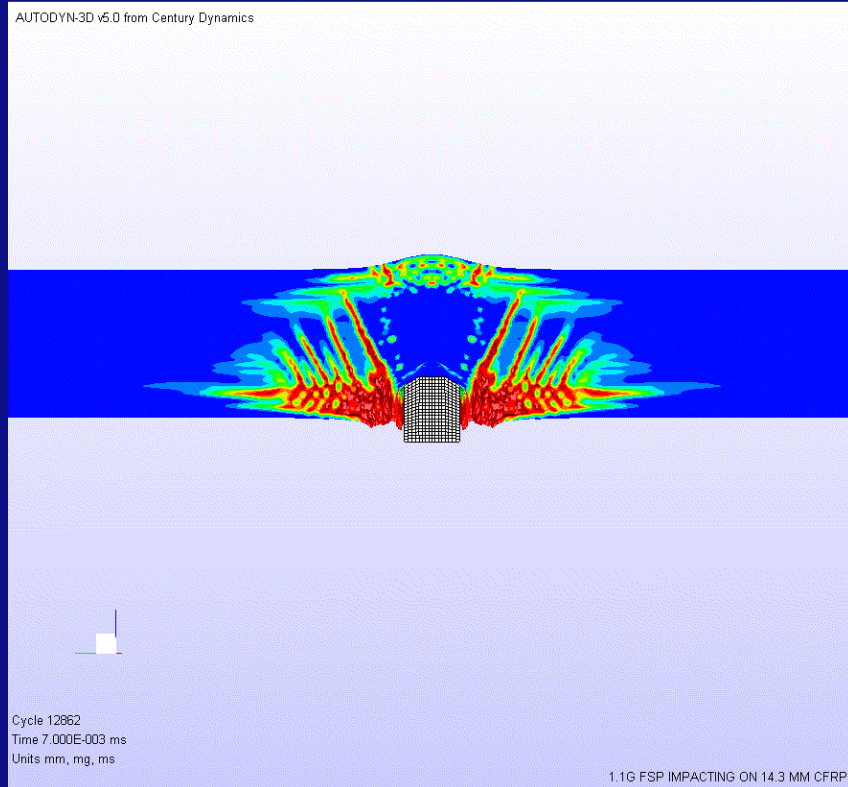
Fiber failure



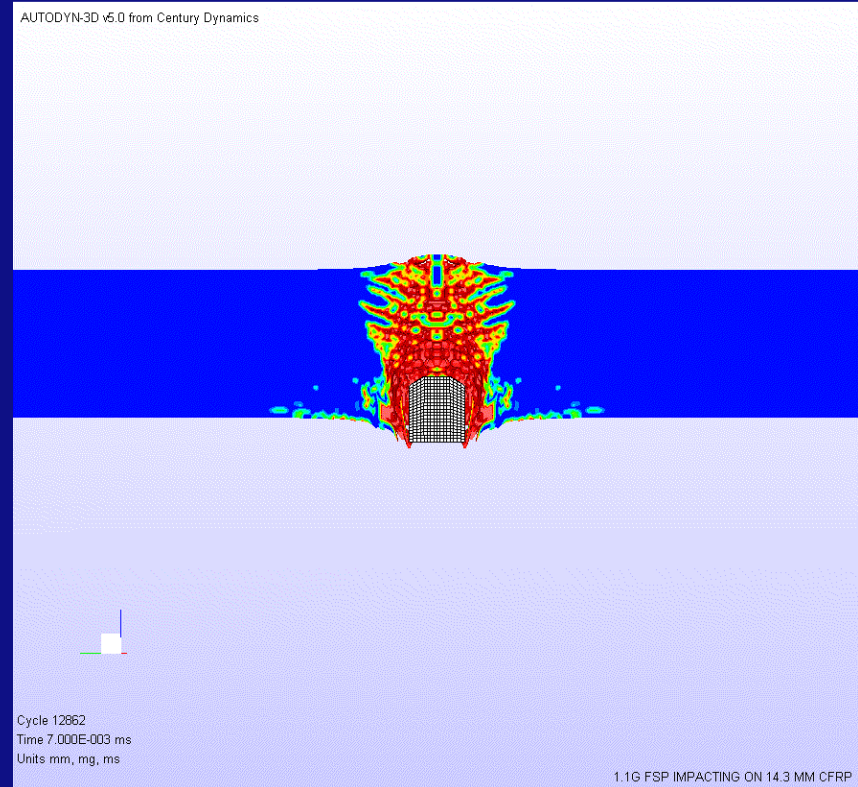
Simulation results

$V_{Impact} = 597 \text{ m/s}$, thickness = 14.3 mm

Delamination



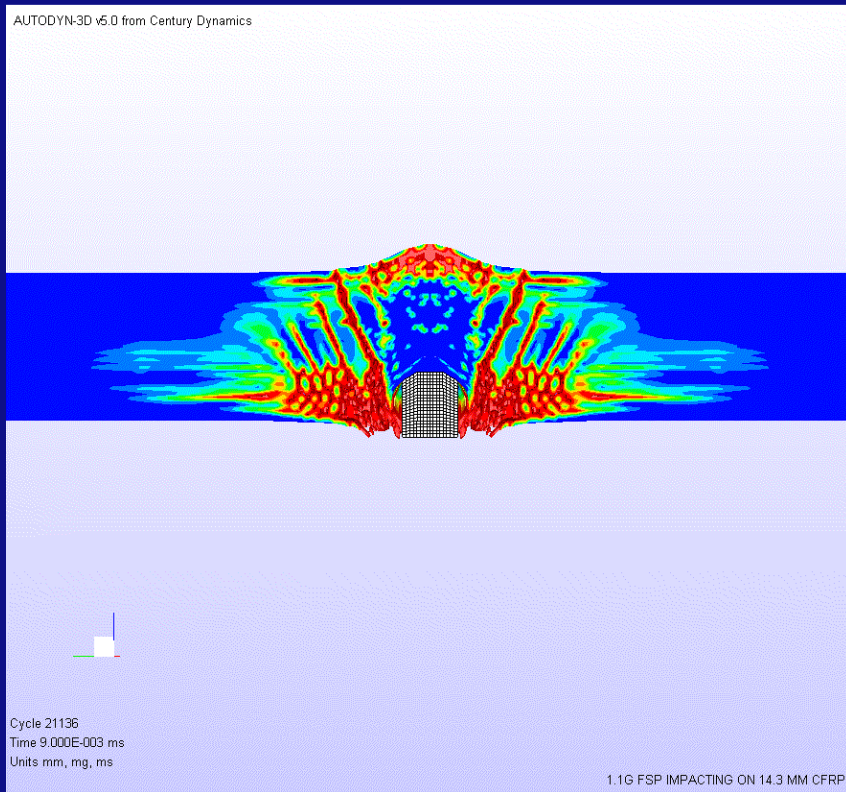
Fiber failure



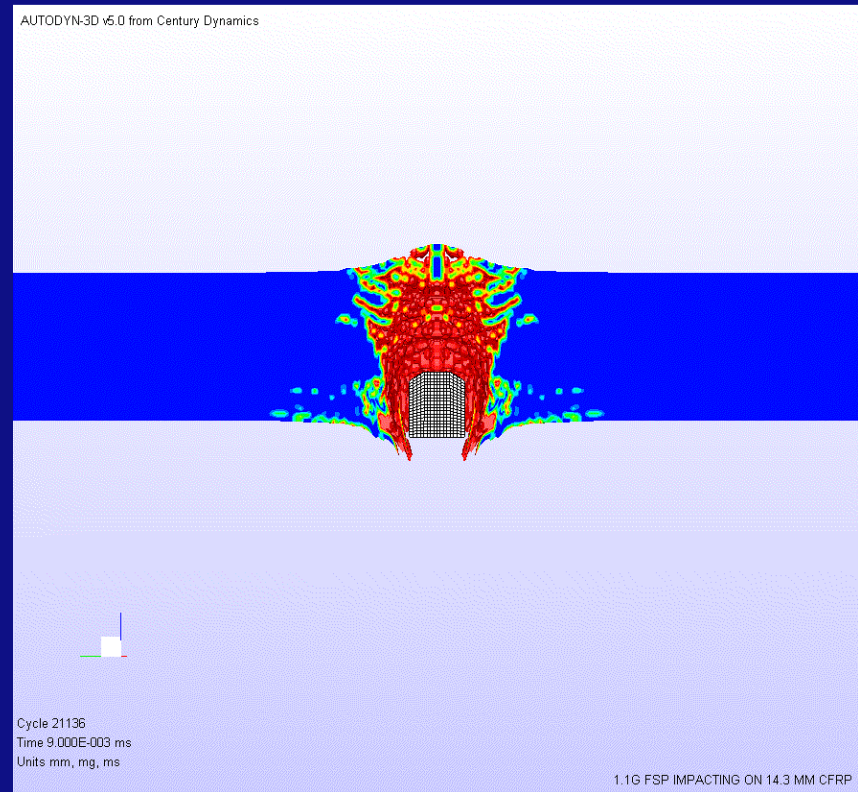
Simulation results

$V_{Impact} = 597 \text{ m/s}$, thickness = 14.3 mm

Delamination



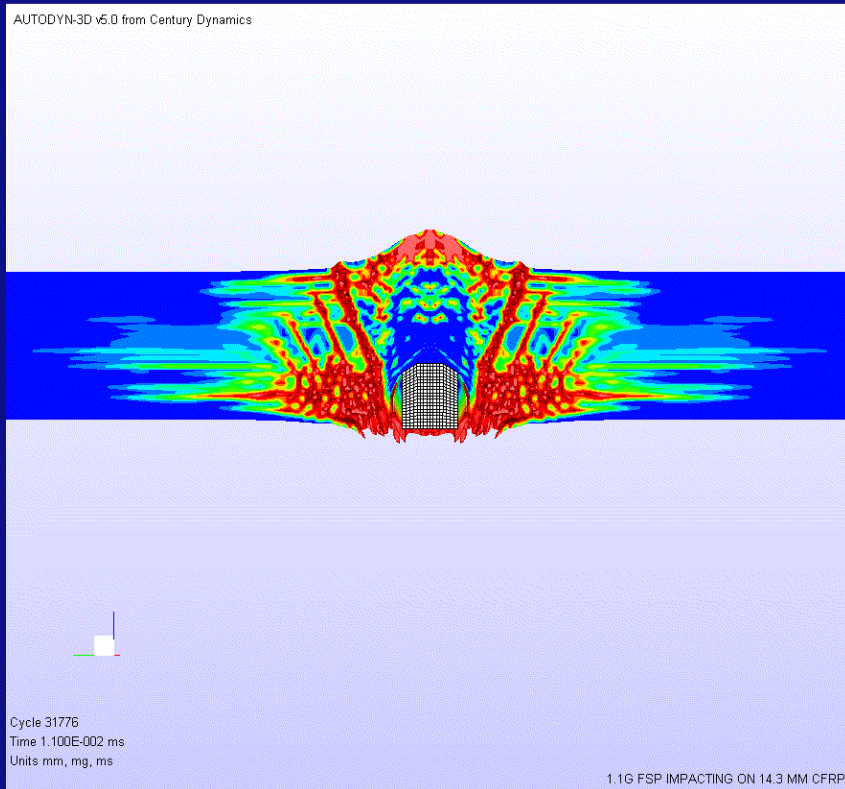
Fiber failure



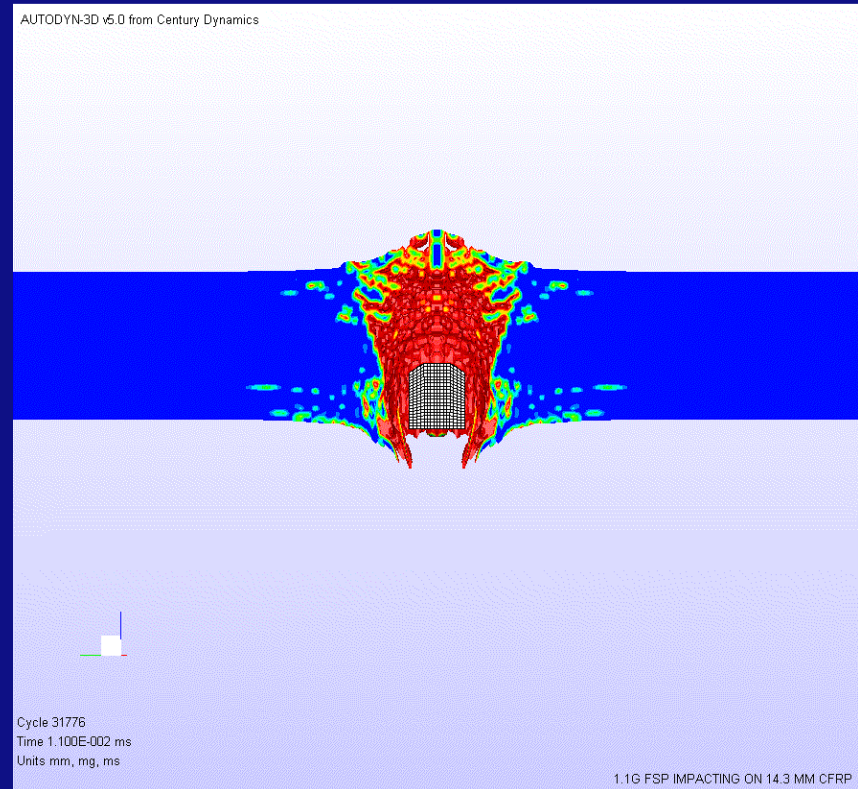
Simulation results

$V_{Impact} = 597 \text{ m/s}$, thickness = 14.3 mm

Delamination



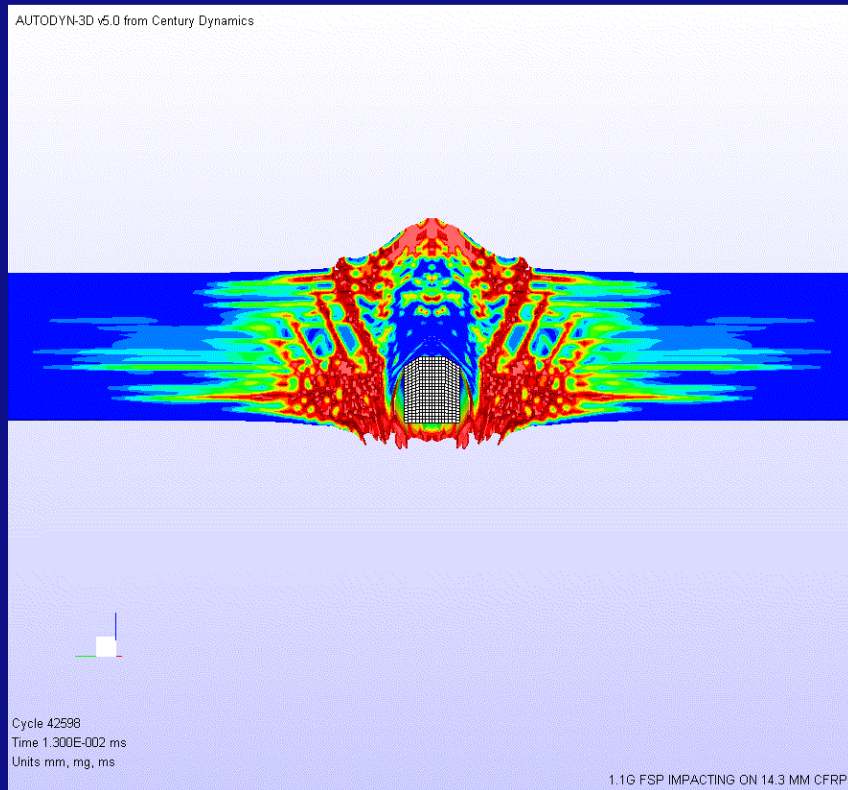
Fiber failure



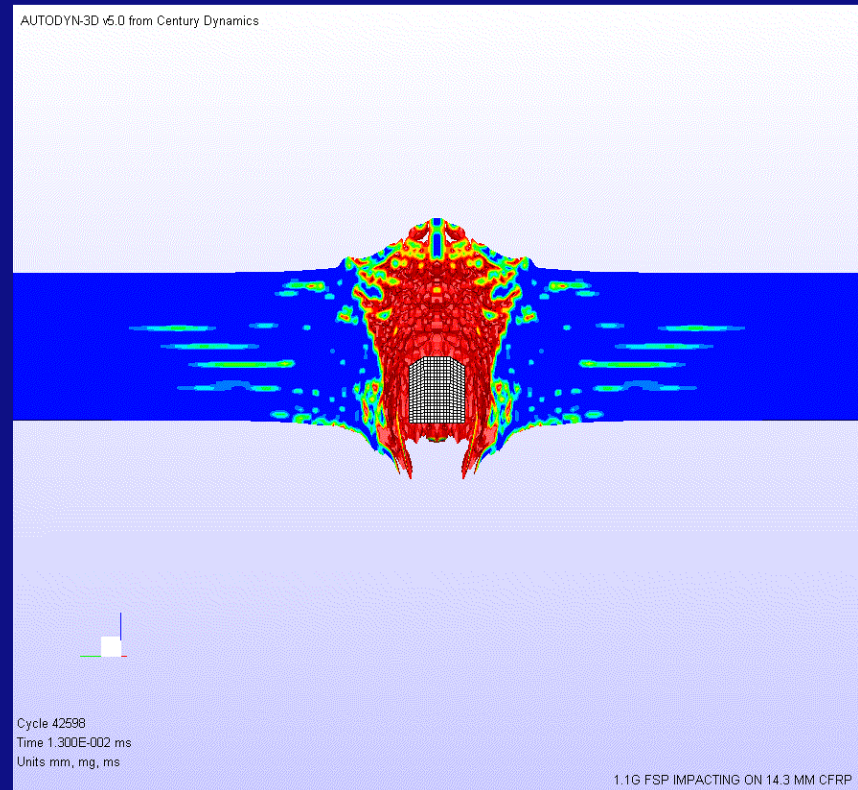
Simulation results

$V_{Impact} = 597 \text{ m/s}$, thickness = 14.3 mm

Delamination

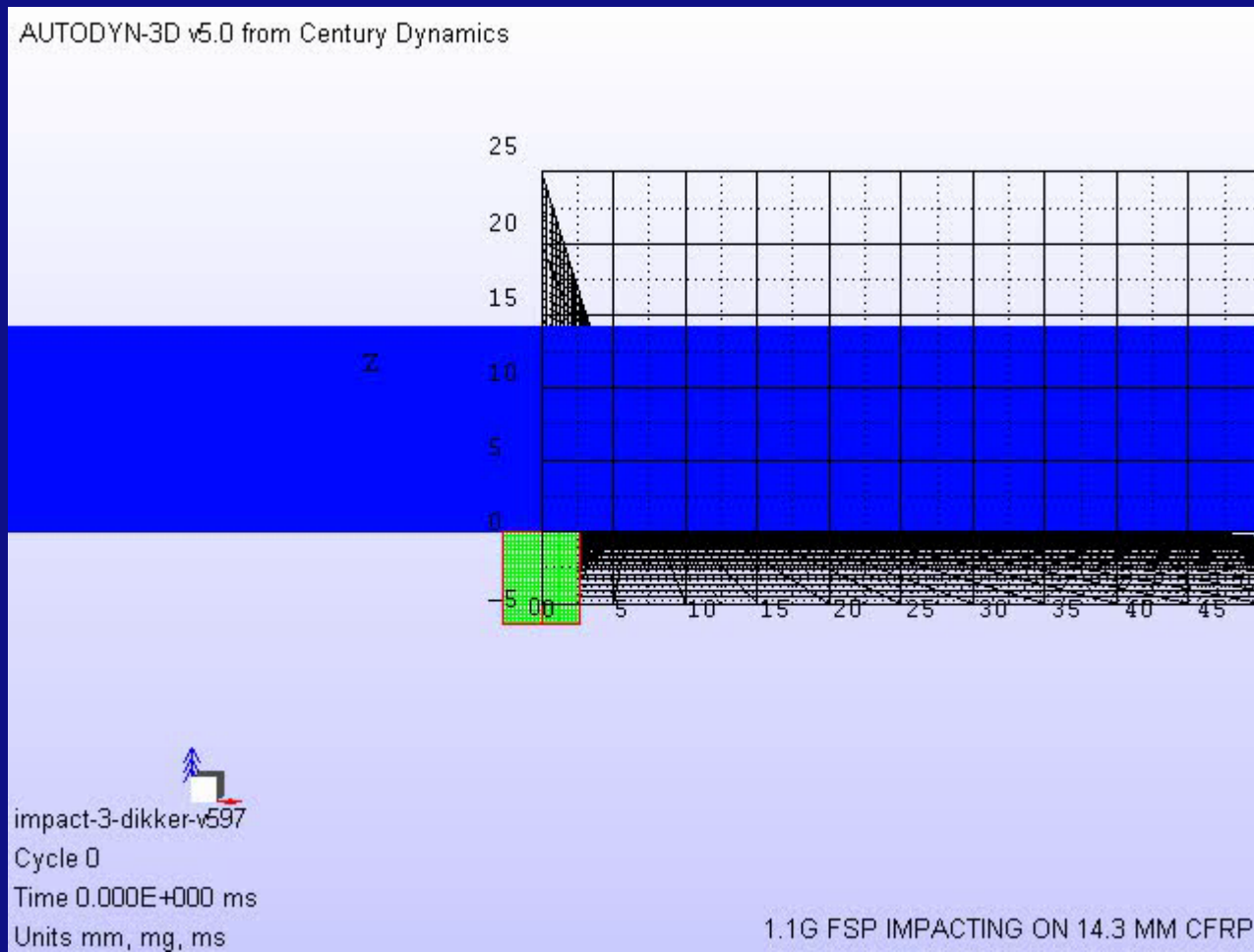


Fiber failure

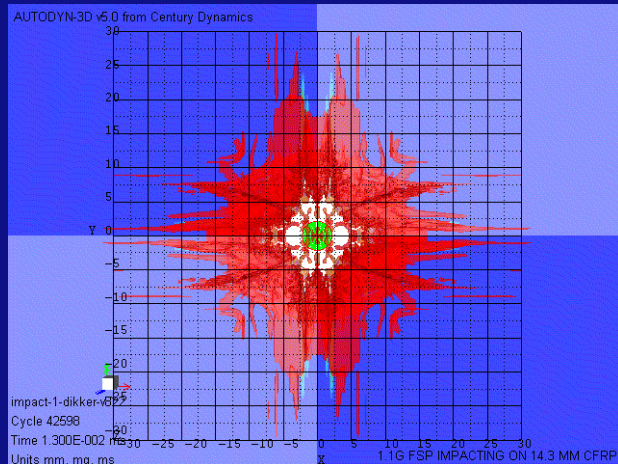
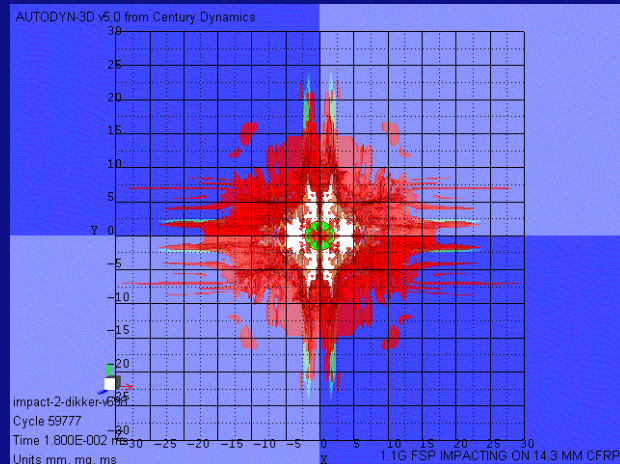
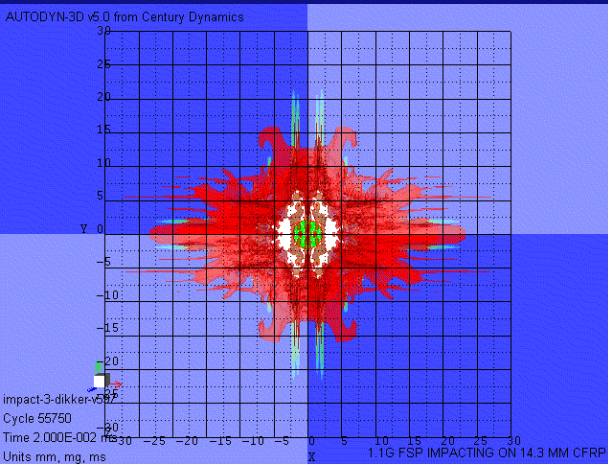


Simulation results, total internal damage

$V_{Impact} = 597 \text{ m/s}$, thickness = 14.3 mm



Total internal damage (comparison)



$$V_{impact} = 597 \text{ m/s}$$

$$V_{impact} = 698 \text{ m/s}$$

$$V_{impact} = 822 \text{ m/s}$$

Total internal damage (comparison)

- Quantitative comparison is very difficult → No direct link

Experiments:

- C-scan with 20 dB threshold
- Damage radius $\approx 22 - 27$ mm
- Little difference in damaged area within velocity range
- However small trend:
 V_{impact} increases \Rightarrow damaged area decreases

Simulations:

- “C-scan” with 60 % threshold
- Damage radius $\approx 20 - 25$ mm
- Little difference in damaged area within velocity range
- However small trend:
 V_{impact} increases \Rightarrow damaged area increases

Improvements can be made by measuring the softening behaviour in thickness direction and by performing inverse flyer plate tests

Conclusions and future research

- With limited material tests → good material behaviour
- Simulation results are consistent with experimental residual velocity
- Internal damage is difficult to compare with experiments
- The damage observed is in the same order of magnitude, however the trend is inconsistent with the experiments.

Future research:

- Further improvement of material model (softening, flyer plate)
- Combine blast loading with fragment impacts on construction
- Translate damaged area into strength reduction of construction
- With the knowledge from the FEM models → improve the current vulnerability and survivability tools

Soft-Recovery of Explosively Formed Penetrators

December 2005



David Lambert*, Matthew Pope

Air Force Research Laboratory

Munitions Directorate

Eglin Air Force Base, FL 32542-6810

*(850)882-7991, david.lambert@eglin.af.mil

Stanley E. Jones, Jonathan Muse

Aerospace Engineering and Mechanics

University of Alabama

Tuscaloosa, Alabama 35487-0280



Outline



Munitions Directorate

- **Introduction**
- **Model Description**
- **Experimental Setup**
- **Results**
- **Discussion/Conclusions**

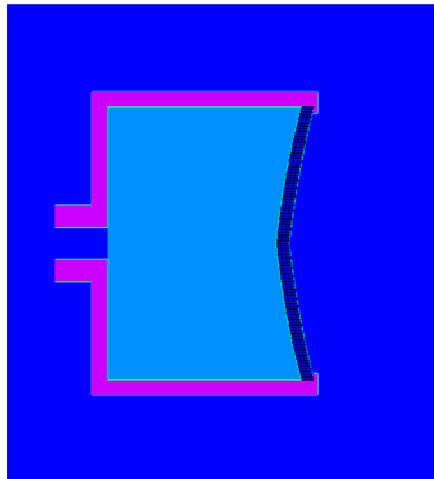


Why Soft-Recovery?

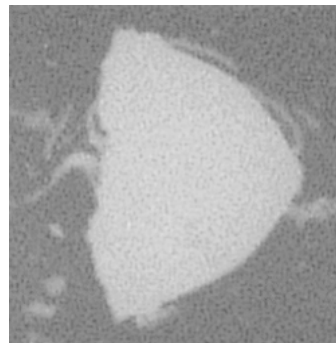


Munitions Directorate

- Improved design of EFPs (Explosively Formed Projectiles) using **state-of-the-art constitutive descriptions** require *ab initio* information of the high-rate, multi-axis stress deformation path
 - Explosive shock effects
 - Predominate crystallographic orientation (i.e. texture) and its dynamic evolution
 - Classical flash radiography and high-speed photography only captures geometry information
- Collaboration with Dr. Paul Maudlin, Los Alamos National Lab., TCG-I



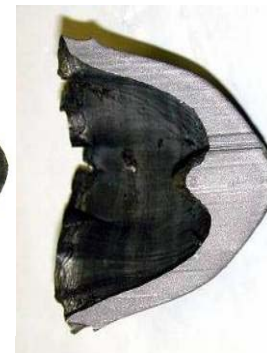
Example EFP Formation



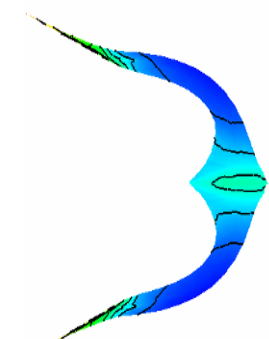
Flash Radiograph of an EFP in flight



Recovered EFP



Cross-section of recovered EFP



Code simulation, EPIC Anisotropic MTS



Developmental Engineering Tools

3D, Anisotropic Material Descriptions



Munitions Directorate

Material Processing

- Conventional
- Unconventional

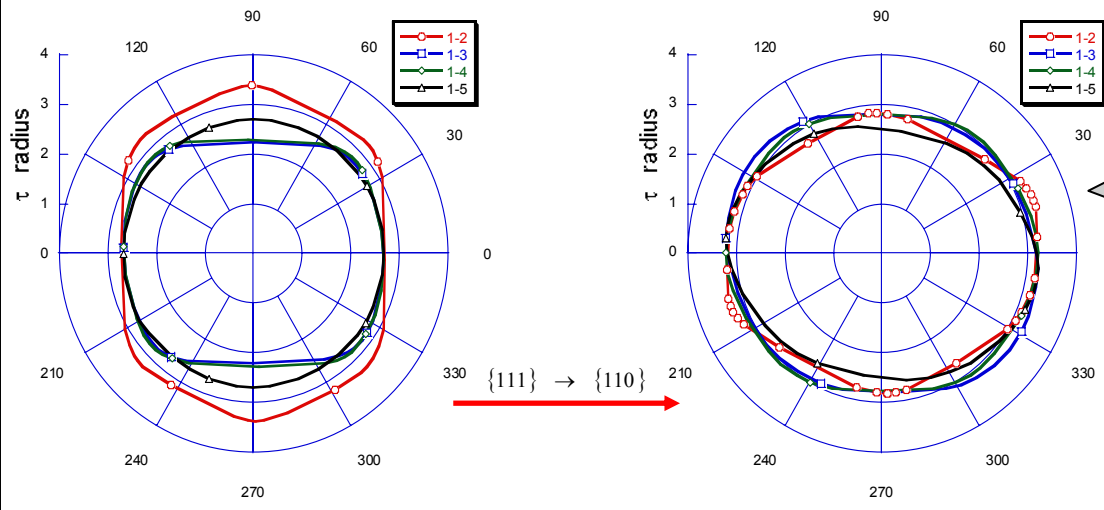
Physical Characterization

- Grain size
- Chemistry
- Crystallography

Mechanical Characterization

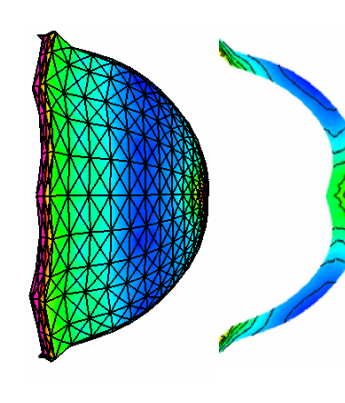
- Low Rate & High Rate
- Temperature
- Uniaxial
- Taylor Impact

Yield Surface Projections



Explosive Metal Forming Experiments

- Shock loading
- High-rate
- Tri-axial stress



Calculations by Dr. Paul Maudlin, LANL, under TCG-I
"Computational Mechanics and Material Models", EPIC-3D



The Approach Taken Here



Munitions Directorate

- **Apply a simplistic, but adequate equation-of-motion for the projectile through the media**
- **Arrange mathematical relationships that relate to the physical experiment and instrumentation capability**
- **Conduct experiments from which the data is used to calibrate the soft-recovery media**
- **Compare results of the general model with specific experiments**
- **Use the model and calibrated media constants for tailored design and construct of soft-recovery apparatus**



Mathematical Model



Munitions Directorate

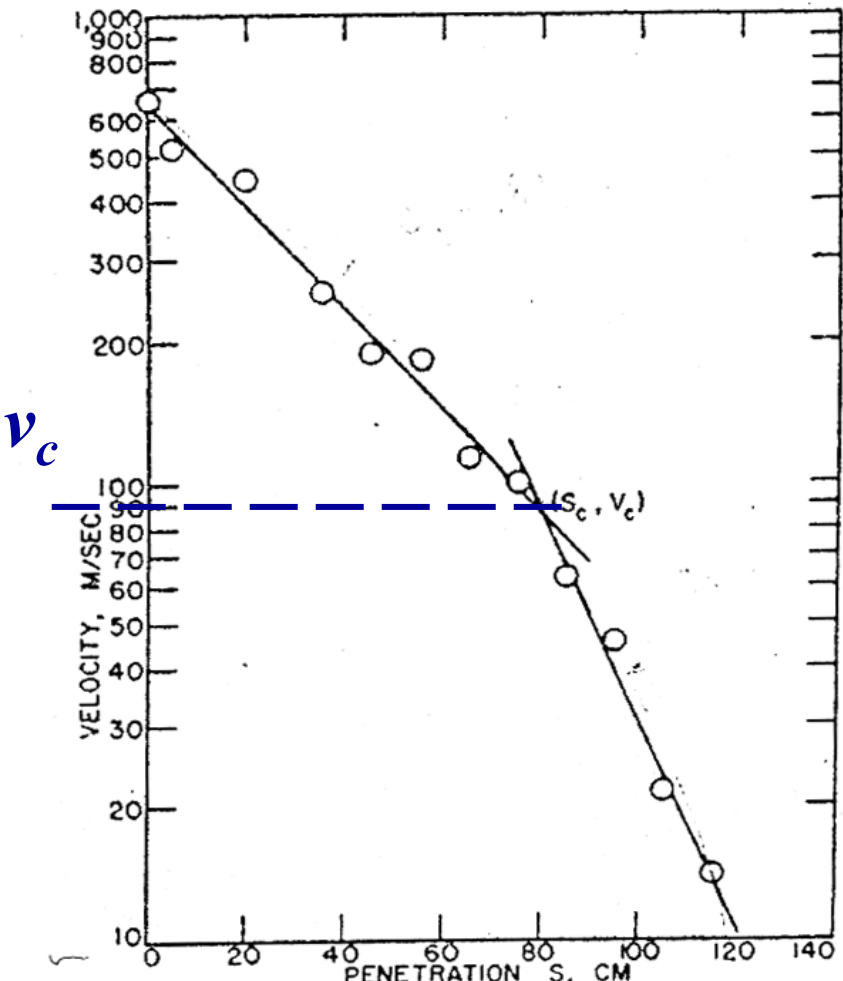
Region 1: Drag Force Model

$$m \dot{v} = -\frac{1}{2} C_D A \rho v^2, \quad v > v_c$$

Region 2: Poncelet Form

$$m \dot{v} = -A(\beta v^2 + R), \quad v < v_c$$

- *m* is mass of the projectile
- *v* is current projectile velocity,
- *A* is projectile cross-section area
- *ρ* is the density of the target medium
- *C_D* is a dimensionless drag coefficient
- *β* is a coefficient (dim. of density)
- *R* is a target strength factor (dim. of stress)



Allen, et al. J. Applied Physics, 1957



Mathematical Model (cont'd)



Munitions Directorate

Assumptions made on the solution:

- Model will be applied for soft-catch sections where $v > v_c$
- Drag coefficient is not dependent on velocity

Direct integration of the Drag-Force model gives:

$$\frac{1}{2} \frac{C_D A \rho}{m} z = \ln \left(\frac{v_0}{v} \right)$$

and

$$\frac{1}{2} \frac{C_D A \rho}{m} t = \frac{1}{v} - \frac{1}{v_0}$$

where:

- z is the displacement into that section of the soft catch
- t is the experimentally obtained time at the displacement z
- v_0 is the entrance velocity to that section
- v is the exit velocity from that section



Mathematical Model (cont'd)



Munitions Directorate

- By dividing the prior two equations, a single relationship is obtained, ***dependent only on parameters*** that can be directly obtained during an experiment.

$$\frac{z}{t} \left(\frac{v_0}{v} - 1 \right) = v_0 \ln \left(\frac{v_0}{v} \right)$$

where:

- ***z is the displacement into that section of the soft catch***
- ***t is the experimentally obtained time at the displacement z***
- ***v₀ is the entrance velocity to that section***
- ***v is the exit velocity from that section***



Solution Steps



Munitions Directorate

Step 1:

$$\frac{z}{t} \left(\frac{v_0}{v} - 1 \right) = v_0 \ln \left(\frac{v_0}{v} \right)$$

Is applied to each catch section with experimental time-position data, using Newton's method for convergence on an iterative root solution to get the ratio v_0/v , where v_0 is the exit velocity from the previous section and v is our unknown

Step 2:

$$\frac{1}{2} \frac{C_D A \rho}{m} z = \ln \left(\frac{v_0}{v} \right)$$

The ratio v_0/v is then put back into this equation to obtain a C_D for each penetrator/soft-catch material combination

Step 3:

$$\frac{1}{2} \frac{C_D A \rho}{m} t = - \frac{1}{v} - \frac{1}{v_0}$$

The C_D for sections of each material are averaged, and then used to obtain an estimated exit time, t , for comparison to the experimental values

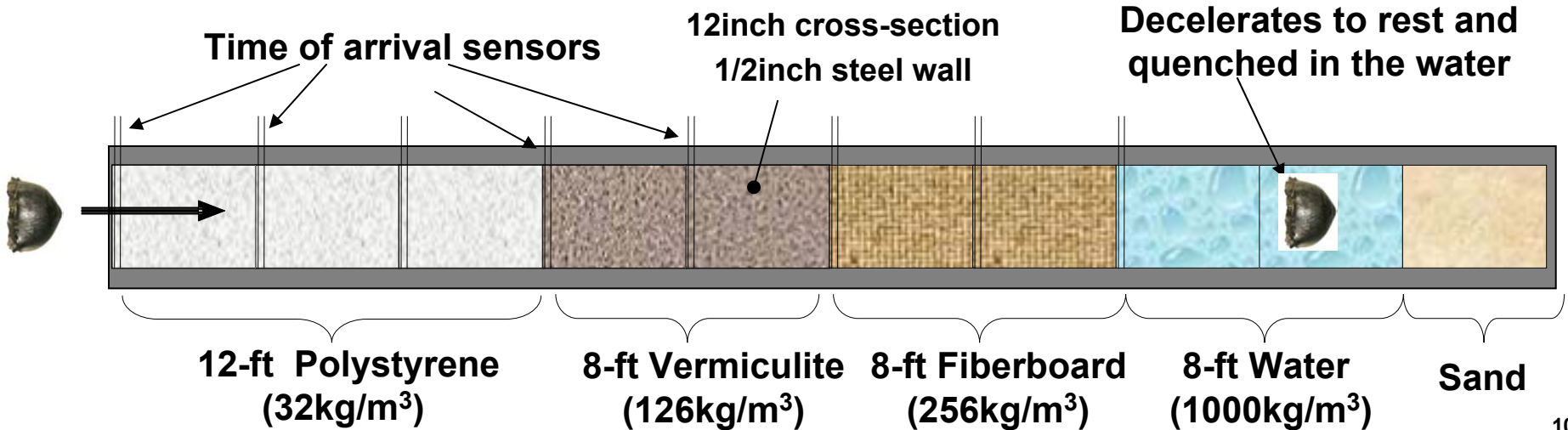


The Soft-Catch Process



Munitions Directorate

- A gradient in the media density safely decelerates the projectile
- Instrumented shotline captures the time, position, and velocity data to feed the transcendental relationship
- The section of water not only provides a gradual increase in media density, but also serves to quench the projectile
- Dual, orthogonal radiographs were used in pre-impact, free-flight to establish external geometry and entrance velocity



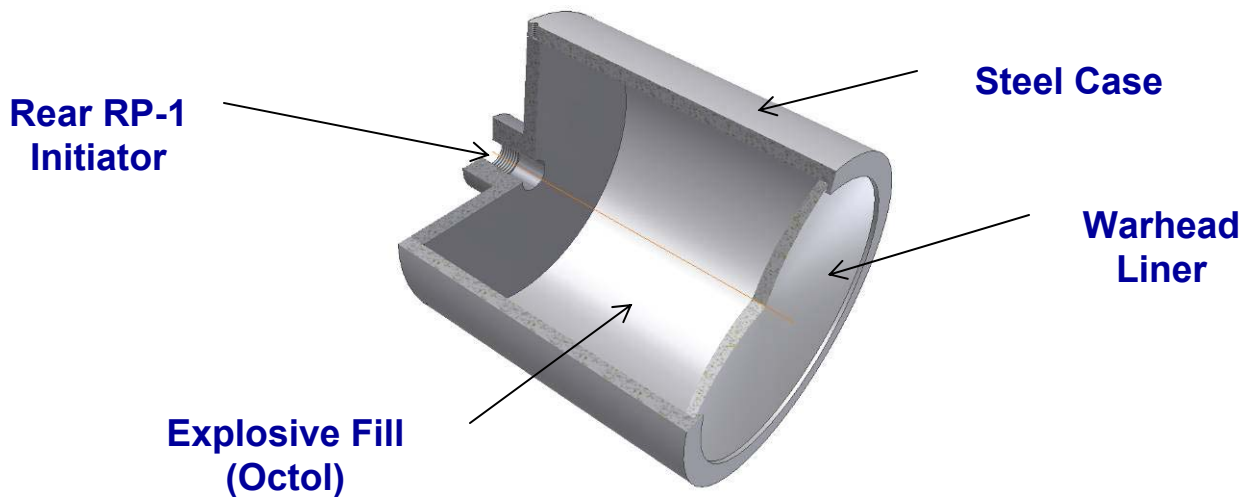


Experimental Setup



Munitions Directorate

1. Three warhead liner types were shot
 - 3 shots with “Tantalum Design 1”
 - 2 shots with “Tantalum Design 2”
 - 1 shot with “Cu EFP”
2. Fine Grain Octol explosive (65%HMX, 35% TNT)
3. Design was for a simple ‘fold-over’ projectile
 - Explosive shock conditions
 - Representative strain-rate and strain paths





Results from Applying the Model



Munitions Directorate

TABLE I. DRAG COEFFICIENTS, C_D , FOR ALL EFP TYPES

	Polystyrene ($\rho = 32.0 \text{ kg/m}^3$)	Vermiculite [©] ($\rho = 126.4 \text{ kg/m}^3$)	Fiberboard ($\rho = 256 \text{ kg/m}^3$)
Ta Design 1 (avg. of 3 shots)	0.777	1.534	0.395
Ta Design 2 (avg. of 2 shots)	0.84	0.88	0.86
Cu EFP (1 shot)	0.77	0.94	0.76



Comparison with the Theory



Munitions Directorate

TABLE II. MODEL COMPARISON WITH “TA DESIGN 2, SHOT 1”

Tantalum Design 2, Shot 1: Impact Velocity = 1440 m/s					
Media	Experiment Velocity (m/s)	est. Exit Velocity (m/s)	Experiment Exit time (us)	est. Exit time (us)	Difference in time (%)
Polystyrene	1395	1381	437	432	-1.1%
	1382	1324	878	883	0.6%
	1273	1270	1357	1353	-0.3%
	1229	1218	1853	1844	-0.5%
	1212	1168	2356	2355	-0.1%
	1146	1120	2888	2888	0.0%
Vermiculite	1039	941	3475	3482	0.2%
	872	791	4174	4190	0.4%
	721	665	5019	5032	0.3%
	615	559	6010	6033	0.4%
	512	469	7201	7225	0.3%
	419	395	8656	8644	-0.1%
Cellotex	325	280	10529	10488	-0.4%
	235	198	13119	13092	-0.2%

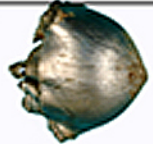
- Excellent results validate the assumption of simple drag-force relationship, $v > v_c$
- Note, penetration velocities are below that reported in Mayfield, et al for v_c



Recovered Projectiles



Munitions Directorate

Shot	Impact Velocity (m/s)	Recovered Mass (kg) (%initial)	Location Recovered	Cross-section	Picture
Ta Design 1 Shot 1	1423	0.726 (83.4%)	12-in into sand		
Ta Design 1 Shot 2	1397	0.720 (82%)	24-in into sand		
Ta Design 1 Shot 3	1389	Not Available	18-in into water	Not available	
Ta Design 2 Shot 1	1440	0.738 (92.6%)	41-in into fiberboard		
Ta Design 2 Shot 2	1422	0.761 (93.4%)	60-in into fiberboard		
Cu EFP	2030	0.409 (90.8%)	fiberboard section		



Discussions/Conclusions



Munitions Directorate

Areas for further investigation:

1. Determine if the tacit assumption that $v > v_c$ used is valid
 - Find v_c in these media
2. Determine if C_D is independent of velocity as assumed (velocities were in a relatively narrow band)
 - Find C_D for a wider range of velocities in each media and compare
3. Use constants for predictive design of soft-catch build up and capture higher velocity, more tactical (collapsed) projectiles



Discussions/Conclusions



Munitions Directorate

An alternative approach to calibrating projectile/media constants:

- 1. Construct a soft catch with just one catch material at a time to obtain C_D for all velocities above and below v_c**
- 2. Place velocity screens at closer intervals for better resolution such that v_c might be obtained**

Total penetration depth $z = S$ is found when $v = 0$, i.e. projectile comes to rest

The original equations of motion can be arranged to solve for total penetration into the single media and extract v_c

$$S = \frac{2m}{C_D A \rho} \cdot \ln\left(\frac{v_o}{v_c}\right) + \frac{m}{2\beta A} \cdot \ln\left(\frac{\beta v_c^2}{R} + 1\right)$$



Summary



Munitions Directorate

- **A simple theory has been successfully applied for the design of a soft-catch apparatus**
- **Model, thus far, yields excellent agreement with experimental time data**
- **Further experiments needed to support underlying assumptions**
- **These interest items will be the subject of future experiments**



Sources



Munitions Directorate

- [1] Draxler, V.C. 1993. "Softcatch Method for Explosively Formed Penetrators," presented at the 44th Meeting of the Aeroballistic Range Association, Munich, Germany, September 13-17, 1993.
- [2] Allen, W.A., E.B. Mayfield, and Morrison, Harvey L., 1957. "Dynamics of a Projectile Penetrating Sand," *J. Applied Physics*, 28(3):370-376, 1957.
- [3] Poncelet, J.V. 1829. *Cours de Mecanique Industrielle*, 1829.
- [4] Allen, W.A., E.B. Mayfield, and Morrison, Harvey L., 1957. "Dynamics of a Projectile Penetrating Sand, Part II" *J. Applied Physics*, 28(11):1331-1335, 1957.



THE INFLUENCE OF POST DETONATION BURNING PROCESS ON BLAST WAVE PARAMETERS IN AIR

E.Muzychuk¹, M.Mayseless², I.Belsky²

¹ *IDF, Armor Branch*

² *IMI, Central Laboratory Division*

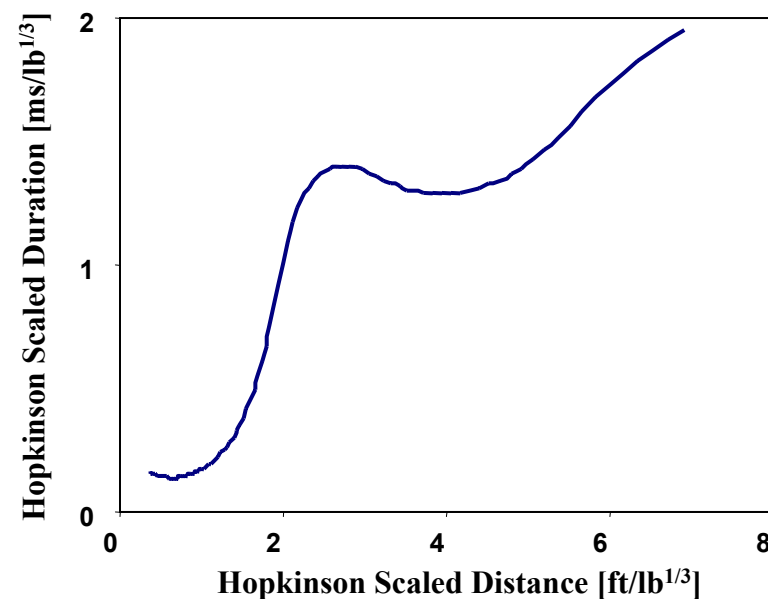


Outline

- Motivation
- Non ideal blast waves
- Goal
- Model
- Simulations
- Experimental work
- Calibration
- Summary

Motivation

- An unexplained non-monotonicity of the scaled blast duration is evident in CONWEP data.
- A possible explanation might be related to non-ideality of the explosion (post-detonation burning).



Non-Ideal Blast Waves

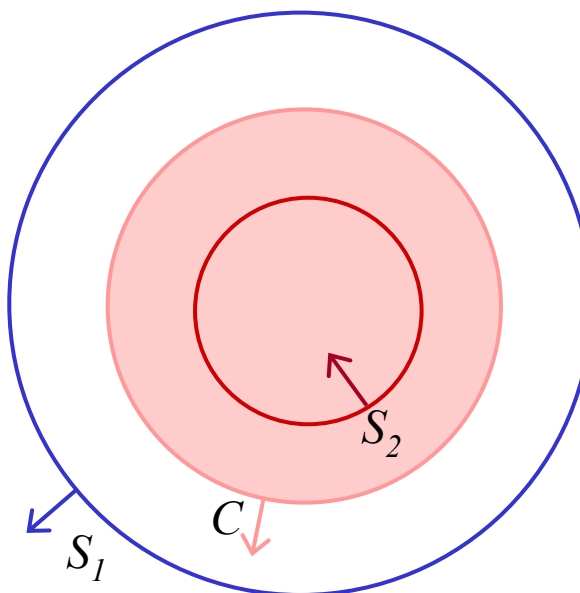
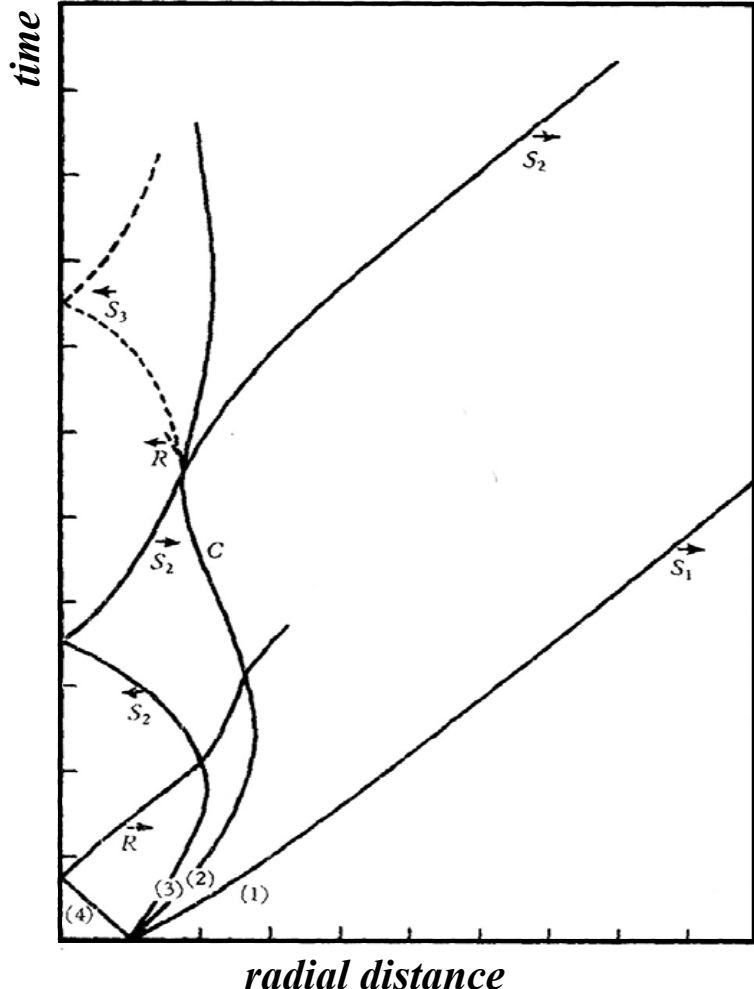
Ideal Explosion	Non Ideal Explosion
All chemical energy is extracted in the detonation front	Some energy remain due to negative oxygen balance
Gas diffusion and surface turbulence are neglected.	Gas diffusion and surface turbulence taken into account
Detonation products do not burn	Detonation products burn when oxygen is supplied



The Goal of our Study

To model effectively the non ideal blast effects (i.e. gas diffusion and burning) in order to understand their influence on the blast profile.

Spherical Explosion Shock Wave Dynamics



C – Det. products – air surface.
 S_1 – Primary shock wave
 R – Rarefaction shock wave.
 S_2 – Secondary shock wave.

Gas Diffusion

- Classically, the diffusion of two gases controlled by three gradients:
 - Concentration
 - Pressure
 - Temperature
- Concentration estimated diffusion velocity:
500-1500 m/s

Model Hypothesis

- All gases are ideal gases with various adiabatic constants.
- Adiabatic constant of mixed gas is a concentration weighted average.
- The burning process affects only the internal energy and the adiabatic constant of the gas.

Relative concentrations inside detonation products cloud:

- η - air
- ξ - Pre-burned gas
- β - burning products

$$\left. \begin{array}{l} \eta + \xi + \beta = 1 \end{array} \right\}$$

Energy release dynamics

Initial conditions (det. products cloud): $\eta = 0$; $\xi = 1$; $\beta = 0$

Diffusion:

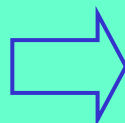
$$\eta(r, t) = \eta_0 \exp\left(-\frac{r_c - r}{ut}\right)$$

Rate of change in internal energy: $\dot{E}_b = \min\left(\frac{5}{7}\eta, \xi\right) \cdot \dot{E}_b^0$

Burning Products concentrations:

$$\beta(t) = \frac{E_b(t)}{E_b^{final}}$$

Pre-burned gas concentration: $\xi = 1 - \beta - \eta$



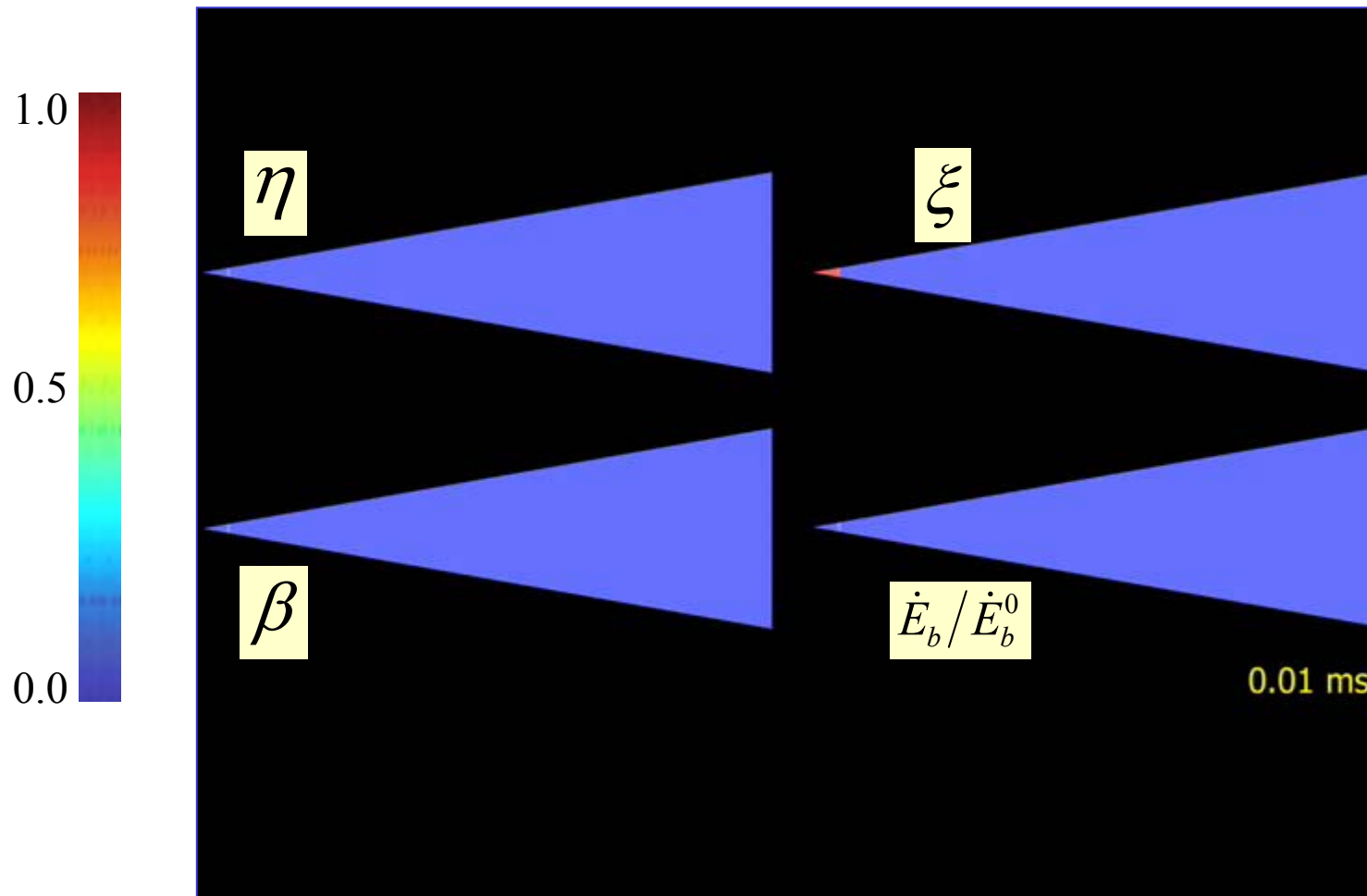
$$\dot{E}_b = \min\left(\frac{5}{7}\eta(r, t), \left(1 - \eta(r, t) - \frac{E_b}{E_b^{final}}\right)\right) \cdot \dot{E}_b^0$$

Numerical Simulation

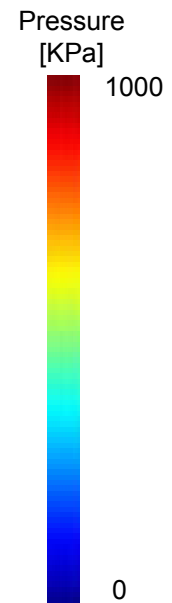
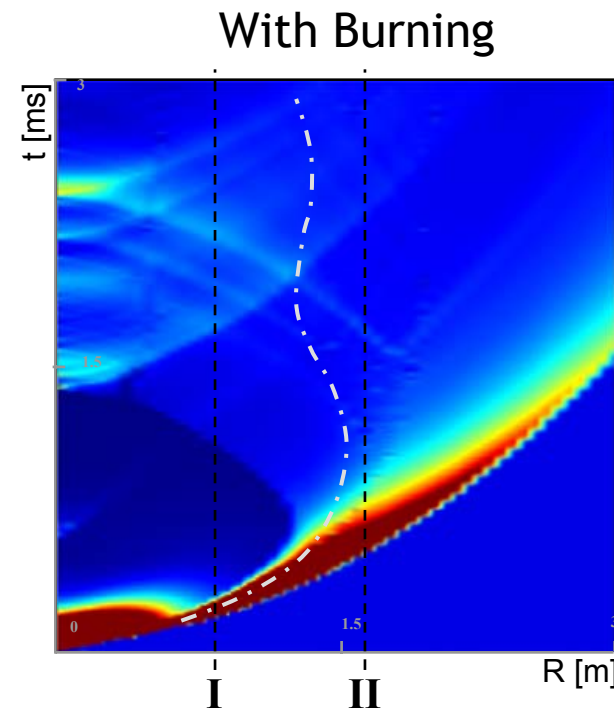
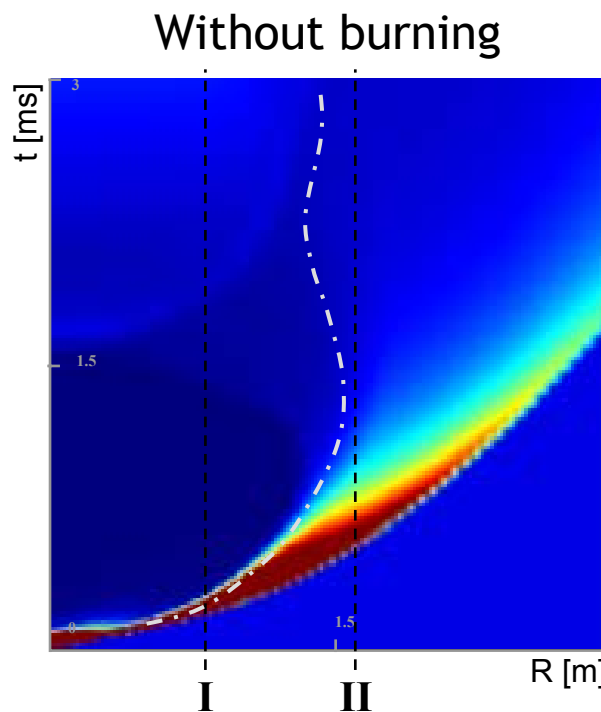
- Simulation conducted using AUTODYN ver. 6.0.
- New EOS (based on ideal gas) was defined in order to implement the model.
- Two stages simulation:
 - Detonation
 - Blast propagation & burning
- The simulation set-up was a spherically symmetrical explosion of 5kg TNT charge.

Numerical Simulation

1D axially symmetrical explosion

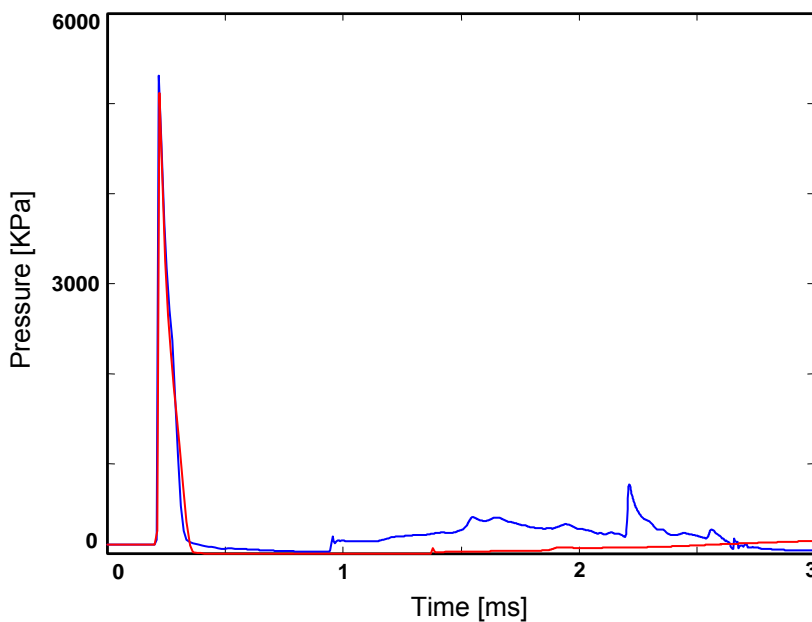


Simulation results

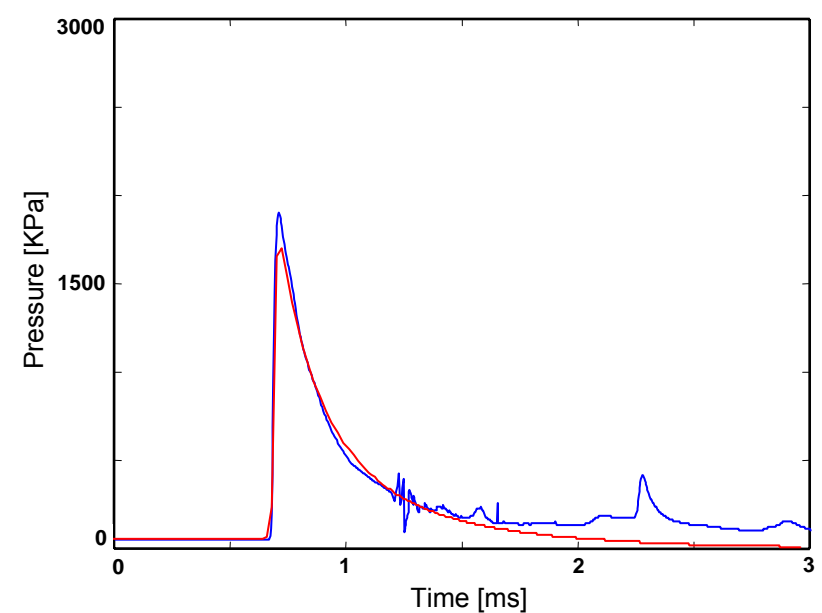


Simulation Results

(I)
 $r=0.8\text{ m}$



(II)
 $r=1.6\text{ m}$



— Without Burning
— With Burning

Experimental Set Up

- Two energy equivalent free field explosion tests conducted:
 - 5 kg TNT
 - 4.2 kg C-4

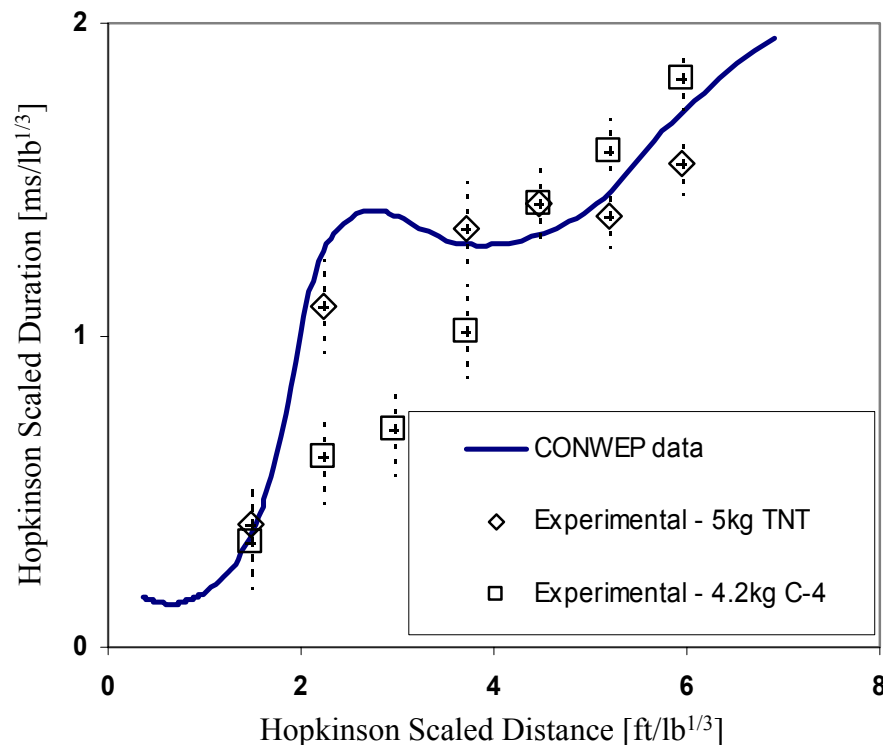


Detonation Products of TNT and C-4

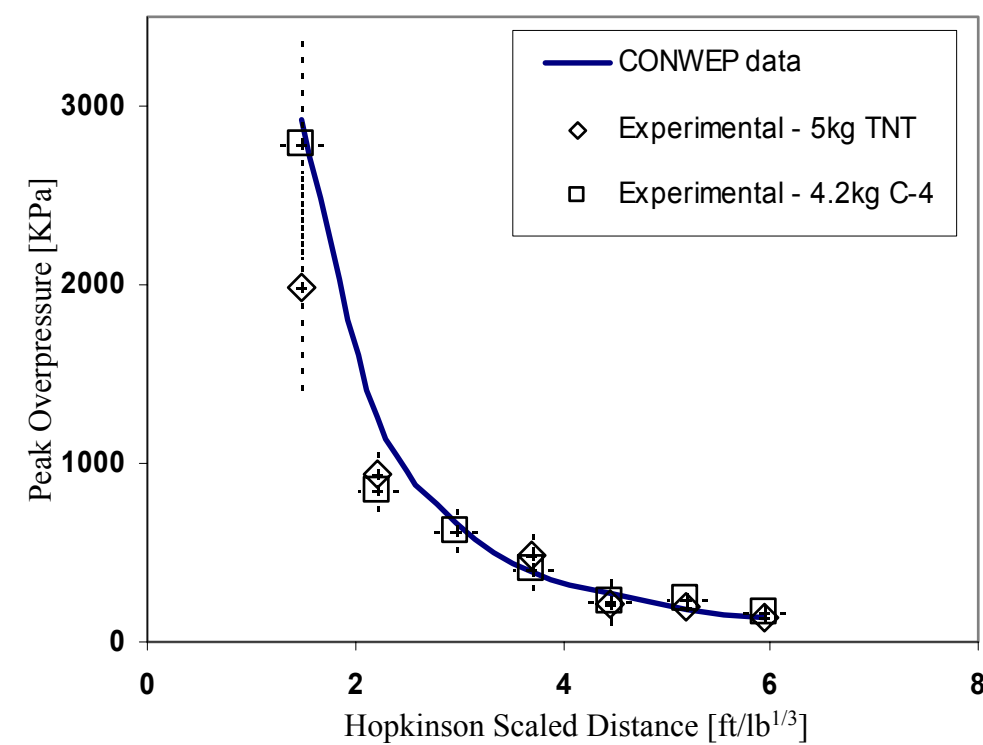
	TNT [%mole]	C-4 [%mole]
H ₂	21.4	12.6
CO	54.5	22.0
CO ₂	5.5	10.5
H ₂ O	1.5	18.0
N ₂	12.5	28.0
Others	5.5	9.9
CO+H ₂	76%	35%

Experimental Results

Pulse durations



Pulse pressure peak



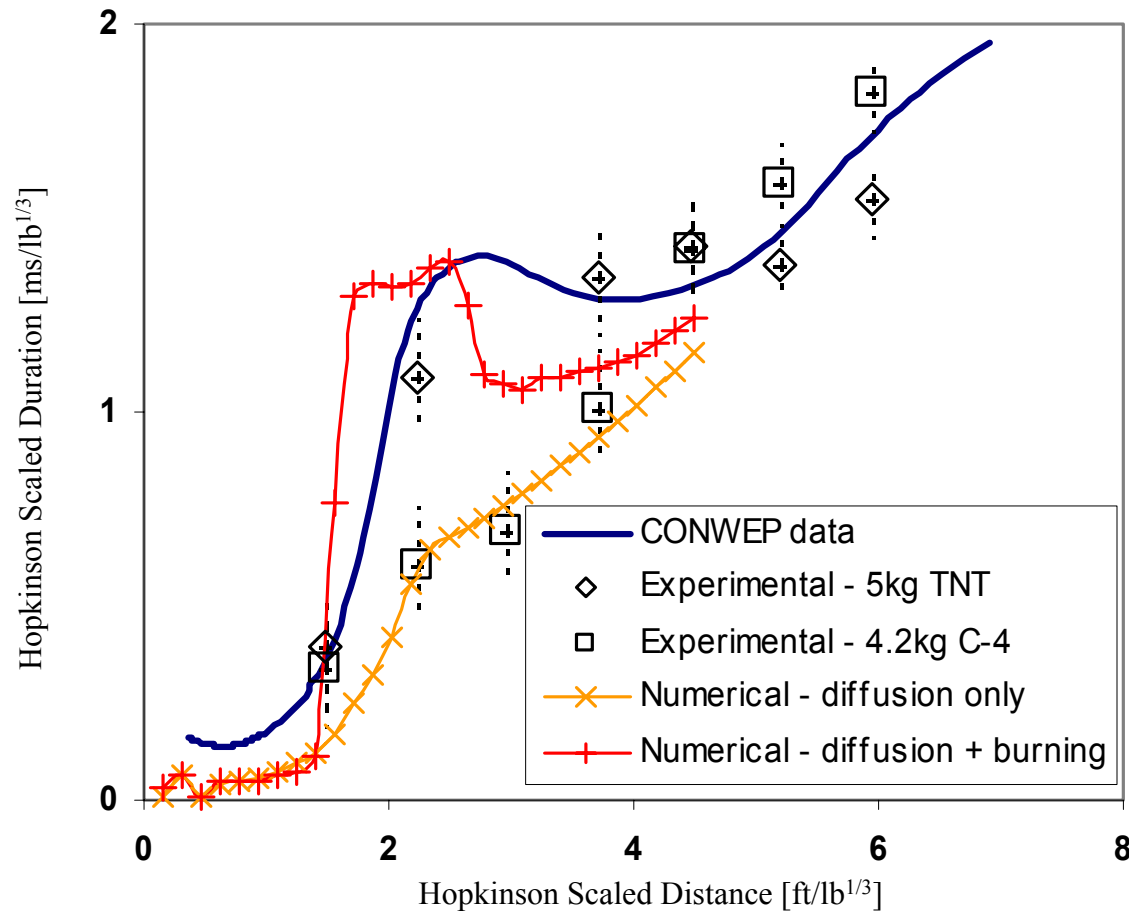
Model Calibration

- Calibration parameters:

$$u, \eta_0, \dot{E}_b^0$$

- The model was calibrated employing:
 - CONWEP data
 - Experimental results

Results



Summary

- An effective model is proposed, capable of reproducing the burning effect on a non-ideal blast waves.
- Good agreement obtained between numerical and experimental results.
- Post detonation burning affects the blast profile in the near field (scaled distance $< 4 \text{ ft/lb}^{1/3}$).
- When non ideal blast effects are important the TNT equivalence convention must be reconsidered.



Acknowledgements

- We would like to thank Dr. Eitan Hirsch for the fruitful discussions of the topic

22nd International Symposium on Ballistics

**November 14-18, 2005
Vancouver, Convention Centre
Vancouver, BC, Canada**

THE ROLE OF RAYLEIGH TAYLOR INSTABILITY IN SHAPED CHARGE JETS FORMATION AND STABILITY

***Dr. Simcha Miller, Mr. Gershon Kliminz**

Rafael Ballistic Center, P.O. Box 2250 (M4), HAIFA, ISRAEL

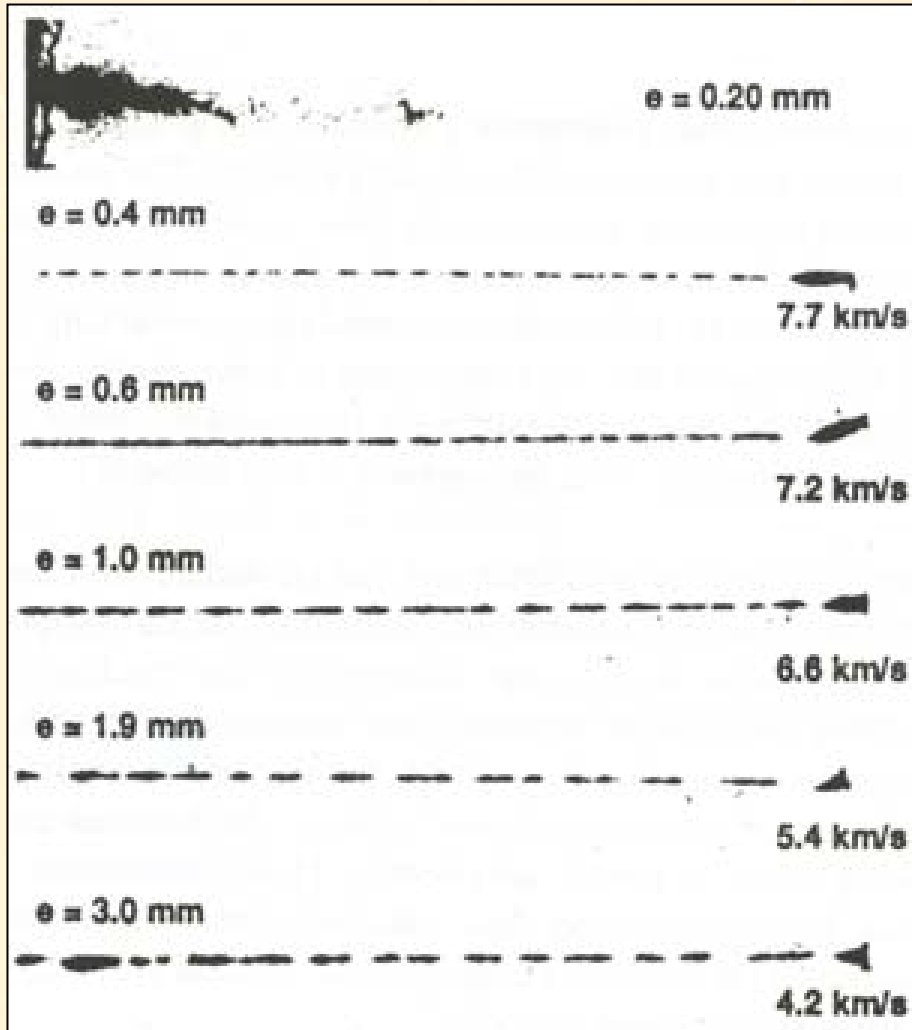
17th International Symposium on Ballistics, Midrand, South Africa, 23-27 March 1998

ABOUT VARYING SHAPED CHARGE LINER THICKNESS

Pierre Y. Chanteret, André Lichtenberger

ISL, French-German Research Institute of Saint-Louis,
BP 34 F68301 Saint-Louis, France

The influence of linear wall thickness on shaped charged jet behavior is investigated. X-ray pictures are presented of jets from 60° copper liners with thickness ranging from 0.4% to 7% of the charge diameter. **First, it is shown that under a minimal thickness, about 0.25 mm, no compact copper jet is formed.** Then, the influence of liner wall thickness on jet fragmentation is studied and a variation of the characteristic velocity difference between consecutive fragments is reported. Introducing this variation in a 1D-code allows for reproducing the jet fragmentation behavior for the whole range of liner thickness considered.



Experiments in plate cutting by shaped high explosive charges

By A.I.O. Zaid, J.B. Hawkyard and W. Johnson

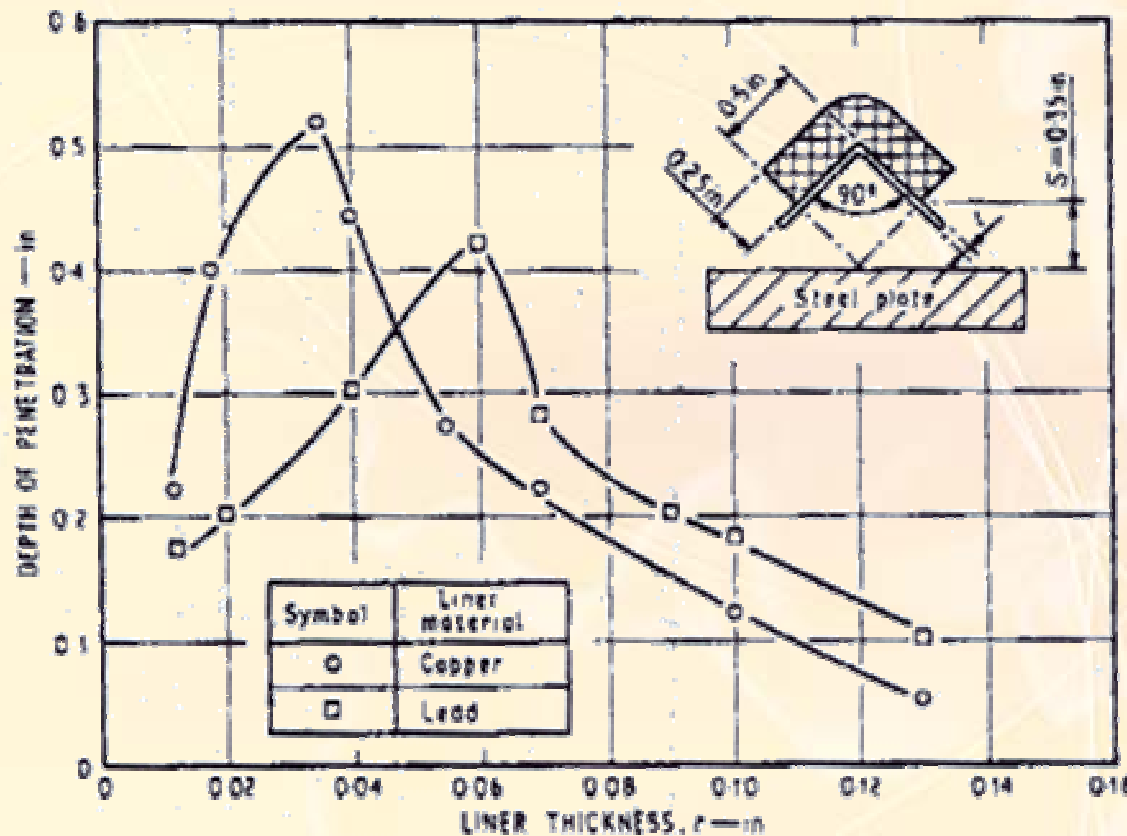
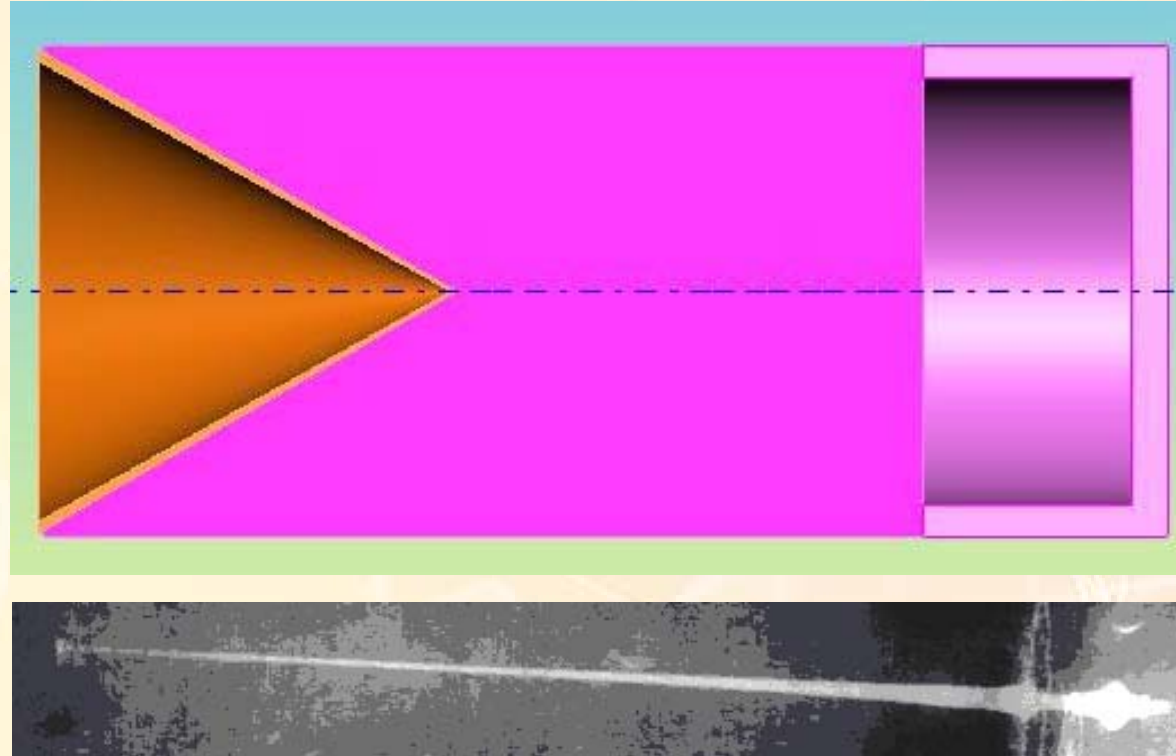
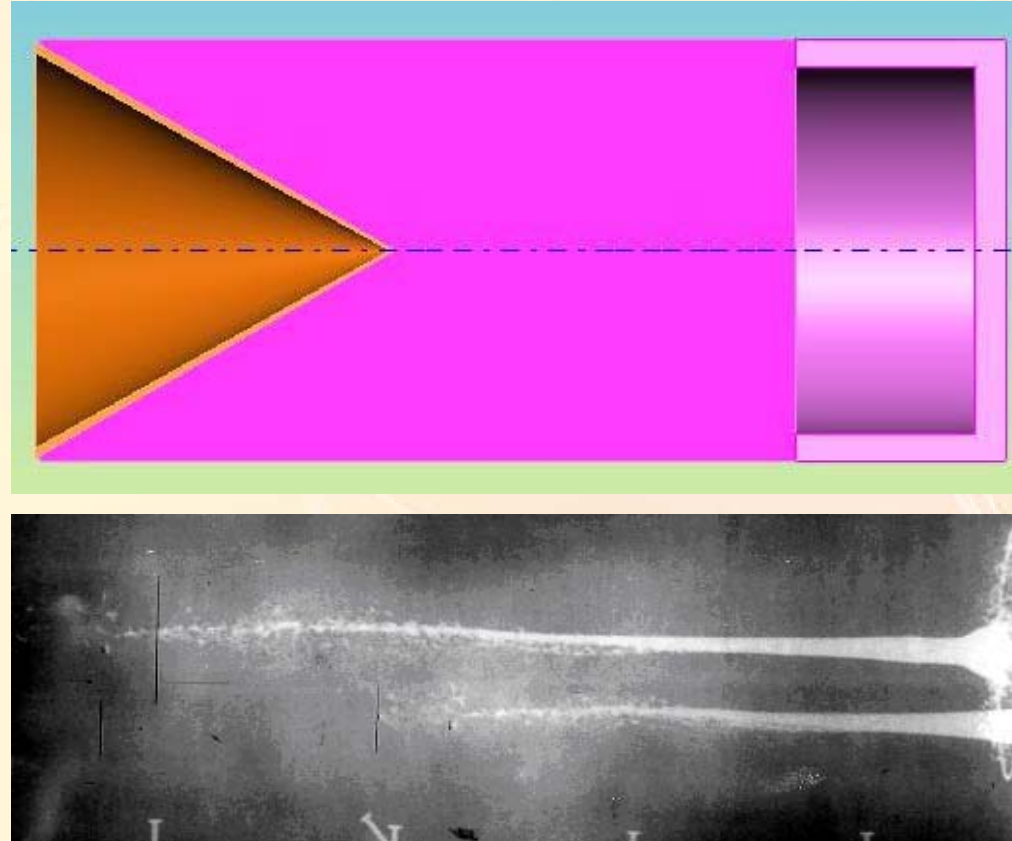


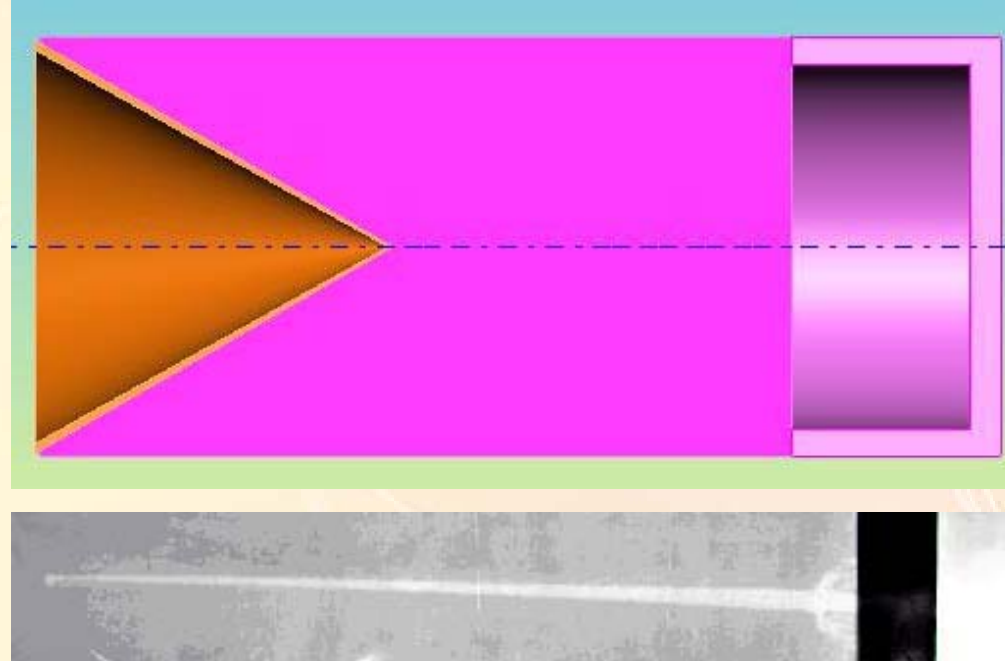
Fig. 8. Effect of liner thickness on penetration



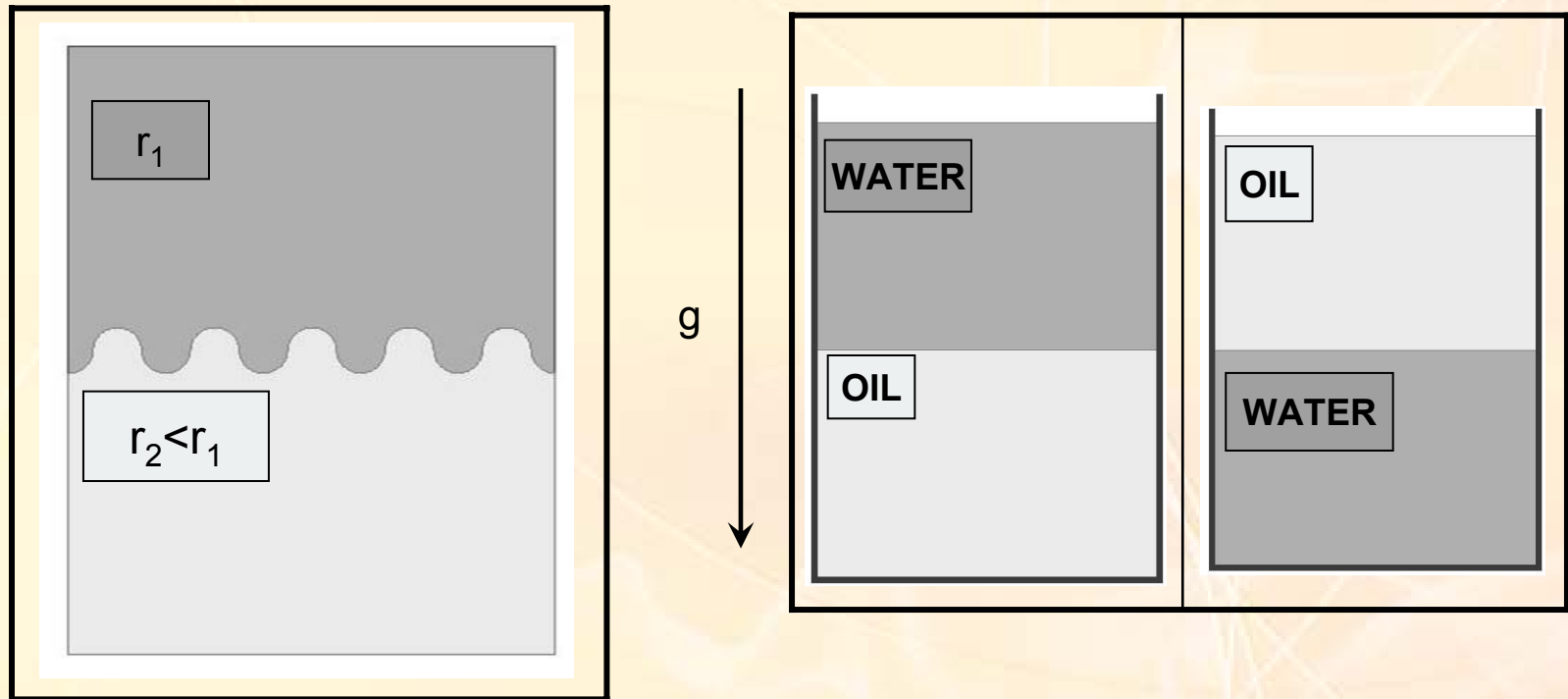
Charge configuration, using high quality explosive PBX – LX07,
based on 90% HMX and 10% Viton.



Same charge configuration with different explosives PEX01, based on 93 wt% HMX and siliconic binder and formed by injection molding into a cylindrical shape. After polymerization (curing) the hollow cone is machined to its final dimension.



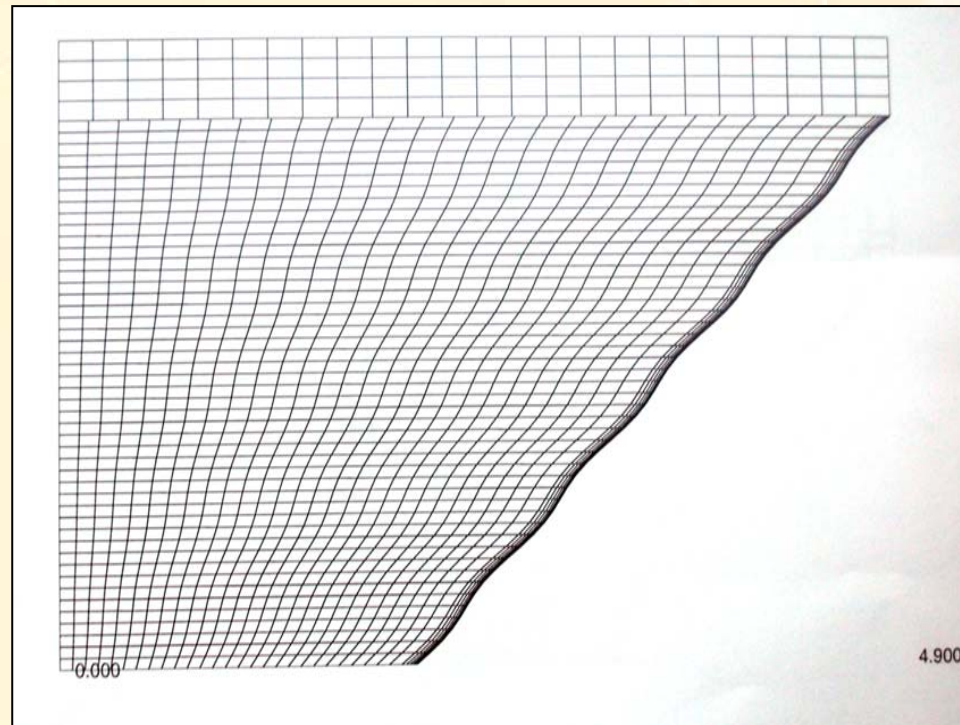
Same charge, same explosive PEX01, but this time the charge is formed by direct injection of the explosive on the liner.



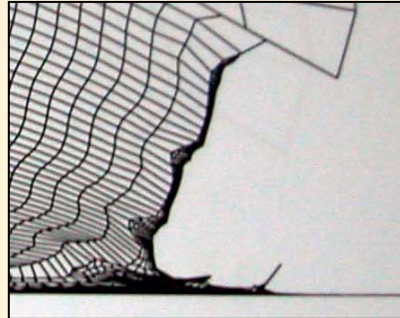
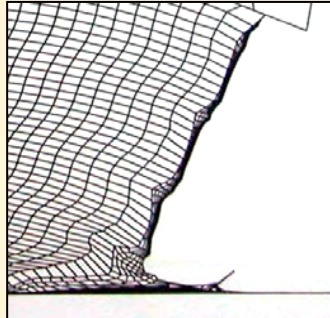
$$a = a_0 \exp \left[\left(\frac{2\pi}{\lambda} \frac{\rho_1 - \rho_2}{\rho_1 + \rho_2} g \right)^{1/2} t \right]$$

Simple demonstration of Rayleigh Taylor Instability

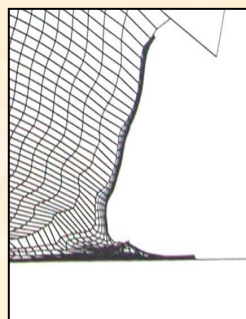
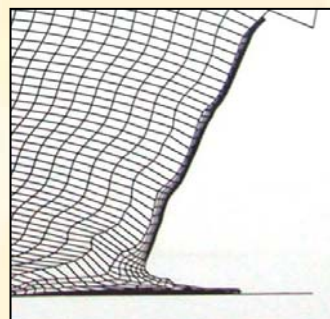
Demonstration of the relevance of the RTI
to shaped charge jet formation.



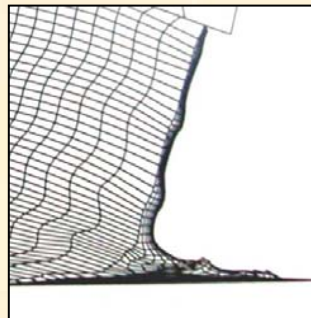
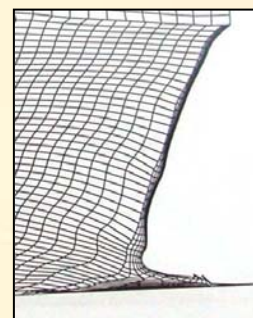
Initial grid setup with a sinusoidal liner.



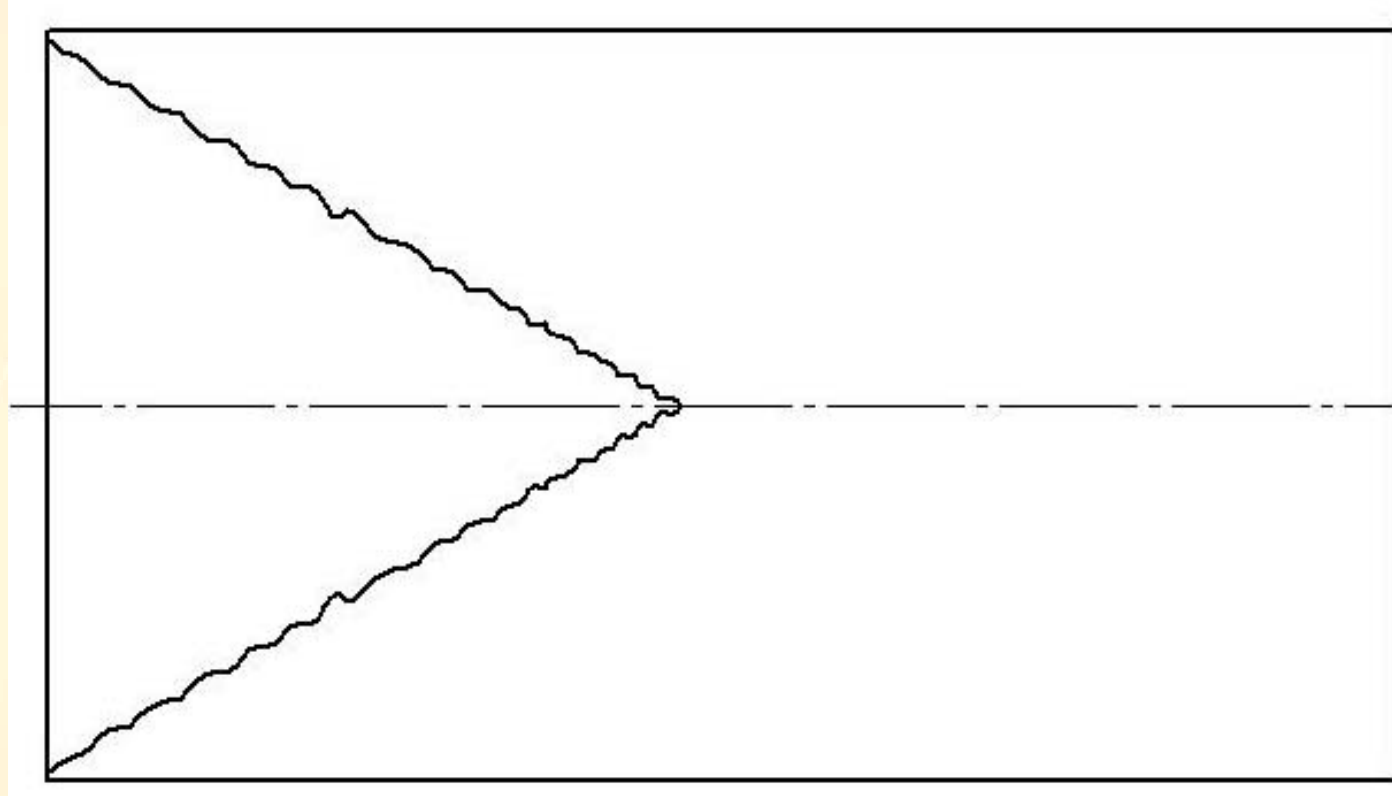
The growth of the initial grid during collapse with a liner made of copper (nominal strength).

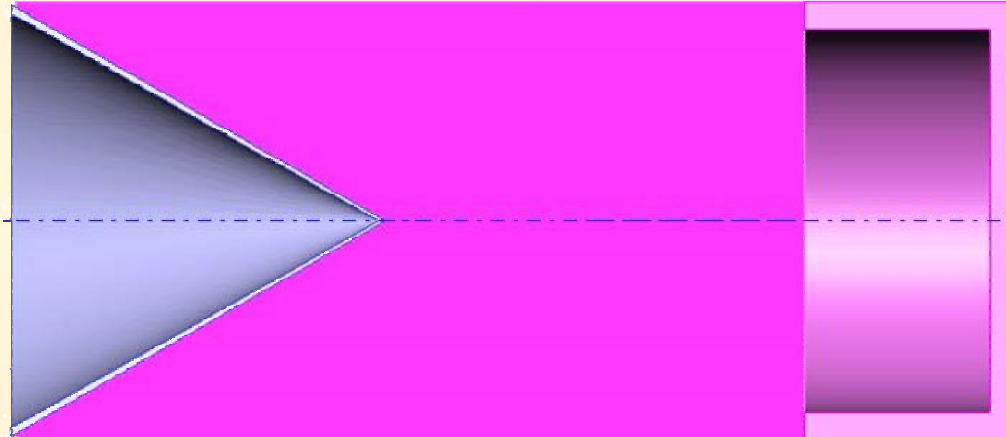


No change in shape during collapse if the simulation is performed with increased strength by a factor of 4.

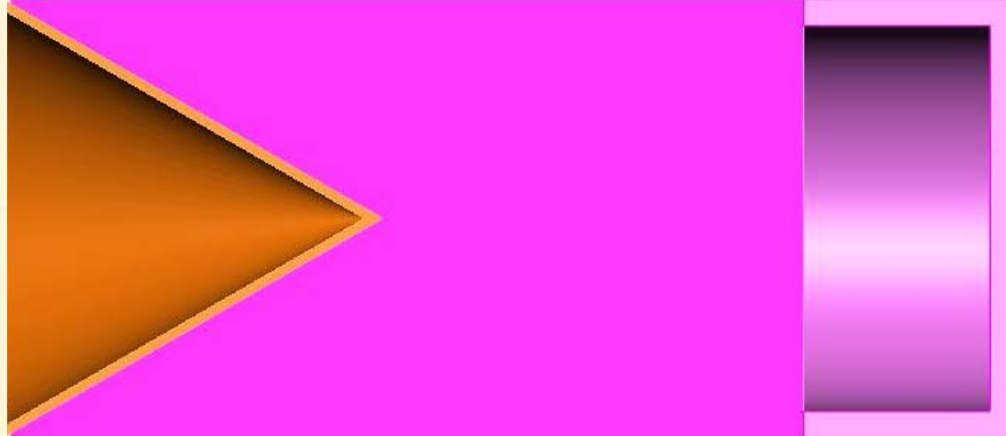


The same initial charge configuration except for the liner. This is the simulation results with aluminum liner (nominal strength). Actually, the interface between the liner and the explosive tends to be smoothed to a straight line.

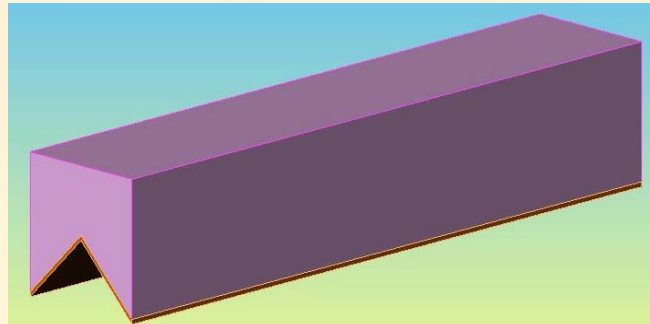




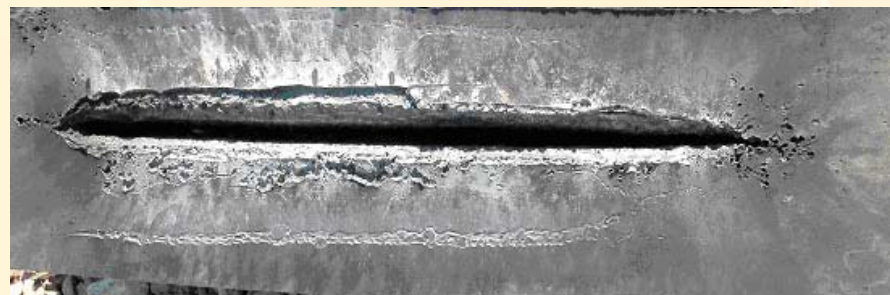
Repeating the experiment with the machined cone in the PEX01 explosives, but with Molybdenum liner.



Repeating the experiment with the machined cone in the PEX01 explosives with 2% copper liner.



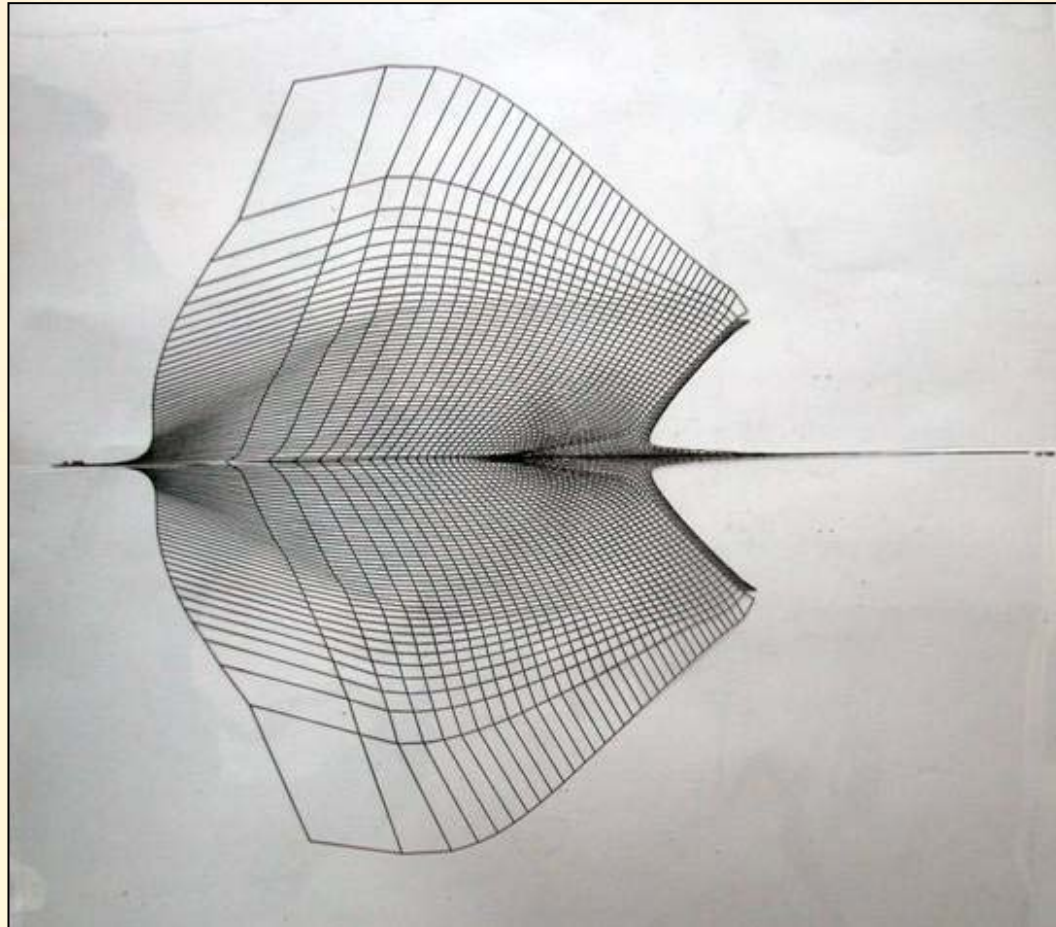
Schematic description of a linear shaped charge configuration.



The crater opening on aluminum target by a configuration with 3% CW thickness copper liner.



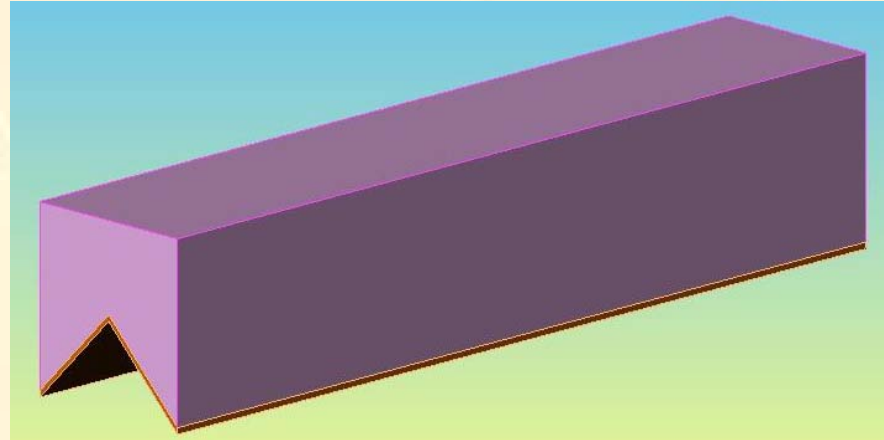
Same as above, but with a variable thickness copper liner from 1% CW near the apex to 3% CW near the base.



summary

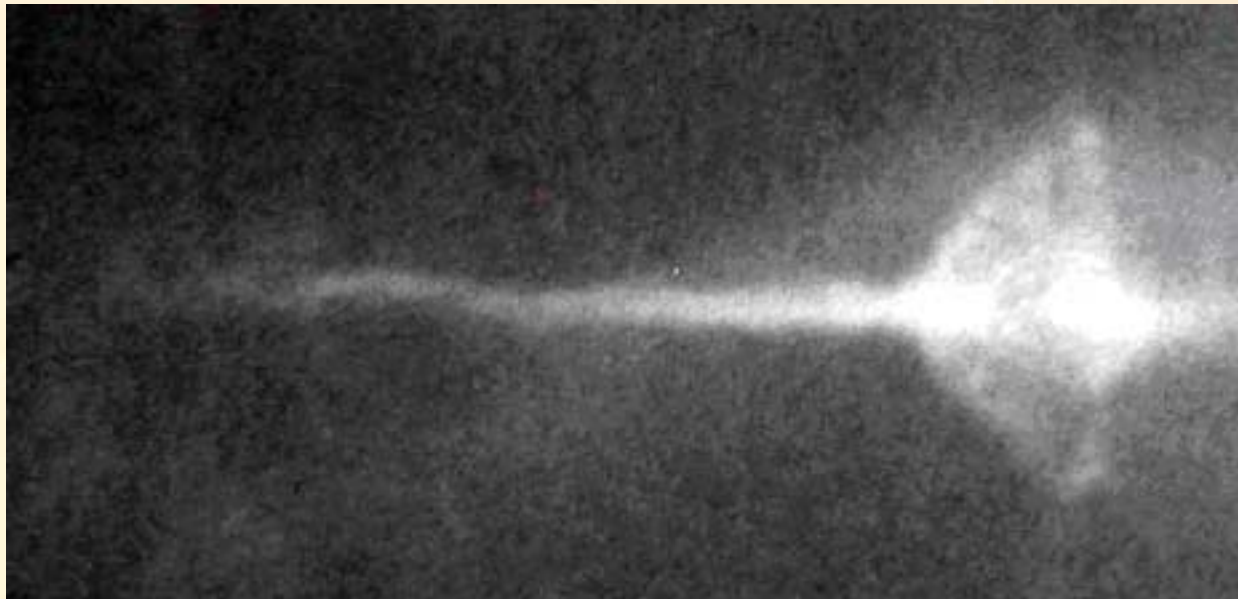
The RTI might have a destructive role in jet formation unless the charge configuration is designed beyond certain threshold limits:

- Minimum liner thickness which depends on liner density and strength.
- Explosive quality, especially near the contact surface with the liner.
- Linear charges experiments have proven to be much more sensitive to initiate instabilities. Some reasonable assumptions have been offered to explain the difference between conical and linear charges. Further investigation is needed in order to gain a conclusive understanding.

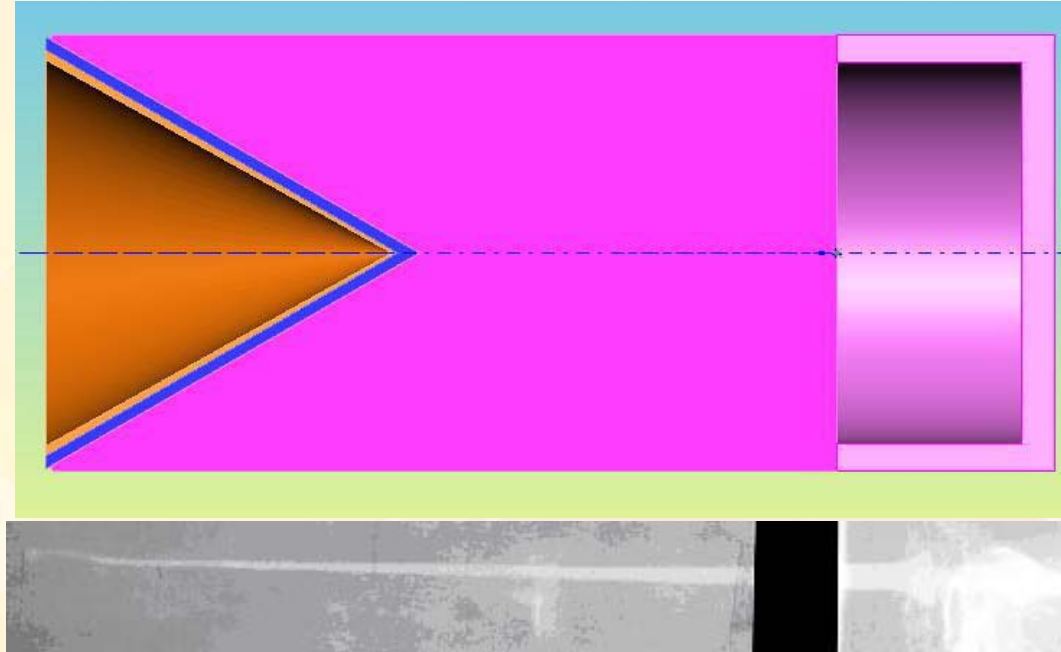


$$a = a_0 \exp \left[\left(\frac{2\pi v \sqrt{\rho_1 \rho_2}}{\lambda(\rho_1 \rho_2)} \right) t \right]$$

$$a = a_0, v = \frac{2\pi\Delta U}{\lambda} a_0 \frac{\rho_1 - \rho_2}{\rho_1 + \rho_2}$$



The charged configuration with PBX-LX07 scaled down by factor 6. Liner thickness around 0.08 mm.



Repeating the experiment with the machined cone in the PEX01 explosives, but with a thin layer of lexan (2 mm thick) inserted between the liner and the explosive.

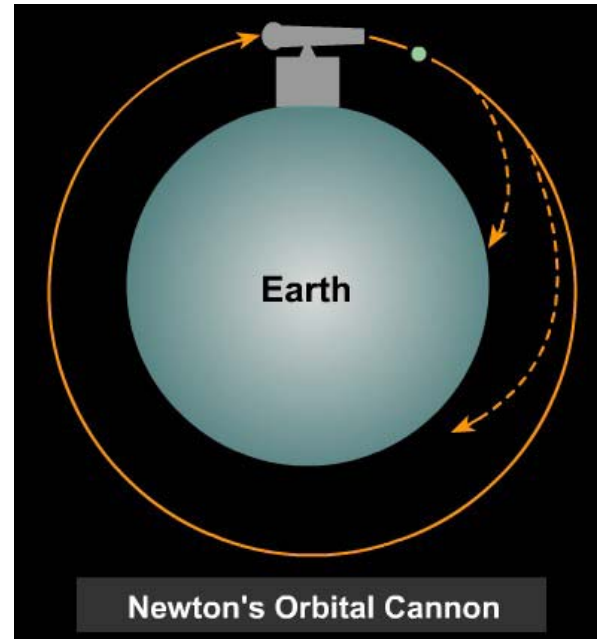
MANOR DIVISION

RAFAEL
ARMAMENT DEVELOPMENT AUTHORITY Ltd.

Dr. SIMCHA MILLER
Chief Scientist
Explosive Systems Department

P.O.B. 2250(M4), Haifa 31021, ISRAEL Tel: +972-4-8795251 Fax: +972-4-8792704
E-mail: simcham@rafael.co.il

Ballistic Launch to Space



Ed Schmidt and Mark Bundy
Army Research Laboratory
November 2005

Background

- Rocket based lift to orbit costs between \$4000 to \$14,000 per pound depending on launcher and payload
- For the Mars mission, NASA anticipates a need for large quantities of supplies and material delivered to earth orbit
- NASA is interested in the possibility of earth launch to space of acceleration tolerant payloads
 - Low Earth Orbit (LEO)
 - 500 kg payload
 - 1000-2000 kg total launch mass
- ARL asked to lead examination of selected launcher technologies:
 - Slingatron
 - Blast Wave Accelerator
 - EM Coil Gun
 - EM Rail Gun

Launch Calculations

Consider orbit of International Space Station (ISS):

- 359 km at 51.4° inclination to the equator
- Orbital velocity 7.7 km/s

Flight Body:



- 10° half angle blunted conical nose
- Base diameter, $D = 0.46$ m
- Cylindrical section, $L = 2.5 D$
- Nose radius, $r_n = 0.0575$ m
- Total flight mass, $m = 1000$ kg

Launch Calculations

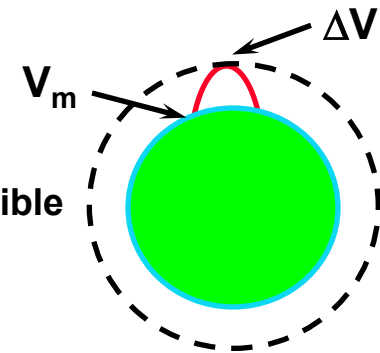
Assume:

- Projectile just reaches apogee at ISS orbit
- Newtonian flow theory applies $\Rightarrow C_D = 0.119$
- Use Rice, et al [5] to estimate velocity at exit from sensible atmosphere:

$$V_e/V_m = \exp[-C_D \rho_o A/2m\beta \sin\theta]$$

where β is the atmospheric lapse rate $= 1.1 \times 10^{-4}/m$

- 50% structural mass, 85% rocket mass fraction, $I_{sp} = 305$ s



Compute muzzle velocity, insertion velocity, and payload mass versus elevation angle for 1000 kg launch mass.

θ (deg)	10	20	30	40	50	60	70	80	90	
V_m (km/s)	13.48	7.88	5.74	4.52	3.81	3.35	3.08	2.93	2.88	
ΔV (km/s)	1.03	2.62	3.89	4.91	5.66	6.28	6.80	7.28	7.70	
m_{pl} (kg)	329	156	72.5	26.3	0.94	Propellant system mass equals or exceeds available non-structural mass				

High Altitude Research Project



HARP:

First serious attempt at gun launch to space.

Double length 16" Naval gun.

Achieved altitude of 180 km ($V_m = 2.1$ km/s) in 1966 firing at Yuma Proving Ground.

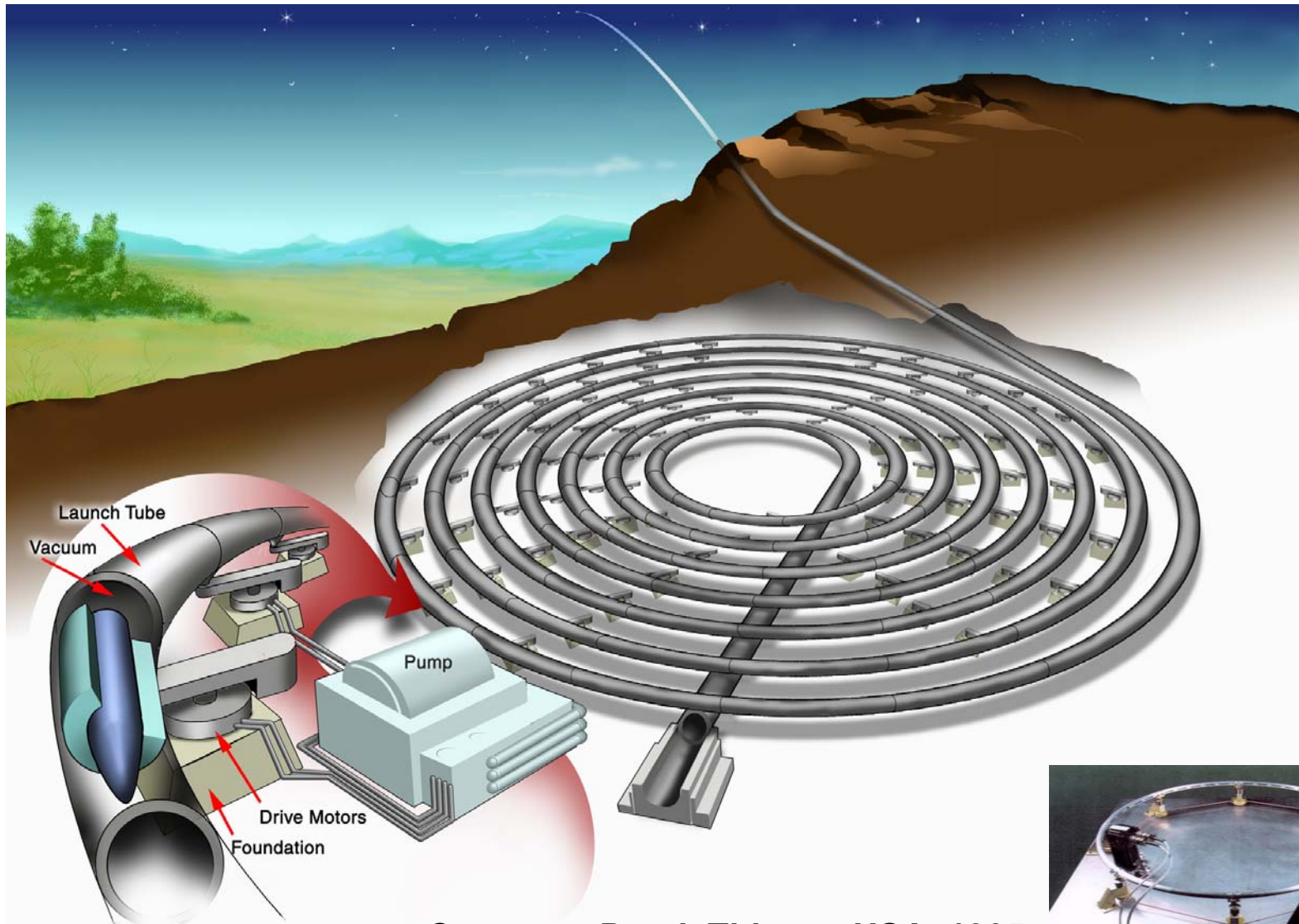
Plans underway for rocket propulsion for orbital insertion.

Project cancelled in 1967.



**Martlet 2: launch mass up to 215 kg capable of 25 kGee. Cost: \$3000 each
Launch Interval: 1 per hour**

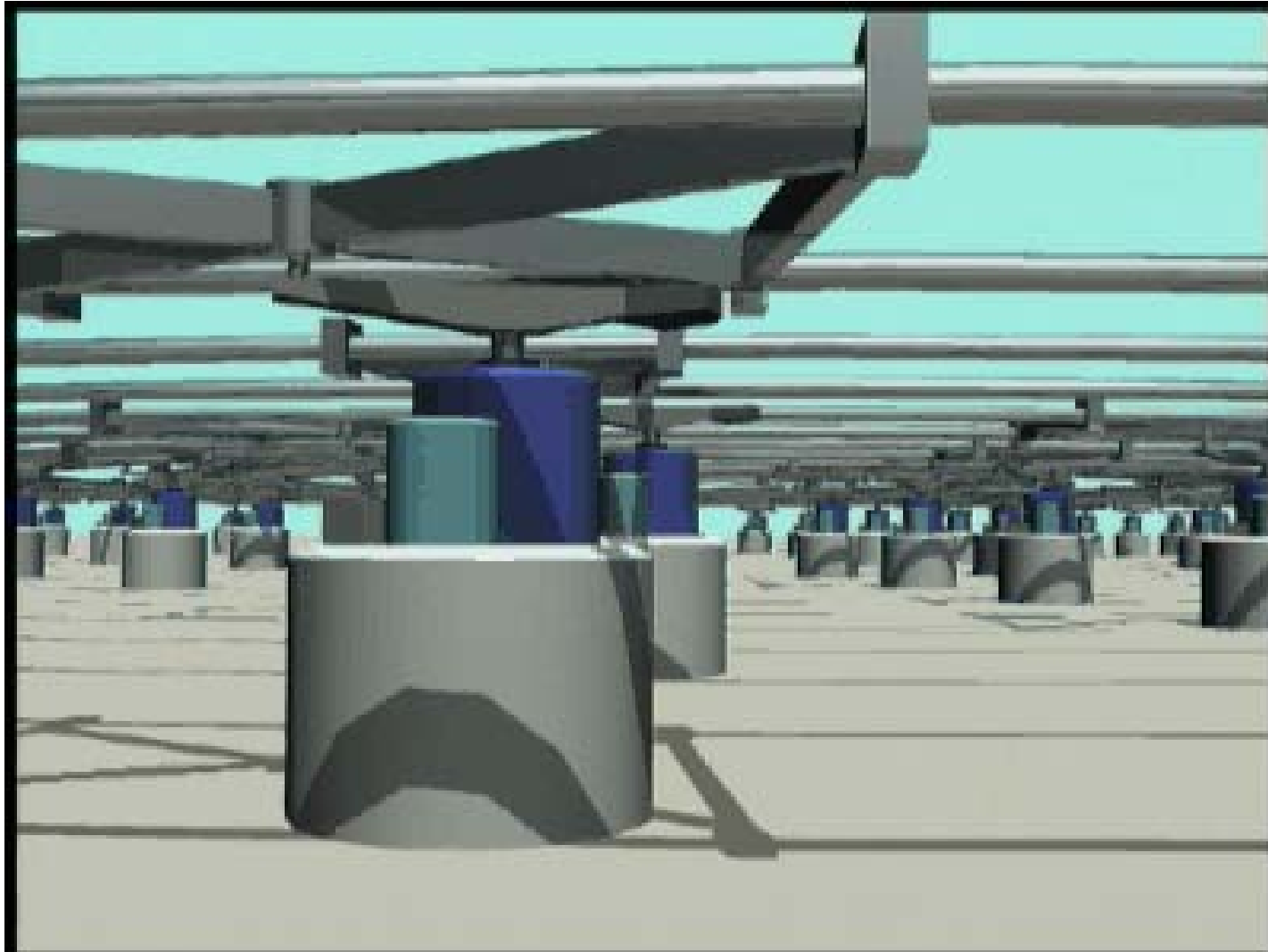
Slingatron



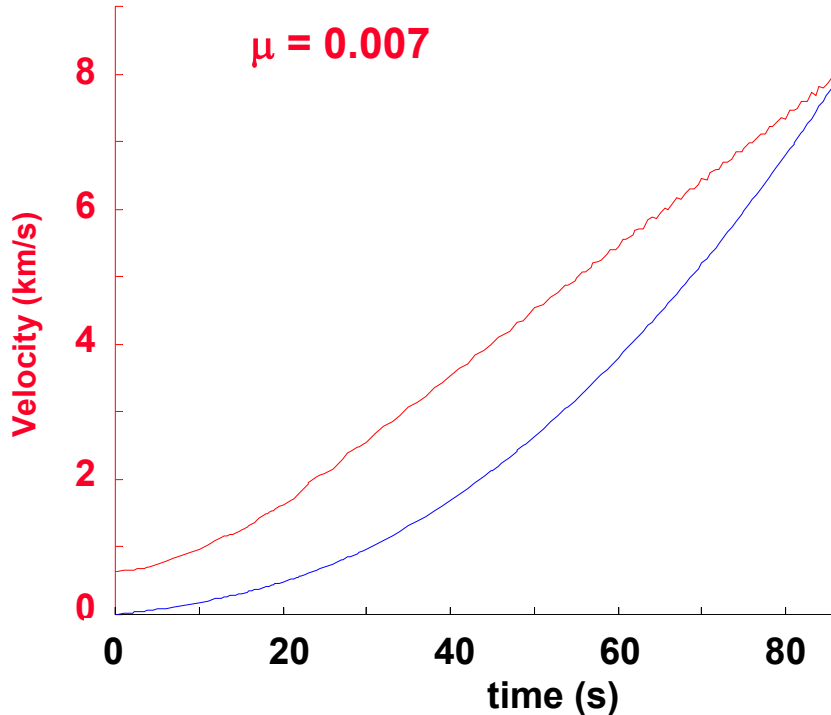
Concept: Derek Tidman, USA, 1995
Table top demo => 100 m/s



Slingatron Functioning



ARL MATLAB Simulation



ARL simulation agreed with Tidman's analysis. Slingatron can in theory accelerate a body to high velocity, but there are significant unknowns – one of which is high speed friction.

Slingatron Launcher

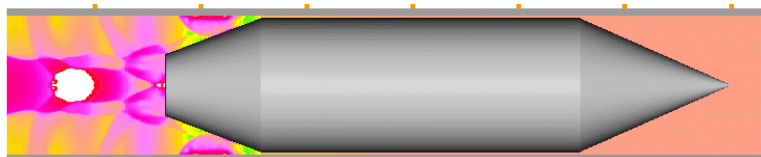
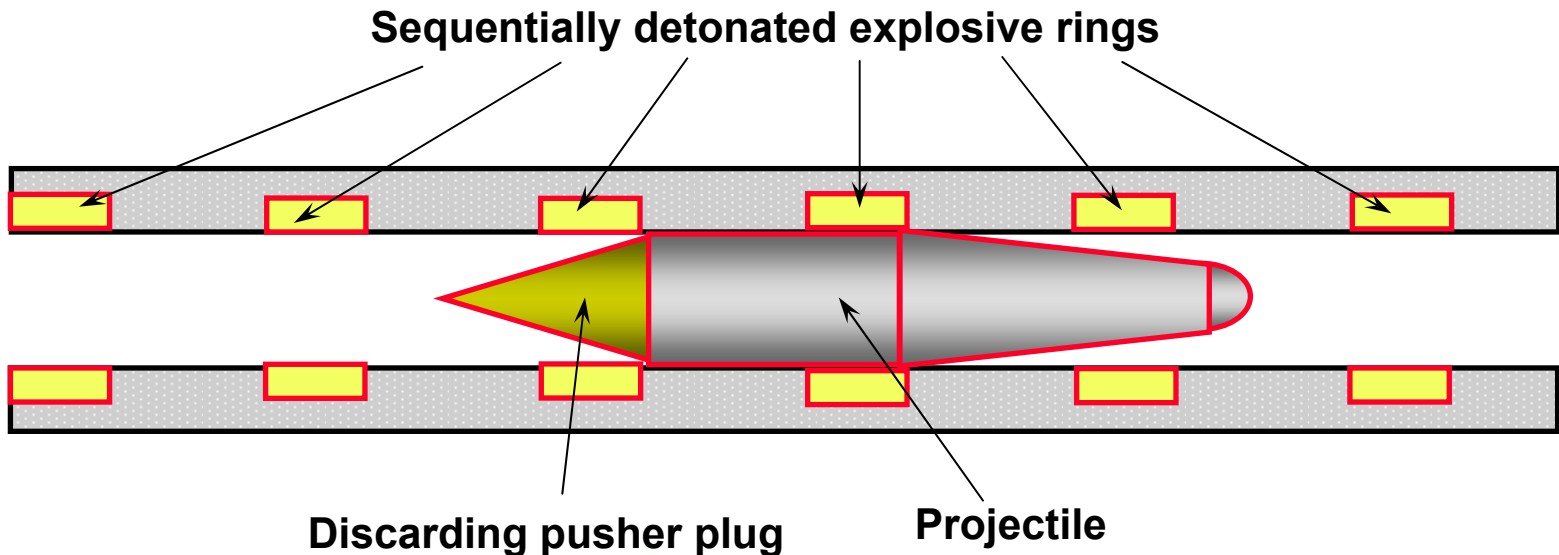
- For 1,000 kg launch mass at 8,000 m/s, a Slingatron solution:
 - Circuit Diameter = 300 m**
 - Tube Diameter = 0.4 m**
 - Tube Wall Thickness up to 0.25 m**
 - Gyration Frequency = 9 cycles/sec**
 - Weight = 20,000 tons**
- Issues:
 - Structural integrity**
 - Friction and surface wear**
 - In-Bore stability**
 - Fabrication of curved guide tube**
 - Drive and support system design integrity**
 - Synchronization of multiple drives**
 - Power to bring to speed and maintain during firing**
 - Reacting the acceleration and centrifugal recoil load**

Blast Wave Accelerator



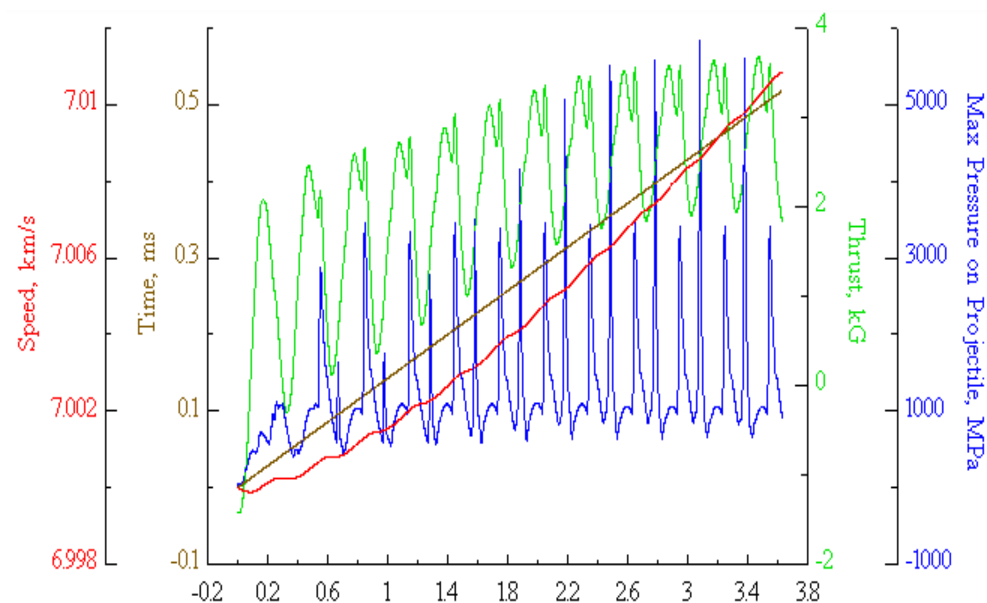
Concept: T Bakirov and V. Mitrofanov, USSR, 1976

Blast Wave Accelerator Concept



CFD calculation of D. Wilson.

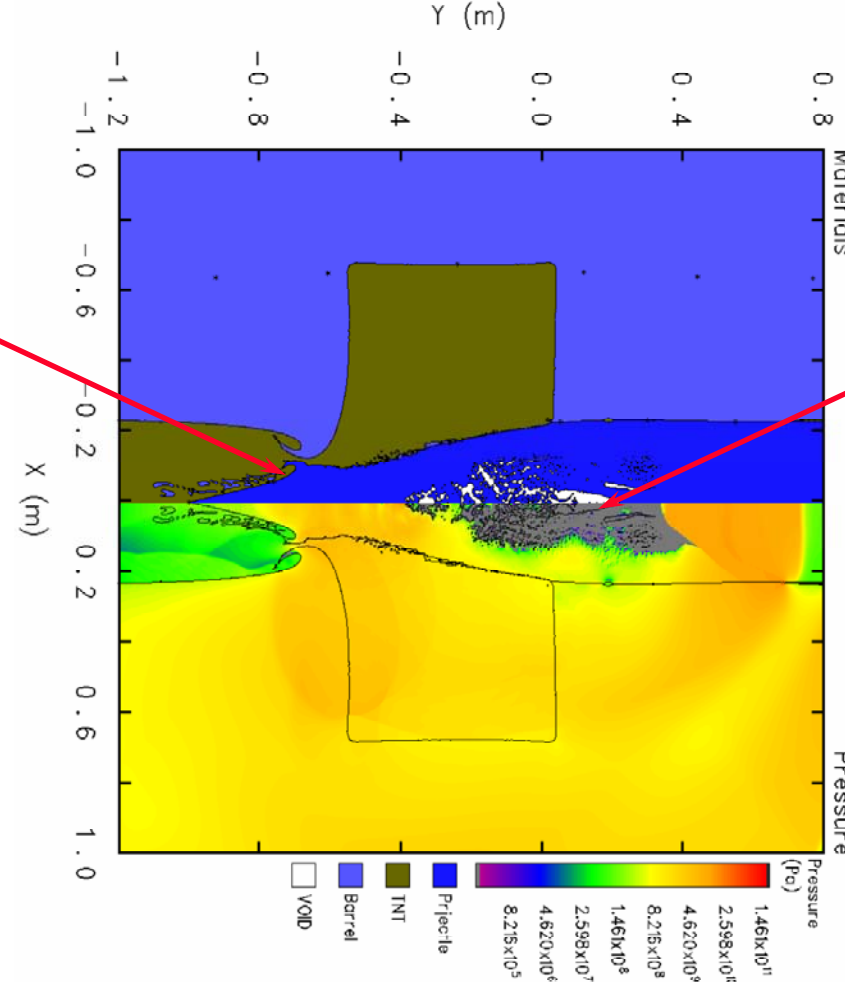
ARL calculations in agreement.



ARL CTH Results

Surface
Deformation

Internal
Cracking



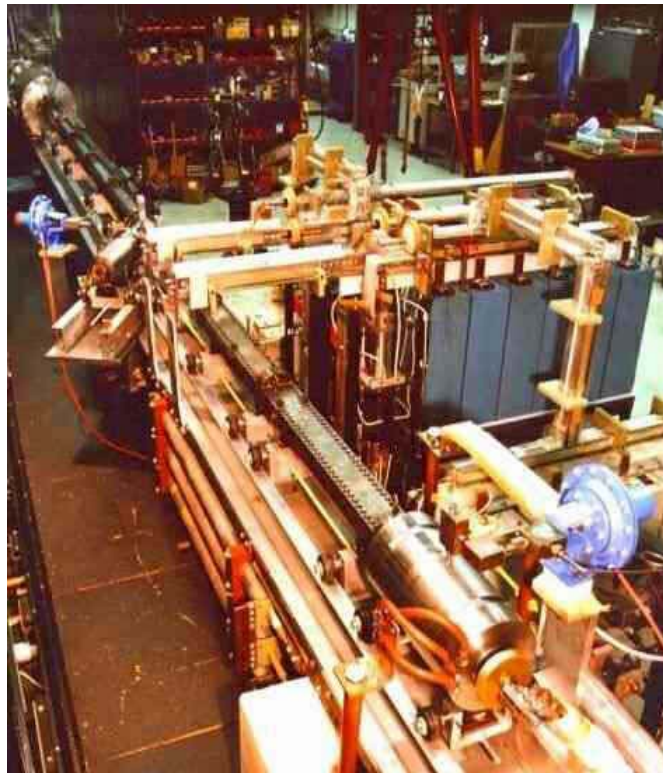
Simulations showed structural damage to mild steel projectile.

Blast Wave Launcher

- For 1,000 kg launch mass at 8,000 m/s:
 Charge mass per Stage = 10 kg
 Number of Stages = 2870
 Gun Length = 861 m
- Issues:
 Projectile integrity
 Launcher integrity (repetitive firings)
 Timing of sequential detonation
 Explosive detonation uniformity
 In-bore stability
 Detonation of 30,000 kg of explosive

Electromagnetic Guns

Sandia Electromagnetic Coilgun



Coilgun has launched 230 g to 1000 m/s

Greenfarm Electromagnetic Railgun

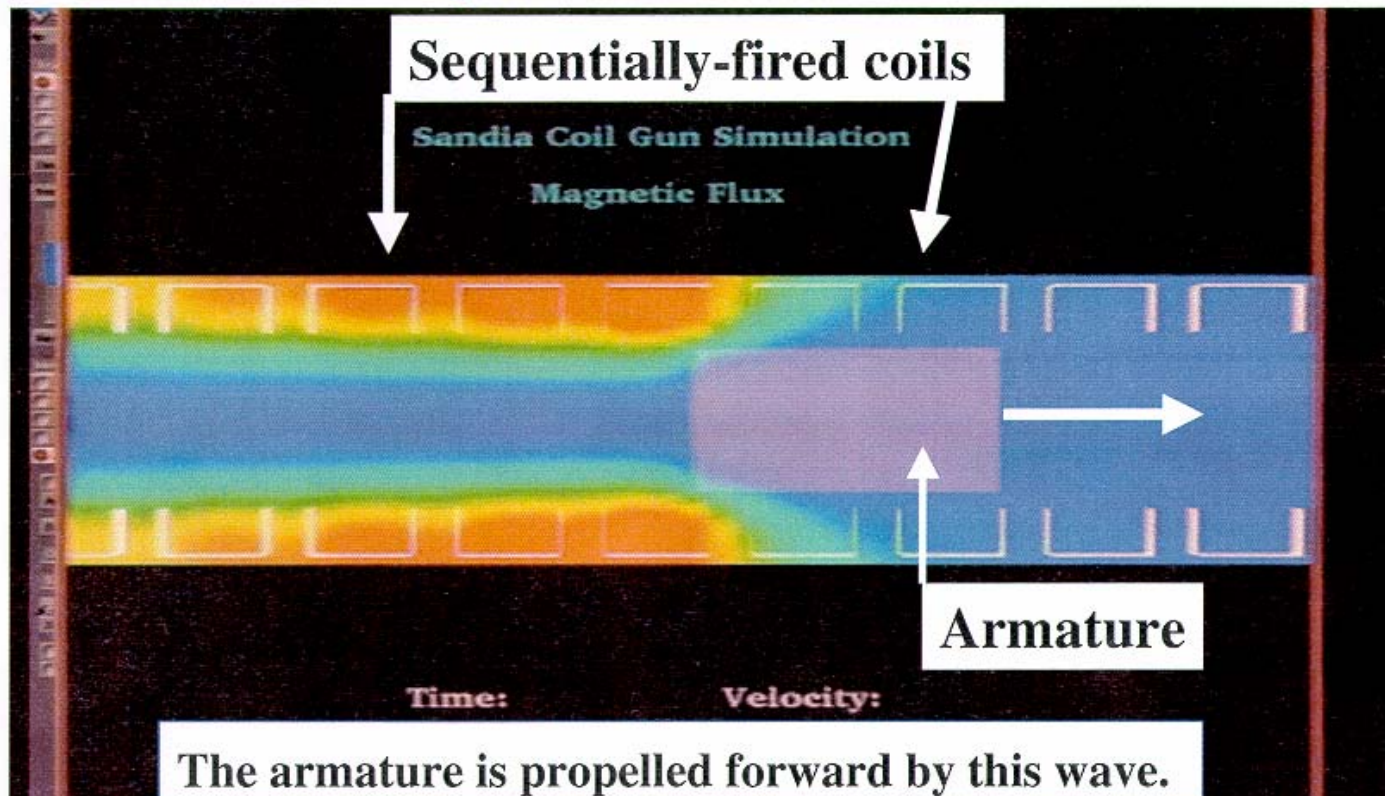


Railguns have launched ~2 kg to 3000 m/s (1 g to 7000⁺ m/s)

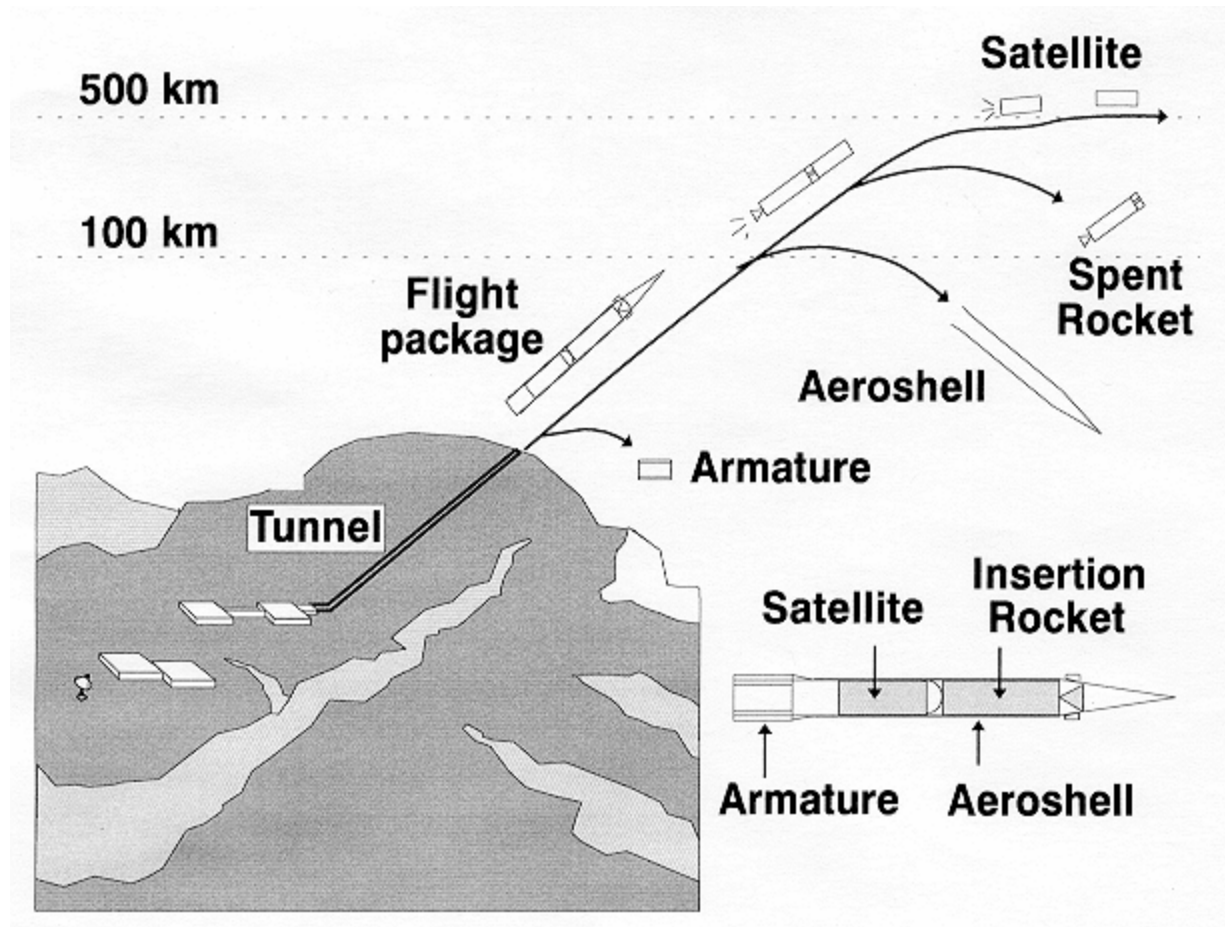
EM Coilgun

A magnetic travelling wave is created by synchronized sequential switching of individual coils.

Strong centering force “levitates” projectile for minimal wall contact



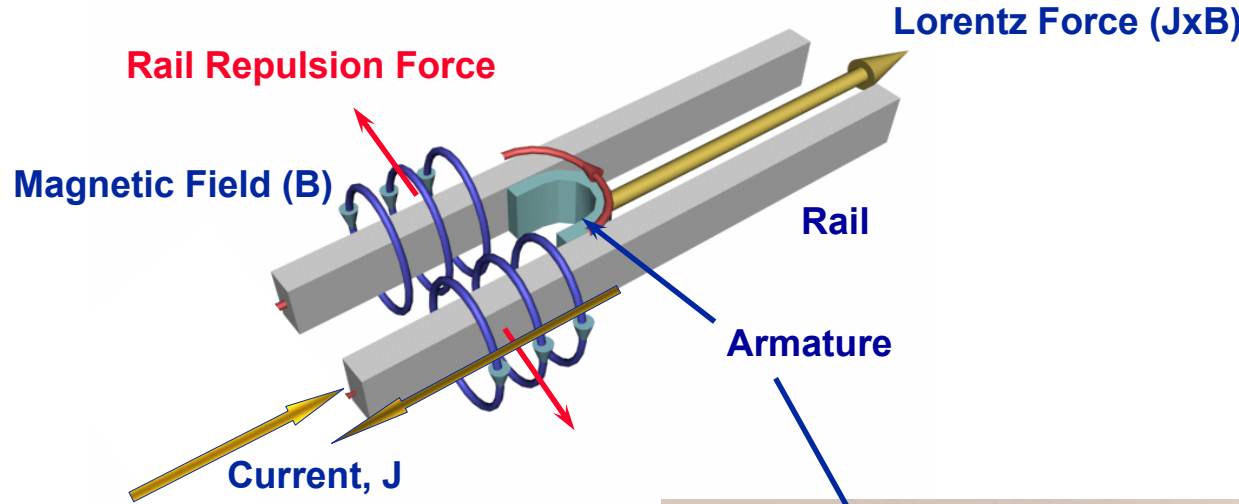
Sandia Coilgun Concept



Coilgun Launcher

- For 837 kg launch mass at 7,000 m/s:
 - Launcher Length = 400 m**
 - Tube Diameter = 1.0 m**
- Issues:
 - Structural integrity of projectile and launcher**
 - Pulsed power supply**
 - Switching**
 - In-bore stability of levitating projectile**

EM Railgun



For velocity > 3 km/s a plasma armature is used.

Firing similar to coilgun – near equator, at high altitude, and from an evacuated launch tube.



Railgun Launcher

- For 1,250 kg launch mass at 7,500 m/s:
 Launcher Length = 1600 m
 Tube Diameter = 1.1 m
- Issues:
 Structural integrity projectile and launcher
 Rail life
 Pulsed power supply
 Switching
 Plasma armature performance

Summary

Comparison of launchers:

	V_m (m/s)	M_{proj} (kg)	E_m (GJ)	L_{tube} (m)	A_{max} (kG)
Slingatron	8000	1000	32	$D = 300$ m	43
BWA	8000	1000	32	861	55
Coil Gun	7000	837	21	400	7
Railgun	7500	1250	35	1600	2

Conclusions:

- Achieving an 8 km/s muzzle velocity did not violate any laws of physics
- All had serious engineering and materials issues
- Significant research is required
- Facilitation costs would be high
- All are high risk



Caseless Ammunition and Advances in the Characterization of High Ignition Temperature Propellant (HITP)

Erin K. Hardmeyer

Armaments Engineering and Technology Center
US Army Armament Research Development Engineering Center

Ben Ashcroft

*Alliant Technical Systems
Thiokol Propulsion*

NDIA 22nd International Symposium on Ballistics
November 14-18, 2005
Vancouver BC, Canada



St. Marks Powder
A GENERAL DYNAMICS COMPANY





Outline

- Objective
- Background
- Overall Program Requirements
- Advantages
- Technical Approach
- Status
- Summary
- Future Plans



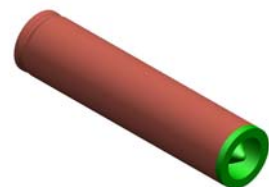
St. Marks Powder
A GENERAL DYNAMICS COMPANY





Caseless Program Objectives

- Characterize the HITP
- Demonstrate a function and production capability
- Identify & address technical challenges/potential risk areas
- Deliver prototype Caseless ammunition for ballistic demonstration in support of the Lightweight Small Arms Technologies (LSAT) Defense Technology Objective
 - 5.56mm cartridge configuration
- Transfer technology to industry



St. Marks Powder
A GENERAL DYNAMICS COMPANY





Background

- Original work performed under the Advanced Combat Rifle (ACR) Program
- Technology Development funded by US (ARDEC) and Germany to Heckler & Koch(H&K)/Dynamit Nobel(DNAG)
- Successful Demonstration of a Caseless Ammunition Rifle System
- Technology Licensed & Transferred to the US at ARDEC

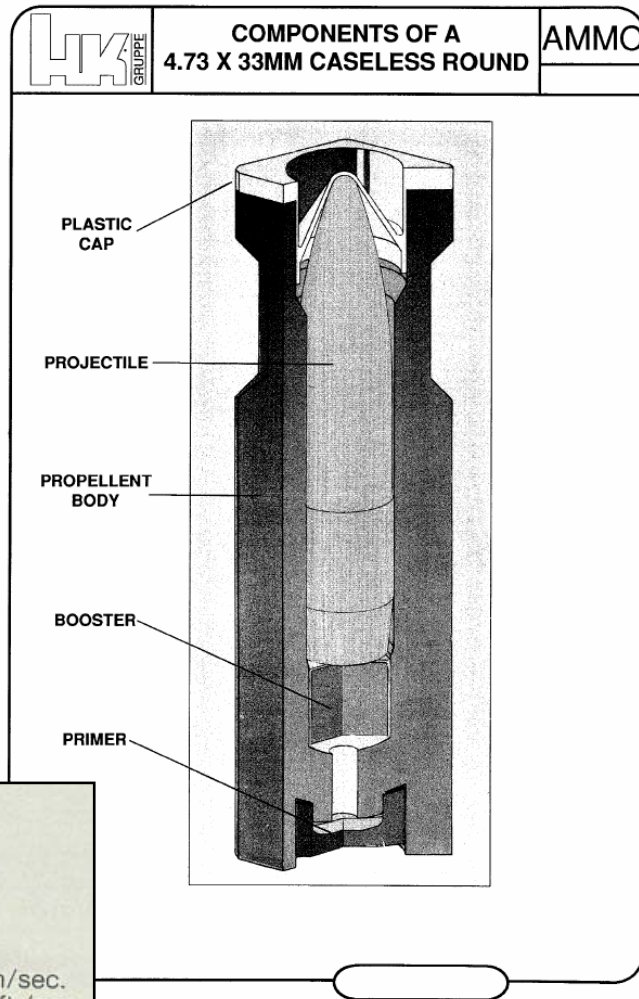
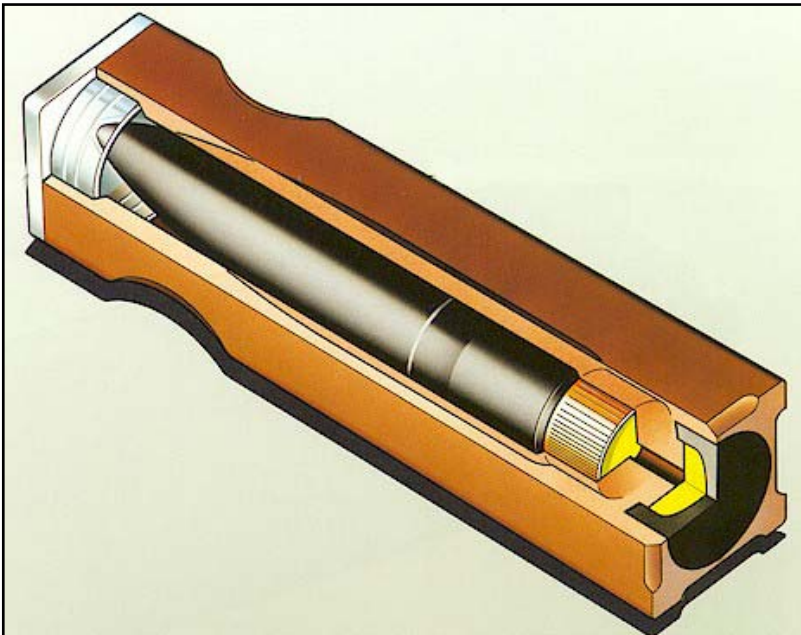


St. Marks Powder
A GENERAL DYNAMICS COMPANY

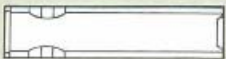




G-11 Open Source Data



Caseless ammunition



Length
Cross-section
Total weight
Projectile weight

33 mm/1.29 in.
8 x 8 mm/0.32 in.
5.20 g/0.18 oz.
3.25 g/0.12 oz.

Ignition
Mean gas pressure
Muzzle velocity V_0

mechanical
3850 bar
approx. 930 m/sec.
3051 ft./sec.



Overall Program Requirements

Threshold requirements

- 25% Decrease in ammunition weight
- Same lethality as the 5.56mm M855 cartridge
- Environmentally friendly alternatives for processing
- Low life-cycle costs

Desired requirements

- Additional decrease in ammunition weight
- Increased lethality over the 5.56mm M855 cartridge
- Same cost/round as current 5.56mm M855 ammunition



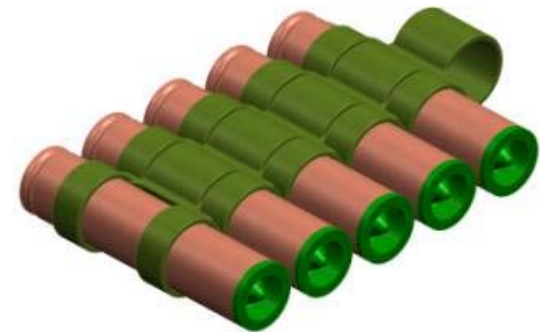
St. Marks Powder
A GENERAL DYNAMICS COMPANY





Why Caseless Ammunition?

- Lightweight
 - Force Multiplier
 - Decreased Logistics Burden
- High Ignition Temperature Propellant (HITP) Provides Improved Propellant Characteristics & Energetic Behavior
- Technology with other potential applications



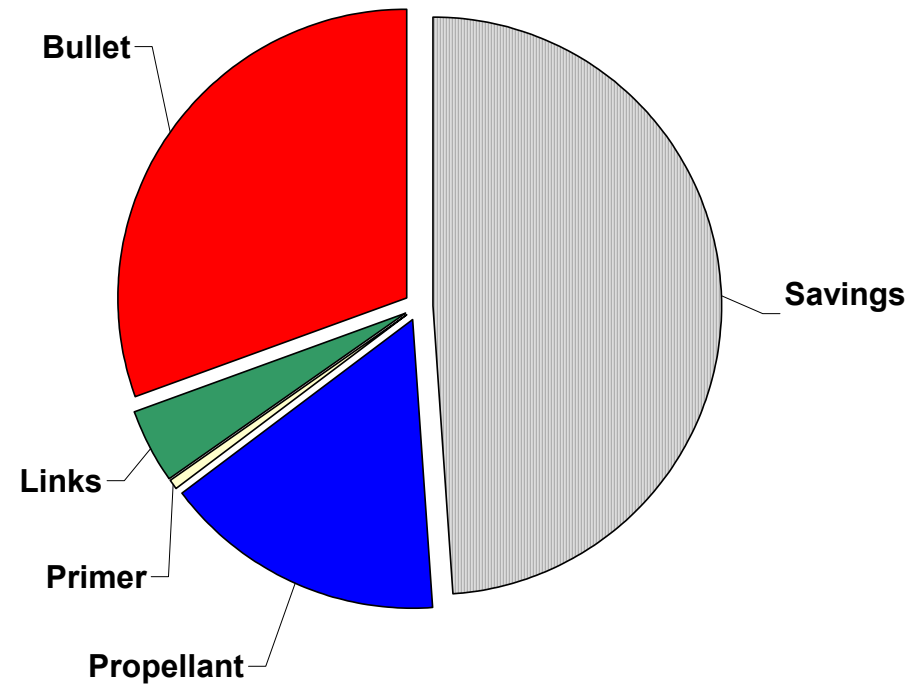
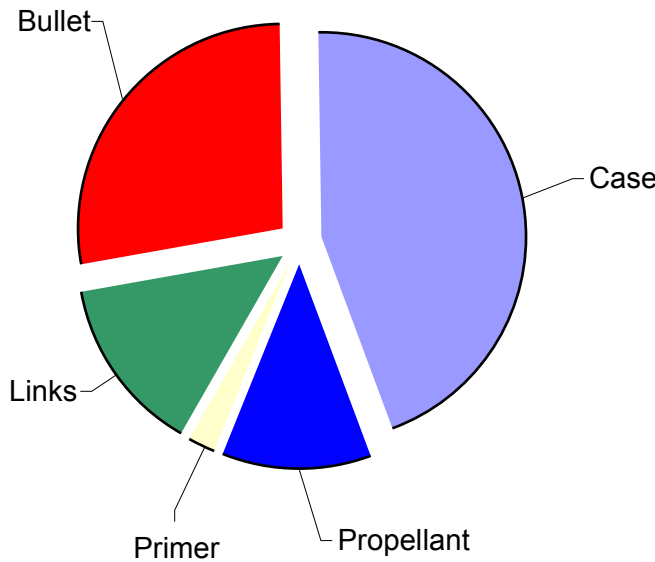
St. Marks Powder
A GENERAL DYNAMICS COMPANY





Weight Reduction Potential

- The brass cases account for 50 % of total ammunition weight!
- Current Ammo Weight (600 rds): 20.8 lbs
- Target Ammo Weight (600 rds): 10.2 lbs \approx 50% Weight Reduction





Why Use an HITP?

- Advantages of Brass Casing
 - Barrel & chamber temperature:
 - Brass is a heat sink that is discharged with each round fired
 - Brass has a long history in small caliber ammunition
 - Brass provides structural strength to ammunition
 - Brass provides gas seal in weapon
- **Advantages of HITP**
 - Weight savings with elimination of the brass case
 - Potential for high firing rates with the elimination of the case ejection cycle
 - High thermal stability over typical ball powder
 - Structural integrity over a wide temperature range



St. Marks Powder
A GENERAL DYNAMICS COMPANY





Initial Caseless Development

ARDEC



St. Marks Powder
A GENERAL DYNAMICS COMPANY





Caseless Program Status

- **Overall ARDEC In-house Progress**
- HITP formulation verified by ARDEC/ATK
- Viable material sources identified
- Producibility demonstrated
 - Several hundred rounds have been produced from lab-scale propellant mixes
- Conducted three ballistic firings
- Continue manufacturing processes and prototyping



St. Marks Powder
A GENERAL DYNAMICS COMPANY





Caseless Program Status

- Conducted three ballistic firings in Mann Barrel at Armament Technology Facility at ARDEC
- Test Firing I**
 - Five Shots
 - Chamber Pressure (8190-11314 psi)
 - Muzzle Velocity (589-1204 fps)
- Test Firing II** (Addition of Booster Charge)
 - 12 Shots
 - Chamber Pressure (14372-62225 psi)
 - Muzzle Velocity (1489-2795 fps)
- Test Firing III**
 - 14 Shots
 - Chamber Pressure (15992-24579 psi)
 - Muzzle Velocity (1000-1686 fps)



St. Marks Powder
A GENERAL DYNAMICS COMPANY





Caseless Program Status

- **Material Characterization**
- Cooperative effort between ARDEC & ATK
- Original & New HTP
 - Chemical Analysis
 - Density
 - Thermal Properties/Ignition Temperature
 - Heat of Explosion



St. Marks Powder
A GENERAL DYNAMICS COMPANY

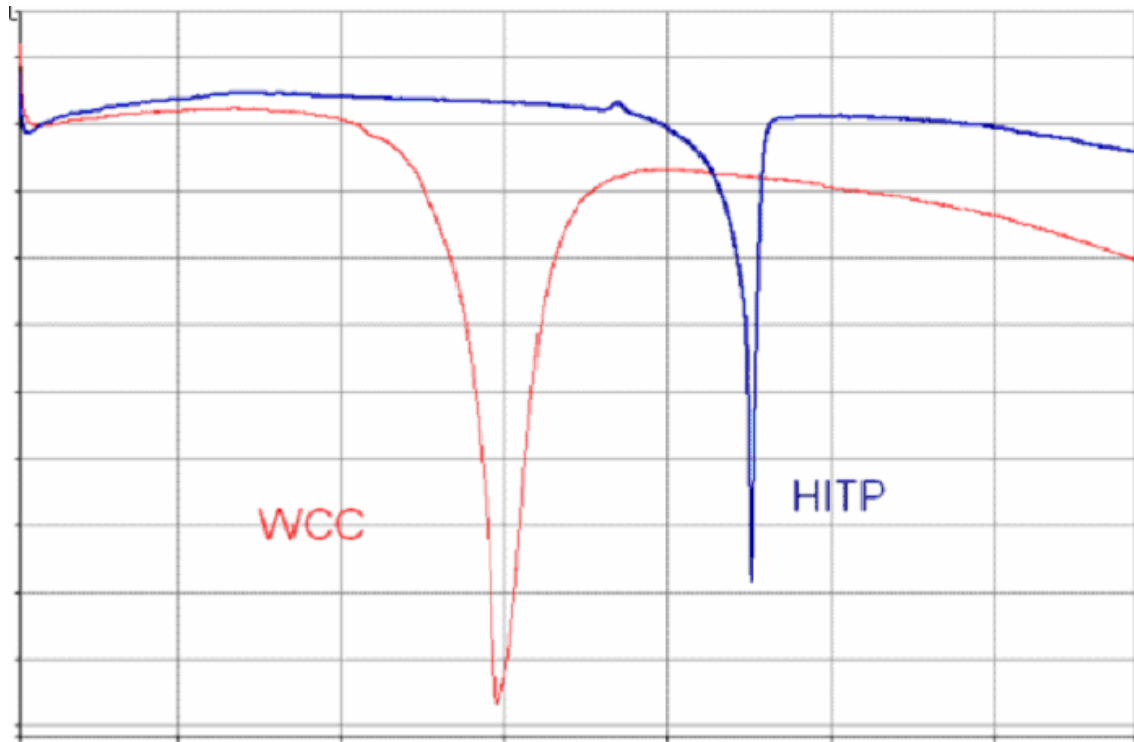




Caseless Program Status

- **HITP Characterization**

- Differential Scanning Calorimetry - Thermal Properties of HITP in comparison to Nitrocellulose based Propellant



St. Marks Powder
A GENERAL DYNAMICS COMPANY





Formulation & Process Development

ATK Thiokol



St. Marks Powder
A GENERAL DYNAMICS COMPANY





Caseless Program Status

- **Overall Formulation & Process Development Progress**
- HTP Characterization
 - Formulation verified
- Material sources identified - CONUS and OCONUS
- Raw materials procured or synthesized
- Compatibilities verified between ingredients
- Hazard Analysis
- HTP Mixing & Processing
 - Identifying manufacturing processes & limitations
- Closed Bomb Testing and Modeling



St. Marks Powder
A GENERAL DYNAMICS COMPANY





Caseless Program Status

- Hazard Analysis
- Safety Data Determined
 - Propellant ingredients
 - HITP

ABL Impact (cm)	ABL Friction (lbs @ fps)	TC ESD (J)
>80	>800 @ 8	>8

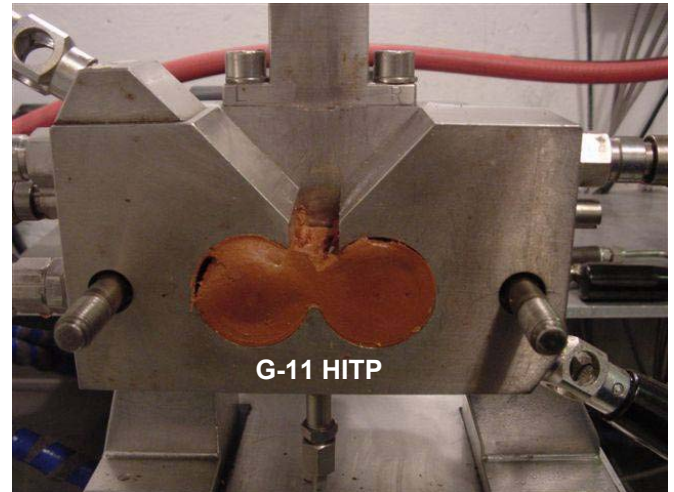
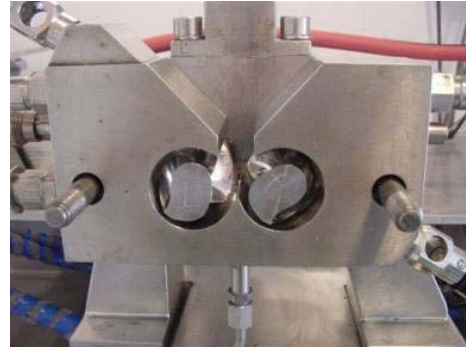


Caseless Program Status

- **HITP Characterization- Mixing**
- Four HITP hand mixes produced
 - Safety testing/Lab analysis
 - Original HITP re-processed for lessons-learned
 - Multiple sub-scale HITP mixes in progress-Design of Experiment (DOE)



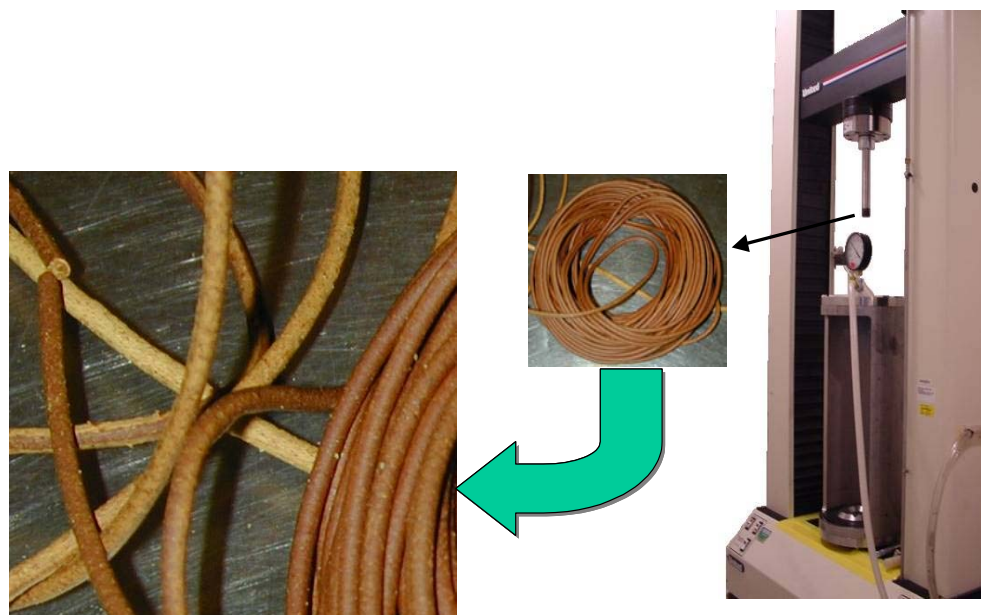
Rheochord Viscometer ideal for sub-scale
(≈100-gr) mixing





Caseless Program Status

- **HITP Processing**
 - HITP Rheology and molding studies
 - Material characteristics and processability testing with Capillary Rheometer



Capillary Rheometer



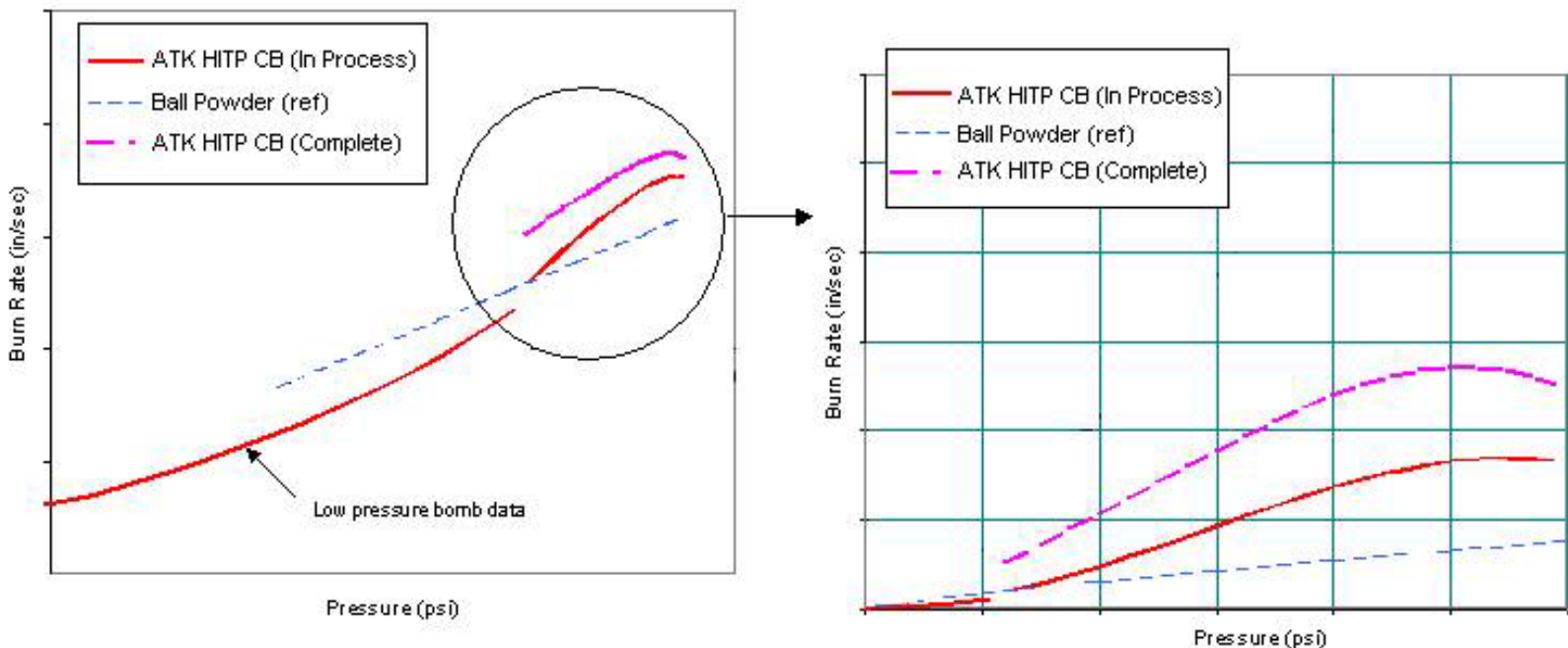
St. Marks Powder
A GENERAL DYNAMICS COMPANY





Caseless Program Status

- **HITP Testing**
 - Low & High Pressure Bomb analysis

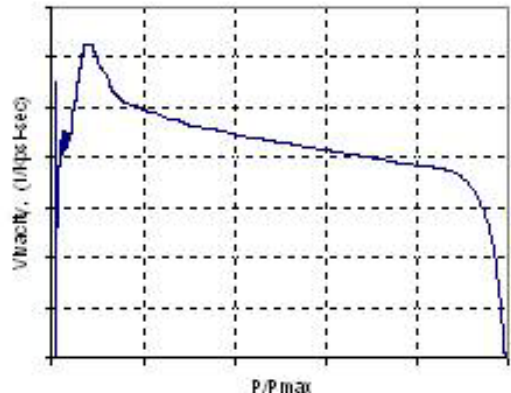




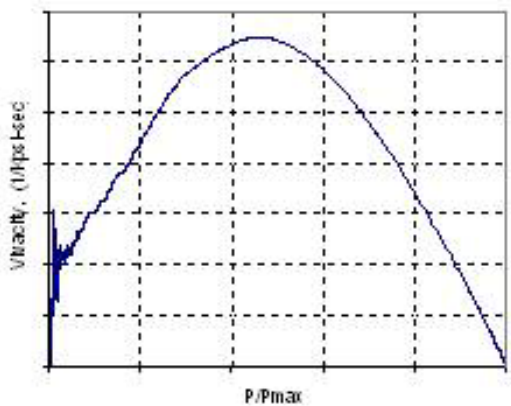
Caseless Program Status

- **HITP Modeling**

- Initial closed bomb testing gave repeatable but unexpected results
 - The CB data from the HITP tests show the vivacity plots to be inconsistent with regressive burnback
 - Grains did not appear to burn with the expected type form function
 - Additional testing is planned to understand this issue



Typical Regressive Vivacity Plot



Obtained Progressive Vivacity Plot



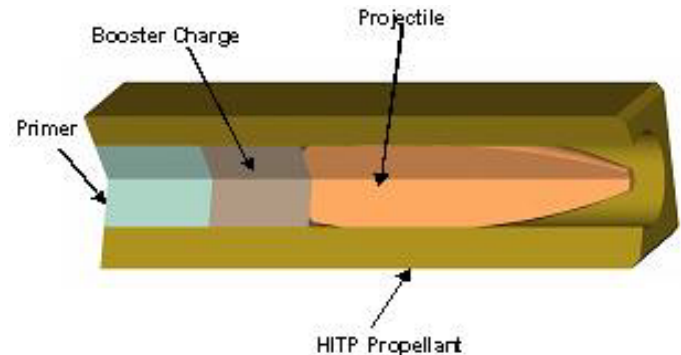
St. Marks Powder
A GENERAL DYNAMICS COMPANY





Caseless Program Status

- **HITP Modeling** – cont
 - JHU/APL Status
 - ACR 1B sequence recreated
 - Modeled as single perf grain
 - HITP burn data
 - Reasonable results given limited data
 - Pressure & velocity close
 - Sensitivity analysis of several parameters generally consistent
 - Model will be updated as additional data becomes available





Caseless Program Status

- **Future Plans**

- Complete HITP Development DOE
 - Identify critical formulation and process parameters
- Produce first prototype Spring 2006
 - Begin Mann barrel testing to screen DOE mixes
- 1st Delivery of test articles for validation testing by Summer of 2006
 - Primary goal is to deliver cartridges for proof-of-concept
- Secure material sources for process scale-up work
 - Some materials require a 6-month lead time
- Support follow-on process improvements



Caseless Program Summary

- **Technical**

- Initial mixing and processing very promising
- Fabrication solutions appear viable
- Interior ballistic modeling is underway that is critical to cartridge design – can be accomplished with additional testing

- **Schedule**

- Mix process DOE has been prepared and set for completion in Spring 2006
- Smaller DOE will likely follow to finalize process/formulation parameters – Summer 2006
- Cartridge fabrication for testing and demonstration – Summer 2006



St. Marks Powder
A GENERAL DYNAMICS COMPANY



CONTACT INFO



• **Name:** Chris Weiland

• **Phone:** 540.250.1267

• **Affiliation:** Virginia Tech Mechanical Engineering

• **Email:** cweiland@vt.edu

A Novel Launcher for Cavitating Weapons

Chris Weiland and Pavlos Vlachos
Virginia Polytechnic Institute and State University
Mechanical Engineering Department
Blacksburg, VA

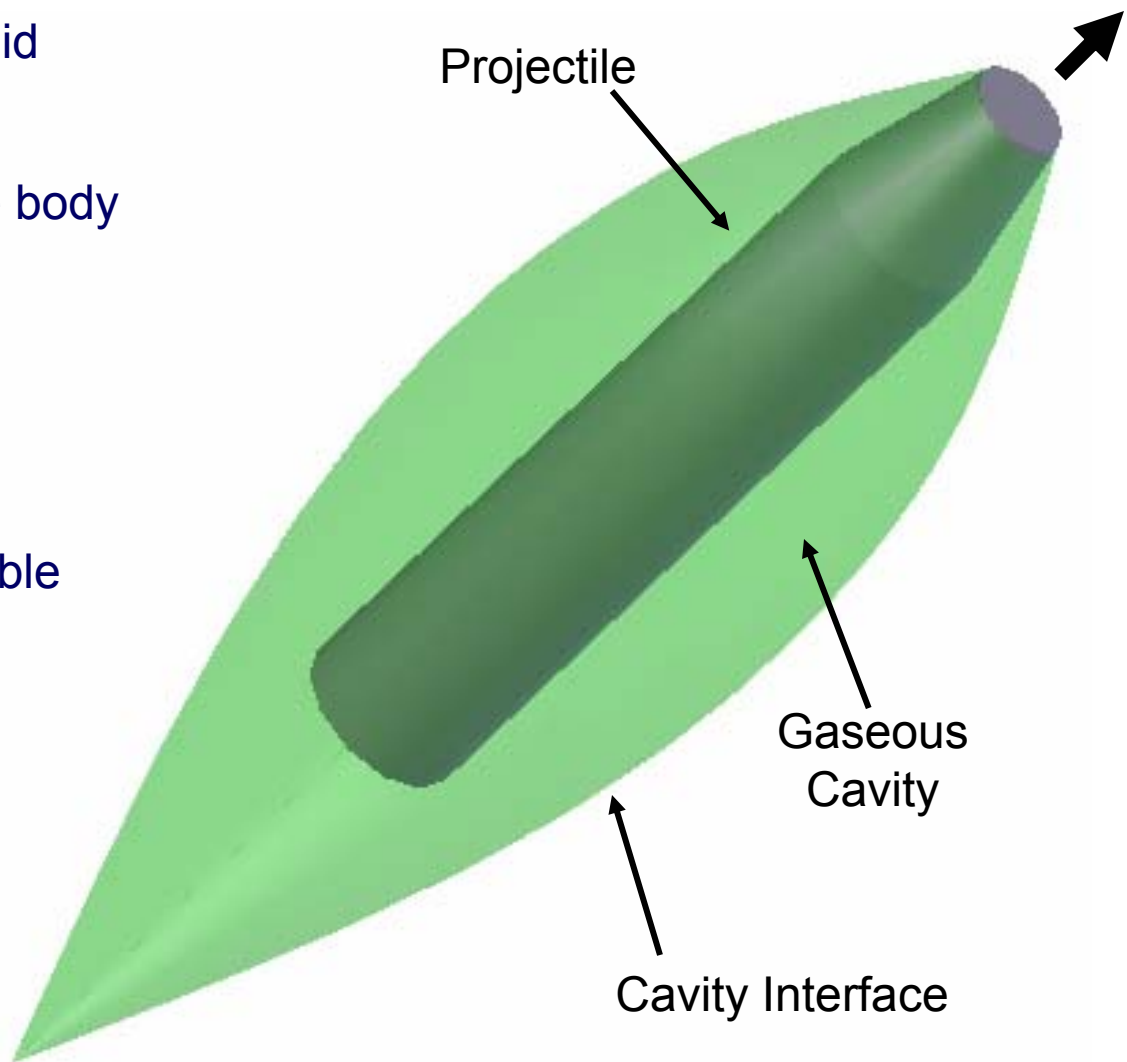
Jon Yagla
Naval Surface Warfare Center
Engagement Systems Department
Dahlgren, VA

*This work was supported by the Mechanical Engineering Department at
Virginia Tech*

Supercavitation

- Stresses exerted on ambient fluid drops below a critical value
- A gaseous cavity envelopes the body and moves with it
- Viscous interaction between projectile surface and water is alleviated (i.e. drag reduction)
- Large underwater speeds possible

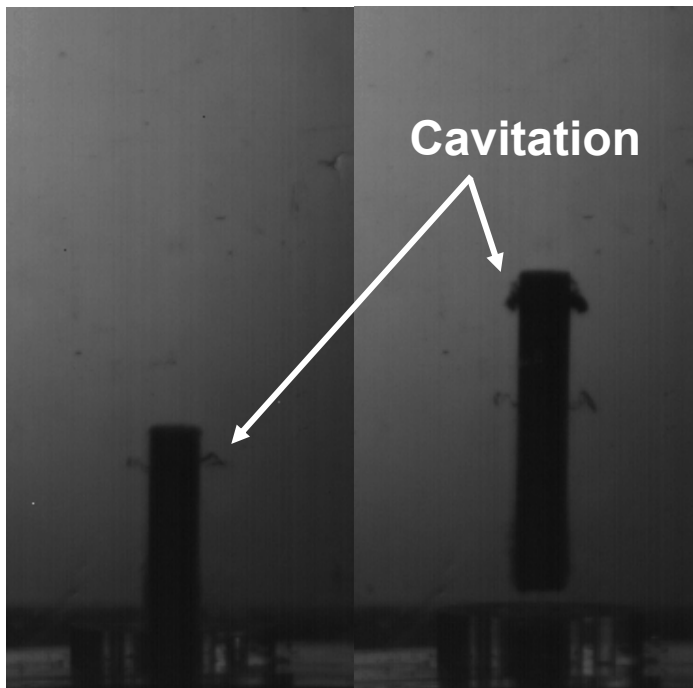
$$\sigma = \frac{p_h - p_c}{\frac{1}{2} \rho U^2}$$



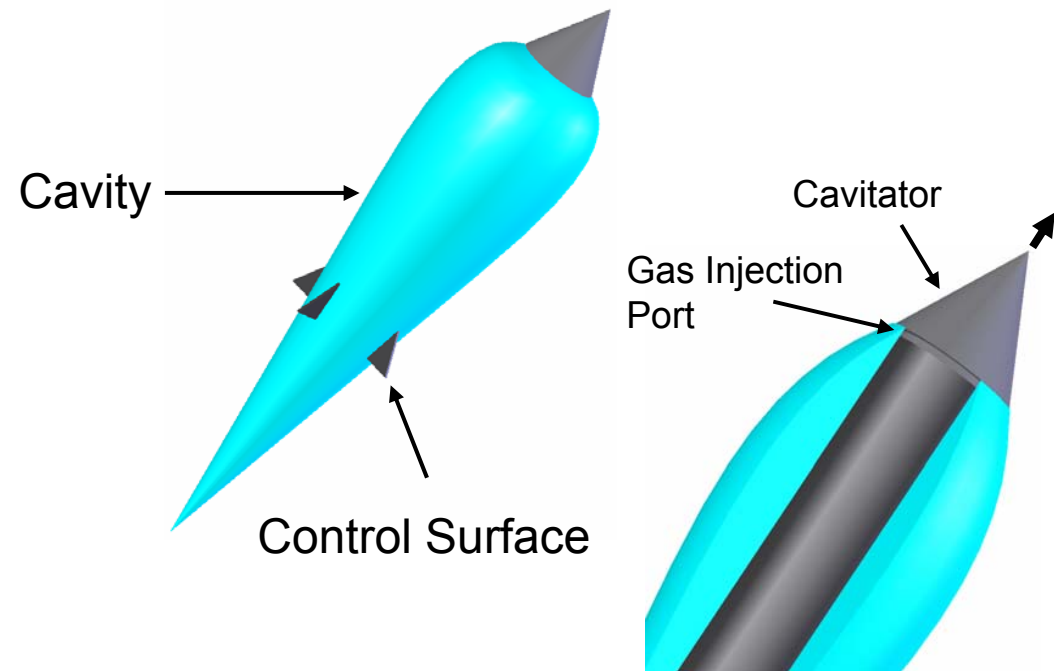
Supercavitation Inception

- **Pure Hydrodynamic Cavitation –** Naturally occurring nuclei (small gas bubbles) explosively grow due to fluctuating pressure field in the separated flow region.

Extremely High Speeds Required For Pure Hydrodynamic Supercavitation



- **Artificial (Ventilated) Cavitation –** Pressurized gas is injected behind the cavitator. Supercavitation at lower speeds is possible.
Requires a Pressurized Source of Gas to be Carried On-Board or Plumbing to Re-Direct Exhaust Gases

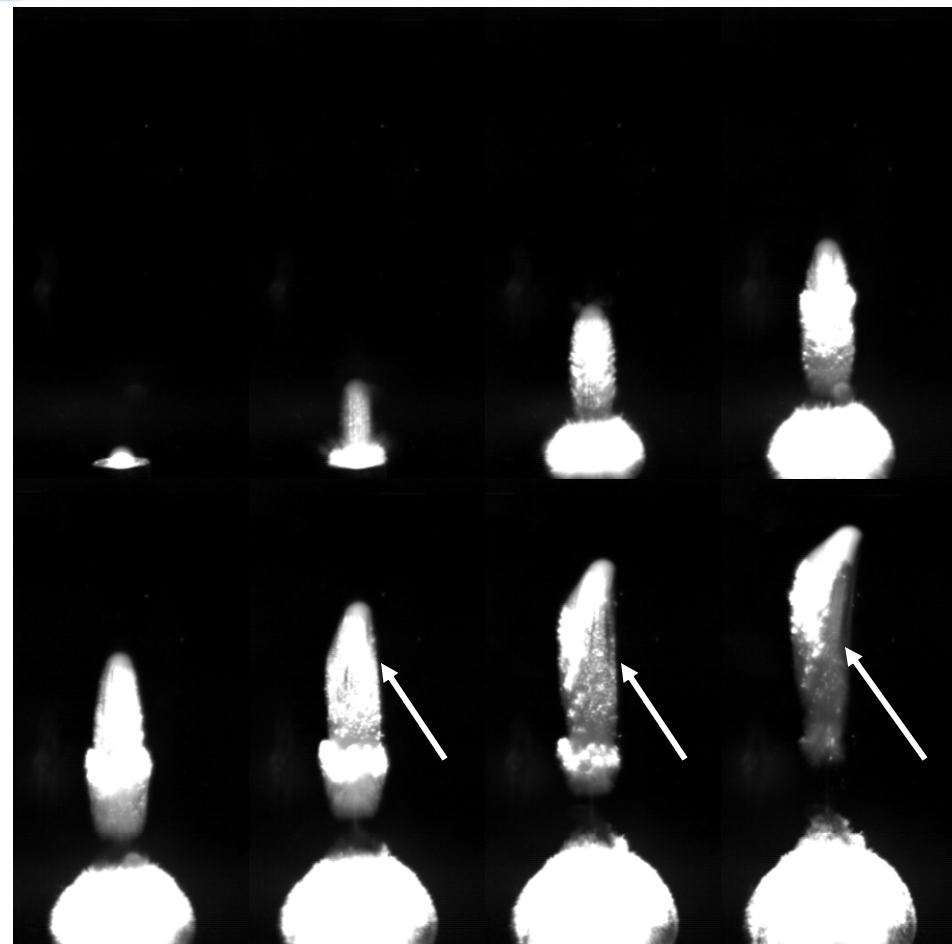


Inception via Gas Entrainment

How Can We Achieve the Best of Both Worlds?

- Pressurized gas is injected during launch
- The pressurized gas fills the separated flow region, resulting in a fully developed cavity
- Velocity required to initiate supercavitation is drastically reduced

**Allows a state of supercavitation
to be prematurely attained until
pure hydrodynamic
supercavitation can ensue**



$$U_0 = 45 \text{ m/s}$$

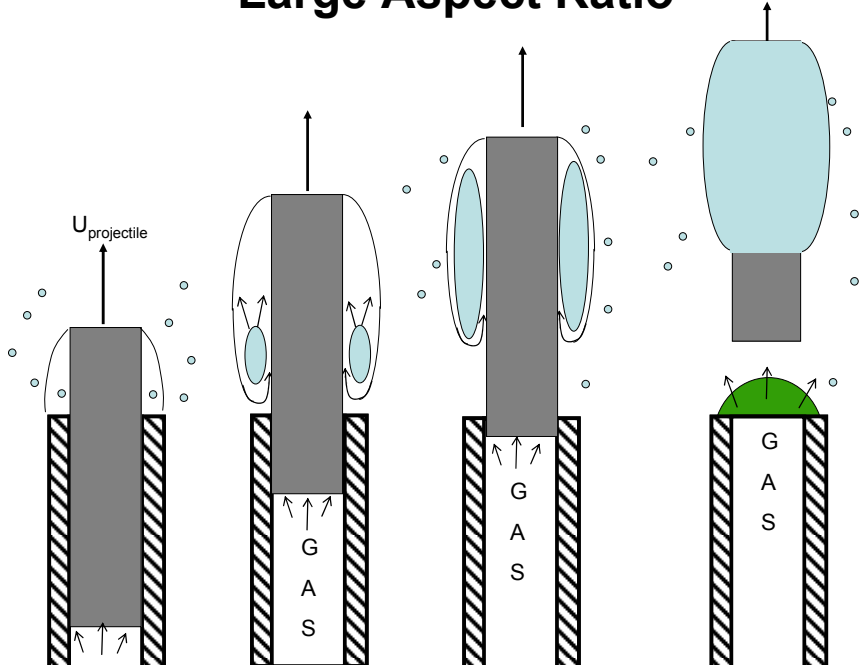
$$\sigma = 0.1$$

(not accounting for injected gas)

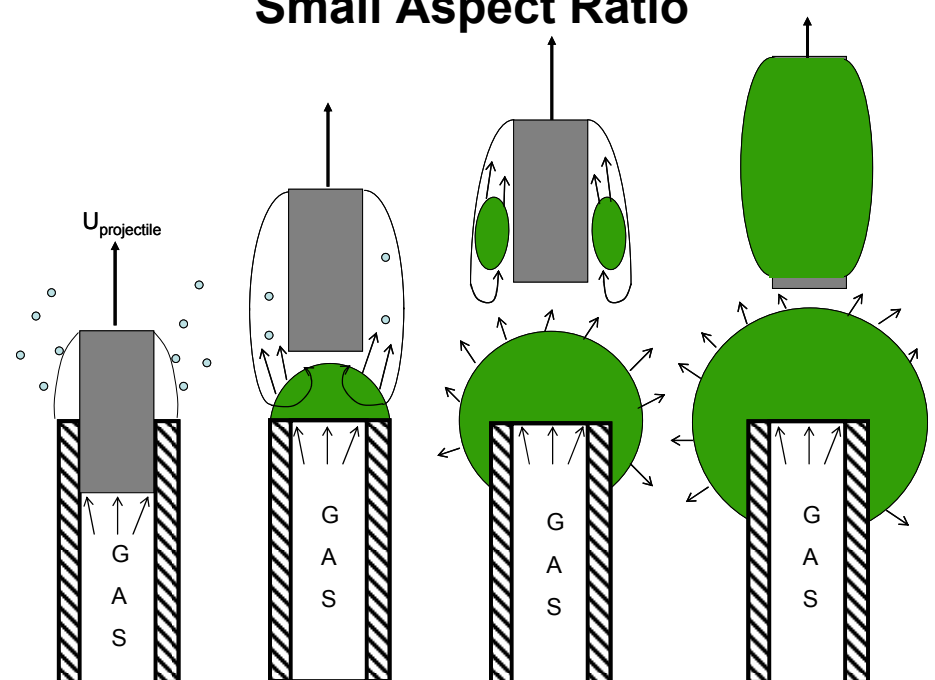
Gas Gun Method

- The projectile leaves the launcher under the force of expanding gases (i.e. gun launch)
- The driving gases are the source of cavitation nuclei
- Degree of supercavitation initiation is aspect ratio dependent – reattachment point is important

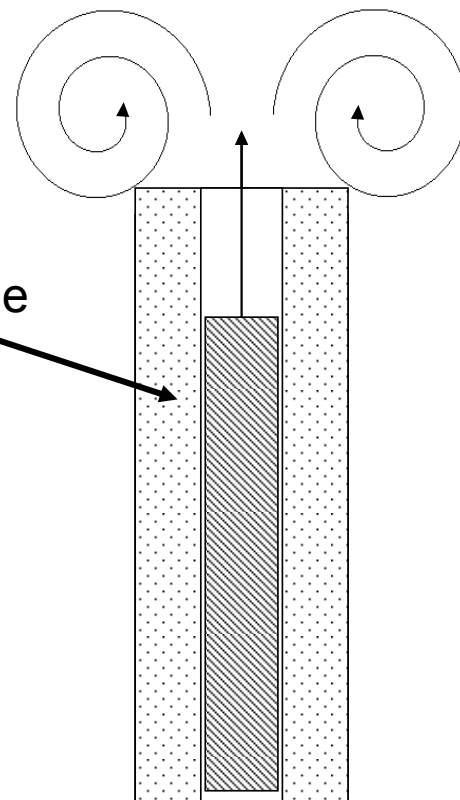
Large Aspect Ratio



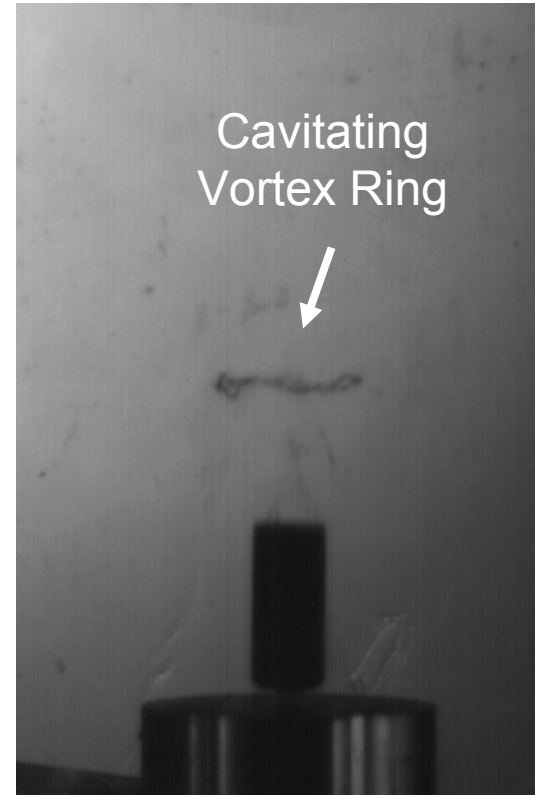
Small Aspect Ratio



Vortex-Body Interaction



The formation of a vortex ring.

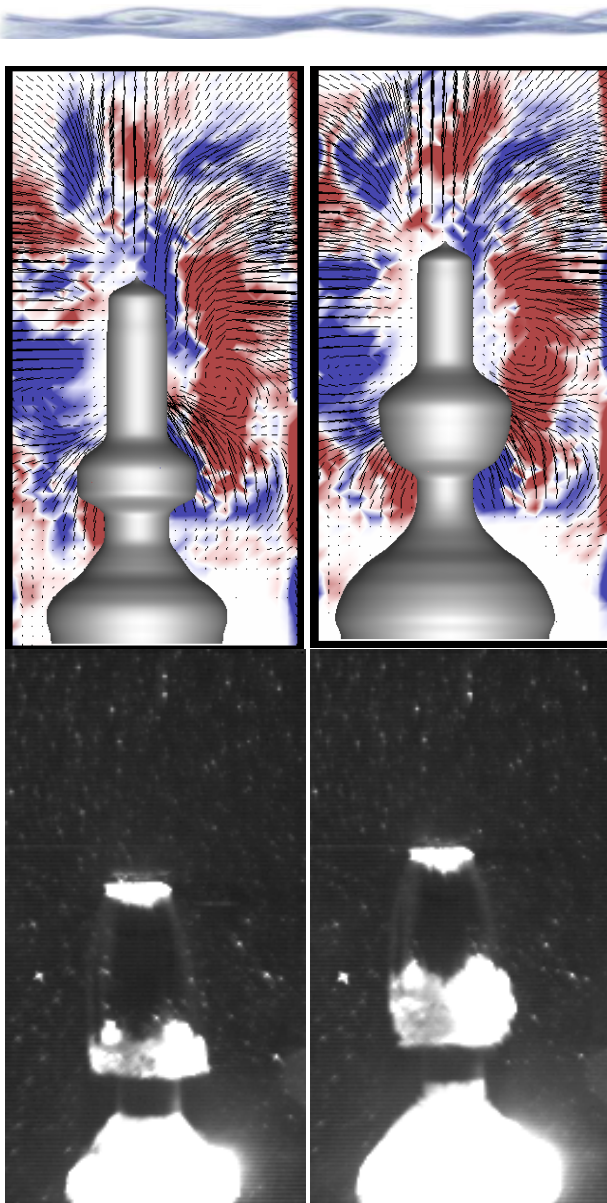


Generation of a cavitating vortex ring.



Interaction of the vortex ring and projectile.

Gas Gun Method



Blunt Cylindrical
Projectile

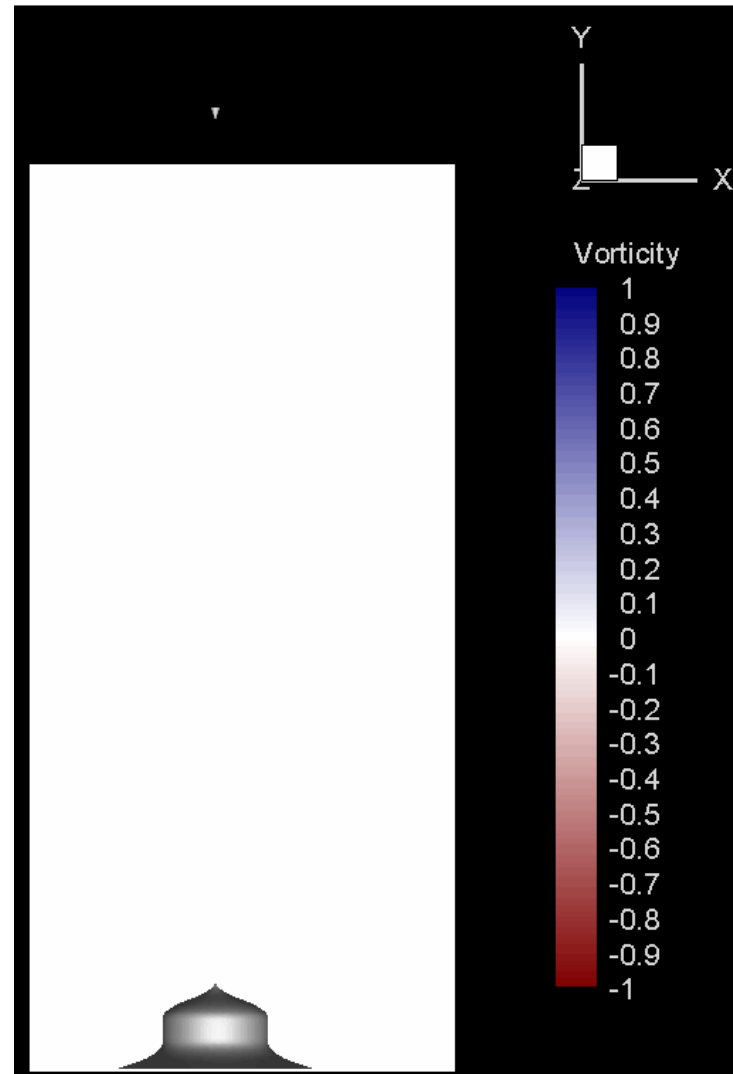
Aspect Ratio 5

$$U_0 = 27 \text{ m/s}$$

$$\sigma = 0.29$$

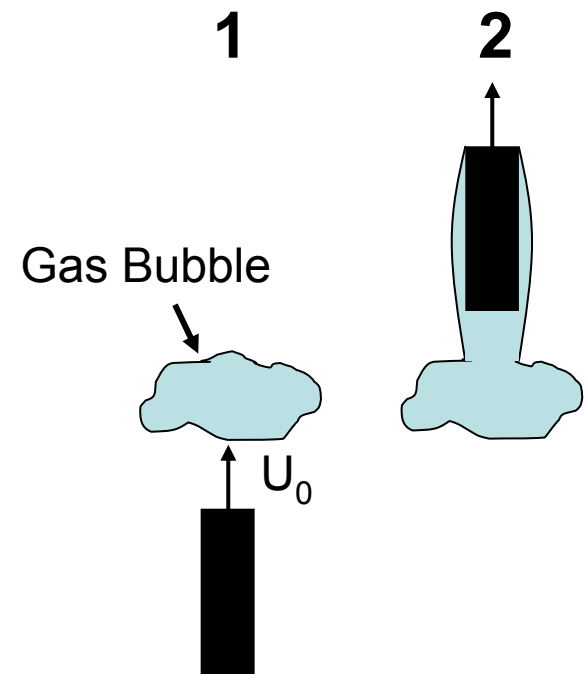
(not accounting for
injected gas)

- A large degree of fluid structure interaction takes place
- Asymmetric vortices can cause instability in projectile flight



Gas Injection Method

- Pressurized gas is injected in the trajectory of the projectile prior to launch
- The supercavity is fully developed before the projectile interacts with the surrounding fluid



$$U_0 = 12 \text{ m/s}$$

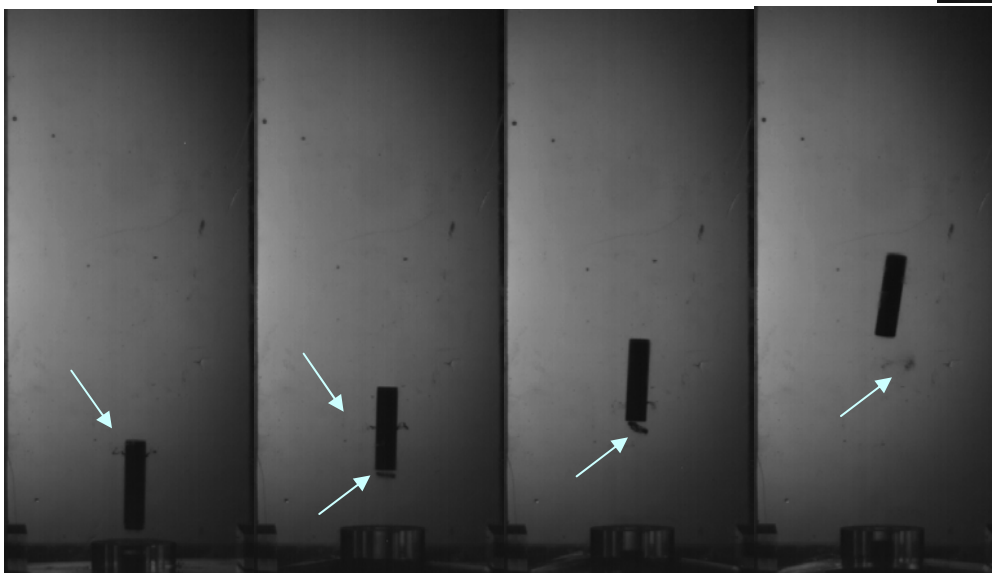
$\sigma = 1.48$ (not accounting for injected gas)

Gas Injection Effect

$$U_0 = 12.8 \text{ m/s}$$

$$\sigma = 1.48$$

(not accounting for
injected gas)



$$U_0 = 13.8 \text{ m/s}$$

$$\sigma = 1.12$$

Gas Injection Method

Square Projectile

No Gas Injection

$$U_0 = 14.4 \text{ m/s}, \sigma = 1.03$$



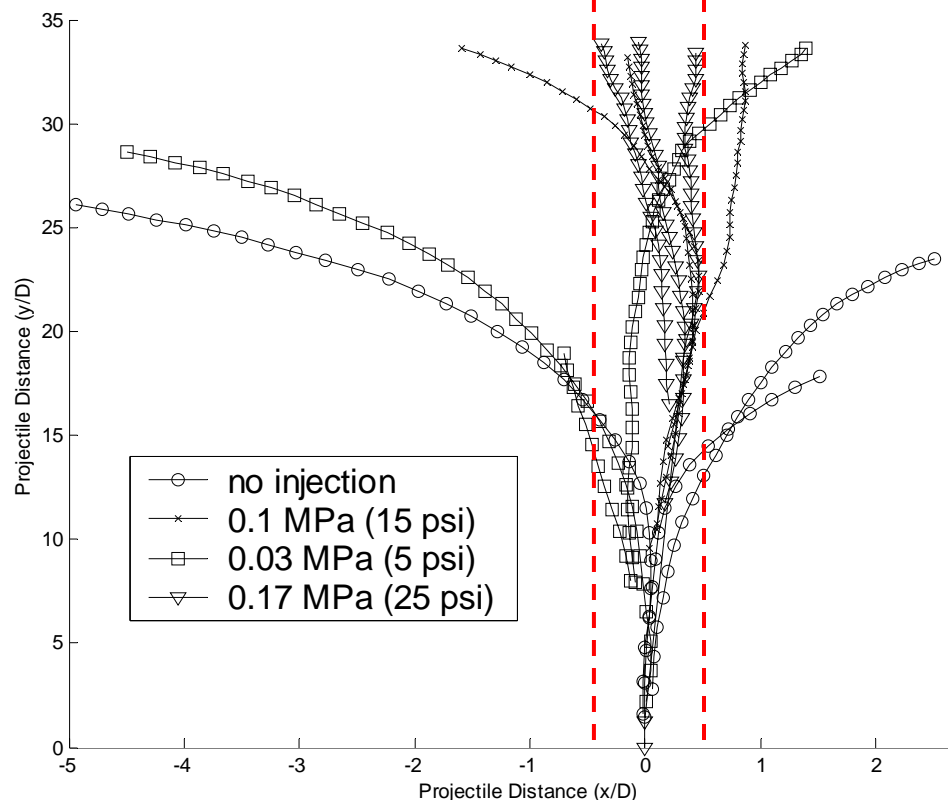
Square Projectile

Gas Injection

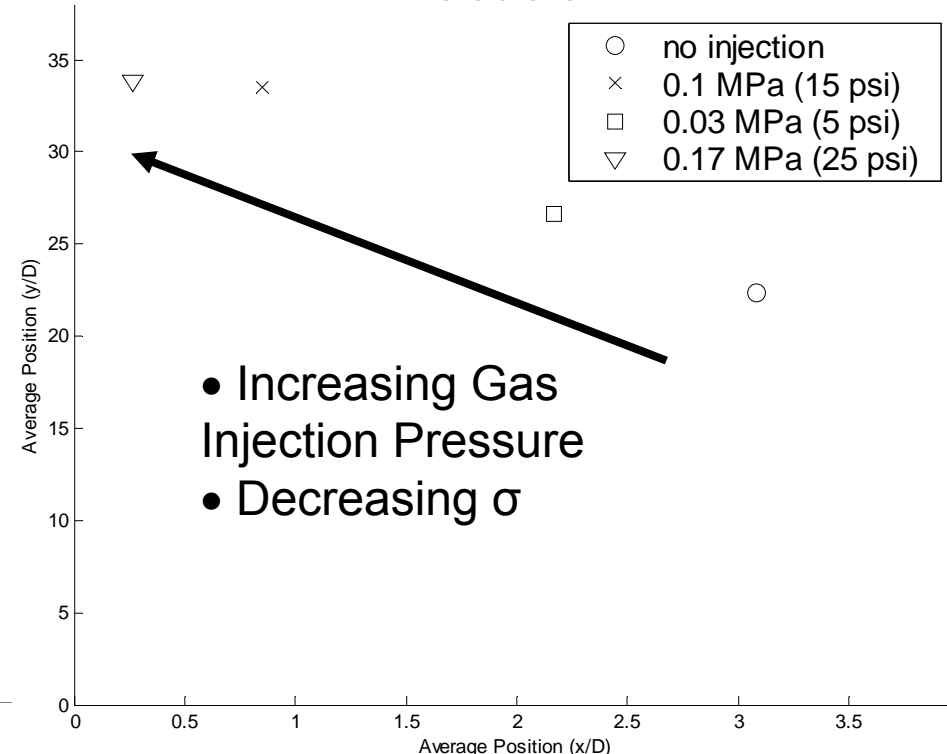
$$U_0 = 11.4 \text{ m/s}, \sigma = 1.64$$

Gas Injection Method

Projectile Trajectories



Average Projectile Ending Location



Higher Gas Injection Pressures Results in Stronger Cavity Development and Better Projectile Stability

Conclusions

- The gas injection method allows the projectile to reach a state of “instant supercavitation,” thereby mitigating any fluid structure that could lead to its instability during launch
- The gas injection method allows supercavitation at greatly reduced speeds
- The gas injection method increases projectile lateral stability and decreases viscous drag



22nd International Symposium on Ballistics

Vancouver, BC Canada



Wind Tunnel Verification of the Performance of a Smart Material Canard Actuator

P. Weinacht, W.F. Drysdale, T. Bogetti, R. Don
US Army Research Laboratory

J.T. Arters, J.R. Vinson, A.R. Hickman
University of Delaware

L. Auman
US Army Aviation and Missile RD&E Center

O. Rabinovitch
Technion Israel Institute of Technology



Aerodynamics Branch

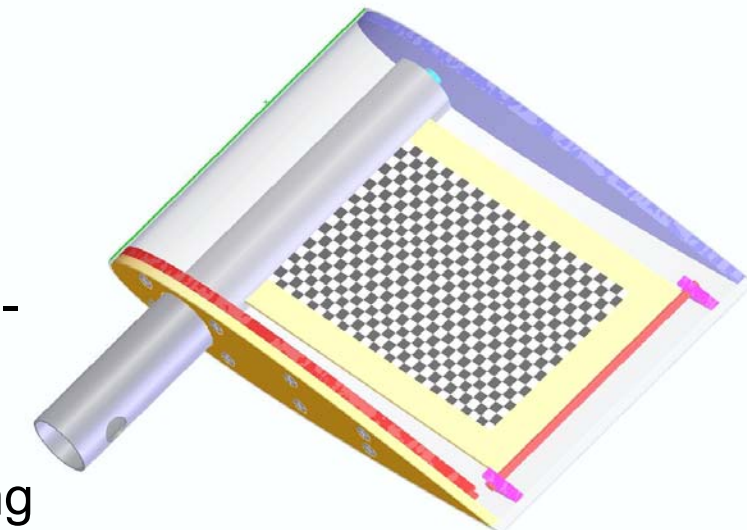




Smart Material Canard Actuator Design

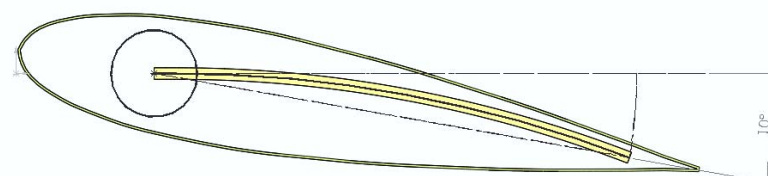
Actuator Characteristics

- Hollow NACA 0018 aeroshell surrounds actuator mechanism.
- Actuator Mechanism consists of two Macro Fiber Composite (MFC) patches bonded to e-glass plate.
 - Differential voltage applied to MFC patches produces deflection at trailing edge of plate and rotation of aeroshell



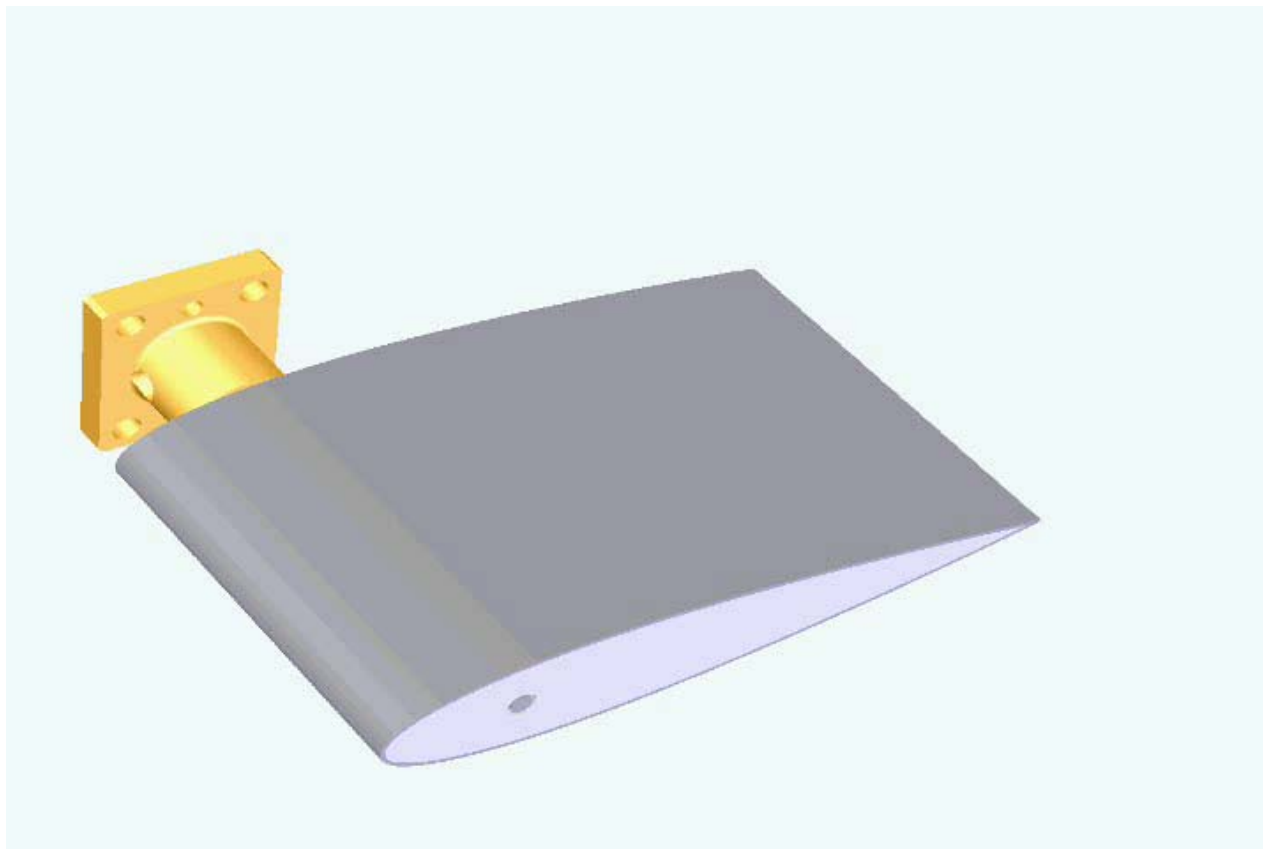
Benefits of actuator concept:

- Minimizes volume intrusion of actuator into munition payload
- Potential weight savings





Smart Material Canard Actuator Design

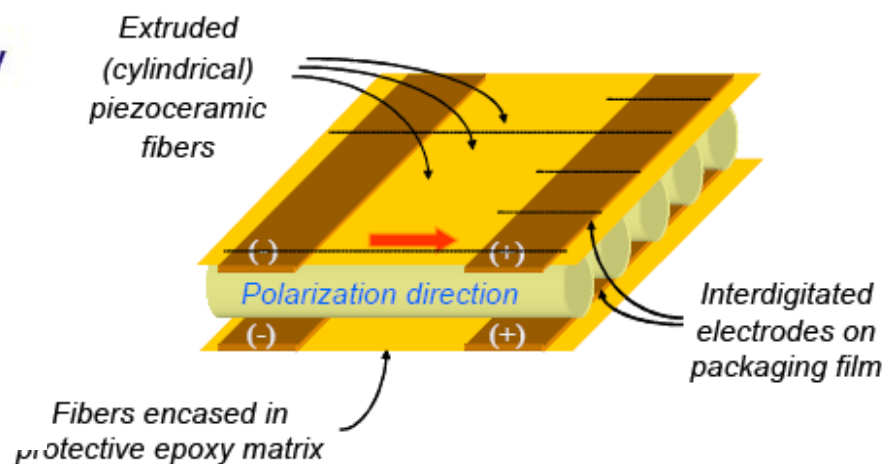
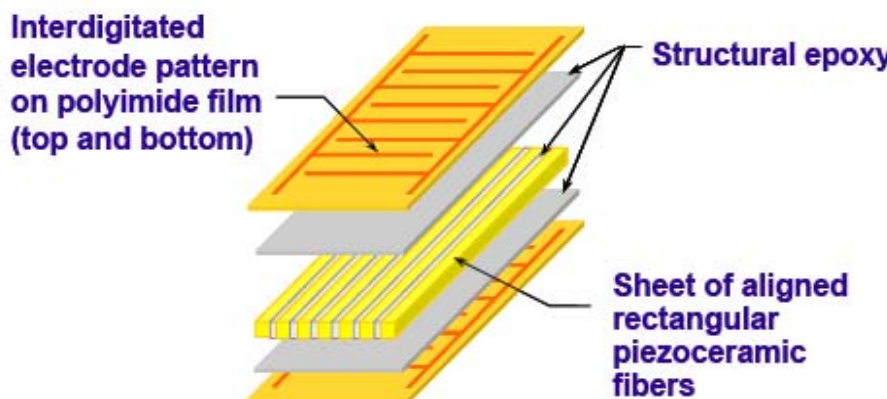




Macro Fiber Composite Patches



- Active layer consists of Macro Fiber Composites (FMC) produced by Smart Material Corp.
- FMCs utilize uniaxially aligned fibers surrounded by a polymeric matrix.
- Interdigitated electrode pattern is used to deliver an electric field along the length of the fiber.





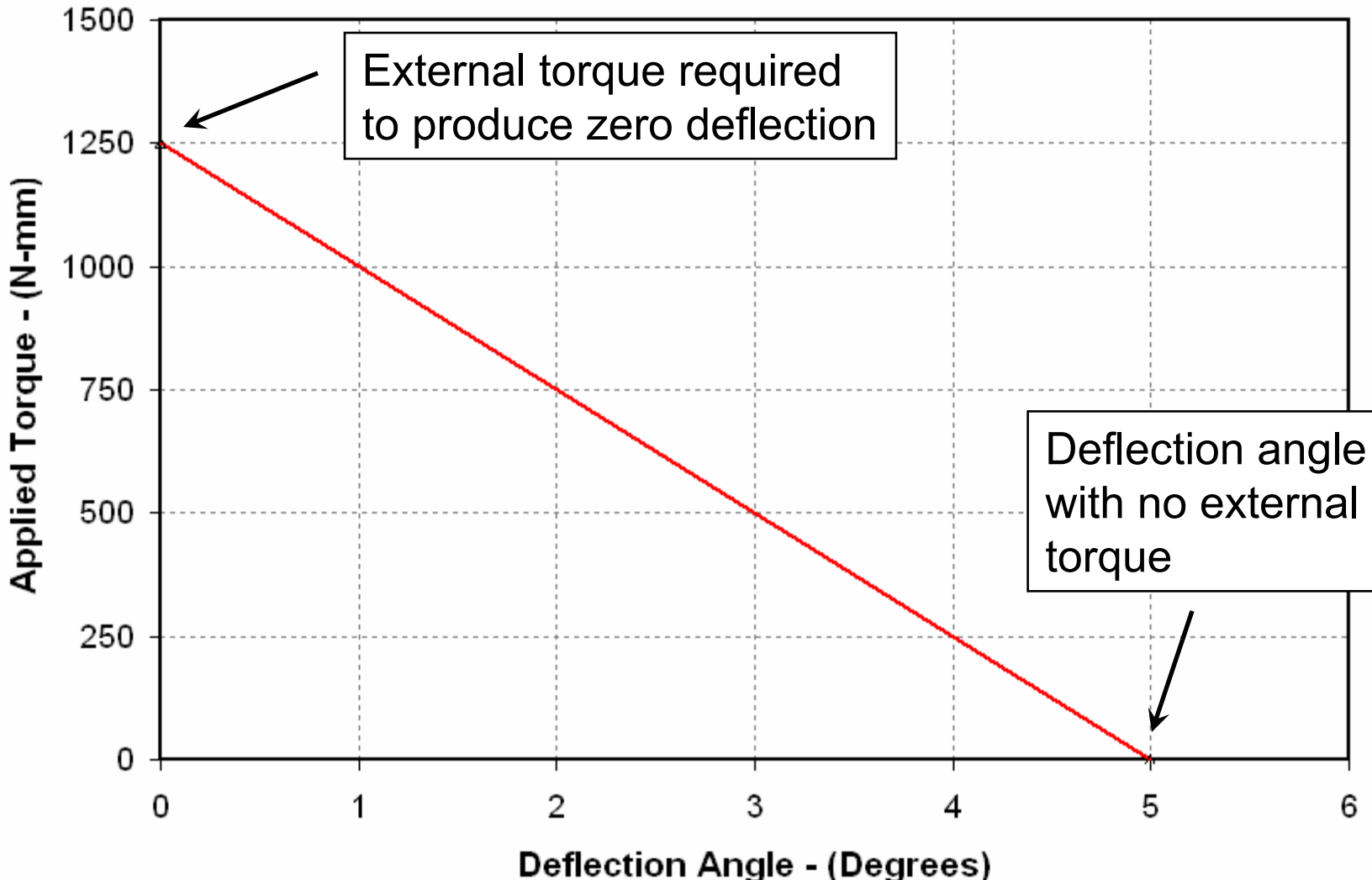
Design Approach

- Multi-disciplinary design approach - coupled structures and aerodynamics.
- In general, there is a trade-off between fin deflection angle and available torque to overcome aerodynamic hinge moment.
- ARL/University of Delaware design - maximize fin deflection angle ~ Mach 0.3-0.5.
- It is possible to obtain more deflection if aerodynamic torque is ignored.



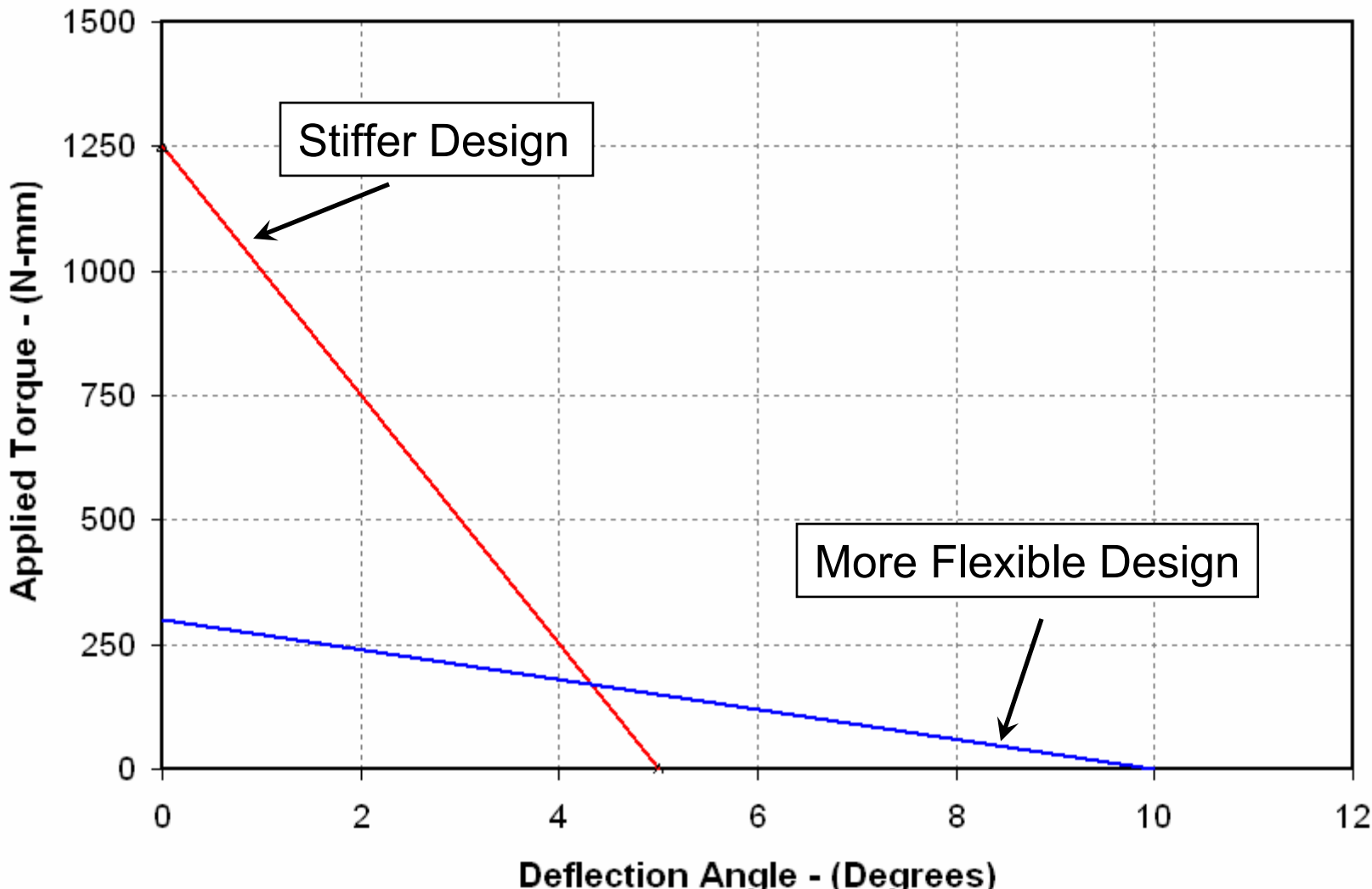


Design Approach (Cont.)





Trade-Off Between Maximum Deflection Angle and Torsional Stiffness

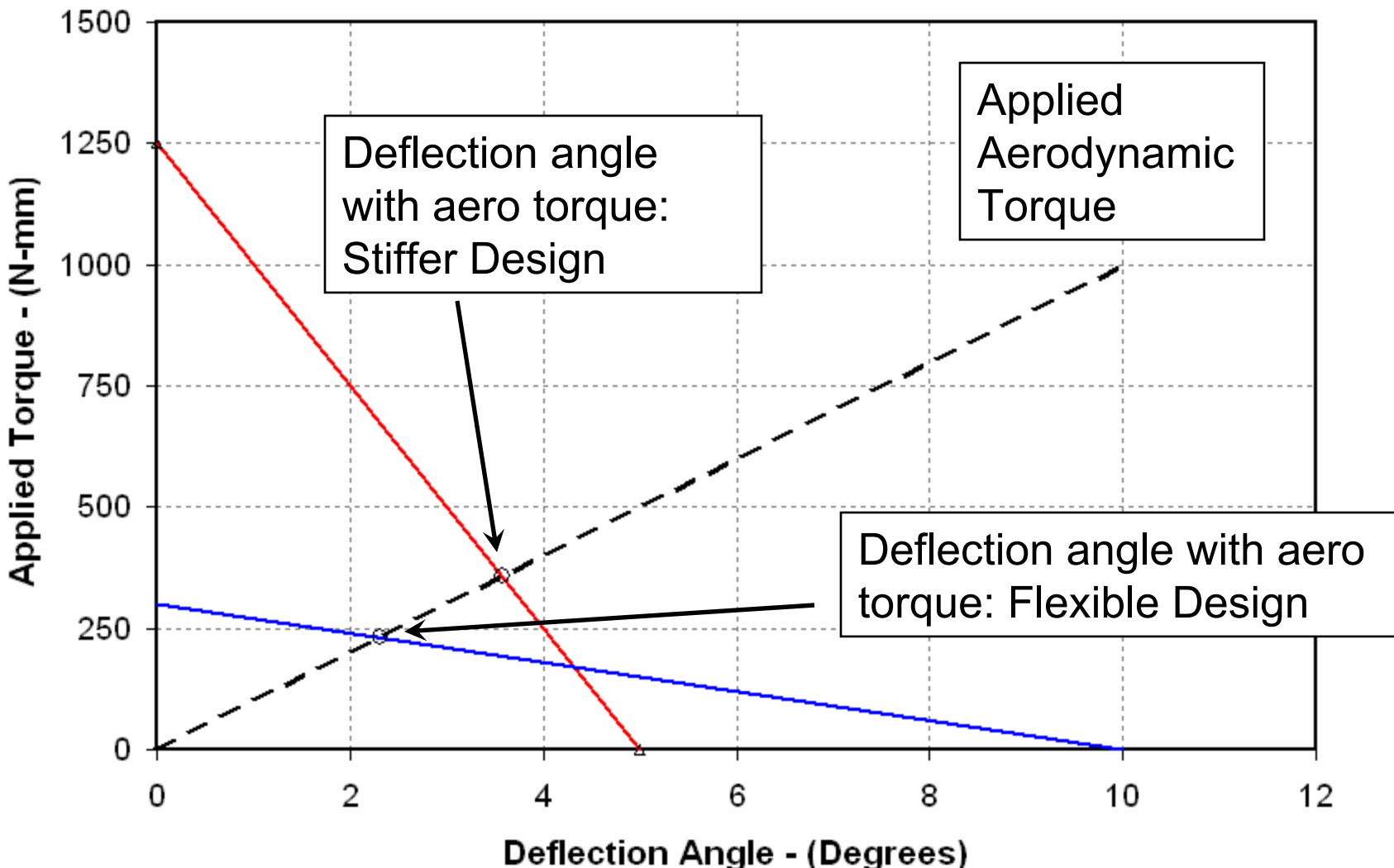


Aerodynamics Branch





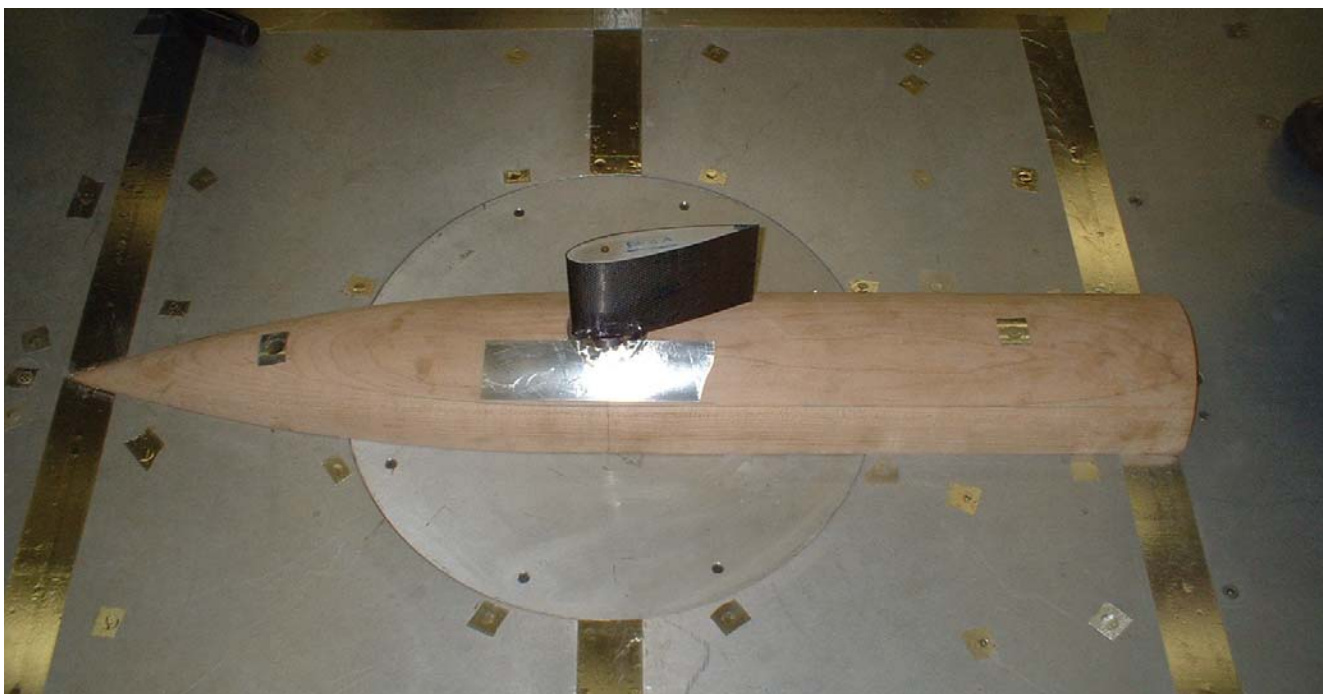
Deflection Angles in Presence of Aerodynamic Torque





Wind Tunnel Testing at U. of Maryland

- Sponsored by ARL, U. Delaware
- Fin mounted to balance on tunnel floor – half missile body fairing used.
- Purpose of Wind Tunnel Test:
 - Determine response of fin in presence of aerodynamic load.
 - Measure and quantify aerodynamic loads.
 - Determine whether flutter is an issue.



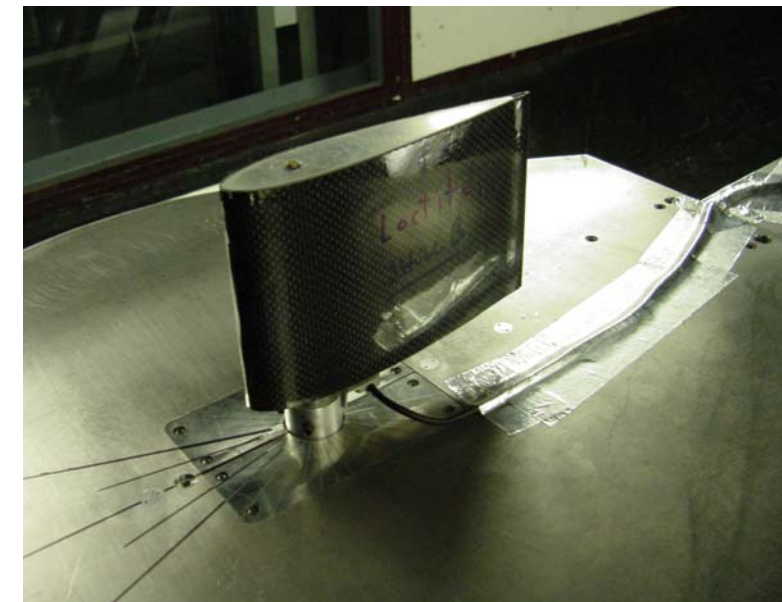
Aerodynamics Branch





Wind Tunnel Testing at Texas A&M

- Collaboration between AMRDEC Aero. Branch, ARL, U. Delaware
- Testing at Texas A&M University
- AMRDEC provided splitter plate, force/moment balance, testing time.
- Purpose of Wind Tunnel Test:
 - Determine response of fin in presence of aerodynamic load
 - Measure and quantify aerodynamic loads
 - Determine whether flutter is an issue.



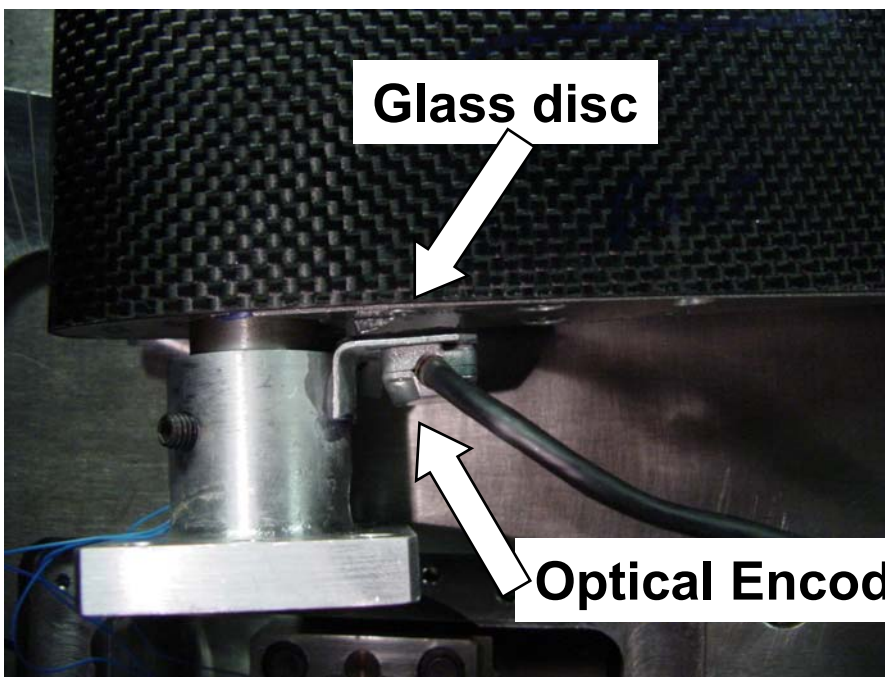
Aerodynamics Branch





Optical Encoder

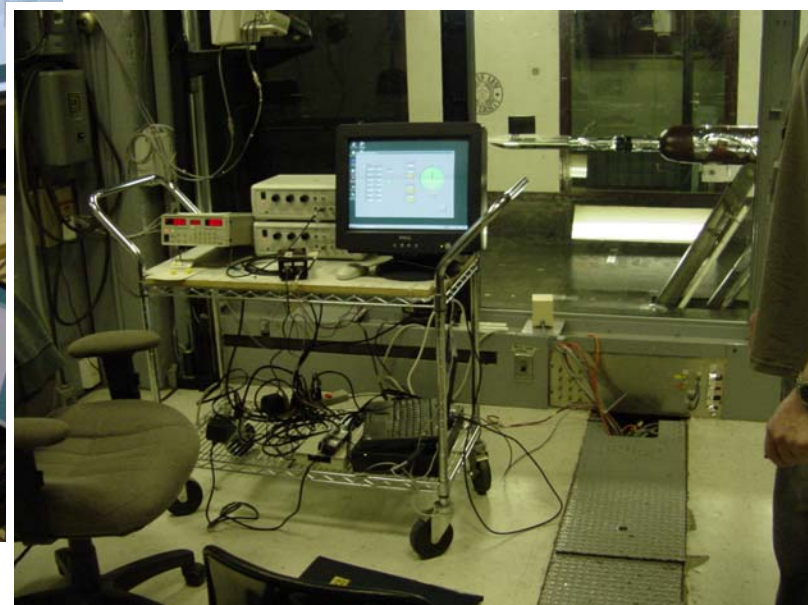
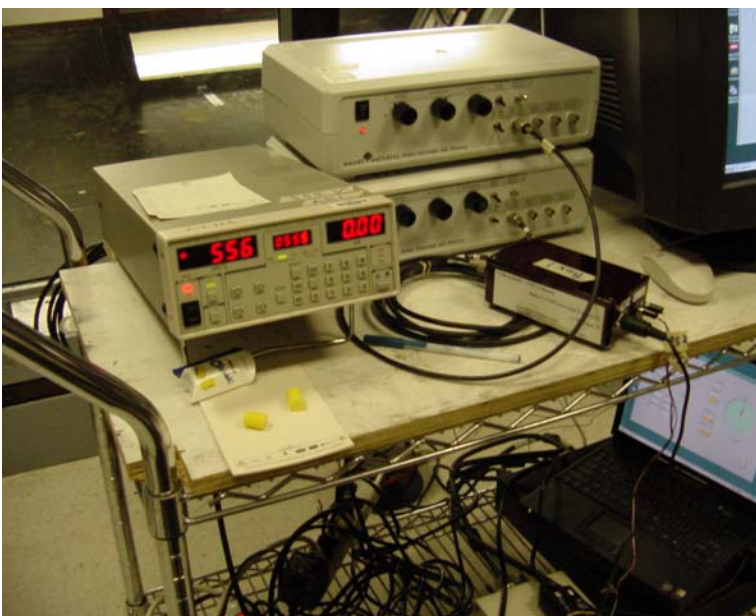
- Measures fin deflection angle
- Sensor mounted on fin base
- Sensor reads deflection from graduated glass disc glued to bottom of fin
- Time-dependent sensor output acquired on laptop





Fin Power Sources

- Three power sources provide voltage to both smart material patches
- Power controlled through laptop
- Continuous range of voltage available -500V to +1500V



Aerodynamics Branch





Wind-Off Response

- Several wind-off tests were run to obtain the response of the fin without aerodynamic load
- Results have some bearing on experimental approach and interpretation of results
- Static Deflection Tests

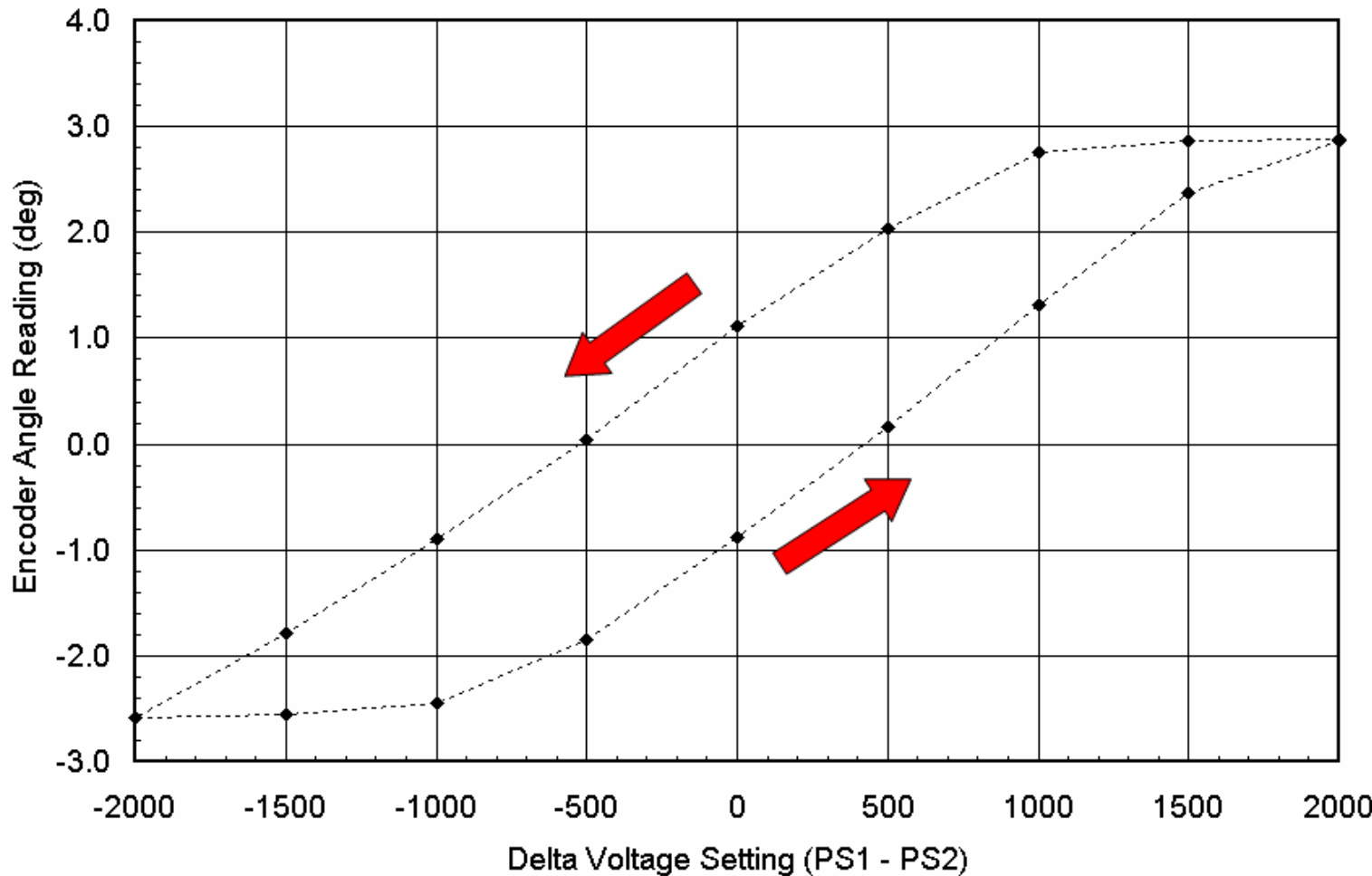
	<i>Peak-to-Peak Deflection</i>	<i>Torsional Stiffness</i>
<i>250°F Fin</i>	<i>5.3 deg</i>	<i>179 N-mm/deg</i>
<i>Loctite Fin</i>	<i>5.5 deg</i>	<i>279 N-mm/deg</i>

- Hysteresis
- Time-Dependent Response





Wind-Off Hysteresis

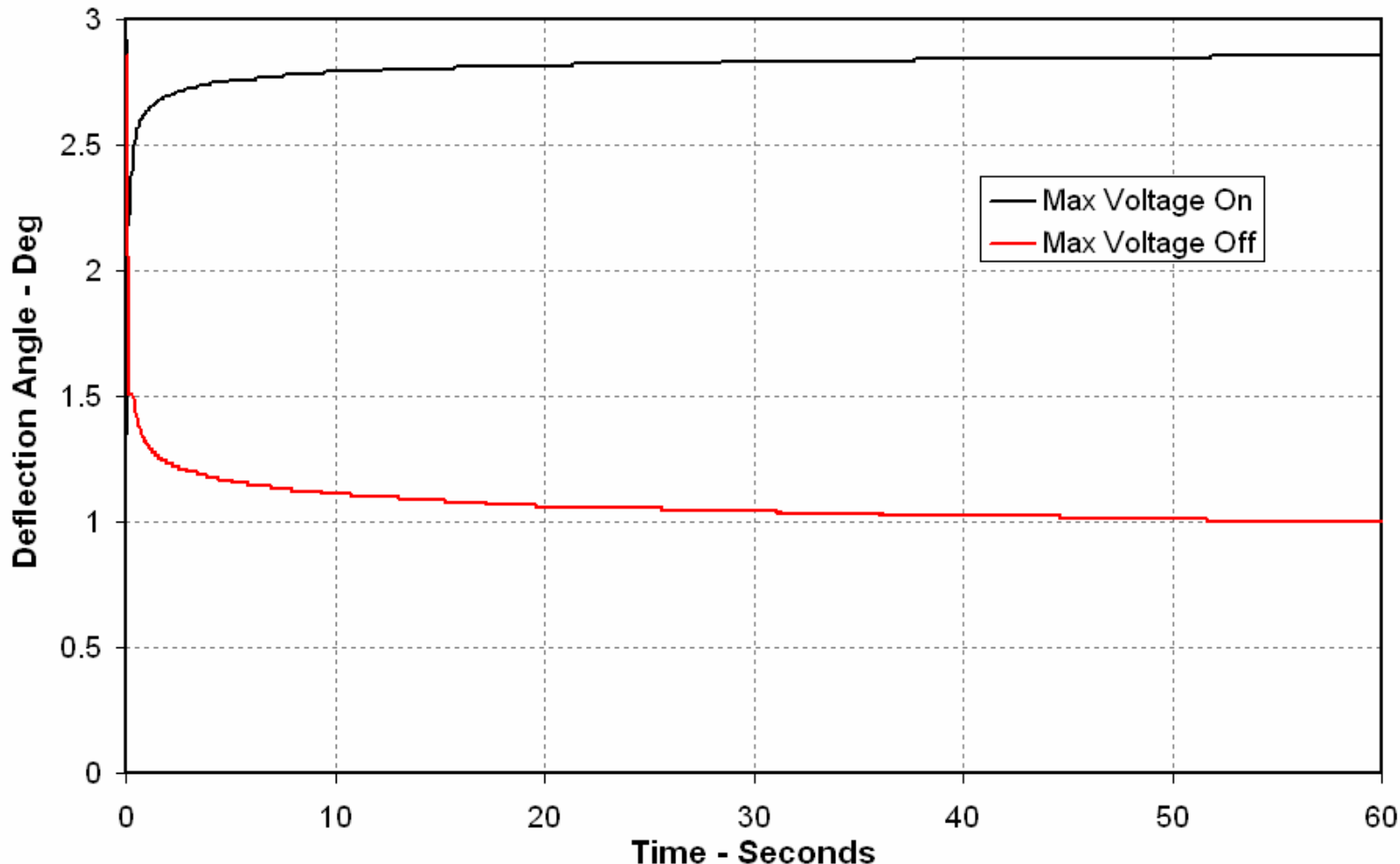


Aerodynamics Branch





Time-Dependent Response





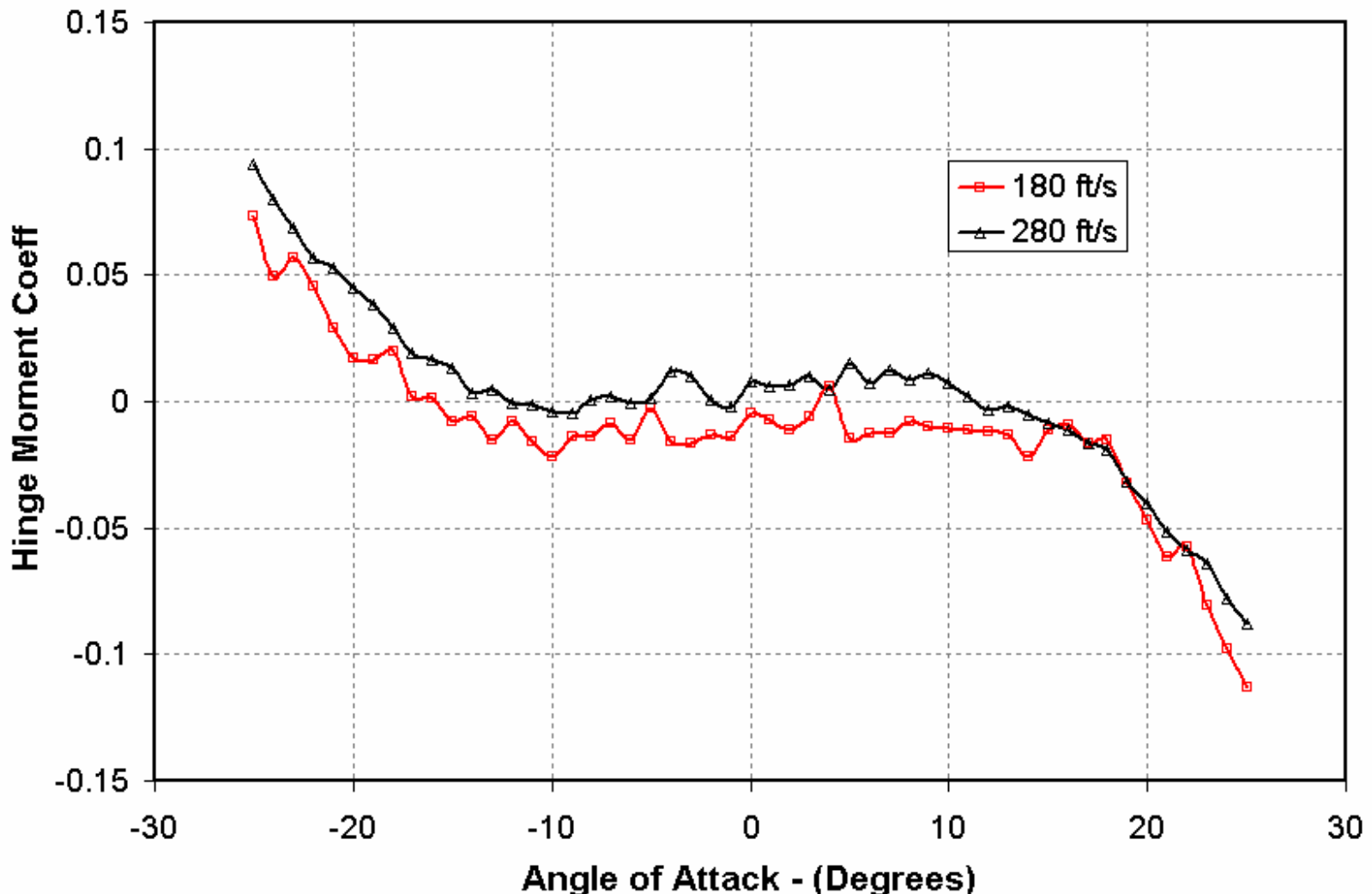
Rigid Fin Tests

- The pure aerodynamic response of the fin was examined using a rigid fin (no actuator):
- Aerodynamic forces and moments measured to ± 25 deg angle of attack (AoA).
- “Hinge” line located at 20% of chord length from leading edge.
- Small difference between rigid fin and fins with actuator
 - Fin was mounted $\frac{1}{4}$ inch higher off splitter plate than for fins with actuator.
 - No optical encoder mounted.
- Considered two velocities 180 ft/s and 280 ft/s
- Measured six force/moment components





Hinge Moment





Smart Material Actuator Fin Tests



- The smart material actuator fin was tested in number of modes:
 - Unpowered (No applied voltage)
 - \pm Maximum Voltage
 - Varying Voltage
 - Tests performed at 180ft/s, 280ft/s
 - AoA -14° to 14°
- Two versions of actuator tested
 - Differ only by adhesive used to bond patch to host
 - 250°F epoxy
 - Loctite epoxy
- Force/moment balance measurements taken.
- Fin deflection measured with optical encoder.

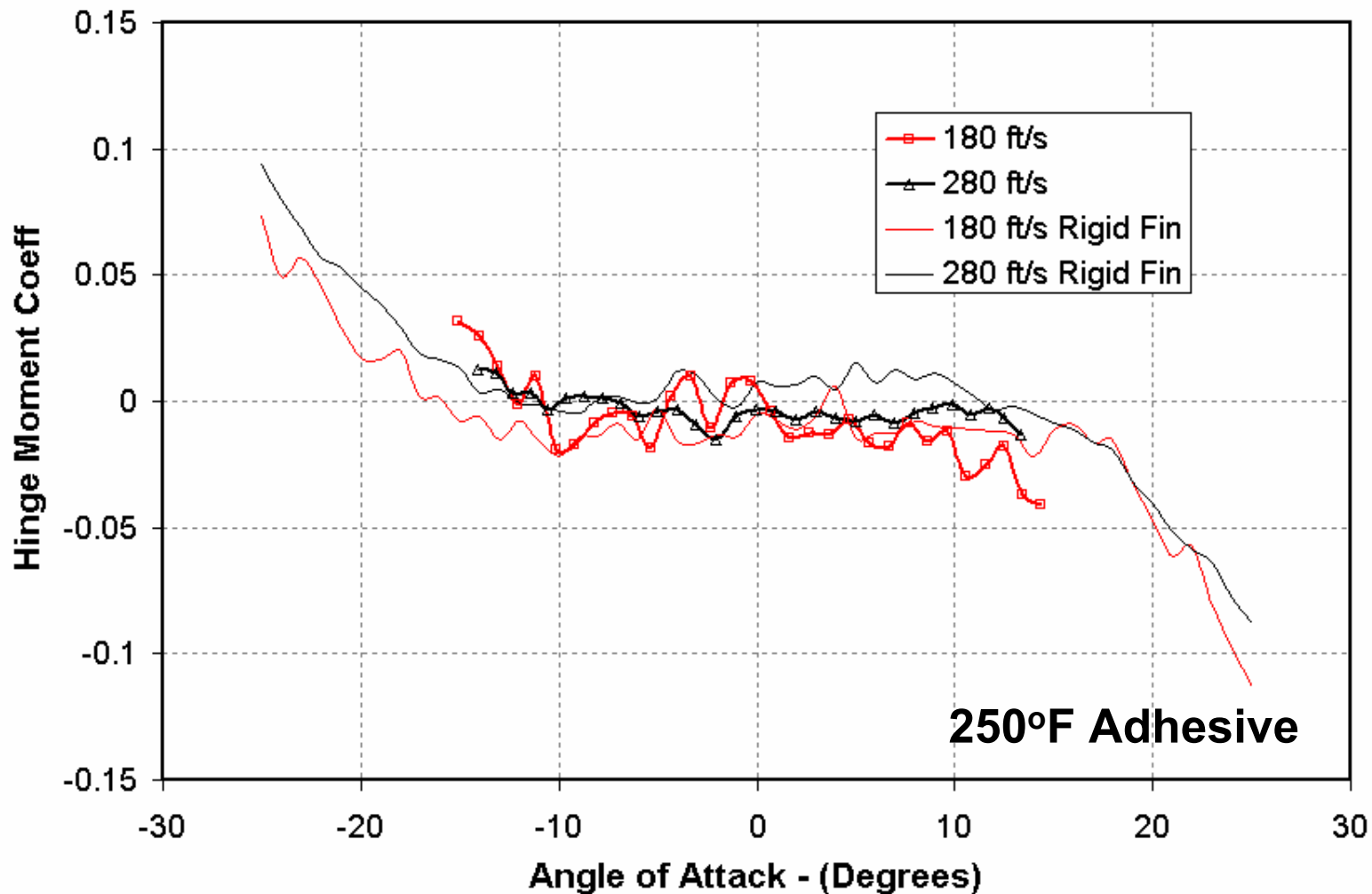


Aerodynamics Branch



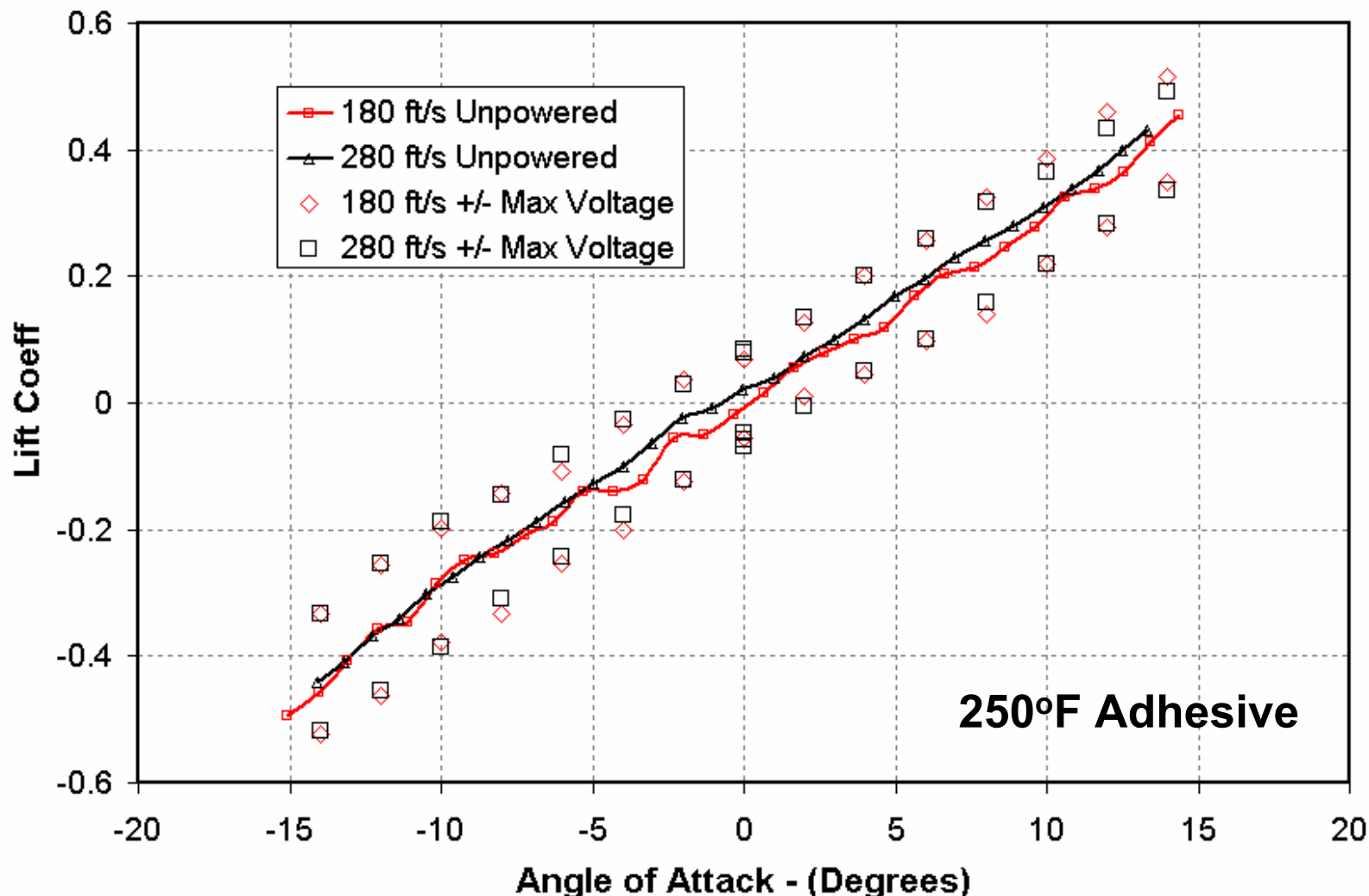


Hinge Moments



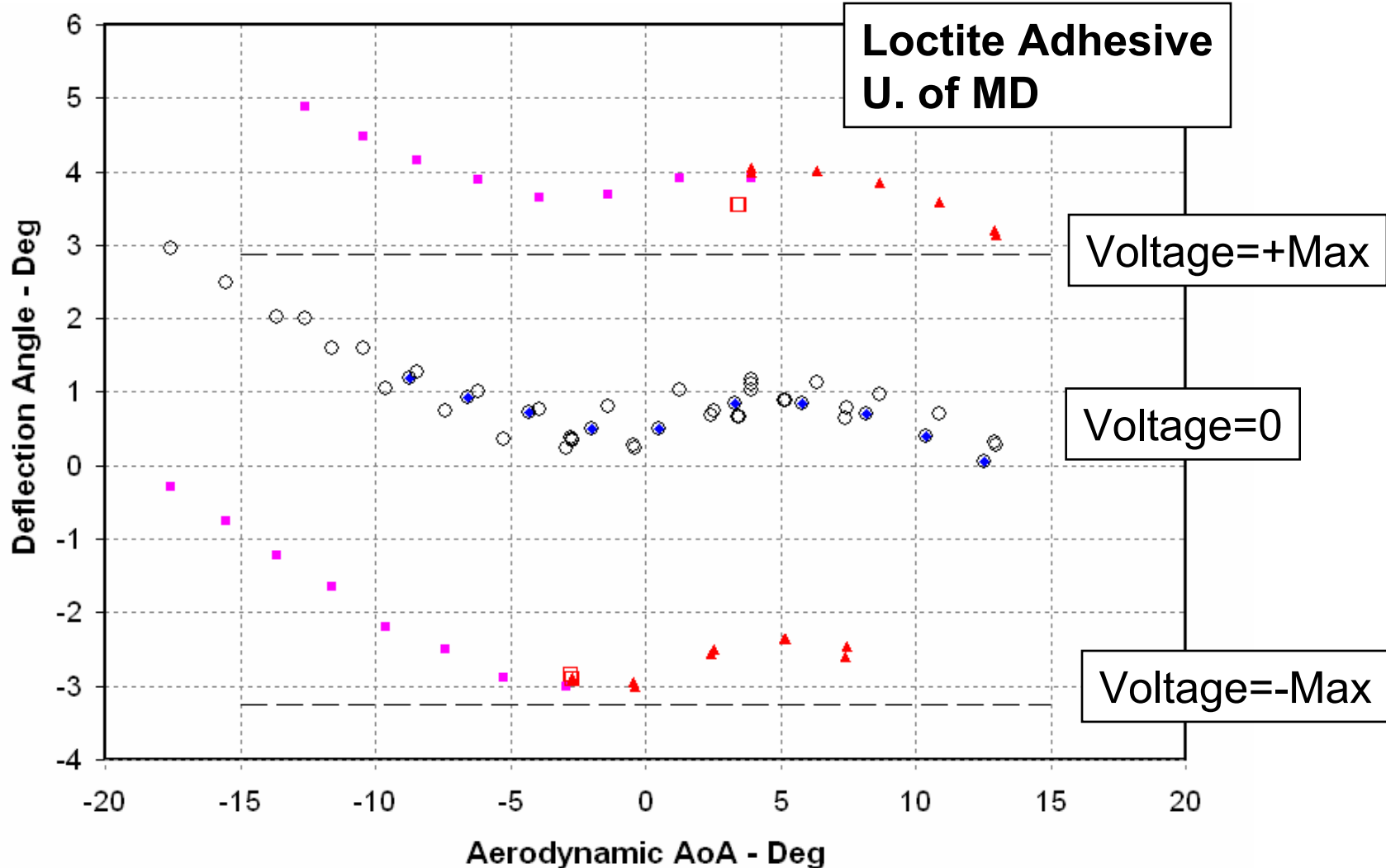


Lift Force Generated by Deflection



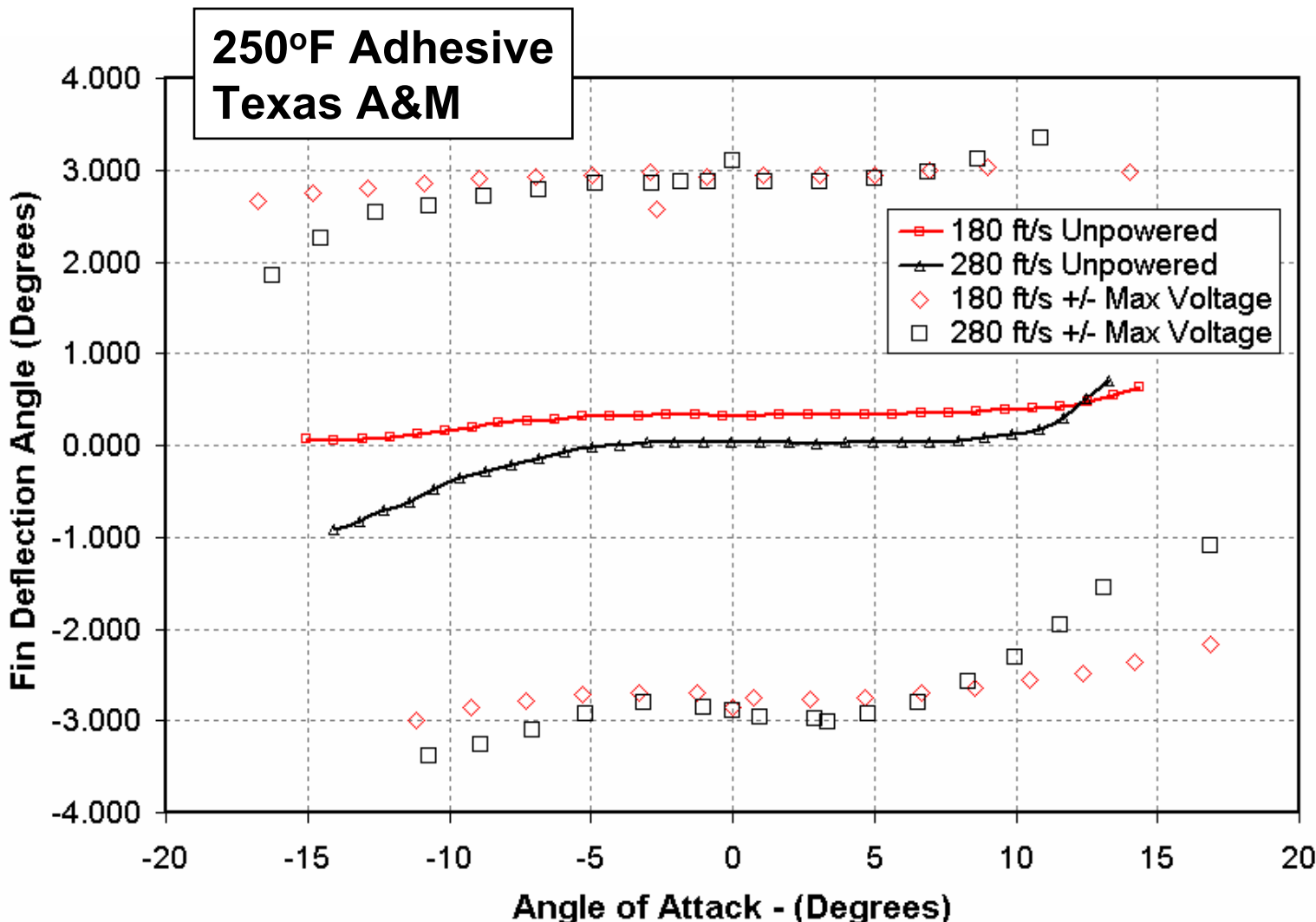


Fin Deflection Angle vs. Angle of Attack





Fin Deflection Angle vs. Angle of Attack





Conclusions

- Within one year, a canard actuator based on smart materials was designed, constructed and wind-tunnel tested.
- Design shows promise for application to munition systems.
 - Coupled structural/aerodynamic analysis required for the design of these flexible structures.
 - MFC actuators: rugged and robust – a requirement for gun-launched munitions.
 - Flutter not an issue for velocity range tested.
- Improved performance possible with existing design using better manufacturing techniques.
- Alternative designs, improved MFC patches being investigated.



The Study on Lethality Simulation Method for Fragmentation Warhead

Yang Yunbin Qu Ming Qian Lixin



Institute of Structural Mechanics

November, 2005

Table of contents



INTRODUCTION



LETHALITY SIMULATION METHOD



EXAMPLE ANALYSIS



CONCLUSION



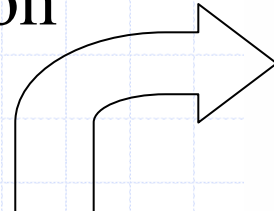
FUTURE WORK



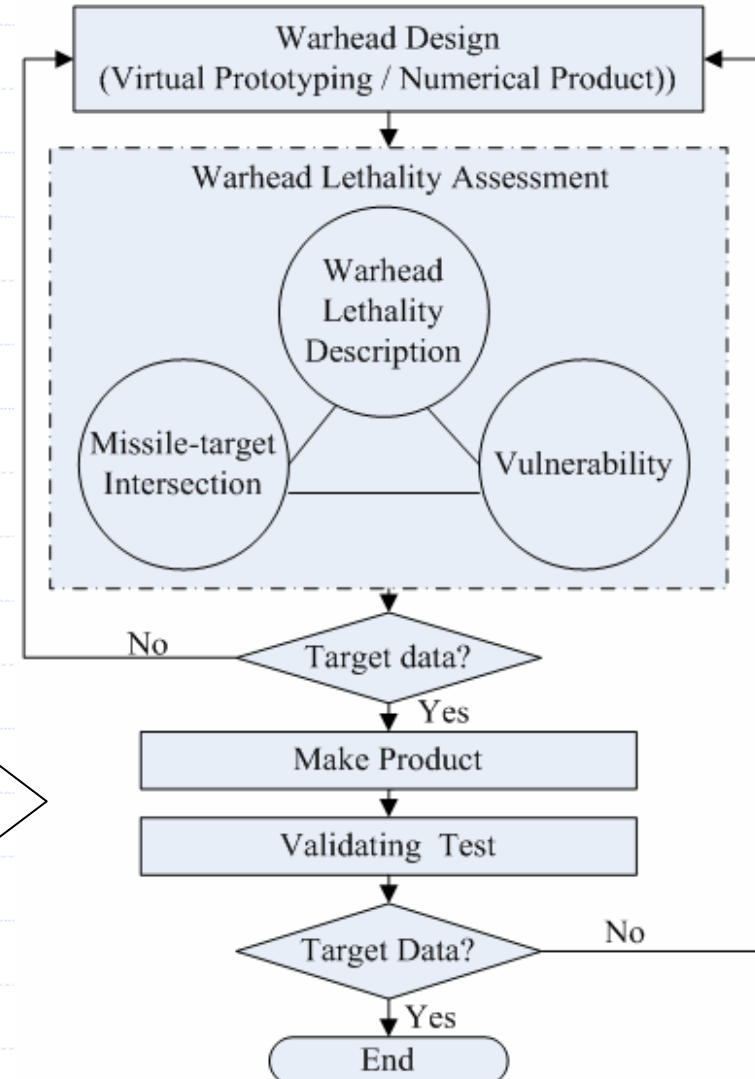
THANKS

INTRODUCTION

👉 Warhead lethality assessment is an important factor of warhead study. It always warhead lethality description, missile-target intersection and vulnerability.



A work flow of warhead study

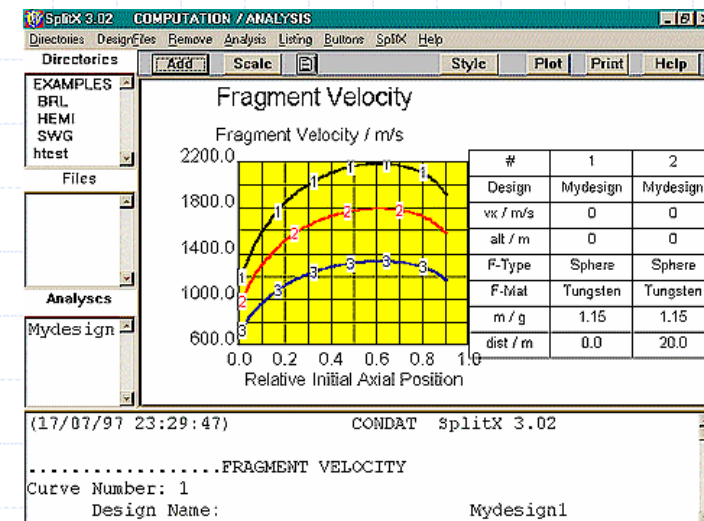


INTRODUCTION

- 👉 With the development of numerical simulation, many new methods of lethality assessment come forth
- 👉 Lethality test simulation could examine whether lethality target data is satisfied with design requirement before making the product, so development cycle is shorten and outlay is reduced.
- 👉 Test method, analytical method and numerical simulation method are widely adopted .

Analytical method

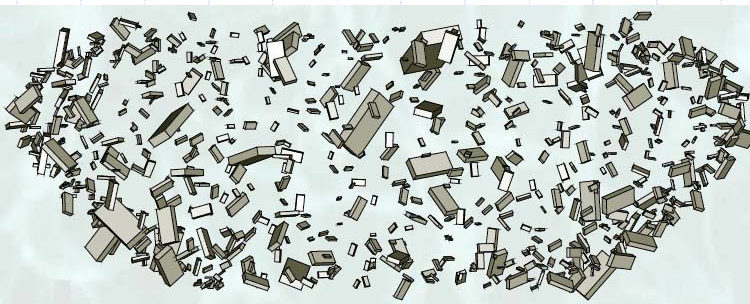
- Analytical methods are often used. Such as SplitX and LATFW, they have been applied largely in design and assessment of warhead .
- SplitX of CONDAT Company is an expert system for the design of fragmentation warhead.
- Assess warhead by analytical method



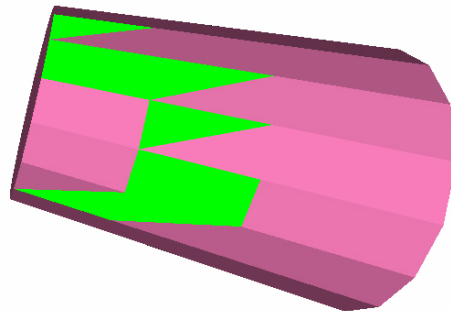
(a) Fragment Velocity Distribution

Analytical method

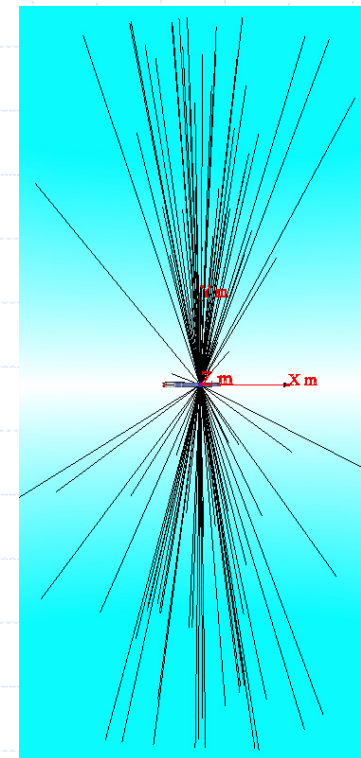
► LATFW (L lethality Assessment of Typical Fragmentation Warhead) is achieved by our institute in China.



(a) Fragment fields simulation



(b) damage effect of one cabin



(c) Shotline simulation

Analytical method

👉 Virtue

- It can be used to rapidly assess a new or existing warhead design.
- Warhead design is accomplished based on the method in a short space of time.

👉 Shortcoming

- The deviation can be introduced if the methods do not be verified or modified by test data .
- The methods are limited by specifically condition.

Numerical simulation method

- ☞ The prediction results by the numerical simulation method are more accurate than those by forenamed methods. It can make structural analysis, detonation calculation and so on.
- ☞ The method is fit for the multifarious warheads, such as the axisymmetric warhead and unsymmetrical warhead.
- ☞ Thinking over calculation scale and complication. The method is adopted in one stage of lethality assessment process.

Test method

👉 Early, the lethality assessment method is warhead test. However, a large number of lethality tests may prolong development cycle and increase outlay.

In present, the integrated method including test method, analytical method and numerical simulation method is commonly adopted.

Our Study

- 👉 How do we make lethality simulation for fragmentation warhead when efficiency and precision must be considered?
- 👉 By integrating Numerical simulation method and analytical method, lethality simulation method for fragmentation warhead is established.
- 👉 By numerical simulation method, the fragment initial fields are gained. Based on analytical method, fragment movement model and fragment impact model on target are established.

Our Study

- 👉 The whole process description of fragment field formed, fragment movement, and fragment impacting on target is achieved by using the method.
- 👉 In my topic, I only present my outlook of our study. I want to validate whether the method is feasibility. We analyze the powerful parameters that affect warhead lethality based on example analysis.

LETALITY SIMULATION METHOD

- ☞ L lethality simulation method of fragmentation warhead consists of numerical simulation model, fragment movement model, lethality parameter model, damage analysis model and fragment field simulation model.
- Fragment initial fields are gained based on numerical results.
- Fragment movement model calculates fragment trajectory. Damage analysis model analyzes fragment damage performance to target.

LETALITY SIMULATION METHOD

- Lethality parameter model analyzes fragment hitting density distribution and the dispersal angle distribution of fragments.
- Fragment field formed, fragment movement, and fragment impacting on target are achieved by fragment field simulation model.

Numerical simulation model

➤ Numerical simulation model includes numerical simulation and Interface middleware. Numerical simulation is accomplished by LS-DYNA. Because LS-DYNA only outputs node velocity and location, interface middleware is developed to achieve fragment velocity and location. Using interface middleware, fragment initial field is gained and saved.

Fragment No	Location			Velocity		
	X m	Y m	Z m	Vx m/s	Vy m/s	Vz m/s
1	0.0011	0.6993	0.01557	29.68	2627.00	36.60
2	0.0089	0.7145	0.07378	34.43	2723.90	27.81
.....						

File format of fragment initial fields

Numerical simulation model

■ Interface middleware is builded based on modified former code. Numerical results are dealed through calling interface middleware, so data exchange between numerical simulation model with fragment movement model.

Fragment movement model

- In fragment movement stage, fragment characteristic parameters are calculated in fragment field. Because of small fragment mass and short fragment trajectory as well as high fragment velocity, fragment gravitational effect is ignored and we assume fragment trajectory is linear.
- Assuming the air drag coefficient is invariable, fragment residual velocity is calculated by

$$V_r = V_0 \exp \left(- \left(\frac{C_D \rho_0 H(Y) A_s g}{2q} \right) r \right)$$

$$C_D = C_{Dsphere} + \frac{S_n - S_{nsphere}}{S_{nnature} - S_{nsphere}} (C_{Dnature} - C_{Dsphere})$$

Fragment movement model

- In this analytical model, we don't think over the effect of fragment tumbling.
- In the paper (Fragment Shot-line Model for Air-Defense Warhead, PEP 25, No.2□2000), the analytical model including the effect of fragment tumbling and air drag on fragment trajectory is presented by our team.

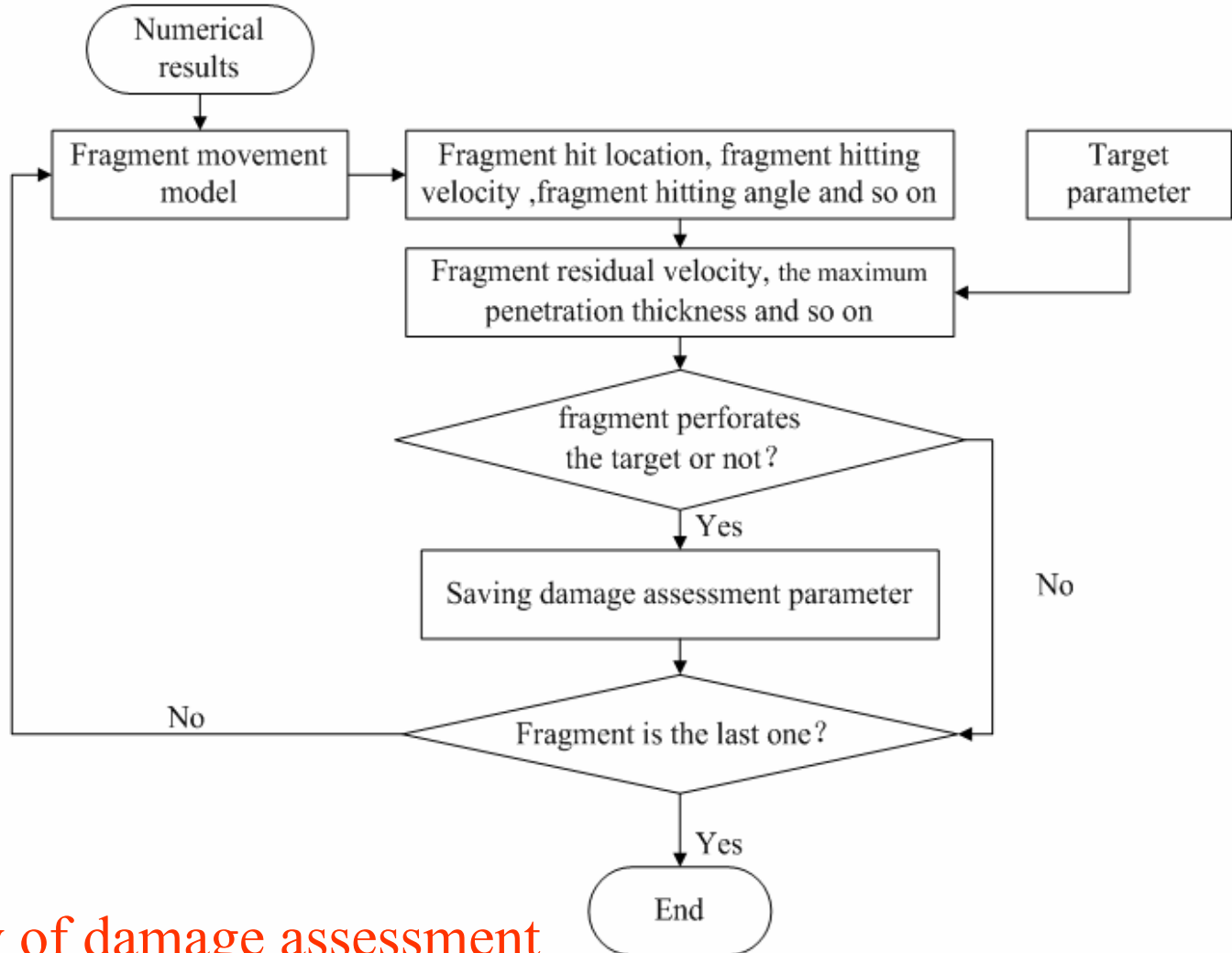
Damage analysis model

- THOR method is adopted to assessment the maximum penetration thickness, the residual mass and the residual velocity.
 - THOR fits for steel fragment impacting on the metallic and nonmetallic target, especially it fits for fragment of high detonator warhead

$$\begin{cases} V_r = V_s - 0.3048 \times 10^{c_{11}} (61023.75hA)^{c_{12}} (15432.1m_s)^{c_{13}} (\sec \theta)^{c_{14}} (3.28084 V_s)^{c_{15}} \\ m_r = m_s - 6.48 \times 10^{c_{21}} (61023.75hA)^{c_{22}} (15432.1m_s)^{c_{23}} (\sec \theta)^{c_{24}} (3.28084 V_s)^{c_{25}} \end{cases}$$

$$h_{\max} = 1.638706 \times 10^{-5-c_{11}/c_{12}} A^{-1} (15432.1m_s)^{-c_{13}/c_{12}} (\sec \theta)^{-c_{14}/c_{12}} (3.28084 V_s)^{(1-c_{15})/c_{12}}$$

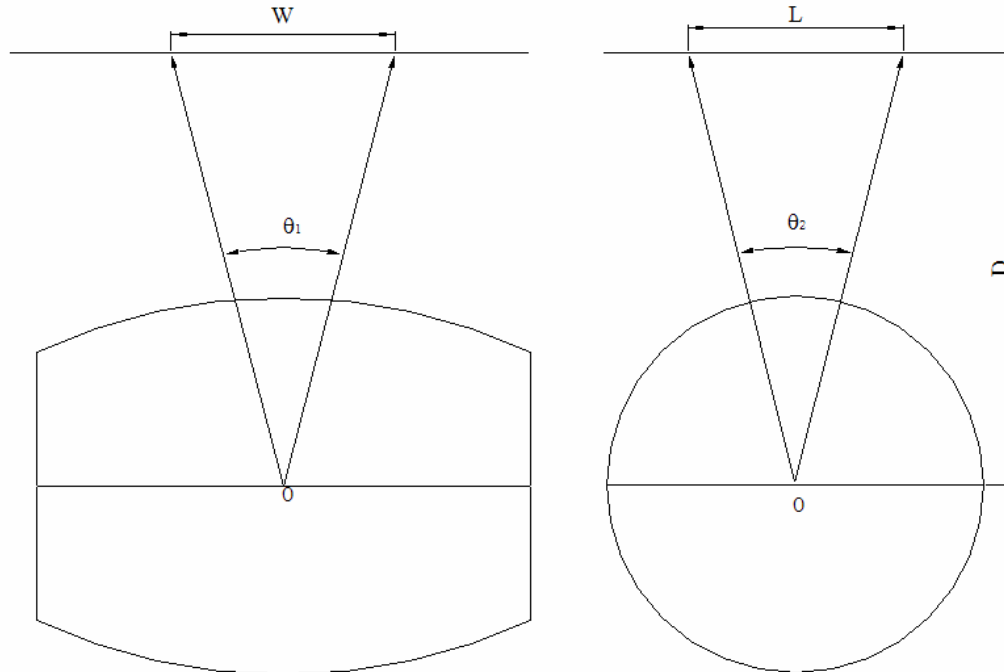
Damage analysis model



Work flow of damage assessment

Lethality parameter model

☞ Definitions of the variables



W—Width of statistical area L—Length of statistical area.

θ_1 —Fragment projection angle θ_2 —Warhead radius angle.

D—Target distance.

Lethality parameter model

Fragment density is affected by statistical area. In order that statistical results are accurate the length of statistical area is ascertained according to warhead radius angle. According to the dispersal angle of fragments the width of statistical area is calculated, the work flow:

$$(1) \quad \theta_1 = 2 \arctan\left(\frac{W}{2D}\right)$$

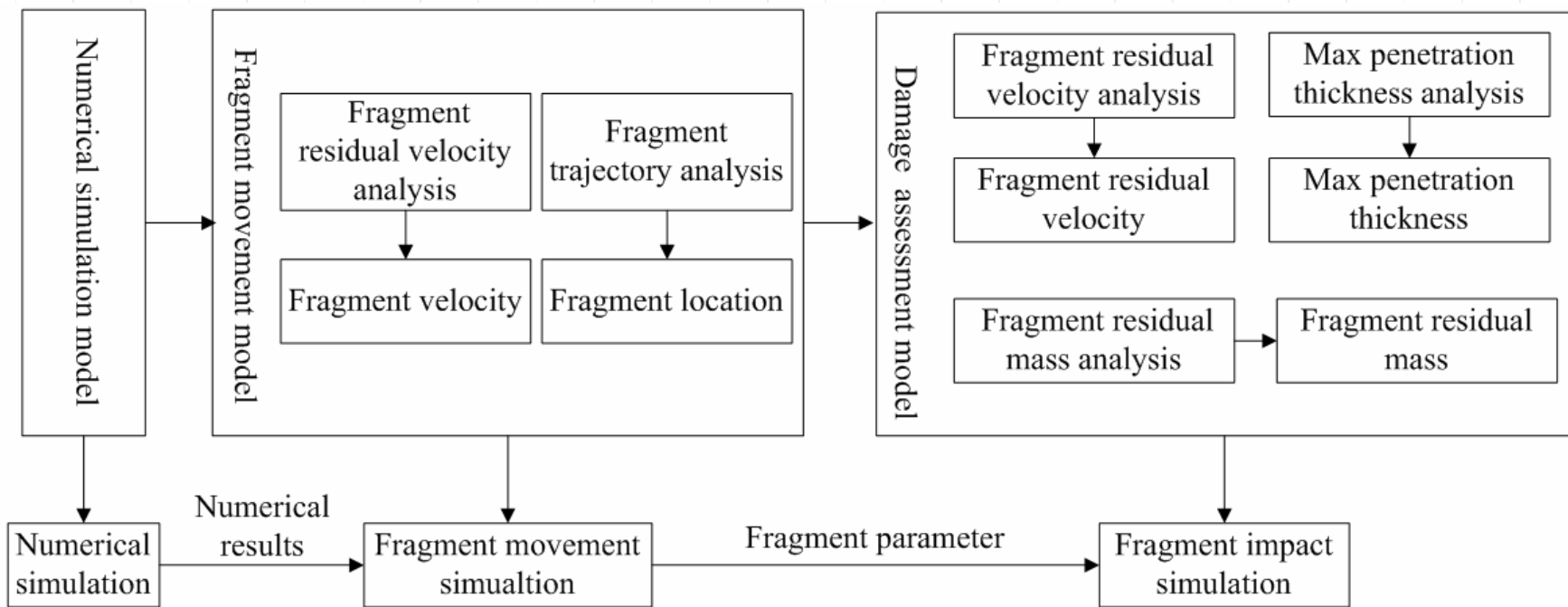
$$(2) \quad L = 2D \cdot \tan\left(\frac{\theta_2}{2}\right)$$

$$(3) \quad \rho = \frac{0.9 N_{\text{frag}}}{L \times W}$$

(4) Based on warhead radius angle the statistical number is ascertained, for the whole target. Fragment density of each statistical area is gained by the step(1)~(3)□

Simulation model

System simulation model divides into three stages.



System simulation model

Simulation model

- System simulation model calculates trajectory, velocity, residual velocity and residual mass.
- In order to investigate fragment field in different time simulation data is saved, and fragment field simulation is displayed in other CAD software.

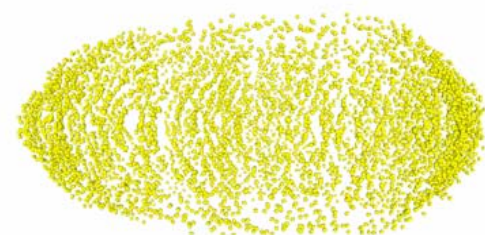
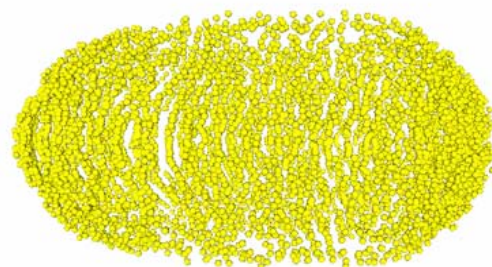
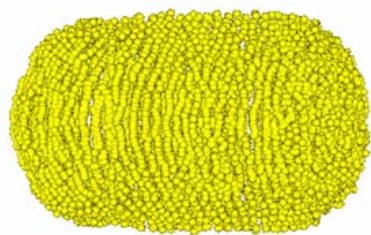
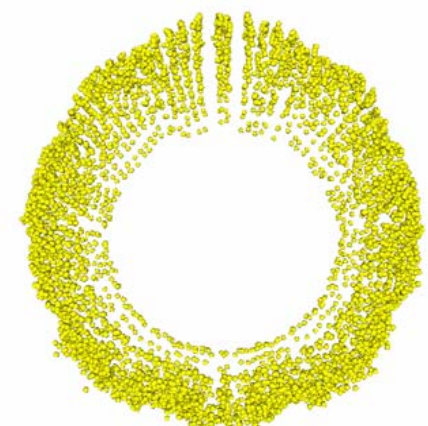
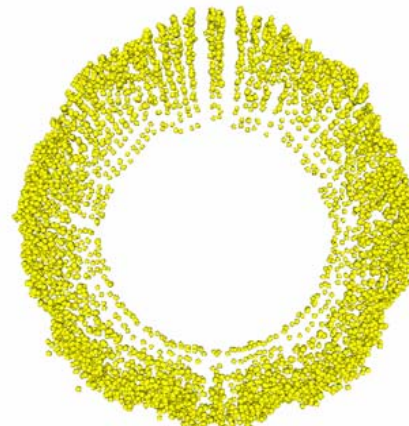
EXAMPLE ANALYSIS

On the basis of the simulation method, lethality simulation code is developed. One example of an aimable warhead is examined.

- ❖ **System visualization**
- ❖ **Analysis of fragment density**
- ❖ **Analysis of fragment projection angle**

System visualization

👉 Fragment field simulation



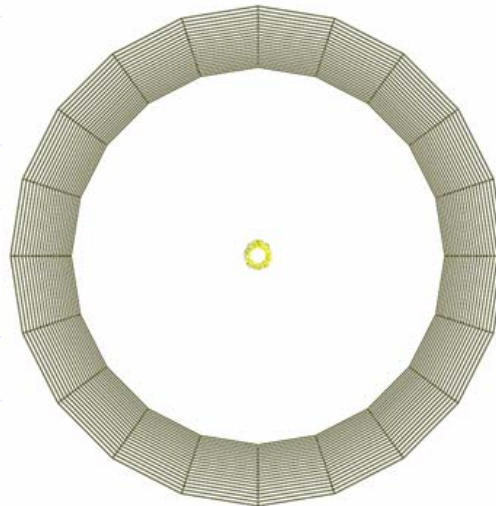
(a) $\tau = 0.25$ ms

(b) $\tau = 0.46$ ms

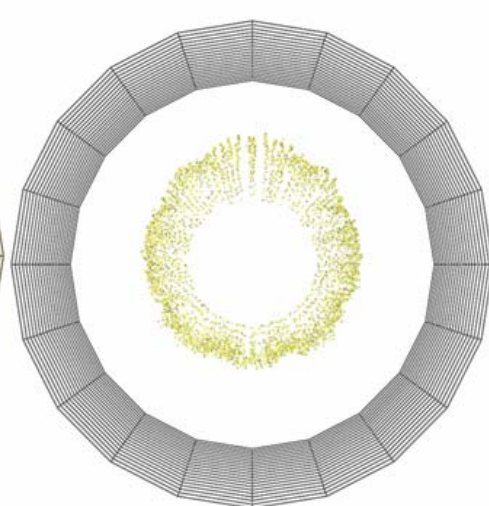
(c) $\tau = 0.80$ ms

System visualization

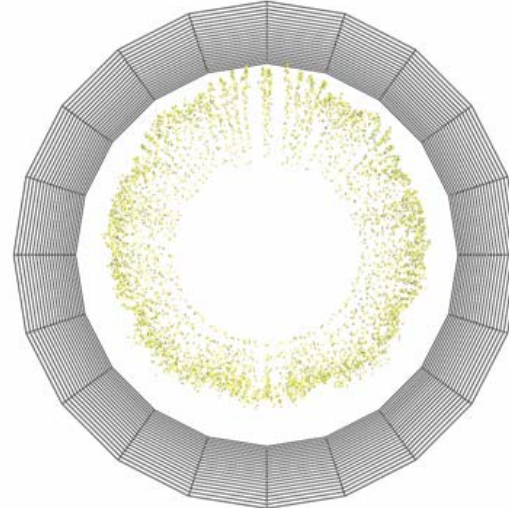
👉 Fragment field simulation



(a) 0.25 ms



(b) 1.98 ms

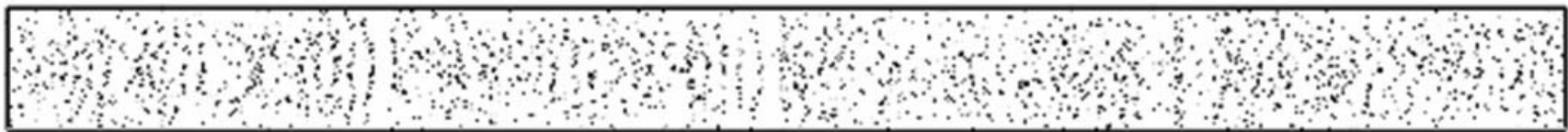


(c) 2.88 ms

➤ The aimable area is not obvious at 0.25 ms. The fragment velocity in aimable area is higher than those in non-aimable area at 2.88 ms. Aimable fragments firstly hit target.

System visualization

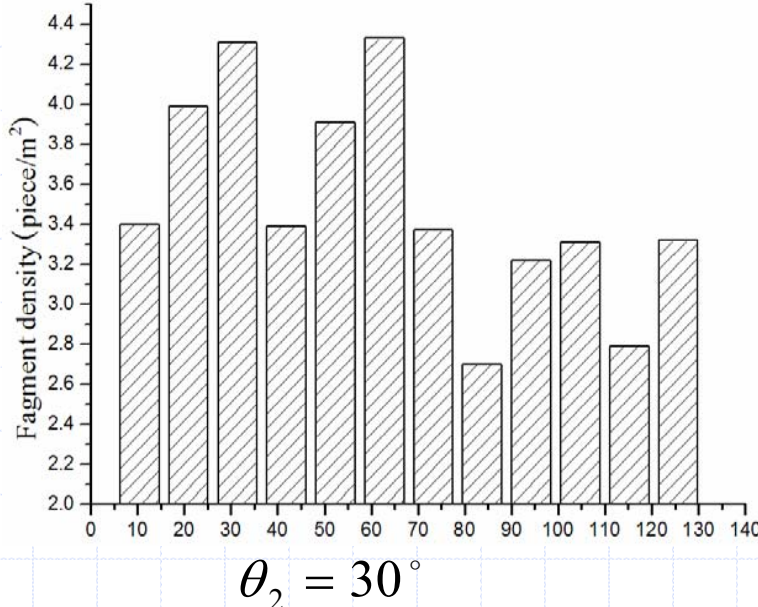
👉 Fragment field simulation



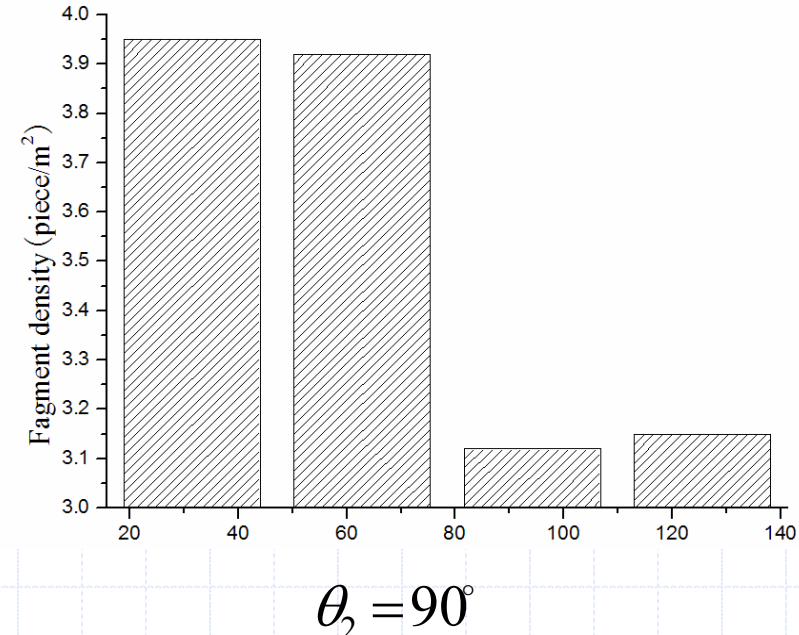
➤ This graph shows visualization graph of fragment distribution on target. Target height is 10m and target distance is 20m. The circle target is unwrapped in order to represent fragment distribution clearly.

Analysis of fragment density

Two cases



$$\theta_2 = 30^\circ$$



$$\theta_2 = 90^\circ$$

- At 30° fragment density fluctuates heavily in each statistical area, The aimable area is not obvious.
- At 90° the aimable area is obvious.

Analysis of fragment density

👉 Results

- According to the analytical results, the variational trend of fragment density is similar when θ_2 is same even if the target distance is different.
- Suppose fragment trajectory is linear, when θ_2 is same fragment density is in inverse proportion to the square of target distance that is match with analytical results.

Analysis of fragment projection angle

- 👉 Considering the relationship between fragment projection angle and warhead radius angle, fragment projection angle corresponding is the average value of projection angle in different statistical area.
- 👉 Fragment projection angle is not sensitive to θ_2 and the statistical error is less than 1° . Fragment projection angle ranges from 42° to 43° .

Analysis of fragment projection angle

Results

- Fragment projection angle in different statistical area fluctuates when θ_2 is same.
- At the same time fragment project angle fluctuates with the change of warhead radius angle but the extent is small.
- Fragment project angle distribution of aimable warhead is unsymmetrical and fluctuates heavily. The factor must be considered. It's better to point out which area projection angel is in aimable area, non-aimable area or all the area.

CONCLUSION

- 👉 Lethality simulation method includes numerical simulation and theoretical analysis, so the method fits for different kinds of the warhead by generalizing it.
- 👉 Based on the method, lethality simulation system is constructed, and numerical simulation of fragmentation warhead lethality are achieved by the system, and analytical results are directly applicable for warhead lethality assessment.
- 👉 Based on the test, the method is an effective method of validating numerical simulation.

FUTURE WORK

- 👉 How to assess Virtual Prototyping (Numerical Products) of warhead thinking over precision and efficiency?
- 👉 How to integrate lethality assessment and warhead design, and establish the composite design environment of warhead study.
- 👉 Our thinking
 - Lethality simulation method and code are studied by integrating analytical method, numerical simulation method in warhead lethality description, missile-target intersection and vulnerability.

FUTURE WORK

☞ Warhead lethality description

- Warhead lethality description for different kinds of the warhead is studied by the integrated method.

☞ Missile-target intersection

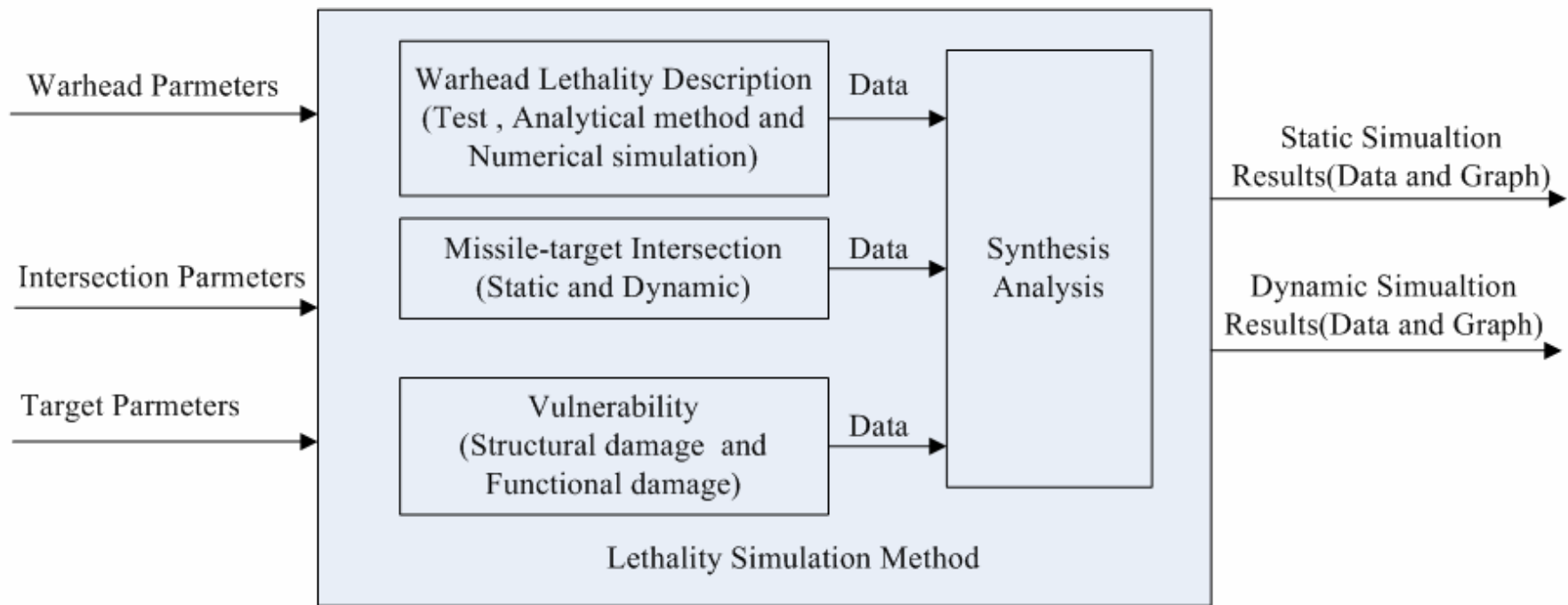
- Static intersection → Dynamic intersection.

☞ Vulnerability

- Vulnerability analysis method is traced and analyzed.
- Structural damage and functional damage.

FUTURE WORK

☞ Lethality Simulation Code



➤ This code is easy to integrate with the compositive design environment.

THANKS

Thank you
for your attention!